Polymorphism in Pharmaceutical Solids

Edited by
Harry G. Brittain

Discovery Laboratories, Inc.
Milford, New Jersey

MARCEL DEKKER, INC.
NEW YORK BASEL

UM00016531
NOVARTIS EXHIBIT 1517
Novartis v. Regents, IPR2023-01347
Page 3513 of 4460

ISBN: 0-8247-0237-9

This book is printed on acid-free paper.

Headquarters
Marcel Dekker, Inc.
270 Madison Avenue, New York, NY 10016
tel:212-696-9000; fax:212-685-4540

Eastern Hemisphere Distribution
Marcel Dekker AG
Hutgasse 4, Postfach 812, CH-4001 Basel, Switzerland
tel:44-61-261-8482; fax:44-61-261-8896

World Wide Web
http://www.dekker.com

The publisher offers discounts on this book when ordered in bulk quantities. For more information, write to Special Sales/Professional Marketing at the headquarters address above.

Copyright ©1999 by Marcel Dekker, Inc. All Rights Reserved.

Neither this book nor any part may be reproduced or transmitted in any form or by any means, electronic or mechanical, including photocopying, microfilming, and recording, or by any information storage and retrieval system, without permission in writing from the publisher.

Current printing (last digit):
10 9 8 7 6 5 4 3 2 1

PRINTED IN THE UNITED STATES OF AMERICA

UM00016532
NOVARTIS EXHIBIT 1517
Novartis v. Regents, IPR2023-01347
Page 3514 of 4460

5
Generation of Polymorphs, Hydrates, Solvates, and Amorphous Solids

J. Keith Guillory
The University of Iowa
Iowa City, Iowa

I. Methods Employed to Obtain Unique Polymorphic Forms 184

A. Sublimation 186

B. Crystallization from a Single Solvent 188

C. Evaporation from a Binary Mixture of Solvents 194

D. Vapor Diffusion 195

E. Thermal Treatment 195

F. Crystallization from the Melt 197

G. Rapidly Changing Solution pH to Precipitate Acidic or Basic Substances 198

H. Thermal Desolvation of Crystalline Solvates 199

I. Growth in the Presence of Additives 201

J. Grinding 202

II. Methods Employed to Obtain Hydrate Forms 202

III. Methods Employed to Obtain Solvate Forms 205

UM00016533
NOVARTIS EXHIBIT 1517
Novartis v. Regents, IPR2023-01347
Page 3515 of 4460

the crystal free to grow at the opposite pole. Since it is bound at the slow growing NH_{3+} end of the polar axis, it does not interfere with the fast growing CO_{2-} end.

J. Grinding

Polymorphic transformations have been observed to occur on grinding of certain materials, such as sulfathiazole, barbital, phenylbutazone, cephalexin, chloramphenicol palmitate, indomethacin, and chlorpropamide. Byrn [46] has stated that polymorphic transformations in the solid state require the three steps of (a) molecular loosening (nucleation by separation from the lattice), (b) solid solution formation, and (c) separation of the product (crystallization of the new phase). Depending on the material and the conditions employed, grinding can result in conversion to an amorphous substance. With the exercise of care, different polymorphic forms can be obtained. Otsuka et al. [57] showed that metastable Forms B and C of chloramphenicol palmitate were transformed into stable Form A upon grinding at room temperature. Indomethacin was transformed into a noncrystalline solid during grinding at 4°C, and into metastable Form A by grinding at 30°C. Caffeine Form II is converted into Form I with grinding, and a 95% phase conversion was obtained following 60 hours of grinding time [38].

II. Methods Employed To Obtain Hydrate Forms

Pharmaceutical solids may come into contact with water during processing steps, such as crystallization, lyophilization, wet granulation, aqueous film-coating, or spray-drying. Moreover, they may be exposed to water during storage in an atmosphere containing water vapor, or in a dosage form consisting of materials that contain water (e.g., excipients) and are capable of transferring it to other ingredients. Water may be adsorbed onto the solid surface and/or may be absorbed in the bulk solid structure. When water is incorporated into the crystal lattice of the compound in stoichiometric proportions, the molecular adduct or adducts formed are referred to as hydrates [58]. More than 90 hydrates

UM00016534
NOVARTIS EXHIBIT 1517
Novartis v. Regents, IPR2023-01347
Page 3516 of 4460

are described in various USP monographs. Hydrates can be prepared by recrystallization from water or from mixed aqueous solvents. They can also result, in some instances, from exposure of crystal solvates (such as methanolates or ethanolates) to an atmosphere containing water vapor.

Crystalline substances often form with water molecules located at specific sites in the crystal lattice, which are held in coordination complexes around lattice cations. This type of water is denoted as water of crystallization and is common for inorganic compounds. For example, nickel sulfate forms a well-defined hexahydrate, where the waters of hydration are bound directly to the Ni(II) ion. Extraneous inclusion of water molecules can occur if a coprecipitated cation carries solvation molecules with it. Water also can be incorporated into random pockets as a result of physical entrapment of the mother liquor. Well-defined multiple hydrate species can also form with organic molecules. For example, raffinose forms a pentahydrate.

Although most hydrates exhibit a whole-number-ratio stoichiometry, an unusual case is the metastable hydrate of caffeine, which contains only 0.8 moles of water per mole of caffeine. Only in a saturated water vapor atmosphere will additional amounts of water be adsorbed at the surface of the 4/5-hydrate to yield a 5/6 hydrate [59].

In some instances, a compound of a given hydration state may crystallize in more than one form, so that the hydrates themselves exhibit polymorphism. One such example is nitrofurantoin, which forms two monohydrates that have distinctly different temperatures and enthalpies of dehydration. The monohydrates have quite different packing arrangements, with Form I possessing a layer structure and Form II exhibiting a herringbone motif. The included water molecules play a major role in stabilizing the crystal structures. Whereas water molecules are contained in isolated cavities in Form II, in Form I they are located in continuous channels, and this apparently facilitates the escape of water when these crystals are heated [60].

Another example of hydrate polymorphism is amiloride hydrochloride [61], which can be obtained in two polymorphic dihydrate forms. These forms are indistinguishable by techniques other than x-ray powder diffraction.

It is interesting that scopolamine hydrobromide has been reported

UM00016535
NOVARTIS EXHIBIT 1517
Novartis v. Regents, IPR2023-01347
Page 3517 of 4460

to exist as the anhydrous form, a "hemihydrate," a sesquihydrate, and a trihydrate [62], while the unit cell parameters and the molecular geometry of these are all the same as those of the hemihydrate. This finding suggests that the "hemihydrate" is actually a partially desolvated sesquihydrate.

Ouabaine is another example of a compound that exhibits many different hydration levels, the most hydrated form being stable at the lowest temperature. Thus the nonahydrate phase of ouabaine is obtained from water at 0–15°C, the octahydrate phase at 15–28°C, and the dihydrate phase at 28–90°C. In addition, ouabaine phases corresponding to 4.5 H_2O, 4 H_2O, and 3 H_2O may be obtained from mixtures of water with other solvents. The anhydrous phase of ouabaine anhydrate is crystallized from ethanol at high temperatures [63].

Typically, hydrates are obtained by recrystallization from water. For example, trazodone hydrochloride tetrahydrate was prepared by dissolving the anhydrate in hot distilled water, allowing the solution to remain at room temperature overnight, and storing the collected crystals at 75% relative humidity and 25°C until they reached constant weight [64].

Hydrates can sometimes be obtained by simply suspending the anhydrous material in water, whereupon a form of Ostwald ripening occurs. For instance, aqueous suspensions of anhydrous metronidazole benzoate are metastable, and storage at temperatures lower then 38°C leads to monohydrate formation accompanied by crystal growth [65]. Sorbitol provides another example of this behavior, where slow cooling of a saturated aqueous solution yields long thin needles of sorbitol hydrate [66]. When suspended in water, anhydrous carbamazepine is transformed to carbamazepine dihydrate [67]. In other instances, hydrates can be obtained from mixed solvent systems. Acemetacin monohydrate can be obtained by slow evaporation from a mixture of acetone and water at room temperature [68].

Simply exposing an anhydrous powder to high relative humidity can often lead to formation of a hydrate. On exposure to a relative humidity of 100%, dexmedetomidine hydrochloride is converted to a monohydrate [69]. Droloxifene citrate is an example of a compound that is not very hygroscopic and yet forms a hydrate. Only after storage of the anhydrous form at 85% relative humidity does some sorption of

UM00016536
NOVARTIS EXHIBIT 1517
Novartis v. Regents, IPR2023-01347
Page 3518 of 4460

water occur. The monohydrate phase can be formed by exposing the anhydrous form to 98% relative humidity for ten days at 24°C [70].

III. Methods Employed To Obtain Solvate Forms

Often, when solvents are employed in the purification of new drug substances by recrystallization, it is observed that the isolated crystals include solvent molecules, either entrapped within empty spaces in the lattice or interacting via hydrogen bonding or van der Waals force with molecules constituting the crystal lattice. Solvent molecules also can be found in close association with metal ions, completing the coordination sphere of the metal atom. Coordinated solvent molecules are considered as part of the crystallized molecule. A crystal with large empty channels or cavities is not stable because of packing demands. The size and chemical environment of the cavity or channel determine what kind of solvent molecule can be included in the structure and what kind of interaction occurs between solvent and structure.

Depending on the nature of molecular packing arrangements, it may happen that the inclusion of solvent is necessary to build a stable crystal structure. van Geerestein et al. [71] found during numerous crystallization attempts of 11β-[4-(dimethylamino)phenyl]-17β-hydroxy-17α-(1-propynyl) estra-4,9-diene-3-one] that crystals were only obtainable in the presence of *n*-butyl acetate or *n*-propyl acetate. The crystal structure of the compound crystallized from *n*-butyl acetate/methylcyclohexane was solved, and one solvent molecule was found in the crystal structure that showed no strong interactions with the rest of the structure. Apparently, this solvent molecule was necessary to fill empty space resulting after the molecular packing. Solvates in which the solvent fills empty space are generally nonstoichiometric, such as the nonstoichiometric solvates formed by droloxifene citrate with acetonitrile, 2-propanol, ethanol, 1-propanol, and 1-butanol. Typically such solvates exhibit the same x-ray diffraction pattern as does the nonsolvated compound.

When solvent molecules increase the strength of the crystal lattice, they can affect the stability of the compound to solid-state decom-

UM00016537
NOVARTIS EXHIBIT 1517
Novartis v. Regents, IPR2023-01347
Page 3519 of 4460

position. It has been observed that the four solvated and one nonsolvated structures of prenisolone *tert*-butyl acetate affect the flexibility of the steroid nucleus and the structure-dependent degradation of the compound when exposed to air and light [72].

van der Sluis and Kroon found 1,247 different compounds with cocrystallized solvents in the Cambridge Crystallographic Database [73]. Out of 46,460 total structures, they found 9,464 solvate structures, and 95% of these contained one of the 15 solvents given in Table 2.

The most commonly encountered solvates among pharmaceuticals are those of 1:1 stoichiometry, but occasionally mixed solvate species are encountered. For structures containing more than one solvent type, one generally finds nonpolar solvents crystallizing together on the one hand and polar solvents on the other. For example, the most common solvents found cocrystallizing with water are (in order of im-

Table 2 Distribution of the 15 Most Abundant Solvents in the Cambridge Crystallographic Database, as the Percentage of Solvate Structures

Solvent	Occurrence (%)
Water	61.4
Methylene dichloride	5.9
Benzene	4.7
Methanol	4.1
Acetone	2.8
Chloroform	2.8
Ethanol	2.6
Tetrahydrofuran	2.3
Toluene	2.2
Acetonitrile	1.9
N,N-dimethylformamide	0.9
Diethyl ether	0.9
Pyridine	0.7
Dimethyl sulfoxide	0.5
Dioxane	0.5

Source: From Ref. 73. Reproduced with permission of the copyright owner.

UM00016538
NOVARTIS EXHIBIT 1517
Novartis v. Regents, IPR2023-01347
Page 3520 of 4460

portance) ethanol, methanol, and acetone. An interesting example of a structure containing a polar and a nonpolar solvent is the sodium salt of the antibiotic K-41, *p*-bromobenzoate monohydrate *n*-hexane solvate [74], which is crystallized from *n*-hexane saturated with water. Perhaps the best known mixed solvate is doxycycline hyclate: (doxycycline HCl)$_2$C$_2$H$_6$). H$_2$O. Triamterene also forms a mixed solvate, containing one *N,N*-dimethylformamide molecule and one water molecule within the crystal lattice [75].

The techniques used to obtain solvates are generally similar to the solvent methods used to obtain polymorphs, i.e. crystallization from a single solvent, from mixed solvents, or by vapor diffusion. Sometimes, it is possible to exchange one solvent within the crystal structure for another. When one recrystallizes a hydrate from dry methanol, in most cases one is left with either a methanol solvate or an anhydrous, unsolvated form of the compound.

A large number of solvates have been reported, especially for steroids and antibiotics. It has been observed that cortisone acetate and dexamethasone acetate can be crystallized as 10 different solvates. Dirithromycin, a semisynthetic macrolide antibiotic, crystallizes in two anhydrous polymorphic forms and in at least nine stoichiometric solvate forms. Six of the known solvates are isomorphic, having nearly identical x-ray powder diffraction patterns [76]. In addition to the anhydrate and dihydrate, erythromycin also forms solvates with acetone, chloroform, ethanol, *n*-butanol, and *i*-propanol [77].

It may be instructive to consider some examples of solvate formation. The compound 5-methoxysulphadiazine forms 1:1 host-guest solvates with dioxane, chloroform, and tetrahydrofuran [78]. These were prepared by heating to boiling a solution of the sulfonamide in the appropriate solvent, followed by slow cooling to obtain large crystals. Spironolactone forms 1:1 solvates with methanol, ethanol, ethyl acetate, and benzene. It also forms a 2:1 spironolactone-acetonitrile solvate [79,80]. The spironolactone solvates were prepared by crystallization in a refrigerator from solutions that were nearly saturated at room temperature.

Another steroid that forms solvates is stanozolol [81]. Solvates having 1:1 stoichiometry were prepared by recrystallization from methanol, ethanol, and 2-propanol, by heating the compound in the

UM00016539
NOVARTIS EXHIBIT 1517
Novartis v. Regents, IPR2023-01347
Page 3521 of 4460

appropriate solvent to 60–70°C and then cooling to 0°C in an ice bath to induce crystallization. The compound also forms a monohydrate and two polymorphs. The polymorphs were prepared by heating the solvates to either 130°C (Form II) or 205°C (Form I).

Mefloquine hydrochloride is an interesting case of a compound that forms stoichiometric 1:1 solvates on cooling hot (50°C) saturated acetone solutions (Form B, acetone solvate 1:1), hot (50°C) saturated isopropanol (Form I, isopropanol solvate 1:1), and a nonstoichiometric ethanol solvate (2.12% ethanol) from hot (50°C) saturated ethanol, Form E, whose x-ray powder pattern does not change following heating to 80°C, in spite of a decrease in the ethanol level to 0.12%. Mefloquine hydrochloride can also be obtained in a nonsolvated form from hot (70°C) saturated acetonitrile (Form A) and as two hemihydrates from water (Forms D and C) prepared at room temperature and at 30°C [82].

IV. Methods Employed To Obtain Amorphous Materials

Solids can exist in crystalline or amorphous form. Crystalline materials have defined structures, stoichiometric compositions, and melting points and are characterized by their chemical, thermal, electrical, optical, and mechanical properties [83]. By contrast, amorphous materials have no clearly defined molecular structure and no long-range order, so their structure can be viewed as being similar to that of a frozen liquid but without the thermal fluctuations observed in the liquid phase. As a result, amorphous materials exhibit the classical diffuse "halo" x-ray powder diffraction pattern rather than the sharp peaks observed in the pattern of a crystalline substance. When the halo is broad, it is often difficult to distinguish between a material that is truly amorphous (e.g., a true glass) and one that is merely microcrystalline. This situation exists because when microcrystallites have diameters less than about 50 Å in diameter, a similar "halo" effect is observed.

While crystalline solids offer the advantages of chemical and thermodynamic stability, amorphous solids are occasionally preferred because they undergo dissolution at a faster rate. Rapid dissolution is desirable in the case of solids, which must be dissolved prior to paren-

UM00016540
NOVARTIS EXHIBIT 1517
Novartis v. Regents, IPR2023-01347
Page 3522 of 4460

of sodium fenoprofen, the calcium fenoprofen that precipitates has a low degree of crystallinity [159]. Similarly, when calcium DL-pantothenate is precipitated from methanol or ethanol solution by the addition of acetone, ether, ethyl acetate, or other solvents, the precipitate obtained is found to be amorphous [154].

V. Summary

The pharmaceutical development scientist who is assigned the task of demonstrating that a substance exhibits only one crystalline form, or that of discovering whether additional forms exist, can utilize the techniques outlined in this chapter as a starting point. Upon completion of this program, one can certainly conclude that due diligence has been employed to isolate and characterize the various solid-state forms of any new chemical entity. One should always be aware that nuclei capable of initiating the crystallization of previously undiscovered forms might be lurking around the laboratory, ready to confound the investigator should their effects become known. In addition, the phenomenon of "disappearing polymorphs" can come into play, and techniques that formerly yielded the same crystals every time may subsequently yield crystals of another, more stable form. In the future, the use of computer simulations of alternative crystallographic structures will suggest how much laboratory work might be required to isolate the polymorphs or solvates of a given compound. Until then, the empirical approach remains superior.

References

1. S. R. Byrn, personal communication, October 2, 1996.

2. W. C. McCrone, Jr., *Fusion Methods in Chemical Microscopy,* Interscience, New York, 1957.

3. H. R. Karfunkel, F. J. J. Leusen, and R. J. Gdanitz, *J. Comp.-Aided Mater. Des., 1,* 177 (1993).

4. H. R. Karfunkel, Z. J. Wu, A. Burkhard, G. Rihs, D. Sinnreich, H. M. Buerger, and J. Stanek, *Acta Cryst., B52,* 555 (1996).

5. J. D. Dunitz, and J. Bernstein, *Acc. Chem. Res. 28,* 193 (1995).

UM00016541
NOVARTIS EXHIBIT 1517
Novartis v. Regents, IPR2023-01347
Page 3523 of 4460

Acta Crystallographica Section C
Crystal Structure Communications
ISSN 0108-2701

Neutron diffraction studies of the 1:1 and 2:1 cocrystals of benzene-1,2,4,5-tetracarboxylic acid and 4,4′-bipyridine

John A. Cowan,[a]*‡ Judith A. K. Howard,[a] Sax A. Mason,[b] Garry J. McIntyre,[b] Samuel M.-F. Lo,[c] Toby Mak,[c] Stephen S.-Y. Chui,[c] Jiwen Cai,[c] John A. Cha[c] and Ian D. Williams[c]

[a]Department of Chemistry, University of Durham, Durham DH1 3LE, England, [b]Institut Laue Langevin, 6 Rue Jules Horowitz, BP156, 38042 Grenoble Cedex 9, France, and [c]Department of Chemistry, Hong Kong University of Science and Technology, Clear Water Bay, Hong Kong, People's Republic of China
Correspondence e-mail: j.a.cowan@dl.ac.uk

Received 12 January 2006
Accepted 1 February 2006
Online 11 March 2006

The 1:1 and 2:1 cocrystals of benzene-1,2,4,5-tetracarboxylic acid (BTA) and 4,4′-bipyridine (BPY) have been studied using neutron diffraction at 215 and 20 K, respectively. BTA and BPY crystallize in a 1:1 ratio with 1.8 molecules of water, *viz.* 4,4′-bipyridinium 2,5-dicarboxybenzene-1,4-dicarboxylate 1.8-hydrate, $C_{10}H_{12}N_2^{2+}\cdot C_{10}H_4O_8^{2-}\cdot 1.8H_2O$, (I), in the space group $P\overline{1}$, with both BTA and BPY lying on inversion centres. BTA and BPY crystallize in a 2:1 ratio, *viz.* 4,4′-bipyridinium bis(2,4,5-tricarboxybenzoate), $C_{10}H_{12}N_2^{2+}\cdot 2C_{10}H_5O_8^{-}$, (II), in the space group *Cc*. The crystal structure of the 1:1 cocrystal contains one short N—H···O hydrogen bond [N···O = 2.6047 (19) Å] and one intramolecular O—H···O hydrogen bond [O···O = 2.423 (3) Å]. The crystal structure of the 2:1 cocrystal contains two N—H···O hydrogen bonds [N···O = 2.639 (3) and 2.674 (2) Å], and two intramolecular [O···O = 2.404 (3) and 2.420 (3) Å] and four strong intermolecular O—H···O hydrogen bonds [O···O = 2.613 (3), 2.718 (3), 2.628 (3) and 2.739 (3) Å].

Comment

As part of an investigation into N—H···O and O—H···N hydrogen bonds (Cowan *et al.*, 2001*a*,*b*; Cowan, Howard, Leech *et al.*, 2001; Cowan, Howard, Leech & Williams, 2001), we have produced cocrystals of benzene-1,2,4,5-tetracarboxylic acid (BTA) and 4,4′-bipyridine (BPY). In the short N···O hydrogen bond observed in the cocrystal of 4-methylpyridine and pentachlorophenol (Steiner *et al.*, 2001), the H atom lies closer to the N atom at 20 K, and migrates across the hydrogen bond to lie closer to the O atom at 296 K. We have recently (Cowan *et al.*, 2003) observed an identical phenomenon of H-atom migration in one of the two short N···O hydrogen bonds in the 1:2 cocrystal of BTA and BPY, whose structure was first described by Lough *et al.* (2000). It was speculated that similar novel behaviour may be observed in the N···O hydrogen bonds of the 2:1 and 1:1 cocrystals, the structures of which have recently been reported (Zhu *et al.*, 2003; Ruiz-Pérez *et al.*, 2004; Fabelo *et al.*, 2005).

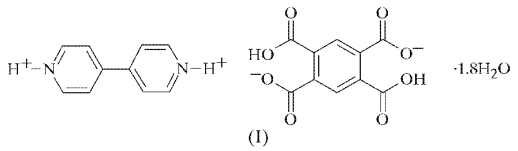

(I)

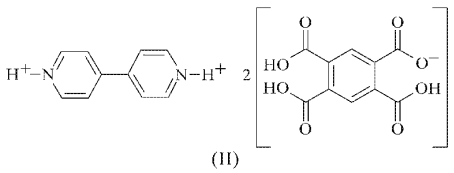

(II)

BTA and BPY crystallize in a 1:1 ratio as a molecular salt, (I), with two molecules of water, in space group $P\overline{1}$. The BTA and BPY molecules are linked by strong N—H···O hydrogen bonds to form infinite one-dimensional chains. The disordered water molecules lie in a channel along the *a* axis between parallel chains of BTA and BPY molecules (Fig. 1). The structure of (I) has been discussed previously by Fabelo *et al.* (2005).

A very short intramolecular hydrogen bond is formed [O11—H1···O21, with O···O = 2.423 (3) Å] between the carboxylic acid group and the carboxylate group. Even though the O···O separation is very short for an O—H···O hydrogen bond, the H atom is asymmetrically positioned. There is no evidence of disorder in the difference Fourier map or in the anisotropic displacement parameters of the H atom (Fig. 2).

A strong charge-assisted N—H···O hydrogen bond [N4—H4···O22, with N···O = 2.6047 (19) Å] (Gilli *et al.*, 1994) is formed between the BTA and BPY molecules. Although this is chemically very similar to the short N—H···O hydrogen bond in the 2:1 cocrystal [N···O = 2.521 (2) Å; Lough *et al.*,

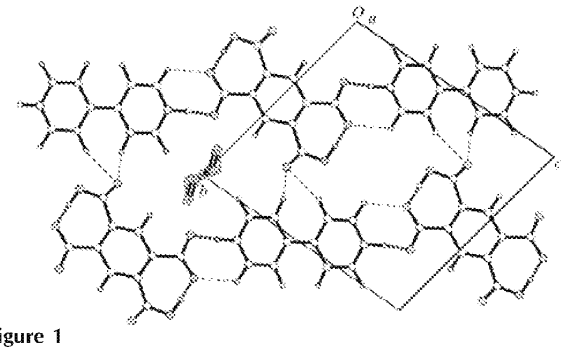

Figure 1
A packing diagram for (I), viewed perpendicular to the hydrogen-bonded chains. Hydrogen bonds are indicated by dashed lines. The disordered water molecules are visible in the large channel.

‡ Present address: Synchrotron Radiation Department, Daresbury Laboratory, Daresbury, Warrington, Cheshire WA4 4AD, England.

 DOI: 10.1107/S0108270106004008 © 2006 International Union of Crystallography

UM00016542
NOVARTIS EXHIBIT 1517
Novartis v. Regents, IPR2023-01347
Page 3524 of 4460

2000], it is much longer. Surprisingly, the longer hydrogen bond is accompanied by a parallel C—H···O hydrogen bond (C9—H9···O21) forming a commonly observed motif, while the shorter hydrogen bond has no parallel C—H···O bond.

The observed deterioration of the crystal below 200 K meant we could not verify the existence or absence of H-atom migration. In the observed cases, H-atom migration has been from the O atom at room temperature to the N atom at low temperature. The H-atom position at 215 K [1.102 (3) Å from the N atom] suggests that significant H-atom migration does not occur. To observe significant H-atom migration, we would expect the N—H distance to be 1.2–1.3 Å at 215 K.

The water molecules were modelled as disordered over four positions, and were refined with the O—H bond lengths and the H—O—H bond angle restrained. Most of the residual nuclear density lies around the water molecules and the model only approximates the true disorder. The occupancy factors of the water molecules were refined and then fixed so that the isotropic displacement parameters were physically reasonable. It was not sensible to refine anisotropic displacement parameters for any of the atoms in the water molecules. The overall occupancy summed to 1.8 water molecules per unit cell.

BTA and BPY crystallize in a 2:1 ratio as a molecular salt, (II), with the formula $C_{10}H_{10}N_2^{2+}\cdot 2C_{10}H_5O_8^-$. The BTA molecules are connected by O—H···O hydrogen bonds in a two-dimensional mesh. The BPY molecules thread through gaps in the mesh and connect the layers together *via* N—H···O hydrogen bonds (Fig. 3). The structure of (II) has been discussed previously by Zhu *et al.* (2003) and Ruiz-Pérez *et al.* (2004).

Our structure of (II) disagrees with both published structures. The structure of Zhu *et al.* (2003) [Cambridge Structural Database (CSD; Allen, 2002) refcode IRETII] was refined in the space group *C*2/*c* with one BTA molecule and one half of a BPY molecule in the asymmetric unit. Refinement of the low-temperature structure of (II) in *C*2/*c* results in unacceptable anisotropic displacement parameters and the refined *R* factor was only ~10%. It is possible that the *C*2/*c* phase occurs at room temperature, or that different crystallization conditions produce a polymorph. The heavy-atom structure and space group of Ruiz-Pérez *et al.* (2004) (CSD refcode IRETII01) agree with our structure. However, their placement of the H atoms is incorrect, including three H atoms curiously attached to the carbonyl O atoms in the carboxylic acid groups.

A short intramolecular hydrogen bond is formed between a carboxylate group and the adjacent carboxylic acid group in both BTA molecules. Again, as in (I), despite the very short O···O separation for an O—H···O hydrogen bond, the H atom is positioned asymmetrically. There is no evidence of disorder in the difference Fourier map or in the isotropic displacement parameters of the H atom (Fig. 4). There are two relatively long N—H···O charge-assisted hydrogen bonds, both with ordered H-atom positions close to the N atoms. No H-atom migration is expected, for the same reasons as stated for (I). Four short but unremarkable O—H···O hydrogen bonds are also formed, linking the BTA molecules into two-dimensional meshes. Full hydrogen-bond parameters are listed in Table 2.

In both (I) and (II), three independent short O—H···O intramolecular hydrogen bonds are formed between a carboxylic acid group and an adjacent carboxylate group attached to a benzene ring. These are among the shortest hydrogen bonds studied by neutron diffraction. In similar short intramolecular hydrogen bonds studied by neutron diffraction, the H atom is rarely found to be equidistant from the O atoms (Wilson, 2000). In the crystal structure of pyridine-2,3-dicarboxylic acid, a short asymmetric intramolecular hydrogen bond is formed and the asymmetry is ascribed to the N atom in the pyridyl ring (Kvick *et al.*, 1974; Takusagawa & Koetzle, 1979). Similar short intramolecular hydrogen bonds between carboxylic acid and carboxylate groups have been studied in detail by neutron diffraction and *ab initio* calculations in maleate ions (Hsu & Schlemper, 1980; Olovsson & Olovsson, 1984; Vanhouteghem *et al.*, 1987; Wilson *et al.*, 2003), and the asymmetry in the H-atom position, when it occurs, is ascribed to intermolecular effects. In imidazolium hydrogen maleate (Sakhawat Hussain *et al.*, 1980), the H atom is found to be centred, but on deuteration the D atom is found to be asymmetrically placed. In the structure of lithium

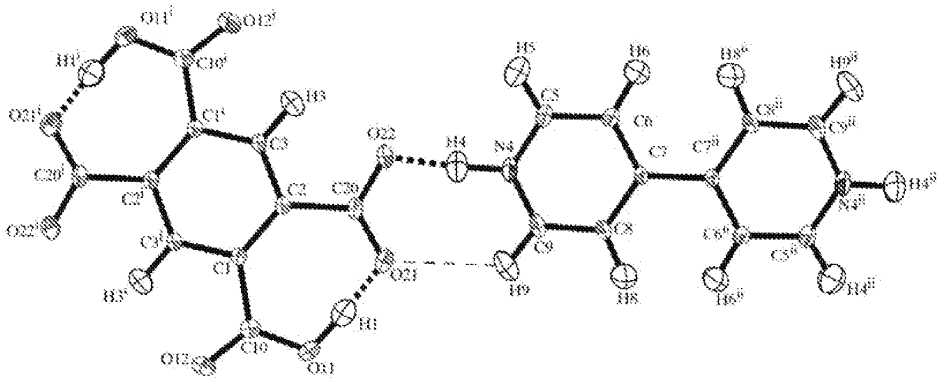

Figure 2
A plot of (I) from the 215 K neutron data. Displacement ellipsoids are drawn at the 50% probability level. The heavy dashed lines indicate strong hydrogen bonds and the thin dashed line indicates a weak C—H···O hydrogen bond. [Symmetry codes: (i) $1-x, 1-y, -z$; (ii) $-x-1, -y, 1-z$.]

UM00016543
NOVARTIS EXHIBIT 1517
Novartis v. Regents, IPR2023-01347
Page 3525 of 4460

hydrogen phthalate (Küppers *et al.*, 1985), there are two phthalate ions forming intramolecular hydrogen bonds, one of which is symmetrical while the other is asymmetrical with respect to the H-atom position.

The asymmetry in the intramolecular hydrogen bonds in structures (I) and (II) is clearly caused by the intermolecular N—H···O hydrogen bonds. The asymmetry in the hydrogen bond is also evident in the C—O distances in the carboxylate/carboxylic acid groups, which are, in (I), characteristic of a carboxylic acid group and a carboxylate group. The carboxylate group acts as the acceptor for both intra- and intermolecular hydrogen bonds. In the cocrystal of BTA and guanidinium (Sun *et al.*, 2002), the H atom was found in the centre of the intramolecular hydrogen bond, although in that case the carboxylate/carboxylic acid groups are both acceptors for similar intermolecular hydrogen bonds and the C—O distances are hybrid between the carboxylate/carboxylic acid cases.

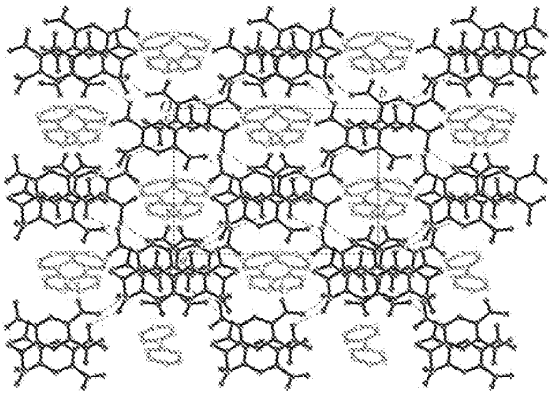

Figure 3
A packing diagram for (II), viewed along the *c* direction. The BPY molecules are shown with hollow bonds and the BTA molecules are shown with solid bonds. H atoms have been omitted for clarity. The two-dimensional BTA networks are parallel to the page and the BPY molecules thread through the gaps.

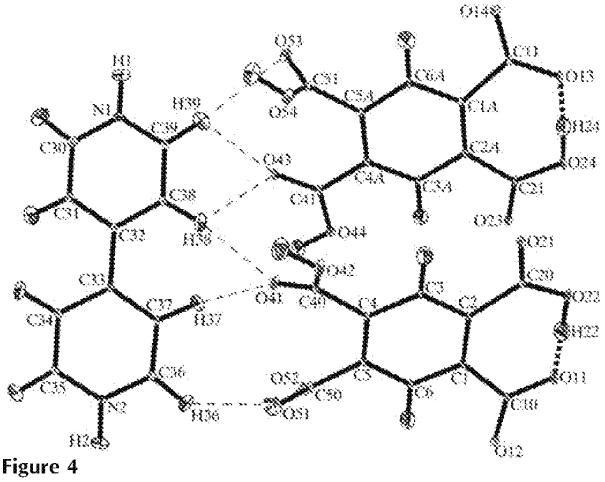

Figure 4
A plot of (II) from the 20 K neutron data. Displacement ellipsoids are drawn at the 50% probability level.

Aromatic interactions between delocalized π-electron systems in crystal structures have long been recognized (Robertson, 1951) and are characterized by perpendicular distances of ~3.4 Å between aromatic rings. Hunter *et al.* (2002) explain π–π interactions by treating the π-electron system and the σ system, in which they include the nuclei and the σ electrons, as separate, and by considering the electrostatic interactions between them.

In structure (I), the BTA molecules form π-stacked columns. In (II), there are no conventional π–π interactions; the BTA molecules do not stack with the delocalized aromatic interactions 'face-to-face', but with the aromatic rings adjacent to the ring formed by the intramolecular hydrogen bonds. The most obvious example of a similar interaction is in the crystal structure of diphthalimidodiethylamine phthalic acid hydrate (Barrett *et al.*, 1998), in which the phthalic acid molecule is pincered between the benzene groups in the the U-shaped diphthalimidodiethylamine. The motif also occurs in cocrystals of BTA and 4-methylpyridine (Biradha & Zaworotko, 1998; centre–centre = 3.538 Å), phenylethylammonium hydrogen phthalate (Kozma *et al.*, 1994; centre–centre = 3.649 Å) and bis(*p*-dimethylaminophenyl)phenylcarbenium hydrogen phthalate phthalic acid (Mitchell *et al.*, 1996; centre–centre = 3.713 Å). This interaction could be interpreted in some cases as a π–π interaction with a large offset between the rings. The description of π–π interactions as electrostatic interactions would include those interactions in which the attraction is between the σ-electron system of the benzene ring and the charges in the polar C—O bonds in the hydrogen-bonded ring. Further examples, with evidence that this motif would form in preference to other possible motifs, are required to determine if these are true intermolecular interactions or simply geometrical coincidences caused by other interactions.

One of the main aims of this study was to obtain neutron diffraction data on short N—H···O/O—H···N hydrogen bonds. The strength of the hydrogen bonds is apparently very sensitive to the intermolecular environment. There is a variation in the N···O distances between 2.5220 (17) and 2.674 (2) Å in the hydrogen bonds formed between BTA and BPY in the three cocrystals of these components.

No hydrogen bonds as short as those in the 2:1 cocrystal (Lough *et al.*, 2000) are observed in (I) and (II), and therefore we do not expect H-atom migration. However, in the cocrystal of BTA and 1,7-phenanthroline (Arora & Pedireddi, 2003), there is an N—H···O hydrogen bond with an N···O distance of 2.562 (2) Å and an N—H distance of 1.31 (3) Å at room temperature. Although this is longer than the values of 2.5220 (17) Å in the 2:1 cocrystal and 2.506 (3) Å in 4-methylpyridine and pentachlorophenol (Steiner *et al.*, 2001), it is likely that H-atom migration may be exhibited upon cooling to low temperature. Neutron diffraction is required to verify this prediction.

Experimental

Cocrystals of BTA and BPY in a 1:1 ratio [compound (I)] were formed in ~80% yield by heating BTA and BPY in a 1:1 ratio (1:1 mmol) in H_2O (1 ml) for 2 d at 453 K in a 23 ml Teflon-lined Parr

UM00016544
NOVARTIS EXHIBIT 1517
Novartis v. Regents, IPR2023-01347
Page 3526 of 4460

vessel under autogenous pressure. Phase purity was established by powder X-ray diffraction and elemental analysis. Typical crystal size was 1–2 mm^3. Larger specimens of up to 5 mm^3 could be obtained by cyclic heating and cooling of the bombs between 373 and 453 K. An identical procedure, using different ratios of the constituents, was used to produce 2:1 cocrystals [compound (II)] of similar size.

Compound (I)

Crystal data

$C_{10}H_{10}N_2^{2+}\cdot C_{10}H_4O_8^{2-}\cdot 1.8H_2O$
M_r = 442.40
Triclinic, $P\overline{1}$
a = 3.7747 (2) Å
b = 10.8587 (5) Å
c = 11.9519 (6) Å
α = 99.626 (3)°
β = 97.726 (3)°
γ = 95.515 (3)°
V = 475.07 (4) Å^3
Z = 1
D_x = 1.546 Mg m^{-3}
Neutron radiation
λ = 1.302 Å
Cell parameters from 1196 reflections
θ = 5–55°
μ = 0.16 mm^{-1}
T = 215 (2) K
Needle, brown
2.0 × 0.8 × 0.5 mm

Data collection

D19 diffractometer, ILL
ω scans
Absorption correction: integration (*D19ABS*; Matthewman *et al.*, 1982)
T_{min} = 0.861, T_{max} = 0.933
1983 measured reflections
1654 independent reflections
1426 reflections with $I > 2\sigma(I)$
R_{int} = 0.017
θ_{max} = 55.0°
$h = -2 \rightarrow 4$
$k = -13 \rightarrow 13$
$l = -14 \rightarrow 14$
3 standard reflections every 100 reflections intensity decay: none

Refinement

Refinement on F^2
$R[F^2 > 2\sigma(F^2)]$ = 0.036
$wR(F^2)$ = 0.081
S = 1.06
1654 reflections
249 parameters
H atoms: see below
$w = 1/[\sigma^2(F_o^2) + (0.0297P)^2 + 1.6121P]$ where $P = (F_o^2 + 2F_c^2)/3$
$(\Delta/\sigma)_{max}$ = 0.001
$\Delta\rho_{max}$ = 0.50 fm Å^{-3}
$\Delta\rho_{min}$ = −0.55 fm Å^{-3}

Table 1
Hydrogen-bond geometry (Å, °) for (I).

D—H···A	D—H	H···A	D···A	D—H···A
O11—H1···O21	1.056 (4)	1.370 (4)	2.423 (3)	174.6 (4)
N4—H4···O22	1.102 (3)	1.505 (3)	2.6047 (19)	175.1 (3)
C6—H6···O12^{i}	1.080 (3)	2.252 (4)	3.199 (2)	145.3 (4)
C8—H8···O12^{ii}	1.083 (4)	2.401 (4)	3.362 (2)	147.2 (4)
C9—H9···O21	1.080 (3)	2.592 (4)	3.302 (2)	122.6 (3)
O1—H1*A*···O22	0.977 (19)	2.10 (2)	2.919 (16)	140 (2)
O2—H2*A*···O22	0.971 (18)	1.922 (15)	2.851 (15)	159 (2)
O3—H3*A*···O22	0.982 (10)	1.849 (12)	2.809 (12)	164.9 (17)
O4—H4*A*···O22^{iii}	0.97 (2)	2.031 (18)	3.00 (2)	174 (3)

Symmetry codes: (i) $x-2, y-1, z$; (ii) $-x+1, -y+1, -z+1$; (iii) $x-1, y, z$.

Compound (II)

Crystal data

$C_{10}H_{10}N_2^{2+}\cdot 2C_{10}H_5O_8^{-}$
M_r = 664.49
Monoclinic, Cc
a = 12.009 (1) Å
b = 15.484 (1) Å
c = 15.221 (1) Å
β = 112.273 (3)°
V = 2619.2 (3) Å^3
Z = 4
D_x = 1.685 Mg m^{-3}
Neutron radiation
λ = 1.3108 (1) Å
Cell parameters from 3055 reflections
θ = 5–50°
μ = 0.14 mm^{-1}
T = 20 (2) K
Bar, yellow
2.2 × 1.0 × 0.7 mm

Data collection

D19 diffractometer, ILL
ω scans
Absorption correction: Gaussian (*D19ABS*; Matthewman *et al.*, 1982)
T_{min} = 0.841, T_{max} = 0.891
3741 measured reflections
2647 independent reflections
2628 reflections with $I > 2\sigma(I)$
R_{int} = 0.019
θ_{max} = 55.2°
$h = -4 \rightarrow 14$
$k = -19 \rightarrow 13$
$l = -19 \rightarrow 17$
2 standard reflections every 100 reflections intensity decay: none

Refinement

Refinement on F^2
$R[F^2 > 2\sigma(F^2)]$ = 0.022
$wR(F^2)$ = 0.048
S = 1.12
2647 reflections
615 parameters
All H-atom parameters refined
$w = 1/[\sigma^2(F_o^2) + (0.0186P)^2 + 12.8939P]$ where $P = (F_o^2 + 2F_c^2)/3$
$(\Delta/\sigma)_{max}$ = 0.001
$\Delta\rho_{max}$ = 0.43 fm Å^{-3}
$\Delta\rho_{min}$ = −0.46 fm Å^{-3}
Extinction correction: *SHELXL97* (Sheldrick, 1997)
Extinction coefficient: 0.000155 (17)
Absolute structure: Flack (1983), with 92 Friedel pairs
Flack parameter: 0 (10)

Table 2
Hydrogen-bond geometry (Å, °) for (II).

D—H···A	D—H	H···A	D···A	D—H···A
O22—H22···O11	1.079 (5)	1.333 (5)	2.404 (3)	172.6 (4)
O24—H24···O13	1.076 (5)	1.348 (5)	2.420 (3)	173.2 (4)
N1—H1···O12^{i}	1.049 (4)	1.635 (4)	2.674 (2)	169.5 (4)
N2—H2···O14^{ii}	1.050 (4)	1.665 (4)	2.639 (2)	151.9 (3)
O42—H42···O11^{iii}	1.011 (5)	1.612 (5)	2.613 (3)	169.8 (4)
O52—H52···O21^{iv}	1.004 (4)	1.717 (4)	2.718 (3)	174.7 (4)
O44—H44···O13^{iv}	1.007 (4)	1.637 (4)	2.629 (3)	167.2 (4)
O54—H54···O23^{iii}	1.004 (5)	1.740 (5)	2.739 (3)	173.2 (4)
C31—H31···O24^{v}	1.085 (4)	2.228 (5)	3.191 (3)	146.7 (4)
C34—H34···O52^{iii}	1.080 (4)	2.482 (5)	3.414 (3)	143.9 (4)
C34—H34···O22^{v}	1.080 (4)	2.467 (4)	3.155 (3)	120.5 (3)
C35—H35···O22^{v}	1.071 (4)	2.549 (5)	3.154 (3)	115.0 (3)
C35—H35···O43^{vi}	1.071 (4)	2.494 (4)	3.042 (3)	110.7 (3)
C36—H36···O51	1.082 (4)	2.364 (5)	3.219 (3)	134.8 (3)
C36—H36···O21^{iv}	1.082 (4)	2.414 (5)	3.134 (3)	122.8 (3)
C37—H37···O41	1.083 (4)	2.193 (5)	3.140 (3)	144.9 (4)
C38—H38···O41	1.081 (4)	2.351 (4)	3.420 (3)	169.7 (3)
C38—H38···O43	1.081 (4)	2.564 (4)	3.044 (3)	106.0 (3)
C39—H39···O23^{iii}	1.082 (4)	2.592 (5)	3.108 (3)	108.4 (3)
C39—H39···O43	1.082 (4)	2.493 (5)	2.994 (3)	107.0 (3)
C39—H39···O53	1.082 (4)	2.692 (5)	3.739 (3)	162.9 (4)

Symmetry codes: (i) $x+\frac{1}{2}, -y+\frac{1}{2}, z-\frac{1}{2}$; (ii) $x-\frac{1}{2}, -y+\frac{1}{2}, z+\frac{1}{2}$; (iii) $x+\frac{1}{2}, y+\frac{1}{2}, z$; (iv) $x-\frac{1}{2}, y+\frac{1}{2}, z$; (v) $x, y+1, z$; (vi) $x, -y+1, z+\frac{1}{2}$.

X-ray diffraction experiments were performed prior to the neutron experiments to verify the identity of the crystals. The initial structural models for the neutron refinements were taken from our X-ray diffraction results. Neutron scattering factors were taken from Sears (1992). All H atoms were refined with anisotropic displacement parameters except for those in the disordered water molecules in (I).

For both compounds, data collection: *MAD* (Barthelemy *et al.*, 1984); cell refinement: *RAFD19* (Filhol, 1998); data reduction: *RETREAT* (Wilkinson *et al.*, 1988); program(s) used to refine structure: *SHELXL97* (Sheldrick, 1997); molecular graphics: *SHELXTL/PC* (Sheldrick, 1999); software used to prepare material for publication: *SHELXTL/PC*.

JAC thanks the ILL and EPSRC for PhD funding. JAKH thanks the EPSRC for a Senior Research Fellowship.

Supplementary data for this paper are available from the IUCr electronic archives (Reference: FG1884). Services for accessing these data are described at the back of the journal.

UM00016545
NOVARTIS EXHIBIT 1517
Novartis v. Regents, IPR2023-01347
Page 3527 of 4460

References

Allen, F. H. (2002). *Acta Cryst.* B**58**, 380–388.
Arora, K. K. & Pedireddi, V. R. (2003). *J. Org. Chem.* **24**, 9177–9185.
Barrett, D. M. Y., Kahwa, I. A., Raduchel, B., White, A. J. P. & Williams, D. J. (1998). *J. Chem. Soc. Perkin Trans. 2*, pp. 1851–1856.
Barthelemy, A., Filhol, A., Rice, P. G., Allibon, J. R. & Turfat, C. (1984). *MAD*. Institut Laue–Langevin, Grenoble, France.
Biradha, K. & Zaworotko, M. J. (1998). *Cryst. Eng.* **1**, 67–78.
Cowan, J. A., Howard, J. A. K. & Leech, M. A. (2001*a*). *Acta Cryst.* C**57**, 302–303.
Cowan, J. A., Howard, J. A. K. & Leech, M. A. (2001*b*). *Acta Cryst.* C**57**, 1196–1198.
Cowan, J. A., Howard, J. A. K., Leech, M. A., Puschmann, H. & Williams, I. D. (2001). *Acta Cryst.* C**57**, 1194–1195.
Cowan, J. A., Howard, J. A. K., Leech, M. A. & Williams, I. D. (2001). *Acta Cryst.* E**57**, o563–o565.
Cowan, J. A., Howard, J. A. K., McIntyre, G. J., Lo, S. M.-F. & Williams, I. D. (2003). *Acta Cryst.* B**59**, 794–801.
Fabelo, O., Cañadillas-Delgado, L., Delgado, F. S., Lorenzo-Luis, P., Laz, M. M., Julve, M. & Ruiz-Pérez, C. (2005). *Cryst. Growth Des.* **5**, 1163–1167.
Filhol, A. (1998). *RAFD19*. Institut Laue–Langevin, Grenoble, France.
Flack, H. D. (1983). *Acta Cryst.* A**39**, 876–881.
Gilli, P., Bertolasi, V., Ferritti, V. & Gilli, G. (1994). *J. Am. Chem. Soc.* **116**, 909–915.
Hsu, B. & Schlemper, E. O. (1980). *Acta Cryst.* B**36**, 3017–3023.
Hunter, C. A., Lawson, K. R., Perkins, J. & Urch, C. J. (2002). *J. Chem. Soc. Perkin Trans. 2*, pp. 651–669.
Kozma, D., Bocskei, Z., Simon, K. & Fogassy, E. (1994). *J. Chem. Soc. Perkin Trans. 2*, pp. 1883–1886.
Küppers, H., Takusagawa, F. & Koetzle, T. F. (1985). *J. Chem. Phys.* **82**, 5636–5647.
Kvick, Å., Koetzle, T. F., Thomas, R. & Takusagawa, F. (1974). *J. Chem. Phys.* **60**, 3866–3874.
Lough, A. J., Wheatley, P. S., Ferguson, G. & Glidewell, C. (2000). *Acta Cryst.* B**56**, 261–272.
Matthewman, J. C., Thompson, P. & Brown, P. J. (1982). *J. Appl. Cryst.* **15**, 167–173.
Mitchell, C. A., Lovell, S., Thomas, K., Savickas, P. & Kahr, B. (1996). *Angew. Chem. Int. Ed. Engl.* **35**, 1021–1023.
Olovsson, G. & Olovsson, I. (1984). *Acta Cryst.* C**40**, 1521–1526.
Robertson, J. M. (1951). *Proc. R. Soc. London Ser. A*, **207**, 101–110.
Ruiz-Pérez, C., Lorenzo-Luis, P. A., Hernández-Molina, M., Laz, M. M., Gilli, P. & Julve, J. (2004). *Cryst. Growth Des.* **4**, 57–61.
Sakhawat Hussain, M., Schlemper, E. O. & Fair, C. K. (1980). *Acta Cryst.* B**36**, 1104–1108.
Sears, V. F. (1992). *Neutron News*, **3**(3), 26–37.
Sheldrick, G. M. (1997). *SHELXL97*. University of Göttingen, Germany.
Sheldrick, G. M. (1999). *SHELXTL/PC*. Version 5.10 for Windows NT. Bruker AXS Inc., Madison, Wisconsin, USA.
Steiner, T., Majerz, I. & Wilson, C. C. (2001). *Angew. Chem. Int. Ed.* **40**, 2651–2654.
Sun, Y.-Q., Zhang, J. & Yang, G.-Y. (2002). *Acta Cryst.* E**58**, o904–o906.
Takusagawa, F. & Koetzle, T. F. (1979). *Acta Cryst.* B**35**, 2126–2135.
Vanhouteghem, F., Lenstra, A. T. H. & Schweiss, P. (1987). *Acta Cryst.* B**43**, 523–528.
Wilkinson, C., Khamis, H. W., Stansfield, R. F. D. & McIntyre, G. J. (1988). *J. Appl. Cryst.* **21**, 471–478.
Wilson, C. C. (2000). *Single Crystal Neutron Diffraction From Molecular Materials*. Singapore: World Scientific Publishing Company.
Wilson, C. C., Thomas, L. H. & Morrison, C. A. (2003). *Chem. Phys. Lett.* **381**, 102–108.
Zhu, N.-W., Zhang, R.-Q. & Sun, T.-H. (2003). *Z. Kristallogr.* **218**, 341–342.

UM00016546
NOVARTIS EXHIBIT 1517
Novartis v. Regents, IPR2023-01347
Page 3528 of 4460

XP-002282989

AN - 1979-65538B [36]
CPY - SUMO
DC - B02
FS - CPI
IC - A61K0/00 ; C07D501/02
MC - B02-C04 B10-E04C
M1 - [01] V031 E680 F570 G100 M531 H181 J111 J321 H401 H441 J521 H521 H592 M431 P220 M511 M521 M540 M782 R000 M412 M902
M2 - [02] H1 J1 J6 H4 J5 H5 M311 M332 M322 M280 M342 M340 M343 M370 M392 E680 F570 G100 M531 H181 J111 J321 H401 H441 J521 H521 H592 M431 P220 M511 M521 M540 M782 R000 M412 M902
- [03] H4 M313 M314 M332 M331 M321 M280 M342 M380 M391 H482 H483 H484 M620 M431 M510 M520 M530 M540 M782 R000 M416 M902
PA - (SUMO) SUMITOMO CHEM CO LTD
PN - JP54095589 A 19790728 DW197936 000pp
- CA1101840 A 19810526 DW198125 000pp
- IT1109398 B 19851216 DW198718 000pp
PR - JP19770160339 19771230
RR - 00094
XIC - A61K-000/00 ; C07D-501/02
AB - J54095589 Prodn, of a solvated cephalosporin antibiotic comprises dissolving 7- D-alpha-amino-alpha-(p-hydroxy-phenyl)acetamido 3-(1,2,3-triazol-5-ylthiomethyl)-3-cephem-4-carboxylic acid or its solvated product in an acidified 1,2-propyleneglycol under substantially anhydrous conditions and neutralising the solution to ppte 7- D-alpha-amino-alpha-(p-hydroxyphenyl)acetamido -3-(1,2,3-triazol-5-ylthiomethyl)-3-cephem-4-carboxylic acid solvated with 1,2-propyleneglycol.
- 7- D-alpha-amino-alpha-(p-hydroxyphenyl)acetamido -3-(1,2,3-triazol-5-ylthiomethyl)-3-cephem-4-carboxylic acid is an antibiotic known as cefatrizine. Its 1,2-propyleneglycol adduct is known also. The present process is characterised by simplified procedures, shortened time required for its execution and minimized decomposition of the material during the procedures.
IW - SOLVATION CEPHALOSPORIN ANTIBIOTIC PRODUCE PROPYLENE GLYCOL ADDUCT
IKW - SOLVATION CEPHALOSPORIN ANTIBIOTIC PRODUCE PROPYLENE GLYCOL ADDUCT
NC - 003
OPD - 1977-12-30
ORD - 1979-07-28
PAW - (SUMO) SUMITOMO CHEM CO LTD
TI - Solvated cephalosporin antibiotic prodn. - i.e. 1,2-propylene glycol adduct of cefatrizine

BEST AVAILABLE COPY

TITLE:
PUBLISHER/PLACE:
VOLUME/ISSUE/PAGES:
DATE:

AMERICAN PHARMACEUTICAL REVIEW
Russell Pub. Indianapolis, IN :
2004;7(1):10,12,14,16,100 - 10,12,14,16;100
2004

Detection of Polymorphism by Powder X-Ray Diffraction: Interference by Preferred Orientation

M. Davidovich[1], J. Z. Gougoutas[2], R. P. Scaringe[1], I. Vitez[1], S. Yin[1]
[1]Bristol-Myers Squibb Pharmaceutical Research Institute, New Brunswick, NJ
[2]Bristol-Myers Squibb Pharmaceutical Research Institute, Lawrenceville, NJ

ABSTRACT:

Polymorphism has important consequences in the development of drugs. The existence of multiple crystal forms with differences in the solid-state properties can translate into significant effects on the bioavailability of the active drug substance, the shelf life of the drug, and manufacturability of drug substance and drug product. Powder X-ray Diffraction (PXRD) is a powerful tool in identifying different crystalline phases by their unique diffraction patterns. The most recent USP has included the criteria in the general chapter on using X-ray powder diffraction for phase identification and for the equivalence of two powder patterns. High-resolution PXRD patterns provide good data to determine the phase composition of crystalline samples, yet morphology and particle shape/size can induce severe preferential orientation that can degrade the utility of PXRD powder data. Small changes in the X-ray powder patterns due to the appearance of new peak(s), additional shoulders or shifts in the peak position can imply the presence of a new polymorph. Although preferred orientation is a well-known phenomenon, its potential to misguide the analyst in the search/identification of polymorphs is under-appreciated and has not been discussed in detail. This article will examine the changes in the powder X-ray powder patterns that arise from artifacts rather than from polymorphism. Many such changes in powder X-ray diffraction patterns are due to particle size/morphology or sample holder geometry. As is well known, grinding the sample can often minimize these effects, but in some cases such artifacts can only be eliminated through the use of a rotating capillary sample holder.

Introduction

A crystal form is defined by the arrangement of the molecules in the solid state. The unit cell and space-group symmetry determines many aspects of the arrangement of the diffraction pattern. This unit cell is the repeating unit of the crystal structure. Polymorphs are a specific type of crystal form system characterized by the ability of a compound to exist in different arrangements and/or conformations in the crystal lattice, but having the same molecular formula (Figure 1) [1].

In the quest of accelerating drug development, the benefits of integrating polymorphic screening in the early phases of development are multifold. High throughput screening capabilities, now common in the Pharmaceutical Industry, will generate an increasing number of potential polymorphs that require characterization. Powder X-ray diffraction (PXRD) provides a highly effective tool for identification of polymorphs, the characterization of their interrelationships, and selection of a suitable stable form as drug candidate [2].

Figure 1. Example of Polymorphs of a Compound Existing in Two Different Conformational Arrangements

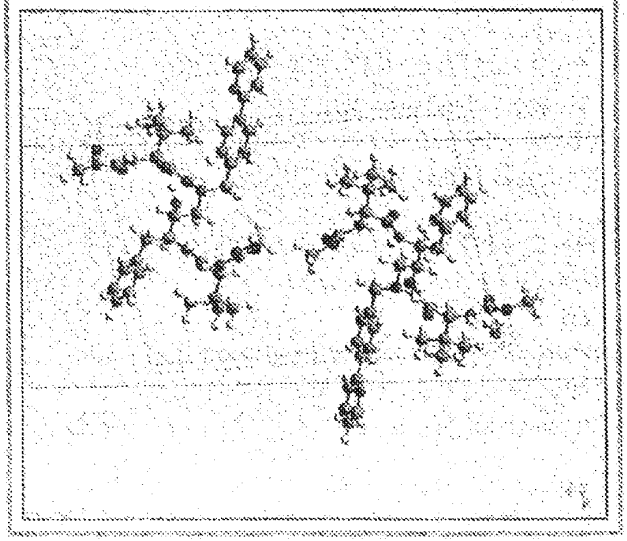

The various methods for preparing different polymorphs of drugs include sublimation, crystallization from melt, and crystallization from supercritical fluids. However, crystallization from solution, employing various solvents and temperature regimes, is often preferred for convenience and efficiency [3]. Polymorphism can be

Material may be protected by copyright law (Title 17, U.S. Code)
UM00016548
NOVARTIS EXHIBIT 1517
Novartis v. Regents, IPR2023-01347
Page 3530 of 4460

introduced in the development of a drug molecule by exchange of a solvent in the last step of synthetic purification. Success in preparing various polymorphs frequently depends on appropriate control of the kinetics rather than the thermodynamics of crystallization. The highly dynamic nature of crystallization can lead to variations in crystal formation [4]. For example, a higher melting form consisting of very long needles can convert to a lower melting polymorph of a platelet-like crystal. Minor variations in the manufacturing procedure can result in significant modification of crystal form.

Understanding the nature of crystalline material and whether it is a single phase is very important and X-ray diffraction is the principle method of characterization. The simplicity and advantages of the powder diffraction technique helped it to become an extensively used tool. Within the Pharmaceutical Industry the FDA has established guidelines to identify the crystal form of the drug substance. This approach for the appropriate characterization of pharmaceutical solids has been summarized [5] by Byrne et al. al. and is part of the ICH Q6A document. The most recent USP includes a general chapter on using X-ray powder diffraction for phase identification and for the equivalence of two powder patterns [6].

Powder X-ray diffraction is one of the most useful and widely used analytical methods to determine polymorphs and quantify the forms present in a mixture. Detection limit determination becomes critical in the analysis of mixtures. The sensitivity to detect small amounts of a given phase relative to another is critical in the characterization of polymorphs especially for patent infringement cases. High-resolution PXRD patterns obtained from X-ray diffraction instruments with polycapillary optics or synchrotron radiation source [7] provide good data to determine pure phases of the crystalline samples. Yet morphology and particle size can induce severe preferential orientation to skew the XRD powder data [8]. Small changes in the X-ray powder patterns due to the appearance of new peak(s), additional shoulders or shifts in the peak position often imply the presence of a new polymorph. Ambiguity in the data arises also from the collapse of the three-dimensional crystallographic information characteristic of single crystal data onto the one-dimensional data of a powder diffraction pattern [9]. Ideal random polycrystalline aggregates are rare in nature and commercial synthetic processes alike. Most naturally occurring crystallites, along with the synthetic counterparts, show specific orientation as a result of growth, during manufacture, mechanical operations, and during powder-sample preparation. All such "orientation" gives the material physical and mechanical properties, which are significantly different from those expected from purely random arrangement [10]. It is important therefore to be able to determine the nature of these properties and X-ray diffraction is the standard method for their characterization. Although, preferred orientation is a well-known phenomenon, its potential to misguide the analyst in the search/identifying polymorphs is under appreciated and has not been discussed in detail. In this article we will show that some of these small changes in the powder X-ray powder patterns arise as artifacts rather than arising from polymorphism. We have found that many small changes in powder X-ray diffraction patterns are due to particle size/morphology or sample holder geometry. As is well known, grinding can often minimize such artifacts but on some cases only the rotating capillary sample preparation method can reduce them to acceptable levels.

Case Study I

Several cGMP lots of drug substance of compound A, manufactured using a new process, exhibited an atypical PXRD pattern. A new crystal form was believed to have been generated. Recrystallization, cooling rate, and slurry studies were conducted to investigate a possible conversion of the known form A to another form during the final crystallization step. The effect of grinding was also investigated to assess the possibility that particle size and/or shape caused the atypical PXRD pattern. The powder pattern of the "as is" material in

Figure 2: XRD Overlay of as is (middle) and Ground (w/o tape) (top) Material versus Simulated Powder Pattern of Form A (bottom)

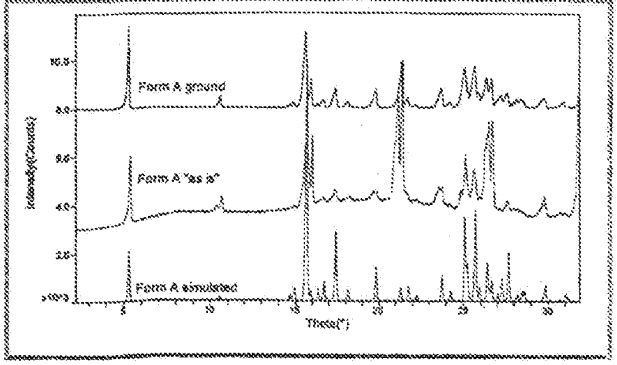

Figure 2 presents some differences in observed peaks as compared to the simulated powder pattern. Note that the peaks at 10.4° and 19.6° 2θ in the "as is" pattern appear as doublets, which are not consistent with the simulated pattern. The amorphous halo present is due to the sample preparation, where the sample in the holder was covered with a Scotch tape film to protect the analyst from the highly potent drug substance. All samples were prepared using back loading sample holders and a conventional Bragg-Brentano geometry diffractometer. Upon light grinding in a mortar and pestle followed by re-analysis without the use of tape, the collected powder pattern still did not fully matched the simulated pattern, especially at 10.4° 2θ, where a spilt in the peak was still present (Figure 3).

Figure 3: XRD Overlay of Expanded View of the Peak at 10.4° 2θ: "As is" (middle) and Ground (top) Material Versus Simulated Pattern of (bottom)

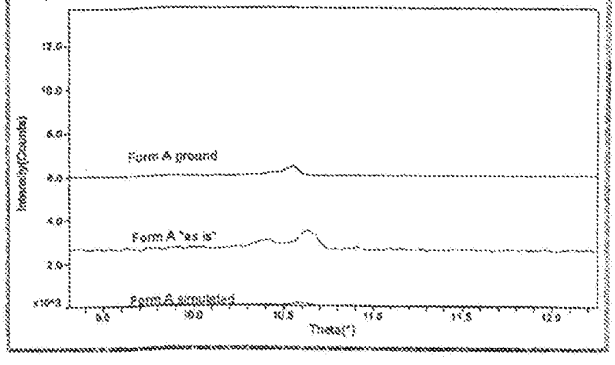

To better understand the significance of the atypical powder pattern, several methods of analysis of the X-ray diffraction patterns were utilized. The experimental pattern exhibiting doublet peaks near 10.4° and 19.6° 2θ was further compared to the simulated pattern and the stick notation, as shown in the bottom of Figure 5. The stick notation indicates the peaks permitted by Bragg's law for form A material based on the single crystal data.

This figure illustrates that, in this limited survey of the diffraction peaks in the 9-10° and 19-20° 2θ regions of the "as is " material, there are 2 peaks or shoulders observed at 10.4° and 20° 2θ which are not predicted by Bragg's Law, as seen by the single stick present at each of the two positions in the bottom diagram. This indicated

Material may be protected by copyright law (Title 17, U.S. Code)
UM00016549
NOVARTIS EXHIBIT 1517
Novartis v. Regents, IPR2023-01347
Page 3531 of 4460

Figure 4: 3D View of the 10.4° 2θ of "as is" (1), Ground (2) and Simulated Pattern (3)

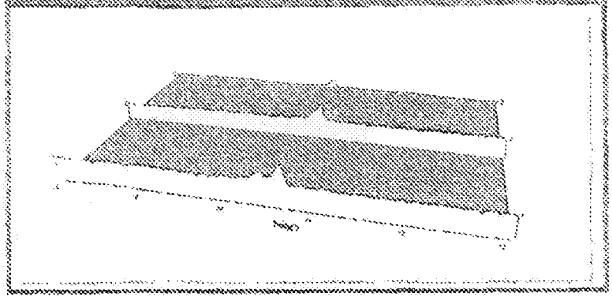

Figure 5: Overlay of Simulated X-Ray Powder Pattern (center) with Stick Diagram of Predicated Diffraction Peaks (bottom) and Experimental Powder Pattern of Form A (top)

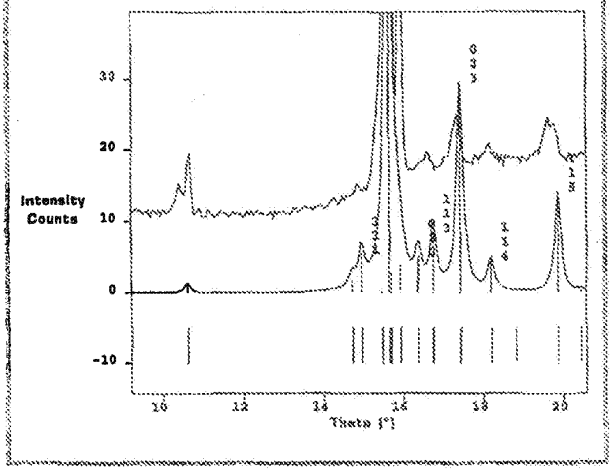

that the extra peaks are either due to some unusual preferential orientation or another phase.

Since the initial grinding of the API material did not resolve the atypical powder pattern, when the sample was analyzed in the presence of the Scotch tape film, further grinding was performed. The re-ground material when it was re-analyzed without using tape showed consistency with the simulated pattern for the known form A. The grinding effect was further checked on the API material of compound A from the different processes A, B, C and D as shown in Figure 6. This overlay shows that form A material from the different processes, when lightly ground and analyzed without tape, exhibits powder patterns consistent with simulated powder pattern.

The effect of grinding on particle size and shape was characterized by SEM (Figure 7). Grinding resulted in the formation of irregular shaped small aggregates in contrast to the individual larger particles with rounded edges exhibited before grinding.

In conclusion, the presence of large particles played a significant role in the generation of atypical powder patterns, introducing the artifact of additional peaks. The Scotch tape film used to cover the "as is" packed material with large rock-like particles, caused the artificial introduction of extra peaks by creating a height difference between material that adhered to the tape and the rest of the sample. The grinding step at the end of the process, as well as removing the tape, eliminated the artifacts from the data in this case.

Figure 6: XRD Overlay of Process A, B, C, and D with Simulated Form A Powder Pattern (bottom)

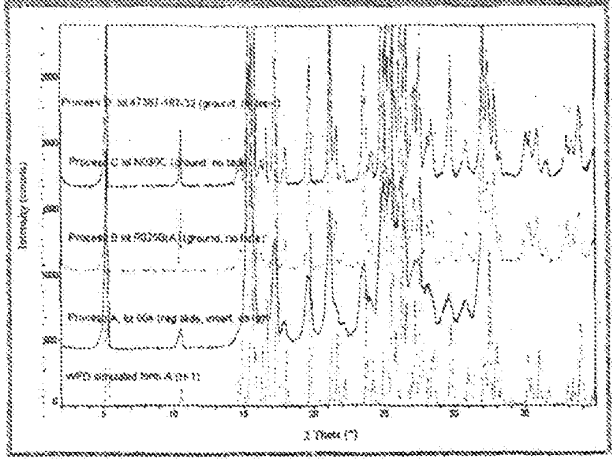

Figure 7: SEM Images of Unground (left) and Ground (right) Form A

Case Study II

In another case, the observed PXRD patterns of bulk materials of compound B, showed unusually higher intensities at positions of 22.5° and 27.2° 2θ, when compared to the simulated pattern of this compound (Figure 8 and Figure 9). The simulated pattern of compound B was calculated from its atomic coordinates determined by single crystal X-ray structural analysis. The intensity differences were immediately considered to be caused by preferential orientation, since the data was collected on a flat geometry (Bragg-Brentano) instrument. The degree of preferred orientation is due to highly asymmetric crystallites, such as plate-like or needle-shaped particles that can result in polycrystalline aggregates, which lack randomness [11]. To minimize particle size, grinding is the simplest process. After lightly grinding (in a mortar and pestle for 3 minutes), the peak at 27.2° 2θ disappeared but the intensity of peak at 22.5° 2θ was almost unchanged. The rest of peaks in the observed powder pattern changed more or less to be equivalent (similar) to the simulated pattern as shown in Figure 8 and Figure 9, respectively. The ground sample was subjected to a second round of grinding (in a mortar and pestle for 3 minutes) and re-analyzed by PXRD. The pattern designated as "ground 2" represents the doubly ground sample. The peak at 22.5° 2θ still showed unusually high intensity, while the rest of peaks offered close similarity in intensity to the simulated pattern. These observations seemed to indicate that there was mainly a pure phase of compound B. However, a second crystal phase or some other orientation phenomenon must be associated with the strong intensity at the 22.5° 2θ peak.

Material may be protected by copyright law (Title 17, U.S. Code)

UM00016550
NOVARTIS EXHIBIT 1517
Novartis v. Regents, IPR2023-01347
Page 3532 of 4460

Figure 8. PXRD Patterns of Simulated (top) and Observed Unground, Ground 1 & Ground 2 of Compound B

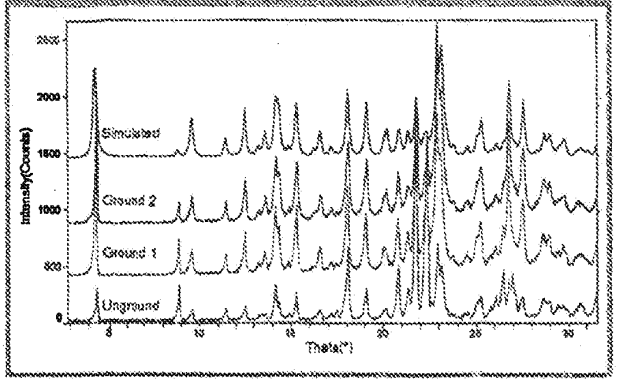

Figure 9. Zoomed in PXRD Patterns of Simulated (top) and Observed Unground, Ground 1 & Ground 2 of Compound B

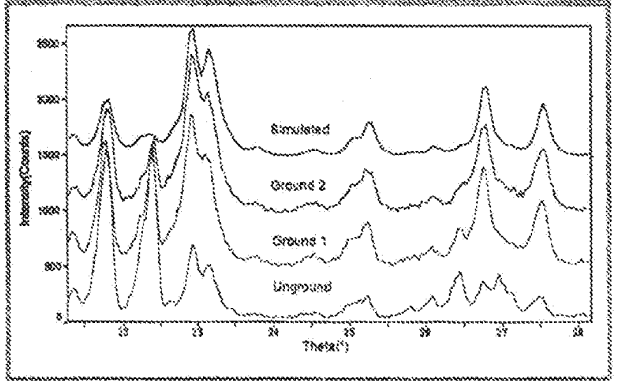

It is well know that the flat-geometry instrument with back-reflection patterns needs randomly oriented specimen. Grinding can reduce the degree of preferred orientation by randomizing the crystallites orientation, but it can not completely eliminate it when a flat-geometry instrument is used. It is evident that generation of a powder reflection is relatively inefficient when a disproportionately small fraction of crystallites are oriented so that they are in the position to satisfy the Bragg reflection condition [12]. In fact, the reflection at 22.3° 2θ is based on (1 0 0 0) plane of the unit cell of this compound, which has the dimensions of a = 4.675 Å, β = 9.380 Å, c = 13.207 Å, β = 103.75°, V = 4894.48Å^3 and the space group of C2. This kind of unit cell usually results in plate-like or blade-like crystal morphology with the basal plane of the plates as (h 0 0) series planes. Thus, the intensities of planes with (h 0 0) reflections, such as (2 0 0), (4 0 0) ....(12 0 0) and (14 0 0), should be enhanced on flat-geometry instruments. In our PXRD patterns for compound B, peaks observed at 4.48°, 8.96°, 13.46°, 17.98°, 22.52°, 27.20° and 31.73° 2θ are reflections of the planes corresponding to (2 0 0), (4 0 0), (6 0 0), (8 0 0), (10 0 0), (12 0 0) and (14 0 0) reflections, respectively. Almost all of these reflections showed higher intensities in our example when compared to the corresponding simulated peak intensities. The intensities of (2 0 0) and (6 0 0) peaks at 4.48° and 13.46° 2θ are lower than their corresponding simulated ones for the unground sample which is probably due to the initial sample preparation. But, for ground samples,

Figure 10. PXRD Patterns of Simulated (2nd to top) and Observed Unground on GADDS (top), Unground, Ground 1 & Ground 2 (on Flat Geometry) of Compound B

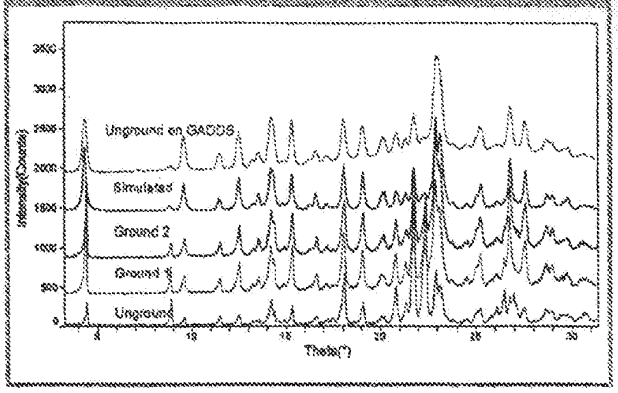

these intensities appear to have increased slightly. After the first grinding preparation, the observed (12 0 0) peak intensity was brought to the simulated level but not the (10 0 0) peak. The intensity for the (10 0 0) peak remained higher than the corresponding simulated peak intensity even after the second round of grinding. Due to the nature of this peak at the (10 0 0) position it was our belief that the abnormal intensity distribution was the result of residual preferential orientation even though the sample had been ground twice.

In order to confirm the case for preferred orientation, about 0.5 mg of unground sample of the same material was loaded into a thin capillary tube (1.0 mm inner diameter). The loaded capillary tube was mounted on Bruker-AXS High Star GADDS system. The capillary tube was rotated during the X-ray diffraction measurement. The collected PXRD pattern from the GADDS unit was overlaid with the patterns generated on a flat-geometry instrument and the simulated powder pattern, as shown in Figure 10. The results clearly show that the pattern collected on GADDS is in very good agreement with simulated pattern in both peak position and peak intensity distribution. This certainly proves that the observed patterns on a flat-geometry instrument are indeed of the pure compound B and also that, the higher intensities of the few peaks related to the (h 0 0) reflection are caused by the preferred orientation characteristic of the flat-geometry X-ray diffraction method.

Conclusion

Small changes in the X-ray powder patterns due to the appearance of new peak(s), additional shoulders, shifts in the peak position, or abnormal intensity distribution can indicate the presence of new polymorphs. Preferred orientation, although a well-known phenomenon has significant potential to misguide the analyst. This article discussed examples of such changes in the powder X-ray powder patterns that resulted from experimental artifacts rather than polymorphism. Most of these changes were due to particle size/morphology, sample holder/preparation, and instrument geometry. Although grinding will usually minimize the effects of sample/instrument geometry it cannot generally eliminate them. Moreover, grinding can introduce new crystal forms through dehydration/desolvation and/or pressure induced phase transitions. Rotating capillary tube sample preparation coupled with the GADDS system can significantly improve the quality of the powder analysis, and confidence in the conclusion drawn from it.

(cont'd on page 100)

Material may be protected by copyright law (Title 17, U.S. Code)

UM00016551
NOVARTIS EXHIBIT 1517
Novartis v. Regents, IPR2023-01347
Page 3533 of 4460

Disintegrants:

12. E.M. Rudnic, C.T. Rhodes, J.F. Bavits, and J.B Schwartz, "Some Effects of Relatively low Levels of Eight Tablet Disintegrants on a Direct Compression System," Drug Dev. Ind. Pharm., 1981, Vol. 7, No.3, pp. 347-358.
13. P-C. Sheen and S-I. Kim, " Comparative Study of Disintegrating Agents in Tiaramide Hydrochloride Tablets," Drug Dev. Ind. Pharm., 1989,Vol. 15, No.3, pp. 401-414.

Glidents:

14. L.L. Augsburger and R.F. Shangraw, " Effects of Glidents in Tableting," J. Pharm Sci., 1966, Vol. 55, No. 4, pp. 418-423.
15. R-K Chang, M. Leonzio, and M.A. Hussian, " Effect of Colloidal Silicon Dioxide on Flowing and Tableting Properties of an Experimental, Crosslinked Polyalkylammonium Polymer," Pharm. Dev. Tech, 1999, Vol. 4, No. 2, pp. 285-289.

Lubricants:

16. M. V. Velasco and A.R. Rajabi-Siahboomi, " Tablet Lubrication: Problems and Perspectives," Pharm. Tech., 1998, Vol. 22, No. 122, pp.40-46.
17. T.A. Miller and P. York, "Pharmaceutical Tablet Lubrication," Int. J. Pharm., 1988, Vol.41, pp. 1-19.

John A. McCarty is president with Pharmaceutical Productions, Inc. (PPI), an international consulting firm. He has held management positions in Research and Development at Key Pharmaceuticals, Schering–Plough, and Pharmavene (acquired by Shire). PPI assists pharmaceutical and biotech companies in developing their therapeutic compounds into efficacious and economical drug delivery systems. PPI provides expertise in developing oral solid dosage forms, biologicals, parenterals, buccals, topicals, transdermals, liquids/semi-solids, aerosols, controlled release and novel drug delivery systems. In addition to dosage form development, PPI assists companies in locating, negotiating and managing outsourced development activities with CROs and CMOs and serves as a technical liaison to the FDA. In addition to these services, PPI has helped clients in assessing technologies, due diligence, preparation of the CMC section of INDs and NDAs and other regulatory applications, OOS and OOT investigations, and manufacturing troubleshooting. Products have been developed for cardiovascular, onocologic, gastrointestinal, CNS, respiratory, pain management, hormone replacement, immunologic and antimicrobial therapies. John McCarty is an inventor on 17 U.S. and foreign patents. Contact: john.mccarty@comcast.net

XRD (cont'd from page 16)

References

1. Grant D.J.W., Theory and origin of polymorphism. In: Brittain HG, editor. Polymorphism in Pharmaceutical Solids. Marcel Dekker, New York, 1999, pp.1-33.
2. R. Jenkins, and R.L. Snyder, Introduction to X-Ray Powder Diffractometry, Vol. 138, (1996), Wiley-Interscience, New York 378, pp.355-556 and 371.
3. Guillory J.K. 1999. Generation of Polymorphs, Hydrates, Solvates and Amorphous Solids. In: Brittain HG, editor. Polymorphism in Pharmaceutical Solids. New York: Marcel Dekker. pp 183-226.
4. Geoff G.Z. Zhang, C. Gu, M.T. Zell, R.T. Burkhardt, E.J. Munson, D.J.W. Grant. Crystallization and Transitions of Sulfamerazine Polymorphs. J.Pharm Sci 91 (2002), pp.1089-1090.
5. Byrne, Pfeiffer, Ganey, Hoiberg, Poochikan, Pharm. Res. 12(7), 1995
6. "X-Ray Diffraction", General Test, 941., United States Pharmacopoeia 25, The United States Pharmacopoeial Convention, Rockville, MD, 2001, pp.2088-2089.
7. P. W. Stephens, What's in Your Pill? What About Theirs? Modern X-ray Analysis in the Pharmaceutical Industry Using Synchrotron Radiation. American Pharmaceutical Review, Vol. 5 (2002) pp. 62-64.
8. M. Davidovich, J. DiMarco, J. Gougoutas, R. Mueller, A. Newman, K. Raghavan , S. Ranadivel I. Vitez, B. Sarsfield. The Role of Powder X-ray Diffraction as a Powerful Tool in Characterization of Various Hydrates of a Drug Substance. American Pharmaceutical Review, Vol. 4 (2001) pp.53-55
9. W. I. F. David, K. Shankland, L.B. McCusker, C. Baerlocher. Structure Determination from Powder Diffraction Data. International Union of Crystallization Oxford University Press, New York. p 1
10. H. P. Klug, L. E. Alexander. X-Ray Diffraction Procedures For Polycrystalline and Amorphous Materials. 2nd Edition, John Wiley & Sons, Inc., 1974 (pp 710).
11. P. Klug, L. E. Alexander. X-Ray Diffraction Procedures For Polycrystalline and Amorphous Materials. 2nd Edition, John Wiley & Sons, Inc., 1974 (pp 709).
12. H. P. Klug, L. E. Alexander. X-Ray Diffraction Procedures For Polycrystalline and Amorphous Materials. 2nd Edition, John Wiley & Sons, Inc., 1974 (pp 177).

Martha Davidovich received her MS degree in Bio-Inorganic Chemistry from C.U.N.Y. (City University of New York) and her BS degree from Yeshiva University, NY. Prior to joining Squibb, she worked for A. Einstein Medical School in Clinical R&D. She joined Bristol-Myers Squibb in 1979 in the QC division. She moved to Pharmaceutics R&D in 1983 and specialized in preformulation and formulation activities. She had spent several years doing computer and analytical instrumentation automation and support in PR&D. In 1997 Martha joined the Materials Science Group of Analytical R&D. In her present position, Martha uses PXRD to characterize pharmaceuticals from drug discovery phase through drug substance and product scale-up. She employs several PXRD techniques to screen for new polymorphic forms, characterize the discovered forms and analyze mixed systems. She has presented at the Pharmaceutical Powder XRD Symposium and has contributed to many papers presented at NATAS, Eastern Analytical conferences and at internal company symposia. She has authored a review article titled "The Role of Powder X-ray Diffraction as a Powerful Tool in Characterization of Various Hydrates of a Drug Substance" for American Pharmaceutical Review.

Material may be protected by copyright law (Title 17. U.S. Code)

UM00016552
NOVARTIS EXHIBIT 1517
Novartis v. Regents, IPR2023-01347
Page 3534 of 4460

DRUG DISPOSITION

Clin Pharmacokinet 2000 Mar; 38 (3): 225-242
0312-5963/00/0003-0225/$20.00/0
© Adis International Limited. All rights reserved.

Clinical Pharmacokinetics and Pharmacodynamics of Celecoxib

A Selective Cyclo-Oxygenase-2 Inhibitor

Neal M. Davies,[1] *Andrew J. McLachlan*,[1] *Ric O. Day*[2] and *Kenneth M. Williams*[2]

1 Faculty of Pharmacy, University of Sydney, Sydney, New South Wales, Australia
2 Department of Clinical Pharmacology and Toxicology, St Vincent's Hospital, University of New South Wales, Sydney, New South Wales, Australia

Contents

Abstract . . . 225
1. Analytical Methods . . . 227
2. Pharmacokinetic Properties . . . 227
   2.1 Absorption . . . 227
   2.2 Distribution . . . 231
      2.2.1 Distribution and Protein Binding . . . 231
      2.2.2 Distribution into Synovial Fluid/Synovium . . . 231
   2.3 Metabolism and Elimination . . . 232
3. Implications of Pharmacokinetic and Pharmacodynamic Properties for Therapeutic Use . . . 232
   3.1 Racial and Genetic Polymorphism . . . 232
   3.2 Specific Inhibition of Cyclo-Oxygenase-2 (COX-2) . . . 232
   3.3 Potential of Selective Inhibitors of COX-2 in Prevention of Myocardial Infarction, Stroke and Angina . . . 233
   3.4 Dosage and Therapeutic Range . . . 234
   3.5 Effectiveness and Safety . . . 235
   3.6 Disease and Celecoxib . . . 236
      3.6.1 Renal Insufficiency . . . 236
      3.6.2 Hepatic Insufficiency . . . 236
      3.6.3 Rheumatic Disorders . . . 237
      3.6.4 Endotoxinaemia . . . 237
      3.6.5 Colorectal Cancer . . . 237
      3.6.6 Alzheimer's Disease . . . 237
   3.7 Influence of Age and Gender on Celecoxib Pharmacokinetics . . . 238
   3.8 Pregnancy and Lactation . . . 238
4. Pharmacokinetic Drug Interactions . . . 239
   4.1 Effect of Other Drugs on the Pharmacokinetics of Celecoxib . . . 239
   4.2 Effect of Celecoxib on the Pharmacokinetics of Other Drugs . . . 239
5. Conclusions . . . 240

Abstract

Celecoxib, a nonsteroidal anti-inflammatory drug (NSAID), is the first specific inhibitor of cyclo-oxygenase-2 (COX-2) approved to treat patients with rheumatism and osteoarthritis. Preliminary data suggest that celecoxib also has

UM00016553
NOVARTIS EXHIBIT 1517
Novartis v. Regents, IPR2023-01347
Page 3535 of 4460

analgesic and anticancer properties. The selective inhibition of COX-2 is thought to lead to a reduction in the unwanted effects of NSAIDs. Upper gastrointestinal complication rates in clinical trials are significantly lower for celecoxib than for traditional nonselective NSAIDs (e.g. naproxen, ibuprofen and diclofenac).

The rate of absorption of celexocib is moderate when given orally (peak plasma drug concentration occurs after 2 to 4 hours), although the extent of absorption is not known. Celexocib is extensively protein bound, primarily to plasma albumin, and has an apparent volume of distribution of 455 ± 166L in humans. The area under the plasma concentration-time curve (AUC) of celecoxib increases in proportion to increasing oral doses between 100 and 800mg. Celecoxib is eliminated following biotransformation to carboxylic acid and glucuronide metabolites that are excreted in urine and faeces, with little drug (2%) being eliminated unchanged in the urine. Celecoxib is metabolised primarily by the cytochrome P450 (CYP) 2C9 isoenzyme and has an elimination half-life of about 11 hours in healthy individuals. Racial differences in drug disposition and pharmacokinetic changes in the elderly have been reported for celecoxib.

Plasma concentrations (AUC) of celecoxib appear to be 43% lower in patients with chronic renal insufficiency [glomerular filtration rate 2.1 to 3.6 L/h (35 to 60 ml/min)] compared with individuals with healthy renal function, with a 47% increase in apparent clearance. Compared with healthy controls, it has been reported that the steady-state AUC is increased by approximately 40% and 180% in patients with mild and moderate hepatic impairment, respectively.

Celecoxib does not appear to interact with warfarin, ketoconazole or methotrexate; however, clinically significant drug interactions with fluconazole and lithium have been documented. As celecoxib is metabolised by CYP2C9, increased clinical vigilance is required during the coadministration of other substrates or inhibitors of this enzyme.

Celecoxib, 4-[5-(4-methylphenyl)-3-trifluoromethyl-1H-pyrazoyl-1-yl]benzene sulphonamide, is a 1,5-diaryl-substituted pyrazole with a pKa of 11.1 (fig. 1). Celecoxib (Celebrex®; Searle-Monsanto and Pfizer) was the first specific inhibitor of cyclooxygenase-2 (COX-2) to be approved by the US Food and Drug Administration (FDA), on December 31, 1998. In the treatment of patients with rheumatoid arthritis, osteoarthritis, and for management of the pain of these conditions, therapeutic doses of celecoxib have proven to be equi-efficacious when compared with other commonly used nonsteroidal anti-inflammatory drugs (NSAIDs), including diclofenac, naproxen and ibuprofen.[1-3] The clinical introduction of celecoxib in 1999 has been the culmination of the important discovery of the COX isoenzymes and the subsequent search for molecules effective in selectively inhibiting COX-2 with little or no effect on COX-1. The major clinical goal was to produce an NSAID that had little or no effects on the gastrointestinal (GI) tract and kidney.

In vitro assays demonstrate that celecoxib is a potent inhibitor of prostaglandin synthesis.[4] *In vitro* assays of inhibition of recombinant human COX-1 and -2 demonstrated that the concentrations of celecoxib required to achieve 50% inhibition of the enzyme (IC_{50}) are 15 ± 1 μg/L for COX-1 and 0.04 ± 0.01 μg/L for COX-2.[5] In cells expressing COX-1 or -2, the IC_{50} values for the COX-1 and -2 isozymes were 13 to 15 and 0.05 μg/L, respectively.[6,7] This suggests that celecoxib possesses a selectivity ratio for COX-1 : COX-2 activity of >375.

© Adis International Limited. All rights reserved.

UM00016554
NOVARTIS EXHIBIT 1517
Novartis v. Regents, IPR2023-01347
Page 3536 of 4460

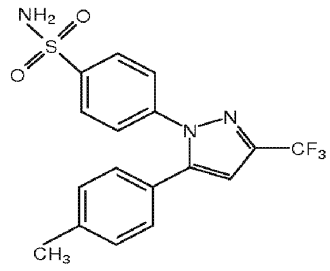

Fig. 1. Structure of celecoxib.

GI complications are the most common adverse effect of the NSAIDs. However, as celecoxib does not inhibit the enzyme COX-1 at concentrations achieved *in vivo* after usual clinical doses, there are putative GI safety advantages compared with other NSAIDs. As celecoxib is structurally a benzene sulphonamide (fig. 1), it should be administered with caution to patients who have demonstrated allergic-type reactions to sulphonamides. A recent meta-analysis suggests that the potential for cross-allergenicity between celecoxib and the sulfanamide-containing medications appears comparable with that of placebo and other nonsulfonamide containing NSAIDs.[8] Prospective trials are needed to confirm these findings. Additionally, celecoxib should not be prescribed for patients who have asthma, urticaria or allergic-type reactions after taking aspirin (acetylsalicylic acid) or NSAIDs.[9]

There are a number of general review articles[10-13] available that deal with the pharmacological properties and therapeutic indications of selective COX-2 inhibition; however, these articles do not discuss, in detail, the clinical pharmacokinetics and pharmacodynamics of celecoxib. In this article, the clinical pharmacokinetics and pharmacodynamics of the first commercially available specific COX-2 inhibitor are reviewed.

1. Analytical Methods

To date there is only one published report describing a method for analysis of celecoxib. Plasma concentrations of celecoxib were determined by high performance liquid chromatography (HPLC) with a quantitation limit of 10 μg/L. This method involved the use of a C18 column and employed ultraviolet detection.[14] There is no information available on analysis of metabolite concentrations.

2. Pharmacokinetic Properties

2.1 Absorption

Celecoxib is administered orally in conventional release capsules, with doses of 100mg and 200mg commercially available. After a single oral 200mg dose to healthy young volunteers the mean maximum drug plasma concentrations (C_{max}) of celecoxib were reached after between 2 and 4 hours[9] (table I). After an oral dose of 300mg, administered as a fine aqueous suspension of the ^{14}C-labelled drug or as a capsule, C_{max} occurred 1.9 hours after administration.[15] Both the C_{max} and area under the concentration-time curve (AUC) were linearly related to dose within the clinical range of 100 to 600mg.[14] Because of the lack of an intravenous form of celecoxib, apparently because of poor solubility, absolute bioavailability studies have not been conducted. Table II provides a summary of the absorption parameters [C_{max}, time to peak concentration (t_{max}) and AUC] for celecoxib in both healthy individuals and patients.

Table I. Concentrations of celecoxib and metabolites (M1, M2 and SC-60613) in plasma. Values are percentages of total radioactivity in plasma samples[9]

Time post-dose (h)	n	Metabolite 1	Metabolite 2	SC-60613	Celecoxib
0.5	8	1.10 ± 0.60	12.1 ± 2.6	2.43 ± 0.89	84.4 ± 3.6
3	8	21.0 ± 4.9	21.2 ± 1.9	0.217 ± 0.182	57.6 ± 6.5
4	2	13.5	21.0	ND	65.6
12	6	23.2 ± 4.1	27.0 ± 5.9	ND	49.9 ± 4.5

n = number of patients; **ND** = not detectable.

© Adis International Limited. All rights reserved.

UM00016555
NOVARTIS EXHIBIT 1517
Novartis v. Regents, IPR2023-01347
Page 3537 of 4460

Table II. Absorption characteristics of celecoxib. Values relate to oral formulations administered as single doses to healthy adults, except where indicated, and are means ± SD where available

Dose (mg)	n	Age (y)[a]	C_{max} (μg/L)	t_{max} (h)	AUC (μg/L • h)	Reference
300 (^{14}C 100μCi)	NR	NR	1527.0 ± 638.0	NR	NR	16
300 (^{14}C 100μCi)	NR	NR	1077.0 ± 649.0	2.0	8764.0	
5	4 (total study 80)	NR	28.0 ± 9.7	1.6 ± 1.1	4.5 ± 0.8	9
25	4 (total study 80)		133.3 ± 45.2	1.3 ± 0.5	10.3 ± 3.8	
50	4 (total study 80)		233.3 ± 45.1	2.0 ± 1.2	7.7 ± 2.7	
100	4 (total study 80)		362.0 ± 156.0	1.4 ± 0.75	8.5 ± 2.9	
200	4 (total study 80)		797.0 ± 498.8	1.8 ± 1.50	7.6 ± 5.5	
200 + high fat breakfast	4 (total study 80)		876.5 ± 749.5	6.3 ± 4.03	9.5 ± 5.6	
400	4 (total study 80)		706.8 ± 104.1	2.3 ± 1.5	7.6 ± 5.5	
400 + high fat breakfast	2 (total study 80)		1355.0 ± 7.1	6.0 ± 2.8	4.2 ± 2.3	
600	4 (total study 80)		1771.0 ± 625.1	1.5 ± 1.0	9.6 ± 3.7	
900	20 (total study 80)		1419.3 ± 683.4	1.9 ± 0.9	10.9 ± 5.2	
1200	4 (total study 80)		2022.5 ± 752.0	2.0 ± 0.8	16.4 ± 17.3	
40	8	(17-44)	197.0 ± 86.0	1.5 ± 0.5	1217.0 ± 328.0	9
200	7		646.0 ± 341.0	1.6 ± 0.7	5986.0 ± 4032.0	
400	8		1433.0 ± 523.0	2.1 ± 0.8	13341.0 ± 3010.0	
40 single dose followed 48h later by bid × 7 days	8		183.0 ± 52.0	1.94 ± 0.9	937.0 ± 288.0	
200 single dose followed 48h later by bid × 7 days	8		1115.0 ± 425.0	1.8 ± 0.7	6726.0 ± 3858.0	
400 single dose followed 48h later by bid × 7 days	8		1833.0 ± 478.0	1.6 ± 1.0	11634.0 ± 3745.00	
40	36	(40-58)	277.0 ± 77.0	3.4 ± 3.5	1928.0 ± 568.0	9
200			759.0 ± 374.0	2.5 ± 1.7	9941.0 ± 4488.0	
400			1103.0 ± 309.0	1.9 ± 0.7	14064.0 ± 5428.00	
40 single dose followed 48h later by bid × 17 days			326.0 ± 119.0	1.7 ± 0.6	1687.0 ± 601.0	
200 single dose followed 48h later by bid × 17 days			1187.0 ± 393.0	2.1 ± 1.0	8155.0 ± 2427.0	
400 single dose followed 48h later by bid × 17 days			1805.0 ± 642.0	3.8 ± 3.6	13355.0 ± 6599.0	
200 (commercial capsule)	36	NR	705.00 ± 38.00	2.8 ± 37.0	7830.0	9
200 (suspension)	36	NR	1229.00	0.8	8001.0	
200 (2 × 100 Phase II capsule)	36	NR	620.00	3.0	7562.0	
200 fasting	24	NR	806.0 ± 411	2.4 ± 0.8	5884.0 ± 2293.0	9
200 high fat meal			1042.0 ± 355	3.4 ± 1.3	7141.0 ± 2787.0	
200 medium fat meal			952 ± 244	3.7 ± 0.8	6607.0 ± 2719.0	
200 + antacid			507 ± 259	2.5 ± 1.1	5729.0 ± 2628.0	
50 fasting	24	NR	321.0 ± 178.0	2.9 ± 1.6	2694.0 ± 2592.0	9
50 fed			354.0 ± 130.0	4.5 ± 1.4	2759.0 ± 2281.0	
100 fasting			455.0 ± 275.0	2.6 ± 1.2	5127.0 ± 4020.0	
100 fed			747.0 ± 382.0	5.0 ± 2.4	5419.0 ± 3890.0	
200	NR	NR	1052.0 ± 324.0	4.0 ± 1.2	NR	9
200 bid × 7 days			1255.0 ± 406.0	3.8 ± 0.5	NR	
400 daily			1760.0 ± 634.0	4.6 ± 1.2	NR	
400 single dose AM	NR	NR	2893.0 ± 930.0	3.1 ± 1.2	22160.0 ± 7463.0	9
400 single dose followed 3 days later by 400 at 08.00h with low fat meal × 10 days			2565.0 ± 738.0	3.2 ± 0.6	18955.0 ± 6001.0	
400 single dose followed 3 days later by 400 at 19.00h with low fat meal × 10 days			2214.0 ± 758.0	4.5 ± 1.9	21034.0 ± 7703.0	

© Adis International Limited. All rights reserved.

UM00016556
NOVARTIS EXHIBIT 1517
Novartis v. Regents, IPR2023-01347
Page 3538 of 4460

Table II. Contd

Dose (mg)	n	Age (y)[a]	C_{max} (μg/L)	t_{max} (h)	AUC (μg/L • h)	Reference
200 day 1, followed by 200 bid begun on day 3 and ending after a single morning dose on day 10	24	<50	598.3 973.2	3.4 2.7	6694.0 9697.0	9
200 day 1, followed by 200 bid begun on day 3 and ending after a single morning dose on day 10	24	>65	1019.0 1808.0	1.9 2.4	10143.0 19446.0	
200	12 male	>65	1254.0	NR	8238.0	9
200	11 male	<50	1089.0	NR	6440.0	
200	12 female	>65	2362.0	NR	15466.0	
200	13 female	<50	875.3	NR	5389.0	
200 bid × 5 days 400 bid × 5 days	24 (GFR 60-130 ml/min/1.73 m^2)	(65-85)	1588.0 2824.0	3.3 3.8	10313.0 20027.0	9
200 bid × 7 days - day 1 200 bid × 7 days - day 7	22 (GFR 34-48 ml/min/1.73 m^2)	(43-78)	509.0 662.0	4.5 4.3	2457.0 5003.0	9
100 day 1 followed by 100 bid × 8 days - day 1	12 mild HI	(43-78)	526.0	2.2	3791.0	9
100 day 1 followed by 100 bid × 8 days - day 8			629.0	1.9	3518.0	
100 day 1 followed by 100 bid × 8 days - day 1	12 healthy control		342.2	2.17	2999.0	
100 day 1 followed by 100 bid × 8 days - day 8			421.8	2.08	2575.0	
100 day 1 followed by 100 bid × 8 days - day 1	12 moderate HI	(43-78)	459.0	2.8	6554.0	9
100 day 1 followed by 100 bid × 8 days - day 8			952.0	2.0	6458.0	
100 day 1 followed by 100 bid × 8 days - day 1	12 healthy control		326.0	2.9	2663.0	
100 day 1 followed by 100 bid × 8 days - day 8			425.0	1.9	2288.0	
200 bid	24	NR	850.7 ± 296.0	2.8 ± 1.0	8696.0 ± 3611.0	9
200 bid + lithium CR 450 bid			996.1 ± 385.8	2.4 ± 0.8	8932.0 ± 4113.0	
200 bid + glibenclamide 5 daily or 10 bid	10 NIDDM	NR	1211.0 ± 373.3	2.5 ± 0.8	8177.7 ± 3965.1	9
200 bid + glibenclamide 10 bid	14 NIDDM		1435.9 ± 767.0	2.5 ± 0.8	9748.1 ± 6289.2	
200, day 1	17	NR	753.3 ± 289.0	2.9 ± 1.3	8133.5 ± 2679.2	17
200/day, day 9	17	NR	649.0 ± 322.0	2.6 ± 0.82.8	7397.3 ± 2819.7	
200, day 1 + KNZ 200/day × 7 days	17	NR	4567.4 ± 320.3	3.5 ± 1.9	7850.5 ± 2294.0	
200, day 1 + FNZ 200/day × 7 days	17	NR	1038.7 ± 377.3	3.4 ± 1.6	17103.8 ± 5424.0	
100	37	(21-49)	550.0 ± 65.0	4.1 ± 0.6	4514.0 ± 531.0	14
400			971.0 ± 115.0	4.3 ± 0.9	11282.0 ± 1339.0	
800			2 929.0 ± 437.0	4.0 ± 0.1	23109.0 ± 6318.0	

a Mean age; range in parentheses.

AUC = area under the concentration-time curve; **bid** = twice daily; **C_{max}** = peak plasma drug concentration; **CR** = controlled release; **FNZ** = fluconazole; **GFR** = glomerular filtration rate; **HI** = hepatic impairment; **KNZ** = ketoconazole; **NIDDM** = type 2 (non–insulin-dependent) diabetes mellitus; **NR** = not reported; **t_{max}** = time taken to achieve C_{max}.

In single dose studies, coadministration of a high fat (75g) meal led to a delay in the C_{max} of between 1 and 2 hours and the AUC was increased significantly, by 10 to 20%, compared with fasting conditions.[9] Coadministration of celecoxib with aluminium- or magnesium-containing antacids resulted in a 37% decrease in the C_{max} and a 10% decrease in AUC.[9]

© Adis International Limited. All rights reserved.

UM00016557
NOVARTIS EXHIBIT 1517
Novartis v. Regents, IPR2023-01347
Page 3539 of 4460

Table III. Pharmacokinetic properties of celecoxib in healthy volunteers. Values are for oral immediate release dosage forms administered as single doses, except where indicated, and are means ± SD where available

Dose (mg)	n	Age (y)[a]	$t_{½\beta}$ (h)	V/F (L/kg)	CL/F (L/h)	Reference
300 (^{14}C 100μCi)	NR	NR	15.6	NR	NR	16
300 (^{14}C 100μCi)	NR	NR	NR	NR	NR	
5	4 (total study 80)	NR	4.5 ± 0.8	NR	NR	9
25	4 (total study 80)		10.3 ± 3.8	NR	NR	
50	4 (total study 80)		7.7 ± 2.7	NR	NR	
100	4 (total study 80)		8.5 ± 2.9	NR	NR	
200	4 (total study 80)		7.6 ± 5.6	NR	NR	
200 + high fat breakfast	4 (total study 80)		9.5 ± 5.6	NR	NR	
400	4 (total study 80)		7.5 ± 2.4	NR	NR	
400 + high fat breakfast	2 (total study 80)		4.2 ± 2.3	NR	NR	
600	4 (total study 80)		9.6 ± 3.7	NR	NR	
900	20 (total study 80)		10.9 ± 5.2	NR	NR	
1200	4 (total study 80)		16.4 ± 17.3	NR	NR	
40	8	(17-44)	4.2 ± 2.0	194.0 ± 81.5	34.3 ± 9.6	9
200	7		8.0 ± 2.3	483.0 ± 260.0	40.1 ± 14.4	
400	8		8.9 ± 3.6	408.0 ± 208.0	31.4 ± 6.9	
40 single dose followed 48h later by bid × 7 days	8		3.9 ± 1.6	239.0 ± 98.0	45.1 ± 14.4	
200 single dose followed 48h later by bid × 7 days	8		7.1 ± 2.33	346.0 ± 176.0	33.9 ± 10.8	
400 single dose followed 48h later by bid × 7 days	8		9.6 ± 4.2	557.0 ± 407.0	38.2 ± 13.8	
40	36	(40-58)	7.7 ± 2.9	244.0 ± 107.0	22.6 ± 7.5	9
200			15.2 ± 7.6	467.0 ± 196.0	25.1 ± 15.2	
400			14.5 ± 5.7	649.0 ± 269.0	32.7 ± 13.6	
40 single dose followed 48h later by bid × 17 days			7.4 ± 1.7	270.0 ± 78.0	26.2 ± 8.4	
200 single dose followed 48h later by bid × 17 days			12.1 ± 3.7	465.0 ± 205.0	26.2 ± 6.6	
400 single dose followed 48h later by bid × 17 days			14.2 ± 4.5	796.0 ± 517.0	36.4 ± 15.7	
200 (commercial capsule)	36	NR	11.9	NR	27.7	9
200 (suspension)	36	NR	13.3	NR	27.1	
200 (2 × 100 Phase II capsule)	36	NR	14.0	NR	29.0	
200 fasting	24	NR	14.1 ± 11.4	NR	NR	9
200 high fat meal			6.3 ± 2.8	NR	NR	
200 medium fat meal			6.2 ± 2.5	NR	NR	
200 antacid			10.6 ± 3.1	NR	NR	
50 fasting	24	NR	11.0 ± 6.7	NR	NR	9
50 fed			6.5 ± 3.9	NR	NR	
100 fasting			16.0 ± 10.2	NR	NR	
100 fed			6.9 ± 3.0	NR	NR	
400 single dose AM	NR	NR	7.7 ± 2.4	NR	NR	9
400 single dose followed 3 days later by 400 at 08.00h with low fat meal × 10 days			10.1 ± 8.7	NR	NR	
400 single dose followed 3 days later by 400 at 19.00h with low fat meal × 10 days			7.3 ± 2.8	NR	NR	
200 day 1, followed by 200 bid begun on day 3 and ending after a single morning dose on day 10	24	<50	11.7 11.3	533.0 630.0	31.7 38.4	9
200 day 1, followed by 200 bid begun on day 3 and ending after a single morning dose on day 10	24	>65	12.8 12.4	390.0 448.0	22.3 23.7	
200	12 male	>65	NR	NR	26.0	9
200	11 male	<50	NR	NR	35.1	
200	12 female	>65	NR	NR	22.3	
200	13 female	<50	NR	NR	42.0	

© Adis International Limited. All rights reserved.

UM00016558
NOVARTIS EXHIBIT 1517
Novartis v. Regents, IPR2023-01347
Page 3540 of 4460

Table III. Contd

Dose (mg)	n	Age (y)[a]	$t_{1/2\beta}$ (h)	V/F (L/kg)	CL/F (L/h)	Reference
200 bid × 5 days	24 (GFR 60-130 ml/min/1.73 m^2)	(65-85)	NR	NR	21.3	9
400 bid × 5 days			NR	NR	21.7	
200 bid × 7 days - day 1	22 (GFR 34-48 ml/min/1.73 m^2)		NR	NR	NR	9
200 bid × 7 days - day 7			NR	NR	41.5	
100 day 1 followed by 100 bid × 8 days - day 1	12 mild HI	(43-78)	11.2	NR	34.5	9
100 day 1 followed by 100 bid × 8 days - day 8			11.0	NR	32.9	
100 day 1 followed by 100 bid × 8 days - day 1	12 healthy controls		10.8	NR	37.1	
100 day 1 followed by 100 bid × 8 days - day 8			10.4	NR	38.0	
100 day 1 followed by 100 bid × 8 days - day 1	12 moderate HI	(43-78)	14.0	NR	18.8	9
100 day 1 followed by 100 bid × 8 days - day 8			13.6	NR	16.2	
100 day 1 followed by 100 bid × 8 days - day 1	12 healthy controls		11.0	NR	40.5	
100 day 1 followed by 100 bid × 8 days - day 8			10.7	NR	43.4	
200 day 1	17	NR	9.6	NR	NR	17
200/day - day 9	17	NR	11.0	NR	NR	
200 day 1 + KNZ 200/day × 7 days	17	NR	11.2	NR	NR	
200 day 1 + FNZ 200/day × 7 days	17	NR	11.2	NR	NR	

a Mean age; range in parentheses.

bid = twice daily; **CL/F** = apparent clearance of drug from plasma after oral administration; **FNZ** = fluconazole; **GFR** = glomerular filtration rate; **HI** = hepatic impairment; **KNZ** = ketoconazole; **n** = number of participants; **NR** = not reported; **$t_{1/2\beta}$** = elimination half-life; **V/F** = apparent volume of distribution after oral administration.

2.2 Distribution

2.2.1 Distribution and Protein Binding

Most traditional NSAIDs are highly (>98%) protein bound to albumin and have an apparent volume of distribution (V/F) ranging from 0.1 to 0.3 L/kg. This volume of distribution is much lower than the volume of total body water (0.6 L/kg) and is equivalent to plasma or blood volume.[15] Celecoxib is also extensively (>97%) protein bound, primarily to albumin. The fraction of unbound drug remains essentially constant (mean 2.6% unbound) at total plasma celecoxib concentrations up to 4000 μg/L.[9] Based on measurement of total ^{14}C radioactivity, celecoxib is evenly distributed between erythrocytes and plasma (red blood cell/plasma = 0.89).[18] Celecoxib has an V/F of 455 ± 166L in humans (5.7 to 7.1 L/kg) [table II].[9,18] This larger than expected V/F when compared with other NSAIDs may relate to the lipophilic nature of celecoxib or be reflective of a low bioavailability.

2.2.2 Distribution into Synovial Fluid/Synovium

Recent preclinical studies suggest that increased prostanoid production in inflammation requires increased COX-2 expression and increased substrate, arachidonic acid. The supply of arachidonic acid to COX-2 may determine the effectiveness of NSAIDs, as supplying arachidonic acid leads to increased prostanoid production and subsequently reduces the effectiveness of NSAIDs, including selective COX-2 inhibitors.[19] NSAIDs may inhibit prostanoid production in a manner that is inversely related to arachidonic acid supply. It has been suggested that COX-2 inhibitors are less effective at more inflamed sites where phospholipase A_2 activity is increased.[19] This may provide a rational explanation for the observation that higher dosages of celecoxib are required for the management of patients with rheumatoid arthritis as compared with patients with osteoarthritis.[20]

The distribution of specific COX-2 inhibitors into the synovium may be an extremely important determinant of the effectiveness of this class of compounds. However, there are no published data on either synovial fluid or synovium concentrations of celecoxib. Based on the relatively high protein binding and intermediate elimination half-life ($t_{1/2\beta}$), one might expect the relative distribution between blood and synovial fluid to be similar to the synovial fluid concentrations displayed by naproxen.[20]

© Adis International Limited. All rights reserved.

UM00016559
NOVARTIS EXHIBIT 1517
Novartis v. Regents, IPR2023-01347
Page 3541 of 4460

The impact of the lipophilic properties of celecoxib on trans-synovial transport is unclear.

NSAIDs account for a high percentage of reported serious adverse drug reactions.[21] As a consequence, there has been considerable interest in the development of topical NSAIDs in recent years with the aim of providing local action without systemic adverse effects. When applied topically, these drugs are formulated to penetrate the skin barrier in sufficient amounts to reach the subadjacent joints and muscles and exert therapeutic activity. Local enhanced topical delivery may also allow the clinician to deliver a specific COX-2 inhibitor to the site of action and increase the therapeutic ratio even further.[22] At this time, there is no information regarding a topical formulation of celecoxib.

2.3 Metabolism and Elimination

Table III presents a summary of the pharmacokinetic parameters of celecoxib. The $t_{1/2\beta}$ of celecoxib is reported to be between 11.2 and 15.6 hours and the apparent clearance (CL/F) is approximately 30 L/h (500 ml/min).[9] Celecoxib undergoes extensive hepatic metabolism in humans. Less than 2% is excreted unchanged in urine and only 2.6% is excreted unchanged in faeces.[9,11,18]

Three metabolites of celecoxib have been found in plasma: SC-60613, SC-62087 and the glucuronide conjugate of SC-62807. SC-60613 is the product of partial oxidation of the methyl moiety of celecoxib to a hydroxyl group and is a minor circulating metabolite. SC-62807 (M2) is the result of complete oxidation of the methyl moiety of celecoxib to a carboxyl group. Glucuronidation of the carboxyl metabolite forms M1[9] (table I). The carboxylic acid metabolite (SC-62807) constitutes 19% and 54% of the dose excreted in urine and faeces, respectively, with low amounts of the glucuronide metabolite also appearing in urine.[9,18]

In vitro studies using human liver microsomes and heterogeneously expressed CYP protein indicate that CYP2C9 is the major isoform responsible for this metabolism.[18]

3. Implications of Pharmacokinetic and Pharmacodynamic Properties for Therapeutic Use

3.1 Racial and Genetic Polymorphism

A meta-analysis of pharmacokinetic studies has suggested an approximately 40% higher AUC and 11% lower CL/F of celecoxib in Blacks compared with Caucasians.[9] The reason for these pharmacokinetic differences is unclear.

Variants at several amino acid residues lead to genetic polymorphism in the coding region of the CYP2C9 gene.[23] Markedly diminished metabolic capacity for CYP2C9 substrates and wide variability in the elimination and/or dose requirements of CYP2C9 substrates occur as a result.[24] Very high concentrations (3 to 9 times mean values) were observed in 2 out of several hundred individuals receiving celecoxib, and it was suggested that they had CYP2C9 deficiency.[9] The clinical significance and the underlying mechanism for these pharmacokinetic differences remain unknown.

Individualisation of the dose may be necessary as a result. There are now many examples where inborn errors of drug metabolism and racial differences in drug disposition may have clinically significant sequelae and account for interindividual variability in the dose requirement for, and response to, a drug [e.g. ethanol (alcohol), warfarin, isoniazid, phenacetin and mephenytoin].[25]

3.2 Specific Inhibition of Cyclo-Oxygenase-2 (COX-2)

It has now been determined that COX exists as at least 2 isoenzymes.[18,19] Generally, COX-1 is a constitutively expressed cellular 'house keeping' isoenzyme that is present in many tissues and regulates gastric cytoprotection, as well as vascular homeostasis.[26] By contrast, COX-2 is an inducible isoenzyme that is predominantly expressed in inflamed tissue although it is constitutively expressed in parts of the brain and kidney.[27] COX-2 is induced by a variety of stimuli, including cytokines, endotoxin, hormones, growth factors and mitogens.

© Adis International Limited. All rights reserved.

UM00016560
NOVARTIS EXHIBIT 1517
Novartis v. Regents, IPR2023-01347
Page 3542 of 4460

It was postulated that inhibition of COX-1 reduced synthesis of cytoprotective compounds, such as prostaglandin (PG) E_2, whereas inhibition of COX-2 reduced inflammation, and that NSAIDs with a high COX-2 : COX-1 inhibitory concentration ratio would have the potential to cause more gastric erosion as the concentration required to elicit beneficial effects exceeds that which causes gastric toxicity.[10] However, some critical points regarding the COX-2 : COX-1 hypothesis can be raised:

- the results of *in vitro* experiments should be cautiously related to the *in vivo* situation because of the pharmacokinetic properties and subsequently different *in vivo* temporal concentration profiles of NSAIDs in various tissues (i.e. synovium, GI tract and kidney)
- *in vitro* experiments cannot take into account the impact of formulation
- *in vitro* experiments cannot predict organ- and tissue-specific adverse effects of NSAIDs
- the relative COX-2 : COX-1 inhibitory activity of an individual NSAID depends on the *in vitro* system or laboratory model used
- there may be more than 2 COX-isoenzymes
- the COX-2 : COX-1 inhibitory activity is only one aspect of an individual NSAID, and other mechanisms of action in terms of anti-inflammatory and adverse effects are possible (e.g. effects on oxidative phosphorylation)[28]
- the effects of suppression of constitutively expressed COX-2
- *in vitro* experiments cannot take into account the role of prosatglandin receptors and the tissue and substrate selectivities of these receptors.

The pathogenesis of NSAID-induced GI and kidney damage has not been clearly delineated. Recent work using transgenic knockout mice deficient in the isoenzymes for COX-1 and -2 has shed light on the specific signalling roles of the 2 prostaglandin biosynthetic pathways defined by these enzymes, although there may be problems of extrapolating physiological responses in knockout mice to the clinical situation. Interestingly, COX-1 knockout mice exhibited no spontaneous GI abnormalities but showed decreased platelet aggregation and a decreased inflammatory response to arachidonic acid but not to the mitogenic stimulator tetradecanylphorbol acetate.[29] COX-2 knockout mice developed severe nephropathy and had an altered but present inflammatory response. In addition, COX-2 knockout mice had increased incidence of peritonitis.[30,31] It remains possible that some of the adverse effects of NSAIDs may be related to their ability to suppress COX-2 and that prostanoids derived via COX-1 contribute to the therapeutic action. Further research derived from these transgenic animals may be valuable for understanding the pathophysiological roles of the COX isoenzymes.

NSAIDs also have a 'topical' or direct local toxicity on the GI mucosa causing ulceration, which is independent of COX inhibition. In contrast to current nonselective NSAIDs, celecoxib is nonacidic and part of its favourable tolerability profile may be due to both the lack of the 'topical' action on GI tissues as well as the lack of inhibitory effects on COX-1 and as yet other unidentified effects. It is unlikely, however, that highly selective inhibitors of COX-2 will be more efficacious than nonselective NSAIDs, since many of the existing NSAIDs are very potent inhibitors of this isoenzyme.

3.3 Potential of Selective Inhibitors of COX-2 in Prevention of Myocardial Infarction, Stroke and Angina

COX-1 is the isoenzyme that mediates the antithrombotic properties of NSAIDs through inhibition of thromboxane synthesis by platelets.[32] Specific COX-2 inhibitors do not have a therapeutic basis as antithrombotic agents in the context of the prevention of myocardial infarction and stroke. However, in patients with unstable angina, it is possible to have an episodic increase in thromboxane synthesis. This can also occur in patients with unstable angina receiving aspirin, resulting in aspirin-resistant thromboxane biosynthesis.[33] Recent data indicate that COX-2 is expressed in the plaques of coronary arteries and in monocytes, which suggests a possible alternative mechanism, i.e. that the benefits of aspirin are mediated via

© Adis International Limited. All rights reserved.

UM00016561
NOVARTIS EXHIBIT 1517
Novartis v. Regents, IPR2023-01347
Page 3543 of 4460

inhibition of COX-2 activity.[34] Thus specific COX-2 inhibition may have a role in protection against unstable angina.

3.4 Dosage and Therapeutic Range

The usual recommended initial dosage of celecoxib for patients with osteoarthritis is 200mg daily, administered as a single dose or as 100mg twice daily. For patients with rheumatoid arthritis, the recommended therapeutic dosage is 100 to 200mg twice daily.[1]

There have been several clinical trials that support the use of celecoxib in pain management, including 4 single dose post-third molar dental extraction studies, and 2 multiple dose (between 3 and 5 days), post-general and orthopaedic surgical studies. Celecoxib has yet to receive FDA approval for use as analgesia, but the drug has been shown to be efficacious in post-surgical dental pain at doses ranging from 50 to 400mg.[3,35]

However, although celecoxib demonstrated analgesic activity in single dose dental pain studies, it appeared to be less effective than ibuprofen or naproxen sodium at equivalent doses, and it did not demonstrate statistically significant effectiveness in the treatment of pain in 2 multiple dose, 3- to 5-day post-operative trials compared with placebo.[9]

In vitro studies of celecoxib on COX-1 activity with U937 cell microsomes, human platelets and CHO cells expressing COX-1 demonstrate IC_{50} values of 52 ± 9, 660 ± 20 and 320 ± 120 μg/L, respectively, in protein-free media.[36] In parallel with these findings, initial studies suggest that celecoxib lacks effect on COX-1 derived thromboxane B_2 levels *in vivo* and has no significant effect on platelet aggregation or bleeding time.[37] A more recent study[14] has shown that at therapeutic doses celecoxib poorly inhibits thromboxane A_2-dependent platelet aggregation induced by arachidonic acid *ex vivo*. Celecoxib did, however, tend to inhibit aggregation by up to 10% as the dose was increased.[14]

Celecoxib also suppressed serum thromboxane B_2 compared with placebo at the 800mg dose. It appears that there is a linear relationship between plasma concentration of celecoxib and the degree of inhibition of serum thromboxane B_2.[14] Celecoxib tends to suppress the urinary excretion of 11-dehydrothromboxane B_2, an index of *in vivo* thromboxane A_2 synthesis. In addition, celecoxib suppressed urinary excretion of the prostacyclin metabolite 2,3-dinitro-6-keto-$PGF_{1\alpha}$, an index of systemic prostacyclin biosynthesis, by a similar degree after a single 400 and 800mg dose of celecoxib was administered. This may imply a major role for COX-2 in the biosynthesis of either systemic or renal PGI_2 under physiological conditions. COX-2 is constitutively expressed in the macula densa of the kidney.[30] Celecoxib is not completely selective for this isoenzyme *in vivo* in the dose range employed.[14,36] The IC_{50} for the hydroxymethyl metabolite against isolated recombinant human COX-1 and -2 are >200 and 93.3 μg/L, respectively. The IC_{50} for the carboxy metabolite against recombinant human COX-1 and -2 are >250 and 11.2 μg/L, respectively.[5]

A recent controlled trial of 10 days' duration conducted in 24 healthy adults compared the effects on platelet function of a dose of celecoxib (600mg twice daily) with a standard dose of naproxen (500mg twice daily). *Ex vivo* platelet aggregation in response to agonists [collagen, arachidonate, or U46619 (a thromboxane A_2 receptor agonist)], bleeding time, and serum thromboxane B_2 level were measured. Naproxen produced statistically significant reductions in platelet aggregation and serum thromboxane B_2 levels and increased bleeding time whereas celcoxib and placebo did not. The results suggest that at supratherapeutic doses, celecoxib does not interfere with platelet aggregation and haemostasis.[38]

The effect of protein binding on the relative activities has not been determined, but would be predicted to increase these values (in terms of total plasma or blood concentration) in proportion to the degree of protein binding.

The C_{max} and AUC of celecoxib are linearly related to dose (fig. 2).[14] There is, however, considerable variability in *ex vivo* COX-2 inhibition by celecoxib and this relationship actually appears to be sigmoidal. A dose-response relationship for celecoxib in patients with arthritis has not yet been

© Adis International Limited. All rights reserved.

UM00016562
NOVARTIS EXHIBIT 1517
Novartis v. Regents, IPR2023-01347
Page 3544 of 4460

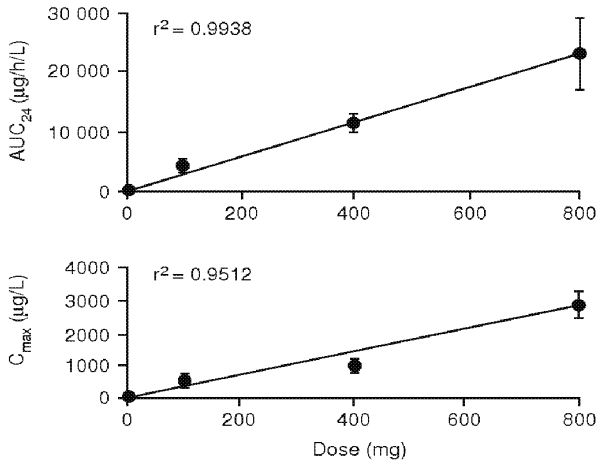

Fig. 2. Relationship between dose and (**top**) area under the concentration-time curve over 24 hours (AUC_{24}) and (**bottom**) peak plasma drug concentration at 4 hours (C_{max}) after administration of single doses of celecoxib to healthy volunteers.[14]

elucidated despite published studies which aimed to establish such a relationship.[2,14] This is a common finding for many NSAIDs, although a linear relationship between anti-inflammatory actions and the dose or plasma concentration of naproxen has been demonstrated in patients with rheumatoid arthritis.[39] A lack of a dose-response relationship for celecoxib may be because celecoxib 100 and 200mg twice daily is already at the upper end of the dose-response curve. This is supported by the observation that for patients with rheumatoid arthritis, doses of 200 and 400mg twice daily are not distinguishable from each other with respect to effectiveness.[2,14] These doses may, therefore, be at the maximum achievable clinical response.

It is clear that celecoxib 40mg twice daily (which was significantly less active in this patient group) is at the lower end of the dose-response curve for this drug.[1] Alternatively, these findings may also reflect a lack of correlation between concentration and effect, but more probably suggest a lack of sensitivity of measured end-points, the subjective nature of clinical measures, the need for studies of greater statistical power, interpatient variability in pharmacokinetics and/or pharmacodynamics or the need for more sensitive quantitative surrogate markers of effectiveness of anti-inflammatory drugs.

There are no published data available on the effect of celecoxib on prostaglandin synthesis in human gastric mucosa, although animal studies suggest celecoxib has no effect on the gastric production of prostaglandins.[40]

With respect to evaluating the effectiveness of NSAIDs, it should be recognised that there are possible 'responders' and 'nonresponders' to therapy.[41] Whether selective COX-2 inhibitors of celecoxib demonstrate this pattern of clinical response has yet to be investigated. Few published studies have attempted to correlate the clinical, pharmacokinetic and pharmacological data of celecoxib. Furthermore, there are no data relating celecoxib concentrations to adverse effects. However, in patients who have a known allergy to sulphonamides, aspirin or NSAIDs, the use of celecoxib may be contraindicated.[9] As celecoxib is from a new chemical class of compound it is likely that the incidence and significance of adverse effects will become more apparent during post-marketing surveillance.

3.5 Effectiveness and Safety

Celecoxib has demonstrated effectiveness in both placebo and active-control (or comparator) clinical trials in patients with osteoarthritis and in patients with rheumatoid arthritis.[2,9,42-44]

In moderate to severe post-operative pain following third molar extraction, celecoxib was superior to placebo in both pain relief and intensity. For all pharmacodynamic variables assessing pain relief, celecoxib performed similarly to aspirin.[2,35]

In endoscopic studies, no significant differences in ulcer or ulcer erosion was found between celecoxib and placebo. The incidence of gastric ulcers and gastric erosions/ulcers was significantly higher for naproxen or diclofenac than for placebo or celecoxib.[1,42,45]

A potential problem in evaluating the adverse effects of new COX-2 inhibitors relates to the claim of fewer adverse effects compared with conventional NSAIDs. Thus these newer drugs may be prescribed for patients who are most prone to de-

© Adis International Limited. All rights reserved.

UM00016563
NOVARTIS EXHIBIT 1517
Novartis v. Regents, IPR2023-01347
Page 3545 of 4460

velop such adverse effects. This has the potential to bias early post-marketing safety data and, along with selective reporting of adverse reactions, a product such as celecoxib may appear more rather than less toxic.[46,47] This phenomena has been termed 'channelling' and has the potential to complicate any interpretation of the epidemiology of early adverse effect reporting with the COX-2 inhibitors. Nevertheless, a US FDA Arthritis Advisory Committee has recommended that the labelling should include a comment saying that serious upper GI complications rates of 0.2% for celecoxib and 1.7% for other NSAIDs might be expected. These recommendations come after analysis of the controlled clinical trials of celecoxib involving 11 000 patients.[48]

3.6 Disease and Celecoxib

3.6.1 Renal Insufficiency

Many patients with rheumatism have some degree of renal function impairment, and elderly patients with poor renal function are especially susceptible to further renal impairment by NSAIDs. COX-2 mRNA and immunoreactive protein localise in the macula densa and adjacent cortical thick ascending limb of the renal tubule of the renal cortex. Chronic NaCl restriction increases the expression of this enzyme and appears to control renin release.[49] COX-2 is also constitutively expressed in thick ascending limbs and papillary interstitial cells in rats and dogs, as well as in the glomerular podocytes and small renal blood vessels in monkeys and humans.[49]

In clinical studies, celecoxib and traditional NSAIDs both inhibited PGE_2 and 6-keto-$PGF_{1\alpha}$ excretion and led to the development of clinically significant oedema, worsened hypertension, increased hypophosphataemia and hydrochloraemia.[9] In normotensive salt-depleted patients, the selective inhibition of COX-2 by celecoxib causes sodium and potassium retention and a short term transient decrease in renal blood flow and glomerular filtration rate, but had no effect on systemic blood pressure at a dose of 400mg.[50]

The AUC of celecoxib has been reported to be approximately 47% lower in patients with chronic renal insufficiency [glomerular filtration rate (GFR) 2.04 to 2.88 L/h (34 to 48 ml/min)] than that seen in individuals with normal renal function. However, no significant relationship has been established between the GFR and CL/F of celecoxib.[9] Celecoxib is extensively metabolised and less than 1% of the drug is excreted in urine. It is possible that there are alterations in protein binding in renal impairment that may contribute to changes in hepatic clearance. It is also possible that there may be reduced absorption, or a compensatory increased biliary excretion, when the drug is administered to patients with renal impairment. However, mechanistic studies of these changes in renal impairment with celecoxib are so far lacking. It is possible that there is reduced tubular reabsorption and/or decreased protein binding of celecoxib in renal insufficiency. The unbound fraction of celecoxib was not determined in the pharmacokinetic study in patients with renal insufficiency and should be determined in future studies.

3.6.2 Hepatic Insufficiency

The influence of chronic hepatic impairment on celecoxib pharmacokinetics has not been completely delineated. As celecoxib undergoes significant hepatic metabolism, there may be important pharmacokinetic variations in patients with hepatic disorders (e.g. hepatitis, cholestasis, cirrhosis or ascites). As albumin, globulin and total protein decrease in patients with hepatic disease, this has the potential to increase the plasma free fraction of celecoxib. It has been reported that in patients with mild and moderate (Child-Pugh class I and II) hepatic impairment the AUC of celecoxib at steady state is increased by about 40 and 180%, respectively, compared with healthy controls.[9] Compared with matched controls, patients with moderate and mild hepatic impairment had a significant (63 and 22%, respectively) reduction in the CL/F of celecoxib calculated during steady-state conditions. It would, therefore, seem prudent that celecoxib be administered at a reduced dosage in patients with moderate hepatic impairment.[9]

Nearly all analgesic and anti-inflammatory agents have the potential for hepatic injury. In con-

© Adis International Limited. All rights reserved.

UM00016564
NOVARTIS EXHIBIT 1517
Novartis v. Regents, IPR2023-01347
Page 3546 of 4460

trolled clinical trials of celecoxib, the incidence of borderline elevations of liver function tests was 6% for celecoxib and 5% for placebo, and 0.2% of patients taking celecoxib and 0.3% of patients taking placebo had notable elevations of liver enzymes which resolved on cessation of treatment.[9]

3.6.3 Rheumatic Disorders

The effect of rheumatoid arthritis on the pharmacokinetics of celecoxib has not been reported. Fluctuations in serum albumin caused by disease processes with corresponding protein binding changes may have pharmacokinetic and pharmacodynamic consequences for celecoxib. In addition, disease states such as rheumatoid arthritis may affect the capacity of the liver to metabolise celecoxib, possibly through the effects of inflammatory mediators, hepatic uptake of unbound drug or modulation of intrahepatic processes.

3.6.4 Endotoxinaemia

Endotoxinaemia is associated with the expression of COX-2 and overproduction of arachidonic acid metabolites. Inhibition of COX-2 activity by selective COX-2 inhibitors, including celecoxib, did not attenuate the circulatory failure nor the organ failure caused by endotoxin in a animal model.[51] Thus, COX-2 inhibitors may not be useful in the therapy of circulatory shock. It is possible that the generation of arachidonic acid metabolites by COX-2 is beneficial in conditions of systemic inflammation, such as endotoxin shock, and further studies are required.

3.6.5 Colorectal Cancer

Colorectal cancer is a common malignant tumour and is a leading cause of deaths in Western countries. Reducing the morbidity and mortality of colorectal cancer lies in its prevention and early detection. One promising approach to chemoprevention of these neoplasms and reduction of mortality involves the use of NSAIDs.[52]

The mechanism(s) by which NSAIDs act to reduce colorectal cancer are unknown, but the obvious possibility is that NSAIDs inhibit COX enzymes in the tumour. It has recently been shown that the expression of COX-2 appears to increase in colorectal adenomas and adenocarcinomas.[53,54] The prostaglandins produced by COX-2 may be involved in regulating cellular proliferation and may be involved in the initiation of the cascade of processes required for carcinogenesis, as well as aiding in tumour growth and development.[55] In addition, COX-2 has been shown to map to chromosome 1, one of the loci associated with colon cancer.[56]

Preclinical studies indicate that celecoxib demonstrated dose-dependent chemopreventive activity against colon carcinogenesis.[57-59] Human data have not yet been published. Many of the published reports on the current generation of NSAIDs and chemoprevention of colorectal cancer have used relatively high dosages that have been associated with significant toxicity. Long term administration of a selective COX-2 inhibitor may be more justifiable. However, the ability of these drugs to inhibit colon carcinogenesis with a relative benign toxicity profile has yet to be demonstrated. The chemoprevention of colorectal cancer with selective inhibitors of COX-2 is an intriguing concept, as early colonic neoplastic lesions have an excellent cure rate, but advanced metastatic colon cancer remains incurable. However, the potential chemopreventive benefits of these agents must be weighed against the risk of potential complications.

Colon cancer screening, using newer methods of detecting high risk patients, deserves further study since these patients could then be targeted for chemoprevention with selective COX-2 inhibitors. Further studies and clinical trials need to be done to clarify the potential benefit of selective COX-2 inhibitors in colorectal cancer and in other forms of cancer such as lung carcinoma and skin carcinogenesis.[60-62]

In December 1999 the US FDA expanded the approval for celecoxib as an adjunct to usual care in the management of patients with familial adenomatous polyposis.

3.6.6 Alzheimer's Disease

Evidence is mounting that NSAIDs retard the degenerative changes associated with Alzheimer's disease.[63] Currently, the promise of NSAID use in patients with Alzheimer's disease relies mostly on epidemiological studies that have examined

© Adis International Limited. All rights reserved.

UM00016565
NOVARTIS EXHIBIT 1517
Novartis v. Regents, IPR2023-01347
Page 3547 of 4460

drug exposure, without detailed information about the specific drug, dosage or duration of NSAID treatment. Alzheimer's disease is another potential target for COX-2 inhibitors, since this disease is characterised by inflammatory processes in the brain that are associated with increased COX-2 expression.[16,64]

Currently, there is no information on the potential beneficial effects of celecoxib in the treatment of patients with Alzheimer's disease. Celecoxib is likely to present safety advantages in elderly patients. It is not known whether the large V/F and lipophilicity of celecoxib, which may facilitate high concentrations in the CNS compared with traditional NSAIDs, may influence the clinical outcome in the treatment of Alzheimer's disease.

3.7 Influence of Age and Gender on Celecoxib Pharmacokinetics

Several studies have demonstrated the importance of age on the pharmacokinetics and pharmacodynamics of NSAIDs. However, it is often difficult to separate the effect of age from coincident disease states. Fluctuations in serum albumin concentrations and changes in severity of disease have the potential to alter the pharmacokinetics of highly bound drugs. In addition, the normal aging process can affect the capacity of the liver to metabolise celecoxib. In elderly individuals (over 65 years of age), a 40% higher C_{max} and a 50% higher AUC were evident at steady-state when compared with pharmacokinetic observations in young individuals. Furthermore, in females the C_{max} and AUC are significantly higher than those found in males. and this has been attributed to lower average bodyweight in elderly females.[9]

In young females (<50 years) a 13% lower C_{max} after a single dose and a longer half-life (13.9 *vs* 11.4h after a single dose) was apparent compared with young males.[9] The therapeutic and toxicological implications of the changes in pharmacokinetics with disease states is not known. However, it did not appear that there were age-related increases in adverse experiences in clinical trials.[9]

Therapeutic regimens in paediatric patients are often inappropriately based on the extrapolation of pharmacokinetic data from adults. Unfortunately, there is no information available on the pharmacokinetics or pharmacodynamics in this age group. The utility of celecoxib in the management of paediatric pyrexia and juvenile rheumatoid arthritis remains unexplored.

3.8 Pregnancy and Lactation

Inhibitors of COX given during pregnancy have the potential to cause adverse maternal and foetal effects. Maternal effects include the prolongation of pregnancy and labour, whereas constriction of the ductus arteriosus, renal dysfunction and haemostatic abnormalities can occur in the foetus and neonate. In animal studies, ductus arteriosus of the foetus expressed virtually only COX-1 immunoreactive protein and activity. In contrast, the ductus of the term newborn pig (<45 minutes old) contained proteins of both COX-1 and -2, but the latter contributed to >90% of PGE_2 formation.[17] A selective COX-2 inhibitor, DuP697, reduced PGE_2 levels in the ductus arteriosus, albeit not in plasma, but did not affect ductal patency in the newborn pig (<1.5 hours old).

By contrast, the COX-1 inhibitor valeryl salicylate, like indomethacin, markedly reduced levels of PGE_2 in the plasma and ductus arteriosus, causing significant constriction of this vessel. The ductus arteriosus of the term newborn pig, in contrast with that of the foetus, expresses COX-2, but circulating prostaglandins, arising mostly from COX-1, seem to exert the major control on ductal patency *in vivo*.[17]

Celecoxib may be a better alternative for the foetus than nonselective COX blockers for maternal conditions such as inflammation or tocolysis. Curiously, it has been suggested that in late pregnancy celecoxib should be avoided because it may cause premature closure of ductus arteriosus; however, no clinical studies have been published to support this assertion.[9]

Teratogenicity has not been found in animal studies of celecoxib.[9] Celecoxib is excreted into

© Adis International Limited. All rights reserved.

UM00016566
NOVARTIS EXHIBIT 1517
Novartis v. Regents, IPR2023-01347
Page 3548 of 4460

Table IV. Drugs metabolised by, inhibiting or inducing cytochrome P450 (CYP) 2C9[9,23,24]

Substrates	Inhibitors	Inducers
Celecoxib	Fluconazole	Rifampicin (rifampin)
Tolbutamide	Ketoconazole	Phenobarbital
S-Warfarin	Metronidazole	Carbamazepine
Ibuprofen	Itraconazole	Ethanol
Flurbiprofen	Sulfaphenazole	Secobarbital
Diclofenac	Ritonavir	
Phenytoin	Amiodarone	
Fluoxetine	Fluvastatin	
Amitriptyline	Fluvoxamine	
Glipizide	Isoniazid	
Irbesartan	Lovastatin	
Piroxicam	Paroxetine	
Rosiglitazone	Phenylbutazone	
Sulfamethoxazole	Probenecid	
Tamoxifen	Sertaline	
Torasemide	Trimethoprim	
Losartan	Zafirlukast	

breast milk of lactating rats at concentrations similar to those in plasma. It is not yet known whether this pattern of excretion is extendable to humans and if there are risks to breast-fed infants.

4. Pharmacokinetic Drug Interactions

4.1 Effect of Other Drugs on the Pharmacokinetics of Celecoxib

Celecoxib undergoes extensive hepatic metabolism in humans and *in vitro* studies indicate that CYP2C9 is the major isoform responsible for this metabolism.[65] CYP2C9 is an enzyme of major importance in human drug metabolism[24] (table IV). Substrates for CYP2C9 include losartan, phenytoin, tolbutamide and numerous NSAIDs. CYP2C activity *in vivo* is inducible by rifampicin (rifampin). Evidence also indicates that the metabolism of CYP2C9 substrates may be induced variably by carbamazepine, alcohol and phenobarbital.[24] Clinically significant inhibition of CYP2C9 activity has been demonstrated with coadministration of fluconazole, sulfaphenazole and certain other sulphonamides.[13] The effects of multiple doses of fluconazole, an inhibitor of CYP2C9, or ketoconazole, an inhibitor of CYP3A4, on the single dose pharmacokinetics of celecoxib demonstrate that treatment with fluconazole (but not ketoconazole) produced a 68% increase in C_{max} and 134% increase in AUC, further suggesting that celecoxib metabolism *in vivo* is via the CYP2C9 pathway.[17] In this drug interaction study with fluconazole there was a decrease in C_{max} for the metabolites SC-60613 and SC-62807 compared with when celecoxib was administered alone.[9]

In vitro studies suggest that celecoxib is an inhibitor of CYP2D6 (table V) but not an inhibitor of CYP2C9, 2C19 or 3A4.[9] The implication of this finding with respect to *in vivo* drug interactions remains unclear.

Phenytoin, an anticonvulsant, is metabolised via CYP2C9 and demonstrates a narrow therapeutic range of serum concentrations between 10 and 20 mg/L. Nevertheless, coadministration of celecoxib did not alter the single dose pharmacokinetic profile of phenytoin nor the pharmacokinetics of celecoxib.[9]

Lithium is used to treat manic depressive episodes. The mean plasma concentrations of celecoxib were higher for the first 6 hours post-dose when celecoxib was coadministered with lithium than when it was administered alone. The AUC of celecoxib was not significantly altered by the coadministration of lithium carbonate.[9]

4.2 Effect of Celecoxib on the Pharmacokinetics of Other Drugs

NSAIDs are often coadministered with disease-modifying antirheumatic drugs, such as methotrexate, in patients with rheumatoid arthritis. Celecoxib was studied in patients with rheumatoid

Table V. Drugs metabolised by cytochrome P450 (CYP) 2D6[9,23,24]

Codeine
Metoprolol
Trazadone
Mianserin
3,4-Methylenedioxymethamphetamine (MDMA, Ecstasy)
Propranolol
Perphenazine
Propafenone
Clozapine

© Adis International Limited. All rights reserved.

UM00016567
NOVARTIS EXHIBIT 1517
Novartis v. Regents, IPR2023-01347
Page 3549 of 4460

arthritis receiving a stable weekly oral dose of methotrexate 5 to 20 mg/week for a minimum of 3 months. The bioavailability, renal clearance and t_{max} for total methotrexate were similar when celecoxib or placebo was administered with methotrexate.[17,65] However, the power of the study was very low and the patients studied may not be representative of clinical populations. As long term use of celecoxib may affect renal function, and urinary excretion is an important route of elimination for methotrexate, there may be a potential for reduced clearance of methotrexate after the long term use of celecoxib.

NSAIDs may potentiate the effect of oral anticoagulants by a number of potential mechanisms, including altering drug metabolism, disrupting epithelial integrity and independently affecting the blood clotting system. *S*-Warfarin is a substrate of CYP2C9.[24] However, steady-state concentrations (C_{ss}) of warfarin were not altered by the coadministration of celecoxib. Prothrombin time values were not significantly affected.[16,66] However, the US label of celecoxib has been altered to reflect a small increase in International Normalised Ratio (INR) with the coadministration of celecoxib and the need for a more intense monitoring of prothrombin times when celecoxib is commenced in a patient already taking warfarin.

Many patients with chronic arthropathies have other diseases, such as diabetes and psychiatric disorders. Tolbutamide is a sulfonylurea antidiabetic agent metabolised by CYP2C9. The pharmacokinetics of celecoxib were not altered by the presence of tolbutamide, nor were the pharmacokinetics of tolbutamide or its metabolites carboxytolbutamide or hydroxytolbutamide altered by celecoxib.[9] Celecoxib does not influence the steady-state pharmacokinetics or pharmacodynamics (blood glucose and insulin concentrations) of glibenclamide (glyburide), nor does glibenclamide affect the pharmacokinetics of celecoxib.[9]

The renal clearance of lithium can be reduced by several NSAIDs, potentially resulting in toxic serum lithium concentrations. In healthy individuals receiving controlled release lithium 450mg twice daily with celecoxib 200mg twice daily, the mean C_{ss} of lithium increased approximately 17% and mean renal clearance was 13% lower in individuals receiving lithium and celecoxib as compared with individuals receiving lithium alone.[9] Careful monitoring and titration of lithium dosage is required in patients who receive celecoxib and lithium concurrently.

NSAIDs attenuate the hypotensive response to several antihypertensive medications, including ACE inhibitors, β-blockers, diuretics and vasodilators. Patients on furosemide (frusemide) or possibly other diuretics should be carefully monitored if celecoxib is introduced.

5. Conclusions

Celecoxib is the first selective COX-2 inhibitor to be approved for clinical practice. The safety profile of celecoxib is promising. This may be attributable to the chemical class of the compound and its lack of acidity in addition to its COX-2 selectivity. The therapeutic and toxicological relevance of celecoxib pharmacokinetic data requires further study. There is limited information on the concentration-effect relationships of celecoxib. A relationship between anti-inflammatory effect, analgesic effect and plasma concentrations of the drug has yet to be established. There is a potential for drug interactions, as celecoxib is metabolised by CYP2C9, although all data to date show no significant interactions with CYP2C9 substrates.

Additional studies and post-marketing experience after longer term celecoxib usage in a greater number of patients will add substantially to the understanding of the overall risks and benefits of celecoxib compared with those of the nonselective NSAIDs. The main clinical goal is to solve the problem of NSAID-induced GI and renal toxicity, with the resultant morbidity and mortality, and to obtain optimal therapeutic effect with minimal adverse effects; celecoxib holds such promise, at least with respect to the GI tract. However, its renal effects are likely to be the same as described for nonselective NSAIDs.

In view of the difficulties that have bedevilled this area of clinical investigation over the years, the

© Adis International Limited. All rights reserved.

UM00016568
NOVARTIS EXHIBIT 1517
Novartis v. Regents, IPR2023-01347
Page 3550 of 4460

introduction of selective inhibitors of COX-2 must be tempered with an additional caution that any new therapeutic agent, no matter what the rationale behind its introduction, must be carefully prescribed. True clinical superiority of the selective COX-2 inhibitors above nonselective NSAIDs will need to be demonstrated by a lower incidence of adverse effects that is not offset by any new clinical pharmacokinetic or pharmacodynamic concerns.

Acknowledgements

Professor Ric Day is on the Australian advisory board for celecoxib.

References

1. Simon LS, Lanza FL, Lipsky PE, et al. Preliminary study of the safety and efficacy of SC-58635, a novel cyclooxygenase-2 inhibitor. Arthritis Rheum 1998; 41: 1591-602
2. Hubbard RC, Koepp RJ, Yu S, et al. SC-58635 (celecoxib), a novel COX-2 selective inhibitor, is effective as a treatment for osteoarthritis (OA) in a short-term pilot study [abstract 1188]. Arthritis Rheum 1996; 39 Suppl.: S226
3. Hubbard RC, Mehlisch DR, Jasper DR, et al. SC-58635, a highly selective inhibitor of COX-2, is an effective analgesic in an acute post-surgical pain model [abstract]. J Invest Med 1996; 44: 293A
4. Zhang Y, Shaffer A, Portanova J, et al. Inhibition of cyclooxygenase-2 rapidly reverses inflammatory hyperalgesia and prostaglandin E_2 production. J Pharmacol Exp Ther 1997; 283: 1069-75
5. Penning TD, Talley JJ, Bertenshaw SR, et al. Synthesis and biological evaluation of the 1,5-diarylpyrazole class of cyclooxygenase-2 inhibitors: identification of 4-[5-(4-methylphenyl)-3-trifluoromethyl-1H-pyrazol-1-yl]benzene sulfonamide (SC-58635, celecoxib). J Med Chem 1997; 40: 1347-65
6. Khanna IK, Weier JJ, Yu Y, et al. 1,2-Diarylimidazoles as potent, cyclooxygenase-2 selective, and orally active anti-inflammatory agents. J Med Chem 1997; 40: 1634-47
7. Khanna IK, Weier JJ, Yu Y, et al. 1,2-Diarylimidazoles as potent, and selective inhibitors of cyclooxygenase-2. J Med Chem 1997; 40: 1619-33
8. Patterson R, Bello AE, Lefkowith J. Immunologic tolerability profile of celecoxib. Clin Ther 1999 Dec; 21: 2065-79
9. Food and Drug Administration. New drug application #20998: clinical pharmacology/biopharmaceutics review section celecoxib. Bethesda (MD): FDA, 1998
10. Vane JR, Bakhle YS, Botting RM. Cyclooxygenases 1 and 2. Annu Rev Pharmacol Toxicol 1998; 38: 97-120
11. Cryer B, Dubois A. The advent of highly selective inhibitors of cyclooxygenase: a review. Prost Other Lipid Mediat 1998; 56: 341-61
12. Mitchell JA, Evans TW. Cyclooxygenase-2 as a therapeutic target. Inflamm Res 1998; 47 Suppl. 2: S88-92
13. Bolten WW. Scientific rationale for specific inhibition of COX-2. J Rheumatol 1998; 51 Suppl.: 2-7
14. McAdam BF, Lawson-Catela F, Mardini IS, et al. Systemic biosynthesis of prostacyclin by cyclooxygenase (COX)-2: the human pharmacology of a selective inhibitor of COX-2. Proc Natl Acad Sci USA 1999; 96: 272-7
15. Davies B, Morris T. Physiological parameters in laboratory animals and humans. Pharm Res 1993; 10: 1093-5
16. Karim A, Tolbert D, Piergies A, et al. Celecoxib, a specific COX-2 inhibitor, lacks significant drug-drug interactions with methotrexate or warfarin [abstract 1698]. Arthritis Rheum 1998; 41 (9 Suppl.): S315
17. Karim A, Tolbert D, Piergies A, et al. Celecoxib biotransformation: fluconazole but not ketoconazole substantially increases celecoxib exposure in man [abstract 4022]. Pharm Res 1998; 1 Suppl. 1: S626
18. Karim A, Tolbert D, Burton E, et al. SC-58635 (celecoxib): a highly selective inhibitor of cyclooxygenase-2 disposition kinetics in man and identification of its major CYP 450 isozyme in its biotransformation [abstract 3469]. Pharm Res 1997; 14 Suppl. 11: S617
19. Hamilton LC, Mitchell JA, Tomlinson AM, et al. Synergy between cyclo-oxygenase-2 induction and arachidonic acid supply in vivo: consequences for nonsteroidal antiinflammatory drug efficacy. FASEB J 1999; 13: 245-51
20. Day RO, Francis H, Vial J, et al. Naproxen concentrations in plasma and synovial fluid and effects on prostanoid concentrations. J Rheumatol 1995; 22: 2295-303
21. Henry DA. Side-effects of non-steroidal anti-inflammatory drugs. Baillieres Clin Rheumatol 1988; 2: 425-54
22. Vaile JH, Davis P. Topical NSAIDs for musculoskeletal conditions: a review of the literature. Drugs 1998; 56: 783-99
23. Wang SL, Huang J, Lai MD, et al. Detection of CYP2C9 polymorphism based on the polymerase chain reaction in Chinese. Pharmacogenetics 1995; 5: 37-42
24. Miners JP, Birkett DJ. Cytochrome P4502C9: an enzyme of major importance in human drug metabolism. Br J Cin Pharmacol 1998; 45: 525-38
25. Kalow W. Pharmacogenetics in biological perspective. Pharmacol Rev 1997; 49: 369-79
26. Vane JR, Mitchell JA, Appleton I, et al. Inducible isoforms of cyclooxygenase and nitric-oxide synthetase in inflammation. Proc Natl Acad Sci USA 1994; 91: 2046-50
27. Meade EA, Smith WL, DeWitt DL. Differential inhibition of prostaglandin endoperoxide synthase (cyclooxygenase) isozymes by aspirin and other non-steroidal anti-inflammatory drugs. J Biol Chem 1993; 268: 6610-4
28. Mahmud T, Rafi SS, Scott DL, et al. Nonsteroidal anti-inflammatory drugs and uncoupling of mitochondrial oxidative phosphorylation. Arthritis Rheum 1996; 39: 1998-2003
29. Lagenbach R, Morham SG, Tiano HF, et al. Prostaglandin synthase 1 gene disruption in mice reduces arachidonic acid-induced inflammation and indomethacin-induced gastric ulceration. Cell 1995; 83: 483-92
30. Morham SG, Langenbach RL, Loftin CD, et al. Prostaglandin synthase 2 gene disruption causes severe renal pathology in the mouse. Cell 1995; 83: 473-82
31. Dinchuk JE, Car BD, Focht RJ, et al. Renal abnormalities and an altered inflammatory response in mice lacking cyclooxygenase II. Nature 1995; 378: 406-9
32. Schror K. Aspirin and platelets: the antiplatelet action of aspirin and its role in thrombosis treatment and prophylaxis. Semin Thromb Hemost 1997; 23: 349-56
33. Patrono C. Cyclooxygenase enzymes in human vascular disease. In: Vane J, editor. Selective COX-2 inhibitors: pharmacology, clinical effects and therapeutic potential. London: Kluwer Academic Publishers, 1997

© Adis International Limited. All rights reserved.

UM00016569
NOVARTIS EXHIBIT 1517
Novartis v. Regents, IPR2023-01347
Page 3551 of 4460

34. Baker CS, Hall RJ, Evans TJ, et al. Cyclooxygenase-2 is widely expressed in atherosclerotic lesions affecting native and transplanted human coronary arteries and colocalizes with inducible nitric oxide synthase and nitrotyrosine particularly in macrophages. Arterioscler Thromb Vasc Biol 1999; 19 (3): 646-55
35. Mehlisch DR, Hubbard RC, Isakson P, et al. Analgesic efficacy and plasma levels of a highly selective inhibitor of COX-2 (SC-58635) in patients with post-surgical dental pain [abstract PIII-2]. Clin Pharmacol Ther 1997; 61: 195
36. Riendeau D, Charleson S, Cromlish W, et al. Comparison of the cyclooxygenase-1 inhibitory properties of nonsteroidal anti-inflammatory drugs (NSAIDs) and selective COX-2 inhibitors, using sensitive microsomal and platelet assays. Can J Physiol Pharmacol 1997; 75: 1088-95
37. Gaw-Mengle L, Hubbard RC, Karim A, et al. A study of the platelet effects of SC-58635, a novel COX-2 selective inhibitor [abstract 374]. Arthritis Rheum 1997; 40 Suppl. 9: S93
38. Leese PT, Hubbard RC, Karim A, et al. Effects of celecoxib, a novel cyclooxygenase-2 inhibitor, on platelet function in healthy adults: a randomized, controlled trial. J Clin Pharmacol 2000; 40 (2): 124-32
39. Day RO, Furst DE, Droomgoole SH, et al. Relationship of serum naproxen concentration to efficacy in rheumatoid arthritis. Clin Pharm Ther 1982; 31: 733-40
40. Anderson GD, Hauser SD, Mcgarity KL, et al. Selective inhibition of cyclooxygenase-2 reverses inflammation and expression of COX-2 and interleukin 6 in rat adjuvant arthritis. J Clin Invest 1996; 97: 2672-9
41. Walker JS, Sheather-Reid RB, Carmody JJ, et al. Nonsteroidal antiinflammatory drugs in rheumatoid arthritis and osteoarthritis: support for the concept of 'responders' and 'non-responders'. Arthritis Rheum 1997; 40: 1944-54
42. Zhao SZ, Hatoum HT, Hubbard AC, et al. Effect of celecoxib, a novel COX-2 inhibitor, on health-related quality of life patients with osteoarthritis of the knee [abstract 348]. Arthritis Rheum 1997; 40 suppl. 9: S88
43. Hubbard RC, Geis GS, Woods E, et al. Efficacy, tolerability, and safety of celecoxib, a specific COX-2 inhibitor, in osteoarthritis [abstract 982]. Arthritis Rheum 1998; 41 (9 Suppl.): S196
44. Geis GS, Stead H, Morant S, et al. Efficacy and safety of celecoxib, a specific COX-2 inhibitor, in patients with rheumatoid arthritis [abstract 1990]. Arthritis Rheum 1998; 41 (9 Suppl.): S364
45. Lanza FI, Rack MF, Callison DA, et al. A pilot endoscopic study of the gastroduodenal effects of SC-58635, a novel COX-2 selective inhibitor [abstract A]. Gastroenterology 1997; 112 (4): 194
46. Mohammed S, Croom II DW. Gastropathy due to celecoxib, a cyclooxygenase-2 inhibitor. N Engl J Med 1999; 340: 2005-6
47. Reuben SS, Steinberg R. Gastric perforation associated with the use of celecoxib. Anesthesiology 1999; 91: 1548-9
48. Less GI disorders with celecoxib than conventional NSAIDs. Inpharma 1998 Dec 12; 1167: 22
49. Khan KN, Venturini CM, Bunch RT, et al. Interspecies differences in renal localization of cyclooxygenase isoforms: implications in nonsteroidal antiinflammatory drug-related nephrotoxicity. Toxicol Pathol 1998; 5: 612-20
50. Rossat J, Maillard M, Nussberger J, et al. Renal effects of selective cyclooxygenase-2 inhibition in normotensive salt-depleted subjects. Clin Pharmacol Ther 1999; 66: 76-84
51. Leach M, Hamilton LC, Olbrich A, et al. Effects of inhibitors of the activity of cyclo-oxygenase-2 on the hypotension and multiple organ dysfunction caused by endotoxin: a comparison with dexamethasone. Br J Pharmacol 1998; 124: 586-92
52. Rosenberg L, Palmer JR, Zauber AG, et al. A hypothesis: nonsteroidal anti-inflammatory drugs reduce the incidence of large bowel cancer. J Natl Cancer Inst 1996; 83: 355-8
53. Eberhardt CE, Coffey RJ, Radhika A, et al. Up regulation of cyclooxygenase 2 gene expression in human colorectal adenomas and adenocarcinomas. Gastroenterology 1996; 107: 1183-8
54. Kargman SL, O'Neill GP, Vikers PJ, et al. Expression of prostaglandin G/H synthase-1 and -2 protein in human colorectal cancer. Cancer Res 1991; 55: 2556-9
55. Ryseck RP, Raynoschek C, Macdonald-Bravo H, et al. Identification of an immediate early gene, PGHS B, whose protein product has prostaglandin synthase/cyclooxygenase activity. Cell Gr Diff 1993; 3: 443-50
56. Jones DA, Carlton DP, McIntyre TM, et al. Molecular cloning of human prostaglandin endoperoxide synthase type II and demonstration of expression in response to cytokines. J Biol Chem 1993; 268: 9049-54
57. Kawamori T, Rao CV, Seibert K, et al. Chemopreventative activity of celecoxib, a specific cyclooxygenase-2 inhibitor, against colon carcinogenesis. Cancer Res 1998; 58: 409-12
58. Reddy BS, Rao CV, Seibert K. Evaluation of cyclooxygenase-2 inhibitor for potential chemopreventative properties in colon carcinogenesis. Cancer Res 1996; 56: 4566-9
59. Masferrer J, Leahy K, Kobolt C, et al. Celecoxib: a specific COX-2 inhibitor with anti-inflammatory, analgesic and anticancer activities [abstract]. Naunyn-Schmiedeberg's Arch Pharmacol 1998; 358: 8
60. Fischer SM, Lo HH, Gordon GB, et al. Chemopreventative activity of celecoxib, a specific cyclooxygenase-2 inhibitor, and indomethacin against ultraviolet light-induced skin carcinogenesis. Mol Carcinogen 1999; 25: 231-40
61. Watkins DN, Lenzo JC, Segal A, et al. Expression and localization of cyclo-oxygenase isoforms in non-small cell lung cancer. Eur Respir J 1999; 14: 412-8
62. Kitamura Y, Shimohama S, Koike H, et al. Increased expression of cyclooxygenases and peroxisome proliferator-activated receptor-gamma in Alzheimer's disease brains. Biochem Biophys Res Commun 1999; 254: 582-6
63. McGeer EG, McGeer PL. The importance of inflammatory mechanisms in Alzheimer disease. Exp Gerontol 1998; 33: 371-8
64. Guerguerian AM, Hardy P, Bhattacharya M, et al. Expression of cyclooxygenases in ductus arteriosus of fetal and newborn pigs. Am J Obstet Gynecol 1998; 179 (6 Pt 1): 1618-26
65. Karim A, Tolbert D, Hunt TL, et al. Celecoxib, a specific COX-2 inhibitor, has no significant effect on methotrexate pharmacokinetics in patients with rheumatoid arthritis. J Rheumatol 1999 Dec; 26 (12): 2539-43
66. Karim A, Piergies A, Tolbert D, et al. Selective inhibitor of cyclooxygenase-2 (COX-2) SC-58635 (celecoxib), does not affect kinetics or dynamics of warfarin [abstract 606]. J Clin Pharmacol 1998; 38: 880

Correspondence and offprints: Dr *Neal M. Davies,* Faculty of Pharmacy, University of Sydney, Sydney, NSW 2006, Australia.
E-mail: ndavies@pharm.usyd.edu.au

© Adis International Limited. All rights reserved.

UM00016570
NOVARTIS EXHIBIT 1517
Novartis v. Regents, IPR2023-01347
Page 3552 of 4460

Copyright © 2003 EBSCO Publishing

ANALYTICAL CHEMISTRY HANDBOOK

John A. Dean
Professor Emeritus of Chemistry
University of Tennessee, Knoxville

SCIENTIFIC & TECHNICAL
INFORMATION CENTER
NOV 1 4 1995
PATENT & TRADEMARK OFFICE

McGRAW-HILL, INC.
New York San Francisco Washington, D.C. Auckland Bogotá
Caracas Lisbon London Madrid Mexico City Milan
Montreal New Delhi San Juan Singapore
Sydney Tokyo Toronto

UM00016572
NOVARTIS EXHIBIT 1517
Novartis v. Regents, IPR2023-01347
Page 3554 of 4460

condition one can calculate the interplanar distances of the crystalline material. The interplanar spacings depend solely on the geometry of the crystal's unit cell while the intensities of the diffracted x rays depend on the type of atoms in the crystal and the location of the atoms in the fundamental repetitive unit, the unit cell.

From the rearranged Bragg equation

$$\theta = \sin^{-1}\left(\frac{\lambda}{2d}\right) \tag{10.6}$$

the two factors within the parentheses control the choice of x radiation. Because the parenthetical term cannot exceed unity, the use of long-wavelength radiation limits the number of reflections that are observed, whereas short-wavelength radiation tends to crowd individual reflections very close together. Furthermore, radiation just shorter in wavelength than the absorption edge of an element in the specimen should be avoided because the resulting fluorescent radiation increases the background. For these reasons, a multiwindow x-ray tube with anodes of Ag, Mo, W, and Cu is used.

Diffractometer alignment procedures require the use of a well-prepared polycrystalline specimen. Two standard samples found to be suitable are silicon and α-quartz (including Novaculite). The 2θ values of several of the most intense reflections for these materials are listed in Table 10.8. To convert to d for average $K\overline{\alpha}$ values or to d for $K\alpha_2$, multiply the tabulated d value (Table 10.8) for $K\alpha_1$ by the factor given below:

Element	$K\overline{\alpha}$ (average)	$K\alpha_2$
W	1.007 69	1.023 07
Ag	1.002 63	1.007 89
Mo	1.002 02	1.006 04
Cu	1.000 82	1.002 48
Ni	1.000 77	1.002 32
Co	1.000 77	1.002 16
Fe	1.000 67	1.002 04
Cr	1.000 57	1.001 70

The applications of x-ray diffraction can be conveniently considered under three main headings: powder diffraction, polymer characterization, and single-crystal structure studies. In addition there are many specialized uses.

10.11.2 Powder Diffraction

In the powder method, the sample is a large collection of very small crystals, randomly oriented. A polycrystalline aggregate is formed into a cylinder whose diameter is smaller than the diameter of the incident x-ray beam. The diffraction pattern is a series of nonuniformly spaced cones (as intercepted on the photographic film) whose spacings are determined by the prominent planes of the crystallites.

Metal samples may be machined to a cylindrical configuration, plastic materials can often be extruded through suitable dies, and all other samples are best ground to a fine powder (200 to 300 mesh) and shaped into thin rods after mixing with collodion binder or simply tamped into a uniform glass capillary. Liquids must be converted into crystalline derivatives.

The x-ray pattern of a pure crystalline substance can be considered as a "fingerprint" with each crystalline material having, within limits, a unique diffraction pattern. The ASTM has published the powder diffraction patterns of some 50 000 compounds. An identification of an unknown compound

UM00016573
NOVARTIS EXHIBIT 1517
Novartis v. Regents, IPR2023-01347
Page 3555 of 4460

TABLE 10.8 Interplanar Spacings for $K\alpha_1$ Radiation, d versus 2θ

					α-Quartz (including novaculite)					
hkl	100	101	110	102	200	112	202	211	203	301
d, Å	4.260	3.343	2.458	2.282	2.128	1.817	1.672	1.541	1.375	1.372
W $K\alpha_1$: 2θ	2.81	3.58	4.87	5.25	5.63	6.59	7.17	7.78	8.72	8.74
Ag $K\alpha_1$: 2θ	7.53	9.60	13.07	14.08	15.10	17.71	19.26	20.91	23.47	23.52
Mo $K\alpha_1$: 2θ	9.55	12.18	16.59	17.88	19.19	22.51	24.49	26.61	29.89	29.96
Cu $K\alpha_1$: 2θ	20.83	26.64	36.52	39.45	42.44	50.16	54.86	59.98	68.14	68.31
Ni $K\alpha_1$: 2θ	22.44	28.71	39.42	42.60	45.85	54.28	59.44	65.08	74.15	74.34
Co $K\alpha_1$: 2θ	24.24	31.04	42.68	46.15	49.71	58.98	64.68	70.96	81.16	81.38
Fe $K\alpha_1$: 2θ	26.27	33.66	46.38	50.20	54.11	64.38	70.75	77.83	89.50	89.74
Cr $K\alpha_1$: 2θ	31.18	40.05	55.52	60.22	65.09	78.11	86.42	95.96	112.73	113.11
					Silicon					
hkl	111	220	311	400	331	422	511.333	440	531	620
d, Å	3.1353	1.91997	1.63736	1.357630	1.24584	1.1085	1.0451	0.0959986	0.917922	0.858637
W $K\alpha_1$: 2θ	3.82	6.24	7.32	8.83	9.62	10.82	11.48	12.50	13.07	13.98
Ag $K\alpha_1$: 2θ	10.24	16.75	19.67	23.78	25.95	29.23	31.04	33.88	35.48	38.02
Mo $K\alpha_1$: 2θ	12.99	21.29	25.02	30.28	33.08	37.32	39.67	43.36	45.45	48.79
Cu $K\alpha_1$: 2θ	28.44	47.30	56.12	69.13	76.38	88.03	94.96	106.71	114.10	127.55
Ni $K\alpha_1$: 2θ	30.66	51.16	60.83	75.26	83.42	96.80	104.96	119.42	129.12	149.76
Co $K\alpha_1$: 2θ	33.15	55.53	66.22	82.42	91.77	107.59	117.71	137.42	154.04	
Fe $K\alpha_1$: 2θ	35.97	60.55	72.48	90.96	101.97	121.67	135.70			
Cr $K\alpha_1$: 2θ	42.83	73.21	88.72	114.97	133.53					

Source. *Tables of Interplanar Spacings d vs. Diffraction Angle 2θ for Selected Targets*, Picker Nuclear, White Plains, NY, 1966.

UM00016574
NOVARTIS EXHIBIT 1517
Novartis v. Regents, IPR2023-01347
Page 3556 of 4460

is made by comparing the interplanar spacings of the powder pattern of a sample to the compounds in the ASTM file. The d value for the most intense line of the unknown is looked up first in the file. In a single compound, the d values of the next two most intense lines are matched against the file values. After a suitable match for one component is obtained, all the lines of the identified component are omitted from further consideration. The intensities of the remaining lines are rescaled by setting the strongest intensity equal to 100 and repeating the entire procedure. If x-ray fluorescence data are also added, the comparison is even more definitive. A systematic search, either manual or by computer, usually leads to an identification within an hour. Mixtures of up to nine compounds can often be completely identified. The minimum limit of detection is about 1% to 2% of a single phase.

In addition to identifying the compounds in a powder, the diffraction pattern can also be used to determine the degree of crystalline disorder, crystalline size, texture, and other parameters associated with the state of the crystalline materials. Differentiation among various oxides such as MnO, Mn_2O_3, MnO_2, and Mn_3O_4, or between materials present in such mixtures as NaCl + KBr or KCl + NaBr, is easily accomplished by x-ray diffraction. Identification of various hydrates, such as $Na_2CO_3 \cdot H_2O$ and $Na_2CO_3 \cdot 10H_2O$, is another application.

10.11.3 Polymer Characterization

The following information can be obtained from wide-angle and small-angle x-ray studies of polymers:

1. Degree of crystallinity
2. Crystallite size
3. Degree and type of preferred orientation
4. Polymorphism
5. Microdiffraction patterns
6. Information concerning the macrolattice of the crystallites

Fibers and partially oriented samples show spotty diffraction patterns rather than uniform cones; the more oriented the specimen, the spottier the pattern. The degree of crystallinity and crystallite size can be measured in powders, films, and fibers. This determination usually takes a few hours. The degree of orientation in uniaxially oriented materials, such as fibers, can also be determined in a few hours. If the orientation is other than uniaxial, the type of orientation and an approximate determination of the degree of orientation require similar times.

Polymorphism, the phenomenon in which a chemical compound can exist in more than one crystalline form, is often exhibited by polymers. From a study of the diffraction pattern, the presence of polymorphism can be ascertained and the approximate percentages of the polymorphs present determined. Such a study usually requires 1 to 2 days.

Micro x-ray diffraction can be used to identify inclusions in polymers and other materials. It can also be used to study the relationship of the skin of fibers to their interiors in regard to crystallinity, crystallite size, and orientation. Areas as small as 25 μm^2 can be studied. One limitation is that the specimen must be transparent to the x-ray beam. For most materials, a thickness up to 1 mm can be tolerated. Studies require 1 to 2 days.

Small-angle x-ray scattering is used to obtain information about the macrolattice, which can be defined as a periodic array of matter in space that is greater than 5.0 nm in size. In many polymers the chains fold back on themselves, forming crystallites. This leads to crystalline and amorphous domains ranging in size from less than 10 nm to almost 100 nm. Small-angle scattering studies are used to determine the size, distribution, and orientation of these domains.

UM00016575
NOVARTIS EXHIBIT 1517
Novartis v. Regents, IPR2023-01347
Page 3557 of 4460

1,531,591,467 visitors served.

TEXT

New: Language forums

TheFreeDictionary Google Bing

solvate Search ?

Word / Article Starts with Ends with Text

Dictionary/ thesaurus | Medical dictionary | Legal dictionary | Financial dictionary | Acronyms | Idioms | Encyclopedia | Wikipedia encyclopedia ?

solvate

Also found in: Wikipedia

0.06 sec.

Polymorph Screening
Knowledge & Solutions not just data Extensive Pharmaceutical Experience
www.pharmorphix.com
ADME Studies
Microsome and S9 stability. Permeability using PAMPA.
www.wolfelabs.com
Sterility Testing Paper
White Paper: Critical concepts in medical device sterilization
www.microtestlabs.com

Ads by Google

Thesaurus Legend: Synonyms Related Words Antonyms

Noun 1. solvate - a compound formed by solvation (the combination of solvent molecules with molecules or ions of the solute)

- chemical compound, compound - (chemistry) a substance formed by chemical union of two or more elements or ingredients in definite proportion by weight

Verb 1. solvate - cause a solvation in (a substance)

- chemical science, chemistry - the science of matter; the branch of the natural sciences dealing with the composition of substances and their properties and reactions
- alter, change, modify - cause to change; make different; cause a transformation; "The advent of the automobile may have altered the growth pattern of the city"; "The discussion has changed my thinking about the issue"

Page tools ?
Printer friendly | Feedback
Cite / link | Add definition
Email

Advertisement (Bad banner? Please let us know)

Related Ads
- Crystallization
- Formulation
- Pharmaceutical
- Amorphous Solid
- Polymorphism
- Enzyme Crystals
- Stability Testing
- Protein Crystals
- V1300X PKA
- DSC Analysis

My Word List ?
Add current page to the list

Advertisement (Bad banner? Please let us know)

Charity ?
Feed a hungry child - donate to school feeding program

UM00016576
NOVARTIS EXHIBIT 1517
Novartis v. Regents, IPR2023-01347
Page 3558 of 4460

2. solvate - undergo solvation or convert into a solvate

> chemical science, chemistry - the science of matter; the branch of the natural sciences dealing with the composition of substances and their properties and reactions

> change state, turn - undergo a transformation or a change of position or action; "We turned from Socialism to Capitalism"; "The people turned against the President when he stole the election"

Based on WordNet 3.0, Farlex clipart collection. © 2003-2008 Princeton University, Farlex Inc.

How to thank TFD for its existence? Tell a friend about us, add a link to this page, add the site to iGoogle, or visit webmaster's page for free fun content.

Link to this page: solvate

Please bookmark with social media, your votes are noticed and appreciated:

Solubility Screening
Solubilise "brick dust" API's Significant track record of success
www.agenda1.co.uk

Chemical Analysis Lab
Analysis of organic impurities in products or raw materials
www.m-scan.com

GEA Crystallization
All your crystallization solutions in one group
www.gea-crystallization.com

Ads by Google

Mentioned in ?

agent lipophobic solvating agent

Dictionary/thesaurus browser ?

Full browser ?

UM00016577
NOVARTIS EXHIBIT 1517
Novartis v. Regents, IPR2023-01347
Page 3559 of 4460

solution
Solution of continuity
Solutive
Solutrean
Solvability
solvable
Solvableness
solvate
solvating agent
solvation
Solvay
Solvay process
solve
solved
solvency

solvable
solvable
solvable
Solvable game
Solvable group
Solvable Lie algebra
Solvable Lie group
Solvable subgroup
solvableness
Solvalla
Solvalou
Solvang
Solvang
Solvang ASA
Solvang, CA
Solvang, California

Solvang, Vestfold
Solvant
Solvant
Solvant
Solvant
Solvant
Solvant
Solvatation
solvate
solvated
Solvated electron
solvates
solvating
solvating agent
solvation
solvation
Solvation shell

solvation structures
solvations
Solvatochromic
Solvatochromism
Solvay
Solvay
Solvay (company)
Solvay Business School
Solvay Business School's partners in America
Solvay Conference
Solvay Congress
Solvay Pharmaceutical
Solvay process
Solvay process
Solvay process
Solvay process

TheFreeDictionary Google

Search

Word / Article Starts with Ends with Text

Free Tools: For surfers: Browser extension | Word of the Day | Bookmark | Help
For webmasters: Free content | Linking | Lookup box | Double-click lookup | Partner with us

Disclaimer | Privacy policy | Feedback | Copyright © 2009 Farlex, Inc.

All content on this website, including dictionary, thesaurus, literature, geography, and other reference data is for informational purposes only. This information should not be considered complete, up to date, and is not intended to be used in place of a visit, consultation, or advice of a legal, medical, or any other professional. Terms of Use.

UM00016578
NOVARTIS EXHIBIT 1517
Novartis v. Regents, IPR2023-01347
Page 3560 of 4460

AN 2002:446673 CAPLUS
DN 138:209993
TI Crystalline modifications and polymorphism changes during drug manufacturing
AU Doelker, E.
CS Laboratoire de Pharmacie Galenique, Section de Pharmacie, Universite de Geneve, Geneva, CH-1211, Switz.
SO Annales Pharmaceutiques Francaises (2002), 60(3), 161-176
CODEN: APFRAD; ISSN: 0003-4509
PB Masson Editeur
DT Journal; General Review
LA French
AB A review. More than half of the pharmaceutical compds. exhibit polymorphism or pseudopolymorphism, e.g., they exist as more than one cryst. structure (true polymorphs, hydrates, solvates) or as more or less amorphous products. As such, they show at the solid state different physicochem. properties (m.p., transition point, plasticity, soly., hygroscopicity, chem. reactivity), which in turn may affect the technol. and biopharmaceutical properties of active ingredients or excipients (compactibility, dissoln. rate, bioavailability, pharmacol. activity, stability). When considering a chem. well-defined compd., one may find one or another cryst. state or polymorphic form according to the source or batch considered. One may also observe changes in technol. or biopharmaceutical properties that are due to polymorphic transformations arising from the mech. or heat treatment or from the environmental conditions (solvent-mediated reactions, desolvation) undergone by the product or the dosage form. The present article presents the fundamental aspects related to the above-mentioned phenomena and reviews both classical and recent examples from the literature reporting transformations during milling or grinding, tabletting, prepn. of drug suspensions, granulation, dissoln. or release tests, stability trials, spray drying, freeze-drying or prepn. of adsorbates or complexes.
RE.CNT 96 THERE ARE 96 CITED REFERENCES AVAILABLE FOR THIS RECORD
ALL CITATIONS AVAILABLE IN THE RE FORMAT

UM00016579
NOVARTIS EXHIBIT 1517
Novartis v. Regents, IPR2023-01347
Page 3561 of 4460

© Masson, Paris, 2002
Ann Pharm Fr 2002, 60 : 161-176

Séance thématique
Modifications cristallines et transformations polymorphes au cours des opérations galéniques

E. Doelker (1)

Résumé. Plus de la moitié des composés pharmaceutiques sont sujets au phénomène de polymorphisme ou de pseudo-polymorphisme, c'est-à-dire qu'ils existent sous plus d'une structure cristalline (polymorphes vrais, hydrates, solvates) ou comme produit plus ou moins amorphe. À ce titre, il présentent, à l'état solide, des caractéristiques physico-chimiques (point de fusion, point de transition, plasticité, solubilité, hygroscopicité, réactivité chimique) différentes, qui à leur tour peuvent avoir des incidences sur les propriétés pharmacotechniques et biopharmaceutiques des principes actifs ou des excipients (comprimabilité, vitesse de dissolution, biodisponibilité, activité pharmacologique, stabilité).

Considérant une substance chimiquement bien définie, on peut se trouver en présence de tel ou tel état cristallin ou forme polymorphe en fonction de la source d'approvisionnement ou simplement du lot en question. Mais il se peut aussi que l'on observe des changements de propriétés pharmacotechniques ou biopharmaceutiques dus à des phénomènes de transformations polymorphes, selon le traitement mécanique, thermique ou les conditions environnementales (intervention d'un solvant, désolvatation) qu'a subi le produit ou la forme médicamenteuse.

Le présent article passe en revue les aspects fondamentaux liés à ces phénomènes et présente des exemples de la littérature, classiques ou récents, de transformations observées lors d'un broyage ou d'une trituration, d'une compression, de la mise en suspension d'un principe actif, d'une granulation, de tests de dissolution ou de libération, d'essais de stabilité, d'une nébulisation, d'une lyophilisation ou encore de la préparation d'adsorbats ou de complexes.

Mots-clés : Transformations polymorphes, Amorphisation, Broyage, Trituration, Compression, Granulation, Stabilité, Nébulisation, Lyophilisation, Adsorbats, Complexes.

(1) Laboratoire de pharmacie galénique, Section de pharmacie, Université de Genève, Quai Ernest-Ansermet 30, CH-1211 Genève 4
Tirés à part : E. Doelker, à l'adresse ci-dessus.

Summary. More than half of the pharmaceutical compounds exhibit polymorphism or pseudopolymorphism, e.g., they exist as more than one crystalline structure (true polymorphs, hydrates, solvates) or as more or less amorphous products. As such, they show at the solid state different physicochemical properties (melting point, transition point, plasticity, solubility, hygroscopicity, chemical reactivity), which in turn may affect the technological and biopharmaceutical properties of active ingredients or excipients (compactibility, dissolution rate, bioavailability, pharmacological activity, stability).

When considering a chemically well-defined compound, one may find one or another crystalline state or polymorphic form according to the source or batch considered. One may also observe changes in technological or biopharmaceutical properties that are due to polymorphic transformations arising from the mechanical or heat treatment or from the environmental conditions (solvent-mediated reactions, desolvation) undergone by the product or the dosage form.

The present article presents the fundamental aspects related to the above-mentioned phenomena and reviews both classical and recent examples from the literature reporting transformations during milling or grinding, tabletting, preparation of drug suspensions, granulation, dissolution or release tests, stability trials, spray drying, freeze-drying or preparation of adsorbates or complexes.

***Key-words:** Polymorphic transformations, Amorphisation, Milling, Grinding, Tabletting, Granulation, Dissolution, Stability, Spray drying, Freeze-drying, Adsorbates, Complexes.*

Crystalline modifications and polymorphism changes during drug manufacture. E. Doelker. *Ann Pharm Fr* 2002, *60* : 161-176.

Material may be protected by copyright law (Title 17, U.S. Code)

UM00016580
NOVARTIS EXHIBIT 1517
Novartis v. Regents, IPR2023-01347
Page 3562 of 4460

Introduction

Depuis plus d'une quarantaine d'années, les milieux pharmaceutiques ont pris progressivement conscience du rôle joué par le polymorphisme et le pseudopolymorphisme dans les propriétés des médicaments. Le nombre d'articles, de revues et d'ouvrages sur le sujet en témoigne, qu'ils traitent des aspects généraux ou des méthodes d'analyse [1-32]. Cet intérêt se justifie également si l'on considère que plus de la moitié des substances organiques de la Pharmacopée Européenne (Ph. Eur.) existent sous plusieurs formes cristallines, selon la répartition suivante [33] :

— substances uniquement monomorphes (42 %) ;
— substances uniquement amorphes (2 %) ;
— polymorphes, hydrates et/ou solvates (56 %) dont :
- polymorphes (58 %) ;
- hydrates (57 %) ;
- solvates (20 %).

Ces chiffres rejoignent de précédentes analyses [34] et surtout corroborent la constatation classique que le polymorphisme vrai est un phénomène qui touche environ un tiers des substances organiques, un autre tiers existant sous forme d'hydrates et de solvates [26]. Il est cependant curieux de constater que ce n'est que dans la quatrième édition de la Ph. Eur., en 2002, qu'apparaît vraiment la notion de polymorphisme (monographie « Substances pour usage pharmaceutique »).

En raison de leur structure cristalline différente, les polymorphes et pseudopolymorphes présentent des caractéristiques physico-chimiques qui varient d'une forme à l'autre, telles que point de fusion, point de transition, plasticité, solubilité, hygroscopicité, réactivité chimique, qui à leur tour peuvent avoir des incidences sur les propriétés pharmaceutiques des principe actifs ou des excipients. On pense en premier lieu à leur comprimabilité, leur mouillabilité, leur vitesse de dissolution, leur biodisponibilité, leur activité pharmacologique et leur stabilité.

Il est toutefois utile de relever que d'autres raisons que le polymorphisme peuvent être à la base des variations observées : forme des particules (habitus, faciès), taille, présence d'impuretés de synthèse ou de dégradation. Cet aspect ne sera pas abordé ici, mais le lecteur peut se référer à un article récent [32].

Considérant une substance chimiquement bien définie, on peut se trouver en présence de différents polymorphes ou pseudopolymorphes en fonction de la source d'approvisionnement ou simplement du lot en question. Mais il se peut aussi que l'on observe des changements de propriétés pharmacotechniques ou biopharmaceutiques dus à des phénomènes de transformations polymorphes, selon le traitement mécanique (broyage, compression) ou les conditions environnementales (intervention d'un solvant, désolvatation) qu'a subi le produit. Byrn [15] parle d'interconversion de polymorphes par transformation de phase ou par un processus médié par un solvant.

Le présent article explique les mécanismes impliqués dans ces transitions et passe en revue les travaux de la littérature, classiques ou récents, relatant de tels phénomènes observés au cours d'opérations galéniques *(tableau I)*. L'impact de ces traitements sur la stabilité chimique proprement dite n'est pas traité ici.

Désordre moléculaire

Sauf exception, un cristal est très imparfait, en ce sens qu'il contient soit des défauts qui viennent interrompre l'alignement des molécules ou des atomes, soit carrément des régions de structure amorphe.

Tableau I. — Opérations galéniques concernées par les transformations polymorphes ou pseudopolymorphes
Pharmaceutical operations concerned with polymorphic or pseudo-polymorphic transformations

• Traitement mécanique
— broyage, trituration
— compression, compactage
• Intervention de l'eau ou d'un solvant
— formulation de suspensions
— étape de fabrication d'une forme sèche (granulation, enrobage)
— tests de dissolution ou de libération
— essais de stabilité en atmosphère contrôlée, stockage
• Déshydratation ou désolvatation
— nébulisation
— lyophilisation
— préparation d'adsorbats

Material may be protected by copyright law (Title 17, U.S. Code)

UM00016581
NOVARTIS EXHIBIT 1517
Novartis v. Regents, IPR2023-01347
Page 3563 of 4460

D'un point de vue morphologique, mais aussi énergétique, on distingue deux grandes catégories de défauts cristallins :

— les défauts ponctuels : lacunes, molécules étrangères ou non placées dans des interstices ou encore molécules étrangères de substitution ;

— les défauts de réseau : linéaires (dislocations) ou bidimensionnels (joints de grain).

Les phases cristallines se caractérisent par un ordre à longue distance, supérieure à 1 000 Å, et contiennent typiquement de 10^3 à 10^6 dislocations (les défauts les plus fréquents) par cm^3. Par comparaison, dans les zones amorphes, l'ordre est à courte distance, inférieure à 100 Å. Ajoutons encore que, la plupart du temps, les « cristaux » sont en fait de nature polycristalline c'est-à-dire que les particules sont en réalité formées de multiples cristaux.

Les défauts ponctuels sont thermodynamiquement stables. Au contraire, les défauts de réseau et les régions amorphes constituent des zones à potentiel chimique et à énergie interne élevés, caractérisées par une grande réactivité. Ces zones favorisent (et même rendent possible) la déformation plastique ou la fracture des cristaux, elles augmentent leur solubilité et donc leur vitesse de dissolution, mais aussi leur instabilité chimique et physique.

Désorganisation de la matière solide sous l'effet d'un stress

Lorsqu'un matériau est soumis à un traitement mécanique (broyage, compression) ou thermique (séchage, chauffage), on assiste généralement à une augmentation considérable du nombre de défauts cristallins (typiquement d'un facteur de 10^4 à 10^6), à leur migration et à un changement de leur nature. Des zones amorphes peuvent également apparaître, notamment à la surface des particules en raison de frictions. L'amorphisation complète du produit est même parfois observée. Il s'ensuit une mobilité moléculaire accrue, ainsi qu'une éventuelle exposition de groupements chimiques plus réactifs.

Si le traitement mécanique ou thermique se prolonge, ou tout simplement spontanément, le produit peut recouvrer un état énergétique plus stable, en recristallisant dans la forme d'origine ou dans une autre forme cristalline (transformation polymorphe). Si l'on assiste à la recristallisation d'une variété amorphe, on parle de dévitrification.

Sur des bases thermodynamiques, Hüttenrauch [35-37] a proposé la notion d'activation-désactivation, qui fait partie du concept plus général de pharmacie galénique moléculaire. L'augmentation de la densité de dislocations (ou l'apparition de zones amorphes) sous l'effet d'un stress s'accompagne d'un accroissement de l'énergie interne du solide, qui conduit à un stade activé.

Une partie plus ou moins importante de l'énergie délivrée au matériau est conservée de manière réversible sous forme de densité de défauts cristallins accrue (ou de zones amorphes). L'autre partie, de nature réversible, est restituée et utilisée sous différentes formes d'énergie pour aboutir à une réorganisation de la matière. C'est le processus de désactivation, appelé aussi passivation.

Point de transition vitreuse des substances amorphes

Comme on le verra plus loin, de nombreuses transitions de phase solide-solide passent par un état amorphe ou semi-cristallin. Or, les matériaux amorphes ou semi-cristallins, à l'instar des polymères, possèdent un point de transition vitreuse T_v (les produits semi-cristallins subissent en outre une fusion à température plus élevée). À titre d'exemple, citons quelques valeurs de T_v :

- Eau : – 134 °C [38] ;
- Aspirine : – 30°C [39] ;
- Phénylbutazone : 4 °C [39] ;
- Paracétamol : 22,6 °C [40] ;
- Cholécalciférol : 23 °C [39] ;
- Indométacine : 42 °C [41] ;
- Phenobarbital : 48 °C [39] ;
- Sulfathiazol : 61 °C [39] ;
- Estradiol : 73 °C [39] ;
- Mannitol : 10,7 °C [42] ;
- Saccharose : 54 °C [38], 74 °C [43] ;
- Lactose : 108 °C [43] ;
- Tréhalose : 115 °C [43] ;
- Povidone : 175 °C [44].

Material may be protected by copyright law (Title 17, U.S. Code)

UM00016582
NOVARTIS EXHIBIT 1517
Novartis v. Regents, IPR2023-01347
Page 3564 of 4460

Au-dessous de la température de transition interne, le matériau est à l'état vitreux ; au-dessous, il se trouve à l'état caoutchoutique.

La viscosité passe d'environ 10^{12} Pa. s au point de transition vitreuse à 10^{7} Pa. s à 20 °C au-dessus de T_v [38], avec un accroissement considérable de la mobilité moléculaire favorisant les cristallisations. À ce propos, il faut signaler que si les cristallisations ont lieu rapidement et le plus souvent à l'état caoutchoutique, elles peuvent parfois également survenir dans des temps mesurables à des températures inférieures à T_v [41].

Les corps amorphes ont par ailleurs la capacité d'absorber l'eau (les corps cristallins l'adsorbent) en quantité appréciable. Cette eau, par un effet plastifiant, abaisse le point de transition vitreuse du produit et permet ainsi une cristallisation à une température inférieure à celle du matériau anhydre. Considérant le cas d'un solide semi-cristallin, Ahlneck et Zografi [38] rapportent, pour les zones amorphes, les valeurs de T_v suivantes pour du saccharose qui contiendrait :

- 0,1 % d'humidité au total avec :
  - 0,5 % de matière amorphe : 9 °C ;
  - 5 % de matière amorphe : 49 °C.
- 0,5 % d'humidité au total avec :
  - 0,5 % de matière amorphe : – 73 °C ;
  - 5 % de matière amorphe : 27 °C.

Ainsi, du saccharose à 99,5 % cristallin et qui contiendrait 0,5 % d'humidité au total comporterait des zones amorphes qui seraient à l'état caoutchoutique à la température ambiante, caractérisées par une grande mobilité moléculaire et une réactivité très importante.

Par ailleurs, en raison justement de leur énergie interne élevée, les produits amorphes présentent des solubilités considérablement supérieures à celles de leurs homologues cristallins. Hancock et Parks [45] font mention, à partir de données expérimentales de la littérature, de rapports de solubilité de 1,1 à 24 (1,1 à 4,0 pour des formes cristallines). À noter que les valeurs prédites de rapports de solubilité seraient respectivement de 10 à 1 600 et de 1,1 à 3,6. La différence entre valeurs expérimentales et valeurs prédites s'explique par le fait qu'une certaine cristallisation de la forme amorphe a lieu au cours de l'essai pratique en milieu liquide. De façon intéressante, ces auteurs concluent également que de faibles fractions amorphes (< 10 %), telles que celles que peut engendrer un traitement mécanique, peuvent déjà aboutir à un doublement de la solubilité par rapport à un produit entièrement cristallin.

Traitement mécanique

Les cas de transformations observés après broyage (trituration) et compression sont traités séparément, mais il va sans dire que très souvent les effets des deux opérations ont été décrits dans les mêmes travaux ou, tout au moins, étudiés par les mêmes équipes.

Broyage, trituration

Le *tableau II* répertorie des exemples récents et significatifs de transformations observées à la suite d'un broyage ou d'une trituration. On constate une variété de processus : formation de défauts à la surface de cristaux, amorphisation directe, amorphisation après transition polymorphe, transition polymorphe, y compris à partir de la forme stable.

Examinons les incidences, constatées ou attendues, de telles transformations. Le cas du palmitate de chloramphénicol est intéressant et complexe. Soumises à un broyage, aussi bien la forme A que la forme B (la forme active) se transforment partiellement ou majoritairement en l'autre forme jusqu'à une valeur d'équilibre, atteinte toutefois après des temps différents [46, 47]. Les auteurs observent également que la présence de seulement 1 % de forme A dans la forme B accélère considérablement la conversion. Sachant que la valeur d'équilibre après broyage est d'environ 80 % de forme A, inactive, il y a tout lieu de penser qu'une réduction particulaire d'un échantillon de palmitate de chloramphénicol conforme à la Pharmacopée (qui prévoit l'identification de la forme B par IR) aboutirait à une mauvaise biodisponibilité. Il est à noter que dans le cas de cet ester, qui est en fait un précurseur du chloramphénicol, la différence d'activité des deux formes n'est pas due à une différence

Material may be protected by copyright law (Title 17, U.S. Code)

UM00016583
NOVARTIS EXHIBIT 1517
Novartis v. Regents, IPR2023-01347
Page 3565 of 4460

Tableau II. — Exemples de transformations observées sous l'effet d'un broyage ou d'une trituration (adapté de [32])
Examples of transformations obtained by milling or grinding (adapted from [32])

Substance	Type de transformation	Auteur	(Année)
Albutérol, sulfate	Formation de défauts à la surface des cristaux	Ward	(1995)
Aspartame hémihydrate	Transition polymorphe forme I → II	Leung	(1998)
Caféine	Transition polymorphe forme II → I	Pirttimäki	(1993)
Carbamazépine	Transition polymorphe formes I et II → III	Kala	(1986)
Céfalexine	Forme IV : amorphisation	Otsuka	(1982, 1983)
Céfalotine sodique	Formation de défauts à la surface des cristaux	Otsuka	(1990)
Céfixime trihydrate	Amorphisation	Kitamura	(1989)
Cimétidine	Transition polymorphe formes B → A et C → B	Bauer-Brandle	(1996)
Chloramphénicol, palmitate	Forme A : amorphisation	Kaneniwa	(1985)
	Transitions polymorphes A → B et B → A	Otsuka	(1986)
Chloramphénicol, stéarate	Transition polymorphe forme A → B → amorphe	Forni	(1988)
Cyclophosphonamide monohydrate	Amorphisation	Ketolainen	(1995)
Griséofulvine	Amorphisation	Elamin	(1985)
Indométacine	Formes α et γ : amorphisation	Otsuka	(1986)
Lactoses	Amorphisation et isomérisation	Otsuka	(1993)
Phénylbutazone	Transition polymorphe formes α, β et δ → ξ	Matsumoto	(1988)
Probucol	Transition polymorphe forme III → I	Gerber	(1992)
Sulfathiazol	Transition polymorphe formes I → III et III → I	Shakhtshneider	(1993)

de solubilité, mais à une différence de sensibilité aux estérases.

Dans le cas de la cimétidine, une transition de la forme B en la forme A est observée [48]. Or, c'est justement la forme commerciale A qui est la plus efficace contre les ulcères d'estomac.

Il est courant, lors de la préparation de comprimés, de gélules ou de suppositoires, de broyer ou de triturer le principe actif en vue d'assurer sa bonne dispersion dans la masse. Dans le cas de l'indométacine, on aboutit à un produit amorphe, dont il a été démontré qu'il était mieux résorbé qu'une forme cristalline, aussi bien par voie orale que rectale [49]. On peut relever avec intérêt que le produit amorphe est stable au moins deux ans à la température ordinaire. Le broyage de la griséofulvine conduit aussi à son amorphisation, avec une augmentation de solubilité d'un facteur 2 [50]. Un effet bénéfique sur la biodisponibilité pourrait être attendu.

Terminons avec deux remarques. Lorsqu'un broyage est nécessaire, il convient de se souvenir que le processus d'amorphisation est de nature logarithmique et que la teneur en produit amorphe atteint généralement un plateau [51].

Par ailleurs, on constate parfois une agglomération des produits après broyage. Ward et Schultz [52] proposent le mécanisme schématisé dans la *figure 1* aboutissant à des soudures (frittage) entre particules.

Material may be protected by copyright law (Title 17, U.S. Code)

UM00016584
NOVARTIS EXHIBIT 1517
Novartis v. Regents, IPR2023-01347
Page 3566 of 4460

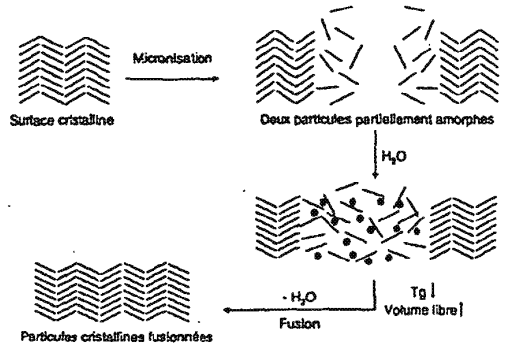

Figure 1. Représentation schématique des surfaces de particules avant et après broyage.
Schematic representation of particle surface before and after milling.

Le broyage entraîne une amorphisation de la surface des particules. Les régions amorphes absorbent suffisamment d'eau (cercles) pour augmenter le volume libre et abaisser le point de transition vitreuse. Les molécules, à mobilité accrue, se réarrangent en une structure cristalline stable (en expulsant l'eau) avec formation d'un pont entre deux particules (adapté de [52]).
Milling leads to amorphous regions at the surface of the particles. Amorphous regions absorb a sufficient quantity of water (circles) to increase the free volume and lower the glass transition temperature. The molecules, now having increased mobility, rearrange into a stable structure (expelling the water) forming a bridge between two particles (adapted from [52]).

Compression, compactage

La compression conduit généralement aux mêmes observations qu'avec un broyage *(tableau III)*.

Ainsi, le cas du chlorpropamide confirme que même une forme stable peut se convertir en forme métastable par un processus d'activation [53]. On observe à la fois une conversion dans l'autre forme et une certaine amorphisation qui dépend de la pression appliquée, donc de l'énergie mécanique fournie.

Nos propres études ont porté notamment sur la caféine [34] et sur le sulfabenzamide [54]. Concernant la caféine, nous avons montré que seule la forme A se transforme en forme B lors d'une compression et que le taux de conversion variait selon la zone du comprimé *(fig. 2)*.

La forme II du sulfabenzamide se transforme en forme I également lors d'une compression. Dans ce cas, nous avons pu mettre en évidence le rôle protecteur de certains excipients vis-à-vis de cette conversion, qui atteint 80 à 90 % même à faible pression. Le stéarate de magnésium s'est révélé plus efficace que l'acide stéarique, la silice colloïdale et la cellulose microcristalline.

Tableau III. — Exemples de transformations observées sous l'effet d'une compression (adapté de [32])
Examples of transformations obtained by tabletting (adapted from [32])

Substance	Type de transformation	Auteurs	(année)
Caféine	Transition polymorphe forme I → II forme A → B	 Chan Pirttimäki	 (1985) (1993)
Carbamazépine	Transition polymorphe forme II → III	Kala	(1986)
Céfaléxine	Forme IV : amorphisation	Kaneniwa	(1985)
Chlorpropamide	Transition polymorphe formes A ⇒ C et C ⇒ A et amorphisation	Otsuka	(1989, 1993)
Cyclophosphonamide monohydrate	Déshydratation via forme métastable	Ketolainen	(1995)
Piroxicam	Transition polymorphe forme α ⇒ β	Ghan	(1992)

Material may be protected by copyright law (Title 17 U.S. Code)

UM00016585
NOVARTIS EXHIBIT 1517
Novartis v. Regents, IPR2023-01347
Page 3567 of 4460

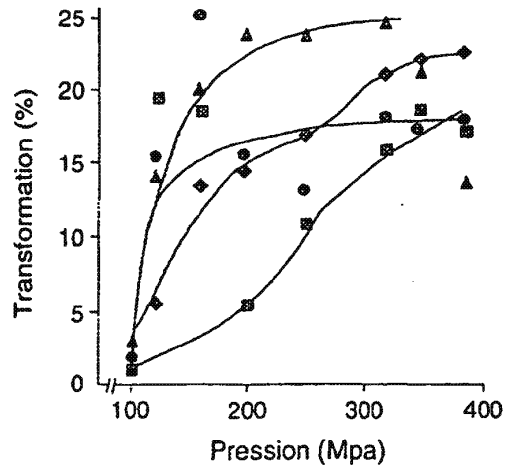

Figure 2. Pourcentage de caféine forme A transformée en forme B en fonction de la pression appliquée et de différentes zones du comprimé [33]. Face supérieure (▲), Face inférieure (■), région centrale (●), et tranche (◆).

Percentage of caffeine form A transformed into form B as a function of applied pressure and zone of the tablet. Upper surface (▲), lower surface (■), middle region (●),and side (◆).[33]

Un changement de structure peut avoir également une incidence pratique sur la fabrication de comprimés. Ainsi, si le cyclophosphonamide monohydraté est comprimé dans des conditions normales, on observe un collage et une certaine gélification du comprimé, en raison de la formation d'un état métastable partiellement déshydraté [55]. La fabrication doit donc se dérouler à basse température (8 à 12 °C) pour prévenir ces aléas.

Il demeure que si divers types de transformations de la matière peuvent survenir, c'est le plus souvent une amorphisation qui intervient, suivie à plus ou moins long terme d'une éventuelle désactivation par recristallisation, avec pour effet de modifier les propriétés des comprimés (ralentissement de la désagrégation et de la dissolution).

Intervention de l'eau ou d'un solvant

L'eau et les solvants organiques interviennent à de multiples stades de la préparation des médicaments. L'humidité est également présente lors d'essais de stabilité des produits finis en atmosphère contrôlée, ainsi que lors du stockage des préparations. Les occasions sont donc nombreuses de rencontrer des transitions de phase médiées par un liquide.

Mise en suspension

Un premier effet que l'on peut observer lorsque l'on dissout en quantité appréciable un composé anhydre est la précipitation d'un hydrate. De même si un produit anhydre est mis en suspension, on assiste souvent à une croissance des particules, par transformation en hydrate. Rappelons en effet qu'une forme anhydre est quasiment toujours plus soluble que l'hydrate correspondant. Ceci résulte du fait que l'hydrate a déjà interagi avec l'eau, et donc l'énergie libre libérée en présence d'eau est moindre pour l'hydrate que pour la forme anhydre [56]. Un exemple de transformation est celui de la conversion complète en une heure de la carbamazépine anhydre en forme dihydratée lorsqu'elle est en suspension dans de l'eau à 25 °C [57]. Quant à une poudre de théophylline anhydre est mise en suspension dans l'eau, elle forme de grandes aiguilles par apparition d'un monohydrate [58]. Un autre cas est la transformation du benzoate de métronidazole anhydre en monohydrate, suivie d'une croissance particulaire importante aboutissant à une instabilité de la suspension [59], mais cette transition de phase et cette croissance cristalline sont inhibées si un complexe d'inclusion est formé entre le principe actif et la β-cyclodextrine [60].

La transition ne correspond pas toujours à une hydratation. Ainsi, la forme A (commerciale) de la cimétidine se transforme en trois mois en forme B, lorsque mise en suspension [48]. Certains lots de suspensions de forme A d'oxyclonazide, passées au broyeur à billes, se transforment en forme B en quelques jours, avec apparition de longues aiguilles. D'autres lots ne subissent aucun changement [58].

La novobiocine acide constitue l'exemple type de l'impact d'une dévitrification. La forme amorphe, très bien résorbée, se transforme en 22 jours à 37°C (en trois mois à 25 °C) en novobiocine acide cristalline, non biodisponible. L'ajout de 1 % de méthylcellulose maintient la novobiocine à l'état amorphe pendant plus d'un an [61].

Material may be protected by copyright law (Title 17, U.S. Code)

UM00016586
NOVARTIS EXHIBIT 1517
Novartis v. Regents, IPR2023-01347
Page 3568 of 4460

Le choix de la forme cristalline est donc à étudier précautionneusement dans le cas de la conception d'une suspension. Cependant, la mise en suspension d'un principe actif dans de l'eau constitue également, au stade de la préformation, un excellent test de mise en évidence du phénomène de polymorphisme.

Étape de fabrication d'une forme sèche

Le recours à de l'eau ou à un solvant intervient la plupart du temps à une étape ou à une autre de la préparation des médicaments : solubilisation du principe actif, granulation, enrobage par exemple. Les occasions d'engendrer des transformations sont nombreuses.

Ainsi, traitée avec de l'isopropanol, la forme B de maléate de flupirtine se transforme rapidement en forme A [62]. Pour leur part, dans le cadre de la conception d'une préparation semi-solide topique Csòka et coll. [63], notent l'apparition de deux formes différentes de piroxicam en fonction du solvant utilisé et du procédé de fabrication.

La granulation à l'aide d'un solvant organique ou d'eau est également en cause. Abordons tout d'abord le procédé de granulation consistant à traiter une substance médicamenteuse avec simplement un solvant (sans agent liant) dans le but d'améliorer sa comprimabilité.

Plusieurs auteurs ont montré qu'un tel traitement peut engendrer une transition de phase ([30], pages 339-341). C'est le cas de la granulation du chlorhydrate de chlorpromazine à l'aide d'un mélange éthanol-eau qui entraîne la formation d'un hémihydrate [64]. Ce dernier est ensuite partiellement déshydraté lors du séchage habituel, ce qui conduit à un produit comprimable, contrairement au produit d'origine (forme II, métastable à la température ordinaire). À noter que l'hémihydrate et le produit partiellement déshydraté peuvent être convertis en chlorhydrate de chlorpromazine anhydre (forme I), qui à son tour peut être réhydraté sans changement de structure cristalline. Il s'agit d'un bon exemple de pseudopolymorphisme au sens de Byrn [15]. Les exemples de granulation humide classique sont nombreux. Cruaud et coll. [65] mettent en évidence une transformation du sulfanilamide (forme II) lors d'une telle opération, ainsi qu'un certain effet de protection d'un excipient comme le phosphate dicalcique vis-à-vis de cette transformation (à noter que ce sulfamidé se modifie aussi sous l'effet d'un traitement mécanique). Morris ([30], pages 125-181) rapporte la conversion de la forme stable A de fosinopril sodique en forme B. Joachim et coll. [66] notent un ralentissement de la dissolution de comprimés de lorazépam, en raison de la formation d'un solvate lors de la granulation avec de l'isopropanol. Herman et coll. [67] mettent en évidence la formation de théophylline monohydratée lors de la granulation d'un mélange de théophyline anhydre et de cellulose microcristalline. La dissolution des grains séchés se prolonge d'autant plus que la quantité d'eau ajoutée et la fraction de cellulose microcristalline ajoutée sont importantes. À noter qu'en l'absence d'excipient la conversion n'a pas lieu.

Une intéressante étude sur les conditions de granulation de la carbamazépine a récemment été publiée [68, 69]. Un mélange composé de carbamazépine (forme I), de lactose monohydraté et d'amidon de blé a été humecté avec trois liquides différents contenant 5 % d'hydroxypropylcellulose comme liant. Après malaxage, granulation à travers un extrudeur, il s'avère que le mélange traité avec une solution de liant dans l'éthanol 50 % entraîne la formation de la forme IV de carbamazépine (dihydrate). Cette transformation ne se produit pas avec l'eau ou l'éthanol pur. Les granulés obtenus avec l'éthanol 50 %, plus tendres et offrant une surface spécifique supérieure, aboutissent aux comprimés les plus résistants [68].

Dans un second article [69], les auteurs examinent le comportement de quatre formes de carbamazépine soumises à une granulation à l'eau. Après malaxage et séchage, les formes I, II et III se transforment en dihydrate (forme IV), respectivement à raison de 2,5, 80, 3 et 35,2 %. Le séchage des grains entraîne la conversion du dihydrate en forme III. Les auteurs observent également que les formes II et III nécessitent l'ajout supplémentaire d'eau pour obtenir un rendement satisfaisant de granulé. Ils notent enfin de grandes différences de résistance mécanique des comprimés, de temps de désagrégation et de dissolution.

Material may be protected by copyright law (Title 17, U.S. Code)

UM00016587
NOVARTIS EXHIBIT 1517
Novartis v. Regents, IPR2023-01347
Page 3569 of 4460

Tests de dissolution ou de libération

Les exemples foisonnent montrant une transition de phase lors d'un essai de solubilité, de dissolution de poudre, ou encore de dissolution intrinsèque. Par contre, peu nombreux sont les cas relatant de telles transformations lors d'essais de dissolution ou de libération de formes galéniques.

La comparaison du comportement à la conservation et à la dissolution de comprimés contenant la forme anhydre I (celle de l'USP) de théophylline ou une forme métastable I' (obtenue par déshydratation de la théophylline monohydratée II) est intéressante [70]. La forme I ne subit pas de transformation au cours de la conservation des comprimés, dont les profils de dissolution ne changent pas quelles que soient les conditions ambiantes. Il est à rappeler qu'au contact de l'eau, la forme I ne se transforme que très lentement en forme monohydratée II. Les profils de dissolution reflètent donc la mise en solution de la forme originale I. En revanche, la forme métastable I' se transforme en quelques jours dans le comprimé en forme anhydre I. Par ailleurs, la forme I' se convertit quasi instantanément en forme monohydratée II en présence du milieu de dissolution, avec des profils ralentis qui reflètent donc en grande partie la mise en solution de la forme hydratée, formée *in situ*.

Une autre étude récente relate la vitesse de dissolution et l'absorption chez le chien des formes I, II, III et IV du tolbutamide [71] *(fig. 3)*.

Les profils de dissolution *(fig. 3)* à gauche) montrent que les formes II et IV se dissolvent le plus rapidement, quasiment à la même vitesse, malgré des solubilités différentes [72]. Ceci est dû à la transformation de la forme VI en forme II observée en deux heures.

Cependant les profils de dissolution ne reflètent pas la mise en solution de la forme I, bien que les auteurs aient mis en évidence une transformation supplémentaire de la forme II en forme I. Cette étape est donc trop lente pour intervenir et explique de surcroît les profils différents des formes II et I. Les cinétiques de dissolution des formes sont en bonne corrélation avec les données de biodisponibilité (à droite), en particulier si l'on considère la partie initiale des profils de dissolution.

Essais de stabilité en atmosphère controlée, stockage

Conservées dans certaines conditions d'humidité relative (HR), les substances organiques subissent souvent des changements de phase. On pense bien entendu à la formation d'hydrates avec une élévation du taux d'humidité. Mais les cas d'amorphisation ou de transition polymorphe pur existent aussi.

Quatre exemples illustrent ces différents types de modifications à la température ambiante.

La forme A du chlorhydrate d'oxytétracycline est stable jusqu'à une humidité relative pratiquement de 100 % [73]. La forme B se transforme progressivement en forme A au-dessus de 51 % HR, pour aboutir à la forme A pure à HR élevée. Quant à la forme C, elle devient partiellement amorphe à 75 % HR, totalement amorphe à 84 % HR, puis cristallise en forme A à 92 % HR.

La prémafloxacine illustre le cas le plus courant [74]. La forme III est stable tout au long de l'isotherme de sorption. La forme I est également stable jusqu'à 70 % HR, mais forme un monohydrate au-dessus de 80 % HR. À noter également que la forme I, dès une température de 40°C, se transforme en forme III à 51 % HR.

L'aspartame existe sous deux formes hémihydratées (dont une commerciale), qui sont stables jusqu'à 42 % HR [75]. Au-dessus, elles se transforment toutes les deux en un hydrate avec 2,5 molécules d'eau. Enfin, la dévitrification de l'indométacine illustre bien aussi la complexité des phénomènes pouvant survenir [41]. En-dessous de 43 % HR, seule la forme γ stable apparaît. Le composé se trouve à l'état vitreux car la teneur en humidité (au maximum environ 1 %) n'est pas suffisante pour abaisser le T_v (42 °C) en dessous de température ambiante. A une HR supérieure, c'est la forme β qui cristallise, car cette fois-ci l'indométacine est à l'état caoutchoutique. L'eau présente a permis d'abaisser le point de transition vitreuse en-dessous de la température ambiante. Il convient également de relever que très souvent la règle des phases, qui voudrait qu'une seule espèce chimique existe à une humidité relative donnée, n'est pas suivie. Certains des exemples précédents le montrent. Ceci est particulièrement fréquent lorsqu'une forme est obtenue par la déshydrata-

Material may be protected by copyright law (Title 17, U.S. Code)

UM00016588
NOVARTIS EXHIBIT 1517
Novartis v. Regents, IPR2023-01347
Page 3570 of 4460

AN 2000:10870 CAPLUS
DN 132:325872
TI Physicochemical behavior of active substances. Consequences for the feasibility and stability of pharmaceutical forms
AU Doelker, E.
CS Section de pharmacie, Universite dc Geneve, Geneva, 1211/4, Switz.
SO S.T.P. Pharma Pratiques (1999), 9(5), 399-409
CODEN: SPPRER; ISSN: 1157-1497
PB Editions de Sante
DT Journal; General Review
LA French
AB A review with 72 refs. Depending on its origin or the particular batch, a given drug, although chem. well defined, may exhibit quite different behavior. Process conditions (grinding, tableting, granulation, drying) may also affect secondary (derived) properties of the drug, such as compactibility, wettability, soly., dissoln. rate, bioavailability and even pharmacol. activity. Property changes may also be due to the storage conditions of the dosage form. In solids, these differences, which may exist initially or be generated by some treatment, arise directly from the primary characteristics of the crystals, i.e. the cryst. structure, both internal (polymorphism , pseudopolymorphism, amorphous state) and external (habitus, facies), crystal defects (dislocations) or the presence of impurities. In this respect, crystal doping by foreign substances may be envisaged as a means to improve drug properties of technol. or biopharmaceutical interest. This review article explains these concepts using classical or more recently published examples from the literature.
RE.CNT 72 THERE ARE 72 CITED REFERENCES AVAILABLE FOR THIS RECORD
ALL CITATIONS AVAILABLE IN THE RE FORMAT

BEST AVAILABLE COPY

UM00016589
NOVARTIS EXHIBIT 1517
Novartis v. Regents, IPR2023-01347
Page 3571 of 4460

CARACTÈRES PHYSICOCHIMIQUES DES PRINCIPES ACTIFS LEURS CONSÉQUENCES SUR LA FAISABILITÉ ET LA STABILITÉ DES FORMES GALÉNIQUES

E. DOELKER

Selon son origine ou le lot considéré, un principe actif, pourtant bien défini chimiquement, peut se comporter de façon très différente. Les opérations galéniques qu'il subit (broyage, compression, granulation, séchage) peuvent également entraîner des modifications des propriétés secondaires (dérivées) du principe actif que sont la comprimabilité, la mouillabilité, la solubilité, la vitesse de dissolution, la biodisponibilité et même l'activité pharmacologique. Des changements de propriétés peuvent aussi survenir en fonction des conditions de conservation des formes pharmaceutiques (humidité relative, température). Dans les corps solides, ces différences de propriétés, qu'elles existent initialement ou soient engendrées par un quelconque traitement, sont directement liées aux caractéristiques primaires des cristaux, c'est-à-dire à leur structure cristalline, à la fois interne (polymorphisme, pseudopolymorphisme, état amorphe) et externe (habitus, faciès cristallin), à la densité des défauts cristallins (dislocations) ainsi qu'à la présence d'impuretés. Le « dopage » de cristaux à l'aide de substances étrangères peut d'ailleurs faire partie des moyens susceptibles d'améliorer les propriétés d'intérêt technologique ou biopharmaceutique. La présente revue explique ces concepts à travers des exemples classiques ou plus récemment publiés dans la littérature.

Mots clefs : Physique de l'état solide — Structure cristalline — Polymorphisme — Hydrates — Solvates — Habitus cristallin — Défauts cristallins — Impuretés — Comprimabilité — Broyage — Compression — Granulation — Séchage — Conditions de conservation.

Depending on its origin or the particular batch, a given drug, although chemically well defined, may exhibit quite different behaviour. Process conditions (grinding, tabletting, granulation, drying) may also affect secondary (derived) properties of the drug, such as compactibility, wettability, solubility, dissolution rate, bioavailability and even pharmacological activity. Property changes may also be due to the storage conditions of the dosage form. In solids, these differences, which may exist initially or be generated by some treatment, arise directly from the primary characteristics of the crystals, i.e. the crystalline structure, both internal (polymorphism, pseudopolymorphism, amorphous state) and external (habitus, facies), crystal defects (dislocations) or the presence of impurities. In this respect, crystal « doping » by foreign substances may be envisaged as a means to improve drug properties of technological or biopharmaceutical interest. This review article explains these concepts using classical or more recently published examples from the literature.

Key words: Solid state physics — Crystalline structure — Polymorphism — Hydrates — Solvates — Crystalline habitus — Crystal defect — Impurities — Compactibility — Tabletting — Grinding — Granulation — Drying — Storage conditions.

Il a été observé de longue date qu'un même principe actif peut, selon sa source, le traitement mécanique ou les conditions environnementales qu'il a subis, se comporter de façon très variable à l'état solide, tant en ce qui a trait à la fabrication, à la stabilité, qu'aux caractéristiques de dissolution et même d'absorption d'une forme galénique. Les aspects à la fois pharmacotechniques et biopharmaceutiques sont donc concernés. Les raisons à l'origine des variations observées sont multiples : taille et forme (habitus, faciès) des particules, polymorphisme et pseudopolymorphisme (hydrates, solvates), impuretés. Ces facteurs exercent leur influence au travers des propriétés physiques et physicochimiques (énergie de surface, solubilité) du principe actif.

Les différences entre sources et lots d'une substance active peuvent être présentes initialement. Une analyse approfondie du matériau de départ permet de s'en rendre compte et d'y remédier. Les caractéristiques d'un principe actif peuvent également se trouver changées lors des différentes étapes de la préparation d'une forme galénique (granulation, broyage, compression) ou de sa conservation. Les raisons à l'origine des variations des propriétés des solides sont multiples ; elles ont fait l'objet de revues partielles et déjà anciennes [1-3]. Ici, une synthèse est effectuée en examinant en particulier les incidences sur la réalisation des formes médicamenteuses et en s'appuyant, dans la mesure du possible, sur des exemples récemment publiés.

Pour bien comprendre les causes des variations des propriétés qui ont une importance en formulation et qui sont généralement des propriétés dérivées, il convient de s'intéresser aux propriétés fondamentales, c'est-à-dire à la structure cristalline et à la morphologie des particules. Ces propriétés fondamentales peuvent, à leur tour, se trouver affectées par la présence d'impuretés, résultant de la cristallisation ou ajoutées intentionnellement. Des facteurs d'agression, tels qu'un stress mécanique, la température et la présence d'humidité, sont également susceptibles de modifier les propriétés fondamentales de la matière et par là les propriétés dérivées. La *figure 1* donne une liste des propriétés fondamentales et déri-

Material may be protected by copyright law (Title 17, U.S. Code)

UM00016590
NOVARTIS EXHIBIT 1517
Novartis v. Regents, IPR2023-01347
Page 3572 of 4460

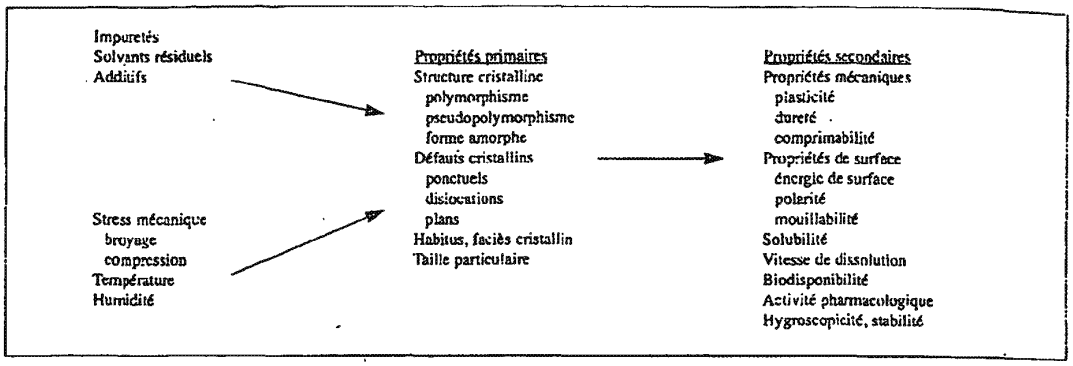

Figure 1 - Relations entre propriétés primaires et propriétés secondaires (dérivées) de l'état solide et sources de modifications.

vées de l'état particulaire solide ; elle mentionne également les facteurs influant dans ce contexte.

Les différentes parties de cette revue illustreront successivement, grâce à des exemples, les aspects suivants :
- les conséquences directes des propriétés fondamentales sur les propriétés intéressant le galéniste,
- les effets sur ces propriétés de la présence, voulue ou non, d'impuretés,
- les effets d'un traitement mécanique sur les deux types de propriétés,
- les effets des conditions de conservation sur l'évolution de ces propriétés.

I. INCIDENCE DE LA STRUCTURE CRISTALLINE ET DE LA MORPHOLOGIE DES PARTICULES SUR LES PROPRIÉTÉS DÉRIVÉES DE L'ÉTAT SOLIDE

La première cause d'un comportement différent d'une même entité chimique est bien évidemment à rechercher dans la structure cristalline, expression qui concerne aussi bien la structure interne d'un solide que son aspect externe, appelé habitus ou faciès cristallin (*figure 2*). La taille particulaire proprement dite ne sera pas abordée ici car elle n'est pas reliée directement à la structure cristalline, hormis à la densité de défauts cristallins. Rappelons que le polymorphisme vrai, au sens chimique, est la possibilité, pour un composé chimique donné, de présenter aux moins deux structures internes différentes, c'est-à-dire deux arrangements différents des molécules ou des atomes. En solution ou à l'état fondu, les polymorphes ne sont en revanche plus reconnaissables. Le pseudopolymorphisme, un phénomène voisin, se rapporte aux composés moléculaires qui comportent au moins deux constituants différents ayant cristallisé en une seule entité. Les solvates et hydrates sont bien évidemment concernés au premier chef. Par ailleurs, la plupart des auteurs incluent aujourd'hui dans le polymorphisme, au sens large, le polymorphisme conformationnel et le polymorphisme configurationnel, à condition toutefois qu'une interconversion très rapide entre les différentes formes soit possible à l'état fondu ou en solution [4-7]. Les formes amorphes, elles, se caractérisent par l'absence d'organisation des molécules ou des atomes (cf. I.4.). Il faut toutefois noter qu'il n'existe pas une distinction nette entre l'état cristallin et l'état amorphe. On parle d'état semi-cristallin lorsque l'organisation est partielle, et il est important de rappeler à ce stade que l'état amorphe est moins stable thermodynamiquement que l'état cristallin [8]. Quant à l'expression « variété polymorphe », elle se rapporte à la fois aux polymorphes, aux pseudopolymorphes et aux formes amorphes. Pour davantage de détails, il est conseillé de lire l'article de Bauer (cf. *supra* [9]).

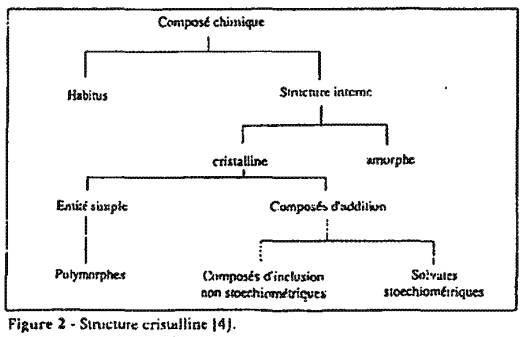

Figure 2 - Structure cristalline [4].

Le polymorphisme vrai est un phénomène qui touche environ un tiers des substances organiques, un autre tiers existant sous forme d'hydrates et de solvates, c'est-à-dire de pseudopolymorphes [10]. Une telle fréquence se retrouve parmi les principes actifs pharmaceutiques, à savoir :
- 40% de substances de l'USP avec monographies comportant un test de dissolution [11],
- plus de cent substances de la Ph. Eur. [12].

Dans un récent article, Henck *et al.* [13] ont même calculé les pourcentages de variétés polymorphes des substances de la Ph. Eur., en y incluant les produits existant seulement à l'état amorphe (*figure 3*).

1. VARIÉTÉS POLYMORPHES

La littérature cite plusieurs exemples de produits dont les polymorphes démontrent des caractéristiques de compression différentes : barbital, sulfathiazol, tartrate de métoprolol, phénobarbital, sulfamétrol. D'une manière générale, il est difficile

Material may be protected by copyright law (Title 17, U.S. Code)

UM00016591
NOVARTIS EXHIBIT 1517
Novartis v. Regents, IPR2023-01347
Page 3573 of 4460

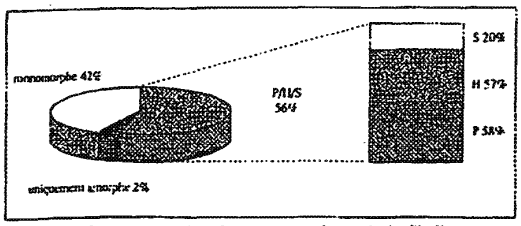

Figure 3 - Pourcentages de substances organiques de la Ph. Eur. monomorphes, uniquement amorphes ou existant sous différentes formes cristallines [13].
P : polymorphe. H : hydrate. S : solvate.

d'établir une relation entre la stabilité thermodynamique des formes (c'est-à-dire leur énergie interne) et leur comprimabilité, en raison de l'effet primordial de la nature du réseau cristallin sur la plasticité. Les formes métastables, aux réseaux cristallins moins denses, sont davantage plastiques et susceptibles de créer de larges surfaces de contact, mais les liaisons en leur sein sont moins fortes. La résistance mécanique dépendra de la balance entre ces deux paramètres.

Le *tableau I* compare les caractéristiques de compression de la forme I, stable, à celles de deux formes métastables du phénobarbital.

Tableau I - Caractéristiques de compression (à 158 MPa) de trois formes de phénobarbital [14].

Caractéristiques	Forme I	Forme II	Forme III
Energie brute de compression (J)	4,7	4,8	4,0
Pression radiale résiduelle (MPa)	9,7	9,3	16,1
Récupération élastique (%)	10,5	11,3	7,1
Force d'éjection (N)	706	661	1150
Seuil d'écoulement Eq. Heckel (MPa)	107	80	130
Résistance radiale (N/cm²)	29	31	95
Résistance en flexion (N/cm²)	123	131	229
Rapport d'isotropie*	4,2	4,2	3,2

* Rapport d'isotropie = résistance en flexion/résistance radiale.

Dans le cas présent, la forme métastable III, bien que moins plastique (seuil d'écoulement plus élevé), donne des comprimés plus résistants. La transmission plus homogène des contraintes (bas rapport d'isotropie) et la faible élasticité du matériau (récupération élastique moindre) en sont les causes. Pour ce qui est de la comprimabilité, le recours à la forme métastable III, en lieu et place de la forme II, présente le plus souvent dans les produits du commerce, pourrait donc paraître judicieux, à condition que d'autres critères, en premier lieu la stabilité chimique et l'activité pharmacologique, soient satisfaits.

Les polymorphes et les pseudopolymorphes peuvent également présenter des propriétés de surface et donc une mouillabilité quelque peu différentes, comme l'attestent les valeurs suivantes d'angle de contact avec l'eau :
- palmitate de chloramphénicol : forme α 122°, forme β 108°,
- furosémide : forme I 90°, forme II 75°,
- ampicilline : anhydre 35°, trihydratée 25°.

La solubilité et la vitesse de dissolution sont deux propriétés importantes qui dépendent de la structure cristalline, en fait de l'énergie de cohésion des molécules. Les formes métastables, d'énergie libre supérieure, sont plus solubles que les formes stables, en général de l'ordre de 50%. Il convient toutefois de rappeler que le rapport des solubilités dépend de la température et du milieu en question, et qu'il peut s'inverser au-dessus de la température de transition polymorphique dans le cas des systèmes énantiotropes. Ajoutons en outre que les formes métastables peuvent, en milieu liquide, se transformer facilement en formes plus stables, de solubilité moindre (*tableau II*).

Tableau II - Solubilité à 37°C de trois formes de cyclopenthiazide [15].

Forme	Solubilité				Chaleur de dissolution (kJ/mol)
	Eau	Ethanol 10%	HCl 0,01 M	NaOH 0,01M	
I*	35	201	24	133	5,91
II**	62	496	63	306	6,14
III***	18	132	13	129	15,00

* Forme métastable, ne se convertit pas dans les milieux testés.
** Forme métastable, se convertit dans HCl 0,01M.
*** Forme thermodynamiquement la plus stable.

Les exemples foisonnent montrant une amélioration de la biodisponibilité ou de l'activité pharmacologique par l'administration d'un polymorphe plutôt qu'un autre [3]. Citons le parfait parallélisme rapporté par des auteurs japonais [16, 17] entre la vitesse de dissolution de quatre formes de cimétidine et le taux d'inhibition d'ulcères gastriques chez le rat (*figure 4*).

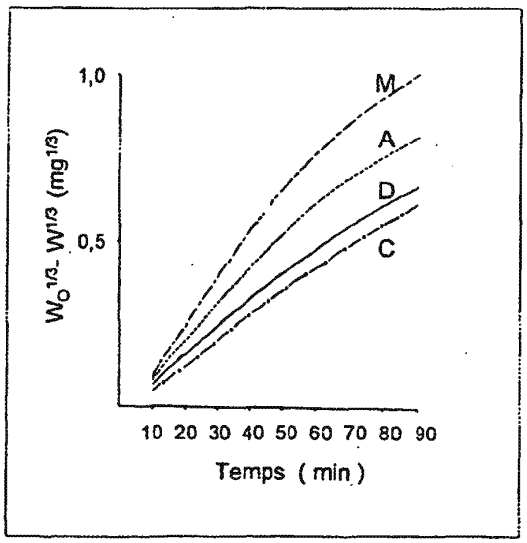

Figure 4 - Profils de dissolution des formes A, C, D et du monohydrate (M) de cimétidine (présentés selon la loi de la racine cubique) [16, 17].
Taux d'inhibition (dose de 12,5 mg/kg) d'ulcères gastriques chez le rat (%) : témoin 0, forme M 87,4, forme A 69,3, forme D 64,1, forme C 60,3.

Material may be protected by copyright law (Title 17, U.S. Code)

UM00016592
NOVARTIS EXHIBIT 1517
Novartis v. Regents, IPR2023-01347
Page 3574 of 4460

Les formes amorphes, non stables thermodynamiquement, présentent en particulier une solubilité élevée, susceptible d'accroître la vitesse de dissolution et la biodisponibilité, comme l'exemple désormais classique de la novobiocine acide l'a démontré. La novobiocine acide amorphe se transforme toutefois en forme cristalline, non résorbable, en six mois à la température ambiante, phénomène qu'il est possible de combattre en ajoutant de la méthylcellulose.

La meilleure biodisponibilité d'un polymorphe n'est toutefois pas toujours attribuable à une plus grande solubilité. Le cas du palmitate de chloramphénicol est là pour nous le rappeler. Il a ainsi été démontré que les taux sériques élevés observés avec la forme « active » B par rapport à la forme « inactive » A proviennent avant tout de sa sensibilité accrue à l'hydrolyse par les estérases. Il faut en effet savoir que le palmitate de chloramphénicol est un précurseur médicamenteux (*prodrug*) qui doit subir une hydrolyse enzymatique dans le tube digestif pour être absorbé et développer son activité antibiotique au niveau sanguin.

L'hygroscopicité et la stabilité sont deux autres propriétés qui dépendent de la variété polymorphique considérée. Les isothermes de sorption/désorption diffèrent, avec souvent une transition polymorphique à des humidités relatives élevées. Le chlorhydrate de paroxétine peut servir d'exemple [18]. Cet antidépresseur existe sous deux formes. La forme I est un hémihydrate, non hygroscopique et thermodynamiquement stable. La forme II, anhydre, est métastable, hygroscopique et davantage soluble. A humidité relative élevée, elle se convertit en forme I, si toutefois des germes de forme I sont présents comme impuretés. Il est à noter que d'une manière générale, l'établissement des isothermes de sorption constitue une méthode simple et efficace pour mettre en évidence l'existence de différentes variétés polymorphes ainsi que leur interconversion.

Les deux exemples suivants illustrent le rôle joué par le polymorphisme dans la stabilité des principes actifs. Parmi les cinq formes de *tert*-butylacétate d'hydrocortisone synthétisées, seules deux se sont révélées insensibles à une exposition aux UV [19]. Quant aux deux formes de fenrétinide, seule la forme I, quel que soit le lot examiné, démontre une stabilité à la chaleur (*tableau III*).

Tableau III - Pourcentage de fenrétinide intacte après 15 j de conservation à trois températures différentes [20].

Forme	Lot	4°C	25°C	40°C
I	A	100,0	100,3	99,1
	B	-	100,5*	100,0**
II	C	97,0	91,9	79,8
	D	93,1	91,2	87,4

* 98,0% à 24 mois. ** 98,6% à 18 mois.

2. SOLVATES DÉSOLVATÉS

Une place particulière doit être réservée aux formes anhydres obtenues par départ du solvant de cristallisation d'un solvate ou d'un hydrate particulier [21]. La plupart du temps, ces « solvates désolvatés » conservent la structure du solvate d'origine, avec relativement peu de changement des paramètres du réseau cristallin. Leur degré d'organisation structurale est cependant moindre et leur masse volumique est particulièrement basse. Il s'ensuit donc des comportements qui diffèrent non seulement de ceux des produits d'origine mais aussi de ceux des formes anhydres obtenues conventionnellement. Les propriétés de ces « solvates désolvatés » dépendent du solvate d'origine. Byrn *et al.* [22] observent ainsi une hygroscopicité croissante, avec formation d'hydrates, de la céfaloridine anhydre préparée à partir respectivement du diméthanolate, du monométhanolate et de l'hydrate.

L'intérêt de disposer d'« hydrates déshydratés » est illustré par le cas de la solution injectable de gluceptate (glucoheptonate) de calcium. Le recours à une forme anhydre obtenue par déshydratation de la forme hydratée permet d'obtenir un injectable conforme à l'USP par augmentation de la solubilité par un facteur de 19 [23].

Il convient également de citer le cas des formes anhydres de théophylline. Une forme métastable I* a été récemment préparée par déshydratation de la théophylline monohydratée II. Cette forme, notamment lorsqu'elle est incorporée dans des comprimés, se comporte différemment de la forme anhydre I de l'USP, tant à la conservation qu'à la dissolution [24] (*figure 5*). La forme anhydre I ne subit pas de

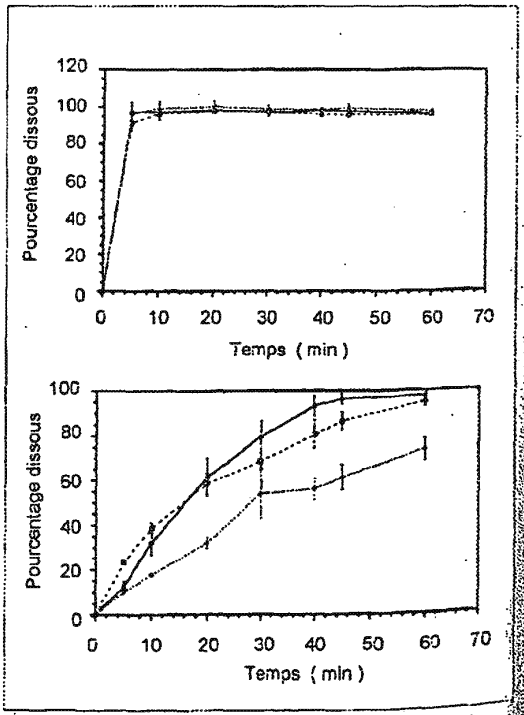

Figure 5 - Profils de dissolution de comprimés de théophylline préparés avec la forme anhydre stable I (haut) et la forme métastable I* (bas) [24]. ● : comprimés fraîchement préparés. ◆ : comprimés conservés 4 j à 52% HR. ■ : comprimés conservés 10 j à 33% HR.

STP Pharma Pratiques 3 (5) 390-400 1993
Material may be protected by copyright law (Title 17, U.S. Code)

UM00016593
NOVARTIS EXHIBIT 1517
Novartis v. Regents, IPR2023-01347
Page 3575 of 4460

transformation au cours de la conservation des comprimés, qui présentent les mêmes profils de dissolution quelles que soient les conditions ambiantes. A noter qu'une fois en contact avec le milieu liquide, la forme I ne se transforme que très lentement en forme monohydratée II. Les profils de dissolution reflètent donc la mise en solution de la forme anhydre I. En comparaison, la forme métastable I* se transforme peu à peu dans le comprimé en forme anhydre stable I (conversion complète en moins de 4 j à 52% HR et en moins de 10 j à 33% HR). De surcroît, la forme I* se convertit quasiment instantanément en forme monohydratée II en présence du milieu liquide, avec des profils ralentis. Les profils reflètent donc en grande partie la dissolution de la forme monohydratée II, formée *in situ*.

Terminons en disant que si la formation d'un produit anhydre par désolvatation peut être souhaitée au stade de la synthèse, elle peut aussi survenir tout à fait insidieusement lors d'une opération de séchage qui suit une granulation. Par ailleurs, un traitement thermique prolongé peut aussi entraîner la transformation du solvate désolvaté en un produit cristallin autre, plus stable thermodynamiquement.

3. HABITUS, FACIÈS CRISTALLIN

Une poudre de structure cristalline donnée peut prendre différentes apparences extérieures (on parle d'habitus ou de faciès), qui sont susceptibles d'entraîner des comportements très variables. Une différence d'habitus se traduit par exemple pour la nitrofurantoïne par des caractéristiques de compression différentes [25]. La modification du faciès cristallin du paracétamol par recristallisation dans différents solvants a permis d'obtenir une qualité apte à la compression directe [26]. Des techniques particulières, dites de cristallisation sphérique, permettent aussi d'améliorer les propriétés d'écoulement et comprimabilité de produits peu favorables, comme la bucillamine [27].

La forme des cristaux affecte également leur vitesse de dissolution au travers de la surface exposée au milieu liquide, paramètre qui entre dans l'équation de Noyes-Whitney. Or, à masse et à diamètre moyen identiques, plus les particules sont irrégulières, plus importants seront la surface offerte et donc le flux de matière. Cet effet a été démontré pour un sel de diclofénac recristallisé dans différents solvants (*figure 6*). Les auteurs [28] obtiennent même une excellente relation inverse entre l'efficacité de dissolution du sel et le facteur de forme, défini ainsi à partir de mesures au microscope électronique à balayage :

facteur de forme = 4π (surface projetée)/(périmètre)^2

Une autre équipe [29] a également mis en évidence l'incidence de la forme des cristaux en combinant les résultats obtenus avec plusieurs principes actifs peu solubles et en corrigeant les valeurs de vitesse de dissolution spécifique par l'effet de la solubilité. Dans ce travail, le rôle de la taille particulaire a également été démontré, en insistant sur le fait qu'une réduction du diamètre entraîne non seulement une augmentation de la surface offerte au milieu de dissolution, mais aussi une diminution de la couche limite de diffusion.

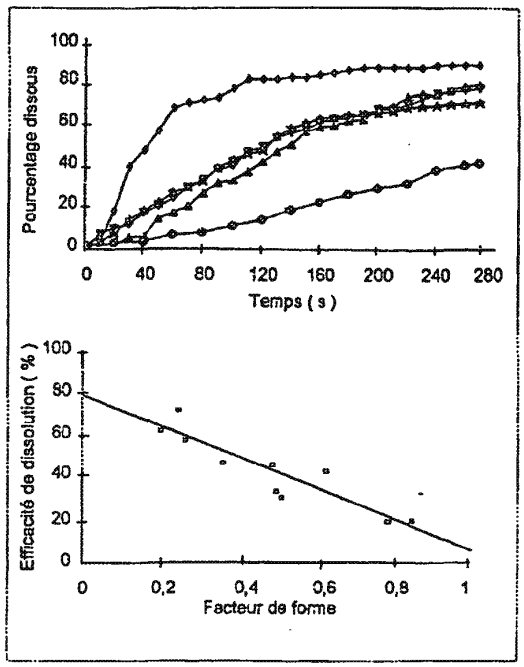

Figure 6 - Profils de dissolution d'un sel de diclofénac recristallisé dans différents solvants (haut) et relation entre l'efficacité de dissolution et le facteur de forme (bas) [28].

4. DÉFAUTS CRISTALLINS

Un cristal est toujours imparfait, en ce sens qu'il contient des défauts qui viennent interrompre l'alignement des molécules ou atomes. Ces défauts sont classés en défauts ponctuels et en défauts de réseau. Les défauts ponctuels, qui sont stables thermodynamiquement, correspondent à des lacunes, à des molécules étrangères ou non placées dans des interstices, ou encore à des molécules étrangères de substitution.

Les défauts de réseau sont constitués à la fois par les défauts linéaires (dislocations) et par les défauts bidimensionnels (joints de grains), qui sont en fait des rangées de dislocations. Pour donner une idée de l'importance du degré d'organisation des solides, qu'il s'agisse d'un cristal parfait, d'un cristal réel ou d'un corps amorphe, on peut faire appel à la notion de degré d'ordre et à celle de distance d'ordre, estimée également en unité de rayon atomique (*figure 7*).

Cristal amorphe		Cristal réel		Cristal parfait
$s \approx 0$	→	$s < 1$	→	$s = 1$
d.o. < 100 Å		d.o. > 1000 Å		d.o. = ∞
$r_o = 3\text{-}10$		$r_o > 100$		$r_o = \infty$

Figure 7 - Degré d'ordre au sein des solides.
s : degré d'ordre, d.o. : distance d'ordre, r_o : rayon moléculaire.

Material may be protected by copyright law (Title 17, U.S. Code)

UM00016594
NOVARTIS EXHIBIT 1517
Novartis v. Regents, IPR2023-01347
Page 3576 of 4460

Les défauts de réseau constituent des zones à potentiel chimique et énergie libre élevés ; ils sont thermodynamiquement instables et responsables d'une réactivité accrue. D'une manière générale, ces imperfections favorisent (et même rendent possible) la déformation plastique des cristaux, diminuent leur stabilité chimique ou physique et accélèrent leur dissolution. La littérature ne cite pas d'exemples de substances pharmaceutiques mettant en relation la densité des dislocations et la vitesse de dissolution des cristaux. En revanche, des différences de densité des dislocations ont souvent été invoquées pour expliquer des différences de cinétique de dissolution. C'est notamment le cas pour l'aspirine, pour laquelle les différences avaient été attribuées, dans un premier temps, au phénomène de polymorphisme.

5. IMPURETÉS

Les composés contiennent tous une certaine quantité d'impuretés (au minimum 1 ppb), même lorsque ces dernières ne sont pas ajoutées délibérément pour modifier certaines propriétés de cristaux. Les impuretés sont de plusieurs natures :
- produits de la synthèse ou même de la purification,
- polymorphes ou pseudopolymorphes en traces,
- excès d'énantiomère,
- solvants résiduels.

Ces molécules étrangères viennent occuper des interstices ou se substituer aux molécules au sein du réseau cristallin. Une seule molécule d'impureté suffit d'ailleurs à influencer la position et l'énergie de plusieurs centaines de molécules. La présence d'impuretés entraîne deux sortes d'effets. Lorsque le principe actif est en contact avec un milieu liquide (par exemple lors d'une granulation ou d'un essai de libération), les impuretés entrent en solution et peuvent venir s'adsorber à la surface des cristaux. Elles vont ensuite inhiber la dissolution des cristaux ; on parle d'« empoisonnement des cristaux ». Mais les impuretés, comme source de défauts du réseau cristallin, ont avant tout pour effet de provoquer une désorganisation de la structure interne (un « indice de disruption » quantifiant le désordre du réseau cristallin, basé sur des mesures d'enthalpie de fusion, a d'ailleurs été proposé [30-33]). Les défauts ainsi créés, comme il a été discuté précédemment (cf. II. 4), constituent des zones de haute énergie qui viennent modifier les propriétés du matériau. L'effet global des impuretés provient cependant à la fois de la désorganisation de la structure cristalline interne et d'une modification de l'habitus. Ainsi, la présence de solvant résiduel influe sur les caractéristiques de compression du paracétamol [34], probablement au travers de la plasticité. Burger et Griesser [35] notent une influence des impuretés sur la transformation polymorphique du succinylsulfathiazol en présence d'une humidité relative élevée. Mais ce sont surtout la solubilité et donc la vitesse de dissolution des composés qui sont affectées. Les impuretés, en particulier lorsqu'elles proviennent de l'étape de synthèse du principe actif, sont en général plus solubles que le principe actif à l'état pur. Il s'ensuit une solubilité apparente plus élevée, qu'il est bon de mettre en évidence en établissant un diagramme de phases, tel que le préconise l'USP <i171>, par exemple à la monographie « Mecamylamine Hydrochloride ». Ce type de diagramme permet d'ailleurs de déterminer le pourcentage d'impuretés sans en connaître la nature, à condition qu'elles soient plus solubles que le corps pur.

Une augmentation de la solubilité de surface due à la présence, dans de nouveaux lots d'un principe actif, d'une impureté soluble a entraîné des difficultés de mise en œuvre de l'opération de granulation. Un lavage des cristaux a permis de retrouver les conditions d'origine [36]. La présence d'impuretés peut avoir des effets bénéfiques. Elles ont permis d'éviter la recristallisation d'estradiol incorporé dans des implants de poly(diméthylsiloxane) [37]. Dans le cas de suspensions d'oxyclozanide, les impuretés de surface, en passant en solution et en s'adsorbant à la surface des cristaux, ont empêché, par un phénomène d'empoisonnement, la transformation de la forme métastable II en forme stable I [38].

Les exemples sont nombreux illustrant l'influence d'impuretés sur la vitesse de dissolution de principes actifs. Ainsi, différents lots de digoxine et de digitoxine ont montré des différences de solubilité jusqu'à un facteur de 4, que les auteurs expliquent par la présence de traces d'autres polymorphes [39]. Li et Grant [40] ont montré que la solubilité et la vitesse de dissolution du racémate de 2-naphtalènesulfonate d'éphédrine atteignaient un maximum lorsque les cristaux contenaient un excès d'un des énantiomère d'environ 1,5 mol % [40]. En revanche, un léger excès d'un énantiomère au sein de l'autre énantiomère de ce même composé chimique se traduit par une réduction de la vitesse de dissolution [41].

6. « DOPAGE » DE CRISTAUX

L'addition délibérée d'une substance étrangère au sein d'un matériau en vue d'en améliorer les performances est un procédé bien connu dans un domaine comme la métallurgie. Cette opération, qui fait partie des techniques dites de « *crystal engineering* » [42], a fait l'objet d'études depuis une dizaine d'années. L'exemple présenté ci-dessus se rapporte d'ailleurs à des cristaux dopés. Les impuretés ajoutées intentionnellement lors de l'étape de recristallisation sont de deux sortes :
- des substances apparentées chimiquement au produit « pur » (réactifs de synthèse, polymorphes, excès d'énantiomère, produits de dégradation),
- des additifs de nature chimique différente (polymères, tensioactifs).

Une série de travaux canadiens ont montré l'influence des substances apparentées sur certaines propriétés de principes actifs. Ainsi, des cristaux d'acide adipique « dopés » à l'acide octanoïque ont montré une comprimabilité bien supérieure à celle du produit pur [43]. Des cristaux de phénytoïne ont été préparés à partir de solutions méthanoliques contenant des composés voisins (en fait des *prodrugs*) en quantités croissantes [44-47]. Les profils de dissolution de cristaux grossis en présence de 3-acétoxyméthyl-5,5-diphénylhydantoïne (AMDPH) font apparaître une augmentation de la vitesse de dissolution. Un accroissement maximal (environ 3,5 fois) est obtenu avec une solution contenant 9 g/l d'AMDPH, correspondant à un taux d'incorporation de 0,54 mol % [42]. Quant à la vitesse de dissolution intrinsèque (vitesse de dissolution initiale di

Material may be protected by copyright law (Title 17, U.S. Code)

UM00016595
NOVARTIS EXHIBIT 1517
Novartis v. Regents, IPR2023-01347
Page 3577 of 4460

par la surface initiale des cristaux), elle montre encore une augmentation maximale d'un facteur de 2 à 3, obtenue cette fois-ci à une concentration de 5 g/l d'AMDPH (*figure 8*). La rapidité plus grande de dissolution provenait donc non seulement d'une augmentation de la surface spécifique par changement d'habitus mais aussi de l'accroissement de la densité des dislocations dû à la présence de l'impureté. Il est à noter que des essais similaires avaient été conduits en recristallisant le paracétamol en présence de p-acétoxyacétynilide, une impureté de synthèse, substance par ailleurs également proposée comme *prodrug* du paracétamol [48-50]. Des augmentations de vitesse de dissolution des cristaux avaient bien été observées, mais elles semblaient largement attribuables à la modification de l'habitus, comme l'ont démontré des tests de dissolution de comprimés de paracétamol à surface exposée constante [50]. L'étude a aussi montré que l'augmentation de la vitesse de dissolution pouvait provenir de l'excellente mouillabilité du produit dopant adsorbé en surface. Ce serait le cas par exemple avec le BMDPH (3-butanoyloxyméthyl-5,5-diphénylhydantoïne), comme l'attestent les valeurs d'angle de contact avec l'eau des cristaux « dopés » [47].

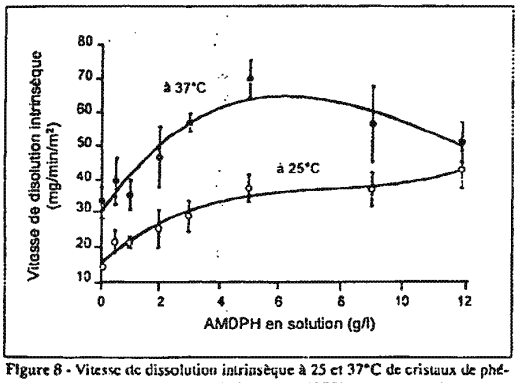

Figure 8 - Vitesse de dissolution intrinsèque à 25 et 37°C de cristaux de phénytoïne ayant grossi dans des solutions d'AMDPH en concentrations croissantes [44].

Une modification des propriétés cristallines peut également être obtenue en recristallisant les substances actives en présence d'additifs. Ces additifs (polymères, tensioactifs) ne sont en principe pas apparentés chimiquement aux produits « purs » ; leur taille diffère également sensiblement. Il en découle que les molécules d'additifs viennent occuper des sites interstitiels plutôt que des sites de substitution. Ces molécules peuvent ainsi entraîner une certaine perturbation de l'arrangement cristallin. Néanmoins, elles influent avant tout sur l'habitus en modifiant la vitesse de croissance des faces des cristaux en fonction de leur polarité. D'une manière générale, peu de données de base sont fournies dans les travaux de la littérature qui permettraient d'étayer les mécanismes mis en jeu. Il n'en reste pas moins que les avantages apportés par cette forme de « dopage » de cristaux peuvent se révéler déterminants. Ainsi, aucun signe de décalottage des comprimés de paracétamol n'apparaît lorsque les cristaux sont préparés en présence d'agar-agar ou de gélatine [51]. Dans le cas du second hydrocolloïde, la vitesse de dissolution est la même que celle des cristaux sans additif. Une autre étude intéressante, quoique déjà ancienne, concerne la phénylbutazone [52, 53]. L'adjonction d'hydroxypropylméthylcellulose (HPMC) dans le milieu de croissance aboutit à un doublement de la vitesse de dissolution intrinsèque (maximum à 2% d'HPMC). Les auteurs incriminent un phénomène de complexation des constituants et celui de désorganisation du réseau cristallin. Cependant, les mêmes auteurs, comparant des cristaux contenant de l'HPMC ou du poloxamère 188 et préparés par cristallisation ou par nébulisation, observent que la phénylbutazone subit une dégradation qui n'a pas lieu en absence d'additif.

Dans les techniques de cristallisation sphérique, des polymères et des tensioactifs sont souvent mis en œuvre pour obtenir des produits à propriétés d'écoulement et de compression favorables, ainsi que pour accroître la vitesse de dissolution. Dans un travail comparant les effets de l'HPMC, de la carboxyméthylcellulose sodique, de l'huile de ricin hydrogénée et du stéarate de polyoxyéthylène 40, Sano *et al.* [54] notent une augmentation de la vitesse de dissolution du tolbutamide par un facteur de huit.

II. INFLUENCE DES TRAITEMENTS ET DE LA CONSERVATION SUR LA TRANSFORMATION DES SOLIDES

Les exemples traités jusqu'ici ont permis d'illustrer les relations entre la structure cristalline du principe actif, telle qu'elle existe à l'origine ou qu'elle a été modifiée intentionnellement, sur certaines propriétés dérivées d'intérêt pour la formulation, comme la comprimabilité, la solubilité, la vitesse de dissolution et la stabilité. Dans la pratique cependant, il peut arriver que certaines opérations pharmaceutiques ou des conditions particulières de stockage du médicament entraînent un changement de la structure cristalline initiale du principe actif et par là même ses propriétés dérivées. Ces « facteurs d'agression » sont de deux ordres :

- un stress mécanique, comme le broyage ou la compression de la poudre,
- la mise en suspension de la poudre dans un liquide, la phase d'humectation lors de l'opération de granulation, le séchage ou les conditions de conservation de la forme pharmaceutique.

1. STRESS MÉCANIQUE

Les opérations de broyage et de compression des poudres, par les contraintes de cisaillement qu'elles engendrent, entraînent un glissement des plans cristallins. Cette déformation plastique est rendue possible par les défauts cristallins déjà présents (en particulier les plus fréquents, à savoir les dislocations), qui représentent des points de moindre résistance, mais elle entraîne également la multiplication de ces défauts. Un cristal réel contient de 10^3 à 10^6 dislocations par cm², alors qu'après déformation la densité des dislocations se situe entre 10^7 et 10^{12} par cm². Il y a donc accroissement de la désorganisation de la structure cristalline (cf. II.4). Le traitement méca-

Material may be protected by copyright law (Title 17, U.S. Code)

UM00016596
NOVARTIS EXHIBIT 1517
Novartis v. Regents, IPR2023-01347
Page 3578 of 4460

nique peut conduire jusqu'à une destruction quasi totale du réseau cristallin, c'est-à-dire à une amorphisation du produit. Le produit devient ainsi plus instable, avec un risque de se retransformer dans la forme initiale ou dans une forme différente.

Il y a plusieurs années déjà, Hüttenrauch [55, 56] a proposé une théorie, basée sur des concepts thermodynamiques, permettant d'expliquer les processus concernés. Selon la théorie de l'activation mécanique, qui fait partie du concept plus général de pharmacie galénique moléculaire, l'augmentation de la densité des dislocations sous l'effet d'un stress mécanique s'accompagne d'un accroissement de l'énergie interne du solide qui conduit à un stade activé instable. Une partie plus ou moins importante de l'énergie apportée en matériau va être conservée de façon irréversible sous forme d'une densité de dislocations accrue. L'autre partie, réversible, va être restituée et utilisée sous différentes formes d'énergie. C'est le processus de désactivation (passivation), plus ou moins complet et rapide, qui conduira à une recristallisation du produit, soit dans la forme cristalline originale, soit dans une autre forme (transformation polymorphique), à une racémisation ou encore à une décomposition du produit. Il est à noter que d'autres opérations entraînent une activation des composés, comme la congélation et la déshydratation dont il a déjà été question (cf. II.2). De même, une passivation peut être obtenue par chauffage, ainsi que par broyage ou compression prolongée du produit.

Les exemples les plus nombreux de transition de phase due à une sollicitation mécanique sont fort nombreux, en particulier pour ce qui est de l'effet du broyage ou d'une simple trituration au mortier (*tableau IV*). A titre d'exemples, on peut noter que chacune des formes A ou B du palmitate de chloramphénicol se transforme en l'autre forme jusqu'à une même valeur d'équilibre, atteinte toutefois après des durées de broyage différentes [57, 58]. L'expérience montre aussi que la présence de seulement 1% de forme A dans la forme B accélère considérablement la conversion de cette dernière. On observe aussi souvent une amorphisation du produit sous l'effet du broyage. C'est le cas du sulfate sodique de prastérone, dont le degré de cristallinité chute à 72,2% après 30 min de broyage, sachant que le produit ne perd pas ses deux molécules d'eau [59]. Les auteurs constatent par ailleurs que la sensibilité à la dégradation est d'autant plus grande que la durée de broyage est élevée, et donc le taux de cristallinité bas. Quant à Hüttenrauch et Fricke [60], ils observent une oxydation de l'acétate de trenbolone à la suite d'une trituration, dont l'importance dépend de l'excipient présent.

La compression entraîne le même type d'effets que le broyage (*tableau V*). Le cas du chlorpropamide, dont les formes A et C s'interconvertissent sous pression [61, 62], prouve bien que même une forme stable peut se transformer en forme métastable par un processus d'activation. Pour ce qui est de la caféine, nous avons montré que seule la modification A se transforme en modification B sous l'effet d'une pression, le taux de transformation variant en fonction de la zone du comprimé examinée [63]. Quant à l'acétate de trenbolone, il subit une oxydation lorsqu'il est soumis à une pression, à

Tableau IV - Quelques exemples de transformations observées sous l'effet d'un broyage.

Substance	Type de transformation	Auteur (année)
Albutérol, sulfate	Formation de défauts en surface des cristaux	Wärd (1995)
Caféine	Transition polymorphique forme I → II	Pirttimäki (1993)
Céfalotine sodique	Formation de défauts en surface des cristaux	Otsuka (1990)
Céfixime, trihydrate	Amorphisation	Kitamura (1989)
Cimétidine	Transition polymorphique formes B → A et C → B	Bauer-Brandl (1996)
Chloramphénicol, stéarate	Transition polymorphique forme A → B → amorphe	Forni (1988)
Cyclophosphonamide, monohydrate	Amorphisation	Ketolainen (1995)
Phénylbutazone	Transition polymorphique formes α, β et δ → ζ	Matsumoto (1988)
Probucol	Transition polymorphique forme III → I	Gerber (1992)
Sulfathiazol	Transition polymorphique formes I → III et III → I	Shakhtshneider (1993)

Tableau V - Quelques exemples de transformations observées sous l'effet d'une compression.

Substance	Type de transformation	Auteur (année)
Caféine	Transition polymorphique forme I → II	Pirttimäki (1993)
Chlorpropamide	Transition polymorphique formes A → C et C → A	Otsuka (1989, 1993)
Cyclophosphonamide, monohydrate	Amorphisation	Ketolainen (1995)
Piroxicam	Transition polymorphique forme α → β	Ghun (1992)

l'instar de ce qui se passe lors d'un broyage. La compression n'entraîne en revanche pas d'hydrolyse de l'aspirine [60]. L'ergocalciférol, lorsqu'il est comprimé, subit une première dégradation à partir d'une certaine pression, en même temps qu'une amorphisation, processus qui se poursuit lors d'une période de conservation et dont l'intensité dépend de la force à laquelle le comprimé a été préparé [64]. Un tel phénomène a également été observé lors du broyage de l'ergocalciférol [64]. L'exemple du cyclophosphonamide monohydraté illustre également bien l'incidence du polymorphisme. Sa mise en forme de comprimés doit se dérouler à basse température (8 à 12°C) pour prévenir tout collage et gélification de cet anticancéreux. Or, ces aléas proviennent justement de la formation d'une forme intermédiaire métastable de cyclophosphonamide [65]. Il reste cependant que si divers types de changements de la matière peuvent survenir sous l'effet d'une contrainte mécanique, les plus fréquents ont trait à une amorphisation en surface ou en profondeur des cristaux, avec toutes les conséquences sur les propriétés technologiques et biopharmaceutiques des formes galéniques. Une désactivation par recristallisation ou par transformation polymorphique à plus ou moins long terme n'est pas non plus à exclure.

Material may be protected by copyright law (Title 17, U.S. Code)

UM00016597
NOVARTIS EXHIBIT 1517
Novartis v. Regents, IPR2023-01347
Page 3579 of 4460

2. MODIFICATIONS SOUS L'EFFET D'EAU OU D'UN SOLVANT

Il est bien connu que les changements d'état des solides sont favorisés par la présence d'eau ou de solvants. Ainsi, l'essai consistant à placer des cristaux en suspension dans un liquide ou à les exposer à des vapeurs constitue un moyen rapide et sûr de mettre en évidence d'éventuelles transformations. La transformation en forme cristalline de la novobiocine acide amorphe en suspension dans l'eau a déjà été évoquée. La forme commercialisée A de la cimétidine se comporte différemment selon le solvant considéré. En suspension dans l'eau, elle se transforme en forme B, tandis qu'en présence d'éthanol à 50% la forme D apparaît [66]. On peut donc imaginer qu'une granulation avec un solvant ou un autre pourra avoir des répercussion très différentes. Le cas des trois formes de chlorhydrate d'oxytétracycline montre, lui, la complexité des transformations pouvant survenir en présence d'humidité [67]. Si la forme A, stable, n'est pas hygroscopique et ne se transforme pas, même à humidité relative élevée, il n'en va pas de même des formes B et C. Les auteurs observent une transformation tout d'abord partielle de la forme B en forme A dès 62,5% d'humidité relative, puis complète à partir de 84% d'humidité relative. Quant à la forme C, elle s'amorphise dès 75% d'humidité relative, puis se transforme en forme A à 92% d'humidité relative. Ces transformations, qui sont susceptibles d'apparaître dans certaines conditions de conservation, peuvent avoir des répercussions d'ordre galénique. Ainsi, des comprimés de forme III de méprobamate ont vu leur résistance à l'écrasement très rapidement augmenter lorsqu'ils étaient placés déjà à une humidité relative de 43 ou 51%. Les auteurs expliquent ce phénomène par l'apparition de la forme II [68]. De même, la FDA a adressé une mise en garde, en 1980, concernant une perte d'activité d'environ un tiers de comprimés de carbamazépine conservés en conditions humides [69]. L'augmentation de la dureté des comprimés et le ralentissement de la dissolution ont pu être attribués à la modification en forme dihydratée du principe actif.

Des transformations défavorables n'ont toutefois pas lieu seulement lors de la conservation de la forme médicamenteuse. Il peut arriver qu'elles surviennent au cours d'une étape de fabrication qui fait intervenir de l'eau ou un solvant. Herman *et al.* [70] rapportent la formation de théophylline monohydratée lors de la granulation de mélanges de théophylline anhydre et de cellulose microcristalline. Le retard de dissolution des grains séchés est d'autant plus grand que la quantité d'eau ajoutée et la fraction de cellulose microcristalline sont importantes. A noter qu'en l'absence de l'excipient, la conversion n'a pas lieu (*figure 9*). Quant à Joachim *et al.* [71], ils observent un ralentissement de la dissolution de comprimés de lorazépam, en raison de la formation d'un solvate lors de la granulation avec de l'isopropanol.

*
* *

Les caractéristiques des formes galéniques solides ou semi-solides, aussi bien technologiques que biopharmaceutiques, dépendent de l'état cristallin du principe actif, en plus bien sûr du rôle joué par les excipients. L'état solide du principe actif est dicté par la structure cristalline (polymorphisme, pseudopolymorphisme, amorphisme), l'habitus cristallin (forme des particules) et la présence de défauts cristallins ou d'impuretés. Ces propriétés de base sont susceptibles d'agir, entre autres, sur la plasticité des produits, leur mouillabilité, leur solubilité, leur vitesse de dissolution, la biodisponibilité et l'activité pharmacologique. Ces propriétés dérivées sont très souvent interdépendantes, de même que les propriétés primaires. Ainsi, les impuretés, toujours présentes au sein des cristaux, vont accroître la densité de défauts cristallins, modifier l'habitus des cristaux ou favoriser une transformation polymorphique. Le solide va à son tour voir sa plasticité augmenter (avec formation facilitée de comprimés) ou sa solubilité s'accroître et par voie de conséquence sa cinétique de dissolution et sa biodisponibilité. La découverte de l'origine de certaines variations de propriétés de lots d'un même principe actif n'est toutefois pas toujours aisée. L'exemple de l'étude statistique de 66 variables sur la vitesse de dissolution de 35 lots de prednimustine le montre bien [72].

Les variabilités entre sources ou lots de principes actifs peuvent exister à l'origine ou être engendrées par des contraintes mécaniques (broyage, compression) ou par la présence d'eau ou d'un solvant. Cette présence peut intervenir au stade de la préparation de la forme galénique (mise en suspension, granulation) ou de sa conservation en conditions relativement humides. L'opération de séchage (étuve, nébulisation, lyophilisation) entre évidemment également en jeu. Il y a donc tout intérêt à connaître les relations complexes et les transformations entre les différentes formes cristallines d'un principe actif. De façon plus générale, il y a nécessité absolue de caractériser à fond chaque lot de principe actif, afin de minimiser les problèmes susceptibles de survenir lors de la préparation et de la conservation des formes pharmaceutiques. Cela paraît d'autant plus justifié que 70 à 90% des formes galéniques, selon les auteurs, sont solides.

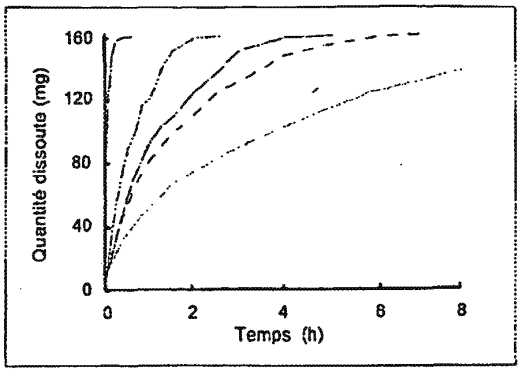

Figure 9 - Influence sur la vitesse de dissolution de la formation de théophylline monohydratée au cours de la granulation d'un mélange théophylline anhydre/cellulose microcristalline 60/40 [70].
Quantité d'eau ajoutée : 0% (—), 25% (-·-·), 40% (·-·-), 60% (-·-), 70% (····).

Material may be protected by copyright law (Title 17, U.S. Code)

UM00016598
NOVARTIS EXHIBIT 1517
Novartis v. Regents, IPR2023-01347
Page 3580 of 4460

BIBLIOGRAPHIE

1. YORK P. - Solid-state properties of powders in the formulation and processing of solid dosage forms. - Int. J. Pharm., 14, 1-28, 1983.
2. DUCHÊNE D., PONCHEL G. - Solid particles, compression and bioavailability. - STP Pharma, 3, 676-687, 1987.
3. GIRON D. - Influence de la qualité des matières premières sur la vitesse de dissolution et sur la biodisponibilité. - STP Pharma, 4, 330-340, 1988.
4. HALEBLIAN J.K. - Characterization of habits and crystalline modification of solids and their pharmaceutical applications. - J. Pharm. Sci., 64, 1269-1288, 1975.
5. BOUCHÉ R., DRAGUET-BRUGHMANS T.M. - Le polymorphisme des substances organiques médicamenteuses. - J. Pharm. Belg., 32, 23-51, 1977.
6. BERNSTEIN J. - Polymorphism in drug design and delivery. - Prog. Clin. Biol. Res., 289, 203-215, 1989.
7. DUNITZ J.D. - Phase transitions in molecular crystals from a chemical viewpoint. - Pure Appl. Chem., 63, 177-185, 1991.
8. HANCOCK B.C., ZOGRAFI G. - Characteristics and significance of the amorphous state in pharmaceutical systems. - J. Pharm. Sci., 86, 1-12, 1997.
9. BAUER M. - Le polymorphisme, son origine, ses caractéristiques, ses conséquences dans le domaine pharmaceutique. - STP Pharma Prat., 9, 5, 354-362, 1999.
10. THRELFALL T.L. - Analysis of organic polymorphs. A review. - Analyst, 120, 2435-1460, 1995.
11. CHAN H.K. - Polymorphic transformation of drugs under mechanical treatment. - Thèse, Université de Genève, 1986.
12. BORKA L. - Review of crystal polymorphism of substances in the European Pharmacopoeia. - Pharm. Acta Helv., 66, 16-28, 1991.
13. HENCK J.O., GRIESSER U.J., BURGER A. - Polymorphie von Arzneistoffen. Eine wirtschaftliche Herausforderung ? - Pharm. Ind., 59, 165-169, 1997
14. KOPP-KÜBEL S., BEYER C., GRAF E., KÜBEL F., DOELKER E. - Einfluss der Polymorphie von Phenobarbital auf Tabletteneigenschaften. - Eur. J. Pharm. Biopharm., 38, 17-25, 1992.
15. GERBER J.J., VANDERWATT J.G., LÖTTER A.P. - Physical characterization of solid forms of cyclopenthiazide. - Int. J. Pharm., 73, 137-145, 1991.
16. SUBATA M., KOKUBO H., MORIMOTO K. - X-ray structural studies and physicochemical properties of cimetidine polymorphism. - J. Pharm. Sci., 72, 1983.
17. KOKUBO H., MORIMOTO K., ISHIDA T., INOUE M., MORISAKA K. - Bioavailability and inhibitory effect for stress ulcer of cimetidine polymorphs in rats. - Int. J. Pharm., 35, 181-183, 1987.
18. BUXTON P.C., LYNCH I.R., ROE J.M. - Solid-state forms of paroxetine hydrochloride. - Int. J. Pharm., 42, 135-143, 1988.
19. LIN C.T., PERRIER P., CLAY G.G., SUTTON P.A., BYRN S.R. - Solid-state photooxidation of 21-cortisol tert-butylacetate to 21-cortisone tert-butylacetate. - J. Org. Chem., 47, 2978-2981, 1982.
20. WALKLING W.D., SISCO W.R., NEWTON M.P., FEEBLY B.J., PLAMPIN J.N., CHRZANOWSKI F.A. - Stability of fenretinide polymorphs. - Acta Pharm. Technol., 32, 10-12, 1986.
21. BYRN S.R., PFEIFFER R.R., STEPHENSON G., GRANT D.J.W., GLEASON W.B. - Solid-state pharmaceutical chemistry. - Chem. Mater., 6, 1148-1158, 1994.
22. BYRN S.R., PFEIFFER R.R., GANEY M., HOIBERG C., POOCHIKIAN G. - Pharmaceutical solids: A strategic approach to regulatory considerations. - Pharm. Res., 12, 945-954, 1995.
23. SURYANARAYANAN R., MITCHELL A.G. - Evaluation of two concepts of crystallinity using calcium gluceptate as a model compound. - Int. J. Pharm., 24, 1-17, 1985.
24. PHADNIS N.V., SURYANARAYANAN R. - Polymorphism in anhydrous theophylline - implications on the dissolution rate of theophylline tablets. - J. Pharm. Sci., 86, 1256-1263, 1997.
25. PONCHEL G., DUCHÊNE D., DOELKER E. - Influence de la taille particulaire et de l'habitus cristallin sur les caractéristiques de compression de la nitrofurantoïne, implications sur la résistance mécanique et la vitesse de dissolution des comprimés. - 4e Congrès international de technologie pharmaceutique (APGI), Paris, 1986, p. 105-114.
26. FACHAUX J.M., GUYOT-HERMANN A.M., GUYOT J.C., CONFLANT P., DRACHE M., HUVENNE J.P., BOUCHE R. - Compression ability improvement by solvation/desolvation process: application to paracetamol for direct compression. - Int. J. Pharm., 99, 99-107, 1993.
27. KAWASHIMA Y., MORISHIMA K., TAKEUCHI H. - Crystal design for direct tabletting and coating by the spherical crystallization technique. - AIChE Symposium Series, 87 (284), p. 26, 1991.
28. PINI A., FAZIO G., FERNÁNDEZ-HERVÁS M.J., HOLGADO M.A., RABASCO A.M. - Influence of crystallization solvent and dissolution behaviour for a diclofenac salt. - Int. J. Pharm., 121, 19-26, 1995.
29. MOSHARRAF M., NYSTRÖM C. - The effect of particle size and shape on the surface specific dissolution rate of microsized practically insoluble drugs. - Int. J. Pharm., 122, 35, 1995.
30. YORK P., GRANT D.J.W. - A disruption index for quantifying the solid state disorder induced by additives or impurities. I. Definition and evaluation from heat of fusion. - Int. J. Pharm., 25, 57-72, 1985.
31. GRANT D.J.W., YORK P. - A disruption index for quantifying the solid state disorder induced by additives or impurities. II. Evaluation from heat of solution. - Int. J. Pharm., 28, 103-112, 1986.
32. GRANT D.J.W., YORK P. - Entropy of processing: a new quantity for comparing the solid state disorder of pharmaceutical materials. - Int. J. Pharm., 30, 161-180, 1986.
33. PIKAL M.J., GRANT D.J.W. - A theoretical treatment of changes in energy and entropy of solids caused by additives or impurities in solid solution. - Int. J. Pharm., 39, 243-253, 1987.
34. BARTHELEMY C., DI MARTINO P., GUYOT-HERMANN A.M. - Influence of drying conditions on residual solvent contents in crystals. - Pharmazie, 40, 607-609, 1995.
35. BURGER A., GRIESSER U.J. - Influence of the degree of chemical purity on the transformation behaviour and physical stability of succinylsulfathiazole crystal forms. - Sci. Pharm., 58, 423-430, 1990.
36. LEFEBVRE-RINGARD C., GUYOT-HERMANN A.M., BOUCHÉ R., RINGARD J. - Répercussion de l'augmentation de solubilité de surface de particules sur leur aptitude à la granulation humide. - STP Pharma, 6, 228-232, 1990.
37. NEEDHAM G.F., PFEIFFER R.R., ENGEL G.L., RUTHERFORD B.S., ALLEN D.J. - Effect of impurities on estradiol crystallization in a sustained-release implant. - J. Pharm. Sci., 81, 1012-1014, 1992.
38. PEARSON J.T., VARNEY G. - The anomalous behaviour of some oxyclozanide polymorphs. - J. Pharm. Pharmacol., 25, Suppl., 62P-70P, 1973.
39. CHIOU W.J., KYLE L.E. - Differential thermal, solubility, and aging studies on various sources of digoxin and digitoxin powder: biopharmaceutical implications. - J. Pharm. Sci., 68, 1224-1229, 1979.
40. LI Z.J., GRANT D.J.W. - Effects of excess enantiomer on the crystal properties of a racemic compound: ephedrinium 2-naphthalenesulfonate. - Int. J. Pharm., 137, 21-31, 1996.
41. DUDDU S.P., FUNG F.K.Y., GRANT D.J.W. - Effect of the opposite enantiomer on the physicochemical properties of (-)-ephedrinium 2-naphthalenesulfonate crystals. - Int. J. Pharm., 94, 171-179, 1994.
42. FÜHRER C. - Crystal-engineering. - Acta Pharm. Technol., 32, 161-163, 1986.
43. LAW D., GRANT D.J.W. - Effect of doping with n-octanoic acid on the indices of tabletting performance of adipic acid. - Pharm. Res., 10, S-152, 1992.
44. CHOW A.H.L., HSIA C.K. - Modification of phenytoin crystals: influence of 3-acetoxymethyl-5,5-diphenylhydantoin on solution-phase crystallization and related crystal properties. - Int. J. Pharm., 75, 219-230, 1991.
45. GORDON J.D., CHOW A.H.L. - Modification of phenytoin crystals. II. Influence of 3-propanoyloxymethyl-5,5-diphenylhydantoin on solution-phase crystallization and related crystal properties. - Int. J. Pharm., 79, 171-181, 1992.
46. CHOW A.H.L., GORDON J.D., SZEITZ A., YOUNG J.W.M. - Modification of phenytoin crystals. III. Influence of 3-butanoyloxymethyl-5,5-diphenylhydantoin on solution-phase crystallization and related crystal properties. - Int. J. Pharm., 126, 11-19, 1995.
47. CHOW A.H.L., HSIA C.K., GORDON J.D., YOUNG J.W.M., VARGHA-BUTLER E.I. - Assessment of wettability and its relationship to the intrinsic dissolution rate of doped phenytoin crystals. - Int. J. Pharm., 126, 21-28, 1995.
48. CHOW A.H.L., CHOW P.K.K., ZHONGHAN W., GRANT D.J.W. - Modification of acetaminophen crystals: influence of growth in aqueous solutions containing p-acetoxyacetanilide on crystal properties. - Int. J. Pharm., 24, 239-258, 1985.
49. CHOW A.H.L., GRANT D.J.W. - Modification of acetaminophen crystals. II. Influence of stirring rate during solution-phase growth on crystal properties in the presence and absence of p-acetoxyacetaniilde. - Int. J. Pharm., 41, 29-39, 1988.

Material may be protected by copyright law (Title 17, U.S. Code)

UM00016599
NOVARTIS EXHIBIT 1517
Novartis v. Regents, IPR2023-01347
Page 3581 of 4460

50. CHAN H.K., GRANT D.J.W. - Influence of compaction on the intrinsic dissolution rate of modified acetaminophen and adipic acid crystals. - Int. J. Pharm., 57, 117-124, 1989.
51. FEMI-OYEWO M.N., SPRING M.S. - Studies on paracetamol crystals produced by growth in aqueous solutions. - Int. J. Pharm., 112, 17-28, 1994.
52. AL-MESHAL M., YORK P. - Studies on phenylbutazone-hydroxypropyl methylcellulose high energy compounds. - J. Pharm. Pharmacol., 36, 18P, 1984.
53. YORK P., AL-MESHAL M. - Crystallographic and chemical stability of modified phenylbutazone crystals containing low level polymer additives. - J. Pharm. Pharmacol., 38, 49P, 1986.
54. SANO A., KURIKI T., HANDA T., TAKEUCHI H., KAWASHIMA Y. - Particle design of tolbutamide in the presence of soluble polymer or surfactant by the spherical crystallization technique: improvement of dissolution rate. - J. Pharm. Sci., 76, 471-474, 1987.
55. HÜTTENRAUCH R. - Molekulargalenik als Grundlage moderner Arzneiformung. - Acta Pharm. Technol., 24, suppl. 6, 55-127, 1978.
56. HÜTTENRAUCH R. - Molecular pharmaceutics. - Pharm. Int., 3, 131-136, 1982.
57. KANENIWA N., OTSUKA M. - Effect of grinding on the transformations of polymorphs of chloramphenicol palmitate. - Chem. Pharm. Bull., 33, 1660-1668, 1985.
58. OTSUKA M., KANENIWA N. - Effect of seed crystals on solid-state transformation of polymorphs of chloramphenicol palmitate during grinding. - J. Pharm. Sci., 75, 506-511, 1986.
59. NAKAGAWA H., TAKAHASHI Y., SUGIMOTO I. - The effects of grinding and drying on the solid state stability of sodium prasterone sulfate. - Chem. Pharm. Bull., 30, 242-248, 1982.
60. HÜTTENRAUCH R., FRICKE S. - Mechano-chemical decomposition of drugs through galenic processes. - Int. J. Pharm., 3, 289-290, 1979.
61. OTSUKA M., MATSUMOTO T., KANENIWA N. - Effects of the mechanical energy of multi-tabletting compression on the polymorphic transformations of chlorpropamide. - J. Pharm. Pharmacol., 41, 665-669, 1989.
62. OTSUKA M., MATSUDA Y. - Effect of environmental temperature and compression energy of polymorphic transformation during tabletting. - Drug Dev. Ind. Pharm., 19, 2241-2269, 1993.
63. CHAN H.K., DOELKER E. - Polymorphic transformation of some drugs under compression. - Drug Dev. Ind. Pharm., 11, 315-332, 1985.
64. HÜTTENRAUCH R., FRICKE S., ZIELKE P. - Mechanical activation of pharmaceutical systems. - Pharm. Res., 2, 302-306, 1985.
65. KETOLAINEN J., POSO A., VIITASAARI V., GYNTHER J., PIRTTIMAKI J., LAINE E., PARONEN P. - Changes in solid-state structure of cyclophosphamide monohydrate induced by mechanical treatment and storage. - Pharm. Res., 12, 299-304, 1995.
66. BAUER-BRANDL A. - Polymorphic transitions of cimetidine during manufacture of solid dosage forms. - Int. J. Pharm., 140, 195-206, 1996.
67. BURGER A., BROX W., RATZ A.W. - Unterschiedliche Hygroskopizität von drei Kristallformen von Oxytetracyclinhydrochlorid und ihr Einfluss auf die Stabilität von Kapselpräparaten. - Acta Pharm. Technol., 31, 230-235, 1985.
68. BURGER A., RAMBERGER R., SCHMIDT W. - Nachhärtung und Zerfallscharakteristik bei Tabletten aus metastabilen polymorphen Modifikationen (Meprobamat). - Pharmazie, 35, 711, 1980.
69. LOWES M.M.J. - More information on hardening of carbamazepine tablets. - Am. J. Hosp. Pharm., 48, 2130-2131, 1991.
70. HERMAN J., REMON J.P., VISAVARUNGROJ N., SCHWARTZ J.B., KLINGER G.H. - Formation of theophylline monohydrate during the pelletisation of microcrystalline cellulose – anhydrous theophylline blends. Int. J. Pharm., 42, 15-18, 1988.
71. JOACHIM J., OPOTA D.O., JOACHIM G., REYNIER J.P., MONGES P., MAURY L. - Effect of solvate formation on lyoavailability of lorazepam during wet granulation. - STP Pharma, 5, 486-488, 1995.
72. LINDBERG N.O., LUNDSTEDT T. - Multivariate data analysis of variables influencing the dissolution rate of prednimustine: A case of disconformity with the Noyes-Whitney equation. - Eur. J. Pharm. Biopharm., 41, 101-113, 1995.

ADRESSE DE L'AUTEUR

Eric Doelker, Section de pharmacie, Université de Genève, Quai Ernest-Ansermet 30, 1211 Genève 4, Suisse.

CEBIPHAR

Votre partenaire privilégié

ETUDES DE STABILITÉ ICH

NOS CONDITIONS DE STOCKAGE :
• 4 chambres de stockage ICH standard :
34 m³ - 21 m³ - 12 m³ - 21 m³
• 3 enceintes 30°C - 70% HR.
• 1 enceinte ICH lumière.
• 1 enceinte contenants semi-perméables.

NOS INSTALLATIONS SONT QUALIFIÉES ET SÉCURISÉES.

NOS 20 ANS D'EXPÉRIENCE en développement pharmaceutique nous permettent de vous proposer des services sur mesure dans de nombreux domaines :
- Analyses physico-chimiques et microbiologiques.
- Développement et validation de méthodes.
- Constitution de Dossiers Pharmaceutiques, (partie II), DMF...
- Expertises pharmaceutiques.
- Conseil en développement pharmaceutique.

NOTRE DÉPARTEMENT ASSURANCE-QUALITÉ vous apporte le meilleur niveau de garantie.

Coupon réponse
Société : .....
Personne à contacter : .....
Fonction : .....
Adresse : .....
Tél. : .....
Fax : .....

A adresser à : CEBIPHAR
M. Christian MAGNET, Expert Pharmaceutique
BP 8 - 37230 FONDETTES
TÉL. : 02 47 42 48 48 - FAX : 02 47 42 03 28
email : cebiphar@ creaweb.fr

Material may be protected by copyright law (Title 17, U.S. Code)

UM00016600
NOVARTIS EXHIBIT 1517
Novartis v. Regents, IPR2023-01347
Page 3582 of 4460

This Page is Inserted by IFW Indexing and Scanning Operations and is not part of the Official Record

BEST AVAILABLE IMAGES

Defective images within this document are accurate representations of the original documents submitted by the applicant.

Defects in the images include but are not limited to the items checked:

- ☒ BLACK BORDERS
- ☐ IMAGE CUT OFF AT TOP, BOTTOM OR SIDES
- ☑ FADED TEXT OR DRAWING
- ☐ BLURRED OR ILLEGIBLE TEXT OR DRAWING
- ☐ SKEWED/SLANTED IMAGES
- ☐ COLOR OR BLACK AND WHITE PHOTOGRAPHS
- ☐ GRAY SCALE DOCUMENTS
- ☐ LINES OR MARKS ON ORIGINAL DOCUMENT
- ☐ REFERENCE(S) OR EXHIBIT(S) SUBMITTED ARE POOR QUALITY
- ☐ OTHER: _____

IMAGES ARE BEST AVAILABLE COPY.
As rescanning these documents will not correct the image problems checked, please do not report these problems to the IFW Image Problem Mailbox.

FOCUS ARTICLE

ChemComm
www.rsc.org/chemcomm

Are crystal structures predictable?

Jack D. Dunitz

Chemistry Department LOC, ETH-Hönggerberg, CH-8093 Zurich, Switzerland. E-mail: dunitz@org.chem.ethz.ch

The one-word answer to the title question is still "No", although at certain levels of discussion a "Maybe", or even a conditional "Yes", may be entertained as possible responses.

Are crystal structures predictable? Eight years ago, a terse monosyllabic negative reply to this question was given by Gavezzotti.[1] Has anything important happened since then to change the answer? Experts in the field have tried their skills in two blind tests and discussed their methods, together with their successes and failures, at two meetings organized by the Cambridge Crystallographic Data Centre in 1999 and 2001.[2,3] Although some successes were reported, no method gave consistently reliable predictions. How is it that, although physicists believe we are approaching a theory of everything, we still lack a theory of crystallization? Is the formation of a crystal more complicated and difficult to understand than the formation of the universe? Or do we mean different things when we say we understand crystallization or galaxy formation?

There is no problem about understanding *why* crystals form. The Gibbs equation $G = H - TS$ expresses the balance between the tendency towards maximal disorder of the molecules in a system and the opposing tendency for attractive intermolecular forces to bring the system into a state where its potential energy is minimized. As the temperature is lowered, the second tendency gains the upper hand. The attractive forces cause the system to condense into a liquid and on further cooling into the state of maximum order, which is crystalline. The entropy S of a perfectly ordered crystal is zero; the location of every molecule can in principle be described by an address, a set of numbers specifying its position in the three-dimensionally periodic array. In fact, real crystals are not perfectly ordered but this does not seriously affect the argument. Crystals form because the state of minimal potential energy is perfectly ordered.

Nowadays it is no great problem to calculate the potential energy of a crystal built from small to medium-sized organic molecules (with up to, say, 20–30 non-hydrogen atoms) by pairwise addition of atom-atom potentials, such as, *e.g.*, $E = \Sigma_i\Sigma_j A \exp(-BR_{ij}) - CR_{ij}^{-6}$ where R_{ij} is the distance between atoms i and j in different molecules. In the summation, i runs over the atoms of a reference molecule and j over atoms of all surrounding molecules. The exponential term represents the repulsion that sets in at short interatomic distance, and the inverse sixth power term represents the attraction in the form of a dispersion (van der Waals) interaction between the given atom pair. The parameters A, B, C need to be calibrated either against experimental data or theoretical calculations, and additional terms $q_iq_jR_{ij}^{-1}$ may be added to represent the electrostatic interaction between atoms with assigned charges at the nuclear positions. Usually the summation converges once the summation goes past the first coordination shell. For a stable crystal structure, E is negative, its first derivatives are zero, and its second derivatives are positive with respect to the various degrees of freedom.

Given a molecular structure, assumed for the moment to be rigid, why not simply calculate E for very many hypothetical crystalline arrangements and find the one with the lowest potential energy? Thousands (millions) of possible structures can be generated by grid search or random search techniques, or by systematic generation of dimers or strings of molecules over crystal space group symmetry elements, and these (or a selection of them) can be used as starting points for energy minimization calculations. The problem is that such calculations typically lead not to a single crystal structure that is much more stable than any of its competitors but rather to many possible crystal structures within a quite small energy range. This kind of result is compatible with the frequent occurrence of polymorphic forms of closely similar energy, but it is obtained also for compounds for which no

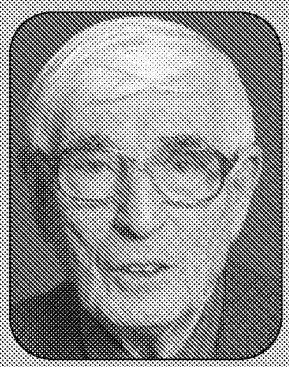

Jack Dunitz (b. 1923) studied chemistry at Glasgow University. After a decade of peripatetic research at Oxford University, Caltech, N.I.H. and the Royal Institution in London, in 1957 he was appointed Professor of Chemical Crystallography at the Swiss Federal Institute of Technology (E.T.H.) in Zurich, a position that he held until his retirement in 1990. As a survivor of the heroic age of X-ray crystallography before the advent of computers, automatic diffractometers and direct methods, he has witnessed how the subject has developed over the last half-century. He has written more than 350 scientific papers and is the author of *X-Ray Analysis and the Structure of Organic Molecules* (Cornell University Press, 1979; Verlag HCA, Basel, 1995) and *Reflections on Symmetry in Chemistry ... and Elsewhere* (with E. Heilbronner, Verlag HCA, Basel, 1993).

DOI: 10.1039/b211531j

This journal is © The Royal Society of Chemistry 2003

UM00016602
NOVARTIS EXHIBIT 1517
Novartis v. Regents, IPR2023-01347
Page 3584 of 4460

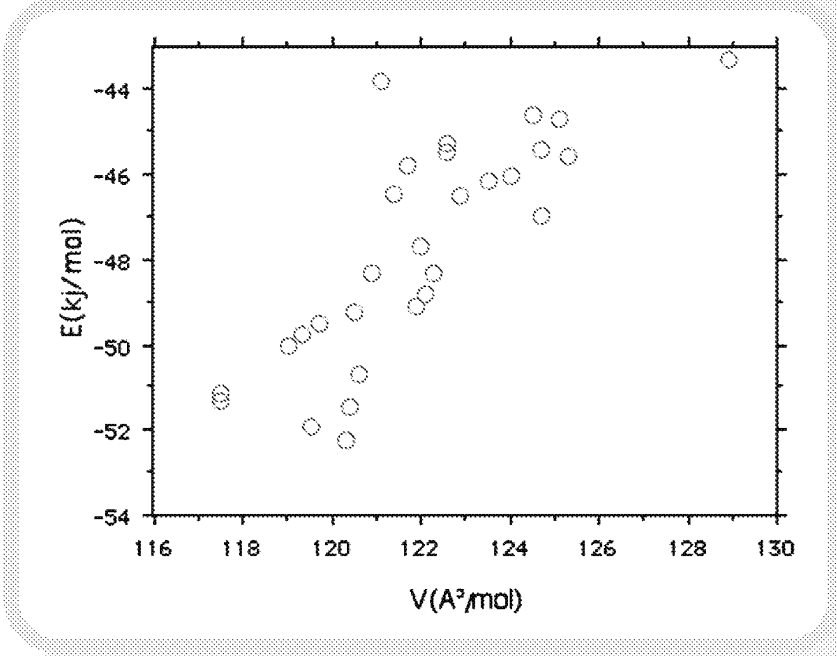

Fig. 1 Scatter plot of calculated lattice energy versus net molecular volume (unit cell volume divided by number of molecules in unit cell) for 30 possible crystal structures of benzene within an energy window of 10 kJ mol–1, based on results from ref. 6. Clearly low energy structures tend to be associated with tighter packing. The structure with the lowest lattice energy corresponds to the normal crystal structure of benzene, the one with the smallest volume to the structure at 25 kbar.

polymorphic forms are known.

For example, benzene. Under normal laboratory conditions benzene crystallizes in the orthorhombic space group *Pbca* and retains this structure down to very low temperatures.[4] At high pressure (circa 25 kbar) an alternative monoclinic structure is obtained.[5] According to a thorough recent study,[6] however, there are at least 30 possible crystal structures with calculated potential energies within a 10 kJ mol^{-1} range (Fig. 1). Indeed, the one with the lowest calculated energy corresponds to the known *Pbca* structure, but it is only a small fraction of a kJ mol^{-1} more stable that its nearest competitors. Also, the one with the highest calculated density corresponds to the known high-pressure structure.

The problem is not so much a matter of generating stable crystal structures but rather one of selecting one or more from many almost equi-energetic possibilities (Fig. 2). Fine details of the calculation and of the parametrization can easily alter the energy ranking. Moreover, the potential energies estimated by such force-field calculations refer to collections of atoms at rest and take no account of the fact that in the real crystal the molecules are vibrating about their equilibrium positions and orientations. It is possible to allow for the vibrational energies and entropies of the calculated structures by making suitable approximations but this does not usually lead to more confident predictions. On the contrary, the less tightly packed the structure, the higher the potential energy tends to be, and also the larger the vibrational entropy.[7] Thus a slightly less favorable potential energy can be compensated at 300 K by a more favorable entropy, and the energy ranking becomes even more uncertain. In any case, any prediction based on the calculated energy ranking would implicitly assume that crystal formation depends on thermodynamic factors rather than kinetic ones.

The question of *how* crystals form is even more problematic, that is to say, very little is known for certain and it is much more difficult to make realistic computer calculations. Crystallization is not an equilibrium process. It requires supercooling or supersaturation. At low degree of supercooling or supersaturation, molecular clusters are presumably being formed and dispersed. As supercooling or supersaturation increases, one type of cluster may tend to grow faster than the others, and such clusters may develop into crystal nuclei. This nucleation process is probably the rate-limiting step in crystal formation, but one may not assume that the fastest forming nuclei necessarily correspond to those of the most stable crystal structure. Indeed, there are many cases known where the crystals first formed from solution or from a melt do not correspond to the thermodynamically stable crystal under normal laboratory conditions.

Thus, computational methods for predicting crystal structures of organic compounds cannot yet be regarded as reliable. From a more qualitative and descriptive viewpoint has come the notion that certain groupings in organic molecules exercise attractive intermolecular interactions and so guide the molecules into distinctive patterns in their crystal structures — structure directing 'synthons'.[8] This indeed has become one of the tenets of crystal engineering. The prime example of a structure directing interaction is, of course, the hydrogen bond, an interaction that has been widened from its original sense (F–H…F⁻, O–H…O, N–H…O, etc.) to include gradually weaker interactions such as C–H…O, C–H…F, C–H…π, and so on into virtual nothingness. One can *describe* almost any observed crystal structure in terms of such interactions. The trouble with this approach is that its physical basis is shaky and its predictive capacity is poor. Of course, inspired guessing may occasionally lead to a correct prediction with any approach. Clearly, the preoccupation with those particular atoms or groupings on the peripheries of different molecules that come 'into contact' with one another is compatible with the r^{-6} dependence of the main attractive term in the usual atom-atom pair potentials referred to earlier (for any given interaction, a 12% increase in interatomic distance corresponds to a halving of the attraction energy).

Indeed, the atom-atom pair potentials described above place the main emphasis on dispersion energy as the dominating attraction term, with electrostatic energy appearing only as a correction term and then in a vastly oversimplified manner with assigned electric charges at the nuclear positions. In more elaborate models for individual molecules, electrostatic effects are expressed in terms of distributed multipoles to simulate not only atomic charges but also features such as lone pairs and π electrons.[9] However, the main emphasis is still provided by the repulsion–dispersion model, and crystal structure predictions using potentials based on the distributed multipole approach are only marginally more successful than those based on simple transferable atom–atom potentials.[2,3]

Very recently, Gavezzotti has described a new procedure for calculating intermolecular interaction energies by direct numerical integration over electron densities.[10] The method is being extended to the calculation of polarization, exchange

This journal is © The Royal Society of Chemistry 2003

UM00016603
NOVARTIS EXHIBIT 1517
Novartis v. Regents, IPR2023-01347
Page 3585 of 4460

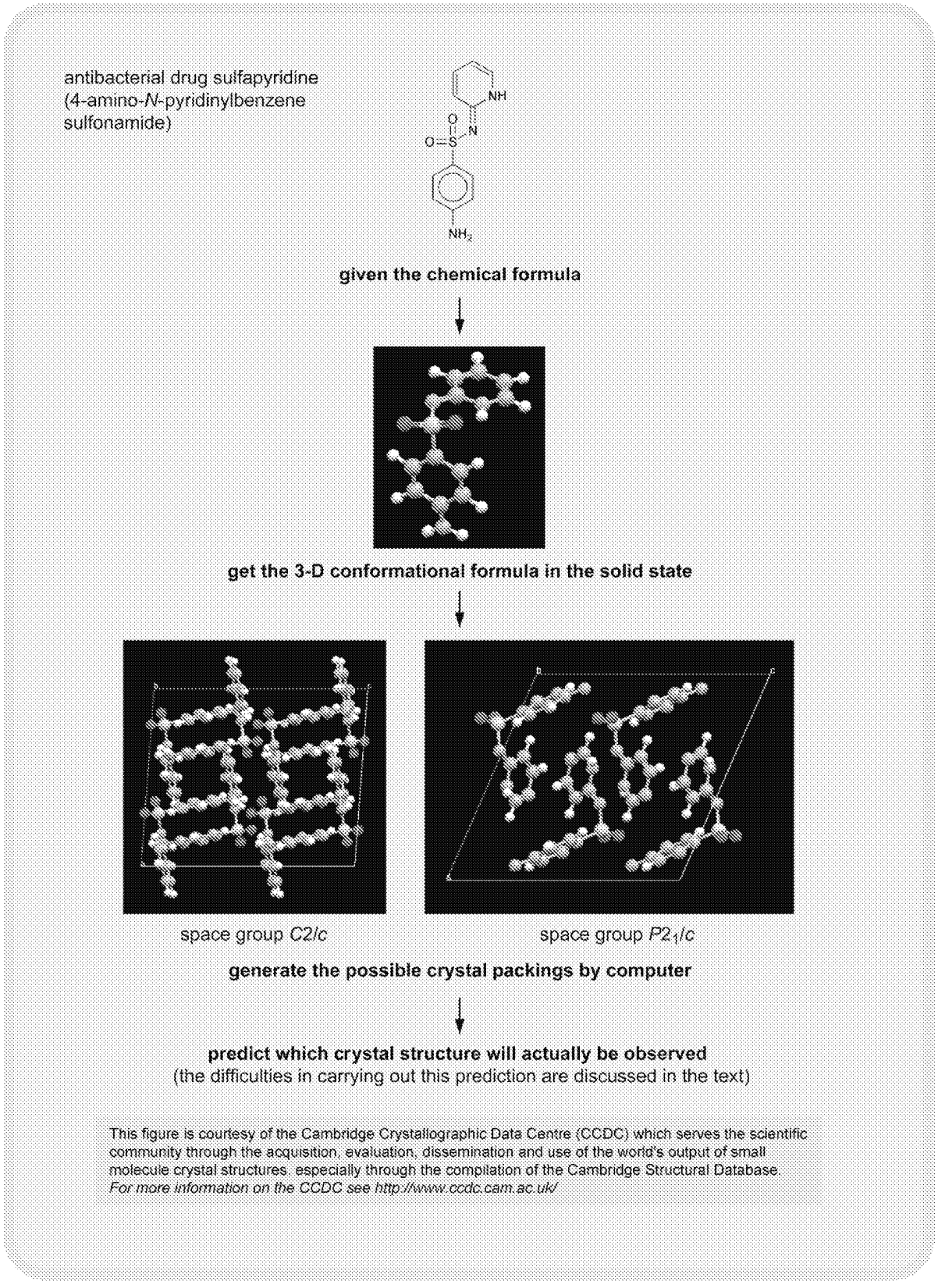

Fig. 2 Crystal structure prediction.

UM00016604
NOVARTIS EXHIBIT 1517
Novartis v. Regents, IPR2023-01347
Page 3586 of 4460

repulsion, and dispersion terms.[11] In place of the many adjustable parameters of atom-atom pair potential schemes, the new method includes only three disposable numerical parameters and seems to be applicable to a wide range of molecular systems. Sublimation energies of many organic crystals are well reproduced. Although destabilization and repulsion at very short distances are not correctly reproduced, the new method seems to provide reliable intermolecular energies at distances characteristic of molecular crystals, where 'penetration energy' arising from overlap of molecular electron densities is not necessarily repulsive. In particular, at such distances, electrostatic energies calculated with this procedure bear little relation to those obtained with point-charge or distributed multipole models. They are generally much larger. It is too early to judge whether this new approach will be more successful than others in the challenge of crystal structure prediction. What it does seem to show is that interpretations of intermolecular attractions and repulsions based mainly or exclusively on r^{-6} interactions between atoms in close contact may be misleading. In fact, it suggests that although the widely used atom-atom approximation is moderately successful in calculating packing energies of crystals, it lacks any sound physical basis. Does this matter?

What next? Doubtless we can look forward to improved force fields tailor-made for individual molecules. Better methods of converting 0 K potential energies into free energies would tell us about the temperatures where free-energy curves cross and hence about the range of thermodynamic stability of hypothetical crystal structures. Faster computing should enable extensions of these methods to more complex molecules with additional degrees of conformational freedom and also to co-crystals, including hydrates and other solvates. Thus, given a molecular formula, we should be able to obtain a list of perhaps 10–20 crystal structures within an energy window of a few kJ mol^{-1}, among which all observable polymorphs are likely to be found. Since energy differences between polymorphs are indeed often very small, we could then claim that the crystal structure problem is more or less solved. However, the ideally periodic structures that serve as models for the energy calculations are far from the physical reality. The free energies of real crystals depend on strains associated with defects and imperfections, accidents of their growth. To go any further with our predictions we would need to ask exactly what we are supposed to predict. How are the crystals to be prepared? By sublimation? By cooling the melt? From solution? In what solvent? At what temperature? At what cooling rate? Besides, it is well known that crystallization experiments are sometimes not reproducible, as witnessed by the phenomenon of 'disappearing polymorphs'.[12] We have a long way to go before we can think of predicting which polymorph will be obtained under any given circumstances.

There are obvious similarities between the crystal-packing problem and the protein-folding problem. Both involve delicate balances between attractions and repulsions at the atomic level, between potential energy and entropic contributions to the free energy, and between thermodynamic and kinetic factors. There are even analogies between the use of 'tailor-made additives' to inhibit formation of a more stable polymorph[13] and Nature's use of chaperone proteins to prevent improper associations and thus ensure biologically correct behavior of their charges.[14] If anything, the protein-folding problem may be even more difficult since it involves interactions between different side chains rather than between identical molecules. Moreover, to allow the flexibility necessary for function, the packing density in a protein molecule must be somewhat less than in a crystal, so even more structures may be attainable within a narrow energy range. The biggest difference, perhaps, is that because of its bio-medical importance vastly more money and effort is being invested in the protein-folding problem.

References

1 A. Gavezzotti, *Acc. Chem. Res*, 1994, **27**, 309.
2 J. P. M. Lommerse, W. D. S. Motherwell, H. L. Ammon, J. D. Dunitz, A. Gavezzotti, D. W. M. Hofmann, F. J. J. Leusen, W. T. M. Mooij, S. L. Price, B. Schweizer, M. U. Schmidt, B. P. van Eijck, P. Verwer and D. E. Williams, *Acta Crystallogr., Sect. B*, 2000, **56**, 697.
3 W. D. S. Motherwell, H. L. Ammon, J. D. Dunitz, A. Dzyabchenko, A. Gavezzotti, D. W. M. Hofmann, F. J. J. Leusen, J. P. M. Lommerse, W. T. M. Mooij, S. L. Price, H. Scheraga, B. Schweizer, M. U. Schmidt, B. P. van Eijck, P. Verwer and D. E. Williams, *Acta Crystallogr., Sect. B*, 2002, **58**, 647.
4 G. J. Jeffrey, J. R. Ruble, R. K. McMullan and J. A. Pople, *Proc. R. Soc. London, Ser. A*, 1987, **414**, 47.
5 G. J. Piermarini, A. D. Mighell, C. E. Weir and S. Block, *Science*, 1969, **165**, 1250.
6 B. P. van Eijck, A. L. Spek, W. T. M. Mooij and J. Kroon, *Acta Crystallogr., Sect. B*, 1998, **54**, 291.
7 J. D. Dunitz, G. Filippini and A. Gavezzotti, *Helv. Chim. Acta*, 2000, **83**, 2317.
8 G. R. Desiraju, *Angew. Chem. Int. Ed. Engl.*, 1995, **34**, 2311.
9 S. L. Price, *J. Chem. Soc., Faraday Trans*, 1996, **92**, 2997.
10 A. Gavezzotti, *J. Phys. Chem., Sect. B*, 2002, **106**, 4145.
11 A. Gavezzotti, personal communication.
12 J. D. Dunitz and J. Bernstein, *Acc. Chem. Res*, 1995, **28**, 193.
13 R. J. Davey, N. Blagden, G. D. Potts and R. Docherty, *J. Am. Chem. Soc*, 1997, **119**, 1767.
14 See, for example, D. Voet and J. G. Voet, *Biochemistry, 2nd Edition*, Wiley, New York, 1995, p. 201.

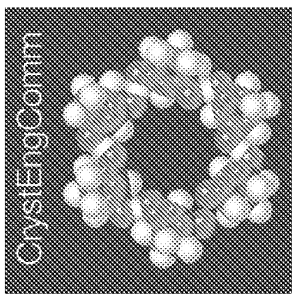

CrystEngComm (ISSN 1466-8033) is an electronic only journal from the Royal Society of Chemistry, dedicated to publishing full papers and communications describing innovative research convering all aspects of crystal engineering. The e-only nature of the journal allows research to be presented in ways that are not possible in printed journals. Authors are encouraged to use colour, movies and animated graphics.

See http://www.rsc.org/CrystEngComm for submission and subscription details.

This journal is © The Royal Society of Chemistry 2003

UM00016605
NOVARTIS EXHIBIT 1517
Novartis v. Regents, IPR2023-01347
Page 3587 of 4460

ISSN 0023-

АКАДЕМИЯ НАУК СССР

КРИСТАЛЛОГРАФИЯ

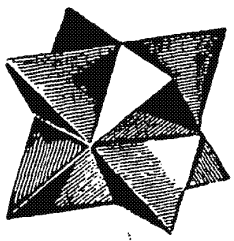

ТОМ 35
ВЫПУСК 3

·НАУКА·
1990

Best Available Copy

UM00016606
NOVARTIS EXHIBIT 1517
Novartis v. Regents, IPR2023-01347
Page 3588 of 4460

К Р И С Т А Л Л О Г Р А Ф И Я

Том 35 1990 Вып. 3

УДК 548.736

© 1990 г.

ДВОРКИН А. А., СИМОНОВ Ю. А., ЛИПКОВСКИЙ ЯНУШ,
ФОНАРЬ М. С., МАЛИНОВСКИЙ Т. И., ГАНИН Э. В.,
КОТЛЯР С. А.

КРИСТАЛЛИЧЕСКАЯ И МОЛЕКУЛЯРНАЯ СТРУКТУРА КОМПЛЕКСА 18-КРАУН-6 С 6-ХЛОР-7-СУЛЬФАМИДО-3,4-ДИГИДРО-1,2,4-БЕНЗО — ТИАДИАЗИН-1,1-ДИОКСИДОМ (ГИПОТИАЗИДОМ) СОСТАВА 1 : 1

Методом рентгеноструктурного анализа определено строение молекулярного комплекса 18-краун-6 с гипотиазидом с соотношением 1 : 1. Структура относится к комплексам типа «хозяин – гость». Особенностью вхождения гипотиазида в кристалл является его мостиковая функция. Впервые найдено, что иминогруппа циклической системы принимает участие в образовании Н-связей с эфирными атомами кислорода. В целом структура цепочечная.

При образовании соединений включения на основе краун-эфиров важным является вопрос о характере связывания «хозяина» (краун-эфира) и «гостя» (нейтральная протонодонорная молекула). В таких соединениях в формировании кристаллической структуры определяющим являются взаимодействия X—H ... O [1]. Характер взаимодействия зависит от нескольких факторов: природы донорных групп и их количества в молекуле «гостя» и стерических особенностей молекул «хозяина» и «гостя».

Оба этих фактора определяют типы образованных Н-связей, стехиометрию молекулярного комплекса и конформацию краун-эфира.

Предметом настоящей публикации является комплекс физиологически активного сульфамидного препарата гипотиазида (6-хлор-7-сульфамидо-3,4-дигидро-1,2,4-бензотиадиазин-1,1-диоксид) с конформационно подвижным краун-эфиром 18-краун-6. Для свободного 18-краун-6 характерно наличие «угловых» фрагментов с двумя *гош*-связями разного знака, сходящимися в них [2]. Такое строение стабилизирует конформацию посредством внутримолекулярных взаимодействий C—H ... O.

Для комплексов с «гостем», содержащим аминогруппу, характерны две конформации с симметрией D_{3d} («гости» — 4-нитроанилин, хлоротилсульфонамид [3, 4]) или C_i (2,4-динитроанилин, бензосульфамид [5, 6]). В последнем случае в краун-эфире имеют место угловые фрагменты типа *гош*$^{\pm}$, *гош*$^{\pm}$.

В гипотиазиде имеется два типа донорных групп — NH_2 (амино) и NH (имино), которые способны образовывать Н-связи с краун-эфиром. Вышеприведенные примеры [3—6] относятся к связыванию NH_2-групп. Литературные данные о связывании нейтральных молекул, имеющих два различных типа донорных групп, ограничены комплексом 18-краун-6 с монометилтиомочевиной [7]. Для выяснения стехиометрического соотношения «хозяин – гость», выявления характера связывания «гостя», конформационных особенностей 18-краун-6 предпринято рентгеноструктурное исследование.

Экспериментальная часть

Синтез комплекса проводили в ацетоне. В 200 мл ацетона при 56 С растворили 6-хлор-7-сульфамидо-3,4-дигидро-1,2,4-бензотиадиазин-1,1-диоксида 2,97 г (0,01 моль). К полученному раствору добавляли 2,65 г

Коор

Атом
S1A
S2A
Cl
O1A
O2A
O3A
O4A
N1A
C1A
C2A
C3A
C4A
C5A
C6A
C7A
N2A
N3A
O1
C2
C3
O4
C5
C6
O7
C8
C9
O10
C11
C12
O13
C14
C15
O16
C17
C18

(0,01 моль) 18-краун-6, ра
и оставляли кристаллизо
кристаллы промывали аце

Бесцветные прозрачны
изопропаноле плавятся с
29, KBr), ν, см$^{-1}$: 33 330
1340 (Ar), 1340 (SO_2), 11
δ, м.д.: 3,56 с (24H, H_2C
Результаты химического
S — 11:50, вычислено, %: N

Для рентгеноструктурн
тического габитуса с разм
моноклинной сингонии с п
b=10.172(6), c=15,023(7
$C_{19}H_{32}ClO_5N_3S_2$, ρ(выч)=
получен в дифрактометре
вано 2762 отражения, 254
тов. Сканирование прово
8°/мин. $(\sin\theta/\lambda)_{max}$=0.6 А
ках программы SHELXS-8
для неводородных атомов
экспериментальной весовой
координаты базисных а

Best Available Copy

UM00016607
NOVARTIS EXHIBIT 1517
Novartis v. Regents, IPR2023-01347
Page 3589 of 4460

Таблица 1

Координаты базисных атомов (×10⁴)

Атом	x/a	y/b	z/c
S1A	1740(1)	901(1)	4239(1)
S2A	3678(1)	3272(2)	4229(1)
Cl	2156(1)	6559(1)	3691(1)
O1A	1650(2)	777(4)	5175(2)
O2A	2349(2)	−371(4)	3774(2)
O3A	3612(2)	4515(4)	4750(2)
O4A	4121(2)	1774(4)	4571(2)
N1A	4059(2)	3313(4)	3294(2)
C1A	2712(2)	3567(5)	4057(3)
C2A	2068(2)	4939(5)	3836(3)
C3A	1329(3)	5111(5)	3719(3)
C4A	1199(2)	3882(5)	3852(3)
C5A	1853(2)	2491(5)	4073(3)
C6A	2594(2)	2352(5)	4162(3)
C7A	291(3)	2894(6)	4024(3)
N2A	908(2)	1374(4)	3760(2)
N3A	460(2)	4085(4)	3775(2)
O1	4843(2)	6042(3)	2793(2)
C2	5373(3)	5624(6)	3539(4)
C3	5657(4)	4098(7)	3846(3)
O4	6093(2)	2985(4)	3262(2)
C5	6582(3)	1544(6)	3633(4)
C6	6202(3)	633(6)	3832(3)
O7	5930(2)	308(4)	3036(2)
C8	5622(3)	−686(5)	3176(3)
C9	5233(3)	−753(5)	2348(3)
O10	5430(2)	610(4)	2216(2)
C11	4153(3)	652(6)	1396(4)
C12	3398(3)	2081(6)	1345(3)
O13	3553(2)	3300(4)	1300(2)
C14	2870(3)	4699(6)	1362(3)
C15	3069(3)	5938(6)	1308(3)
O16	3545(2)	5856(3)	2058(2)
C17	3555(3)	7222(5)	2222(3)
C18	4052(3)	7011(5)	3020(3)

(0,01 моль) 18-краун-6, растворенного в 20 мл ацетона, защищали от пыли и оставляли кристаллизоваться при комнатной температуре. Выпавшие кристаллы промывали ацетоном и сушили на воздухе.

Бесцветные прозрачные кристаллы растворяются в ацетоне, метаноле, изопропаноле плавятся с разложением при 209–211° С. ИК спектр (ИКС 29, KBr), ν, см$^{-1}$: 33330–3000 (N–H), 2970–2850 (C–H), 1575 (Ar), 1340 (Ar), 1340 (SO_2), 1110 (C–O–C и Ar–Cl). ПМР-спектр (CF_3COOH), δ, м.д.: 3,56 с (24H, H_2CO), 4,76 с (2H, HCN), 7,02–8,02 с (2H, Ar). Результаты химического анализа: найдено, % для комплекса: N – 7,55, S – 11,50, вычислено, %: N – 7,48, S – 11,41.

Для рентгеноструктурного исследования отобран монокристалл призматического габитуса с размерами 0,3×0,4×0,6 мм. Кристалл относится к моноклинной сингонии с параметрами элементарной ячейки a=19,533(11), b=10,172(6), c=15,023(7) Å, γ=60,79(3)°, пр.гр. $P2_1/a$, Z=4 состава $C_{19}H_{32}ClO_5N_3S_2$, ρ(выч)=1,422(8) гсм$^{-3}$. Экспериментальный материал получен в дифрактометре РЭД-4 на MoK_α-излучении. Всего зарегистрировано 2762 отражения, 2545 из которых с $I \geqslant 3\sigma$ использованы для расчетов. Сканирование проводилось ω-методом с постоянной скоростью 8°/мин, $(\sin\theta/\lambda)_{max}$=0,6 Å^{-1}. Структура решена прямым методом в рамках программы SHELXS-86 и уточнена МНК в анизотропном варианте для неводородных атомов и изотропном для атомов водорода с учетом экспериментальной весовой схемы, R=0,053 (R_w=0,041).

Координаты базисных атомов приведены в табл. 1.

Best Available Copy

UM00016608
NOVARTIS EXHIBIT 1517
Novartis v. Regents, IPR2023-01347
Page 3590 of 4460

Описание и обсуждение структуры

В результате проведенного рентгеноструктурного анализа установлено, что в структуре реализован молекулярный комплекс «хозяин – гость» 1 : 1. Фрагмент кристаллической структуры в проекции на плоскость гетероатомов макроцикла представлен на рисунке. Молекулы «гостя» соединяют молекулы «краун-эфира» связями NH...O между амино-группами сульфамидного фрагмента гипотиазида и NH-группами краун-эфира. Эфирные атомы кислорода O10 и O16 участвуют в водородной связи с NH_2-группой «гостя» через H-связи N1*A*–H...O16 2,935 Å (O...H 2,04 Å, угол при H 156°) и N1*A*–H...O10 2,925 Å (1,99 Å и 179°) соответственно. Топологически NH_2-группа соответствует фрагменту O10...O16 в

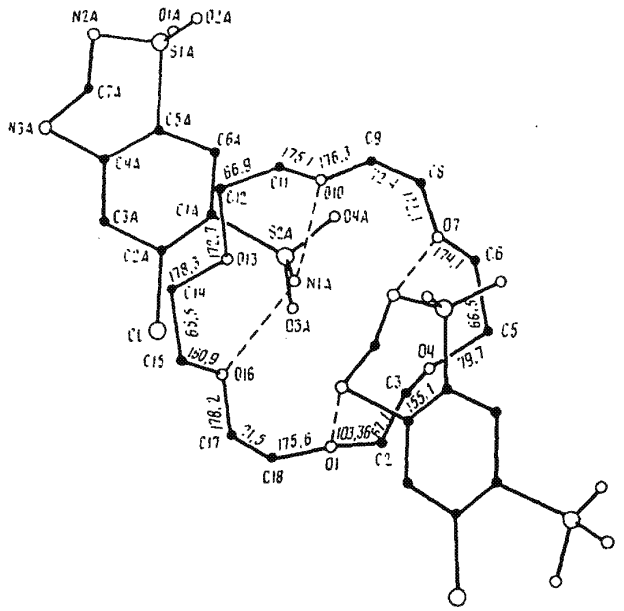

Проекция фрагмента структуры на плоскость эфирных атомов O
Указаны значения торсионных углов (град)

краун-эфире. Подобная ситуация реализована и в большинстве других структур [3–6], упомянутых выше.

Во взаимодействии с O1 и O7 принимает участие ...N3*A*–C7*A*–N2*A*... фрагмент молекулы «гостя» через H-связи: N2*A*–H...O7 2,901 Å (O...H 1,90 Å, угол при H 151°) и N3*A*–H...O1 2,936 Å (2,04 Å, 152°). Донорные группы разделены CH_2-группой (C7) и для топологического соответствия «гостя» и «хозяина» необходимо раздвинуть акцепторные атомы краун-эфира. Таким образом, молекула «гостя» соединяет два краун-эфира – базисный и полученный преобразованием симметрии $x-1/2, y, -z+1/2$. При этом получается полимерная цепочка, направленная вдоль оси x кристалла. Необычным способом связывания определяется необычная конформация молекулы 18-краун-6. Отметим сразу новый набор торсионных углов по связям, существенно отличный как для симметрии D_{3d}, так и для C_i. Если фрагмент краун-эфира ...C6–O7...C18–O1... составлен из оксиэтиленовых фрагментов O–CH_2–CH_2 с *гош-транс*-конфигурацией, то в оставшейся части имеют место существенные конформационные напряжения. Так, по связям O4–C5 и O1–C2 реализуются ротамеры с торсионными углами 82,7 и 105,5°. Кроме того, значение торсионного угла по связи C3–O4 более чем на 20° отличается от идеаль-

Межатомные р

	Рассто
N1*A*–O10	2,9
N1*A*–O16	2,9
O1–C2	1,4
C2–C3	1,4
C3–C4	1,3
O4–C5	1,4
C5–C6	1,4
C6–C7	1,4
O7–C8	1,4
C8–C9	1,4
C9–O10	1,4
C18O1C2	113,6
O1C2C3	114,1
C2C3O4	116,4
C3O4C5	116,1
O4C5C6	115,9
C5C6O7	109,7
C6O7C8	112,3
O7C8C9	108,3
C8C9O10	110,4
C1*A*–C2*A*	1,3
C2*A*–C3*A*	1,3
C3*A*–C4*A*	1,4
C4*A*–C5*A*	1,4
C5*A*–C6*A*	1,3
C6*A*–C1*A*	1,3
C1*A*–S2*A*	1,7
S2*A*–N1*A*	1,5
S2*A*–O3*A*	1,4
O1*A*S1*A*O2*A*	118,6
O1*A*S1*A*C5*A*	107,3
O1*A*S1*A*N2*A*	108,2
O2*A*S1*A*C5*A*	109,8
O2*A*S1*A*N2*A*	108,6
C5*A*S1*A*N2*A*	102,8
O3*A*S2*A*O4*A*	119,2
O3*A*S2*A*C1*A*	107,3
O3*A*S2*A*N1*A*	107,3
O4*A*S2*A*C1*A*	105,7
O4*A*S2*A*N1*A*	107,1
C1*A*S2*A*N1*A*	109,6
S2*A*C1*A*C2*A*	124,7
S2*A*C1*A*C6*A*	117,5
C2*A*C1*A*C6*A*	117,7

ного значения 180°. Такая искажениям в молекуле кр аннулярных расстояниях O 5,155 Å.

Таким образом, методом присоединения «гостя» чер кой конформационной под вающейся к особенностям г

Межатомные расстояния эфира средние расстояния для этой молекулы [3–6]. рода в цепи увеличены до нековалентными внутримолек ра. Эфирные атомы O суще кулы. Отклонения лежат в

В молекуле гипотиазида

Best Available Copy

UM00016609
NOVARTIS EXHIBIT 1517
Novartis v. Regents, IPR2023-01347
Page 3591 of 4460

Таблица 2

Межатомные расстояния (Å) и валентные углы (град)

Расстояния донор — акцептор в Н-связях			
N1A–O10	2,925	N2A–O7	2,901
N1A–O16	2,935	N3A–O1	2,936
Краун-эфир			
O1–C2	1,442(7)	O10–C11	1,426(7)
C2–C3	1,446(8)	C11–C12	1,484(8)
C3–C4	1,356(7)	C12–O13	1,414(7)
O4–C5	1,416(7)	O13–C14	1,400(6)
C5–C6	1,474(9)	C14–C15	1,493(8)
C6–C7	1,411(6)	C15–O16	1,437(6)
O7–C8	1,422(7)	O16–C17	1,419(6)
C8–C9	1,477(7)	C17–C18	1,492(7)
C9–O10	1,409(6)	C18–O1	1,410(6)
C18O1C2	113,6(4)	C9O10C11	113,0(4)
O1C2C3	114,1(5)	O10C11C12	109,0(5)
C2C3O4	116,4(5)	C11C12O13	109,0(5)
C3O4C5	116,1(5)	C12O13C14	112,4(4)
O4C5C6	115,9(5)	O13C14C15	110,0(4)
C5C6O7	109,7(5)	C14C15O16	109,6(4)
C6O7C8	112,3(4)	C15O16C17	113,3(4)
O7C8C9	108,3(4)	O16C17C18	108,4(4)
C8C9O10	110,4(4)	C17C18O1	108,7(4)
Молекула гипотиазида			
C1A–C2A	1,388(6)	S2A–O4A	1,431(4)
C2A–C3A	1,377(8)	C2A–Cl	1,752(5)
C3A–C4A	1,406(7)	C4A–N3A	1,360(7)
C4A–C5A	1,406(6)	N3A–C7A	1,451(7)
C5A–C6A	1,390(7)	C7A–N2A	1,477(6)
C6A–C1A	1,372(7)	N2A–S1A	1,621(5)
C1A–S2A	1,779(5)	S1A–C5A	1,753(5)
S2A–N1A	1,599(4)	S1A–O1A	1,430(3)
S2A–O3A	1,438(4)	S1A–O2A	1,440(4)
O1AS1AO2A	118,6(2)	ClC2AC1A	121,2(4)
O1AS1AC5A	107,3(2)	ClC2AC3A	116,2(4)
O1AS1AN2A	108,2(2)	C1AC2AC3A	122,5(5)
O2AS1AC5A	109,8(2)	C2AC3AC4A	120,0(4)
O2AS1AN2A	108,6(2)	C3AC4AC5A	117,3(4)
C5AS1AN2A	102,8(2)	C3AC4AN3A	119,4(4)
O3AS2AO4A	119,2(2)	C5AC4AN3A	123,2(4)
O3AS2AC1A	107,3(2)	S1ACHAC4A	120,0(3)
O3AS2AN1A	107,3(2)	S1AC5AC6A	119,0(3)
O4AS2AC1A	105,7(2)	C4AC5AC6A	120,9(4)
O4AS2AN1A	107,1(2)	C1AC6AC5A	121,3(4)
C1AS2AN1A	109,6(2)	C4AN3AC7A	120,5(4)
S2AC1AC2A	124,7(4)	N3AC7AN2A	113,7(4)
S2AC1AC6A	117,5(3)	S1AN2AC7A	112,2(3)
C2AC1AC6A	117,7(4)		

ного значения 180°. Такая конформация цикла приводит к линейным искажениям в молекуле краун-эфира и существенным различиям в *транс*-аннулярных расстояниях O . . . O. Так, O10 . . . O16 равно 4,713, а O1–O7 — 5,155 Å.

Таким образом, методом рентгеноструктурного анализа доказан факт присоединения «гостя» через различные донорные группы и факт высокой конформационной подвижности молекулы 18-краун-6, приспосабливающейся к особенностям геометрии «гостя».

Межатомные расстояния в комплексе приведены в табл. 2. Для краун-эфира средние расстояния C–O равны 1,43, C–C 1,50 Å, что характерно для этой молекулы [3–6]. Некоторые валентные углы при атомах углерода в цепи увеличены до 114,1° (табл. 2). Такое увеличение связано с нековалентными внутримолекулярными контактами в молекуле краун-эфира. Эфирные атомы O существенно выходят из средней плоскости молекулы. Отклонения лежат в пределах от −0,280(O16) до +0,394(O13) Å.

В молекуле гипотиазида ароматический цикл плоский со средними рас-

Best Available Copy

UM00016610
NOVARTIS EXHIBIT 1517
Novartis v. Regents, IPR2023-01347
Page 3592 of 4460

стояниями C–O 1,39 Å и эндоциклическими углами от 118,0 до 123,5°. Широкий диапазон угловых характеристик определяется разной природой заместителей в цикле. Гетероцикл имеет конформацию конверта с выходом из плоского фрагмента N2A на 0,644 Å. Угол между циклами в молекуле равен 4,9°. Расстояния в сульфамидных группах обычные.

Между собой цепи связаны ван-дер-ваальсовскими взаимодействиями.

Список литературы

1. *Weber E.* // Progress in macrocyclic chemistry. V. 3. Ed. *R. M. Izatt, J. J. Christensen*, New York: Wiley, 1987. P. 337.
2. *Maverick E., Seiler P., Schweizer W. B., Dunitz J. D.* // Acta cryst. 1980. V. B36. P. 615.
3. *Weber G.* // Z. Naturforsch. 1981. B. B36. S. 896.
4. *Elvasyouny A., Brügge H. J., von Deuten K. et al.* // J. Amer. Chem. Soc. 1983. V. 105. P. 6568.
5. *Weber G., Sheldrick G. M.* // Acta cryst. 1981. V. B37. P. 2108.
6. *Knöchel A., Kopf J., Oechler J. et al.* // J. Chem. Soc. Chem. Commun. 1978. P. 595.
7. *Watson W. H., Galloy J., Grossie D. A. et al.* // J. Organ. Chem. 1984. V. 49. P. 347.

Институт прикладной физики
АН МССР
Институт физической химии
ПАН, Варшава

Поступила в редакцию
26.09.1988

К Р И С
Том 35

УДК 548.736.5

© 1990 г.

ОБОДОВСКАЯ А
ИВАНОВ Ю. А

КРИСТАЛЛИЧЕСКАЯ
2,2,4-ТРИМ

Рентгеноструктурным ис
дигидрохинолина представля
лекула неплоская – угол ме
и ТГХ) 88,0°. Геометрия и
ются от найденных в соотв
можные причины неравноце
в реакциях ацилирования и

Впервые димер 2,2,4-т
получен в 1938 г. [1]. Д
димеру приписывали стр
рые соответствуют прин
жению 3,4′ (А) или 6,4′ (

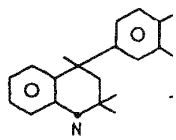

Б

С целью установлени
структурное исследовани
из этанола, $T_{пл}$=93–95°.

Съемка, расшифровка
фрактометрической систе
монохроматор, ω/2θ-скани

С кристалла размером
(θ_{max}=26°). Параметры м
c=16,050(6) Å, β=99,43(

Структура решена пр
лучшими оценками найде
и атомы H локализованы
МНК (1105 отражений с
поэтапно: сначала уточне
том атомов H, а затем ат
атомов. Окончательные з
c=0,66(2)·10⁻⁶, R=0,051,

Координаты атомов пр
рис. 1, длины связей и в
кулы – на рис. 3 и 4.

Димер представляет со
тетрагидрохинолин-4′)-1,2
формуле Б. Молекула неп
тичными плоскостями ди
ветственно ДГХ и ТГХ) 8

Best Available Copy

UM00016611
NOVARTIS EXHIBIT 1517
Novartis v. Regents, IPR2023-01347
Page 3593 of 4460

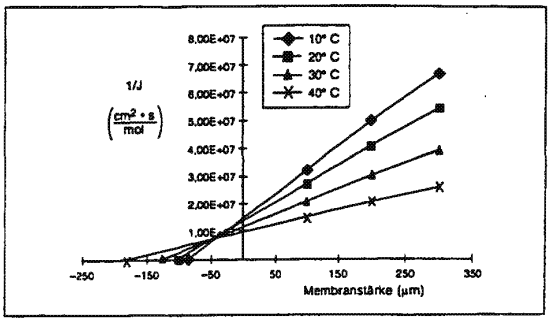

Abb. 7: Darstellung des reziproken Flusses gegen die Membranstärke für das Modell Kaliumchlorid/Wasser

tionswiderstands erfolgte aus den reziproken Diffusionsflüssen für die Schichtdicke x = 0 (Abb. 7).
Die errechneten Permeationsgrößen sind in Tabelle 2 aufgelistet.

Tabelle 2: Permeationswerte für die ungerührten Schichten im KCl-Modell

Temperatur (°C)	1/J (10^{-7} cm² · s/mol)	J (10^{-8} mol/cm² · s)	P (10^{-4} cm/s)	R (s/cm)
10	1,49	6,71	6,71	1490
20	1,35	7,40	7,40	1350
30	1,15	8,69	8,69	1150
40	0,965	10,36	10,36	965

Der Anteil der ungerührten Schichten am Gesamtpermeationswiderstand bei den Untersuchungen mit den amphiphilen Netzwerken lag je nach Temperatur, Membrandicke und Permeabilität zwischen 0,1% und 3%.

3. Diskussion

Die vorgestellte Diffusionszelle hat sich in der Praxis bewährt. Dies beruht auf der einfachen Variation von einzelnen Faktoren wie beispielsweise Akzeptor/Donatorvolumina, Rührbedingungen, Einsatz verschiedener Medien und Membranmaterialien sowie an dem relativ geringen apparativen Aufwand.
Untersuchungen mit unterschiedlichen Medien haben gezeigt, daß der Anteil der ungerührten Schichten am Gesamtwiderstand bei der verwendeten Apparatur erhebliche Ausmaße (bis zu 15%, je nach Versuchsbedingungen) annehmen kann. Aufgrund der Abhängigkeit des Permeationswiderstandes dieser „Bereiche ohne Konvektion" von der Temperatur, vom Medium, v m untersuchten Stoff, von den Rührbedingungen und v n der Geometrie der Diffusionszelle können Abschätzungen nicht zu befriedigenden Ergebnissen führen. Es muß daher grundsätzlich die Bestimmung des Widerstandes der ungerührten Schichten im Rahmen von Diffusionsexperimenten empfohlen werden.

4. Experimenteller Teil

Die Rührgeschwindigkeiten für alle Diffusionsmodelle und Versuche waren gleich und wurden konstant gehalten (100 U/min). Es wurden jeweils Rührstäbe der gleichen Größe und Geometrie eingesetzt.

4.1. Bestimmung der ungerührten Schichten

Für die Bestimmung wurde Dialysierschlauch mit Schichtdicken von 0,1 mm, 0,2 mm und 0,3 mm verwendet. Es wurden Messungen bei vier unterschiedlichen Temperaturen (10 °C, 20 °C, 30 °C, 40 °C) durchgeführt. Der Diffusionsfluß wurde über einen Zeitraum von mindestens 3 h gemessen. Jede Messung wurde mindestens dreimal wiederholt.

4.2. Flavon-Modell

Die Meßdauer für einen Temperaturwert betrug 3 h.
Akzeptor: 100 ml Paraffin. Donator: ca. 5 ml Paraffin. Donatorkonzentration: 0,1 mmol/l Flavon.
Die Ermittlung der Konzentration erfolgte diskontinuierlich im Abstand von etwa 20 min UV-spektrometrisch bei λ = 252 nm.

4.3. KCl-Modell

Die Volumina betrugen 600 ml für den Akzeptor und ca. 8 ml für den Donator. Die eingesetzte Donator-Konzentration war 0,1 h KCl. Die Bestimmung des Diffusionsflusses erfolgte durch kontinuierliche Messung der Leitfähigkeitsänderung im Donatorkompartiment. Dazu wurde eine WTW LTA-100-Leitfähigkeitsmeßzelle eingesetzt. Die Meßdauer für einen Temperaturwert betrug mindestens 3 h.

Literatur

1 Barry, P. H., Diamond, J. M.: Physiol. Rev. 64, 763 (1984)
2 Ginzburg, B. Z.; Katachalsky, A.: J. Gen. Physiol. 47, 403 (1963)
3 Trautmann, H.: Diss. Univ. Freiburg 1990
4 Hermes, R.; Bauer K. H.: Pharmazie 50, 481 (1995)

Eingegangen am 4. Dezember 1995
Angenommen am 16. Februar 1996

Prof. Dr. K. H. Bauer
FMF Freiburger Material-Forschungszentrum
Stefan-Meierstr. 21
D-79104 Freiburg

Department of Pharmaceutical Sciences, National Research Centre, Dokki, Cairo, Egypt

Physico-chemical characteristics of carbamazepine-β-cyclodextrin inclusion compounds and carbamazepine-PEG solid dispersions

S.A. El-Nahhas

[PD. 00/12/96
p-960 - 963 = (4)]

Carbamazepine (CBZ) was found to form an inclusion complex with β-cyclodextrin (β-CD). The solubility of CBZ increased on addition of β-CD displaying a linear relationship. A stability constant of 404 mol^{-1} was calculated. The complex obtained had a stoichiometry of 1:1. A comparison of the complex was carried out with polyethylene glycol 6000 solid dispersion prepared by either the comelting or coevaporate method using IR spectrophotometry and differential thermal analysis. Dissolution profiles in 0.1 N HCl medium of CBZ-comelt, coevoporate and inclusion complex demonstrated a faster dissolution rate of the inclusion complex compared to solid dispersions and CBZ alone.

NSDOCID: <XP 633833A I >

UM00016612
NOVARTIS EXHIBIT 1517
Novartis v. Regents, IPR2023-01347
Page 3594 of 4460

Physikochemische Charakteristiken von β-Cycl dextrin-Einschlußverbindungen und festen Polyethylenglycol-Dispersionen des Carbamazepins

Carbamazepin (CBZ) bildet einen 1 : 1-Einschlußkomplex mit β-Cyclodextrin (β-CD). Die Löslichkeit von CBZ wächst linear mit der Zugabe von β-CD. Für den Komplex wurde eine Stabilitätskonstante von 404 mol^{-1} ermittelt. Die IR- und DTA-Befunde des Komplexes wurden mit denen von CBZ-Polyethylenglycol(PEG)-6000-Dispersionen, hergestellt durch Schmelz- oder Coevaporationsverfahren, verglichen. Die Dissolution in 0,1 HCl verläuft beim β-CD-Komplex schneller als bei den PEG-Dispersionen.

1. Introduction

Since the first description of a solid dispersion in order to increase the dissolution and oral absorption of poorly water soluble drugs by Sekiguchi et al. [1], the tremendous amount of research carried out in this field led only to a very limited range of patented products on the world market. More recently, complexation with cyclodextrin has been extensively applied to improve the solubility, stability and bioavailability of various drugs [2–4].

The objective of the present study was to investigate the potentiality of interaction of carbamazepine (CBZ), a practically insoluble drug with β-cyclodextrin (β-CD) and to assess the implication of such an interaction on improving certain pharmaceutical properties of the drug. On the other hand, comparing the results with those achieved via dispersing the drug with polyethylene glycol (PEG 6000) in the form of a comelt or a coevaporate was a major objective.

2. Investigations, results and discussion

2.1. Potentiality of interaction of carbamazepine with β-cyclodextrin

A differential UV absorption spectrum of CBZ solution was monitored in presence of different concentrations of β-CD. The extinction of the drug is remarkably increased as a function of the β-CD concentration. Also, there is a bathochromic shift in the λ_{max} of the drug in presence of β-CD from 285 to 288 nm. These spectral changes most probably reflect a sort of molecular interaction between the drug and β-CD.

The absorbance of a solution of a fixed total concentration (0.03 mmol/l) and different mole fractions of CBZ and β-CD was measured at 285 nm. The difference between the measured absorbance values and those expected if no complexation takes place, as a function of the mole fraction is illustrated in Fig. 1. Since for a constant total concentrations of the two species of a complex, the complex is at its high concentration at the point which they occur in the complex, it can be concluded that CBZ forms an 1 : 1 complex with β-CD.

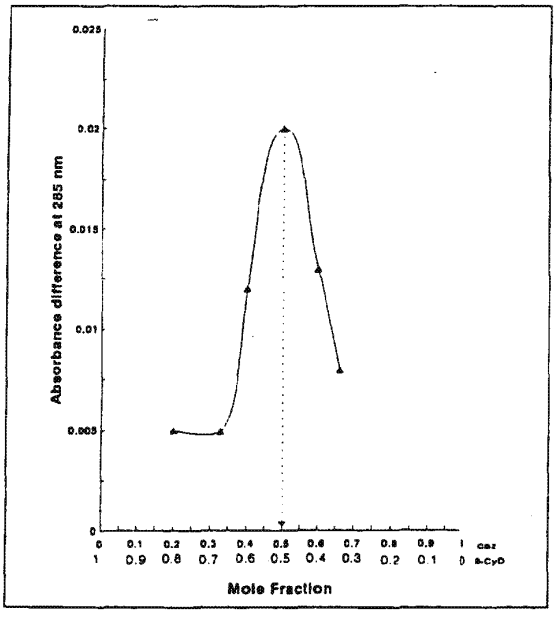

Fig. 1: Elucidation of the stoichiometric ratio of carbamazepine-β-cyclodextrin complex by the spectrophotometric method

2.2. Phase solubility

The graphical representation of the amount of CBZ dissolved as a function of β-CD concentration reveals enhancement of water-solubility of the drug in presence of β-CD (Fig. 2). The solubility increased with an increasing β-CD concentration, whereby a linear relationship exists between the maximum additive concentration of the drug and β-CD concentration. The stability constant of the

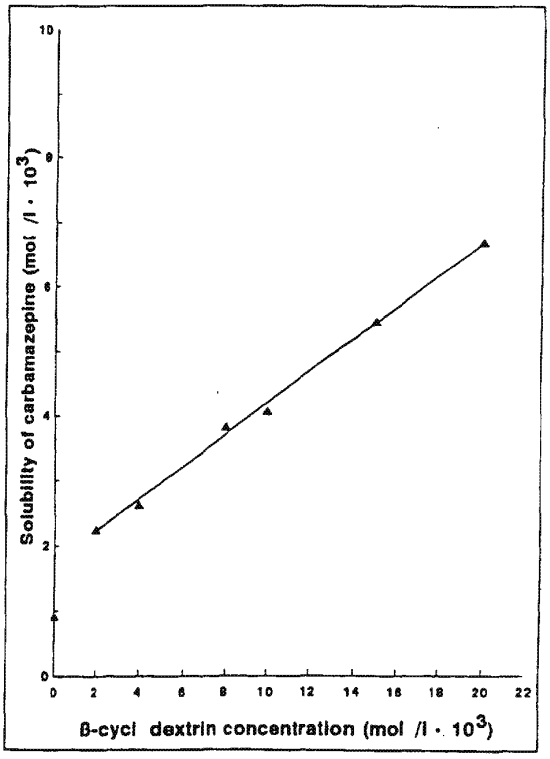

Fig. 2: Effect of β-cyclodextrin on the solubility of carbamazepine in water at 25 °C

ISDOCID: <XP 633833A 1 >

UM00016613
NOVARTIS EXHIBIT 1517
Novartis v. Regents, IPR2023-01347
Page 3595 of 4460

Table: IR specta of the carbamazepine/β-cyclodextrin inclusion complex and the carbamazepine/PEG 6000 coevaporate or comelt

System	I	II	III	IV	V	VI	VII	VIII	IX	X
CBZ	765		1245	1305	1390		1490	1590	1690	3450
β-CD	1020	1150							1670	3350
CBZ/β-CD complex	1020	1150							1690	3350
CBZ/PEG coevaprate		1110	1240	1280	1390		1490	1590	1700	3450
CBZ/PEG comelt		1105	1240	1280	1360	1470	1490	1590	1695	3450

CBZ/β-CD complex was determined from the slope of this linear relationship according to the equation of Higuchi et al. [5].

$$K = \text{slope}/S_0(1 - \text{slope})$$

where S_0 is the solubility of the drug in water.
The stability constant of CBZ/β-CD complex was found to be 404 mol^{-1}.

2.3. *Infrared spectra*

The IR spectra of the inclusion complex of the drug in β-CD as well as its comelt and coevaporate with PEG 6000 generally appeared to be the consequence of the superposition of those of the pure compounds i.e. CBZ and the host molecule.
In case of the β-CD complex, the major bands of CBZ are covered by the host molecule (Table). This is due to the inclusion of the drug in the β-CD cavity. Also, the carbonyl stretching at 1690 cm^{-1} for the drug is shifted to a lower wave number 1670 cm^{-1} in the inclusion complex. The formation of hydrogen bonds between CBZ and the host molecule may account for such shifts. In case of solid dispersions, the drug is also covered with the host and there is a clear shift in all main bands of the drug in both of the comelt and coevaporate (Table). Also there is a lack of some of the characteristic peaks of CBZ. This refers to some sort of interaction between CBZ and PEG via hydrogen bonding.

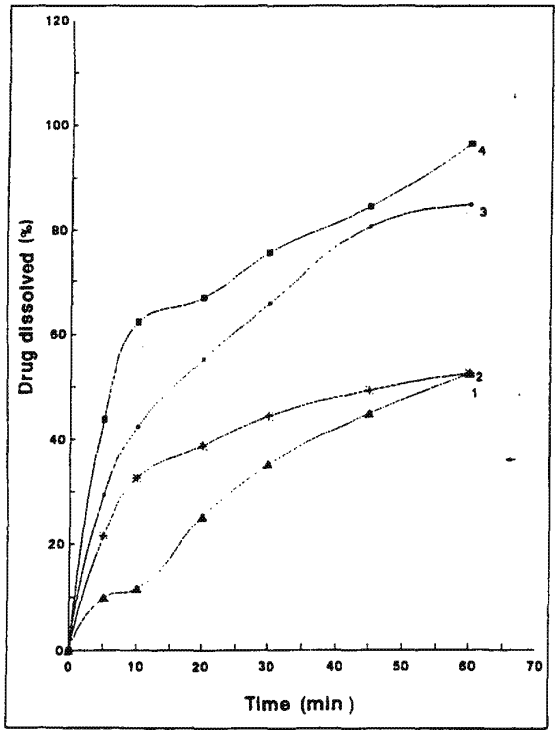

Fig. 3: Dissolution profiles of carbamazepine (1), carbamazepine – PEG 6000 coevaporate (2), carbamazepine – PEG 6000 comelt (3), and carbamazepine – β-cyclodextrin complex (4) in 0.1 N HCl at 37 °C

2.4. *Differential thermal analysis*

The differential thermal analysis displays one endothermal CBZ peak at 222 °C. PEG shows a single peak at 349 °C. The two endothermic peaks at approximately 220 °C and 350 °C represent the two solid dispersions, i.e. comelt and coevaporate, since its height corresponds to about half that of PEG or CBZ peak for an amount of 200 mg of each sample. These results suggest that the CBZ peak is decreased to its half height in presence of PEG solid dispersion.
The thermograms of CBZ and β-CD show that β-CD has two endothermic peaks at 65 °C and 276 °C. The thermogram of the inclusion complex shows the complete disappearance of the endothermic peak of CBZ at 222 °C. The appearance of two peaks at 60 °C and 292 °C are due to the presence of β-CD. This result confirms that an inclusion complex has been formed [6].

2.5. *Dissolution*

The dissolution profiles presented in Fig. 3 confirm that incorporation of CBZ in a water-soluble carrier significantly enhances the dissolution rate of the drug compared to the free drug. Thus, it can be seen that the dissolution rate of the CBZ/β-CD complex is higher than that of the comelt or coevaporate of the drug with PEG 6000. This is very evident by comparing the amount of drug dissolved from the complex with that from the comelt or coevaporate during the initial 5 min of the dissolution run. The former is about twice that of the latter. On the other hand, considering the values of the dissolution efficiency of the drug, complex, comelt and coevaporate (31, 71, 61 and 41%, respectively), it can be seen that the dissolution rate of the drug from its comelt with PEG 6000 is higher than that of the corresponding coevaporate. The dissolution rate of the drug from its inclusion complex with β-CD is higher than from its solid dispersions with PEG 6000.
In conclusion, inclusion complexation of CBZ in β-CD results in a very pronounced enhancement in the dissolution properties of the drug compared to the approach of solid dispersing the drug with water-soluble polymers. This result which runs parallel with more or less similar findings reported for tolbutamide [7], suggests the use of β-CD to improve the biological performance of CBZ.

3. Experimental

3.1. *Materials*

Carbamazepine (CBZ) (Aldrich, Milwaukee WI 53201 USA). Polyethylene glycol 6000, β-cyclodextrin (Merck, Darmstadt, Germany). All other reagents and solvents were of analytical grade.

3NSDOCID: <XP 633833A 1 >

UM00016614
NOVARTIS EXHIBIT 1517
Novartis v. Regents, IPR2023-01347
Page 3596 of 4460

3.2. Methods

3.2.1. Differential spectrum

Differential UV absorption spectrum of 0.02 mol/l of CBZ solution in presence of different concentrations of β-CD (5, 15, 20 mmol/l) was determined using a LKB spectrophotometer at the wave length range from 240 to 320 nm.

3.2.2. Continuous variation method

The continuous variation method described by Job [8] was used to determine the stoichiometric ratio of CBZ/β-CD complex by spectrophotometric measurements at 285 nm.

3.2.3. Phase solubility studies

Phase solubility studies were performed according to the method reported by Higuchi et al. [5]. CBZ 20 mg was weighed out into 25 ml stoppered flasks. A constant volume of 5 ml distilled water was added to each container, then successively increasing portions of β-CD (0.002–0.0025 M) were added to these vessels which were closed and brought to a solubility equilibrium. The contents of the flasks were filtered through a Millipore membrane (HA 0.45 µm). The CBZ concentration in the filtered solution was determined spectrophotometrically at 285 nm.

3.2.4. Sample preparation

3.2.4.1. Preparation of the CBZ comelt

CBZ and PEG 6000 (1 : 1) were melted together by first heating the PEG 6000 in an aluminum dish over an oil bath at 80 °C. The drug was then dissolved in the molten carrier and stirred to obtain a homogenous dispersion. Flash cooling of the dispersion by immersion in a bath of dry ice and acetone was employed. Indeed, it has been shown that rapid cooling give rise to faster dispersion rates. The dispersion was then dried under vacuum at room temperature for 24 h.

3.2.4.2. Preparation of the CBZ coevaporate

A mixture of CBZ and PEG 6000 (1 : 1) was dissolved in a sufficient volume of absolute ethanol and evaporation was carried out in vacuo at 25 °C. The hardened mass was removed from the container and dried under vacuum at room temperature for 24 h.

3.2.4.3. Preparation of the solid complex

The CBZ/β-CD complex was prepared according to the kneading method. In this method, least amount of water was used, CD was kneaded like a paste with a small amount of water to which CBZ has been added without a solvent. The paste made of CD and CBZ was ground in a mortar, then dried under vacuum in presence of phosphorous pentoxide as drying agent at room temperature.

Each sample of comelt, coevaporate and solid complex, was – after drying – passed through a 250 µm mesh. These samples were retained for the dissolution study as well as IR spectrophotometry and differential scanning calorimetry investigation.

3.2.5.4. IR spectrophotometry

The IR were measured as KBr disc using a Shimadzu 435 µ – 04 IR spectrophotometer.

3.2.6. Thermal measurements

The thermal behavior of the investigated samples were traced by differential thermal analysis (DTA). The DTA scans were carried out using a computerized Perkin Elmer DTA/TGA series under a dynamic N_2 purging gas atmosphere (at a constant rate of 50 cm^3/min) and a heating rate of 5 °C/min.

3.2.7. Dissolution studies

Drug dissolution tests were performed according to the USP XXI method with the apparatus 2. For each sample, 900 ml of 0.1 N hydrochloric acid were stirred at 50 r.p.m. and maintained at 37 ± 0.5 °C. An amount of each sample equivalent to 25 mg CBZ was added to the medium after the equilibrium temperature was reached. Samples (5 ml) were withdrawn at various time intervals and filtered through a 0.22 µm filter. The volume in the vessel was replaced with pure 0.1 N HCl after each sampling. The concentration of CBZ dissolved in the medium was determined spectrophotometrically at 285 nm.

References

1 Sekiguchi, K.; Obi, N.; Ueda, Y.; Chem. Pharm. Bull. 9, 866 (1961)
2 Saenger, W.: Chem. Int. Ed. Engl. 19, 344 (1980)
3 Uekama, K.; Hirayama, F.; Wakuda, T.; Otagiri, M.: Chem. Pharm. Bull. 29, 213 (1981)
4 Nakai, Y.; Yamamoto, K.; Tereda, K.; Akimoto, K. O.: Chem. Pharm. Bull. 32, 685 (1984)
5 Higuchi, T.; Connors, K. A.: Advances in Analytical Chemistry and Instrumentation, p. 117 Interscience Publishers, New York 1965
6 Mura, P.; Liguori, A.; Bramanti; Poggi, L.: Acta Pharm. Technol. 34, 77 (1988)
7 Kedzierewicz, F.; Hoffman, M.; Maincent, P.: Int. J. Pharm. 58, 221 (1990)
8 Martin, A.; Swarbrick, J.; Cammarata, A.: Physical Chemical Principles in the Pharmaceutical Sciences, 3rd edn., Complexation and Protein Binding, p. 314, Lea and Febiger, Philadelphia 1983

Received December 12, 1995
Accepted January 18, 1996

Dr. Soheir A. El-Nahhas
Dept. of Pharmaceutical Sciences
National Research Centre
Dokki, Cairo
Egypt

Laboratoire de Pharmacologie, Pharmacocinétique et Pharmacie Clinique[1], Faculté des Sciences Pharmaceutiques et Biologique, Lille and Laboratoires Macopharma[2], Tourcoing, France

Stability and compatibility studies of cefazoline, ceftriaxone, cefotaxime and latamoxef with PVC infusion bags

M. A. Faouzi[1], F. Khalfi[1], T. Dine[1], B. Gressier[1], J. Kablan[1], M. Luyckx[1], L. Ballester[1], F. Goudaliez[2], C. Brunet[1], M. Cazin[1] and J. C. Cazin[1]

A rapid isocratic technique for the analysis of four cephalosporins, cefazoline, cefotaxime, ceftriaxone and latamoxef, in parenteral solutions by HPLC with UV detection and a C_{18} column was developed. The stability and compatibility of drugs from solutions infused via plastic infusion bags through plastic administration sets have been examined. No significant drugs loss was observed during the simulated infusion (n = 4) for 1 h. No significant difference was found between infusion solutions (5% glucose or 0.9% sodium chloride). The stability of drugs was also studied in solution in PVC bags after storage at room temperature without protection from light and at +4 °C with protection from light. The results show the stability of drugs after 24 h at room temperature and 48 h storage at +4 °C to be satisfactory, irrespective of the infusion solution (5% glucose or 0.9% sodium chloride), except for the ceftriaxone solution that should not be used after 8 h at room temperature without protection from light.

ISDOCID: <XP 633833A 1 >

UM00016615
NOVARTIS EXHIBIT 1517
Novartis v. Regents, IPR2023-01347
Page 3597 of 4460

D.6 **CONCENTRATION RELATED EFFECTS OF VIGABATRIN ON GABA UPTAKE IN CULTURED RODENT ASTROCYTES**

John Paul Leach, Graeme Sills, George Thompson, Gerard Forrest, Elaine Butler, and Martin J Brodie.
Epilepsy Research Unit, Western Infirmary, Glasgow, UK

Rationale
Vigabatrin is an effective anticonvulsant when used as add-on therapy. The clinical efficacy of vigabatrin was previously believed to be due solely to the inhibition of GABA-transaminase (GABA-T) activity. We have shown that vigabatrin also inhibits the reuptake of GABA by astrocytes. Here we describe how this effect varies with the concentration of vigabatrin.

Methods
Astrocytes were cultured from the cerebral cortices of 1-day old rat pups. After three weeks in culture, the rate of GABA uptake was assessed by exposure to [^{14}C]-labelled GABA. GABA uptake into cells following 1 hour pre-treatment with vigabatrin (1 to 500uM) was compared to that of cells exposed to control conditions.

Results
At concentrations of 1uM,10uM, and 50uM, vigabatrin did not significantly alter the rate of GABA uptake. At 100uM however, vigabatrin significantly decreased GABA uptake, the mean values at 100uM being 80% of the mean control values ($p<0.05$), an effect that persists at 250uM. Exposure to vigabatrin at 500uM, however, significantly *increased* the mean rate of GABA uptake by 32% ($p<0.01$).

Conclusions
While it was previously felt that vigabatrin had only one action on the GABAergic system, it is now clear that it also has significant dose-dependant effects on the rate of GABA uptake. The clinical relevance of this is unclear, but this inhibition at levels known to decrease GABA-T activity may be at least partly responsible for the anticonvulsant action of vigabatrin.

D.8 **TOPIRAMATE: DOUBLE-BLIND TRIAL AS MONOTHERAPY**

Authors: S. K. Sachdeo, MD, Rajesh C. Sachdeo, MD, UMDNJ, New Brunswick, NJ, Ross A. Reife, MD, Pilar Lim, Gordon Pledger, Ph.D., RWJ Pharmaceutical Research Institute, Raritan, NJ.

Rationale: Topiramate has shown efficacy in treating adults with refractory partial-onset seizures in five trials. In these double-blind trials, patients were randomized to add either topiramate or placebo to their existing anti-epileptic drug (AED) regimen. The percent reduction in seizures over baseline was compared for the two groups. The current trial assessed efficacy in the same population using a different design.
Methods: In this double-blind trial, 48 patients were randomized to receive either the minimum efficacious dose of topiramate [100 mg/day] or a higher dose [1000 mg/day or maximum tolerated dose (MTD)]. Concomitant AEDs were withdrawn during the first 35 days of the double-blind period. The patient continued monotherapy of either 100 mg/day or 1000 mg/day (or MTD) of topiramate for the duration of the 112-day double-blind phase or until the patient met exit criteria. The exit criteria were pre-defined to indicate a worsening of seizures over baseline.
Results: The time to exit was longer in the 1000 mg/day group than in the 100 mg/day group ($p=0.0017$). The number of patients who remained in the trial for the entire 112 days was also greater in the 1000 mg/day group ($p=0.002$).
Conclusions: In a different trial design than those previously reported with topiramate, 1000 mg/day (or MTD) of topiramate monotherapy is effective as treatment for refractory partial onset seizures in adults.

Supported by RWJ Pharmaceutical Research Institute

Ross A. Reife, Pilar Lim, and Gordon Pledger, Ph.D., are employees of RWJ Pharmaceutical Research Institute, the sponsor of the research. As such they receive salaries from RWJ Pharmaceutical Research Institute and may hold equity positions and/or receive stock options. Drs. S. K. Sachdeo and Rajesh C. Sachdeo have received a grant for doing the above study.

D.7 **DOSE-RANGING TRIAL WITH HIGHER DOSES OF TOPIRAMATE IN PATIENTS WITH RESISTANT PARTIAL SEIZURES** Michael Privitera,[1] Richard Fincham,[2] J. Kiffin Penry,[3] Ross Reife,[4] Lynn Kramer,[5] Gordon Pledger,[4] R. Karim,[4] and the Topiramate YE Study Group 1.University of Cincinnati Medical Center, 2.University of Iowa Hospitals, 3.Bowman Gray School of Medicine, 4.R.W. Johnson Pharmaceutical Research Institute, 5.Ciba-Geigy Pharmaceuticals Division

RATIONALE: We conducted a double-blind, parallel group, placebo-controlled trial in 190 patients to evaluate the safety and efficacy of three dosages of topiramate, an investigational antiepileptic drug (AED) as adjunctive therapy for refractory partial epilepsy. **METHODS**: During a 12 week baseline period, patients were required to have at least one partial-onset seizure per week while receiving one or two standard AEDs at therapeutic concentrations. Patients were randomized to 600 mg/day, 800 mg/day, 1000 mg/day or placebo in a bid regimen. A 6 week titration period was followed by a 12-week maintenance period. **RESULTS**: Median percent reductions from baseline in monthly seizure rates were 1% for placebo, 41% for topiramate 600 mg/day and topiramate 800 mg/day, and 38% for topiramate 1000 mg/day. A 50% or greater reduction in baseline seizure frequency during the treatment phase was observed in 9% of placebo, 44% of topiramate 600 mg/day, 40% of topiramate 800 mg/day and 35% of topiramate 1000 mg/day patients. No placebo patients improved by 75-100%, but 20% of topiramate patients had this degree of improvement. All analyses were intent-to-treat drug-placebo comparisons and significantly ($p \leq 0.02$) favored topiramate. Treatment-emergent adverse events consisted mainly of neurological symptoms commonly observed during standard AED therapy. Sixteen percent of topiramate patients discontinued due to adverse events. **CONCLUSIONS**: Topiramate is a highly efficacious and generally well tolerated new AED. When large groups of patients are compared, incremental efficacy in the add-on setting is not observed above 600 mg/day; however, higher doses may prove beneficial to individual patients who tolerate them.

Dr. Privitera has performed consulting for R.W. Johnson PRI. Drs. Reife, Pledger, and Karim are currently employees of R.W. Johnson PRI. Dr. Kramer was an employee of R.W. Johnson PRI at the time the trial was completed, however, he no longer works for them.

D.9 TOPIRAMATE DOSE-RANGING TRIAL IN REFRACTORY PARTIAL EPILEPSY. Edward Faught, B.J. Wilder, R. Eugene Ramsay, Ross A. Reife, Lynn D. Kramer, Gordon W. Pledger, Rezaul M. Karim and the Topiramate YD Study Group. University of Alabama at Birmingham, Birmingham, AL 35294.

RATIONALE: We conducted a randomized, double-blind comparison of three dosages of topiramate to placebo as adjunctive therapy in refractory partial onset epilepsy.
METHODS: 181 patients completed a 12-week baseline during which they had at least one partial-onset seizure per week. All received one or two other drugs at therapeutic concentrations. Patients were randomized to 200 mg/day, 400 mg/day, 600 mg/day or placebo. A four-week titration preceded a 12-week maintenance period.
RESULTS: The median percent seizure reductions relative to baseline, using an intent to treat analysis, were: 30% for topiramate 200 mg/day ($p = 0.051$), 48% for topiramate 400 mg/day ($p = 0.007$), 45% for topiramate 600 mg/day ($p = 0.001$) and 13% for placebo. Percent responders (> 50% reduction in seizure frequency) were 27% for topiramate 200 mg/day, 47% for topiramate 400 mg/day ($p = 0.013$), 46% for topiramate 600 mg/day ($p = 0.027$) and 18% for placebo. A significant ($p = 0.003$) reduction in secondarily generalized tonic clonic seizures with topiramate was demonstrated.
Mild or moderate central nervous system symptoms were the primary treatment-emergent adverse events, but treatment-limiting adverse events occurred in only 9% of topiramate patients compared to 7% of placebo patients.
CONCLUSIONS: Topiramate is effective and well-tolerated in refractory partial epilepsy.

Edward Faught, M.D., received research support and an honorarium for speaking from R.W. Johnson Pharmaceutical Research Institute.

UM00016616
NOVARTIS EXHIBIT 1517
Novartis v. Regents, IPR2023-01347
Page 3598 of 4460

Drug Therapy

ALASTAIR J.J. WOOD, M.D., *Editor*

THE COXIBS, SELECTIVE INHIBITORS OF CYCLOOXYGENASE-2

GARRET A. FITZGERALD, M.D., AND CARLO PATRONO, M.D.

NONSTEROIDAL antiinflammatory drugs (NSAIDs) are widely used to treat arthritis, menstrual pain, and headache. Although they are effective, their long-term use is limited by gastrointestinal effects such as dyspepsia and abdominal pain and, less often, gastric or duodenal perforation or bleeding. Development of the coxibs, a new group of antiinflammatory drugs, represents a response to the unsatisfactory therapeutic profile of NSAIDs. Both groups of drugs inhibit prostaglandin G/H synthase, the enzyme that catalyzes the transformation of arachidonic acid to a range of lipid mediators, termed prostaglandins and thromboxanes (Fig. 1). However, whereas NSAIDs inhibit the two recognized forms of the enzyme, also referred to as cyclooxygenase-1 and cyclooxygenase-2, the coxibs are selective inhibitors of cyclooxygenase-2. The inhibition of cyclooxygenase-2 has been more directly implicated in ameliorating inflammation, whereas the inhibition of cyclooxygenase-1 has been related to adverse effects in the gastrointestinal tract. Therefore, it was hoped that coxibs would be better tolerated than nonselective NSAIDs but equally efficacious. This review will assess the evidence that has emerged in support of that hypothesis.

Prostaglandin G/H synthase has both cyclooxygenase and hydroperoxidase activity.[1] Neither coxibs nor NSAIDs inhibit the activity of hydroperoxidase. Aspirin inhibits the activity of cyclooxygenase by irreversibly acetylating a serine residue at position 529 in the only form of the enzyme expressed in platelets, cyclooxygenase-1.[2] There were several early suggestions of a second form of cyclooxygenase.[3-5] Analysis of unrelated genes identified one that was highly homologous to the gene for cyclooxygenase-1.[6-8] This isoform, termed cyclooxygenase-2, can be up-regulated by cytokines, growth factors, and tumor promoters,[6-10] suggesting its relevance to inflammation and cancer.

Although cyclooxygenase-1 has the structural features of a "housekeeping" enzyme, its expression may also be regulated.[11,12] The expression of both cyclooxygenase-1 and cyclooxygenase-2 is increased in the synovia of inflamed joints and in atherosclerotic plaques.[13,14] Although the catalytic activities and tertiary structures of cyclooxygenase-1 and cyclooxygenase-2 are also remarkably similar,[2,15,16] cyclooxygenase-2 has a broader affinity for substrates because the hydrophobic channel leading to the active site of this enzyme is more accommodating. However, distinguishing cyclooxygenase-1 as a constitutive enzyme and cyclooxygenase-2 as an inducible enzyme that accounts for the formation of prostanoid in disease is an oversimplification of the biologic reality.

SELECTIVE AND NONSELECTIVE INHIBITION OF CYCLOOXYGENASE ISOFORMS

Three broad classes of cyclooxygenase inhibitors have emerged: aspirin synthesized from salicylic acid; indomethacin and other NSAIDs, whose chemical modifications were based largely on findings in models of inflammation and gastric mucosal damage; and the first selective cyclooxygenase-2 inhibitors, the coxibs (e.g., celecoxib and rofecoxib). Other selective cyclooxygenase-2 inhibitors, such as valdecoxib[17] and etoricoxib,[18] are being developed.

Selectivity for cyclooxygenase-2 may be expressed at several levels. A compound may be biochemically selective for cyclooxygenase-2. Drug companies assess selectivity by in vitro assays during screening, because these assays are relatively rapid and simple. However, they do not necessarily reflect the complexity of the drug–enzyme interaction in vivo. To address this concern, whole-blood assays of cyclooxygenase-isoform activity have been developed.[19,20] These assays are based on the production of thromboxane B_2 during blood clotting (an index of platelet cyclooxygenase-1 activity) and the production of prostaglandin E_2 by bacterial lipopolysaccharide in whole blood (an index of monocyte cyclooxygenase-2 activity). Clinical selectivity has been based on either surrogates for clinical toxicity (e.g., endoscopically visualized gastroduodenal ulcers) or actual clinical end points at antiinflammatory doses of an inhibitor.

There are two basic requirements to test the hypothesis that cyclooxygenase-2 inhibitors are better tolerated than nonselective NSAIDs but just as efficacious. First, the drug must not inhibit cyclooxygenase-1 activity in clinically relevant targets (gastrointestinal mucosa and platelets) at therapeutic plasma concentrations. Second, the clinical end points assessed must reflect cyclooxygenase-1–dependent gastrointestinal toxicity. When symptoms are the end point, a limitation is that the dependence of cyclooxygenase-1 on the signal is uncertain, and symptoms may not correlate with lesions. When endoscopically visualized lesions are the end point, the situation is

From the Center for Experimental Therapeutics, University of Pennsylvania, Philadelphia (G.A.F.); and the Department of Medicine and Center of Excellence on Aging, University of Chieti, Chieti, Italy (C.P.). Address reprint requests to Dr. FitzGerald at the Department of Pharmacology, 153 Johnson Pavilion, 3620 Hamilton Walk, University of Pennsylvania, Philadelphia, PA 19104-6084, or at garret@spirit.gcrc.upenn.edu.

Downloaded from www.nejm.org at FLAMEDLIB on May 13, 2009 .
Copyright © 2001 Massachusetts Medical Society. All rights reserved.

UM00016617
NOVARTIS EXHIBIT 1517
Novartis v. Regents, IPR2023-01347
Page 3599 of 4460

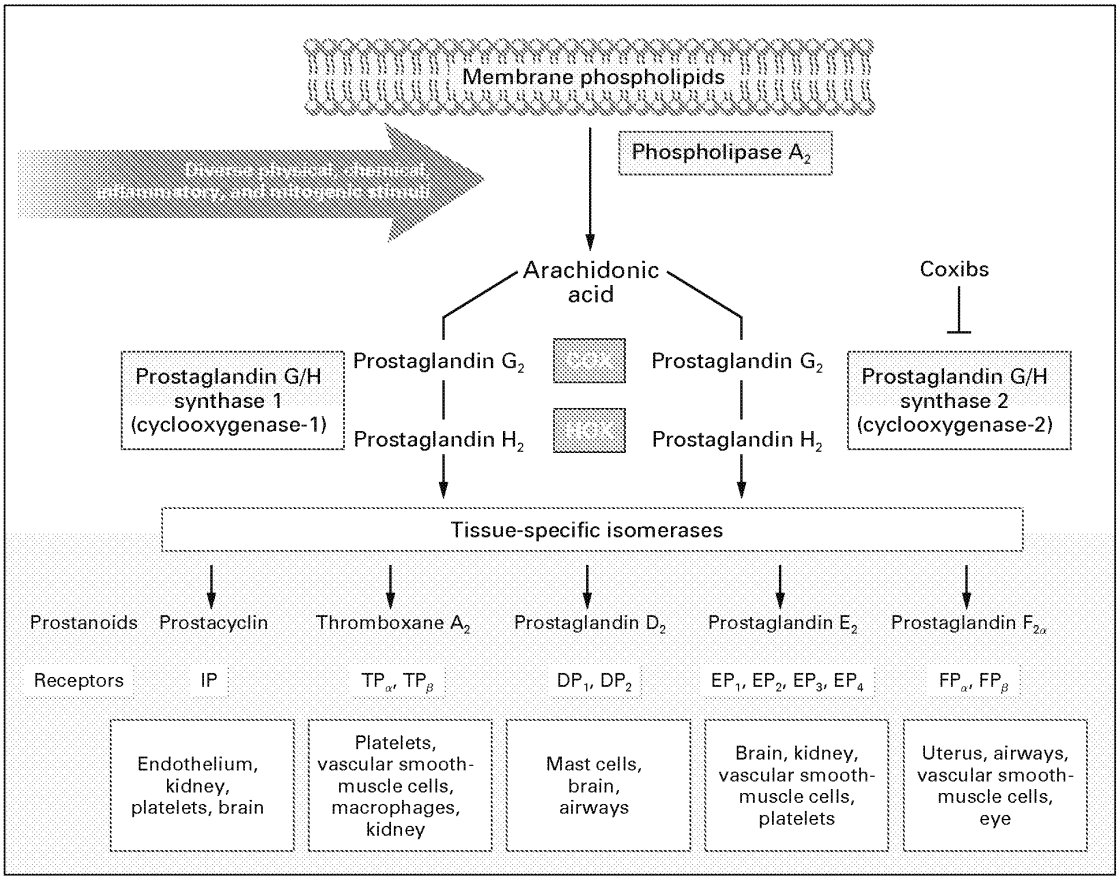

Figure 1. Production and Actions of Prostaglandins and Thromboxane.

Arachidonic acid, a 20-carbon fatty acid containing four double bonds, is liberated from the *sn*2 position in membrane phospholipids by phospholipase A_2, which is activated by diverse stimuli. Arachidonic acid is converted by cytosolic prostaglandin G/H synthases, which have both cyclooxygenase (COX) and hydroperoxidase (HOX) activity, to the unstable intermediate prostaglandin H_2. The synthases are colloquially termed cyclooxygenases and exist in two forms, cyclooxygenase-1 and cyclooxygenase-2. Coxibs selectively inhibit cyclooxygenase-2. Prostaglandin H_2 is converted by tissue-specific isomerases to multiple prostanoids. These bioactive lipids activate specific cell-membrane receptors of the superfamily of G-protein–coupled receptors. Some of the tissues in which individual prostanoids exert prominent effects are indicated. IP denotes prostacyclin receptor, TP thromboxane receptor, DP prostaglandin D_2 receptor, EP prostaglandin E_2 receptor, and FP prostaglandin $F_{2\alpha}$ receptor.

different. The dependence of the lesions on cyclooxygenase-1 has been established, but it is uncertain whether the finding of lesions on endoscopy is actually predictive of the likelihood of serious gastrointestinal complications, such as perforation, obstruction, and bleeding. Indeed, the hemorrhagic nature of most serious gastrointestinal end points makes it likely that they primarily reflect the inhibition of cyclooxygenase-1 activity in platelets, rather than in gastric mucosa. Finally, the low incidence of these events means that many patients must be studied for prolonged periods of treatment to detect the differences between drugs reliably.[21,22]

The biochemical selectivity of a particular drug, as assessed in vitro, is critically dependent on its concentration. One can summarize such selectivity profiles by plotting the drug concentrations necessary to inhibit the activity of cyclooxygenase-2 and cyclooxygenase-1 by 50 percent (Fig. 2).[23-26] However, given the concentration dependence of these estimates, it is not useful to attempt to discriminate between existing NSAIDs on the basis of small differences in biochemical selectivity with the use of terms such as "preferential cyclooxygenase-2 inhibitor."

How well do the results of these in vitro assays predict selectivity when the measurements are per-

Downloaded from www.nejm.org at FLAMEDLIB on May 13, 2009 .
Copyright © 2001 Massachusetts Medical Society. All rights reserved.

UM00016618
NOVARTIS EXHIBIT 1517
Novartis v. Regents, IPR2023-01347
Page 3600 of 4460

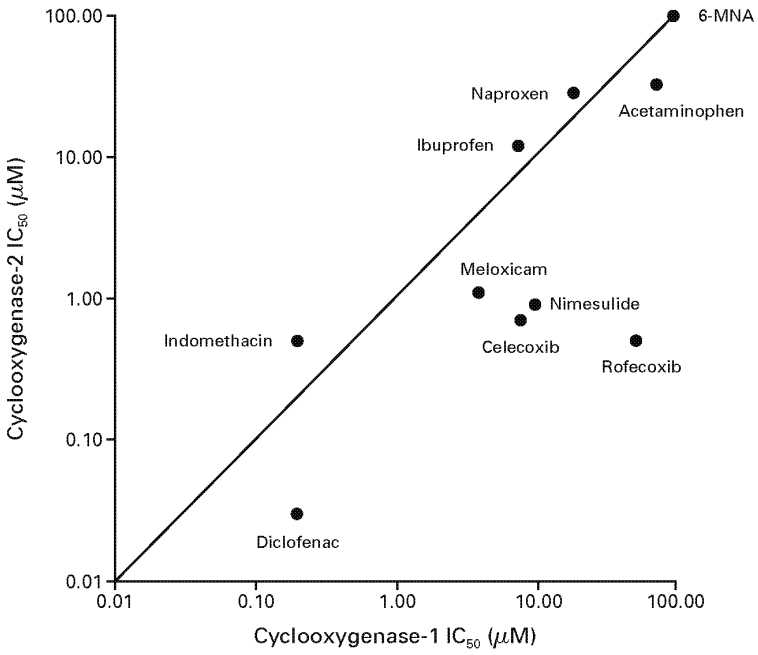

Figure 2. Concentrations of Various Drugs Required to Inhibit the Activity of Cyclooxygenase-1 and Cyclooxygenase-2 by 50 Percent (IC_{50}) in Assays of Whole Blood.

Each point is the mean of three or four values.[23-26] Drugs plotted below the diagonal line indicating equivalence are more potent inhibitors of cyclooxygenase-2 than drugs plotted on or above the line. 6-MNA denotes 6-methoxy-2-naphthylacetic acid.

formed in blood samples obtained from patients given cyclooxygenase inhibitors? Although the curves plotted from the in vitro data fit the plasma data well, the variance of the latter assays is much greater (Fig. 3). This variance reflects substantial variability between patients in plasma concentrations of the cyclooxygenase inhibitor after oral administration of a standard therapeutic dose and in the degree of inhibition of cyclooxygenase isoforms corresponding to any given concentration of inhibitor. Indeed, many factors determine the clinical response to a cyclooxygenase-2 inhibitor (Fig. 4). Thus, genetic variability in the target protein or metabolizing enzymes, interactions between drugs, and the characteristics of the patient, such as a history of peptic ulcer,[29,30] may all influence both the efficacy and the adverse effects of cyclooxygenase-2 inhibitors in clinical trials.

PHARMACOKINETICS AND DRUG INTERACTIONS

The pharmacokinetics, metabolism, and drug interactions of celecoxib[31-34] and rofecoxib[35-39] are summarized in Table 1. The clinically important differences between the two drugs are related to oral bioavailability, half-life, and main pathways of hepatic metabolism. Differences in the pathways of hepatic metabolism may have smaller effects on the pharmacokinetics of rofecoxib than on those of celecoxib.

CLINICAL VERIFICATION OF THE CYCLOOXYGENASE-2 HYPOTHESIS

Both celecoxib and rofecoxib are superior to placebo in the relief of both subjective and objective measurements of pain and inflammation in patients with osteoarthritis of the hip and knee[40-45] and in the relief of symptoms in patients with rheumatoid arthritis.[22,46] Moreover, analgesic efficacy has been demonstrated in clinical models of acute pain, such as that after dental surgery, after orthopedic surgery, and during dysmenorrhea. On the basis of the results of various phase 3 studies, the Food and Drug Administration (FDA) approved celecoxib for the treatment of patients with osteoarthritis and rheumatoid arthritis, and rofecoxib for the treatment of patients with osteoarthritis and acute musculoskeletal pain.

Similar indications have now been approved worldwide. However, whether rofecoxib and celecoxib are equally efficacious is not known. In all of these stud-

Downloaded from www.nejm.org at FLAMEDLIB on May 13, 2009 .
Copyright © 2001 Massachusetts Medical Society. All rights reserved.

UM00016619
NOVARTIS EXHIBIT 1517
Novartis v. Regents, IPR2023-01347
Page 3601 of 4460

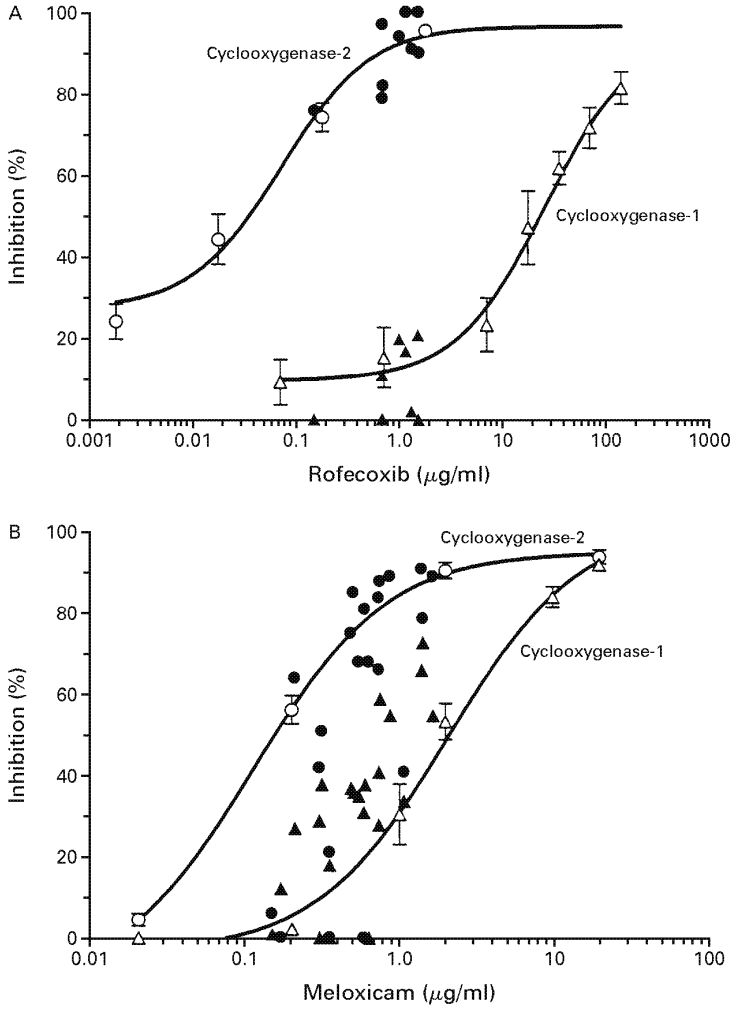

Figure 3. Relations between Mean (±SE) Steady-State Plasma Concentrations of Rofecoxib (Panel A) and Meloxicam (Panel B) and Inhibition of Cyclooxygenase-1 and Cyclooxygenase-2, as Measured in Vitro.

Data were obtained from 9 patients with rheumatoid arthritis who were given 50 mg of rofecoxib once daily for seven days[27] and from 21 normal subjects who received 7.5 or 15 mg of meloxicam once daily for seven days.[28] Blood was drawn 4 hours after the last dose of rofecoxib and 24 hours after the last dose of meloxicam. Superimposed on the same graphs are concentration–effect curves for the degree of inhibition of cyclooxygenase-2 and cyclooxygenase-1 induced by rofecoxib and meloxicam in vitro. In these studies, increasing concentrations of rofecoxib or meloxicam were incubated with 1-ml samples of heparin-treated whole blood in the presence of lipopolysaccharide for 24 hours, and plasma prostaglandin E_2 was measured as an index of cyclooxygenase-2 activity in monocytes. Rofecoxib or meloxicam was also incubated with 1-ml samples of whole blood that had been allowed to clot for 60 minutes, and serum thromboxane B_2 was measured as an index of cyclooxygenase-1 activity in platelets. Sigmoidal concentration–response curves fitting the experimental data were generated by ALLFIT analysis.[28]

ies,[22,40-46] a nonselective NSAID — that is, a drug that nonselectively inhibits cyclooxygenase-1 and cyclooxygenase-2 at therapeutic plasma concentrations — was included. However, the trials were designed to detect equivalence of efficacy between the NSAID and the coxib, rather than any small, but potentially important, difference between the treatments. Thus, although cyclooxygenase-1 may be a minor source of the prostaglandins produced in response to inflammation in humans,[47] and although both cyclooxygenase isoforms are expressed in inflamed synovia,[13] the studies of the efficacy of coxibs were not designed to de-

Downloaded from www.nejm.org at FLAMEDLIB on May 13, 2009 .
Copyright © 2001 Massachusetts Medical Society. All rights reserved.

UM00016620
NOVARTIS EXHIBIT 1517
Novartis v. Regents, IPR2023-01347
Page 3602 of 4460

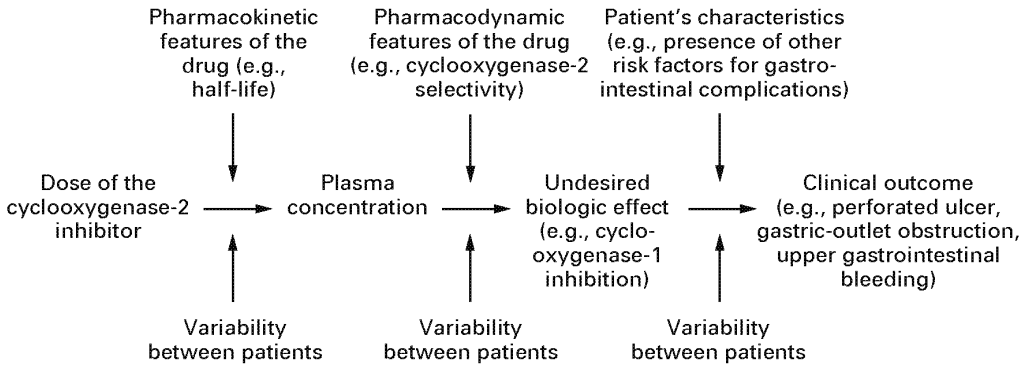

Figure 4. Factors That May Influence the Clinical Selectivity and Safety of a Cyclooxygenase-2 Inhibitor in an Individual Patient. These factors include pharmacokinetic and pharmacodynamic variables, as well as the interaction of the drug with preexisting risk factors for drug-dependent adverse effects. All these factors are subject to variability from patient to patient.

TABLE 1. PHARMACOKINETICS, METABOLISM, AND DRUG INTERACTIONS OF ROFECOXIB AND CELECOXIB.*

FEATURE	ROFECOXIB	CELECOXIB
Oral bioavailability (%)	92–93	22–40
Effect of food	Minimal	None
Time to maximal plasma concentration (hr)	2–3	2–4
Elimination half-life (hr)	10–17	Approximately 11
Volume of distribution (liters)	86–91	455±166
Extent of binding to plasma proteins (%)	86	>97
Main pathway of liver metabolism	Cytosolic reduction	Oxidation by cytochrome P-450 2C9, 3A4
Interaction with cytochrome P-450 inhibitors	No	Yes
Interaction with digoxin	No	Not tested
Interaction with warfarin	Causes 10% increase in INR	No
Interaction with methotrexate	At supratherapeutic doses	No
Interaction with antihypertensive drugs	Increases blood pressure	Increases blood pressure
Influence of renal insufficiency	Has little effect	AUC 43% lower
Influence of hepatic impairment	AUC 30–70% higher	AUC 40–180% higher
Approved daily doses (mg)		
For osteoarthritis	12.5–25	100–200
For rheumatoid arthritis	Not approved	200–400
For acute pain	Up to 50	Not approved

*INR denotes international normalized ratio, and AUC area under the curve. Plus–minus value is the mean ±SD.

tect a small difference in efficacy that might result from the coincidental inhibition of both isoforms, rather than from the inhibition of cyclooxygenase-2 alone. Moreover, it should be emphasized that the clinical-efficacy end points used in these trials have a rather poor ratio of signal (the drug effect) to noise (the placebo effect), making detection of moderate differences in efficacy between drugs an unrealistic exercise. Furthermore, although the efficacy of coxibs is similar to that of nonselective NSAIDs in animal models of acute inflammation,[48] they may exacerbate a late phase of inflammation characterized by the generation of antiinflammatory prostaglandins by cyclooxygenase-2.[49]

Two large trials have addressed the efficacy of coxibs and the associated risk of gastrointestinal complications, the Vioxx Gastrointestinal Outcomes Research (VIGOR) trial and the Celecoxib Long-Term Arthri-

Downloaded from www.nejm.org at FLAMEDLIB on May 13, 2009 .
Copyright © 2001 Massachusetts Medical Society. All rights reserved.

UM00016621
NOVARTIS EXHIBIT 1517
Novartis v. Regents, IPR2023-01347
Page 3603 of 4460

tis Safety Study (CLASS) trial. In the VIGOR trial,[22] a daily dose of 50 mg of rofecoxib was compared with a twice-daily dose of 500 mg of naproxen in 8076 patients with rheumatoid arthritis who were treated for a median of nine months. The mean age of the patients was 58 years, and 80 percent were women. Almost 60 percent were receiving long-term glucocorticoid therapy, and 8 percent had a history of gastrointestinal perforation, gastrointestinal hemorrhage, or symptomatic peptic ulcer. Both drugs were similarly effective, according to either the patient's or the investigator's Global Assessment of Disease Activity scores or the Modified Health Assessment scores. The rates of discontinuation of treatment owing to a lack of efficacy were low in both groups (6.3 percent in the rofecoxib group and 6.5 percent in the naproxen group). The incidence of gastrointestinal perforation, gastrointestinal hemorrhage, or symptomatic peptic ulcer was 4.5 per 100 patient-years in the naproxen group and 2.1 per 100 patient-years in the rofecoxib group, a difference of 54 percent ($P<0.001$). The results in these patients with rheumatoid arthritis were consistent with those of an overview analysis of gastrointestinal side effects in patients with osteoarthritis treated with rofecoxib or nonselective NSAIDs.[50]

The CLASS trial[21] consisted of two separate studies. In one, celecoxib (400 mg twice daily) was compared with diclofenac (75 mg twice daily); in the other, celecoxib was compared with ibuprofen (800 mg three times daily). In contrast to ibuprofen, which is a nonselective NSAID, the selectivity of diclofenac for cyclooxygenase-1 and cyclooxygenase-2 was similar to that of celecoxib (Fig. 2). Seventy-two percent of the patients had osteoarthritis, and 68.5 percent were women. The study lasted 13 months, but only the data from 6 months of follow-up have been published. The patients in the CLASS trial were permitted to take aspirin in doses of up to 325 mg per day. There was no statistically significant difference between the groups in the incidence of the primary end point of ulcer perforation, gastric-outlet obstruction, or upper gastrointestinal bleeding (0.8 percent in the celecoxib group vs. 1.5 percent in either NSAID group, $P=0.09$). The CLASS study was not designed to compare the efficacy of the drugs, and the choice of dosing regimens was based on an analysis of prescription patterns, rather than evidence of similar efficacy.[21] More patients withdrew from the combined NSAID groups than from the celecoxib group (14.8 percent vs. 12.6 percent, $P=0.005$) because of lack of efficacy. The reasons for the higher withdrawal rates in the CLASS trial than in the VIGOR trial are unclear.

Despite the evidence that a coxib is safer than a nonselective NSAID, there are some caveats. The likelihood of a gastrointestinal complication in patients who are taking NSAIDs depends on preexisting risk factors, including age and a history of peptic ulcer and gastrointestinal bleeding, which are likely to be relevant to the gastrointestinal effects of cyclooxygenase-2 inhibitors. Patients with a history of peptic ulcer and gastrointestinal bleeding who are given an NSAID have a risk of a complicated ulcer of about 5 percent per year, in contrast to an incidence of 0.4 percent in patients with no such history.[51] Although patients with peptic ulcers were excluded from both the VIGOR and the CLASS trials, many of those enrolled still had risk factors for gastrointestinal events. Analysis of the VIGOR results revealed an absolute reduction in the risk of peptic ulcers or gastrointestinal bleeding of 2.4 percent in the patients treated with rofecoxib, suggesting that 41 patients needed to be treated for one year to prevent one such event.

The distinct roles of the two cyclooxygenase enzymes in patients with peptic ulcers are unknown. For example, cyclooxygenase-2, as well as cyclooxygenase-1, has been detected in apparently normal gastrointestinal epithelium, and therefore, it may also help protect the gastric mucosa.[52] However, the results of both the VIGOR and the CLASS trials suggest that cyclooxygenase-1 has the main cytoprotective role. Perhaps of more concern is that the expression of gastrointestinal epithelial cyclooxygenase-2 is increased by traumatic and inflammatory stimuli, as well as by *Helicobacter pylori* infection.[53,54] Expression is increased in the margin of healing ulcers, and cyclooxygenase-2 inhibitors impair ulcer healing in mice.[55,56] We still have much to learn about the potential risks of the inhibition of cyclooxygenase-2 in the gastrointestinal tract. For example, cyclooxygenase-2 inhibitors impair tolerance of dietary antigens[57] and exacerbate experimental colitis in rodents.[58,59]

CYCLOOXYGENASE-2, COXIBS, AND CARDIOVASCULAR DISEASE

Cyclooxygenase-1 is constitutively expressed in cultured endothelial and vascular smooth-muscle cells. The expression of cyclooxygenase-2 is increased by cytokines, growth factors, phorbol esters, and lipopolysaccharide in both types of cells and by injury to smooth-muscle cells. These observations suggest that cyclooxygenase-2 has an important role in the increase in prostacyclin formation that occurs in clinical syndromes of platelet activation.[60] Expression of both cyclooxygenase-2 and cyclooxygenase-1 is upregulated in the foam cells and smooth-muscle cells of atherosclerotic plaques.[14] Cyclooxygenase-2 may well be important under physiologic conditions also. For example, cyclooxygenase-2 inhibitors decrease urinary excretion of prostacyclin metabolites in normal subjects,[61-63] indicating that the production of prostacyclin is also decreased.[64-66] Laminar shear forces increase the expression of cyclooxygenase-2 in endothelial cells in vitro[67] and may do so in endothelial cells in normal subjects.[61] Prostacyclin is thought to be part of a homeostatic defense mechanism that limits the consequences of platelet activation in vivo.[60]

Downloaded from www.nejm.org at FLAMEDLIB on May 13, 2009 .
Copyright © 2001 Massachusetts Medical Society. All rights reserved.

UM00016622
NOVARTIS EXHIBIT 1517
Novartis v. Regents, IPR2023-01347
Page 3604 of 4460

In mice, deletion of the prostacyclin receptor increased the sensitivity to thrombotic stimuli but did not increase the risk of spontaneous thrombosis.[68]

What are the implications of these observations with respect to selective cyclooxygenase-2 inhibitors? If they are associated with a risk of thrombosis, the risk should be small, because of the presence of other endothelium-derived substances, such as nitric oxide, that protect against thrombosis. However, thrombosis would be expected to occur in patients who are already at increased risk because of other underlying conditions. In fact, arterial thrombosis occurred after the initiation of celecoxib therapy in four patients with lupus anticoagulant.[69]

In the VIGOR trial, 4 percent of the patients met the FDA criteria for the use of aspirin therapy for secondary prevention of major vascular events, but patients who were taking aspirin were excluded from the trial.[22] The rates of nonfatal myocardial infarction, nonfatal stroke, and death from any vascular event were higher in the rofecoxib group than in the naproxen group (0.8 percent vs. 0.4 percent, $P<0.05$). This difference was largely due to a difference in the incidence of myocardial infarction (0.4 percent in the rofecoxib group vs. 0.1 percent in the naproxen group, $P<0.01$). In contrast, in the CLASS trial, in which 21 percent of the patients took aspirin, there was no significant difference between the treatment groups in the incidence of major cardiovascular events.[21]

The difference in major cardiovascular events in the VIGOR trial may reflect the play of chance. The end point was prespecified, and the difference in the frequency of events was statistically significant, but the absolute number of cardiovascular events was small (less than 70). Although an effect of this magnitude would be surprising, it would be consistent with the formation of thromboxane in the absence of the concomitant generation of prostacyclin. This would be a drug-class–specific effect, but a difference in rates of cardiovascular events may not have been revealed in the CLASS trial because of differences in the study patients, the use of aspirin by some patients, or the nature of the nonselective NSAIDs used in the two trials. Patients with rheumatoid arthritis, such as those in the VIGOR trial, may have an increased risk of thrombotic events.[70,71] This is not true of patients with osteoarthritis, who constituted most of the patients in the CLASS trial. Naproxen, the nonselective NSAID used in the VIGOR trial, may be protective against cardiovascular events.[22] Naproxen has an extended half-life and may have completely suppressed the capacity of platelets to make thromboxane A_2 throughout its dosing interval,[72] although this feature of naproxen has been disputed.[73] There is no convincing evidence from epidemiologic studies that NSAIDs, including naproxen, protect against cardiovascular events.[74] Clearly, more information is needed on the cardiovascular effect of selective inhibitors of cyclooxygenase-2 and their combination with antiplatelet drugs.

In the interim, what approach to cardioprotection might be taken in patients with arthritis? Patients who have had a major cardiovascular event should be treated with low-dose aspirin.[75] For such patients who need antiarthritic therapy, the additional suppressive effect on the synthesis of prostacyclin of either a coxib or a nonselective NSAID should be indistinguishable,[61-63] whereas the profile of adverse gastrointestinal effects may favor the former. However, whether this combination maintains the advantage of a coxib over a nonselective NSAID with respect to gastrointestinal side effects remains to be tested. The incidence of serious gastrointestinal bleeding in patients taking low doses of aspirin, although low, is roughly double the incidence in those taking placebos.[76] Aside from potentially increasing the rate of acute events, such as myocardial infarction, cyclooxygenase-2 inhibitors may have relevance to other aspects of cardiovascular biology, such as cardiac function and atherogenesis.[77-79]

CYCLOOXYGENASE-2 AND RENAL FUNCTION

Cyclooxygenase-2–dependent prostaglandin formation is necessary for normal renal development. In mice, the complete absence of cyclooxygenase-2 results in severe renal dysplasia characterized by a postnatal arrest of maturation in the subcapsular nephrogenic zone and progressive deterioration with increasing age.[80] Antenatal exposure of both mice and rats to an inhibitor of cyclooxygenase-2, but not of cyclooxygenase-1, had similar effects.[81]

Cyclooxygenase-2 has been localized to the renal vasculature, the cortical macula densa, and the medullary interstitial cells of the kidney, and its content in these areas increases with age. By contrast, cyclooxygenase-1 is found in the vasculature, the collecting ducts, and the thin loops of Henle.[82] The presence of both isoforms in the vasculature raises the question of which is the predominant source of the increased production of vasodilator prostaglandins that are critical to the preservation of renal blood flow in the presence of volume depletion. Inhibition of this homeostatic response accounts for the most common renal side effects associated with nonselective NSAID therapy.[83]

Remarkably little information on the renal pharmacology of cyclooxygenase-2 inhibitors in humans is available. In normal salt-replete subjects who were 59 to 80 years of age, the administration of 50 mg of rofecoxib once daily or 50 mg of indomethacin three times daily transiently decreased urinary sodium excretion by approximately 20 percent but did not cause detectable edema or hypertension. The glomerular filtration rate, measured after 14 days, declined by an average of 5 percent in the indomethacin group but did not change in the rofecoxib group ($P=0.005$).[63]

Downloaded from www.nejm.org at FLAMEDLIB on May 13, 2009 .
Copyright © 2001 Massachusetts Medical Society. All rights reserved.

UM00016623
NOVARTIS EXHIBIT 1517
Novartis v. Regents, IPR2023-01347
Page 3605 of 4460

By contrast, 12.5 or 25 mg of rofecoxib once daily and 50 mg of indomethacin three times daily reduced the glomerular filtration rate in salt-depleted elderly subjects, but to a similar degree.[84]

An analysis of the post-marketing data for celecoxib revealed that edema occurred in 2.1 percent of patients, hypertension in 0.8 percent, and exacerbation of preexisting hypertension in 0.6 percent — a profile and incidence similar to those of nonselective NSAIDs.[85] Similarly, post hoc analysis of the rofecoxib data base revealed that peripheral edema occurred in 3.8 percent of the patients who received a dose of 25 mg per day.[86] Controlled comparisons of the coxibs with each other and with nonselective NSAIDs are necessary to assess the risk of hypertension. These should be designed to match the degree and duration of cyclooxygenase-2 inhibition throughout the dosing interval.

EFFECTS OF OTHER CYCLOOXYGENASE-2 INHIBITORS

Two older drugs, nimesulide and meloxicam, the latter recently approved for use in the United States, exhibit cyclooxygenase-2 selectivity similar to that of celecoxib in vitro (Fig. 2). It is not clear whether their effects are similar to those of rofecoxib or celecoxib in clinical practice. Variability between patients in plasma drug concentrations is an important determinant of the selectivity of these agents for cyclooxygenase-2. Thus, in the case of nimesulide, a daily dose of 100 mg reduced cyclooxygenase-1 activity measured ex vivo in normal subjects in one study[87] but not in another.[62] Meloxicam caused dose-dependent inhibition of cyclooxygenase-2 and cyclooxygenase-1, but the extent of inhibition varied greatly among the subjects (Fig. 3).[28,88]

The clinical selectivity of these drugs has not been addressed in large trials with statistical power similar to that of the VIGOR and CLASS trials. Thus, although post hoc analyses of small studies have suggested that gastrointestinal side effects are less frequent with nimesulide than with nonselective NSAIDs,[89] prospective studies of the efficacy and gastrointestinal safety have been small, involving 60 to 392 patients who were treated for eight days to three months.[90-93] There was no significant difference in the incidence of serious gastrointestinal side effects among patients who were taking 7.5 mg of meloxicam daily, those who were taking 100 mg of slow-release diclofenac daily, and those who were taking 20 mg of piroxicam daily for 28 days in two large studies, the Meloxicam Large-Scale International Study Safety Assessment[94] and the Safety and Efficacy Large-Scale Evaluation of COX-Inhibiting Therapies.[95] A meta-analysis of six trials, including these two large trials, suggested a relative risk of serious upper gastrointestinal side effects of 0.5 for meloxicam as compared with NSAIDs, with the upper bound of the 95 percent confidence interval approaching 1.0.[96] In contrast, a small observational study suggested that the risk of upper gastrointestinal complications associated with meloxicam was similar to that of conventional NSAIDs.[30]

CONCLUSIONS

In less than a decade after the discovery of cyclooxygenase-2, clinical trials have demonstrated that treatment with highly selective cyclooxygenase-2 inhibitors causes significantly fewer serious gastrointestinal adverse events than does treatment with nonselective NSAIDs. More selective coxibs are already being developed. We must gather additional information on the pharmacology of the coxibs. Given the cardiovascular findings in the VIGOR trial and the association of both rofecoxib and celecoxib with small, but potentially clinically relevant, changes in blood pressure, elucidation of the cardiovascular and renal effects of these drugs and their interactions with potential adjuvant therapies, such as low-dose aspirin, is imperative.

Supported by grants from the National Institutes of Health (HL 62250, HL 57847, and M01 RR00040) and the Italian Ministry of University and Research (9706570507-005).

Dr. FitzGerald has received grant support from Bayer, Johnson & Johnson, Merck, and Searle and has served as a consultant to Boehringer Ingelheim, Bristol-Myers Squibb, Johnson & Johnson, Merck, and Searle. Dr. Patrono has received grant support from Bayer, Merck, and McNeil and has served as a consultant to Merck, Pharmacia & Upjohn, and Novartis.

REFERENCES

1. Marnett LJ, Rowlinson SW, Goodwin DC, Kalgutkar AS, Lanzo CA. Arachidonic acid oxygenation by COX-1 and COX-2: mechanisms of catalysis and inhibition. J Biol Chem 1999;274:22903-6.
2. Loll PJ, Picot D, Garavito RM. The structural basis of aspirin activity inferred from the crystal structure of inactivated prostaglandin H_2 synthase. Nat Struct Biol 1995;2:637-43.
3. Pash JM, Bailey JM. Inhibition by corticosteroids of epidermal growth factor-induced recovery of cyclooxygenase after aspirin inactivation. FASEB J 1988;2:2613-8.
4. Sebaldt RJ, Sheller JR, Oates JA, Roberts LJ II, FitzGerald GA. Inhibition of eicosanoid biosynthesis by glucocorticoids in humans. Proc Natl Acad Sci U S A 1990;87:6974-8.
5. Masferrer JL, Zweifel BS, Seibert K, Needleman P. Selective regulation of cellular cyclooxygenase by dexamethasone and endotoxin in mice. J Clin Invest 1990;86:1375-9.
6. Xie W, Chipman JG, Robertson DL, Erikson RL, Simmons DL. Expression of a mitogen-responsive gene encoding prostaglandin synthase is regulated by mRNA splicing. Proc Natl Acad Sci U S A 1991;88:2692-6.
7. Kujubu DA, Herschman HR. Dexamethasone inhibits mitogen induction of the T1S10 prostaglandin synthase/cyclooxygenase gene. J Biol Chem 1992;267:7991-4.
8. O'Banion MK, Winn VD, Young DA. cDNA cloning and functional activity of a glucocorticoid-regulated inflammatory cyclooxygenase. Proc Natl Acad Sci U S A 1992;89:4888-92.
9. Lee SH, Soyoola E, Chanmugam P, et al. Selective expression of mitogen-inducible cyclooxygenase in macrophages stimulated with lipopolysaccharide. J Biol Chem 1992;267:25934-8.
10. Sheng H, Shao J, Dixon DA, et al. Transforming growth factor-β1 enhances Ha-*ras*-induced expression of cyclooxygenase-2 in intestinal epithelial cells via stabilization of mRNA. J Biol Chem 2000;275:6628-35.
11. Smith CJ, Morrow JD, Roberts LJ II, Marnett LJ. Induction of prostaglandin endoperoxide synthase-1 (COX-1) in a human promonocytic cell line by treatment with the differentiating agent TPA. Adv Exp Med Biol 1997;400A:99-106.
12. Rocca B, Spain LM, Pure E, Laugenbach R, Patrono C, FitzGerald GA. Distinct roles of prostaglandin H synthases 1 and 2 in T-cell development. J Clin Invest 1999;103:1469-77.

Downloaded from www.nejm.org at FLAMEDLIB on May 13, 2009 .
Copyright © 2001 Massachusetts Medical Society. All rights reserved.

UM00016624
NOVARTIS EXHIBIT 1517
Novartis v. Regents, IPR2023-01347
Page 3606 of 4460

13. Crofford LJ, Wilder RL, Ristimäki AP, et al. Cyclooxygenase-1 and -2 expression in rheumatoid synovial tissues: effects of interleukin-1β, phorbol ester, and corticosteroids. J Clin Invest 1994;93:1095-101.
14. Schonbeck U, Sukhova GK, Graber P, Coulter S, Libby P. Augmented expression of cyclooxygenase-2 in human atherosclerotic lesions. Am J Pathol 1999;155:1281-91.
15. Kurumbail RG, Stevens AM, Gierse JK, et al. Structural basis for selective inhibition of cyclooxygenase-2 by anti-inflammatory agents. Nature 1996;384:644-8. [Erratum, Nature 1997;385:555.]
16. Malkowski MG, Ginell SL, Smith WL, Garavito RM. The productive conformation of arachidonic acid bound to prostaglandin synthase. Science 2000;289:1933-7.
17. Talley JJ, Brown DL, Carter JS, et al. 4-[5-Methyl-3-phenylisoxazol-4-yl]-benzenesulfonamide, valdecoxib: a potent and selective inhibitor of COX-2. J Med Chem 2000;43:775-7.
18. Riendeau D, Percival MD, Brideau C, et al. Etoricoxib (MK-0663): preclinical profile and comparison with other agents that selectively inhibit cyclooxygenase-2. J Pharmacol Exp Ther 2001;296:558-66.
19. Patrono C, Ciabattoni G, Pinca E, et al. Low dose aspirin and inhibition of thromboxane B_2 production in healthy subjects. Thromb Res 1980; 17:317-27.
20. Patrignani P, Panara MR, Greco A, et al. Biochemical and pharmacological characterization of the cyclooxygenase activity of human blood prostaglandin endoperoxide synthases. J Pharmacol Exp Ther 1994;271: 1705-12.
21. Silverstein FE, Faich G, Goldstein JL, et al. Gastrointestinal toxicity with celecoxib vs nonsteroidal anti-inflammatory drugs for osteoarthritis and rheumatoid arthritis: the CLASS study: a randomized controlled trial. JAMA 2000;284:1247-55.
22. Bombardier C, Laine L, Reicin A, et al. Comparison of upper gastrointestinal toxicity of rofecoxib and naproxen in patients with rheumatoid arthritis. N Engl J Med 2000;343:1520-8.
23. Patrignani P, Panara MR, Sciulli MG, Santini G, Renda G, Patrono C. Differential inhibition of human prostaglandin endoperoxide synthase-1 and -2 by nonsteroidal anti-inflammatory drugs. J Physiol Pharmacol 1997; 48:623-31.
24. Chan C-C, Boyes S, Brideau C, et al. Rofecoxib [Vioxx, MK-0966; 4-(4′-methylsulfonylphenyl)-3-phenyl-2-(5H)-furanone]: a potent and orally active cyclooxygenase-2 inhibitor: pharmacological and biochemical profiles. J Pharmacol Exp Ther 1999;290:551-60.
25. Warner TD, Giuliano F, Vojnovic I, Bukasa A, Mitchell JA, Vane JR. Nonsteroid drug selectivities for cyclo-oxygenase-1 rather than cyclo-oxygenase-2 are associated with human gastrointestinal toxicity: a full in vitro analysis. Proc Natl Acad Sci U S A 1999;96:7563-8. [Erratum, Proc Natl Acad Sci U S A 1999;96:9666.]
26. Cryer B, Feldman M. Cyclooxygenase-1 and cyclooxygenase-2 selectivity of widely used nonsteroidal anti-inflammatory drugs. Am J Med 1998;104:413-21.
27. Patrignani P, Panara MR, Santini G, et al. Biochemical selectivity of rofecoxib in rheumatoid arthritis. In: Proceedings of the 11th International Conference on Advances in Prostaglandin and Leukotriene Research: Basic Science and New Clinical Applications, Florence, Italy, June 4–8, 2000:19. abstract.
28. Panara MR, Renda G, Sciulli MG, et al. Dose-dependent inhibition of platelet cyclooxygenase-1 and monocyte cyclooxygenase-2 by meloxicam in healthy subjects. J Pharmacol Exp Ther 1999;290:276-80.
29. Garcia Rodríguez LA, Cattaruzzi C, Troncon MG, Agostinis L. Risk of hospitalization for upper gastrointestinal tract bleeding associated with ketorolac, other nonsteroidal anti-inflammatory drugs, calcium antagonists, and other antihypertensive drugs. Arch Intern Med 1998;158:33-9.
30. Garcia Rodriguez LA, Hernandez-Diaz S. The risk of upper gastrointestinal complications associated with nonsteroidal anti-inflammatory drugs, glucocorticoids, acetaminophen, and combination of these agents. Arthritis Res 2001;3:98-101.
31. Tang C, Shou M, Mei Q, Rushmore TH, Rodrigues AD. Major role of human liver microsomal cytochrome P450 2C9 (CYP2C9) in the oxidative metabolism of celecoxib, a novel cyclooxygenase-II inhibitor. J Pharmacol Exp Ther 2000;293:453-9.
32. Davies NM, McLachlan AJ, Day RO, Williams KM. Clinical pharmacokinetics and pharmacodynamics of celecoxib: a selective cyclo-oxygenase-2 inhibitor. Clin Pharmacokinet 2000;38:225-42.
33. Paulson SK, Hribar JD, Liu NW, et al. Metabolism and excretion of [^{14}C]celecoxib in healthy male volunteers. Drug Metab Dispos 2000;28: 308-14.
34. Karim A, Tolbert DS, Hunt TL, Hubbard RC, Harper KM, Geis GS. Celecoxib, a specific COX-2 inhibitor, has no significant effect on methotrexate pharmacokinetics in patients with rheumatoid arthritis. J Rheumatol 1999;26:2539-43.
35. Porras A, Ko A, Larson P, et al. Single and multiple dose pharmacokinetics (PK) of rofecoxib (R) in healthy subjects. Clin Pharmacol Ther 2000;67:137. abstract.
36. Depre M, Ehrich E, Van Hecken A, et al. Pharmacokinetics, COX-2 specificity, and tolerability of supratherapeutic doses of rofecoxib in humans. Eur J Clin Pharmacol 2000;56:167-74.
37. Schwartz J, Zhao P, Gertz B, et al. Pharmacokinetics of rofecoxib in mild to moderate hepatic insufficiency (H1). Clin Pharmacol Ther 2000; 67:137. abstract.
38. Schwartz JI, Larson PJ, Bugianesi KJ, et al. Effect of rofecoxib (R) on the pharmacodynamics and pharmacokinetics (PK) of warfarin (W). Clin Pharmacol Ther 2000;67:165. abstract.
39. Nicoll-Griffith DA, Yergey JA, Trimble LA, et al. Synthesis, characterization, and activity of metabolites derived from the cyclooxygenase-2 inhibitor rofecoxib (MK-0966, Vioxx). Bioorg Med Chem Lett 2000;10: 2683-6.
40. Hawkey C, Laine L, Simon T, et al. Comparison of the effect of rofecoxib (a cyclooxygenase 2 inhibitor), ibuprofen, and placebo on the gastroduodenal mucosa of patients with osteoarthritis: a randomized, double-blind, placebo-controlled trial. Arthritis Rheum 2000;43:370-7.
41. Simon LS, Lanza FL, Lipsky PE, et al. Preliminary study of the safety and efficacy of SC-58635, a novel cyclooxygenase 2 inhibitor: efficacy and safety in two placebo-controlled trials in osteoarthritis and rheumatoid arthritis, and studies of gastrointestinal and platelet effects. Arthritis Rheum 1998;41:1591-602.
42. Bensen WG, Fiechtner JJ, McMillen JI, et al. Treatment of osteoarthritis with celecoxib, a cyclooxygenase-2 inhibitor: a randomized controlled trial. Mayo Clin Proc 1999;74:1095-105.
43. Clemett D, Goa KL. Celecoxib: a review of its use in osteoarthritis, rheumatoid arthritis and acute pain. Drugs 2000;59:957-80.
44. Cannon GW, Caldwell JR, Holt P, et al. Rofecoxib, a specific inhibitor of cyclooxygenase 2, with clinical efficacy comparable with that of diclofenac sodium: results of a one-year, randomized, clinical trial in patients with osteoarthritis of the knee and hip. Arthritis Rheum 2000;43:978-87.
45. Day R, Morrison B, Luza A, et al. A randomized trial of the efficacy and tolerability of the COX-2 inhibitor rofecoxib vs ibuprofen in patients with osteoarthritis. Arch Intern Med 2000;160:1781-7.
46. Simon LS, Weaver AL, Graham DY, et al. Anti-inflammatory and upper gastrointestinal effects of celecoxib in rheumatoid arthritis: a randomized controlled trial. JAMA 1999;282:1921-8.
47. McAdam BF, Mardini I, Habib A, et al. Effect of regulated expression of human cyclooxygenase isoforms on eicosanoid and isoeicosanoid production in inflammation. J Clin Invest 2000;105:1473-82.
48. Seibert K, Zhang Y, Leahy K, et al. Pharmacological and biochemical demonstration of the role of cyclooxygenase 2 in inflammation and pain. Proc Natl Acad Sci U S A 1994;91:12013-7.
49. Gilroy DW, Colville-Nash PR, Willis D, Chivers J, Paul-Clark MJ, Willoughby DA. Inducible cyclooxygenase may have anti-inflammatory properties. Nat Med 1999;5:698-701.
50. Langman MJ, Jensen DM, Watson DJ, et al. Adverse upper gastrointestinal effects of rofecoxib compared with NSAIDs. JAMA 1999;282: 1929-33.
51. Silverstein FD, Graham DY, Senior JR, et al. Misoprostol reduced serious gastrointestinal complications in patients with rheumatoid arthritis receiving nonsteroidal anti-inflammatory drugs: a randomized, double-blind, placebo-controlled trial. Ann Intern Med 1995;123:241-9.
52. Zimmermann KC, Sarbia M, Schror K, Weber AA. Constitutive cyclooxygenase-2 expression in healthy human and rabbit gastric mucosa. Mol Pharmacol 1998;54:536-40.
53. Sawaoka H, Kawano S, Tsuji S, et al. Helicobacter pylori infection induces cyclooxygenase-2 expression in human gastric mucosa. Prostaglandins Leukot Essent Fatty Acids 1998;59:313-6.
54. McCarthy CJ, Crofford LJ, Greenson J, Scheiman JM. Cyclooxygenase-2 expression in gastric antral mucosa before and after eradication of Helicobacter pylori infection. Am J Gastroenterol 1999;94:1218-23.
55. Mizuno H, Sakamoto C, Matsuda K, et al. Induction of cyclooxygenase 2 in gastric mucosal lesions and its inhibition by the specific antagonist delays healing in mice. Gastroenterology 1997;112:387-97.
56. Prescott SM. Is cyclooxygenase-2 the alpha and the omega in cancer? J Clin Invest 2000;105:1511-3.
57. Newberry RD, Stenson WF, Lorenz RG. Cyclooxygenase-2-dependent arachidonic acid metabolites are essential modulators of the intestinal immune response to dietary antigen. Nat Med 1999;5:900-6.
58. Morteau O, Morham SG, Sellon R, et al. Impaired mucosal defense to acute colonic injury in mice lacking cyclooxygenase-1 or cyclooxygenase-2. J Clin Invest 2000;105:469-78.
59. Reuter BK, Asfaha S, Buret A, Sharkey KA, Wallace JL. Exacerbation of inflammation-associated colonic injury in rat through inhibition of cyclooxygenase-2. J Clin Invest 1996;98:2076-85.
60. FitzGerald GA, Smith B, Pedersen AK, Brash AR. Increased prosta-

Downloaded from www.nejm.org at FLAMEDLIB on May 13, 2009 .
Copyright © 2001 Massachusetts Medical Society. All rights reserved.

UM00016625
NOVARTIS EXHIBIT 1517
Novartis v. Regents, IPR2023-01347
Page 3607 of 4460

cyclin biosynthesis in patients with severe atherosclerosis and platelet activation. N Engl J Med 1984;310:1065-8.
61. McAdam BF, Catella-Lawson F, Mardini IA, Kapoor S, Lawson JA, FitzGerald GA. Systemic biosynthesis of prostacyclin by cyclooxygenase (COX)-2: the human pharmacology of a selective inhibitor of COX-2. Proc Natl Acad Sci U S A 1999;96:272-7. [Erratum, Proc Natl Acad Sci U S A 1999;96:5890.]
62. Cullen L, Kelly L, Connor SO, Fitzgerald DJ. Selective cyclooxygenase-2 inhibition by nimesulide in man. J Pharmacol Exp Ther 1998;287: 578-82.
63. Catella-Lawson F, McAdam B, Morrison BW, et al. Effects of specific inhibition of cyclooxygenase-2 on sodium balance, hemodynamics, and vasoactive eicosanoids. J Pharmacol Exp Ther 1999;289:735-41.
64. FitzGerald GA, Brash AR, Falardeau P, Oates JA. Estimated rate of prostacyclin secretion into the circulation of normal man. J Clin Invest 1981;68:1272-5.
65. Braden GA, Knapp HR, FitzGerald GA. Suppression of eicosanoid biosynthesis during coronary angioplasty by fish oil and aspirin. Circulation 1991;84:679-85.
66. Wennmalm A, FitzGerald GA. Excretion of prostacyclin and thromboxane A_2 metabolites during leg exercise in humans. Am J Physiol 1988; 255:H15-H18.
67. Topper JN, Cai J, Falb D, Gimbrone MA Jr. Identification of vascular endothelial genes differentially responsive to fluid mechanical stimuli: cyclooxygenase-2, manganese superoxide dismutase, and endothelial cell nitric oxide synthase are selectively up-regulated by steady laminar shear stress. Proc Natl Acad Sci U S A 1996;93:10417-22.
68. Murata T, Ushikubi F, Matsuoka T, et al. Altered pain perception and inflammatory response in mice lacking prostacyclin receptor. Nature 1997; 388:678-82.
69. Crofford LJ, Oates JC, McCune WJ, et al. Thrombosis in patients with connective tissue diseases treated with specific cyclooxygenase 2 inhibitors: a report of four cases. Arthritis Rheum 2000;43:1891-6.
70. Wallberg-Jonsson S, Ohman ML, Dahlqvist SR. Cardiovascular morbidity and mortality in patients with seropositive rheumatoid arthritis in northern Sweden. J Rheumatol 1997;24:445-51.
71. Wallberg-Jonsson S, Cederfelt M, Rantapaa Dahlqvist S. Hemostatic factors and cardiovascular disease in active rheumatoid arthritis: an 8 year followup study. J Rheumatol 2000;27:71-5.
72. Van Hecken A, Schwartz JI, Depre M, et al. Comparative inhibitory activity of rofecoxib, meloxicam, diclofenac, ibuprofen, and naproxen on COX-2 versus COX-1 in healthy volunteers. J Clin Pharmacol 2000;40: 1109-20.
73. Knijff-Dutmer EA, Martens A, vd Laar MA. Effects of nabumetone compared with naproxen on platelet aggregation in patients with rheumatoid arthritis. Ann Rheum Dis 1999;58:257-9.
74. Garcia Rodriguez LA, Varas C, Patrono C. Differential effects of aspirin and nonaspirin nonsteroidal antiinflammatory drugs in the primary prevention of myocardial infarction in postmenopausal women. Epidemiology 2000;11:382-7.
75. Antithrombotic Trialists' (ATT) Collaboration. Prevention of death, myocardial infarction and stroke by antiplatelet therapy: collaborative meta-analysis of 266 trials involving 200,000 patients at high risk of occlusive vascular events. BMJ (in press).
76. Patrono C, Coller B, Dalen JE, et al. Platelet-active drugs: the relationships among dose, effectiveness, and side effects. Chest 2001;119: Suppl:39S-63S.
77. Pratico D, Tillman C, Zhang ZB, Li H, FitzGerald GA. Acceleration of atherogenesis by COX-1-dependent prostanoid formation in low density lipoprotein receptor knockout mice. Proc Natl Acad Sci U S A 2001;98:3358-63.
78. Adderley SR, Fitzgerald DJ. Oxidative damage of cardiomyocytes is limited by extracellular regulated kinases 1/2-mediated induction of cyclooxygenase-2. J Biol Chem 1999;274:5038-46.
79. Shinmura K, Tang XL, Wang Y, et al. Cyclooxygenase-2 mediates the cardioprotective effects of the late phase of ischemic preconditioning in conscious rabbits. Proc Natl Acad Sci U S A 2000;97:10197-202.
80. Dinchuk JE, Car BD, Focht RJ, et al. Renal abnormalities and an altered inflammatory response in mice lacking cyclooxygenase II. Nature 1995;378:406-9.
81. Komhoff M, Wang JL, Cheng HF, et al. Cyclooxygenase-2-selective inhibitors impair glomerulogenesis and renal cortical development. Kidney Int 2000;57:414-22.
82. Nantel F, Meadows E, Denis D, Connolly B, Metters KM, Giaid A. Immunolocalization of cyclooxygenase 2 in the macula densa of human elderly. FEBS Lett 1999;457:475-7.
83. Patrono C, Dunn MJ. The clinical significance of inhibition of renal prostaglandin synthesis. Kidney Int 1987;32:1-12.
84. Swan SK, Rudy DW, Lasseter KC, et al. Randomized evaluations of the effects of cyclooxygenase-2 inhibition on renal function in elderly persons receiving a low-salt diet: a randomized, controlled trial. Ann Intern Med 2000;133:1-9.
85. Whelton A, Maurath CJ, Verburg KM, Geis GS. Renal safety and tolerability of celecoxib, a novel cyclooxygenase-2 inhibitor. Am J Ther 2000; 159-75.
86. Whelton A. Renal aspects of treatment with conventional nonsteroidal anti-inflammatory drugs versus cyclooxygenase-2 specific inhibitors. Am J Med 2001;110:Suppl 1:33-42.
87. Panara MR, Padovano R, Sciulli MG, et al. Effects of nimesulide on constitutive and inducible prostanoid biosynthesis in human beings. Clin Pharmacol Ther 1998;63:672-81.
88. Tegeder I, Lotsch J, Krebs S, Muth-Selbach U, Brune K, Geisslinger G. Comparison of inhibitory effects of meloxicam and diclofenac on human thromboxane biosynthesis after single doses and at steady state. Clin Pharmacol Ther 1999;65:533-44.
89. Feldman M, McMahon AT. Do cyclooxygenase-2 inhibitors provide benefits similar to those of traditional nonsteroidal anti-inflammatory drugs, with less gastrointestinal toxicity? Ann Intern Med 2000;132:134-43. [Erratum, Ann Intern Med 2000;132:1011.]
90. Singla AK, Chawla M, Singh A. Nimesulide: some pharmaceutical and pharmacological aspects — an update. J Pharm Pharmacol 2000;52:467-86.
91. Shah AA, Thjodleifsson B, Murray FE, et al. Selective inhibition of COX-2 in humans is associated with less gastrointestinal injury: a comparison of nimesulide and naproxen. Gut 2001;48:339-46.
92. Porto A, Almeida H, Cunha MJ, Macciocchi A. Double-blind study evaluating by endoscopy the tolerability of nimesulide and diclofenac on the gastric mucosa in osteoarthritic patients. Eur J Rheumatol Inflamm 1994;14:33-8.
93. Bourgeois P, Dreiser RL, Lequesne MG, Macciocchi A, Monti T. Multi-centre double-blind study to define the most favourable dose of nimesulide in terms of efficacy/safety ratio in the treatment of osteoarthritis. Eur J Rheumatol Inflamm 1994;14:39-50.
94. Hawkey C, Kahan A, Steinbruck K, et al. Gastrointestinal tolerability of meloxicam compared to diclofenac in osteoarthritis patients. Br J Rheumatol 1998;37:937-45. [Erratum, Br J Rheumatol 1998;37:1142.]
95. Dequeker J, Hawkey C, Kahan A, et al. Improvement in gastrointestinal tolerability of the selective cyclooxygenase (COX)-2 inhibitor, meloxicam, compared with piroxicam: results of the Safety and Efficacy Large-scale Evaluation of COX-inhibiting Therapies (SELECT) trial in osteoarthritis. Br J Rheumatol 1998;37:946-51.
96. Schoenfeld P. Gastrointestinal safety profile of meloxicam: a meta-analysis and systematic review of randomized controlled trials. Am J Med 1999;107:48S-54S.

Copyright © 2001 Massachusetts Medical Society.

Downloaded from www.nejm.org at FLAMEDLIB on May 13, 2009 .
Copyright © 2001 Massachusetts Medical Society. All rights reserved.

UM00016626
NOVARTIS EXHIBIT 1517
Novartis v. Regents, IPR2023-01347
Page 3608 of 4460

CRYSTAL GROWTH & DESIGN
2003
VOL. 3, NO. 6
909–919

Crystal Engineering of the Composition of Pharmaceutical Phases: Multiple-Component Crystalline Solids Involving Carbamazepine

Scott G. Fleischman,[†] Srinivasan S. Kuduva,[†] Jennifer A. McMahon,[†] Brian Moulton,[†] Rosa D. Bailey Walsh,[†] Naír Rodríguez-Hornedo,[‡] and Michael J. Zaworotko*,[†]

Department of Chemistry, University of South Florida, Tampa, Florida 33620-5250, and Department of Pharmaceutical Sciences, College of Pharmacy, University of Michigan, Ann Arbor, Michigan 48109-1065

Received March 3, 2003; Revised Manuscript Received May 14, 2003

Ⓦ **This paper contains enhanced objects available on the Internet at http://pubs.acs.org/crystal.**

ABSTRACT: The crystal engineering design strategy facilitates supramolecular synthesis of 13 new crystalline phases of carbamazepine (CBZ), an analgesic and anticonvulsant with known problems related to solubility and polymorphism. CBZ forms supramolecular complexes with the following molecules, all of which are complementary to CBZ in terms of hydrogen bonding and can therefore act as cocrystal formers: acetone (**1a**); DMSO (**1b**); benzoquinone (**1c**); terephthalaldehyde (**1d**); saccharin (**1e**); nicotinamide (**1f**); acetic acid (**1g**); formic acid (**1h**); butyric acid (**1i**); trimesic acid (**1j**); 5-nitroisophthalic acid (**1k**); adamantane-1,3,5,7-tetracarboxylic acid (**1l**); and formamide (**1m**). Two distinct strategies based upon selection of complementary hydrogen-bond functionalities and previously known supramolecular synthons were utilized: strategy I exploits the exofunctional nature of the carboxamide dimer as either a hydrogen-bond donor or a hydrogen-bond acceptor and thereby retains the carboxamide dimer that is present in all previously isolated forms of CBZ; strategy II perturbs the carboxamide homosynthon by forming a heterosynthon between the carboxamide moiety of CBZ and the carboxylic acid moieties. The latter approach profoundly modifies crystal packing and should therefore affect the physical and pharmaceutical properties of CBZ. A full analysis of crystal packing and a discussion of what these results might mean in the broader context of crystal engineering and pharmaceutical solids is presented.

Introduction

The concept of crystal engineering was introduced by Pepinsky in 1955[1] and was first applied by Schmidt in the context of covalent bond formation in the solid state (i.e., topochemical reactions).[2] The concept continues to attract interest in this context;[3] however, more recent developments have expanded it into areas as diverse as supramolecular synthesis, crystal structure analysis and prediction,[4] and functional materials.[5] Supramolecular synthesis offers a paradigm for the facile design and isolation of supramolecular complexes using self-assembly of different but complementary supramolecular synthons. The subsequent ability to generate a diverse range of multiple-component crystalline solids affords new compositions of matter and an ability to engage in systematic analysis of the factors that control structure/function relationships in the solid state.

Active pharmaceutical ingredients (APIs) represent a particularly great challenge to crystal engineers because of both fundamental and applied reasons. APIs are inherently predisposed for self-assembly since their utility is normally the result of the presence of one or more exofunctional supramolecular synthons. However, the crystal packing of APIs tends to be even less predictable than that of other organics because they often have multiple avenues for self-assembly and are therefore predisposed to exhibit polymorphism.[6] The presence of torsional flexibility further exacerbates matters as it can result in conformational polymorphism.[7] Such issues are of more than academic interest since intellectual property implications are considerable, and physical properties and bioavailability are often critically dependent upon crystal packing.[8] In this paper, we address how the concepts of crystal engineering and supramolecular synthons can be applied to the design of new compositions of matter that are based upon existing APIs and complementary molecules that might be called cocrystal formers. The new compositions that are thereby generated are expected to offer desirable components, structures, and of course, properties.

It should be noted that this approach represents a complementary strategy to the use of techniques such as high throughput crystallization[9] or polymer nucleation[10] for control of polymorphs. Furthermore, in principle it offers a much wider range of possible pharmaceutical compositions without the need for covalent modification of APIs.

The pharmaceutically active molecule carbamazepine (CBZ) [5*H*-dibenz(b,f) azepine-5-carboxamide] was of interest to us because of its limited bioavailability[11] and its eight reported polymorphs[12,13] and pseudopolymorphs.[13] It is an important drug for the treatment of epilepsy and trigeminal neuralgia, and pure CBZ crystallizes as one of four polymorphs: tri-

* To whom correspondence should be addressed. E-mail: xtal@usf.edu. Fax: (813) 974-3203. Tel: (813) 974-4129
† University of South Florida.
‡ University of Michigan.

10.1021/cg034035x CCC: $25.00 © 2003 American Chemical Society
Published on Web 06/17/2003

UM00016627
NOVARTIS EXHIBIT 1517
Novartis v. Regents, IPR2023-01347
Page 3609 of 4460

clinic (form I); trigonal (form II); and monoclinic (forms III and IV). Its relevance, limited solubility, and the fact that it exists in multiple crystalline forms therefore makes CBZ an ideal candidate for a crystal engineering case study.

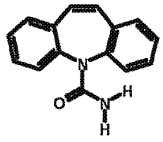

The primary supramolecular synthon in CBZ is the carboxamide moiety, which has already proven to be a reliable supramolecular synthon for the generation of supramolecular architectures.[14] It most commonly forms the cyclic homosynthon[15] I using the syn-oriented N−H group.[16] The anti-oriented N−H group of the carboxamide typically forms either a 5.1 Å translation related hydrogen-bonded tape or a glide or 2_1-screw pattern. In either case, the additional hydrogen-bond acceptor is the amide carbonyl group of the adjacent carboxamide moiety. This centrosymmetric homosynthon is the primary supramolecular synthon observed in crystalline solids that contain carboxamide moieties.

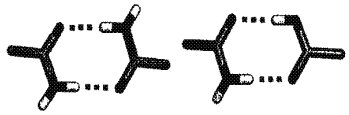

I II

A survey of the Cambridge Structural Database (CSD)[17] and a review of the literature indicated that only five of the eight forms of CBZ isolated thus far have been reported with full structural data (polymorphs II[13b] and III,[13c] a hydrate[14a] with an *R* factor of ~10%, and two multiple-component phases[14]), although the cell parameters of an acetone solvate have also been reported.[13d] Analysis of crystal packing in these structures reveals that the supramolecular homosynthon I generates CBZ dimers in all compounds and that the azepine ring adopts a boat conformation. Form II is trigonal, and form III is a monoclinic phase that contains cavities. The syn-oriented N−H of the carboxamide group forms the expected dimers, while the anti-oriented N−H does not engage in intermolecular interactions. A search of the CSD revealed 440 structures containing an amide homodimer (organics only, NH···O contact is 0−3.3 Å). Of those 440 structures, 30% have an anti-oriented N−H that is not involved in hydrogen bonding, most commonly because of steric hindrance.

As revealed later, the presence of unused hydrogen bond donor and acceptor sites is an important issue in the context of crystal engineering. Furthermore, the different crystal packing motifs in the polymorphs of CBZ might be attributed to the molecular shape of the CBZ dimer and its inability to efficiently pack or utilize the inactivated anti N−H group. Interestingly, an isostructural crystal packing with the trigonal form II was identified from the CSD. *N*-Acetyl-dibenz(b,f)-azepine [CSD REFCODE: BOWWAL] is an analogue of CBZ in which the amide NH_2 group in CBZ is replaced with a CH_3 group; therefore, the supramolecular synthon is the result of a C−H···O=C mediated homosynthon instead of a N−H···O=C homosynthon.[18] Form III has been reported to be the most thermodynamically stable phase at room temperature and the one selected for use herein.[19] Interestingly, the hydrate structure of CBZ forms N−H···O hydrogen bonds via the anti-oriented N−H of the amide group in addition to the homosynthon I and is even less soluble in water than the pure forms.[12] It is this low solubility of CBZ in water that makes it difficult to further extend its utility as a pharmaceutical and justifies CBZ as a candidate for a search for more crystalline phases.

In this contribution, we present two basic strategies for such a search, both of which might be generally applicable to APIs that contain carboxamide moieties. Strategy 1 maintains the carboxamide homosynthon but exploits the exterior H-bond donor and acceptor sites of the carboxamide homosynthon with a nonacid cocrystal former. Strategy 2 breaks the carboxamide homosynthon with carboxylic acid moieties, thereby generating the heterosynthon II.[20]

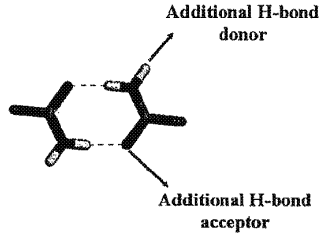

Strategy 1

As revealed herein, both strategies are fruitful, and we report full structural information on the acetone solvate of CBZ along with full structural data on 12 other multiple-component phases of CBZ. All 13 of these phases contain a cocrystal former, which are illustrated schematically in Scheme 1. Those generated from strategy 1 retain the carboxamide dimer motif, but there are three modes by which they exploit their remaining H-bonding sites: H-bond donor of CBZ to the H-bond acceptor of cocrystal former (CBZ/acetone, **1a**, Figure 1; CBZ/DMSO, **1b**, Figure 1; CBZ/benzoquinone, **1c**, Figure 2; and CBZ/terephthalaldehyde, **1d**, Figure 2); H-bond donor of the cocrystal former to the H-bond acceptor in CBZ (CBZ/saccharin, **1e**, Figure 3); and both H-bond donor and H-bond acceptors of the CBZ interacting with the cocrystal former (CBZ/nicotinamide, **1f**, Figure 4). Strategy 2 affords six new phases: CBZ/acetic acid, **1g**, Figure 5; CBZ/formic acid, **1h**, Figure 5; CBZ/butyric acid, **1i**, Figure 5; CBZ/trimesic acid, **1j**, Figure 6; CBZ/5-nitroisophthalic acid, **1k**, Figure 6; and CBZ/adamantane-1,3,5,7-tetracarboxylic acid, **1l**, Figure 7. Understanding the structural packing in these compounds allowed us to generate one more compound that is based upon extending the amide hydrogen-bond pattern with the use of the cocrystal former formamide, **1m**. Throughout the remainder of this paper we refer to **1a**−**1m** as supramolecular complexes and do not separately identify the solvated CBZ structures as peusodopolymorphs.[21]

UM00016628
NOVARTIS EXHIBIT 1517
Novartis v. Regents, IPR2023-01347
Page 3610 of 4460

Table 1. Crystallographic Data for the Supramolecular Complexes 1a–1m

	1a	**1b**	**1c**	**1d**	**1e**	**1f**	**1g**	**1h**	**1i**	**1j**	**1k**	**1l**	**1m**
formula	$C_{18}H_{18}N_2O_2$	$C_{17}H_{18}N_2O_2S_1$	$C_{18}H_{14}N_2O_2$	$C_{19}H_{16}N_2O_2$	$C_{22}H_{17}N_3O_4S_1$	$C_{21}H_{18}N_4O_2$	$C_{17}H_{16}N_2O_3$	$C_{18}H_{14}N_2O_3$	$C_{19}H_{20}N_2O_3$	$C_{24}H_{18}N_2O_7$	$C_{23.5}H_{20}N_3O_3$	$C_{44}H_{40}N_4O_{10}$	$C_{16}H_{15}N_3O_2$
stoichiometry	1:1	1:1	1:0.5	1:0.5	1:1	1:1	1:1	1:1	1:1	1:1	1:1	1:0.5	1:1
mol. wt.	294.34	308.36	290.31	303.33	419.46	358.39	296.32	282.29	324.37	446.40	472.42	784.80	281.31
crystal system	triclinic	triclinic	monoclinic	monoclinic	triclinic	monoclinic	monoclinic	monoclinic	triclinic	monoclinic	monoclinic	monoclinic	triclinic
space group	$P\bar{1}$	$P\bar{1}$	$P2_1/c$	$C2/c$	$P\bar{1}$	$P2_1/n$	$P2_1/c$	$P2_1/c$	$P\bar{1}$	$C2/c$	$C2/c$	$C2/c$	$P\bar{1}$
a (Å)	7.3985(15)	7.3254(19)	10.3335(15)	29.191(16)	7.5140(11)	5.0961(8)	5.1206(4)	5.2031(9)	9.1567(12)	32.531(5)	34.355(8)	18.388(4)	5.1077(11)
b (Å)	8.9054(18)	8.889(2)	27.611(5)	4.962(3)	10.4538(15)	17.596(3)	15.7136(13)	14.741(2)	10.1745(13)	5.2697(8)	5.3795(13)	12.682(3)	16.057(3)
c (Å)	11.873(2)	12.208(3)	4.9960(9)	20.316(11)	12.6826(18)	19.647(3)	18.4986(15)	17.882(3)	10.5116(14)	24.159(4)	23.654(6)	16.429(3)	17.752(4)
α (deg)	95.809(3)	94.840(5)	90	90	83.642(2)	90	90	90	72.850(2)	90	90	90	73.711(3)
β (deg)	93.401(4)	94.926(5)	102.275(3)	92.105(8)	85.697(2)	90.917(3)	96.546(1)	98.132(3)	70.288(2)	98.191(3)	93.952(6)	100.491(6)	89.350(3)
γ (deg)	101.362(3)	100.048(5)	90	90	75.411(2)	90	90	90	67.269(2)	90	90	90	88.636(3)
volume (Å^3)	760.5	775.8(3)	1392.9(4)	2941(3)	957.0(2)	1761.4(5)	1478.8(2)	1357.7(4)	834.91(19)	4099.3(11)	4361.2(2)	3767.1(1)	1397.1(5)
calc density (g cm^{-3})	1.285	1.346	1.232	1.370	1.456	1.352	1.331	1.381	1.290	1.450	1.408	1.384	1.337
Z	2	2	4	8	2	4	4	4	2	8	8	8	4
θ range	1.7–25.0	1.7–25.0	2.02–28.24	1.4–21.8	1.6–28.2	1.5–25.0	1.7–28.4	1.7–28.3	2.1–28.28	1.3–25.0	1.2–25.0	2.0–28.2	1.2–28.33
no. data/params	2449/202	2674/211	2707/199	1559/208	4372/283	3033 /244	3529/203	3191/190	2684/217	3601/303	3839/310	4481/263	4610/379
T (K)	100	200	100	200	200	200	100	100	100	100	200	100	100
solvent	acetone	DMSO	methanol	methanol	ethanol	DMSO-methanol	acetic acid	formic acid	butyric acid	methanol	DMSO-methanol	ethanol	methanol
R1	0.0768	0.0795	0.0545	0.0351	0.0458	0.0522	0.0492	0.0533	0.0499	0.1556	0.0619	0.0433	0.0766
wR2	0.2669	0.2376	0.1358	0.0931	0.1204	0.1124	0.1335	0.1268	0.1137	0.3607	0.1763	0.0913	0.1633

Experimental Procedures

Crystals of **1c**, **1d**, **1e**, **1f**, **1j**, **1k**, **1l**, and **1m** were obtained via slow evaporation of 1:1 molar ratio of CBZ and cocrystal formers in an appropriate solvent. Solutions were not allowed to go to dryness. The remaining crystals were obtained by recrystallization from their respective solvents, which also acted as cocrystal formers. All crystallization experiments were conducted in an unmodified atmosphere, and solvents were dried by standard methods prior to use. All chemicals used are commercially available and were purchased from Aldrich. Melting points for **1a**–**1m** are given in Table 3.

Infrared spectroscopy was conducted using a Nicolet Avatar 320 FTIR. Differential scanning calorimetry was conducted on TA Instruments 2920 DSC. Thermogravimetric analysis was conducted using a TA Instruments 2950 Hi-Resolution TGA. X-ray powder diffraction was conducted on a Rigaku Miniflex Diffractometer using CuKα (λ = 1.540562, 30 kV, 15 mA). The powder data were collected over an angular range of 3–40° 2θ in continuous scan mode using a step size of 0.02° 2θ and a scan speed of 2.0°/min, and melting points were determined on a Mel-temp.

X-ray Crystallography. All single-crystal X-ray data were collected on a Bruker SMART-APEX CCD diffractometer. Lattice parameters were determined from least-squares analysis, and the reflection data were integrated using the program SAINT. Structures were solved by direct methods and refined by full matrix least-squares based on F^2 using SHELXTL.[22] Crystallographic data for **1a**–**1m** are presented in Table 1.

Results and Discussion

1a–**1m** form X-ray quality single crystals via a reaction between CBZ and cocrystal formers as described above. For the 10 new cocrystals reported, approximately 50 cocrystal formers were used with CBZ, giving a success ratio of 20%. The crystal structures of these supramolecular complexes are now described. In all crystal structures reported herein, **1a**–**1m**, the CBZ azepine ring adopts a boat conformation. **1a**–**1e** are related in that they contain the CBZ dimers that are sustained by the robust cyclic carboxamide homosynthon I and pack roughly in an eclipsed manner. This packing mode facilitates the formation of a cavity in which cocrystal formers can exist. Indeed, **1a** and **1b** are isostructural, and the asymmetric unit contains one molecule of CBZ and one solvent molecule.

The CBZ molecules in **1a** and **1b** form homosynthon I, and the voids that exist between adjacent CBZ dimers lie around crystallographic inversion centers. The salient hydrogen-bond distances for **1a** and **1b** are summarized in Table 2 and are within expected ranges for these types of hydrogen bonds.[23] The cocrystal formers interact with the anti N–H of the CBZ dimers to form N–H···O=C/S hydrogen bonds (Figure 1).

1c and **1d** exhibit a similar supramolecular structure to that of **1a** and **1b**, and benzoquinone and terephthalaldehyde molecules lie around crystallographic inversion centers. The asymmetric unit of **1c** and **1d** consists of one molecule of CBZ and a half molecule of benzoquinone and terephthalaldehyde, respectively. The difference between the crystal structures of **1c** and **1d** lies with the symmetry of homosynthon I. In supramolecular complex **1c**, homosynthon I was observed between inversion related CBZ molecules; however, in **1d** a 2_1-screw relates the CBZ molecules. As a result of the two different symmetry operations, the orientation of the CBZ azepine ring changes between **1c** and **1d** and influences the overall crystal packing. In short, the

UM00016629
NOVARTIS EXHIBIT 1517
Novartis v. Regents, IPR2023-01347
Page 3611 of 4460

Scheme 1. Cocrystal Former Structures

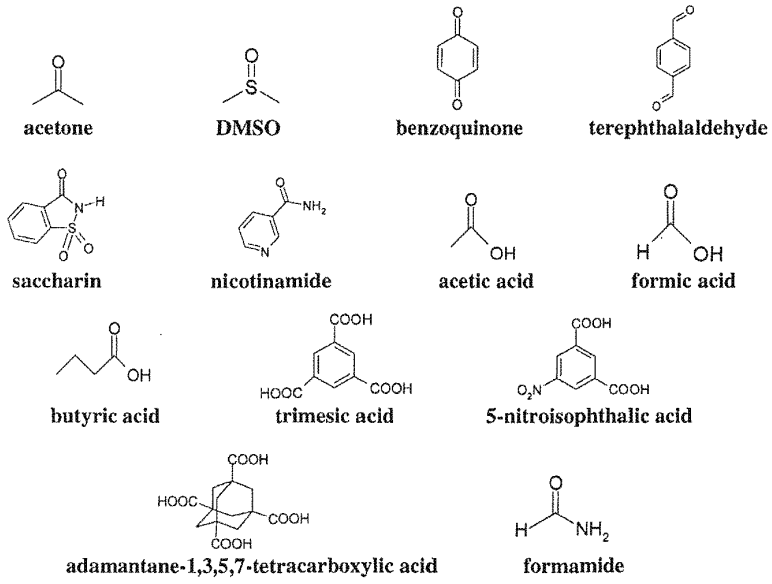

benzoquinone and terephthalaldehyde molecules in **1c** and **1d** provide complementary molecular recognition sites for CBZ dimers in a similar way to those that exist in the acetone and DMSO solvates. However, the net result is a 1-D ribbon because of the presence of two acceptor sites (Figure 2).

In **1e**, homosynthon I is generated by inversion related CBZ molecules. The saccharin molecule acts as both H-bond donor and acceptor. An N−H···O hydrogen bond with the O=C group of the carboxamide is formed, while the anti N−H of the CBZ forms a weak N−H···O=S hydrogen bond with weak metrics (d = 2.47 Å, D = 3.007(2) Å, θ = 113°). The inversion related saccharin molecules form auxiliary C−H···O hydrogen bonds (d = 2.21 Å, D = 3.196(2) Å, θ = 150°), and the overall hydrogen-bonding pattern can therefore be described as a 1-D array (Figure 3). The crystal packing of **1a**−**1e** can all be described as crinkled tape motifs with a zigzag arrangement along the hydrophobic regions of the CBZ azepine ring system.

Given these observations, one might ask what drives the CBZ molecule in the pure forms to adopt crystal

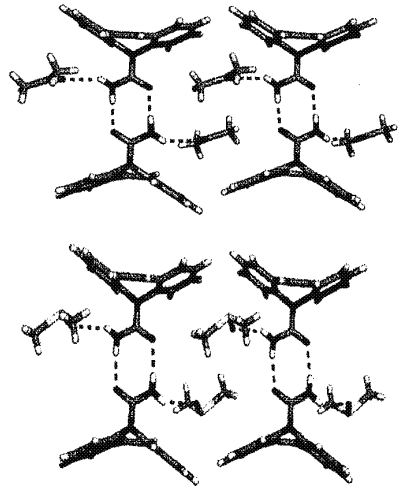

Figure 1. Illustration of the interactions between CBZ dimers and acetone (**1a**) or DMSO (**1b**). The cocrystal formers in these isostructural compounds are held by the anti N−H···O hydrogen bond of the CBZ dimers and thereby generate a void space between the CBZ dimers that is not present in the pure forms of CBZ.

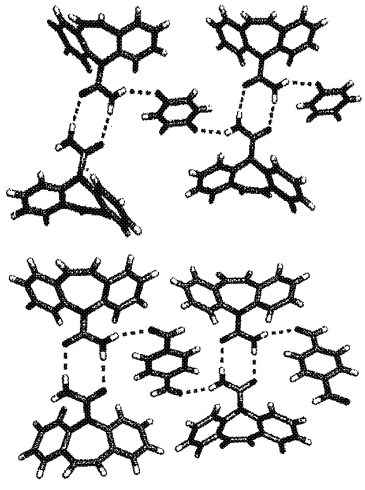

Figure 2. Interaction of CBZ dimers with cocrystal formers in structures **1c** and **1d**. The cocrystal formers are held by the anti N−H···O hydrogen bond of the CBZ dimers and not only generate a void space between the CBZ dimers but also sustain a 1-D hydrogen-bonded network.

UM00016630
NOVARTIS EXHIBIT 1517
Novartis v. Regents, IPR2023-01347
Page 3612 of 4460

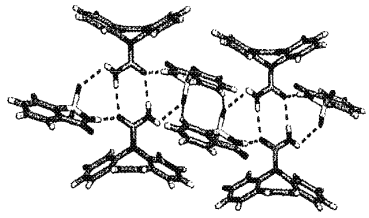

Figure 3. Illustration of the interaction between CBZ dimers and saccharin (**1e**). The cocrystal former in this structure is held by C=O···H–N hydrogen bonds with the CBZ dimers and is elongated into a 1-D network by C–H···O interactions between saccharin molecules.

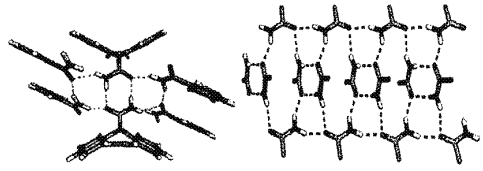

Figure 4. Cocrystal former, nicotinamide, links the CBZ homosynthon by forming a hydrogen-bonded strip in **1e**. For clarity, unwanted atoms are removed, and the hydrogen-bonded strip is shown in the adjacent figure.

packing with unsatisfied amide N–H moieties? Comparison of the supramolecular complexes **1a**–**1e** with the pure forms suggests that approach of two molecules of CBZ via the anti N–H···O=C is sterically disfavored because of the shape of the CBZ dimers. However, the supramolecular complexes satisfy these N–H moieties and facilitate a more open crystal packing (i.e., eclipsed with large cavities in **1a**–**1e** vs staggered with no large cavities but unsatisfied N–H moieties in **1**).

1f also exhibits an inversion related homosynthon I between CBZ molecules. However, an unexpected exterior hydrogen-bonded pattern that is translation related exists between cocrystal former, nicotinamide, and CBZ molecules (Figure 4). In this way, the donors and acceptors of both amide groups are fulfilled. However, the nitrogen atom within the ring structure of the nicotinamide does not form any strong hydrogen bonds. The crystal packing illustrates hydrophobic interlocking rows with $\pi\cdots\pi$ interactions between the CBZ hoods and the nicotinamide rings.

In summary, structures **1a**–**1f** retain the carboxamide homosynthon, I. We now turn our attention to exploitation of heterosynthon II (i.e., strategy 2). One would expect heterosynthon formation to be preferred over homosynthon formation if there is an appropriate complementarity between the two components of the heterosynthon. In the case of carboxamide/carboxylic acid heterosynthons, the strongest hydrogen-bond donor (acid O–H) should hydrogen bond with the best acceptor atom (amide C=O).[24] This leaves the slightly weaker donor (amide N–H) to hydrogen bond to the weaker acceptor group (acid C=O). It should be noted that this heterosynthon minimizes intermolecular lone-pair repulsions that would occur between the acid O–H and carbonyl moieties in hydrogen-bonded chains constructed from the homosynthon and N–H···O hydrogen bonds.[18,23]

X-ray quality single crystals of **1g** were grown from acetic acid and exhibit the expected heterosynthon II. The anti N–H of the amide moiety forms an N–H···O hydrogen bond with the acetic acid carbonyl group instead of its own amide carbonyl group. However, an inversion center relates two adjacent heterosynthons, thereby generating a four-component supramolecular complex (Figure 5). These supramolecular complexes are connected to adjacent supramolecular complexes through C–H···O hydrogen bonds (d = 2.32 Å, D = 3.368(2) Å,

Table 2. Geometric Parameters of Intermolecular Interactions[a]

	interaction	d (Å)	D (Å)	θ (deg)
1a	N–H$_s$···O	1.98	2.928(4)	156
	N–H$_a$···O	2.17	3.018(4)	140
1b	N–H$_s$···O	1.98	2.960(6)	164
	N–H$_a$···O	2.11	2.966(6)	141
1c	N–H$_s$···O	1.90	2.899(2)	171
	N–H$_a$···O	2.21	3.116(2)	148
1d	N–H$_s$···O	2.07	2.947(3)	144
	N–H$_a$···O	2.15	3.079(3)	152
1e	N–H$_s$···O	1.95	2.954(2)	174
	N–H···O=C	1.75	2.724(2)	161
1f	N–H$_s$···O	1.90	2.868(2)	160
	N–H$_a$···O	2.30	3.040(2)	129
	N–H···O=C	1.95	2.871(2)	150
	N–H$_a$···O	2.06	2.986(3)	152
1g	N–H$_s$···O	2.09	3.016(2)	151
	N–H$_a$···O	2.25	2.919(2)	122
	O–H···O=C	1.59	2.553(2)	167
1h	N–H$_s$···O	2.02	2.939(3)	150
	N–H$_a$···O	2.06	2.894(2)	139
	O–H···O=C	1.58	2.548(2)	167
1i	N–H$_s$···O	2.04	2.963(2)	152
	N–H$_a$···O	2.44	2.929(2)	109
	O–H···O=C	1.62	2.589(2)	170
1j	N–H$_s$···O	1.95	2.864(10)	149
	O–H···O=C	1.57	2.542(10)	169
	O–H···O		2.590(9)	
	O–H···O	1.63	2.607(9)	171
1k	N–H$_s$···O	1.96	2.898(4)	153
	O–H···O=C	1.53	2.489(3)	163
	O–H···O	1.63	2.599(3)	166
1l	N–H$_s$···O	1.91	2.895(2)	164
	N–H$_a$···O	2.09	2.899(2)	136
	O–H···O=C	1.66	2.637(2)	170
	O–H···O=C	1.69	2.675(2)	178
1m	N–H$_s$···O	1.94	2.922(2)	164
	N–H$_a$···O	2.11	2.974(3)	142
	N–H$_s$···O	1.87	2.872(3)	171
	N–H$_a$···O	2.04	2.911(3)	144
	N–H$_s$···O	1.94	2.947(3)	172
	N–H$_s$···O	1.94	2.941(3)	172
	N–H$_s$···O	1.89	2.889(3)	170
	N–H$_a$···O	1.95	2.875(3)	150

[a] The syn and anti N–H groups of the carboxamides are referred with subscript s and a, respectively. Neutron normalized hydrogen atom position are used for the intermolecular calculations.

Table 3. Melting Points of CBZ Cocrystals (°C)

carbamazepine (CBZ)	**1**	190–192°
CBZ.acetone (1:1)	**1a**	189°
CBZ.DMSO (1:1)	**1b**	189°
CBZ.benzoquinone (2:1)	**1c**	170°
CBZ.terephthalaldehyde (2:1)	**1d**	124°
CBZ.saccharin (1:1)	**1e**	174°
CBZ.nicotinamide (1:1)	**1f**	151–161°
CBZ.acetic acid (1:1)	**1g**	187°
CBZ.formic acid (1:1)	**1h**	187°
CBZ.butyric acid (1:1)	**1i**	120°
CBZ.trimesic acid (1:1)	**1j**	278° (dec)
CBZ.5-nitroisophthalic acid (1:1)	**1k**	190° (dec)
CBZ.adamantane-1,3,5,7-tetracarboxylic acid (2:1)1	**1l**	258–260°
CBZ.formamide (1:1)	**1m**	142–144°

UM00016631
NOVARTIS EXHIBIT 1517
Novartis v. Regents, IPR2023-01347
Page 3613 of 4460

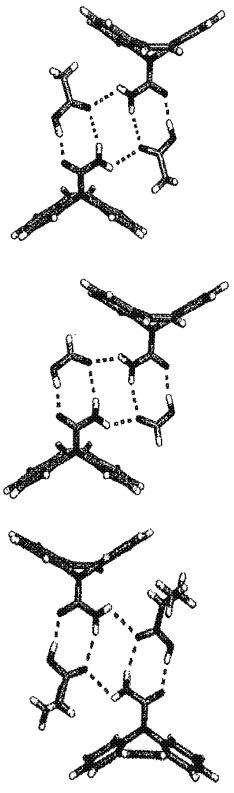

Figure 5. Heterosynthon **II** formed with cocrystal formers, acetic acid (**1g**), formic acid (**1h**), and butyric acid (**1i**). The anti-N−H group of CBZ is utilized to form the inversion related N−H···O hydrogen bond with carboxylic acid C=O of the cocrystal former, thereby generating a four-component supramolecular complex rather than a tape.

θ = 163°) that are glide related. The CBZ azepine ringsorient above and below the hydrogen-bonded patterns and thereby form a hydrophobic region.

Crystallization from formic acid afforded an isostructural four-component supramolecular complex, **1h** (Figure 5). The C−H moiety of the formic acid does not form any strong intermolecular interactions. Crystallization of CBZ from butyric acid resulted in **1i**, which exhibits a similar hydrogen-bonded motif (Figure 5). The butyric alkyl groups fold to facilitate formation of the four-component motif. The anti N−H···O hydrogen bond is bent, presumably because of the relative size of the alkyl group (matrix for the anti N−H···O in structure **1g**: d = 2.25 Å, D = 2.919(2) Å, θ = 122°; **1h**: d = 2.06 Å, D = 2.894(2) Å, θ = 139°; **1i**: d = 2.44 Å, D = 2.929(2) Å, θ = 109°).

The structures presented in Figure 5 suggest that the four-component supramolecular complex would be sterically disfavored if sterically bulky carboxylic acids were to be utilized. The 1:1 supramolecular complex, **1j**, of CBZ and trimesic acid reveals this to be the case. The hydrogen-bonding pattern in the crystal structure of **1j** is 1-D and consists of both acid−acid homosynthons and acid−amide heterosynthons. Two carboxylic acid groups of the trimesic acid are free to form homosynthons, and

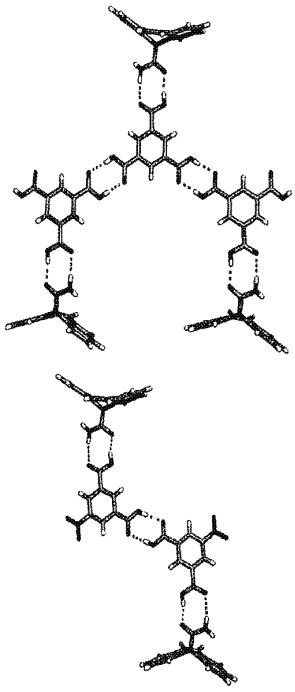

Figure 6. Illustration of portions of the structures observed in compounds **1j** and **1k**. One carboxylic acid group in the cocrystal former is utilized to form a heterosynthon, and the other carboxylic acid groups form homosynthons that propagate a 1-D hydrogen-bonded pattern in **1j** and a 0-D discrete pattern in **1k**.

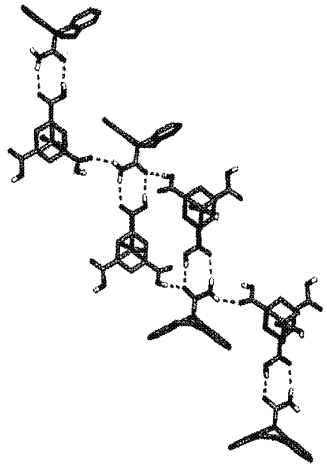

Figure 7. All the hydrogen-bonding sites of the cocrystal former are utilized in **1l**. Notice the heterosynthon **II** and absence of any carboxylic acid dimer homosynthons.

these sustain a 1-D zigzag array. The third carboxylic acid group bonds to CBZ molecules via heterosynthon II. Replacement of one carboxylic acid group in trimesic acid with a size matching nitro group, 5-nitroisophthalic acid, leads to a closely related structure in which a discrete four-component supramolecular complex is

UM00016632
NOVARTIS EXHIBIT 1517
Novartis v. Regents, IPR2023-01347
Page 3614 of 4460

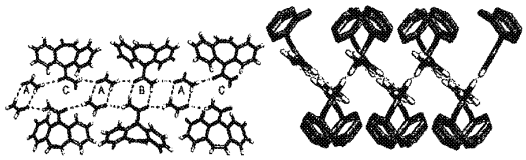

Figure 8. All the hydrogen-bonding sites of the CBZ molecule are utilized with the formamide cocrystal former in the supramolecular complex **1m**. Notice the homosynthon I formed by formamide molecules. The adjacent illustration represents the cross-section view of the hydrogen-bonded 2-D structure.

generated, **1k**. Indeed, **1k** is isostructural with **1j**, and its crystal structure consists of a carboxylic acid homosynthon and a heterosynthon (Figure 6). The anti N−H group of the carboxamide moieties forms N−H···O hydrogen bonds with disordered solvent molecules.

Adamantane-1,3,5,7-tetracarboxylic acid would be expected to increase the dimensionality further. Supramolecular complex **1l** was obtained when the cocrystallization was carried out with a 1:1 ratio of CBZ and adamantane-1,3,5,7-tetracarboxylic acid from either ethanol or methanol. The asymmetric unit of **1l** consists of one molecule of CBZ and a half molecule of adamantane-1,3,5,7-tetracarboxylic acid, which lies at a 2-fold rotation axis. The structure contains heterosynthon II and does not form acid−acid homosynthons (Figure 7). The two carboxylic acid groups of the cocrystal former generate heterosynthon II with two CBZ molecules, and the exterior hydrogen-bond acceptor/donor sites of the CBZ molecules interact with the remaining acid groups by means of anti N−H···O=C and acid O−H···O=C H bonds. In this fashion, all the hydrogen-bonding donor/acceptor sites of CBZ molecule and adamantane tetra acid are satisfied. The resulting H-bond network is 3-D in nature and free of solvent molecules.

Structures **1g**−**1l** confirm that heterosynthon II can indeed be formed reliably and that they can generate supramolecular structures and networks that are rational and prototypal for an even wider range of related structures.

As revealed by Figure 9, there is a considerable degree of superstructural diversity in the crystal packing observed within compounds **1a**−**m**. Indeed, they also differ from the crystal packing exhibited by forms II and III of CBZ itself. An analysis of **1a**−**m** reveals that it is possible for the CBZ carboxamide group to form conventional translation or 2_1-screw/glide symmetry tapes that are commonly observed in amide hydrogen-bonding patterns. However, the conventional motif appears to be impossible in pure CBZ because of the boat shaped azepine ring that sterically blocks the exterior amide hydrogen-bond acceptor/donor. Analysis of the aliphatic acid phases **1g**−**1i** provides the hint that crystallizing CBZ with a simple aliphatic amide might extend the hydrogen-bonded pattern, using the exterior amide acceptor/donor in a manner similar to that observed in the approach as in **1g**−**1i**. Another viable pattern could utilize the exterior hydrogen-bond acceptor/donor of the CBZ homosynthon I with the exterior hydrogen-bond acceptor/donor sites of a carboxamide cocrystal former. A third possibility would be a structure similar to that of supramolecular complex **1f** that does not follow the conventional amide hydrogen-bonded pattern.

1m was prepared to test which of these possible structures occurs. **1m** forms when CBZ is crystallized with formamide in methanol.[25] The asymmetric unit of **1m** consists of two molecules of CBZ and two molecules of formamide in the triclinic space group $P\bar{1}$. Both formamide molecules in the asymmetric unit form homosynthon I, hereafter denoted as A. The two CBZ molecules form two different inversion related homosynthons, denoted B and C, respectively. The exterior of CBZ homosynthon B hydrogen bonds with the two pairs of A homosynthons to generate a six-component planar supramolecular complex, A-B-A. The exterior of the A-B-A supramolecular complex consists of two formamide anti N−H donor groups and two C=O acceptor groups. These donor/acceptor moieties hydrogen bond with the second CBZ dimer, C, of the asymmetric unit. In the hydrogen-bonding pattern, the formamide and the CBZ dimers alternate through exterior hydrogen bonding (Figure 8). In this fashion, a 2-D hydrogen-bonded pattern is generated. **1m** represents a rare example of a crystal structure that contains two chemically different amide groups. Previous examples include a urea-carboxamide cocrystal[26] and an amide-secondary amide cocrystal[27] that could be described as being examples of homosynthons between two different molecules (i.e., amide-amide′ homosynthons). However, **1m** is to our knowledge unprecedented in that it contains two different molecules, both of which form the amide-amide homosynthon, not the amide-amide′ homosynthon.

Conclusion

In summary, we have exercised a paradigm based on modular design in which cocrystal formers can be exploited for their ability to form supramolecular interactions with APIs. The result is a diverse range of multiple-component crystalline phases of a well-known API with previously documented solubility and polymorphism problems. Of particular note is that the multiple-component phases are formed in preference over a low solubility hydrate of CBZ (there were no attempts to eliminate adventitious moisture in our experiments). The immediate implication of our results is that it should be generally possible to exploit APIs that contain amide moieties for formation of a diverse range of new multiple-component crystalline phases if appropriate cocrystal formers are employed. The broader implications are that the cocrystal former strategy might be applied even more generally and that it could ultimately become an essential component in optimization of the drug design, processing, and delivery procedures. Indeed, we recently demonstrated that pyridinecarboxylic acid heterosynthons might be exploited in a similar fashion,[15] and there are numerous examples of other heterosynthons that will be expected to be suitable in the context of APIs. Most importantly, the cocrystal former approach means that the APIs are not covalently modified, and a diverse range of new compositions of matter with different physical properties is readily accessible. Simply put, we have applied new tricks to old procedures and molecules. Future work will concen-

UM00016633
NOVARTIS EXHIBIT 1517
Novartis v. Regents, IPR2023-01347
Page 3615 of 4460

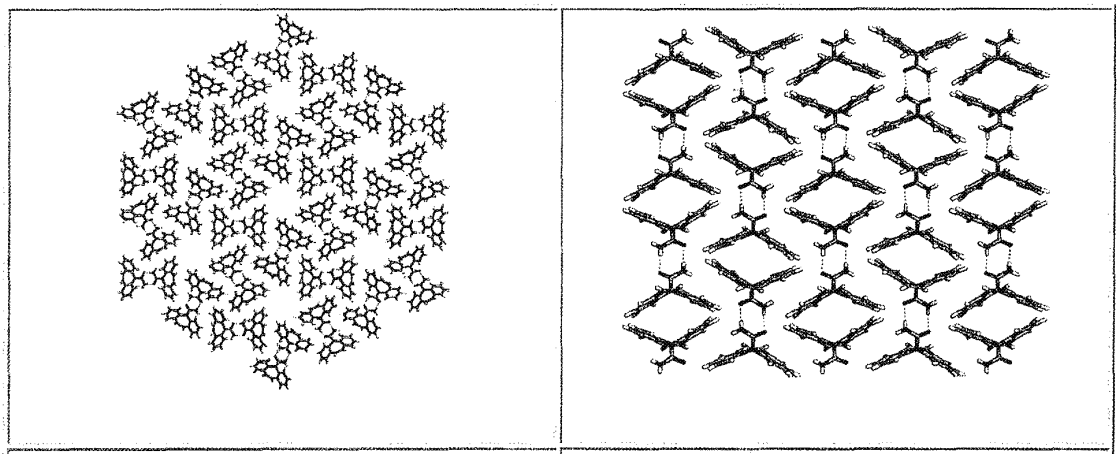

Form II **Form III**

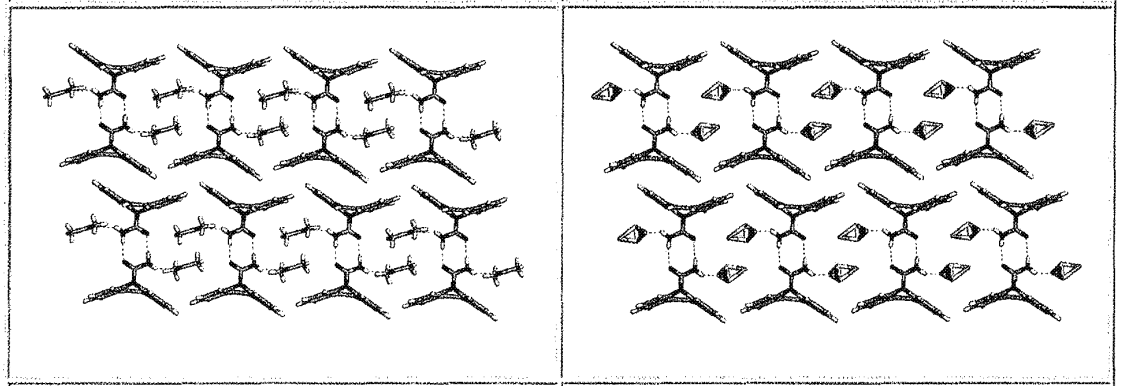

1a **1b**

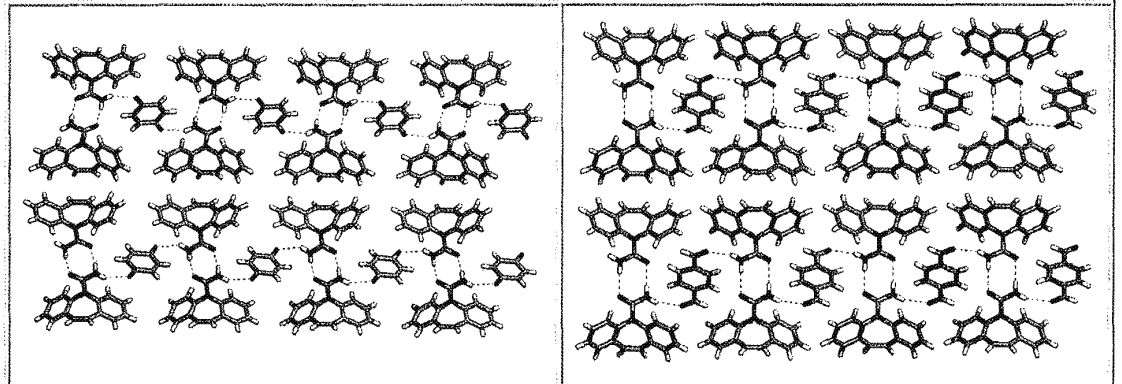

1c **1d**

UM00016634
NOVARTIS EXHIBIT 1517
Novartis v. Regents, IPR2023-01347
Page 3616 of 4460

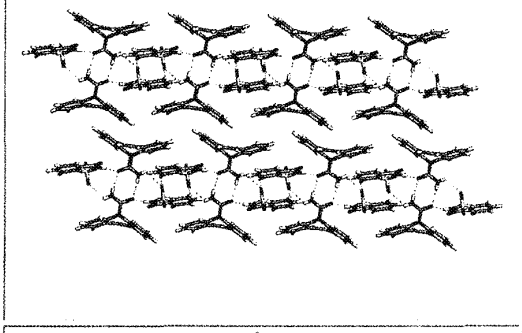

1e

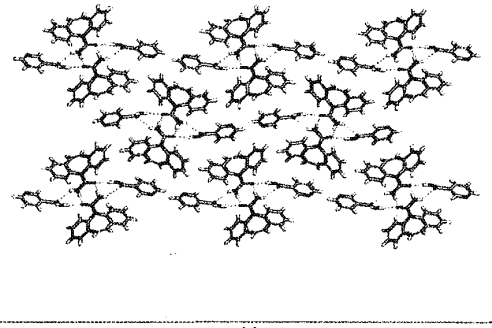

1f

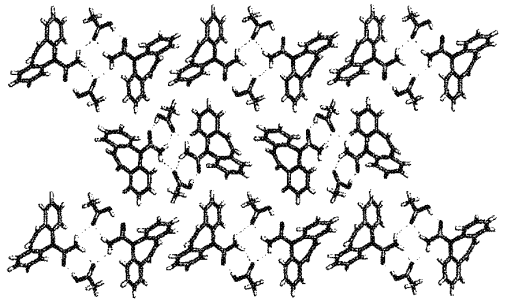

1g

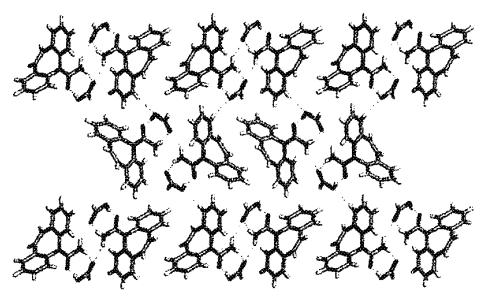

1h

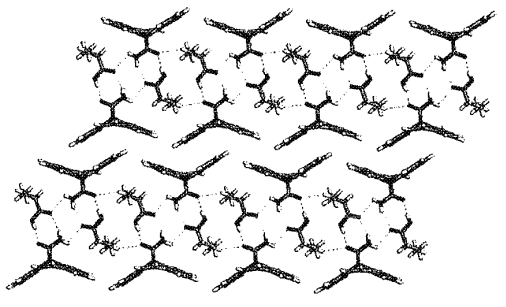

1i

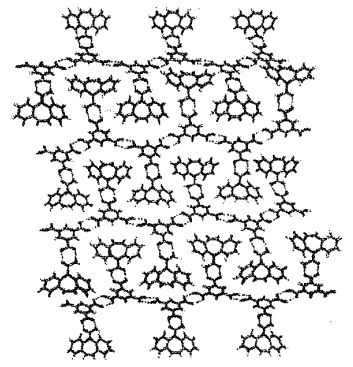

1j

UM00016635
NOVARTIS EXHIBIT 1517
Novartis v. Regents, IPR2023-01347
Page 3617 of 4460

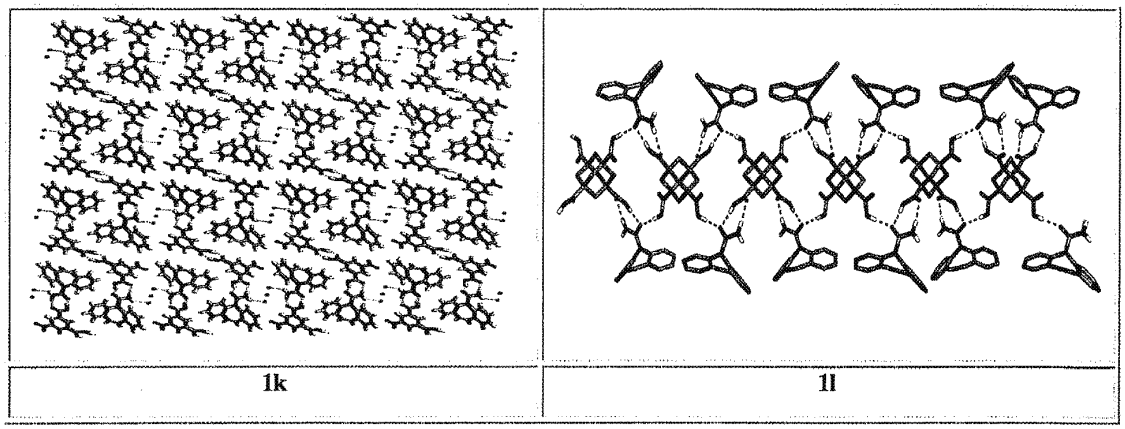

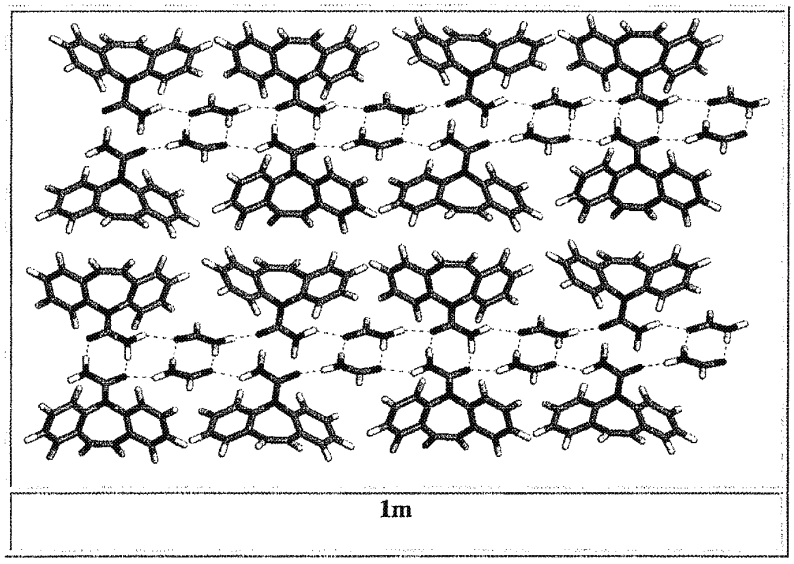

Figure 9. Crystal packing of pure CBZ (forms II and III) and supramolecular complexes **1a**−**1m**.

Ⓦ 3D rotatable images in PDB format of Ⓦ **1f** , Ⓦ **1g** , and Ⓦ **1m** are available.

trate upon other supramolecular synthons, the use ofGRAS[28] or food additives as cocrystal formers,[29] structure/functional property studies, and high-throughput crystallization experiments.

Acknowledgment. M.Z. and N.R.H. gratefully acknowledge partial support from the Vahlteich Research Award from the College of Pharmacy, University of Michigan. We also acknowledge partial support from the National Science Foundation (M.Z., DMR-0101641) and Transform Pharmaceuticals (M.Z.).

Note Added after ASAP Posting

An earlier version of this paper was posted ASAP on the Web on June 17, 2003. Links to web-enhanced files were added to a new electronic version posted October 16, 2003.

Supporting Information Available: Crystallographic information files for compounds **1a**−**1m**. This material is available free of charge via the Internet at http://pubs.acs.org.

References

(1) Pepinsky, R. *Phys. Rev.* **1955**, *100*, 971.
(2) Schmidt, G. M. *J. Pure Appl. Chem.* **1971**, *27*, 647.
(3) (a) Hamilton, T. D.; Papaefstathiou, G. S.; MacGillivray, L. R. *J. Am. Chem. Soc.* **2002**, *124*, 11606. (b) MacGillivray, L. R.; Papaefstathiou, G. S.; Reid, J. L.; Ripmeester, J. A. *Cryst. Growth Des.* **2001**, *1*, 373. (c) Papaefstathiou, G. S.; MacGillivray, L. R. *Angew. Chem., Int. Ed.* **2002**, *41*, 2070. (d) Metzger, J. O. *Angew. Chem., Int. Ed.* **1998**, *37*, 2975. (e) Joy, A.; Ramamurthy, V. *Chem.—Eur. J.* **2000**, *6*, 1287.
(4) (a) Desiraju, G. R. *Crystal Engineering—The Design of Organic Solids*; Elsevier: Amsterdam, 1989. (b) Lehn, J. M. *Supramolecular Chemistry: Concepts and Perspectives*; VCH: Weinheim, Germany, 1995. (c) Philp, D.; Stoddart,

UM00016636
NOVARTIS EXHIBIT 1517
Novartis v. Regents, IPR2023-01347
Page 3618 of 4460

J. F *Angew. Chem., Int. Ed.* **1996**, *35*, 1154. (d) Steed, J. W.; Atwood, J. L. *Supramolecular Chemistry*; John Wiley & Sons: New York, 2000. (e) Desiraju, G. R. in *Stimulating concepts in Chemistry*; Vögtle, F.; Stoddart, J. F.; Shibasaki, M., Eds.; Wiley-VCH, Weinheim, Germany, 2000, p 293. (f) Holman, K. T.; Pivovar, A. M.; Swift, J. A.; Ward, M. D. *Acc. Chem. Res.* **2001**, *34*, 107. (g) Aakeröy, C. B.; Beatty, A. M.; Helfrich, B. A. *Angew. Chem., Int. Ed.* **2001**, *40*, 3240.

(5) (a) Aakeröy, C. B. *Acta Crystallogr.* **1997**, *B53*, 569. (b) Kuduva, S. S.; Craig, D. C.; Nangia A.; Desiraju, G. R. *J. Am. Chem. Soc.* **1999**, *121*, 1936. (c) Zaworotko, M. J. *Chem. Commun.* **2001**, *1*. (d) Nguyen, T. L.; Fowler, F. W.; Lauher, J. W. *J. Am. Chem. Soc.* **2001**, *123*, 11057. (e) Moulton, B.; Zaworotko, M. J. *Chem. Rev.* **2001**, *101*, 1629. (f) Aakeröy, C. B.; Beatty, A. M. *Aust. J. Chem.* **2001**, *54*, 409. (g) Zaworotko, M. J. *Nature* **1999**, *402*, 242. (h) Kahn, O. *Curr. Opin. Solid State Mater. Sci.* **1996**, *1*, 547. (i) Fyfe, M. C. T.; Stoddart, J. F. *Acc. Chem. Res.* **1997**, *30*, 393. (j) Kaes, C.; Katz, A.; Hosseini, M. W. *Chem. Rev.* **2000**, *100*, 3553.

(6) (a) Threlfall, T. L. *Analyst* **1995**, *120*, 2435. (b) Desiraju, G. R. *Science* **1997**, *278*, 404. (c) Henck, J.-O.; Bernstein, J.; Ellern, A.; Boese, R. *J. Am. Chem. Soc.* **2001**, *123*, 1834.

(7) Bernstein, J.; Davey, R. J.; Henck, J.-O. *Angew. Chem., Int. Ed. Engl.* **1999**, *38*, 3440.

(8) Seddon, K. R.; Zaworotko, M. J. *Crystal Engineering: The Design and Application of Functional Solids*, NATO-ASI Series, Vol. 539; Kluwer: Dordrecht, The Netherlands, 1999.

(9) (a) Peterson, M. L.; Morissette, S. L.; McNulty, C.; Goldsweig, A.; Shaw, P.; LeQuesne, M.; Monagle, J.; Encina, N.; Marchionna, J.; Johnson, A.; Gonzalez-Zugasti, J.; Lemmo, A. V.; Ellis, S. J.; Cima, M. J.; Almarsson, Ö. *J. Am. Chem. Soc.* **2002**, *124*, 10958. (b) Morissette, S. L.; Soukasene, S.; Levinson, D.; Cima, M. J.; Almarsson, Ö. *Proc. Natl. Acad. Sci. U.S.A.*, **2003**, *100*, 2180.

(10) Lang, M.; Grzesiak, A. L.; Matzger, A. J. *J. Am. Chem. Soc.* **2002**, *124*, 14834.

(11) Kobayashi, Y.; Ito, S.; Itai, S.; Yamamoto, K. *Int. J. Pharm.* **2000**, *193*, 137.

(12) (a) Himes, V. L.; Mighell, A. D.; De Camp, W. H. *Acta Crystallogr.* **1981**, *B37*, 2242. (b) Reboul, J. P.; Cristau, B.; Soyfer, J. C.; Astier, J. C. *Acta Crystallogr.* **1981**, *B37*, 2242. (c) Lowes, M. M. J.; Cairo, M. R.; Lotter, A. P.; Van der Watt, J. G. *J. Pharm. Sci.* **1987**, *76*, 744. (d) Lisgarten, J. N.; Palmer, R. A.; Saldanha, J. W. *J. Crystallogr. Spectrosc. Res.* **1989**, *19*, 641. (e) Rustichelli, C.; Gamberini, G.; Ferioli, V.; Gamberini, M. C.; Ficarra, R.; Tommasini, S. *J. Pharm. Biomed. Anal.* **2000**, *23*, 41. (f) Ceolin, R.; Toscani, S.; Gardette, M. F.; Dzyabchenko, V. N.; Bachet, B. *J. Pharm. Sci.* **1997**, *86*, 1062. (g) Lang, M.; Kampf, J.; Matzger, A. J. *J. Pharm. Sci.* **2002**, *91(4)*, 1186.

(13) (a) Chang, C. H.; Yang, D. S. C.; Yoo, C. S.; Wang, B. L.; Pletcher, J. *Acta Crystallogr.* **1981**, *A37*, C71. (b) Reck, G.; Dietz, G. *Cryst. Res. Technol.* **1986**, *21*, 1463.

(14) (a) Leiserowitz, L.; Schmidt, G. M. J. *J. Chem. Soc. A* **1969**, 2372. (b) MacDonald, J. C.; Whitesides, G. M. *Chem. Rev.* **1994**, *94*, 2383. (c) Bernstein, J.; Etter, M. C.; Leiserowitz, L. *Structure Correlation*; Burgi, H.-B., Dunitz, J. D., Eds.; VCH: Weinheim, Germany, 1994; Vol. 2, p 431. (d) Whitesides, G. M.; Simanek, E. E.; Mathias, J. P.; Seto, C. T.; Chin, D. N.; Mammen, M.; Gordon, D. M. *Acc. Chem. Res.* **1995**, *28*, 37. (e) Melendez, R. E.; Hamilton, A. D. *Hydrogen-Bonded Ribbons, Tapes, and Sheets as Motifs for Crystal Engineering* in *Design of Organic Solids*; Weber, E., Ed.; Springer: Berlin, 1998, p 130. (f) Rebek, J., Jr. *Acc. Chem. Res.* **1999**, *32*, 278. (g) MacDonald, J. C.; Palmore, G. T. R. *The Role of Amides in the Noncovalent Synthesis of Supramolecular Structures in Solution, at Interfaces and in Solids* in *The Amide Linkage: Selected Structural Aspects in Chemistry, Biochemistry, and Materials Science*; Greenberg, A.; Breneman, C. M.; Liebman, J. F. Eds.; John Wiley & Sons: New York, 2000, p 291.

(15) Bailey Walsh, R. D.; Bradner, M. W.; Fleischman, S.; Morales, L. A.; Moulton, B.; Rodríguez-Hornedo, N.; Zaworotko, M. J. *Chem. Commun.* **2003**, 186.

(16) Allen, F. H.; Motherwell, W. D. S.; Raithby, P. R.; Shields, G. P.; Taylor, R. *New J. Chem.* **1999**, 25.

(17) Allen, F. H.; Kennard, O. *Chem. Des. Automation News* **1993**, *8*, 31.

(18) Harding, M. M. *Acta Crystallogr.* **1983**, *C53*, 397.

(19) Nair, R.; Gonen, S.; Hoag, S. W. *Int. J. Pharm.* **2002**, *240*, 11.

(20) (a) Holy, P.; Zavada, J.; Cisarova, I.; Podlaha, J. *Tetrahedron: Asymmetry* **2001**, *21*, 3035. (b) Leiserowitz, L.; Nader, F. *Acta Crystallogr.* **1977**, *B33*, 2719. (c) Chang, Y.-L.; West, M.-A.; Fowler, F. W.; Lauher, J. W. *J. Am. Chem. Soc.* **1993**, *115*, 5991. (d) Wash, P. L.; Maverick, E.; Chiefari, J.; Lightner, D. A. *J. Am. Chem. Soc.* **1997**, *119*, 3802. (e) Leiserowitz, L.; Hagler, A. T. *Proc. R. Soc. London* **1983**, *A388*, 133. (f) Ohba, S.; Hosomi, H.; Ito, Y. *J. Am. Chem. Soc.* **2001**, *123*, 6349.

(21) (a) Kumar, V. S. S.; Kuduva, S. S.; Desiraju, G. R. *J. Chem. Soc., Perkin Trans. 2*, **1999**, 1069. (b) Nangia, A.; Desiraju, G. R. *Chem. Commun.* **1999**, 605.

(22) Sheldrick, G. M. *SHELXTL*, Release 5.03; Siemans Analytical X-ray Instruments, Inc.: Madison, WI, 1994.

(23) (a) Jeffrey, G. A.; Saenger, W. *Hydrogen bonding in biological structures*; Springer-Verlag: Berlin, 1991. (b) Jeffrey, G. A. *An introduction to hydrogen bonding*; Oxford University Press: New York, 1997. (c) Desiraju, G. R.; Steiner, T. *The Weak hydrogen bond in structural chemistry and biology*; Oxford University Press: Oxford, 1999. (d) Desiraju, G. R. *Acc. Chem. Res.* **2002**, *35*, 565.

(24) Etter, M. C. *Acc. Chem. Res.* **1990**, *23*, 120.

(25) Crystallizing pure CBZ from formamide did not yield X-ray quality crystals.

(26) Emsley, J.; Ma, L. Y. Y.; Hursthouse, M. B.; Karaulov, S. A.; Motevalli, M. *J. Chem. Soc., Perkin Trans. 2*, **1990**, 1077.

(27) Etter, M. C.; Reutzel, S. M. *J. Am. Chem. Soc.* **1991**, *113*, 2586.

(28) FDA GRAS notices can be found at www.cfsan.fda.gov/~dms/eafus.html.

(29) Saccharin, nicotinamide (vitamin B3), and acetic acid are appearing on the Generally Recognized As Safe (GRAS) list.[28] The list is maintained by the US Food and Drug Administration.

CG034035X

UM00016637
NOVARTIS EXHIBIT 1517
Novartis v. Regents, IPR2023-01347
Page 3619 of 4460

The Concentration of Spermine, Spermidine, and Putrescine in Rat Liver

The concentration of polyamines in the liver of two rats was determined by our method. As shown in Table II, the duplicability of the method was quite good. The mean values of spermine, spermidine, and putrescine per gram of liver were 0.69, 0.52, and 0.06 in the first rat, and 0.68, 0.56, and 0.04 in the second rat, respectively. These data are similar to those reported by other workers[6] using electrophoretic analysis. The present method has proved to be rapid and reliable for the estimation of polyamine content in *E. coli* also.

Acknowledgement The authors are grateful to Dr. Y. Yamane of this Faculty for his kind advice during the course of this work. They are also indebted to Dr. B. K. Joyce of Colorado State University for her help in preparing this manuscript. This work was supported in part by a Grant-in-Aid from the Ministry of Education.

6) D.H. Russell, V.J. Medina, and S.H. Snyder, *J. Biol. Chem.*, **245**, 6732 (1970); E. Cavia and T.E. Webb, *Biochem. J.*, **129**, 223 (1972).

[Chem. Pharm. Bull. 22(2) 454—458 (1974)]

UDC 615.011.4.014

Solvent Effects on Comparative Dissolution of Pharmaceutical Solvates[1]

Ho-Leung Fung and Thomas Nealon

Pharmaceutics Department, School of Pharmacy, State University of New York at Buffalo[2]

(Received May 21, 1973)

Two potential applications of organic solvates in pharmaceutical formulation have been suggested, *viz.*: (i) as intermediates to achieve particle size reduction and (ii) as pharmaceutical derivatives to promote dissolution of poorly soluble drugs. While there are evidences which testify to the success of the first application to drugs such as griseofulvin[3] and chloramphenicol,[4] conflicting data exist in the literature about the general ability of solvates to show enhanced dissolution rates over their non-solvated compounds. Thus, while some solvates[5,6] showed higher *in vitro* dissolution rates when compared to their non-solvated forms, others[7,8] demonstrated the reverse behavior. This confusing picture is further complicated by the lack of standardization of dissolution techniques used to study solvate dissolution. In particular, in the dissolution studies of water insoluble drugs, it is often expedient to employ mixed aqueous organic solvent systems to facilitate data collection.[5] This practice does not necessarily lead to ready extrapolation of comparative solvate dissolution data in these media to those in aqueous solutions. This is primarily due to the probable difference in the rate or extent of dissociation of the solvate in these solvent systems, which in turn provides a dif-

1) Partly presented at the 119th Annual Meeting of the American Pharmaceutical Association, Houston, Texas, April 24, 1972.
2) Location: *180 Race Street, Box U, Station B, Buffalo, New York 14207 U.S.A.*
3) K. Sekiguchi, K. Ito, E. Owada, and K. Ueno, *Chem. Pharm. Bull.* (Tokyo), **12**, 1192 (1964).
4) I. Himuro, Y. Tsuda, K. Sekiguchi, I. Horikoshi, and M. Kanke, *Chem. Pharm. Bull.* (Tokyo), **19**, 1034 (1971).
5) E. Shefter and T. Higuchi, *J. Pharm. Sci.*, **52**, 781 (1963).
6) T. Higuchi, K. Uekama, M. Nakano, and C. Huang, "Abstracts, symposia and contributed papers presented to the APhA Academy of Pharmaceutical Sciences," 119th Annual Meeting of the American Pharmaceutical Association, Houston, Texas, April 22—28, 1972.
7) M. Mayersohn and M. Gibaldi, *J. Pharm. Sci.*, **55**, 1324 (1966).
8) J.K. Haleblian, R.T. Koda, and J.A. Biles, *J. Pharm. Sci.*, **60**, 1488 (1971).

NII-Electronic Library Service

UM00016638
NOVARTIS EXHIBIT 1517
Novartis v. Regents, IPR2023-01347
Page 3620 of 4460

ferent thermodynamic driving force for dissolution. In this brief report, we show that it is quite possible to draw erroneous conclusions on the usefulness of particular solvates to give higher dissolution rates based on their comparative dissolution behavior in mixed solvents. As examples, we used the chloroform solvate of griseofulvin and the *t*-butylamine (TBA) disolvate of fluprednisolone, both of which have been shown to exhibit slower dissolution rates than their anhydrous parent compounds in aqueous solutions.

Griseofulvin

Mayersohn and Gibaldi[7] showed that the particulate dissolution rate of griseofulvin chloroform solvate in water was slower than that of microcrystalline griseofulvin. Under our experimental conditions of constant surface area, we also found no significant enhancement in dissolution rate of the solvate over that of the anhydrous non-microcrystalline form, either in the presence or absence of a small percentage (0.005% w/v) of Tween 80. However, when a water miscible organic solvent was added to the dissolution medium, the solvate became the faster dissolving species. For example, when the alcohol content was 50% v/v, the solvate dissolved about three times faster than the non-solvated form (Fig. 1). Table I tabulates the effects of solvent on the initial dissolution rates of griseofulvin and its chloroform solvate. The rates were obtained for dissolution runs in the first twenty minutes during which time the dissolution curves were linear for systems containing twenty or more percent v/v organic solvent and approximately linear for those systems of a lower organic solvent concentration. It can be readily seen that as the concentration of the non-aqueous solvent increased in the dissolution medium, the relative enhancement in initial dissolution rate of the solvate over the anhydrous form also increased. Preliminary data showed that the solvate was also the faster dissolving species in pure polar organic solvents, such as methanol and acetone, but not in cyclohexane (Table I).

Fluprednisolone

It has been shown previously[8] that the TBA disolvate did not exhibit any enhancement in dissolution in water over the anhydrous form. In this study, the dissolution rates of the disolvate and the non-solvated form (Form I) were found to be essentially the same also in 0.1 N hydrochloric acid. The lack of enhancement did not appear to be due to a lack of wetting of the solvate, nor was it diffusion layer limited; since it was found that neither the addition of Tween 80 nor an increase in the stirring rate from 60 to 250 rpm caused significant en-

TABLE I. Initial Dissolution Rates and Rate Ratios for Griseofulvin and Its Chloroform Solvate in Various Dissolution Media

Dissolution media	Rate (anhydrous) ($M \cdot min^{-1}$)	Rate (solvate) ($M \cdot min^{-1}$)	Rate (solvate) / Rate (anhydrous)
Water[a]	(1.38×10^{-2})[b]	(1.38×10^{-2})[b]	1.00
Tetrahydrofuran[c]			
5%	1.15×10^{-7}	1.50×10^{-7}	1.30
10%	2.23×10^{-7}	3.02×10^{-7}	1.35
20%	1.98×10^{-6}	2.96×10^{-6}	1.50
40%	1.04×10^{-5}	2.40×10^{-5}	2.31
Ethanol[a]			
25%	2.78×10^{-7}	4.70×10^{-7}	1.69
50%	0.35×10^{-6}	1.00×10^{-6}	2.84
100%	0.87×10^{-5}	1.01×10^{-5}	1.16
Methanol[d]	7.05×10^{-6}	8.67×10^{-6}	1.23
Acetone[d]	0.74×10^{-5}	1.48×10^{-5}	2.00
Cyclohexane[a]	(1.53×10^{-2})[b]	(1.06×10^{-2})[b]	0.70

a) stirring rate: 750 rpm *b*) absorbance: units/hr *c*) 2000 rpm *d*) 60 rpm

NII-Electronic Library Service

UM00016639
NOVARTIS EXHIBIT 1517
Novartis v. Regents, IPR2023-01347
Page 3621 of 4460

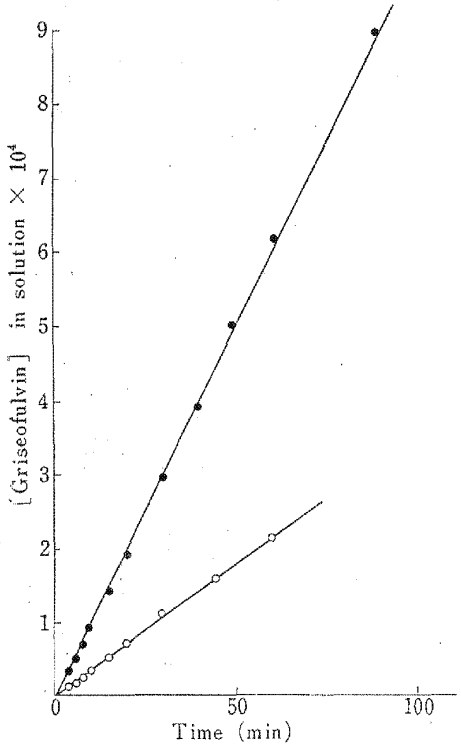

Fig. 1. Initial Dissolution Curves of Griseofulvin (○) and Its Chloroform Solvate (●) in 50% v/v Ethanol

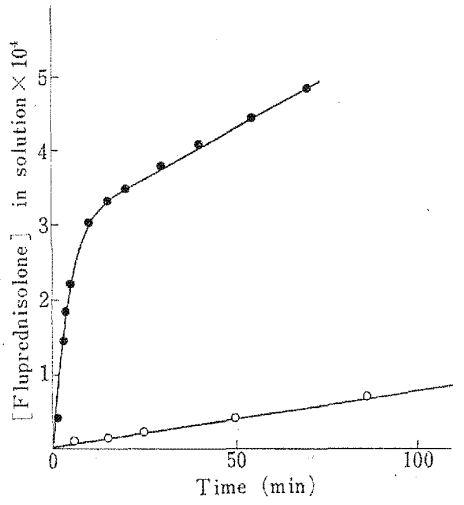

Fig. 2. Initial Dissolution Curves of Fluprednisolone Form I (○) and Its TBA Disolvate (●) in 25% v/v Ethanol

hancement in the relative dissolution rate of the solvate. A change of the dissolution medium to a 0.1N NaOH solution also had little effect on the dissolution of the solvate.

Preliminary data on aqueous alcoholic solvents showed that addition of a small amount of alcohol (10%) caused only a slight increase in dissolution, but when the alcohol content was increased to 25% v/v (Fig. 2), a tremendous difference resulted (Table II). The dissolution rate of the solvate was now very much enhanced. At 5 minutes, the concentration of the drug in solution was more than 50 times higher for the dissolution of the solvate than for the anhydrous form.

Table II. Initial Dissolution Rates and Rate Ratios for Fluprednisolone and Its TBA Disolvate in Various Dissolution Media

Dissolution media[a]	Rate (anhydrous) ($M \cdot min^{-1}$)	Rate (solvate) ($M \cdot min^{-1}$)	Rate (solvate) / Rate (anhydrous)
Water	—	(0.9×10^{-3}) [b]	—
0.1N HCl	(1.2×10^{-2}) [b]	(1.1×10^{-2}) [b]	0.9
0.1N NaOH	—	(1.0×10^{-2}) [b]	—
Ethanol 10%	5.6×10^{-7}	6.3×10^{-7}	1.1
25%	0.8×10^{-6}	$\sim 4.5 \times 10^{-5}$ [c]	55

a) stirring rate: 60 rpm b) absorbance units/min c) initial rate (0—5 min)

These results demonstrated the profound importance of solvent effects in solvate dissolution. We submit, therefore, that the choice of solvent systems in the study of *in vitro* dis-

NII-Electronic Library Service

UM00016640
NOVARTIS EXHIBIT 1517
Novartis v. Regents, IPR2023-01347
Page 3622 of 4460

solution of solvates may be extremely critical, since studies in aqueous organic solvent systems may not accurately reflect the dissolution behavior of these solvates in purely aqueous system, much less the *in vivo* systems in which the dissociation of the solvate is unpredictable.

Further, the data presented here also provided some interesting information with regard to the mechanism of solvate dissolution. In the case of the griseofulvin solvate, the results appeared to be consistent with the dissociation model[5] for solvate dissolution: *i.e.*, the lack of enhancement in dissolution of the solvate in water was apparently due to a lack of favorable molecular interaction between the complexing solvent (chloroform) and water, so that the dissociation of the solvate and its accompanying "dissolution driving force" could not be readily attained. When an interacting solvent such as ethanol, acetone and tetrahydrofuran was provided to solvate the chloroform, dissociation of the solvate became favorable, and enhancement in dissolution rate resulted. Further indication that these observed enhancements in mixed aqueous organic solvents were related to a specific solvation mechanism and not to a decrease in the dielectric constant of the medium was provided by the dissolution data in cyclohexane. In this solvent, no enhancement was observed apparently because cyclohexane could not solvate chloroform favorably and dissociation was, therefore, not promoted. The above conclusions, of course, could be substantiated by measuring the dissociation constant of the solvate and also the rate at which dissociation equilibrium is obtained in each solvent under the same experimental conditions.

The mechanism of dissolution for the TBA disolvate of fluprednisolone is less clear. In the griseofulvin case the complexing solvent (chloroform) is very hydrophobic and may not be expected to dissociate from the drug in water because its interaction with water is not favorable. However, since TBA is very hydrophilic (it is freely miscible with water), its free energy of dilution should be readily available. Thus, based on the dissociation model, it is difficult to rationalize why enhancement of dissolution through this solvate in water is not achieved. One possible answer to this question may be found from the DSC data for the solvate. The enthalpy of desolvation was found to be 34 ± 2 kcal/mole of solvate for the fluprednisolone TBA disolvate and 8.2 ± 0.3 kcal/mole of solvate for the griseofulvin chloroform solvate respectively. It can be seen that approximately four times as much energy was required to completely desolvate the steroid solvate as compared to the griseofulvin solvate. Even after stoichiometric correction, liberation of a TBA molecule from the fluprednisolone disolvate would apparently require at least twice the amount of energy necessary for the release of chloroform from the griseofulvin solvate. It may then be speculated that the *t*-butylamine molecules in the solvate are so strongly bound to the steroid that a large amount of energy may be required to cause dissociation. Apparently this amount of energy cannot be supplied in water because solvation of the steroid and the base by water molecules does not compensate for the energy lost in breaking the solvate bonds. In mixed alcoholic solvents, possible solvation of the steroid may now lead to favorable dissociation of solvate, which is then accompanied by an observed enhancement in dissolution rate.

Interpretation of dissolution data of the TBA disolvate of fluprednisolone is further complicated by possible transformation during dissolution. Haleblian, *et al.*[8] reported that in water, this solvate rapidly transforms to its β-monohydrate and subsequently to its α-monohydrate. It was also stated that the Form I polymorph was converted to the α-monohydrate in water. However, on examination of their dissolution data, it was noted that, at least up to one hour, the dissolution rates of all these forms were significantly different. This tends to suggest that phase transition during initial dissolution is probably not extensive. Thus, the initial dissolution curves shown in Fig. 2 most likely represent predominantly those of the starting material. The abrupt change in slope after 10 minutes in the TBA dissolution curve might be due to gradual buildup of phase-transformed material or might represent a slowing of rate due to higher concentration of the steroid in the dissolution medium.

NII-Electronic Library Service

UM00016641
NOVARTIS EXHIBIT 1517
Novartis v. Regents, IPR2023-01347
Page 3623 of 4460

Experimental

Materials——Griseofulvin[9] and fluprednisolone[10] were obtained from their respective manufacturers and used as the anhydrous compounds without further recrystallization. The latter compound had the same X-ray diffraction pattern as that described for Form I of fluprednisolone.[11]

The chloroform solvate of griseofulvin was prepared by recrystallizing the anhydrous drug in chloroform.[3] Both weight loss and Beer's Law plot confirmed a 1 : 1 drug–solvent stoichiometry. Fluprednisolone-TBA disolvate was obtained by recrystallizing the drug in *t*-butylamine. From a Beer's Law plot the solvate was found to contain two moles of TBA per mole of drug. X-ray powder diffraction patterns of both solvates were distinctly different from those of the anhydrous compounds. In the case of the TBA disolvate, the diffraction data agreed with the published data.[8] Since both solvates were found to desolvate on prolonged standing, dissolution runs were performed with freshly prepared solvates. Dissolution disks were prepared by compressing 500 mg of pure drug material, using a pressure of 1000 psi for 10 seconds. Tetrahydrofuran A.R. was distilled to remove the stabilizer before use.

Dissolution Studies——The rotating disk method of Levy and Sahli[12] was essentially adopted. Temperature was at 25±0.2°. A stirring rate of 60 rpm was used for the fluprednisolone systems. In the case of griseofulvin, where dissolution was quite slow, higher stirring rates were employed for both the tetrahydrofuran systems (2000 rpm) and the alcohol systems (750 rpm). Similar quantitative data, however, were also obtained at low stirring rates. Concentrations were determined from ultraviolet (UV) absorbance readings at the appropriate wavelengths. Where they were determined, both solvates had the same molar absorptivities as the non-solvated forms. In water and cyclohexane systems, where preparation of Beer's Law plots was difficult, due to low solubility of the drug, dissolution rates were expressed in terms of absorbance units per unit time.

DSC Studies——Thermograms were obtained from uncrimped samples at a heating rate of 10° per minute with a Perkin-Elmer DSC-1B calorimeter, calibrated with indium (enthalpy of fusion=6.8 cal/g). Enthalpies of desolvation were determined from areas of desolvation endotherms, as measured by a planimeter.

Acknowledgement The authors wish to express their appreciation to Dr. Eli Shefter for valuable discussions and to Dr. J. Marinsky and the Chemistry Department, SUNYAB for the use of the Perkin-Elmer DSC-1B calorimeter.

This work was supported in part by Institutional Funds, Health Sciences Faculty, SUNYAB, U.S. Publish Health Service Grant Number 5-S05-RR07066-06.

9) McN-R-719, Lot No. 4745 McNeil Laboratories, Inc., Fort Washington, Pa.
10) Lot No. XP738, The Upjohn Company, Kalamazoo, Michigan.
11) J.K. Haleblian, R.T. Koda, and J.A. Biles, *J. Pharm. Sci.*, **60**, 1485 (1971).
12) G. Levy and B. Sahli, *J. Pham. Sci.*, **51**, 58 (1962).

NII-Electronic Library Service

UM00016642
NOVARTIS EXHIBIT 1517
Novartis v. Regents, IPR2023-01347
Page 3624 of 4460

Dystrophic Psoriatic Fingernails Treated with 1% 5-Fluorouracil in a Nail Pen...
E.M.G.J. de Jong; H.E. Menke; M.C.G. van Praag; P.C.M. van de Kerkhof
Dermatology; 1999; 199, 4; Research Library
pg. 313

Pharmacology and Treatment

Dermatology

Dermatology 1999;199:313–318

Received: February 22, 1999
Accepted: August 12, 1999

Dystrophic Psoriatic Fingernails Treated with 1% 5-Fluorouracil in a Nail Penetration-Enhancing Vehicle: A Double-Blind Study

E.M.G.J. de Jong[a] H.E. Menke[b] M.C.G. van Praag[b] P.C.M. van de Kerkhof[a]

[a]Department of Dermatology, University Hospital Nijmegen St. Radboud, Nijmegen, and
[b]Department of Dermatology, Sint Franciscus Gasthuis, Rotterdam, The Netherlands

Key Words
Nail · Psoriasis · Belanyx · 5-Fluorouracil

Abstract
Background: Topically applied nail therapeutics need to permeate the nail plate to reach the nail bed or nail matrix and exert their potential beneficial effect at these locations to obtain a therapeutic benefit. So far only topically applied 5-fluorouracil on affected nails of psoriatic patients has been shown to produce a notable clearance. Vehicle formulations enhancing nail permeation processes are thought to increase the concentration of the active agent and therefore therapeutic efficacy, possibly enabling the use of a low concentration of the active agent thereby lowering the incidence of adverse effects. ***Objective:*** This study was designed to verify whether a recently developed nail penetration enhancer in a lotion formulation, Belanyx® (urea, propylene glycol), improves the efficacy of a low concentration of 5-fluorouracil (1%) in psoriatic fingernail lesions. ***Methods:*** In a randomised, double-blind, left-right study the efficacy of 1% 5-fluorouracil in the Belanyx vehicle was compared to the vehicle preparation Belanyx in dystrophic fingernails of 57 psoriatic patients. Both preparations were applied in a once daily regimen for 12 weeks. Responses and adverse effects of one selected target nail were recorded at screening, at baseline and at weeks 2, 4, 8 and 12 of treatment with a final assessment at week 16: 4 weeks after the end of treatment. As parameter of efficacy was chosen the total nail area severity (NAS) score, consisting of the separate parameters nail pitting area, number of nail pits, subungual keratosis, onycholysis, oil spots and the various scores of overall improvement. ***Results:*** The efficacy of 1% 5-fluorouracil in lotion and that of the vehicle in suppressing the parameters of dystrophy were shown to be similar at the end of treatment ($p = 0.063$) or follow-up ($p = 0.130$). Both preparations produced statistically significant improvements ($p \leq 0.05$) for almost all assessed parameters after 12 weeks of treatment and after the 4 weeks of follow-up. For Belanyx lotion this applied to the nail pitting area, the number of nail pits, subungual keratosis, onycholysis and oil spots. The investigators' and patients' opinion of overall improvement of severity as well as the total NAS score of one target nail likewise showed a statistically significant improvement at the end of treatment and at the end of the observation period ($p \leq 0.05$). With the 1% 5-fluorouracil lotion the same statistically significant improvements were obtained in all of the assessed symptoms with the exception of the number of pits and onycholysis at week 12 and week 16. Possible treatment-related adverse effects were established in 6 patients showing inflammation and infection (3 patients) or discoloration (5 patients); 3 patients on 5-fluorouracil lotion showed onycholysis. ***Conclusion:*** Addition of 1% 5-fluorouracil to the nail permeation enhancer Belanyx does not increase the efficacy of the active agent in psoriatic nail dystrophy of this study population. The obtained results also suggest that Belanyx lotion can be used in this indication since it has shown a favourable efficacy-safety ratio.

Copyright © 2000 S. Karger AG, Basel

KARGER
Fax +41 61 306 12 34
E-Mail karger@karger.ch
www.karger.com

© 1999 S. Karger AG, Basel
1018–8665/99/1994–0313$17.50/0

Accessible online at:
www.karger.com/journals/drm

E.M.G.J. de Jong
Department of Dermatology
University Hospital Nijmegen St. Radboud
René Descartesdreef 1, PO Box 9101
NL–6500 HB Nijmegen (The Netherlands)

Reproduced with permission of the copyright owner. Further reproduction prohibited without permission.

UM00016643
NOVARTIS EXHIBIT 1517
Novartis v. Regents, IPR2023-01347
Page 3625 of 4460

Introduction

The prevalence of nail psoriasis in patients with psoriasis of the skin is high. According to a recent study this amounted to about 80% of 1,728 psoriasis patients [1]. Involvement of finger nails and toenails was observed in roughly 60% of patients whereas in 30% only the fingernails and in 10% only the toenails were affected [1]. In addition 51.8% of patients suffered from pain caused by these nail changes, while about 55% were restricted in their daily activities, including housekeeping or profession. Virtually all patients (93%) indicated to have problems with the cosmetic aspects of the diseased nails. Despite this high prevalence of involvement and complaints and probably therefore a high need for effective treatment, no treatment modalities have shown reliable and satisfactory efficacy-safety ratios and so far have been accepted as the established, recommended treatment of psoriatic nails. Case reports mention the use of intralesional corticosteroids [2], and the use of topical anthralin [3] or topical calcipotriol [4]. Systemic use of methotrexate [5] or local PUVA [6] and use of other types of radiation, e.g. X-ray [7] or grenz ray [8], were also reported.

Somewhat more suitable for use in nail psoriasis is 5-fluorouracil, which has an antimitotic and cytotoxic effect and was already used for psoriasis a few decades ago [9]. Although 5% 5-fluorouracil in a cream base applied for 1 month under occlusion on paronychial warts was reported to have caused onycholysis this was not true for a low concentration of 5-fluorouracil cream base (2%) also applied under occlusion [10]. Using even lower concentrations of 5-fluorouracil (1%) good results in psoriatic nails were obtained provided penetration enhancers such as urea [11] or propylene glycol [12] were used. Based on the results of these studies it was assumed that possibly the presence of urea together with that of propylene glycol in a formulation containing 5-fluorouracil would enhance penetration of 5-fluorouracil in or through the nail plate reaching eventually the nail bed and nail fold exerting its antimitotic effect on the psoriatic lesion present. A lotion formulation mainly composed of a solution of propylene glycol as well as urea in water (Belanyx®, Yamanouchi Europe BV, Leiderdorp, The Netherlands) was developed to serve as carrier for a topical 5-fluorouracil preparation for application on the nail. Both urea and propylene glycol have proteolytic, keratolytic and moisturising or humectant effects softening the nail plate presumably facilitating the penetration of 5-fluorouracil. In an in vitro nail plate diffusion test it was subsequently determined that 1% 5-fluorouracil in Belanyx lotion was the optimal preparation with the highest diffusion rates if compared to other 5-fluorouracil test concentrations [unpubl. data]. Whether this preparation would also show clinical activity was subsequently assessed in this randomised, double-blind, left-right study in psoriasis of the fingernails.

Study Design and Methods

In a randomised, double-blind, left-right trial, psoriasis of the fingernails of 57 adult patients was treated once daily either with 1% 5-fluorouracil in Belanyx lotion or with its vehicle Belanyx lotion. After application the treated nails were covered with plaster. All participating patients were recruited from patient populations of the dermatological centres of Nijmegen and Rotterdam in the Netherlands. The duration of treatment was determined at 12 weeks with subsequently a follow-up assessment period of 4 weeks. At the screening visit female patients were tested for pregnancy and all patients for onychomycosis by means of a KOH test and mycological culture. Positive cases were excluded from the study. Improvement during the course of treatment was recorded and gathered from the changes in nail area severity (NAS) scores of a comparable target nail of each hand. Somewhat analogous to the psoriasis area severity index [13], the parameters of the NAS score were assessed according to a 5-point rating scale (none = 0, very severe = 4). The assessed individual parameters of the NAS were: extent of the nail pitting area (0–100%), in steps of 25% + number of pits (0–>15) the average of which was defined as nail pitting; subungual keratosis (0–>3 mm: measured from nail bed to thickest part); onycholysis (0–100%) and oil spots (0–100%). A minimum NAS score of 5 for the target nail was required for inclusion in this study. The assessments of severity took place at baseline and at weeks 2, 4, 8 and 12 and at the end of a 4-week follow-up period (week 16). Included in the assessment of efficacy were the changes in overall severity score according to the opinion of the investigator or that of the patient also following a 5-point scale (none to very severe).

The safety of treatment, i.e. those presenting systemically, was assessed by means of complete blood chemistry and haematology at screening, baseline and at the end of treatment. Topically the signs of tolerability, notably irritation and contact allergy, were assessed at the start and at each visit. Parameters were erythema, burning and stinging. They were scored in each patient following a 5-point rating scale (0 = none to 4 = severe). All further adverse events occurring during treatment were recorded.

To obtain statistically significant results at the level of 0.05 with 90% power at two-sided testing, at least 42 patients were required. To compensate for possible withdrawals and drop-outs the number of patients was settled at the mentioned 57.

Differences in the reduction of the NAS score between treatment groups were assessed by means of analysis of variance using patient, left-right side and treatment as factors. The individual NAS parameters, overall severity scores and tolerability were analysed using the Mantel-Haenszel χ^2 test or Fisher's exact test in the case of low scores. Written approval of the Ethics Committee was obtained before the start of this study. Consent of all patients included in this study was obtained in writing.

Reproduced with permission of the copyright owner. Further reproduction prohibited without permission.

UM00016644
NOVARTIS EXHIBIT 1517
Novartis v. Regents, IPR2023-01347
Page 3626 of 4460

Table 1. Mean NAS score changes as a result of treatment with 5-fluorouracil (5-FU) in Belanyx lotion or with Belanyx lotion

Parameter	5-FU in Belanyx lotion			Belanyx lotion		
	start	12 weeks	16 weeks	start	12 weeks	16 weeks
Total NAS score (parameters 1–5)	7.1	4.8 (32%)	4.2 (40%)	7.1	4.3 (39%)	3.8 (46%)

The average of parameters 1 and 2 was used here.

Table 2. Mean score changes of the individual symptoms as a result of treatment with 5-fluorouracil (5-FU) in Belanyx lotion or with Belanyx lotion

Parameter	5-FU in Belanyx lotion			Belanyx lotion		
	start	12 weeks	16 weeks	start	12 weeks	16 weeks
(1) Nail pitting area	2.9	2.1 (28%)	1.8 (38%)	2.9	1.7 (41%)	1.4 (51%)
(2) Nail pit number	2.7	2.4 (11%)*	2.0 (26%)	2.8	1.9 (32%)	1.7 (40%)
(3) Subungual keratosis	1.9	1.0 (47%)	1.0 (47%)	1.9	1.0 (47%)	0.9 (53%)
(4) Onycholysis	1.6	1.3 (19%)*	1.1 (31%)	1.6	1.2 (25%)	1.0 (38%)
(5) Oil spots	0.8	0.3 (63%)	0.2 (75%)	0.7	0.3 (57%)	0.3 (57%)
Total	9.9	7.1	6.1	9.9	6.1	5.3

All changes statistically significant ($p < 0.05$) except those marked *.

Results

The results of treatment have also been analysed in the study population which met all the inclusion or exclusion criteria, were without protocol violations as determined by the Data Review Committee and completed the end of treatment visit (week 5) as well as the follow-up visit (week 6). However, since the results of statistical analysis of this so-called efficacy-analysable population were similar, the presented data will only refer to the entire intention-to-treat population of 57 patients. Of these 57 patients, 36 were male and 21 female with a mean age of 45.8 years and a range of 21–77 years. The fingernail psoriasis was present in a mean of 9.9 years (range 0–46 years).

For the NAS score of a target nail of each hand, consisting of the total symptom scores of the 5 parameters nail pitting area, number of nail pits, subungual keratosis, onycholysis and oil spots treated with 1% 5-fluorouracil lotion, a change from baseline severity of 7.1 to 4.8 after 12 and from 7.1 to 4.2 after 16 weeks was observed. This means an improvement of 32 and 40%, respectively. With the vehicle lotion alone, the baseline NAS score improved from 7.1 to 4.3 after 12 weeks and from 7.1 to 3.8 after 16 weeks of treatment, which is an improvement of 39 and 46%, respectively (table 1; fig. 1). These findings are in agreement with improvements recorded for the mean baseline severity of the total of the 5 individual assessed parameters of dystrophy. The baseline score of 9.9 decreased to 7.1 after 12 weeks as a result of treatment with 1% 5-fluorouracil lotion: an improvement of 28%. In the follow-up period of 4 weeks a further decrease of baseline severity to 6.1 or 38% could be obtained (table 2).

With the vehicle lotion alone the total severity of psoriatic nails improved from 9.9 at baseline to 6.1 at the end of 12 weeks: an improvement of 38%. During the observation period of the 4 additional weeks a further reduction to 5.3 (46%) was observed (table 2).

The overall improvement according to the investigator's and to the patient's opinion in the 1% 5-fluorouracil lotion and the vehicle lotion populations after 12 and after 16 weeks has been presented in table 3 and figures 2 and 3.

Statistical analysis of the results obtained for the NAS score after 12 or 16 weeks shows that there is no difference in efficacy between 1% 5-fluorouracil lotion and vehicle lotion alone after 12 weeks ($p = 0.063$) or after 16 weeks ($p = 0.134$). The results of analysis obtained in the 5 parameters (table 2) of psoriatic nails show that 1% 5-fluorouracil in Belanyx lotion induces significant improvement after 12 weeks of treatment in nail pitting area ($p = 0.004$) and in subungal hyperkeratosis or oil spots ($p = 0.001$). Statistical analysis of the overall improvement from baseline according to the investigator's and patient's opinion at week 12 of treatment was also shown to be very significant ($p = 0.001$). No statistically significant improvement could be obtained

Reproduced with permission of the copyright owner. Further reproduction prohibited without permission.

UM00016645
NOVARTIS EXHIBIT 1517
Novartis v. Regents, IPR2023-01347
Page 3627 of 4460

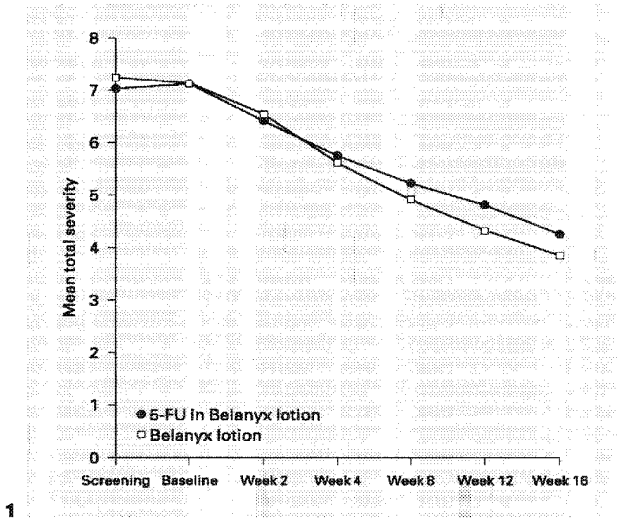

1

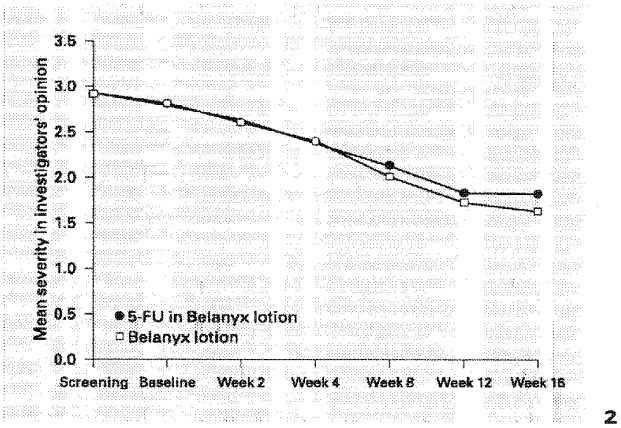

2

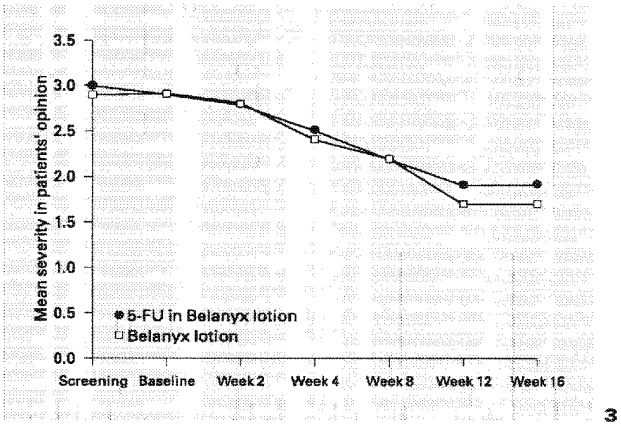

3

Fig. 1. Changes in the mean total NAS score. ● = 5-Fluorouracil in Belanyx lotion; □ = Belanyx lotion.
Fig. 2. Changes in the mean overall severity score, investigators' opinion. ● = 5-Fluorouracil in Belanyx lotion; □ = Belanyx lotion.
Fig. 3. Changes in the mean overall severity score, patients' opinion. ● = 5-Fluorouracil in Belanyx lotion; □ = Belanyx lotion.

with 1% 5-fluorouracil in Belanyx lotion in the number of pits or in onycholysis at the end of treatment. The vehicle lotion treatment alone on the other hand showed significant improvement of all 7 assessed parameters of psoriatic nails at the end of treatment ($p < 0.05$). No statistically significant difference in efficacy between the 2 modes of treatment could be demonstrated in all assessed parameters of the disease.

The efficacy of 1% 5-fluorouracil lotion and of the vehicle lotion as a function of the duration of treatment, on total NAS score or overall improvement according to the investigator's and patient's opinion, has been presented graphically in figures 1–3.

The safety aspects of both preparations were followed closely during the comparative study and although a total of 70 adverse events were reported in 43 of the 57 treated patients only a few were thought to be related to treatment. The most commonly occurring adverse events were associated with the nail itself and concerned symptoms such as pain, swelling, discoloration, inflammation and the nail signs, onycholysis and perforations. These were reported 9 times in 6 patients at the side treated with 1% 5-fluorouracil lotion. Onycholysis was reported to have occurred in 3 of these. Apparently the vehicle lotion formulation itself is tolerated very well since none of the reported adverse effects could be associated with the use of this particular application form.

The two assessed symptoms erythema and burning or stinging, recorded at baseline and scored at weeks 12 and 16, did not show treatment related changes. Erythema scores were very low at the beginning in both groups, remaining virtually the same at the end of treatment. The scores for

Reproduced with permission of the copyright owner. Further reproduction prohibited without permission.

UM00016646
NOVARTIS EXHIBIT 1517
Novartis v. Regents, IPR2023-01347
Page 3628 of 4460

Table 3. The overall improvement according to the investigators' or patients' opinion

Overall improvement	5-FU in Belanyx lotion			Belanyx lotion		
	start	12 weeks	16 weeks	start	12 weeks	16 weeks
Investigators' opinion	2.8	1.8 (36%)	1.8 (43%)	2.8	1.7 (39%)	1.6 (43%)
Patients' opinion	2.9	1.9 (34%)	1.9 (34%)	2.9	1.7 (41%)	1.7 (41%)
Total	5.7	3.7 (35%)	3.7 (35%)	5.7	3.4 (40%)	3.3 (42%)

5-FU = 5-Fluorouracil.

burning and stinging in the 1% 5-fluorouracil lotion group at baseline had increased at the end of treatment and had disappeared at the follow-up assessment. For Belanyx lotion, very low scores for burning and stinging were recorded at baseline; they had disappeared at the end of treatment and at the end of follow-up treatment.

Discussion

The results of this comparative study show that both preparations are effective in improving the dystrophy of psoriatic nails. Apparently, however, the duration of treatment of 12 weeks with these formulations is too short to obtain an improvement of at least 50% in most of the assessed symptoms of dystrophic nails in psoriasis. If the changes in improvement from week 12 to week 16 could be considered representative, a duration of treatment of at least 20 weeks would presumably be necessary to obtain the 60% range of improvement in this indication (fig. 1). Although such a duration of treatment is quite normal for these psoriatic types of nail lesions but may seem rather protracted, this mode would almost certainly be preferable over anaesthesia and complete extraction of the nails, an option which has been mentioned in the past. In addition the results of this study have shown that the quality of the obtained nail improvement was excellent, while it is not certain that dystrophic nails of other diseases would require similar prolonged treatment periods.

An unexpected finding in this study is that the 1% 5-fluorouracil addition to the Belanyx lotion formula, included for its antimitotic or antipsoriatic effect, rather worsened the apparent efficacy of the vehicle lotion in the parameters number of nail pits, area of nail pits and onycholysis. Another unexpected finding is that Belanyx lotion itself showed a remarkable efficacy in the total NAS score and the parameters nail pitting area, subungual keratosis and oil spots at week 12 and week 16. This effect was only observed in the treated nails. The severity of the afflicted nails that were left untreated did not change during treatment and during the post-treatment observation period. No seasonal fluctuations in severity were observed. Possibly the proteolytic and keratolytic activity of urea, together with the humectant activity of propylene glycol, softened and dissolved the various characteristics of dystrophic nails. However, it is clear that nature and type of improvement need to be confirmed by further clinical assessments. In this study both lotion application forms were painted on the nails and subsequently covered with plaster, to keep the medication in place. An improvement of the adhesive power of Belanyx lotion on the nails can probably be obtained by changing the lotion vehicle to a gel formulation which has to be fixed on the nails by means of a spray, which hardens on the nail.

The nature and incidence of adverse effects induced by the 1% 5-fluorouracil lotion preparation were as expected for this irritating substance, while the Belanyx lotion vehicle itself was shown to be non irritant in this selected patient population. The results of this comparative study show that apparently the duration of treatment of 12 weeks is too short to obtain the maximum improvement of the assessed symptoms of dystrophic fingernails in psoriasis. It takes about 6 months for a fingernail to regrow completely, therefore a duration of treatment of at least 26 weeks is presumably necessary to obtain a justified impression of efficacy in dystrophic fingernails of psoriasis.

Conclusion

The results of this double-blind, left-right trial demonstrate that the addition of 1% 5-fluorouracil to Belanyx lotion does not enhance the efficacy of the Belanyx lotion in dystrophic nails of psoriasis. After 12 weeks of treatment, Belanyx lotion itself was shown to induce a statistically

Reproduced with permission of the copyright owner. Further reproduction prohibited without permission.

UM00016647
NOVARTIS EXHIBIT 1517
Novartis v. Regents, IPR2023-01347
Page 3629 of 4460

significant and satisfactory improvement in psoriatic nails. Since the Belanyx vehicle shows a very favourable efficacy-safety ratio compared to the 1% 5-fluorouracil Belanyx nail preparation in the treatment of dystrophic nails of psoriasis, it could probably also be effective in dystrophic nails associated with other dermatological or systemic diseases, although of course this needs further clinical confirmation. Good results of treatment require a duration of treatment of half a year in psoriatic nails, whereas this may be shorter for other types of dystrophic nails.

Contrary to expectation the vehicle Belanyx was shown to be preferable over the 1% 5-fluorouracil Belanyx preparation in dystrophic nails of psoriasis.

References

1 de Jong EMGJ, Seegers BAMPA, Gulinck MK, Boezeman JBM, van de Kerkhof PCM: Psoriasis of the nails associated with disability in a large number of patients: Results of a recent interview with 1,728 patients. Dermatology 1996;193:300–303.

2 Bleeker JJ: Intradermal triamcinolone acetonide treatment of psoriatic nail dystrophy with Port O Jet (letter). Br J Dermatol 1975;92:479.

3 Yamamoto T, Katayama I, Nishioka K: Topical anthralin therapy for refractory nail psoriasis. J Dermatol 1998;25:231–233.

4 Kokelj F, Lavaroni G, Piraccini BM, Tosti A: Nail psoriasis treated with calcipotriol (MC903): An open study. J Dermatol Treat 1994;5:149–150.

5 Nyfors A: Benefits and adverse drug experiences during long-term methotrexate treatment of 248 psoriatics. Dan Med Bull 1978;25:208–211.

6 Handfield-Jones SE, Boyle J, Harman RRM: Local PUVA treatment for nail psoriasis (letter). Br J Dermatol 1987;116:280–281.

7 Finnerty EF: Successful treatment of psoriasis of the nails. Cutis 1979;23:43–44.

8 Lindelof B: Psoriasis of the nails treated with grenz rays: A double-blind, bilateral trial. Acta Derm Venereol (Stockh) 1989;69:80–82.

9 Luger A: 5-Fluorouracil in der Lokalbehandlung der Psoriasis. Z Haut Geschlechtskr 1969;44:361–370.

10 Shelley WB: Onycholysis due to topical 5-fluorouracil. Acta Derm Venereol 1972;52:320–322.

11 Fritz K: Erfolgreiche Lokalbehandlung der Nagelpsoriasis mit 5-Fluorouracil. Z Haut Geschlechtskr 1989;64:1083–1088.

12 Fredriksson T: Topically applied fluorouracil in the treatment of psoriatic nails. Arch Dermatol 1974;110:735–736.

13 Fredriksson T, Lassus A, Salde L: Reproducibility of clinical trials of topical glucocorticosteroids. Int J Dermatol 1983;22:536–539.

Reproduced with permission of the copyright owner. Further reproduction prohibited without permission.

UM00016648
NOVARTIS EXHIBIT 1517
Novartis v. Regents, IPR2023-01347
Page 3630 of 4460

REVIEW ARTICLE

POLYMORPHISM IN PHARMACY

N. K. Jain and (Miss) M. N. Mohammedi

(Received 14 December 85)

A. INTRODUCTION

Polymorphism is the ability of any element or compound to crystallize as more than one distinct crystalline species eg. carbon as a cubic diamond or hexagonal graphite.[1] A polymorph is a solid crystalline phase of a given compound resulting from the possibility of at least two different arrangements of the molecules of the compound in the solid state. The molecule itself may be of different shape in the two polymorphs but that is not necessary and indeed, certain changes in shape involve formation of different molecules and hence do not constitute polymorphism. Geometric isomers or tautomers, even though interconvertible and reversibly so, cannot be called polymorphs, although they may behave in a confusingly similar manner.[2]

The fact that a compound can exist in a crystalline form does not mean that it will always crystallize in one particular crystal system. If a compound can exist in two (or more) forms, these are denoted polymorphs. When polymorphism exists, the molecules can arrange themselves in two (or more) different ways in crystalline state. The molecules in the two forms are chemically identical. Certain shape changes of a molecule in the two forms may occur, but these are not what are known as 'Chemical Changes'. Such non chemical changes encompass resonance structures, rotations about single bonds, and slight bond-distance alterations. A good criterion for distinguishing between polymorphs and chemically different entities is that in the former case the two crystal phases form chemically identical melts and vapours. The composition of saturated solutions and their vapour pressure, however will be different for the two polymorphs and this is of pharmaceutical importance.

The form isolated at any given time may be influenced by the nature of the crystallizing solvent (s) as well as the process or parameters of crystallization. A classical example of polymorphism found in nature, which highlights the physical and chemical differences that can exist between polymorphs is that observed between hexagonal carbon graphite and cubic diamond.[4]

The polymorphs show different solubilities and rates of solution, hence different absorption (bioavailability) tendencies. Thus, polymorphic transformations are structural differences resulting from different arrangements of molecules in the solid state. Polymorphism as it pertains to physical and chemical stability and also to the therapeutic activity has been discussed by a number of researchers.[5]

Different polymorphs of a given compound are in general as different in structure and properties as the crystals of two different compounds. Solubility, melting point, density, hardness, crystal shape, optical and electrical properties, vapour pressure, stability, etc. all vary with the polymorphic forms. In general, it should be possible to obtain different crystal forms of a drug substance and thus modify the performance properties for that compound. To do so requires a knowledge of the behaviour of polymorphs. There are numerous reviews on the subject of polymorphism. In addition, numerous indications of the

Pharmacy Department Faculty of Tech. & Engg., M. S. University of Baroda, BARODA-390 001.

UM00016649
NOVARTIS EXHIBIT 1517
Novartis v. Regents, IPR2023-01347
Page 3631 of 4460

importance of polymorphism in pharmaceuticals are reported in the literature. The work of Kubnert — Brandstatter et al with steroids, barbiturates, and antihistamines probably represents the most intensive study of polymorphism and drugs.[6] They emphasized that almost one in every three compounds exhibit polymorphic behaviour. When the change from one polymorphic form is reversible it is said to be enantiotropic but when the transition takes place in one direction only i.e. from a metastable form to a stable form it is said to be monotropic. Polymorphism is known to occur in many steroids, in sulphonamides and barbiturates, the occurance being frequent in complex molecules, particularly if hydrogen bond formation is possible within the molecules. When a crystalline solid is dissolved in solvent, the crystalline structure is lost so that different polymorphs of the same substance will show the same absorption spectra in solution. Sulphathiazole exists in at least two polymorphic forms, one of which (Form I) undergoes a change in crystal structure at about 174° to form II that melts at 180°; Form I can be prepared by crystallization of sulphathiazole from boiling water or 95% ethanol and seems to be the form commonly met in practice. Cortisone acetate exists in several crystalline forms, only one of which is suitable for preparing stable aqueous suspensions. The unstable forms undergo a polymorphic change in the presence of water which results in crystal growth. The biological activity of chloramphenicol palmitate has been correlated with polymorphic behaviour.[7]

Four different polymorphic forms of oil of theobroma have different melting points. Heating it to 38° completely liquifies the fat but destroys the beta stable crystal (melting point 34.5°) the crystal that are formed being the meta stable, gamma, alpha and beta forms melting at 18°, 22° and 28° respectively so that suppositories tend to melt at room temperature. By melting the oil of theobroma at the lowest possible temperature (about 33°) the stable beta form is not lost and a suppository stable at room temperature is produced. Hydrogenated vegetable oils are also used as suppository bases but as they are unlikely to exist in polymorphic forms they are not affected by slight overheating.[8]

A safe criterion for classification of a system as polymorphic is the following. The polymorphs will be different in crystal structure but identical in the liquid or vapour states. Dynamic isomers will melt at different temperatures, as do polymorphs, but will give melts of different composition. In time, each of these melts changes to an equlibrium mixture of the two isomers with temperature dependent compositions. Some reported cases of polymorphism are undoubtedly dynamic isomerism since the two behave quite similarly.[9]

Methods for obtaining Polymorphs.[10]

The initial task of the performulator is to determine whether or not the drug substance being evaluated exists in more than one crystalline form. The following procedures are usually followed to cause crystallization of a metastable form.[11]

(a) Melt completely a small amount of the compound on a slide and observe the solidification between crossed polars. If after spontaneous freezing, a transformation occurs spontaneously or can be induced by seeding or scratching, the compound probably exists in at least two polymorphic forms. It is essential to prevent nucleation of the stable form by inducing supercooling. Supercooling can be induced by using a small sample size by holding the melt for approximately 30 seconds about 10° above the melting point, by carefully setting aside the compound without physical shock before observing it, and by rapid cooling of the compound.

(b) Heat a sample of the compound on a hot stage and observe whether a solid-solid transformation occurs during heating.

(c) Sublime a small amount of the compound and attempt to induce a transformation between the sublimate and the original sample by mixing the two in a drop of saturated solution of one of them. If the two are polymorphs, the more stable one will be more insoluble and will grow at the expense of the more

UM00016650
NOVARTIS EXHIBIT 1517
Novartis v. Regents, IPR2023-01347
Page 3632 of 4460

soluble metastable form. This process will continue until the metastable form is completely transformed to the stable form. If the samples are not polymorphs, one may dissolve but the other will not grow. If the two are identical forms nothing will occur.

(d) Maintain an excess of the compound in a small amount of solvent held near the melting point of the compound. Isolate the suspended solid. Care should be taken to maintain the temperature during this step. Test the isolated material with an original sample using the procedure outlined in (e).

(c) Recrystallize the compound from solution by shock cooling and observe a portion of the precipitated material suspended in a drop of the mother liquor. The drop may then be seeded with the original compound to check for solution biphase transformation. If the precipitate is a different polymorph, a solution phase transformation should take place. Once it has been established that polymorphism occurs there are procedures which enable the preformulator to prepare the various forms in larger quantities for further evaluation and suitability for incorporation into dosage forms.

Methods of Identification of Polymorphs

Once a compound has been shown to exist in more than one crystalline form, a number of techniques are available to identify the different polymorphic phases present. Each of these techniques could be successful in identifying the phase, but a combination of methods provides a means for isolation, and identification of each crystalline modification. In order to confirm the pressence of more than one crystalline form of a compound it is advisable to identify the modifications present by more than one method. Using only one method for confirming the presence of polymorphs may sometimes be misleading.

i) Microscopy: Optical crystallography is used in the identification of polymorphs. Crystals exist in isotropic and anisotropic forms. When isotropic crystals are present the velocity of light is the same in all directions. While ansotropic crystals have two or three different light velocities or refractive indices. This method requires the services of a trained crystallographer.

ii) Hot Stage Methods : The polarizing microscope fitted with a hot or cold stage is very useful for investigating polymorphs. An experienced microscopist can quickly tell whether polymorphs exist, the degree of stability of the metastable forms, transition temperatures, and melting point, rates of transition under various thermal and physical conditions and whether to pursue polymorphism as a route to improved dosage form. Kodlers and Mc Crone discuss these methods in detail.

iii) X-Ray Powder Diffraction: Crystalline materials in powder form give characteristic x-ray diffraction patterns made up of peaks in certain positions and varying intensities. Each powder pattern of the crystal lattice is characteristic for a given polymorph. This method has the advantage over other identification techniques in that the sample is examined as presented. Some care should be exercised in reducing and maintaining particle size control. A very small sample size is needed and the method is non destructive. This method has been used by several investigators in identifying polymorphs in pharmaceuticals.

iv) Infrared spectroscopy : This procedure is useful in identification of polymorphs. Solid samples must be used since polymorphs of a compound have identical spectra in solution. The technique can be used for both qualitative and quantitative identification.

UM00016651
NOVARTIS EXHIBIT 1517
Novartis v. Regents, IPR2023-01347
Page 3633 of 4460

v) Thermal Methods : Differential scanning calorimetry and differential thermal analysis have been used extensively to identify polymorphs. In both methods the heat loss or gain resulting from physical or chemical changes occuring in sample is recorded as a function of temperature as the substance is heated at a uniform rate. Enthalpic changes both endothermic and exothermic are caused by phase transitions. For example fusion, sublimation, solid-solid transition, and water loss generally produce endothermic effects while crystallization produces exothermic effects. Thermal analysis enables one to calculate the thermodynamic parameters for the system being evaluated. Guillory obtained the heats of fusion for sulfathiazole and methyl prednisolone. Ravin et al utilized differential scanning calorimetry to follow the rate of conversion of sulfathiazole polymorphs.

vi). Dilatometry : Dilatometry measures the change in volume caused by thermal or chemical effects. Ravin & Higuchi,[12] utilized dilatometry to follow the melting behaviour of theobroma oil by measuring the specific volume of both rapidly and slowly cooled, theobrome oil as a function of increasing temperature. The presence of the metastable form was shown by a contraction in the temperature range 20° to 24° C. Dilatometry is extremely accurate, however, it is extremely tedious, and time consuming. It is not widely used.

Proton magnetic resonance, nuclear magnetic resonance and electron microscopy are sometimes used to study polymorphism.[13]

vii) Laser Raman Spectroscopy : Bellows, Chen, and Prasan,[14] determined drug polymorphs by means of the Laser Raman spectroscopy. This Raman Spectroscopy of the lattice vibrations (Phonon) was used to distinguish among various forms of ampicillin (I) and griseofulvin (II). The two anhydrous polymorphs of I and the trihydrate were identified. II solvates with benzene and chloroform were differentiated and the spectra suggested that the II lattice structure expanded to accept chloroform, but that the benzene solvates had a different crystal structures.

I. Preformulation :

Lachman, Swartz, and Huebner in their paper reported (a) the physical and chemical characteristics especially the dissolution properties of three salt forms of 1-(2,3, dihydro-5 methoxy benzo (b) furan -2-yl methyl) -4- (o methoxy phenyl) piperazine (I), a potential antihypertensive compound and (b) the relationship between the salt form and biological activity in dogs.

The dissolution kinetics and thermodynamic parameters of polymorphs of I are considered in part II, of their paper.[15]

II. Biopharmaceutics

A. Kinetics

Shami et al used the differential scanning calorimetry for the determination of sulfathiazole form I in the presence of sulfathiazole form II. An activation energy of 56 kcal/mole was calculated for the system.[16]

The effect of various additives on the rate of transformation of the metastable anhydrous succinyl sulfathiazole (I) form I to the water soluble dihydrate form II in aqueous suspensions was studied by Ebain, Moustafa, and Khalil.[17]

Some structurally related compounds, viscosity imparting agents, surfactants, and colouring agents were used as possible transformation retardants. The effect of including seeds of Form II in the presence and absence of additives was also discussed. Some additives eg. methyl cellulose and pthalylsulfathiazoles showed significant transformation retarding effects. Other additives eg. sulfanilamide and glycerin increased the rate of transformation.

UM00016652
NOVARTIS EXHIBIT 1517
Novartis v. Regents, IPR2023-01347
Page 3634 of 4460

Colouring agents had only slight effects. Utilization of the results in the formulation of physically stable aqueous suspensions of I was discussed.

Using differential scanning calorimetry and thermomicroscopy, Echert and Muller studied the formation and transformation with time of the different polymorphic modifications obtained during the crystallization of I-(5-oxohexyl)-theobromine in vitreous supercooled melts.[18]

B. Dissolution

Andersgaard and Finholt determined the dissolution rates of chloramphenicol palmitate polymorph A and B in phosphate buffer pH. 7.5, containing 0.05% polysorbate 80. This was then compared to the rates of the enzymatic hydrolysis of the two polymorphs by pancreatin in the same phosphate buffer.

The rate of hydrolysis, especially of polymorph B. was so high compared to the rate of dissolution that the first step of the enzymatic process cannot be a dissolution of the ester. It was more likely that chloramphenicol was attached in undissolved state by an enzyme from the pancreas, probably the pancreatic lipase.[19]

Then Frokjaer and Andersen, proposed a model to aid the analysis of the dissolution phenomens occuring with polymorphism in metastable drugs.

The model was tested experimentally by a rotating disk method using testosterone which changes to testosterone monohydrate II in water. It was possible to determine the solubility of testosterone. The rate constants of the transport process and the crystallization process were also estimated. The dissolution process for testosterone and the monohydrate was found to be transport controlled. From the solubilities at various temperatures of the 3 modifications (1 anhydrate and 2 mono-hydrates) the enthalpy changes and the equillibrium temperatures associated with their phase interconversions were determined. The results agree with those from thermoanalytical investigations of the system.[20]

Niazi, found that the dissolution rates of the 2 polymorphic forms of sulfathiazole containing polyethylene glycol 4000(1) were significantly different in water. At higher stirring speeds the dissolution rates in water. At higher stirring speeds the dissolution rates of the stable forms were effected more than the stable form. A high concentration of I seemed to affect the dissolution properties of the metastable polymorph more than the stable polymorph.[21]

Similarly Corrigan, and Timoney found the incorporation of hydroflumethiazide (I) with polyvinyl pyrrolidone (Povidone II), to retard and to enhance the dissolution of the drug from compressed disease, the magnitude of the effect being dependent on the proportion of II present and its method of in corporation.

The most active system dissolved 16 times faster than pure I. Low concentrations of II were also found to decrease the apparent solubility of I while at high concentrations solubility was enhanced. X-Ray and infrared analysis of the systems suggested the presence of an amorphous form of I in coprecipitate systems. The dissolution data were consistent with a physical model which takes account of the roles played by crystalline and amorphous I together with the complexing and crystal growth inhibiting effect of II on I.[22]

Huang and Niazi studied a fast dissolving polymorphic form of mercaptopurine (I) which can be useful in increasing bioavailability.

Differential thermal X-ray diffraction analyses showed 2 polymorphic forms of I which when tested for solubility, showed identical results. However dis-

UM00016653
NOVARTIS EXHIBIT 1517
Novartis v. Regents, IPR2023-01347
Page 3635 of 4460

solution rates for the high energy polymorph were twice those of the lower energy form.[23]

Kohler et al showed that the two polymorphic modifications of 2-sulfanilamido 5-(β-hydroxy ethoxy) pyrimidine were characterized by their different crystal shapes, melting points, IR spectra, and dissolution profiles. In contact with water one polymorph was partialy or completely able to transform into the other form, however it was not possible to quantity this transition.[24]

Differential scanning calorimietry and hot stage microscopy were used by Ford and Rubinstein to obtain phase diagrams of the binary system of indomethacin (I) and polyethlene glycol 6000 (II). The solubility of I in II solutions and the dissolution rate profiles of I and II compressed and melt disks were determined. Results showed that II increased the solubility and dissolution rate of I, an optimum being obtained from the 15% I and 85% II system. The melts exhibited higher dissolution rates than the compressed disks.[25]

Dilute, saturated and supersaturated solutions of cholorothiazide (I) and Polyvinyl Pyrrolidone (Povidone II) coprecipitates and mechanical mixes were prepared and evaluated for permeability through an everted rat intestine by O Driscoll, and Corrigan

Dissolution profiles showed that relative to pure I, coprecipitation enhanced dissolution by a factor of 18.9 and mechanical mixes caused 2.84 fold increase. Reduced permeability from dilute solutions containing II and enhanced dissolution from a mechanical mixture were explained by the formation of a soluble complex. Transport rates from a supersaturated solution were also enhanced in the presence of II.

It was concluded that high dose to solubility ratios were responsible for lack of I transport and that enhanced transport in the presence of II was due to inhibition of I crystallisation.[26]

Merkle prepared by the solvent method coprecipitates containing hydrocortisone (I) or prednisolone (II) and polyvinyl pyrrolidones (Povidone PVP) ranging in molecular weight between 11500 and 10000, and a physiochemical evaluation of the resultant products was undertaken.

Enhanced drug release rates were found only up to a limit of 20% for I and 4% for II. Higher drug fractions led to amorphous or crystalline formations covering the dissolution, surface and severe inhibition of polyme dissolution. Fast drug release was found to be restricted to the low molecular weight polymer formulations. Factors influencing drug release rates in this range were dissolution rate of the polymer and the ratio of drug to polymer weight fractions.[27]

Then Dommeyer et al studied the factors affecting the physiochemical properties of tolbutamide (I) during coprecipitation with polyvinyl pyrrolidone (Povidone).

In ethanolic solutions, I properties varied according to the concentration of the hydrophilic vehicle, cording to the concentration of the hydrophilic vehicle, as well as by direct effects of the solvent. Therefore dif erent crystalline states and one amorphous state of I were found during coprecipitation. Particle size was found to play the most important role in coprecipitation dissolution.[28]

By dissolution rate testing Tuladhar et al evaluated the relative particle size changes for phenylbutazone (I) during compression and crushing and bonding mechanisms associated with the changes.

The effects of polymorphism, compression pressure, drug content and the rate of compression were also studied. Crushing and bonding mechanisms in high concentration of drug were dependent on the original particle size and the polymorphic form of I. With low concentrations diluents protected I particles from bonding. The effects of different types of diluents were also discussed. Decreasing the rate of compression.

UM00016654
NOVARTIS EXHIBIT 1517
Novartis v. Regents, IPR2023-01347
Page 3636 of 4460

decreassed the amount of particle bonding with smaller particles, but larger particles were independent of the compression rates.[29]

Later Tuladhar, and Carless studied the preparation and thermal characterication of 5 phanyl butazone using differential scanning calorimetery, in an aqueous buffer of pH 7.5. Rapid heating rates produced single endothermic peaks due to melting, but slower heating rates resulted in interconversion of 3 polymorphs to the more stable form. Interconversion on grinding the polymorphs was also observed Equilibrium solubility and intrinsic dissolution rates showed that the dissolution process could be described by a Berthoud model. The effect of some tablet excipients on the dissolution processes was also shown.[30]

C. Absorption

Yama moto et al prepared ground mixtures of chloramphenicol palmitate (I) and Micro-crystalline Cellulose using Form A (stable form) and form B (metastable form) of I.

Dissolution and enzymatic hydrolysis rates of the ground mixture were greater than that of Form A. The enzymatic hydrolysis rate of Form B was as fast as that of the ground mixture even when its dissolution rate was not much greater than that of Form A. Four preparations, Form A, Form B, Form A ground mixture, and Form B ground mixture were administered in a random crossover fashion to 5 human subjects and urinary metabolite excretion data were evaluated for drug absorption. After oral administration of the ground mixtures the drug was found to be more uniformly absorbed. A 20 fold increase in absorption was also observed by grinding form A.[31]

Absorption of indomethacin (I) from the rabbit rectum was examined in suppositories containing I polymorphs (α or γ forms) by Yokoyam et al. Rectal suppositories were made with Witespsol H-12. Plasma levels of the 2 α form of I were higher than those of γ form. The commercial product made with polyethylene glycol base was also examined. The plasma levels of I in polyethylene glycol base were similar to those of α form.

The relationship between the thermodynamic activities of I polymorphs and their rectal absorption was also discussed.[32]

D. Bioavailability

The bioavailability of two crystal forms of sulfameter was determined by Khalafallah, and Khalil from the urinary exeretion data of two female and six male volunteers.

One gram of either crystal form was suspended in a mixture previously shown to inhibit polymorphic transformation and immediately administered after an overnight fast period. A crossover study was performed with the same volunteers after one month. Although the urine data revealed a significant difference in the rate of absorption of the two forms, no significant difference was observed in the extent of absorption of both forms as indicated by the 72 hour urinary excretion data. It was suggested that crystal forms of sulfameter may be compared as to their bioavailability by comparing their excretion rate during the absorption phase. Unrinary excretion data are also suggested as a simple alternative to blood level data in studying the kinetics of absorption and deriving absorption parameters that enable the comparison of different formulations of sulfameter.[33]

The determination of the transition temperature and heat of transition between three polymorphic forms of phenobarbittal (I) form 1, form 2, and the hydrate was reported by Kato and Watanabe.

Also the bioavailability of these 3 forms were evaluated by the in vivo absorption test after oral administration to rabbits.

UM00016655
NOVARTIS EXHIBIT 1517
Novartis v. Regents, IPR2023-01347
Page 3637 of 4460

The transition temperature and the heat of transition between form 1, and form 2 and between the hydrate and form 2 were determined to be 80.9 and 0.23 kcal/mole, and 49.1 and 1.52 kcal/mole by the solubility measurement. These values were in agreement with those obtained by other methods. The crystalline energy differences were in agreement with those of the heat of transition by the solubility measurement. In the in vivo absorption test the plasma concentration versus time curves of the 3 forms I in rabbits indicated that each form was similar and these polymorphic states do not effect bioavailability.[34]

Dragnet :- Brughmans and Bouche, investigated polymorphism in 11 samples of pentobarbital using differential scanning calorimetry, thermomicroscopy, IR spectrophotometry, and X-ray diffraction.

The conformity of the samples to European Pharmacopoeia specifications was also studied. The existence of 2 polymorphs was reported in some of the samples. Other samples were mixtures of polymorphs or were pure polymorphs. The different forms had different, solubilities, dissolution rates and bioavailabilities[35].

Camerom et al studied the solvation of chloremphemiol stegrate and chloramphenicol palmitate and various analytical techniques were used to characterize the resulting solvates.

Metastable polymorphic forms of chloramphenicol were formed, however the high crystallinity and low enzymatic hydrolysis rate constants determined in vitro suggested low potential availability.[36]

E. Bioequivalence

Physiochemical characteristics of chloramphenicol palmitate form B, prepared by different methods, were quantified and related to drug bioavailability by Bernobei et al.

The dimensions and morphology of particles, thermo microscopic characteristics, IR spectra, X-ray diffraction results, degree of crystallinity, and the velocity constant of enzymatic hydrolysis in vitro were obtained.

An inverse relationship was found between relative crystallinity and in vitro enzymatic, hydrolysis, suggesting an inverse relationship with bioavailability, Pharmacopoeial tests to standardize the degree of crystallization for chloramphenicol are recommended.[37]

F. Toxicity

Ghielmetti, and Bruzzese found marked differences in LD 50 values between various batches of polyene antibiotics (meparticin and nystatin) after IP administration in suspension to mice. Such differences do not seem attributable to the particle size but to different crystal structures of the products, which modify their solubility and biological availability. In the samples obtained by chemical treatments of some batches of the polyene substances, it has been possible to change the toxicity drastically and then to bring it back to its original value.[38]

III. Manufacturing

Various crystal forms of sulfathiazole, barbital and aspirin were compressed in a single punch tablet machine instrumented to monitor axially applied and radially transmitted forces, and upper punch movement. The effects of this were studied by Summers, Enever, and Carless.

The changes in radial stress during the compression cycle depended upon the polymorphic forms of the compressed material. The results were rationalized in terms of the degree of plastic flow/crushing that occurred with each material, and the degree to which the final compact underwent elastic compression.[39]

UM00016656
NOVARTIS EXHIBIT 1517
Novartis v. Regents, IPR2023-01347
Page 3638 of 4460

A method was described for the preparation of sterile hydrocortisone as the stable polymorph A by evaporation from a mixture of methanol and ethanol by Chrai et al. This procedure can be adopted to large scale manufacture.[40]

Data was collected by Ibrahim from X-ray diffraction, thermal analysis, IR spectroscopy, and solubility studies and were used for identification and characterization of 4 crystalline modifications of phenylbutazone.

The thermal behaviour of the polymorphs under different treatment conditions was also investigated. Compression of the thermodynamically unstable forms, at a compression force of 1590-2040 kg. induced polymorphic changes in the crystals. Similar changes were also produced through grinding. The apparent equilibrium solubilities were determined as was the dissolution as compressed disks in an equeous medium. The small effective surface area possessed by one polymorph resulted in slow dissolution.[41]

Studies on the crystal transformation of methisazone (I) upon grinding was made by Lee and Hersey by X-ray diffraction, IR spectra and differential thermal analysis carried out on freshly ground, unground and micronised I. All these materials give distinctive diffraction patterns indicating the presence of at least 2 polymorphs. There polymorphic changes may explain the increased solubility, biological activity and stability obtained with the use of micronized (I) in pharmaceutical formulations.[42]

Junginger studied the effects of grinding on the various polymorphs of sulfanilamide (I). Grinding of polymorph (I) in a colloid mill produces a 95% phase transformation into polymorph II. On the other hand, when polymorph II is ground under identical conditions, the same phase equilibrium is reached as on grinding phase I. Investigations on the nucleation phase of this phase transformation prove that up to a degree of phase transformation of 50% the Prout Tompkins mechanism is performed. Milling polymorph III under the same conditions produces a quantitative phase transformation into polymorph II. A more extensive grinding leads to the same phase equilibrium consisting of 95% polymorph II and 5% polymorph I. On grinding polymorph III, the nucleation phase of polymorph II is superposed by the milling process, so that Prout-Tompkins mechanism cannot be fulfilled.

The phase transformations were proved by X-ray crystallography (goniometer methods) and by measuring the solution enthalpies of the ground products. In addition, the increase of temperature during the milling process was determined. The temperature increases faster when the milling process is repeated because the need of energy to get smaller particles is lower than for the first milling process.[43]

Florence used infrared spectroscopy, X-ray diffractometry, differential thermal analysis, scanning electron microscoppy, solubility and dissolution rate measurements to demonstrate that pulverization of digoxin (I) crystals resulted in the appearance of an amorphous phase. The study of spironolactone and 17-β estradiol also showed that these compounds undergo changes in their crystallinitiy on grinding. Since the dissolution characteristics of poorly soluble drugs may be complex functions of surface area and crystallinity it was concluded that the most pertinent method for standardizing a sample of a polymorph drug of low solubility is by means of a powder dissolution test.[44]

Conte et al compared the compression properties of 2 polymorphic forms of sulfamethoxydiazine (sulfameter I). Tablets obtained with I crystalline form has better particle size distribution, disintegration time, porosity, and friability, than, the other I polymorphic form. The best formulations were obtained when potato starch and lactose were used as diluents.[45]

The conditions for preparing 2 known crystalline polymorphs of trimethoprim (I) of a new crystalline form and of I monohydrate were studied by Bettin-

UM00016657
NOVARTIS EXHIBIT 1517
Novartis v. Regents, IPR2023-01347
Page 3639 of 4460

atti et al. The crystals were characterized by IR spectroscopy, thermal and thermogravimetric analysis, and by x-ray diffractometry.[46]

The effects of wet granulation, excipients and compression on polymorphic changes in sulfanilamide were studied by Gruaud et al.[47]

The crystal changes during tablet compression were studied by Fuhrer and the compression characteristics of polymorphic compounds were also noted.[48]

IV. Microencapsulation

Takenaka and Kawashima[49] investigated the effects of cellulose acetate phthalate and excipients such as talc colloidal silica and montmorillonite on the polymorphism of sulfamethoxazole in microcapsules.

The surface topography varied with the type of excipient and the pH of the suspending medium. Polymorphic transformations of sulfamethoxazole were attributed to interactions with cellulose acetate phthalate. Talc was the only excipient to contribute to sulfamethoxazole polymorphism.[49]

Various microscapsule formulations of sulfamethoxazole containing either xanthan gum or guargum and colloidal silicon dioxide or cellulose acetate phthalate were evaluated for release behaviour, physicochemical characteristics and drug polymorphism by Kawashima et al. Silica preparations produced increased particle size and improved physical characteristics. Crystalline forms I, II and III of sulfamethoxazole were observed in formulations containing cellulose acetate phthalate. Colloidal silica products showed only form I crystals. Formulations obtained from aqueous solutions had prolonged drug release rates from tablets, while those obtained from ammonium hydroxide exhibited rapid drug releases.[50]

V. ANTIGEN FORMATION :

Using a reversed phase high pressure liquid chromatographic method an investigation of the time courses of formation of ampicillin di and polymers in aqueous solutions of ampicillin sodium (I) at different initial concentrations (1 to 20% w/v) was carried out and studied by Larsen and Bundgaard. In 10 to 20% solutions at room temperature, di, tetra and hexamers account for more than 90% of the products formed by I total degradation. In 1 to 5% solutions the dimer and α amino penicilloic acids constituted the major degradation products. For each individual polymer, ranging in size from the dimer to the octamer quantitative data for the amounts formed during storage of I solutions under practical clinical conditions were calculated, and the influence of storage time of the I solutions on their antigenic activity was discussed.[51]

VI. OINTMENTS

Borka studied the problems of polymorphism in pharmaceutical preparations and emphasized more on the risk of crystal growth in eye ointments due to unstable polymorph conditions.[52]

In order to characterize the crystalline state of hydrophilic ointment (I) as well as of its components, X-ray studies (using Kiessing's low angle technique and goniometric diffractometry) were carried out and studied by Fuhrer et al.

Both cetyl and stearyl alcohols crystallize in a mixture of β_o and γ [4] Polymorphs. Depending on the conditions of crystallization one or the other polymorphic phase is in excess. The mixture of these two alcohols, contostearyl alcohol forms mixed crystals with a uniform Bragg's distance, which is between the 2 β_o polymorphic forms of the single components. On the other hand sodium cetyl sulphate (II) and sodium stearyl sulphate (III) crystallize as seperate entities from their mixtures.

UM00016658
NOVARTIS EXHIBIT 1517
Novartis v. Regents, IPR2023-01347
Page 3640 of 4460

The predominant species in emulsifying wax (90% cetostearyl alcohol and 10% II and III) are mixed crystals which consist mainly of cetyl alcohol, and II and partly of stearyl alcohol. In addition, mixed crystals of stearyl alcohol and III are found in small amounts. In I both types of mixed crystals from a framework of gel in which white soft paraffin and the liquid components of the white petrolatum are immobilized either mechanically or by capillary attraction. Since the wide angle interferences are nearly identical, it may be assumed that the paraffinic carbon chains of all components of the ointment can form similar orthorhombic subcells.[53]

The influence of ointment composition and storage temperature on the conversion of anhydrous prednisolone (I) to its hydrated form in oil in water type cintments was studied using an x-ray diffractometer and a polaring microscope by Kacho et al.

When stearyl alcohol or cetyl alcohol alone was added to the ointment anhydrous I was converted into the hydrate at a low temperature (5°). However, when a mixture of alcohols was used in a proper ratio, the conversion of the anhydrous to the hydrated form was retarded. When stearyl alcohol and cetylalcohol were mixed in the ratio of approx. 2 : 3, the anhydrous form remained most stable. When the ointment was stored at a high temperature (37°) for a long time and then moved to a low temperature (5°) for storage, conversion to the hydrate was difficult. These results were due to the 3 polymorphisims (α r, and β) of long chain alcohols. The ointment structure containing the α form was stable enough to stabilize anhydrous I while that containing the β or r form was less stable.[54]

VII. Suppositories

Nurnberg, Schenk, and Kohr, studied the methods of production, composition and melting behaviour of adeps solidus and the conditions under which polymorphic modifications result were shown experimentally with the aid of differential scanning colorimetry. Thermograms of 7 different suppository bases were illustrated and comparisons between them were made.[55]

Luversidge, & Grant, showed that in order to determine the most suitable compositions for suppository bases from the point of view of melting point, and polymorphic change, complete phase diagrams of binary mixtures of some monoacid triglycerides, namely tricaprin (glyceryl-tri-n-decanoate, Dynasan 110, I), trilaurin (glyceryl-tri-n-di decanoate, Dynasan 112, II), trimyristin (glyceryl, tri-n-hexa tetradecanoate, Dynasan 114, III), tripalmitin (glyceryl tri-n-hexa decanoate, Dynasan 116, IV) and tristearin (glyceryl tri-n-octa dercenoate, glyceryl tristearate, dynasan tri-n-octa decanoate, glyceryl tristearate, dynasen 118, V). Witepsol W 35, Witepsol E 75 and Suppocire A, were derived, using differential thermal analysis as a heating method.

The increase in melting point on storage was found to be closely associated with the conversion of the α and β' polymorphs of the constitutent bases to the more stable β polymorph. The rate of this process was found to decrease with increasing chain length. Tricaprin II, III, IV and V showed eutectic or monotectic behaviour, the eutectic composition of one varying by about 20% from the others next to it, with respect to the higher melting components.

From the results, 2-8% V in I, 3-10% IV in I, 10-25% III in I, 55-65% II in I and 40% II in I (all W/W) were proposed as suppository bases.[56]

Thoma performed an in vitro study of the physical stability of 107 commercial hard fat (Adeps solidus) suppository preparations, comparing the effects of storage conditions on the melting times is presented.

The techniques used included the Erweka Penetration Tester PM 3, the Selnikar — Fantelli method, the suppository melting Tester SSP and the apparatus of the European Pharmacopoeia II.

UM00016659
NOVARTIS EXHIBIT 1517
Novartis v. Regents, IPR2023-01347
Page 3641 of 4460

The observed melting times showed a considerable dependency on the age of the preparations. The changes were due to the polymorphic behaviour of the semi-synthetic triglyceride suppository bases. Subject to the temperature, hard fat crystallizes in an α or β modification and changes to β polymorph within months or years. All bases showed this phase transition as a function of storage temperature.[57]

The influence of the liquid phase on the A and B transition of semisynthetic fatty suppository bases, including Witepsol H-15 and E-75 (trilaurin) during storage was studied by Yosheno et al.

The case where the liquid phase was produced only from the molten vehicle containing no liquid additive was also examined. The activation energy of transition was compared in the presence and absence of liquid additives. The transition mechanism was considered to involve dissolution of the solid A form in the intervening liquid phase followed by crystallization as solid B form.[58]

The polymorphism of hard fat (Adeps solidus) in suppository bases was demonstrated by X-ray diffraction and studied by Thoma, Serno & Precht. Temperature and storage effects on polymorphism were discussed. Differences between several types of base were found to be due to different chain lengths of the triglycerides[59]

Differential thermal analysis was used to demonstrate the 2 polymorphic crystal forms of hard fat (Adeps solidus) suppository bases resulting from solidification of a molten mass, dependent on temperature by Thoma.

Transition from one polymorphic form to the other during storage and effects of the transition on suppository hardening were discussed. Addition of soy lecithin was shown to alter crystal behaviour and stabilize the suppositories.[60]

VII. Stability

Various analytical techniques were used to investigate the physical characteristics of sulfa-methoxazole (I) instability in aqueous suspensions of Graf. Transformation of I to a semihydrate form was found to be the major characteristic to I instability formulation methods for inhibiting this transformation were studied. Methyl cellulose, povidone and sucrose used as suspension additives inhibited the transformation while carmellose sodium (carboxy methyl cellulose sodium) enhanced this effect[61]

IX. Effect of Ageing

The effect of ageing on the disolution of indomethacin (I) solid dispersions in polyethylene glycol 6000 (II) was studied by Ford and Rubinstein using constant surface area disks stored at various temperatures. It was determined that ageing markedly reduces dissolution rates. The changes were complex and dependent upon disk concentrations and storage conditions. Melts stored at 4°C containing 5 or 10% I showed slow decreases in dissolution rates which still decreased even after one year storage. However, melts containing 25% I stored at 35°C exhibited large dissolution rate decreases initially which then remained relatively constant after 10 days storage.

The presence of moisture also played a major role in reducing dissolution rates. Photomicroscopy revealed changes in structure of the melts dependent on concentration which were thought to produce the dissolution rate changes.[62]

X. Forensic Aspects

The forensic aspects of heroin (diacetyl morphine) were examined by Borka in its existence as a polymorph. A form with a slightly lower melting point and an irregular IR Spectroscopy was found. These irregularities donot necessarily indicate impure I, but may be explained by polymorphism.[63]

UM00016660
NOVARTIS EXHIBIT 1517
Novartis v. Regents, IPR2023-01347
Page 3642 of 4460

It may thus be concluded that polymorphism is one of the most important property of drug compounds which might affect various formulation parameters and performance characterestics of dosage forms. It would therefore be desirable that polymorphic behaviour of drug alone and in presence of formulation additives is studied thoroughly.

REFERENCES

1. Arthur Osol. Ed., **Remington's Pharmaceutical Sciences, 16th edition, 1980, Mack Publishing Company. Easton, Pennsylvania, p. 1358.**
2. ibid, p. 1359.
3. J. Thurocarstensen **Theory of Pharmaceutical systems, Vol. II, Academic Press, New York & London, 1973, p. 113.**
4. Kenneth E. Avis, Leon Lachman and Herbert A Liebermann. Eds. **Pharmaceutical Dosage Forms, Parenteral Medications Vol. I. Marcel Dekker, Inc, New York and a Basel, 1984, p. 123.**
5. ibid, p. 151.
6. Arthus Osol, Ed. **Remington's Pharmaceutical Sciences, 16th edition, 1980, Mack Publishing Company. Easton, Pennsylvania p. 1359.**
7. Aguiar. J. A. Kre J. Kinkel, A. W. and Samyer, J. C., **J. Pharm Sci., 1967, 56, 847.**
8. E. A. Rawlins Ed. **Bentley's Textbook of Pharmaceutics, 8th edition Sc 1977, Cassel and Coclear Macmillan Publishers Ltd., London p. 25-26.**
9. Arthur Osol. Ed. **Remington's Pharmaceutical Sciences, 16th, Edition, 1980; Mack Publishing Company, Easton Pennsylvania P. 1359.**
10. **Ibid, p. 1360.**
11. Halebian. M. Mc Crone W; **J. Pharm Sci., 1961, 58, 911.**
12. Ravin, J. Higuchi, T. **J. Am. Pharm. Assoon., Sci. Ed., 1957, 46, 732.**
13. Arthur Osol. Ed; **Remington's Pharmaceutical Sciences; 16th Edition; 1980, Mack Publishing Co., Easton, Pennsylvania; Pp. 1361.**
14. Bellows, J. C. Chen, F. P., and **Prasan P. N Drug Dev. Ind. Pharm, 1977, 3, 451-458.**
15. Lachman, L, Swartz, C. J., and Huebner, C F.; **J. Pharm. Sci., 1972, 61, 1418 : 1430.**
16. Shami; E. G. Bernardo, P. D. Rattic, E. S., and Ravin, L. J., **J. Pharm Sci., 1972, 61, 1313-1320.**
17. Ebain, A. R. Moustafa, M. A. Khalil, S. A., **J: Pharm Sci., 1975, 1481-1484.**
18. Echert, T. Muller, J., **Pharm Acta Helv, 1977, 52, 45-47.**
19. Andersguaald, H, Finholt R., **Acta Pharm Suec, 1974, 11, 239-248.**
20. Frokjaer, S. and Andersen, V. S. **Arch. Pharm. Chemi. (Sci. Ed), 1974, 2, 79-84.**
21. Niazi, S, **J. Pharm Sci., 65, 302-304.**
22. Corrigan, O. I., and Timoney, R. F., **J. Pharm. Pharmacol, 1975, 27, 759-764.**

UM00016661
NOVARTIS EXHIBIT 1517
Novartis v. Regents, IPR2023-01347
Page 3643 of 4460

23 Huang, M L , and Niazi, S; J. Pharm Sci., 1977, 66, 608-609.

24. Kohler, H. J., Soliva, M, and Speiser, P., Pharm Acta, Helv., 1975, 50, 17-24.

25 Ford J. L. and Rubinetein, M. H.. Pharm Acta Helv., 1978, 53, 93-98.

26. O' Driscoll, K. M., and Corrigan, O. I., Drug Dev. Ind. Pharm, 1982, 8, 547-564.

27 Merkle, H P , Acta Pharm, Technol, 1981, 27, 193-203.

28 Dommeyer, A., Boucherat, J., and Buri, F., Acta, Pharm. Technol, 1981, 27, 205-210.

29. Tuladhar, M. D., Carless, J. E., J. Pharm. Pharmacol., 1983, 35, 208-214.

30 Tuladhar, M. D., Carless, J. E., J. Pharm, Pharmacol., 1983, 35, 269-274.

31. Yamamoto K., Matsuda, S, Nakano, M., Yakugakuzasshi; 1977, 97, 367-372.

32. Yokoyam, T, Umeda, T. Kuroda, K. Nagafuku, T. Yamamoto, T., Yakugaku Zasshi, 1979, 99, 837-842.

33 Khalafallah, N., Khalil, S. A., J. Pharm. Sci., 1974, 63, 861-864.

34. Kato. Y., and Watanable, F., Yakugakuzasshi, 1978, 54, 639-648.

35. Dragnet — Brughmans, M., Bouche, R. Pharm. Acta, Helv, 1979, 53 : 140-145.

36. Cameroni, R , Coppi, G, Forni. F. Gambarini, A, and Farcoli, V, Farmaco Ed. Prat., 38, 173-182.

37 Bernobei, M T , Forni, F. Coppi G. Iennucelli, V, and Cameroni, R. Farmaco Ed. Prat, 1983, 384, 391-402.

38 Ghielinetti, G, Bruzzese, T., J. Pharm, Sci, 1976, 65, 905-907.

39 Summers, M P , Enever, R. P., and Carless, J. E., J. Pharm. Pharmacol, 1976, 28, 89-99.

40. Chrai, S. S. and Stupak, E. I , Bull Parenter, Drug Assoc., 1976, 30, 100-103.

41 Ibrahim H G , Pisano F., and Bruno, A , J. Pharm Sci., 1977, 66, 669-673.

42. Leo K. C., and Hersey, J. A.. J. Pharm. Pharmacol., 1976, 29, 249-250.

43 Junginger, H , Dtsch. Apoth. Ztg. 1977, 117, 456-459.

44 Florence, A. T., J. Pharm. Pharmacol, 1976, 28, 637-642.

45 Conte, U. Colomba, P., Carmella, C. Bettinetti, G. P., Giordano, F., Farmaco, Ed. Prat, 1975, 30, 194-206.

46. Bettinetti, G. P., Giordano, F., La Meanna, A., and Giuseppetti, G , Boll. Chim. Farm., 1978, 117, 522-529.

47. Gruaud G., Guchene, D., Puisieux, F., Chauvet, A., and Masse, J. Pharm Belg., 1981, 86, 15-20.

48. Fuhrer, C., Acta. Pharm. Technol., 1970, 24, 129-140.

UM00016662
NOVARTIS EXHIBIT 1517
Novartis v. Regents, IPR2023-01347
Page 3644 of 4460

49. Takenaka, H, Kawashima, V , J. Pharm Sci., 1981, 70, 1256-1260.

50 Kawashimo, Y., Lin, S. Y , and Takenaka H , Chemi., Sci., Ed. 1977, 3, 201-209.

51 Larsen, C and Bundgaard, H., Arch. Pharm Drug Dev. Ind. Pharm. 1983, 9, 1445-1463.

52 Borke, L Norg. Apotelokerforen. Tidsswar, 1977, 85, 440-442.

53 Fuhrer, C., Junginger, H , and Fiiberg, S. J. Soc. Cosmet, Chem., 1978, 29, 703-716.

54 Kacho, F , Takigawa, Y., Ando, A. and Kato, Y., Yakugnku Zasshi., 1979, 99, 1068-1072.

55. Nurnberg, E., Schenk, D., and Kohr., P., Pharm. Ztg., 1077, 122, 1376-1382.

56 Luversidge, G G , Grant, D J. W., Int. J. Pharm., 1981, 7, 211-223.

57. Thoma, K., Pharm.-Ztg., 1982, 427, 980-986.

58 Yosheno, H , Kobayashi, M., and Samajuma, M., Chem. Pharm. Bull, 1982, 30, 2941-2950.

59 Thoma, K., Serno, P , and Frecht, D , Pharm. Ind., 1983, 45, 420-426.

60 Thoma, K , Vesstand Dea Inst. Aur Pharm and Lebenmilted Chemia dez, Ludiving Maximilliens Unio. Sophrenate, 10, 8000, Munich, 2, FRG and Serne, P.

61. Graf, E., Pharm. Ind., 1982, 44, 1071-1074.

62 Ford, J. L , and Rubinstein., M. H , Pharm. Acta. Helv, 1979, 54, 353-358.

63 Borka, L , Acta, Pharm. Suec., 1977, 14, 210-212.

UM00016663
NOVARTIS EXHIBIT 1517
Novartis v. Regents, IPR2023-01347
Page 3645 of 4460

Notice of Reasons for Rejection
(Translation)

Drafting Date:	September 29, 2009
Dispatch Date:	October 8, 2009
Sections Applied:	29 (1), 29(2), 36, and 37

This application is rejected for the reasons stated below. If the Applicant has any arguments against the reasons, such arguments should be submitted within three months from the dispatch date of this *Notice of Reasons for Rejection.*

Rejections

1. This application fails to comply with the requirements under Japanese Patent Law Section 37, for the reasons mentioned below.

2. The inventions claimed in the following claims are not patentable under Japanese Patent Law Section 29(1)(iii), because they have already been described in the documents listed below, which were distributed in or outside of Japan, or made publicly available through electric telecommunication lines, prior to the filing of the present application.

3. The inventions described in the claims indicated below are not patentable under Japanese Patent Law Section 29(2), because they could have easily been made by a person with ordinary skill in the art to which the invention pertains, prior to the filing of this application, on the basis of the inventions described in the documents listed below, which were distributed in or outside of Japan, prior to the filing of this application.

4. The claims of this application fail to comply with the requirements under Japanese Patent Law Section 36(6)(i), for the reasons mentioned below.

5. The claims of this application fail to comply with the requirements under Japanese Patent Law Section 36(6)(ii), for the reasons mentioned below.

Reasons (Regarding the cited documents, see List of Cited Documents)

[A]

Claims: 1-36
Rejection 1
Remarks: Based on the relationship between independent and dependent Claims and categories of the inventions, the Claims can be divided as follows:

-Product inventions relating to Claims 1-19 (Invention 1)
-A product invention relating to Claim 20 (Invention 2)
-A product invention relating to Claim 21 (Invention 3)
-A product invention relating to Claim 22 (Invention 4)
- A product invention relating to Claim 23 (Invention 5)
- A product invention relating to Claim 24 (Invention 6)
-Method inventions relating to Claims 25-28 (Invention 7)
-Method inventions relating to Claims 29-32 (Invention 8)
-Method inventions relating to Claims 33-36 (Invention 9)

Even when any one of Inventions 1-6 is the specified invention, Inventions 7-9 are neither a method of producing the product of the specified invention, a method of using the product of the specified invention, nor a method of dealing with the product of the specified invention. Therefore, it is not recognized that those inventions fulfill the relationship defined in Japanese Patent Law Section 37 (iii).

Since the present application fails to comply with Japanese Patent Law Section 37, the claims other than claims 1-24 have not been further examined for other requirements, except for the requirements under Section 37.

[B]
Claims: 1-24
Rejection 4
Remarks: Claim 1 specifies "a multiple-component phase composition comprising a solid phase that is sustained by intermolecular interactions between two or more independent molecular entities, wherein at least one of said two or more independent molecular entities is a pharmaceutical molecule".

However, having reviewed the descriptions of the specification, what is substantially produced in the Examples is only co-crystals of two kinds of compounds or co-crystals of two kinds of compounds and water.

Therefore, the products encompassed by the above multiple-component phase

composition other than co-crystals are not supported sufficiently by the specification.

Please note that as mentioned above, since the products encompassed by the above multiple-component phase composition other than co-crystals are not supported sufficiently by the specification, in this Notice, the examination regarding novelty and inventive-steps has been conducted assuming that the multiple-component phase composition is co-crystal.

[C]
Claims: 1-19, 21, 23, and 24
Rejections 2 and 3
Cited Documents: 1-9
Remarks: Cited Document 1 describes a 1:1 carbamazepine/formamide co-crystal (See page 508, right column, Schema 2 and the same column, the fourth-third lines from the bottom), which is identical to the co-crystal described in Example 17.

Cited Document 2 describes an inclusion complex of Carbamazepine with β-cyclodextrin (1:1) (See page 960, lines 1-3). In a broader sense, an inclusion complex is a kind of co-crystal.

Cited Document 3 describes "Caboril Complex" which is recognized as a complex of phenyloin, phenobarbitone, and aminohydroxybutiric acid.(See page 1610, column 2).

A complex can be recognized as a kind of co-crystal in a broader sense (Regarding "complex", the same applies to the following Cited Documents.).

Cited Document 4 describes a phenazone/paracetamol (acetaminophene) complex compound in a form of a molecular complex compound having a hydrogen bonding including phenazone and paracetamol in an almost equivalent molar ratio (Page 1, left column, lines 2-9).

Cited Document 5 describes a 1:1 molecular complex of mebendazole with propionic acid. Cited Document 5 also describes that the complex forms intermolecular hydrogen bonding (See page 11, abstract, and page 13, Fig.2 and such).

Cited Document 6 describes a 1:1 complex between 5-chlorosalicylic acid and theophylline. Cited Document 6 also describes that the complex forms intermolecular hydrogen bonding (See page 710, abstract and such).

Cited Document 7 describes a 1:1 molecular complex of theophylline and p-nitoroaniline. Cited Document 7 also describes that the complex forms intermolecular hydrogen bonding in the crystal structure (See page 2390, abstract and page 2391, Figure 2

and such).

Cited Document 8 describes a 1:1 complex of theophylline and p-nitrophenol. Cited Document 8 also describes that the complex forms intermolecular hydrogen bonding (See page 2333, abstracts and such).

Cited Document 9 describes a 2:1 molecular complex of theophylline and 5-fluorouracil as the monohydrate. Cited Document 9 also describes that the complex forms intermolecular hydrogen bonding (See page 1857, abstract and right column, lines 9-12 and such).

Therefore, the inventions of Claims 1-19, 21, 23, and 24 are the inventions described in any one of Cited Documents 1-9 or at least, would have been easily achieved by one skilled in the art on the basis of the descriptions of any one of Cited Documents 1-9.

[D]
Claims: 1-24
Rejection 3
Cited Documents: 1-11
Remarks: As described in Cited Documents 1-9, producing co-crystals regarding various kinds of compounds was frequently conducted from before the priority date of this application.

Furthermore, as described in Cited Documents 10 and 11, it was well known before the priority date of this application that when producing co-crystals with compounds having π-electron systems or having groups which can form hydrogen bonds, intermolecular interactions such as hydrogen bonding or π–π interactions occurred (See Cited Document 10, Figure 1-4, and page 9833, the second-fifth lines counting from the Figure and Cited Document 11, page 5987 abstracts, page 5989 Table 1, and Figure 1-11 and such.).

Therefore, producing co-crystals consisting of two kinds of compounds and confirming the occurred intermolecular interactions in the obtained co-crystals do not present any difficulties for one skilled in the art.

[E]
Claim: 11
Rejection 5
Remarks: (1) The descriptions using parentheses in Claim 11 make the scope of the invention unclear.

(2) "Profen" recited in Claims 9 and 22 is not a usual name of the chemical compound. Therefore, it is unclear what compound this term indicates. (Is this an error of either of "ibuprofen" or "flurbiprofen"?)

(*)When amending, please note that no new matter must be introduced. At the same time, it is desirable that the Applicant clearly indicates in a *Written Argument* support from the original specification and such.

List of Cited Documents

1. H. Wounderlich et al., Pharmazie, 1991, Vol. 46, No. 7, P. 507-509
2. S. A. EL=NAHHAS, Pharmazie, 1996, Vol. 51, No. 12, P. 960-963
3. JAMES E. F. REYNOLDS, Martindale. The extra pharmacopeia, The PHARMACEUTICAL PRESS, 1993, P. 1610
4. Japanese Patent Application Kokoku Publication No. (JP-B) 46-33588 (examined, published Japanese patent application)
5. Mino R. Caira et al., Journal of Chemical Crystallography, 1998, Vol. 28, No. 1, P. 11-15
6. Eli Shefter, Journal of Pharceuticla Sciences, 1969, Vol. 58, No. 6, P. 710-714
7. Shuich Zaitu et al., Acta Crystalllographica Section C, 1995, Vol. 51, P. 2390-2392
8. Katsuyuki Aoki et al., Acta Crystalllographica Section B, 1978, Vol. 34, P. 2333-2336
9. Shuich Zaitu et al., Acta Crystalllographica Section C, 1995, Vol. 51, P. 1857-1859
10. V. R. Pedireddi et al., Tetrahedron Letters, 1998, Vol. 39, P. 9831-9834
11. Md. Badrus Zaman et al., Journal of Organic Chemistry, 2001, Vol. 66, P. 5987-5995

Record of Prior Art Search Results

This record is not a component of the reasons for rejection.

・ Prior art references: None

拒絶理由通知書

特許出願の番号	特願２００３－５７２９４６
起案日	平成２１年　９月２９日
特許庁審査官	三輪　繁　　４１４８　４Ｃ００
特許出願人代理人	清水　初志（外　１名）　様
適用条文	第２９条第１項、第２９条第２項、第３６条、第３７条

この出願は、次の理由によって拒絶をすべきものです。これについて意見がありましたら、この通知書の発送の日から３か月以内に意見書を提出してください。

理　由

１．この出願は、下記の点で特許法第３７条に規定する要件を満たしていない。

２．この出願の下記の請求項に係る発明は、その出願前に日本国内又は外国において、頒布された下記の刊行物に記載された発明又は電気通信回線を通じて公衆に利用可能となった発明であるから、特許法第２９条第１項第３号に該当し、特許を受けることができない。

３．この出願の下記の請求項に係る発明は、その出願前に日本国内又は外国において頒布された下記の刊行物に記載された発明又は電気通信回線を通じて公衆に利用可能となった発明に基いて、その出願前にその発明の属する技術の分野における通常の知識を有する者が容易に発明をすることができたものであるから、特許法第２９条第２項の規定により特許を受けることができない。

４．この出願は、特許請求の範囲の記載が下記の点で、特許法第３６条第６項第１号に規定する要件を満たしていない。

５．この出願は、特許請求の範囲の記載が下記の点で、特許法第３６条第６項第２号に規定する要件を満たしていない。

記　　（引用文献等については引用文献等一覧参照）

［A］

・請求項　　１－３６
・理由　　１

特許請求の範囲の請求項は、独立請求項－従属請求項の関係及び発明のカテゴリーにより、以下のように区分し得る。

・請求項１－１９に係る物の発明（発明１）
・請求項２０に係る物の発明（発明２）
・請求項２１に係る物の発明（発明３）
・請求項２２に係る物の発明（発明４）
・請求項２３に係る物の発明（発明５）
・請求項２４に係る物の発明（発明６）
・請求項２５－２８に係る方法の発明（発明７）
・請求項２９－３２に係る方法の発明（発明８）
・請求項３３－３６に係る方法の発明（発明９）

そして、物の発明である発明１－６のいずれを特定発明としても、該特定発明に対して、方法の発明である発明７－９は、その物を生産する方法の発明、その物を使用する方法の発明、その物を取り扱う方法の発明の関係となっていないから、特許法第３７条第３号の関係を満たしているとはいえない。

よって、この出願は特許法第３７条の規定に違反しているので、請求項１－２４以外の請求項に係る発明については特許法第３７条以外の要件についての審査を行っていない。

［B］
・請求項　　１－２４
・理由　　４

請求項１では、「２種以上の独立した分子実体間の分子間相互作用により維持される固相を含む多構成要素相組成物であって、該２種以上の独立した分子実体のうち少なくとも１種が薬剤分子である、多構成要素相組成物」が特定されている。

しかしながら、本願明細書の発明の詳細な説明を検討すると、実施例において実質的に製造されているのは、２種の化合物又は２種の化合物及び水を組み合わせて結晶化した共結晶が記載されているのみである。

したがって、請求項１－２４規定の多構成要素相組成物に包含される物のうち、共結晶以外については、発明の詳細な説明中に十分なサポートが存在するとは

いえない。

なお、上述のように、共結晶以外の多構成要素相組成物については、発明の詳細な説明中に十分なサポートが存在するとはいえないので、本拒絶理由通知書においては、請求項１－２４規定の「多構成要素相組成物」が「共結晶」であるものとして、新規性・進歩性等の審査を行った。

［C］
・請求項　　１－１９，２１，２３，２４
・理由　　２，３
・引用文献等　１－９
・備考

引用文献１には、カルバマゼピンとホルムアミド（１：１）の共結晶が記載されている（第５０８頁右欄Schema 2及び同欄下から第４行－下から第３行）。

ここで、カルバマゼピンとホルムアミド（１：１）の共結晶は、本願実施例１７に記載されたものと同一である。

引用文献２には、カルバマゼピンとβ－シクロデキストリン（１：１）の包接錯体が記載されている（第９６０頁第１－３行等）。

そして、包接錯体は、広義には、共結晶の一種とみなせる。

引用文献３には、フェニトイン、フェノバルビタール、アミノヒドロキシ酪酸の錯体と認められる「Ｃａｂｏｒｉｌ　Ｃｏｍｐｌｅｘ」が記載されている（第１６１０頁第２欄）。

そして、Ｃｏｍｐｌｅｘ（錯体）は、広義には、共結晶の一種とみなせる。（「錯体」については、以下に引用する文献においても同様である。）。

引用文献４には、結晶性粉末であって、水素結合を有する分子錯化合物の形でほぼ等モル比のフェナゾンとパラセタモールを含んでいる、フェナゾン・パラセタモール（アセトアミノフェン）錯化合物が記載されている（第１頁左欄第２－９行）。

引用文献５には、メベンダゾールとプロピオン酸（１：１）の分子錯体が記載されており、分子間で水素結合が生じることも記載されている（第１１頁要約部、第１３頁Fig. 2等）。

引用文献６には、５－クロロサリチル酸とテオフィリン（１：１）の錯体が記載されており、分子間で水素結合が生じることも記載されている（第７１０頁Abstract等）。

引用文献７には、テオフィリンとｐ－ニトロアニリン（１：１）の分子錯体が記載されており、結晶構造中で水素結合が生じることも記載されている（第２３９０頁からのAbstract、第２３９１頁Fig. 2等）。

UM00016671
NOVARTIS EXHIBIT 1517
Novartis v. Regents, IPR2023-01347
Page 3653 of 4460

引用文献８には、テオフィリンとｐ－ニトロフェノール（１：１）の錯体が記載されており、分子間で水素結合が生じることも記載されている（第２３３３頁からのAbstract等）。

引用文献９には、一水和物としてのテオフィリンと５－フルオロウラシル（２：１）の分子錯体が記載されており、分子間で水素結合が生じることも記載されている（第１８５７頁Abstract、同頁右欄第９－１２行等）。

よって、本願請求項１－１９，２１，２３，２４に係る発明は、引用文献１－９のいずれかに記載された発明であるか、少なくとも引用文献１－９のいずれかから当業者が容易になし得たものである。

［D］
・請求項　　１－２４
・理由　　３
・引用文献等　１－１１
・備考

引用文献１－９に記載のように、様々な化合物について、共結晶を製造することは、本願優先日前から行われていたことである。

そして、引用文献１０，１１に記載のように、π電子系を有する化合物や水素結合を形成する基を有する化合物を共結晶とした場合、水素結合やπ－π相互作用等の分子間相互作用が生じることも本願優先日前から知られていたことである（引用文献１０：Figure 1-4、第９８３３頁Figureの下第２－５行；引用文献１１：第５９８７頁要約部、第５９８９頁Table 1、Figure 1-11等）。

してみれば、２種以上の化合物から構成される共結晶を製造し、得られた共結晶について、生じる分子間相互作用を確認することは、当業者にとり格別困難なことではない。

［E］
・請求項　　１１
・理由　　５

（１）請求項１１の括弧書きを使用した記載は、発明の範囲を不明確にするものである。

（２）請求項９，２２の「プロフェン」は、一般的に使用されている化学物質名ではなく、いかなる化学物質を示すのか明確でない。
（「イブプロフェン」又は「フルルビプロフェン」のことか？）

UM00016672
NOVARTIS EXHIBIT 1517
Novartis v. Regents, IPR2023-01347
Page 3654 of 4460

(*)　補正をするときは、新規事項の追加とならないよう留意されたい。
　またその際、補正の根拠となる明細書又は図面中の該当記載箇所について、意見書中で明示されることが望ましい。

引 用 文 献 等 一 覧

１．H. Wunderlich et al., Pharmazie, １９９１年, Vol. 46, No. 7, p. 507-509
２．S.A. EL-NAHHAS, Pharmazie, １９９６年, Vol. 51, No. 12, p. 960-963
３．JAMES E.F. REYNOLDS, Martindale. The extra pharmacopeia, THE PHARMACEUTICAL PRESS, １９９３年, p. 1610
４.特公昭４６－３３５８８号公報
５．Mino R. Caira et al., Journal of Chemical Crystallography, １９９８年, Vol. 28, No. 1, p. 11-15
６．Eli Shefter, Journal of Pharmaceutical Sciences, １９６９年, Vol. 58, No. 6, p. 710-714
７．Shyuichi Zaitu et al., Acta Crystallographica Section C, １９９５年, Vol. 51, p. 2390-2392
８．Katsuyuki Aoki et al., Acta Crystallographica Section B, １９７８年, Vol. 34, p. 2333-2336
９．Shyuichi Zaitu et al., Acta Crystallographica Section C, １９９５年, Vol. 51, p. 1857-1859
１０．V.R. Pedireddi et al., Tetrahedron Letters, １９９８年, Vol. 39, p. 9831-9834
１１．Md. Badruz Zaman et al., Journal of Organic Chemistry, ２００１年, Vol. 66, p. 5987-5995
（注）法律又は契約等の制限により、提示した非特許文献の一部又は全てが送付されない場合があります。

先行技術文献調査結果の記録

・調査した分野　　ＩＰＣ　Ａ６１Ｋ　９／００
　　４７／００
　　３１／００
　　ＤＢ名　CAplus(STN)

この先行技術文献調査結果の記録は拒絶理由を構成するものではありません。

(*)　この拒絶理由通知の内容に関するお問い合わせ、または面接のご希望がございましたら下記までご連絡下さい。

特許審査第三部　医療　　三輪　繁
ＴＥＬ．０３（３５８１）１１０１　内線３４５１
ＦＡＸ．０３（３５８１）１３４２

DOI: 10.1002/chem.200901314

Co-crystals with Acetylene: Small Is not Simple!

Michael T. Kirchner, Dieter Bläser, and Roland Boese*[a]

Dedicated to Yitzhak Apeloig on occasion of his 65th birthday

Abstract: Acetylene is an amazingly versatile component for the formation of co-crystals. It requires careful handling and special techniques for crystallisation, but the efforts seem to be rewarding when attaining co-crystals with small molecules as partners. Many basic questions such as the dominance of specific heterogeneous intermolecular interactions, their driving force for the formation of multicomponent crystals instead of neat ones are expected to be easily analysed. The underlying packing patterns and resulting stoichiometries based on the known supramolecular synthons seem to be straightforward for such small molecules and crystal engineering, considered as the prototype of supramolecular synthesis, should be a simple task. Nineteen co-crystals with acetylene are presented in this paper, some of which have been previously reported individually. An attempt has been made to find features shared by the groups of co-crystals, including those that could not be co-crystallised. But in spite of clear ideas and experiences from previous experiments, surprisingly almost none of systems reached our expectations. Our intuitive approach was not fulfilled, which demonstrates that multicomponent crystals even of small molecules will remain a great challenge for theoretical methods and the crystal structures shown herein represent good candidates for future testing. On the other hand, we wish to encourage other groups to present their views on the crystal structures with an unbiased approach that may offer a better explanation than we are able to outline in this article.

Keywords: acetylene · aggregation · crystal packing · molecular interactions · X-ray diffraction

Introduction

Organic chemical synthesis in the last century was successful in designing methods for the production of nearly any small organic molecule needed by mankind. This is especially evident in the field of pharmaceutics, but also true of many small compounds with hidden chemical applications in everyday life. The resolution of a difficult task often results in an even more difficult task. Nowadays it is expected that new materials are either all-rounders or have additional functionalities. Functionality implies differentiation, which can lead to multicomponent supermolecules that self-organise. In terms of synthesis, this emphasises weaker intermolecular interactions with binding energies of 5–20 kJ mol^{-1}, which are weak enough to be formed and broken as needed but strong enough, in concert and if designed well, to maintain aggregation of the aggregate. This vision is, of course, inspired by Nature's biochemical examples. Even the key properties of simpler materials are governed by weak intermolecular forces. The study and classification of intermolecular forces as well as their use for assembling molecular aggregates is a new, developing field of research.

Co-crystals are a first step in such multicomponent supramolecular aggregates. They may also be seen as model compounds that are easier to prepare and analyse. The crystallisation of a co-crystal of defined stoichiometry represents a prototype of supramolecular synthesis.[1] In contrast to molecular synthesis, there is no breaking or forming of covalent bonds, everything relies on weak interactions only. To produce multicomponent solids by co-crystallisation might seem anti-intuitive at first because crystallisation is often employed for purification. Therefore the formation of a co-crystal from a mixture of organic materials is rare, even though mixed crystals and solvates are commonplace in inorganic chemistry and mineralogy. This new synthetic approach is still not well understood in terms of strategy or systematic development but it is gaining interest in several industrially important areas.

Pharmaceutical co-crystals are prominent among these areas. In the last decade the development of new active in-

[a] Dr. M. T. Kirchner, D. Bläser, Prof. Dr. R. Boese
Institut für anorganische Chemie, Universität Duisburg Essen
Universitätsstrasse 5, 45117 Essen (Germany)
Fax: (+49) 2011832535
E-mail: roland.boese@uni-due.de

 © 2009 Wiley-VCH Verlag GmbH & Co. KGaA, Weinheim InterScience

These are not the final page numbers! ↗↗

UM00016675
NOVARTIS EXHIBIT 1517
Novartis v. Regents, IPR2023-01347
Page 3657 of 4460

gredients takes increasingly more time and is shifting towards biochemical methods. The slow down in development is partly due to increasing costs within the development itself, but also a result of the testing, marketing and legal procedures, especially the settlement of patent claims in the USA. On this basis, it is not surprising that a substantial amount of pharmaceutical research is devoted to the modification of known active ingredients, including the modification by co-crystallisation.

By co-crystallisation, different molecules with different functionalities or functional groups can be brought together relatively easily compared with the effort of designing a covalently bound molecule with both functions combined. The partners are free to self-organise into an optimal intermolecular arrangement to yield a co-crystal. This might take the form of a molecular complex with ordered molecules in a fixed stoichiometric ratio or a host–guest complex in which the guest fits into the cavities of a host network: it is often disordered and has only partial occupancy.[2] Whereas the mixing of compounds is usually favoured by entropy, the formation of a co-crystal still depends on it being thermodynamically stable relative to the crystals of the neat compounds but it may also be kinetically preferred. As mentioned above, crystallisation from mixtures may be used for purification under which circumstances a co-crystal is not the desired result.

The product of a successful co-crystallisation can be analysed by X-ray diffraction, preferably by single-crystal diffraction if a crystal of appropriate dimensions and quality can be grown. Thus, a three-dimensional structure of the molecules and their relative positions would be available and be the result of all the intermolecular forces acting at the time of crystallisation. To separate the effects of all such forces it has been suggested to select small molecules, which have a lower number of permutations amongst all the possible interactions. This is also attractive in theoretical chemistry in which a smaller number of atoms in a calculation leads to significantly better results at the same time. Co-crystals of small molecules may therefore be considered as model compounds for the study of intermolecular interactions. Unfortunately, small molecules have low melting points and can even be gases under ambient conditions and therefore they must be crystallised at low temperatures or increased pressures. This necessitates special experimental instrumentation and methods as will be outlined below.

The analysis of the packing of a co-crystal is governed by two complementary questions. First, the specialities and geometrical details of the interactions in the co-crystal have to be evaluated. Can those intermolecular interactions that predominantly influence the packing be identified? For this it is important to compare structures with similar functional groups and similar interactions to find patterns and rank their relative robustness. This can be done by studying homologous series of compounds.[3] Highly robust patterns of intermolecular interactions are termed synthons, which suggests their usefulness in supramolecular synthesis.[4] Secondly, the detected principles can be generalised with the aim of predicting the packing of so far unknown co-crystals. Theoretical methods are being developed to help in the prediction and multicomponent systems will be the next great challenge.

For a better understanding of co-crystal formation we decided to use small molecules that only have a few functionalities. Our strategy focused on the combination of a Lewis acid and a Lewis base, which results in the formation of a hydrogen bridge. Although hydrogen bridges are weak in comparison with covalent or ionic bonds, they themselves are divided into strong, medium strong and weak hydrogen bridges.[5] The weak bridges are all bonds from a hydrogen atom attached to a carbon atom with the acceptor usually an oxygen, nitrogen or halogen atom. The chemical bond has so many meanings for chemists that the term hydrogen bond might be misinterpreted whereas the term hydrogen bridge is free of prejudices and is "perhaps a better descriptor", as expressed by Desiraju.[5b]

An ideal co-crystal component with a minimum of functional groups should form co-crystals with a large number of partner molecules. These partner molecules should be small and sparse in their functionality. One of the most versatile molecules in respect of weak intermolecular interactions is probably acetylene. Acetylene is an ellipsoidal molecule rather than rod-shaped, the long axis is 5.5 Å. As a C–H donor it is bifunctional and simultaneously it can act as a π acceptor. This enables acetylene to form networks. The hydrogen bridges from acetylene are expected to be close to linear, however, the flat energy profile allows for a high variation of the C–H···A angle, which increases the flexibility of the networks. Suitable compounds for co-crystallisation with acetylene should show good acceptor abilities and ideally have more acceptors than donors and/or only weaker C–H donor functionalities.

Acetylene: Owing to the carbon≡carbon triple bond and the high positive energy of formation, acetylene is an unstable, highly reactive unsaturated hydrocarbon.[6] The C≡C triple bond and C–H bond lengths are 1.176 and 1.025 Å, respectively.[7]

Under normal conditions acetylene is a colourless, nontoxic and narcotic gas; it is slightly lighter than air. The critical temperature and pressure are 308.32 K and 6.139 MPa. The triple point at 128.3 kPa is 192.4 K. The formation of acetylene is strongly endothermic ($\Delta H_f = +227.5$ kJ mol^{-1} at 298.15 K).

Self-decomposition can be initiated when certain pressure limits above atmospheric pressure are exceeded. Solid acetylene is not critical with regard to decomposition provided it is the only material involved. The crystalline structure of solid acetylene changes at −140.15 °C from a cubic to an orthorhombic phase. The solubility coefficients of acetylene in organic solvents are listed in Table 1.[8] Acetylene is well-suited to co-crystallisation studies because it dissolves well in various organic solvents, which indicates its versatility in intermolecular interactions.

 © 2009 Wiley-VCH Verlag GmbH & Co. KGaA, Weinheim

These are not the final page numbers!

UM00016676
NOVARTIS EXHIBIT 1517
Novartis v. Regents, IPR2023-01347
Page 3658 of 4460

Table 1. Solubility coefficients of C_2H_2 in various solvents.[8]

Solvent	C_2H_2 pressure [bar]	Solubility coefficient [mol kg^{-1} bar^{-1}]	
		20 °C	25 °C
methanol	0.98	1.979	0.569
ethanol	0.98	0.851	0.318
n-hexane	6.90	0.523	0.264
benzene	0.98		0.225
toluene	0.98	0.619	0.214
xylene (tech.)	0.98	0.528	0.189
triethyleneglycol	0.98		0.205
acetone	0.98	4.231	1.069
N-methyl-2-pyrrolidone	0.98	5.687	1.319
N,*N*-dimethylformamide	0.98	5.096	1.501
dimethyl sulfoxide	0.98		1.001
ammonia	0.98	7.052	2.229

Acetylene is used in several processes in chemical engineering and as a welding gas. Because of its tendency to easily deflagrate or to detonate under pressure, acetylene cannot be compressed and stored in gas cylinders like most other gases. To desensitise the gas, acetylene stored in gas cylinders is dissolved in a solvent in which the acetylene is very soluble. This solvent is mostly dispersed in a porous solid that fills the gas cylinder completely. The porous material in the cylinder arrests any local acetylene decomposition when induced, for instance, by flashback. Acetone and dimethylformamide are the preferred solvents for acetylene in cylinders. Owing to the difficulty in the preparation of co-crystals formed by acetylene and these solvents, any study of the underlying interactions were prevented until recently, when the difficulties were overcome by in situ cryocrystallisation techniques.

An overview: Before the results are discussed a generalised experimental method for the preparation of acetylene co-crystals is given and the special difficulties of their growth are discussed. The results (Scheme 1) are arranged not according to their chemical classification but by the similarities of the coordination sphere of the acceptor, starting from a tetrahedral sphere, through distorted octahedral and trigonal-bipyramidal spheres, to an aromatic linear arrangement. This one-by-one presentation of results is interrupted by ad hoc discussions of special features common to a sub-group and exemplified by the structure at hand. The ratio of acetylene-to-acceptor molecules and the distinction of molecular complexes and clathrates are discussed with the example of DMSO. The importance of comparisons with the packing of the neat components is discussed in the section on dioxane. The lengths of the acetylene hydrogen bridges are given in the acetonitrile section. A comparison with the structures of bromine is discussed in the section on methanol. The importance of polymorphism is discussed with the structures of acetone, which was found to be polymorphic. Five of the structures are clathrates, which are discussed in the text when chemically appropriate and in the context of the clathrate of hexafluorobenzene. The discussion is completed by a list of compounds that did not lead to co-crystals.

General experimental procedure: Acetylene is a gas at ambient pressure and temperature and condenses at 189 K. Direct co-crystallisation at ambient pressure therefore is not possible.

To trap the corresponding solutions and to grow single crystals of the complexes, acetylene was condensed at −196 °C in a vacuum line into a quartz capillary (0.3 mm diameter) already filled with the second component, flame-sealed and transferred to the diffractometer, a Bruker Smart1000 CCD-System with an XSTREAM LT device (MSC). The latter provides a very stable cold stream of gas along the omega axis. The goniometer head was equipped with an additional arc and an *x*,*y*,*z* slide, which allows alignment of the capillary along the omega axis. This is used as the scanning axis for data collection with a fixed or at least highly constrained ϕ angle, as provided by the Siemens SMART three-axis platform. The capillary, which withstands pressures of up to about 100 bar, was then cooled to −155 °C and a crystal was grown by our in situ crystallisation technique, that is, by moving an intensity controlled, focused infrared laser beam along the capillary (OHCD).[9] The diffusion processes at the gas/liquid/solid interfaces do not lead to the formation of one single crystal that fills the entire capillary as we usually achieve for neat compounds. Multiple heating/cooling cycles of the acetylene system usually produce several crystals in the same area. They are so close to

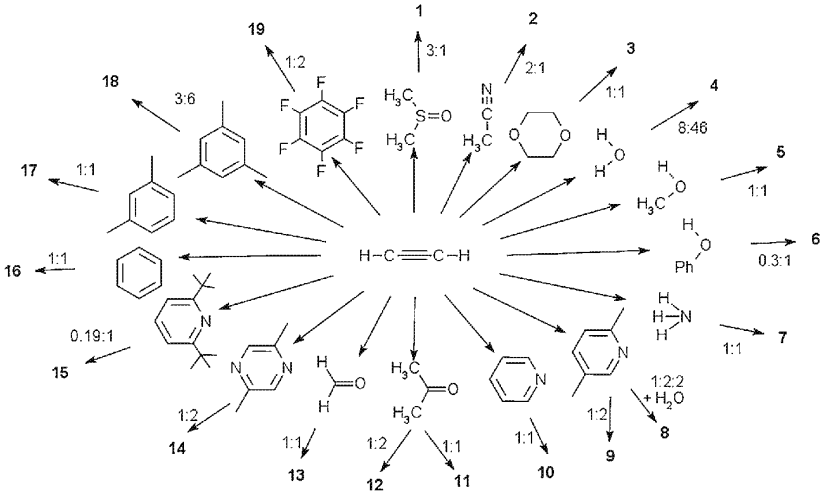

Scheme 1. Overview of the co-crystals formed with acetylene.

© 2009 Wiley-VCH Verlag GmbH & Co. KGaA, Weinheim

UM00016677
NOVARTIS EXHIBIT 1517
Novartis v. Regents, IPR2023-01347
Page 3659 of 4460

each other that all of them diffract simultaneously in the primary X-ray beam. Consequently, the collected data correspond to a superposition of diffraction patterns of several crystals. In a laborious hand-selection and systematic separation procedure utilising the RLATT program in the Bruker-AXS software, we then extracted consistent data sets and indexed, integrated and merged them to refinement. The ease with which this is possible has increased considerably in recent years since we started this procedure with acetylene. Programs like cell_now, twinabs and the twin-handling algorithms in SAINT of the Bruker-AXS suite allow for easy processing of non-merohedral twins. We feel that the procedure we coined "oligo-diffractometry" in 2003 has now evolved into a mature form between single crystal and powder work.[10]

Results and Discussion

Tetrahedral

Dimethyl sulfoxide: The molecular complex **1** of acetylene with dimethyl sulfoxide (DMSO) is a good example of the versatility of acetylene co-crystals.[10] In the crystal the molar ratio of acetylene to DMSO is 2:1. This should not be confused with the three different molecules in the unit cell as two acetylene molecules are placed at a centre of symmetry. The first molecule of acetylene links the DMSO molecules in a zigzag chain, with one short, nearly linear and one longer, side-on C–H···O hydrogen bridge (Figure 1). This zigzag chain is comparable to the zigzag chain in the β-form of the co-crystal with acetone.

The second acetylene molecule forms a two-dimensional network by cross-linking of the chains with two side-on C–H···O hydrogen bridges. This pseudo-hexagonal two-dimensional network of triple acetylene-bridged DMSO oxygen atoms is heavily corrugated. So even when neighbouring layers interlock, they still leave cavities for a third molecule of acetylene that does not participate in C–H···O hydrogen-bridging (C–H···O, $d=5.006$ Å) but is clathrated into the packing (Figure 2). The shortest intermolecular distances are to the other acetylene molecules (C–H···π, $d=2.871$ and 2.877 Å), but the are still above the sum of the van der Waals radii.

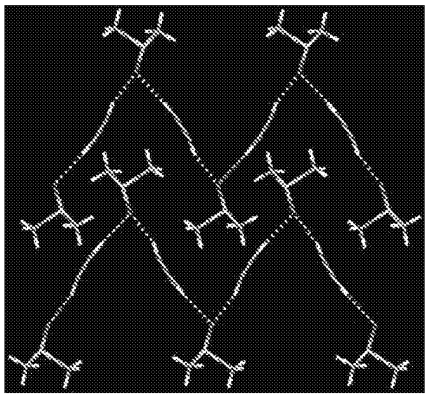

Figure 1. Part of the packing of the 2:1 acetylene/dimethyl sulfoxide co-crystal (**1**). The interaction of the first acetylene is characterised by a zigzag chain (C–H···O, $d=2.085$ Å, $D=3.135$ Å, $\theta=162°$; S=O···C, $\theta=165°$; C–H···O, $d=2.174$ Å, $D=3.252$ Å, $\theta=173°$; S=O···C, $\theta=123°$).

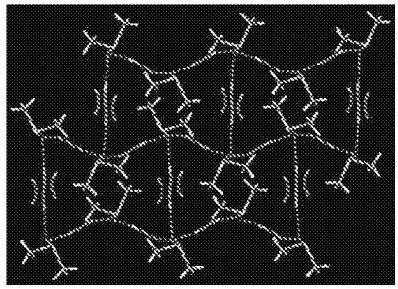

Figure 2. Packing of the 2:1 acetylene/dimethyl sulfoxide co-crystal (**1**). The second acetylene (central vertical) forms cross-links with the zigzag chains (three, horizontal) into a 2D net (C–H···O, $d=2.135$ Å, $D=3.179$ Å, $\theta=161°$; S=O···C, $\theta=120°$). A third molecule of acetylene (left and right vertical) is not incorporated into the network but fills a void.

The molecular complex with DMSO (**1**) examples the ambivalent character inherent in interactions of acetylene. Acetylene is a hydrogen-bridge donor, albeit a weak one. When acceptors are available, it will try to form two interactions. Although this is energetically favourable, it puts geometrical strain on the packing as acetylene is a slim molecule and something has to occupy the space along its side. The situation worsens when more than one acetylene molecule per acceptor must be accommodated. Intermolecular interactions with acetylene generate hollows and produce a need for bumps, otherwise the packing density and subsequently the lattice energy decrease. With DMSO half a molecule of acetylene is clathrated into the hollow that is formed by three molecules forming three hydrogen bridges to the DMSO oxygen atom.

This demonstrates that acetylene is versatile in its interactions. The geometry of the hydrogen bridge is equally variable in the angle to the triple bond (157–178°) and the hydrogen-to-acceptor distance (2.085–2.482 Å). Both sides of the acetylene molecule can be active. Within the structures observed an acetylene molecule can be employed in two, one or no hydrogen bridge. If more than one molecule of acetylene is present, each may be in a different arrangement. If more than one molecule of acetylene binds to a single acceptor molecule, the geometries of the interactions tend to be different. DMSO binds three molecules of acetylene, the highest number of acetylene molecules we found to be bound to a single acceptor atom. There are two acetylene molecules bound to the acceptor atom in the molecular complexes with pyridine and acetone (β-form). In the molecular complexes with ammonia, acetonitrile and formaldehyde the two binding acetylenes are symmetry equivalent.

© 2009 Wiley-VCH Verlag GmbH & Co. KGaA, Weinheim

These are not the final page numbers!

UM00016678
NOVARTIS EXHIBIT 1517
Novartis v. Regents, IPR2023-01347
Page 3660 of 4460

Furthermore, if other donors are present they may compete with acetylene for acceptor atoms. When classifying our results the role of the acetylene molecule as a hydrogen-bridge donor is therefore less relevant and we concentrated on the acceptor and the number and geometrical arrangement of its (inter- and intramolecular) bonding contacts.

The oxygen atom of DMSO in the molecular complex **1** has four contacts: the sulfur is covalently bonded and three acetylene molecules bind intermolecularly. The four contacts adopt an arrangement that is closest to tetrahedral. A coordination number of four and a similar tetrahedral geometry are found in molecular complexes with acetonitrile (**2**), dioxane (**3**), methanol (**5**), ammonia (**7**) and a hydrate of 2,5-dimethylpyridine (**8**).

If there are five contacts, especially in a planar structure with three in-plane contacts and one each above and below the plane, the coordination geometry is trigonal-bipyramidal, as in the molecular complexes formed with formaldehyde (**13**) and 2,5-dimethylpyrazine (**14**).

2,5-Dimethylpyridine (**9**), pyridine (**10**) and acetone (**11**/**12**) form molecular complexes with six contacts to the acceptor leading to a distorted octahedral geometry.

The aromatic π system is special in its acceptor abilities as it usually will accept one hydrogen-bridge donor on each side to form a linear aromatic arrangement.

A final option for the packing of acetylene with other small molecules, especially if no acceptors are available for acetylene, is a clathrate. In the molecular complex with DMSO, the enclathration of one molecule of acetylene is a consequence of the packing of the other two molecules. With water, phenol, 2,6-di-*tert*-butylpyridine and hexafluorobenzene, clathrates are also formed.

Acetonitrile: In the molecular complex with acetonitrile the molar ratio of acetylene to acetonitrile (**2**) is 2:1. The three molecules form a finite aggregate through two hydrogen bridges from the acetylene to the nitrogen atom of the acetonitrile ($d=2.443$ Å). The C-N···C angle is 120.6°.

The aggregates are linked by aliphatic sp^3-C–H···N ($d=2.703$ Å, $D=3.519$ Å, $\theta=132°$) hydrogen bridges. Therefore the nitrogen atom has four contacts (one covalent, two acetylenes and one methyl) in a distorted tetrahedral arrangement (Figure 3). The situation is comparable to the oxygen atom in the molecular complex formed with DMSO (**1**).

The second acetylene hydrogen atoms do not bind to any acceptor. This is not a unique observation and can be seen in the molecular complexes formed with methanol (**5**) and xylene (**17**). As a consequence the network dimension is generally not predictable. The interactions with acetonitrile (**2**), methanol (**5**) and *m*-xylene (**17**) all have a comparably long C–H···X hydrogen bridge (2.376, 2.412 and 2.443 Å, respectively).

The distribution of C–H···X distances is bimodal and it varies between 2.258 and 2.363 Å (Figure 4). The molecular complexes with only half-active acetylenes belong to the group with the longest distances. This group also includes ammonia (**7**; 2.363 Å), 2,5-dimethylpyridine hydrate (**8**; 2.375 Å), pyridine (**10**; 2.464 and 2.482 Å) and β-acetone (**11**; 2.379 Å). As a longer distance usually means a weaker interaction, these co-crystals must compensate for this either by other especially strong interactions or an overall dense packing. Although this might be argued for the other co-crystals, it is not immediately clear for the co-crystal with acetonitrile.

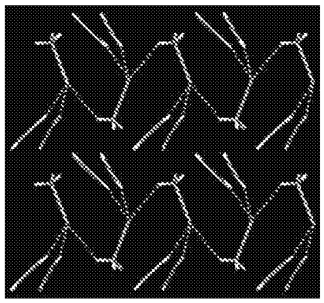

Figure 3. Co-crystal of acetylene with acetonitrile (**2**) (C–H···N, $d=2.443$ Å, $D=3.490$ Å, $\theta=162°$).

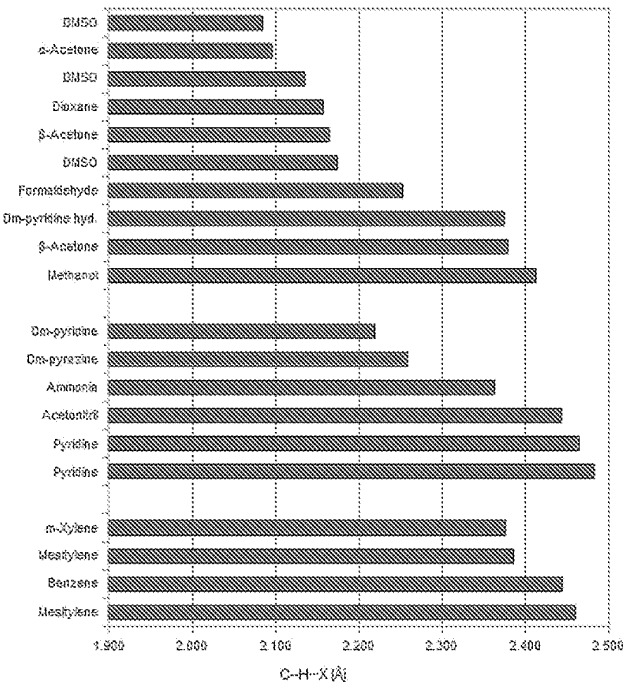

Figure 4. Intermolecular C–H···X hydrogen bridge lengths to oxygen and nitrogen atoms and π acceptors. The distribution for oxygen- and nitrogen-atom acceptors is bimodal with a distinct increase in bridge distances beginning with dimethylpyridine hydrate and ammonia.

The shorter and probably stronger hydrogen bridges are found in the molecular complexes with DMSO (**1**; 2.085, 2.135 and 2.174 Å), dioxane (**3**; 2.157 Å), 2,5-dimethylpyridine (**9**; 2.219 Å), β-acetone (**11**; 2.164 Å), α-acetone (**12**; 2.096 Å), formaldehyde (**13**; 2.253 Å) and 2,5-dimethylpyrazine (**14**; 2.258 Å).

© 2009 Wiley-VCH Verlag GmbH & Co. KGaA, Weinheim

UM00016679
NOVARTIS EXHIBIT 1517
Novartis v. Regents, IPR2023-01347
Page 3661 of 4460

Dioxane: Acetylene and dioxane (**3**) form a 1:1 linear chain (Figure 5).[11] The C–H···O hydrogen bridge is tilted 20° out of the C–O–C plane and 8° out of the plane of bisection of the molecule. The dioxane molecules are stacked in columns. Very weak hydrogen bridges are formed between the oxygen atoms and the methylene hydrogen atoms in the next molecules in the column. In total, the oxygen atoms have four contacts (two intramolecular, one acetylene and one methylene hydrogen) in a distorted tetrahedral geometry.

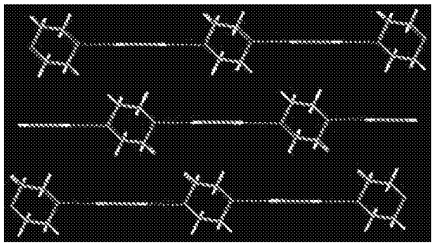

Figure 5. Linear chains of dioxane and acetylene molecules **3** linked by C–H···O ($d = 2.160$ Å, $D = 3.240$ Å, $\theta = 179°$).

The similarities with the packing in neat dioxane are clear; columns are also formed and the layer arrangement is similar. This similarity in the structural motifs between the neat compound and the molecular complex with acetylene is found in several molecular complexes, for example, in methanol (**5**) the O–H···O chains and their stacking in layers, in 2,5-dimethylpyridine (**9**) the C–H···N hydrogen bridge from the *para*-hydrogen atom, in acetone (**12**) the *anti* arrangements of CO dipoles and the sidewise C–H···O bridge from the methyl group.

From the viewpoint of crystal engineering and co-crystallisation there is a fundamental conclusion: the packing motifs of the neat component can be maintained even in co-crystals in which rather strong interactions are present. Of course this is not a general principle: in those cases in which the strong acceptor is blocked by acetylene the previous donors have to find new acceptors, as in pyridine (**10**), or otherwise stay inactive.

Water (clathrate hydrate): The smallest molecule with an oxygen atom as acceptor is water. In hexagonal ice each water molecule acts as hydrogen-bridge acceptor and a donor, which results in a tetrahedral environment of hydrogen bridges around the oxygen atoms. This leads to the rather loose packing of ice in the hexagonal tridymite lattice with unoccupied cavities of 1.5–2.8 Å diameter, low density, and other properties that make the water/ice system "so nice to live in".

These features facilitate the formation of cages in the presence of small guest molecules and results in the encapsulation of the guest.[2] All cages are built of nearly planar, hydrogen-bridged four-, five- and six-membered rings with O···O distances between 2.725 and 2.791 Å. The cages are linked within the host framework by the sharing of common faces.

The structures of the hydrates depend on the size of the guest molecules so that the regular cages will only accommodate molecules up to a maximum size. On the other hand, if not enough guests of the appropriate size are present, the cage structure becomes unstable and hexagonal ice will form. In short, water will form a solid through good interactions (ice) or good space-filling (clathrate hydrate).

Three main structural types of clathrate hydrates have been characterised in their single crystals by using neutron or X-ray diffraction techniques: structure I, $6X{\cdot}2Y{\cdot}46H_2O$, structure II, $8X{\cdot}16Y{\cdot}136H_2O$, and the hexagonal structure H, $1X{\cdot}3Y{\cdot}2Z{\cdot}34H_2O$, in which X, Y and Z represent the different types of cages in the clathrate hydrates.[2] The cages are filled with guest molecules that stabilise the host network.

Structure I is formed when water is co-condensed with acetylene ($Pm\bar{3}n$ space group, $a = 11.877(3)$ Å at 123(2) K).[2] Dodecahedral cages are formed by the oxygen atoms (Figure 6) and adopt a nearly body-centred arrangement with the central dodecahedron turned by 90°. The surrounding tetrakaidecahedra form columns along their hexagonal faces arranged vertically, horizontally and out of the plane.

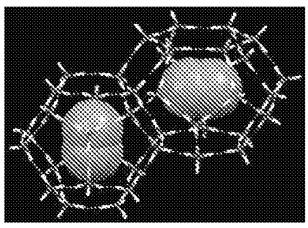

Figure 6. A tetrakaidecahedron and a dodecahedron in structure I clathrate hydrate with acetylene **4** as guest. Each water molecule is disordered; the disorder of the acetylene molecules is not shown.

The low occupation factor 0.6(1) in the dodecahedral cage corresponds to the fact that molecules that are too large to fit easily within the cage will have a lower stoichiometry. The tetrakaidekahedral cage is fully occupied with acetylene.

In the clathrate hydrate with water acetylene is not involved in a hydrogen bridge. Water is the stronger donor and acceptor. Furthermore the number of donors and acceptors match, so the participation of acetylene is not needed. A co-crystal is only formed as a clathrate as the packing density of the O–H···H network is optimised with the enclathration of small molecules. As the same clathrates are also formed with other molecules of gas any special donor abilities of acetylene are not relevant.

We can distinguish between clathrates, in which there is no special interaction between acetylene and the strong host network, intercalates, in which there is a (weak) interaction

© 2009 Wiley-VCH Verlag GmbH & Co. KGaA, Weinheim

These are not the final page numbers!

UM00016680
NOVARTIS EXHIBIT 1517
Novartis v. Regents, IPR2023-01347
Page 3662 of 4460

to a strong network, and molecular complexes, in which acetylene is incorporated into a network of interactions with its partner. All these are co-crystals.

Methanol: If methanol is thought to be derived from water by substitution of one hydrogen atom by a methyl group, the matching of donor and acceptor numbers in water is broken. Methanol may still accept two hydrogen bridges but has only one hydrogen atom to form a hydrogen bridge to another molecule of methanol. In the (disordered) β-form of methanol the O–H···O chain is formed.[12] Co-crystallised **5** with acetylene, methanol also forms chains in [100] with O–H···O hydrogen bridges (d=1.690 Å, D=2.666 Å, θ=171°).[12] Here the packing motif of the neat compound is retained. The acetylene molecules are intercalated into the otherwise intact methanol β-structure and hydrogen-bridged to the oxygen atoms (d=2.399 Å, D=3.358 Å; θ=147°) side-on to the chain ($\approx$45°). Interestingly, only one acetylene hydrogen atom is used for a hydrogen bridge with methanol in the 1:1 molecular complex (Figure 7). The closest contact of the other hydrogen atom of acetylene is to the π system of another acetylene molecule, but the distance is greater than the sum of the van der Waals radii (d=2.823 Å, D=3.857 Å, θ=160°). In total the oxygen atoms have four contacts (two intramolecular, one acetylene and one intermolecular methanol). The arrangement is distorted tetrahedral.

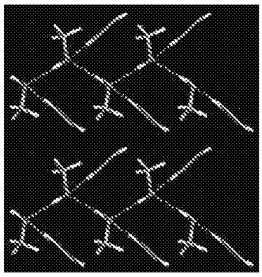

Figure 7. Chain of methanol molecules in the molecular complex with acetylene (**5**) forming a O–H···O chain (d=1.690 Å, D=2.666 Å, θ=171°). Side-on the acetylene is intercalated by weaker C–H···O interactions (d=2.399 Å, D=3.358 Å, θ=147°).

The relationship between the β-phase of methanol and the complex with acetylene is emphasised by a comparison of the cell parameters. The cell axes representing the methanol layer are comparable in length: 4.647/4.565 and 7.220/7.3135 Å. Perpendicular to the methanol layer the distance increases from 6.401 to 13.165 Å to accommodate the acetylene molecules.

The weight ratio of host-to-guest is 1.23 for acetylene/methanol, which is more efficient than in any other co-crystal with acetylene. The co-crystal features both a host network of strong hydrogen bridges enclathrating guests and a molecular complex in which each guest is strongly attached to another molecule.

Methanol and bromine form a similar complex.[13] In the 1:2 molecular complex of methanol with bromine, bromine binds to two molecules of methanol. In this molecular complex the periodicity of the methanol chain is not two (one up, one down) but four (two up, two down), rather similar to the chain of water molecules in the co-crystal of the 1:2:2 acetylene and 2,5-dimethylpyridine hydrate. But although there are some differences in the intermolecular interactions, the similarity of the co-crystals of acetylene and bromine is noteworthy, especially because the nature of the underlying interactions (hydrogen bridge vs. charge transfer) seems to be different. Although the size of both molecules is similar, the similarity in the interactions is supported by the gas-phase measurements of bimolecular complexes formed with Lewis bases. In the crystal structures, even the slight tendency to less linear arrangements of the hydrogen bridge, which was found in gas-phase bimolecular complexes, was reproduced.[14]

Two other molecular complexes of acetylene have counterparts with bromine. The molecular complex of bromine with acetone forms a symmetrical zigzag chain, which in this respect is closer to the co-crystal of acetylene with formaldehyde (**13**). Bromine with dioxane forms a 1:1 chain. The general packing is comparable to the co-crystal formed with acetylene and dioxane (**3**).

Phenol: In methanol an imbalance in the donor-to-acceptor ratio leads to the inclusion of acetylene. This is not necessarily so with all alcohols, as the example of phenol shows.

The co-crystal of acetylene with phenol (**6**) is dominated by a molecular aggregate of 12 molecules of phenol. Six phenol molecules are linked by O–H···O hydrogen bridges (d=1.728/1.729 Å, D=2.702/2.703 Å, θ=170/170°) into a hexagonal ring system. Half of the aromatic systems of these six-membered rings are linked with each other by C–H···π interactions (d_{plane}=2.884 Å) into a "hexagonal prism" (Figure 8). The hexagonal prisms of 12 molecules are arranged in hexagonal close packing. Further C–H···π interactions are found between phenol molecules (d_{plane}=2.866/2.860/2.898 Å).

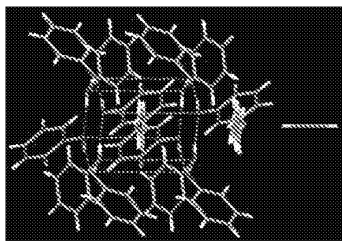

Figure 8. Co-crystal of phenol with acetylene (**6**). Twelve molecules of phenol form a hexagonal prism by O–H···O (d=1.728/1.729 Å, D=2.702/2.703 Å, θ=170°/170°) and C–H···π (d_{plane}=2.884 Å) interactions.

The acetylene molecules are incorporated into two of the cavities of this packing structure of phenol. Within the hex-

 © 2009 Wiley-VCH Verlag GmbH & Co. KGaA, Weinheim

UM00016681
NOVARTIS EXHIBIT 1517
Novartis v. Regents, IPR2023-01347
Page 3663 of 4460

agonal prism one disordered molecule of acetylene (A) is enclathrated. The free diagonal distance between two phenol oxygen atoms is 4.4 Å and too short for the molecule to from a hydrogen bridge. It is therefore stacked flat between the hexagonal ring systems. The second cavity is longer and holds 0.90(2) of an acetylene molecule (B) at both ends, again disordered coplanar to the hexagonal ring system, and 0.77(2) of an acetylene molecule (C) perpendicular to the hexagonal ring systems and the disordered acetylene molecule B. The free cavity distance between two acetylene molecules B is 7.06 Å and too short for two molecules of acetylene, the molecule C is then disordered over two sites forming a C–H···π interaction (d_{plane} = 2.367 Å, D_{plane} = 3.450 Å) to molecule B. The ratio of acetylene to phenol is 2.28:2.

Phenol forms a clathrate with acetylene. The strong enclathrating interactions are the O–H···O hydrogen bridge and the edge-to-face phenyl interaction. Although this leaves oxygen atom acceptor positions open, the cavities in the host framework do not allow for hydrogen bridges from acetylene to phenol.

Ammonia: A change in the donor-to-acceptor ratio is also achieved when adding a third hydrogen atom, as in ammonia. The acceptor position takes the form of a single lone-pair which is especially attractive to hydrogen bridges.

At 143 K ammonia forms a 1:1 zigzag chain with acetylene (**7**) through a C–H···N hydrogen bridge (d = 2.362 Å;[15] Figure 9, top). The molecular ratio of acetylene to ammonia is 1:1. Further N–H···C hydrogen bridges can be identified (d = 2.668/2.819/2.899 Å). The ammonia is disordered over two orientations. In each orientation the lone-pair is pointing towards an acetylene molecule (Figure 9, bottom). If only one of the orientations of disorder is considered, the nitrogen atom adopts a tetrahedral sphere (three intramolecular contacts and one to acetylene).

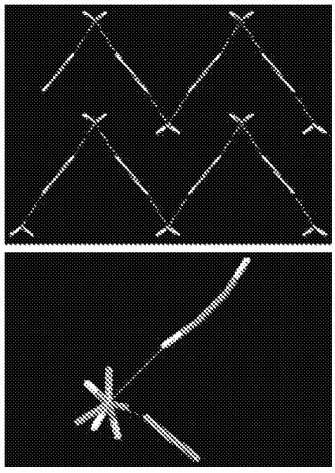

Figure 9. Co-crystal of ammonia with acetylene (**7**). Top: Each ammonia accepts two intermolecular hydrogen bridges and a zigzag chain is formed. Bottom: The ammonia is disordered over two orientations (grey, green). If only one of the orientations of disorder is considered, the tetrahedral sphere of the nitrogen atom is seen.

The 1:1 stoichiometry of the molecular complex is surprising as we expected to find a 2:1 ratio with one hydrogen bridge per lone-pair. The experimental result indicates that the electrostatic component prevails in the interaction. A linear directionality is not necessary for a stable acetylene hydrogen bridge. As other nitrogen-acceptor atoms do only accept one acetylene molecule this means that the dimensionality of the network may not be predicted reliably. Similarly, the dimensionality of oxygen acceptor networks cannot be rationalised before the measurement.

The molecular complex of acetylene with ammonia, $C_2H_2 \cdot NH_3$, is the smallest known organic molecular complex. Although methane with water, $CH_4 \cdot H_2O$, or acetylene with water, $C_2H_2 \cdot H_2O$, would be smaller (or lighter), they form a clathrate hydrate.

2,5-Dimethylpyridine hydrate: 2,5-Dimethylpyridine is hygroscopic and unsurprisingly a 1:2:2 co-crystal dihydrate (**8**) was found even without the purposeful addition of water.[16] The dihydrate **8** in space group $P2_1/c$ has one molecule of acetylene, two molecules of 2,5-dimethylpyridine and two molecules of water in the asymmetric unit. The water molecules form a chain along the O–H···O hydrogen bridges (d = 1.874/1.954 Å, D = 2.827/2.919 Å, θ = 163°/166°) in the [001] direction. 2,5-Dimethylpyridine molecules are attached to this chain through strong O–H···N hydrogen bridges (d = 1.954/1.953 Å, D = 2.931/2.936 Å, θ = 172/177°). This leaves one acceptor site for each water molecule open to accept hydrogen bridges from acetylene. Being bifunctional, one molecule of acetylene connects two chains of water molecules to produce a layer in (010). Owing to the space requirements of 2,5-dimethylpyridine, the chains are separated by 8.243 Å, which is only 0.4 Å less than the sum of the van der Waals radii of the oxygen atoms and the length of the acetylene molecule. It is asymmetrically linked with a shorter and a longer hydrogen bridge (Figure 10).

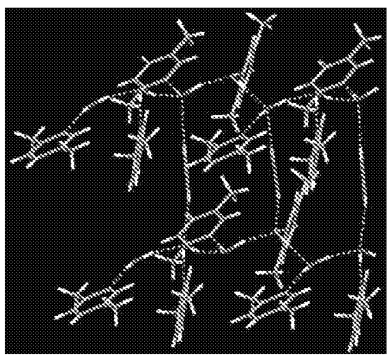

Figure 10. Co-crystal of the dihydrate **8**. Two chains of water molecules with attached molecules of 2,5-dimethylpyridine (O–H···N, d = 1.954/1.953 Å, D = 2.931/2.936 Å, θ = 172/177°) are linked by acetylene molecules (C–H···O, d = 2.375/2.574 Å, D = 3.437/3.656 Å, θ = 167/177°).

© 2009 Wiley-VCH Verlag GmbH & Co. KGaA, Weinheim

These are not the final page numbers!

UM00016682
NOVARTIS EXHIBIT 1517
Novartis v. Regents, IPR2023-01347
Page 3664 of 4460

The oxygen atom in the molecular complex **8** has a tetrahedral sphere of contacts: two intramolecular contacts to its water hydrogen atoms, one intermolecular hydrogen bridge along the water chain and the intermolecular hydrogen bridge from acetylene.

The packing of the dihydrate demonstrates how the equilibrium of hydrogen bridges changes when stronger donors than acetylene are introduced. Acetylene is forced out of its interaction with the strongest acceptor, the nitrogen atom. Its new role depends on the number and character of acceptors added. In this case (adding water) the acceptor-to-donor ratio stays the same and acetylene attaches to the oxygen atom as the second strongest remaining acceptor. This indicates that hydrates of acetylene complexes are possible.

Distorted octahedral

2,5-Dimethylpyridine: If 2,5-dimethylpyridine is crystallised with acetylene but without water the situation of the donors and acceptors changes.[16] The pyridine nitrogen atom is the strongest acceptor, acetylene the strongest donor and they form a hydrogen bridge. No chain is formed but a 1:2 molecular complex (**9**) similar to the 1:2 complex formed with acetone. The hydrogen bridge is not perfectly aligned to the lone-pair, 25° above the plane of the aromatic system and 21° from the molecular axis. The other side of the nitrogen atom is involved in an aromatic C–H···N hydrogen bridge with the aromatic *para*-hydrogen atom. Both the acetylene C–H···N and aromatic C–H···N bridges form a two-dimensional honeycomb network in the (−102) layer (Figure 11).

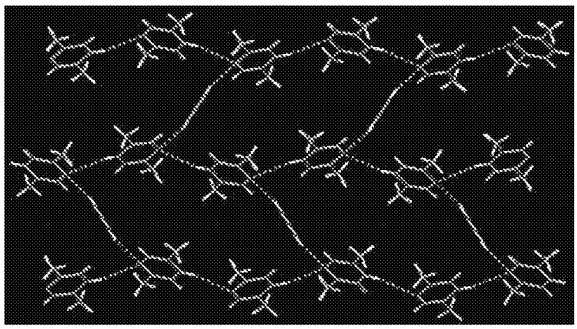

Figure 11. Co-crystal of 2,5-dimethylpyridine and acetylene (**9**) without water. With weak acetylenic C–H···N (d=2.223 Å, D=3.261 Å, θ=160°) and aromatic C–H···N (d=2.693 Å, D=3.671 Å, θ=151°) hydrogen bridges a honeycomb network is formed.

Although the nitrogen atom is the strongest acceptor and its lone-pair accepts two C–H hydrogen bridges, the aromatic system of the pyridine can also accept hydrogen bridges and two weak C–H···N (d=2.877/2.979 Å) links are formed from aliphatic methyl groups to the nitrogen atom in the aromatic system. The nitrogen atom has six contacts (two intramolecular and four intramolecular, one with acetylene C–H, one aromatic C–H and two aliphatic C–H). The coordination geometry is distorted octahedral.

There seems to be a distinction between the interactions of acetylene with a heteroaromatic system and a pure aromatic system. Although the latter often have perpendicular interactions of acetylene to benzene, the nitrogen heteroatom forms one or two interactions to acetylene along the axis of the lone-pair. Acetylene then does not interact further with the aromatic system.

Pyridine: In the high-pressure form of benzene, C–H···π interactions govern the packing in a herringbone arrangement. In neat pyridine, the *ortho*-hydrogen atoms are engaged in C–H···N hydrogen bridges whereas the C–H···π interactions involve *meta*- and *para*-hydrogen atoms that cannot form a herringbone pattern. With the incorporation of acetylene into the co-crystal with pyridine (**10**) the *ortho*-hydrogen atoms are forced out of the C–H···N interaction by the stronger and more versatile acetylene C–H donor so that the heterocycle returns to the herringbone pattern of benzene.[16] In this respect this co-crystal might be compared with the case of methanol in which during intercalation of acetylene the packing is retained. Here, acetylene is intercalated into the packing of benzene with pyridine taking the place of benzene. Also the hydrogen-bridge distances are the longest found in all the molecular complexes with acetylene and there are rather large cavities in the intercalated layer of acetylene.

In the co-crystal of acetylene and pyridine (**10**) one molecule of pyridine is opposed by two half-molecules of acetylene leading to a 1:1 composition. A chain of hydrogen bridges C–H···N (d=2.485/2.467 Å, D=3.440/3.336 Å, θ=147/144°) involving the nitrogen atom of the pyridine and the hydrogen atoms of the acetylene is formed comparable to the chain found in the 1:1 complex of acetone and acetylene (**12**; Figure 12). Here, we find a more side-on interaction (43° out-of-plane) and another more in-plane interaction (−28° out-of-plane).

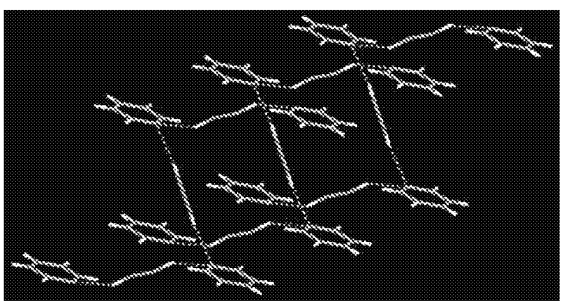

Figure 12. Co-crystal of pyridine with acetylene (**10**) with zigzag chain (C–H···N, d=2.485/2.467 Å, D=3.440/3.336 Å, θ=147°/144°).

The coordination sphere is very much comparable to that of 2,5-dimethylpyridine (**9**). Six contacts (two intramolecular, two intermolecular to acetylene and two intermolecular

 © 2009 Wiley-VCH Verlag GmbH & Co. KGaA, Weinheim

UM00016683
NOVARTIS EXHIBIT 1517
Novartis v. Regents, IPR2023-01347
Page 3665 of 4460

to aromatic C–H in pyridine) resemble a distorted octahedral.

Acetone (1:1): The packing and the interactions of the molecular complexes of acetylene with 2,5-dimethylpyridine (**9**) and pyridine (**10**) are governed by the shape and functionality of the acceptor molecule. They are flat molecules with a dipole. Acetone is similar in both respects. It also forms a (strongly distorted) octahedral sphere of contacts, even though the acceptor is changed from an aromatic nitrogen atom to a double-bonded oxygen. Furthermore, acetone forms two molecular complexes **11** and **12** with different stoichiometries.

In the β-phase (**11**) the ratio of acetylene to acetone is 1:1.[10] The molecules are arranged in a zigzag chain with two hydrogen bridges to the oxygen atom of each acetone molecule (as in the complex with pyridine). One of these hydrogen bridges is nearly linear with respect to the carbonyl group whereas the other occurs side-on (Figure 13).

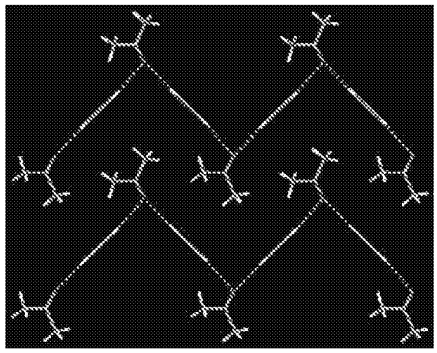

Figure 13. β-Phase of the co-crystal of acetone with acetylene (**11**). The crystal is characterised by a zigzag chain. At the acceptor oxygen atom there is a head-on and a side-on hydrogen bridge (C–H···O, $d=2.164$ Å, $D=3.246$ Å, $\theta=177°$; C=O···C, $\theta=160°$; C–H···O, $d=2.379$ Å, $D=3.431$ Å, $\theta=163°$; C=O···C $\theta=111°$).

The acetone molecule is rather flat and offers a positive polarised carbon atom. A molecule of acetylene is stacked above and below the acetone molecule. On one side the molecules are collinear, the intermolecular C···C distance is short ($D=3.491$ Å). On the other side of the acetone molecule the acetylene is perpendicular lying across the methyl groups and therefore further away from the carbon atom ($D=3.938$ Å).

Another C–H···O hydrogen bridge should be mentioned. It originates from a methyl group ($d=2.629$ Å) and with a second forms a doubly bound circular dimer. This is a packing motif found very often in the packing of neat acetone and in both molecular complexes with acetylene. Although there are other contacts with longer distances these six contacts (one intramolecular, two intermolecular to acetylene C–H, one intermolecular to methyl and two intermolecular to acetylene-π above and below) form a distorted octahedral sphere.

Acetone (1:2): In the α-phase (**12**) the ratio of acetylene to acetone is 1:2 and features a tripart molecular complex with a dumb-bell shape and two almost linear C–H···O hydrogen bridges.[10] The dumb-bells are stacked on one another so that the dipole moments of the acetone molecules are anti-parallel (Figure 14). Basically this anti-parallel arrangement of the linear acetylene–acetone molecular complex can also be seen in the β-form (**11**). There, however, they are not directly on top of each other but somewhat shifted.

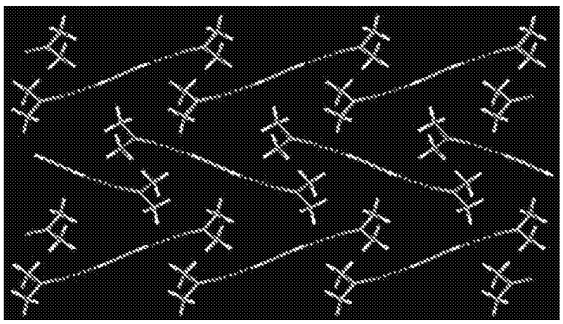

Figure 14. Packing of 1:2 acetylene and acetone α-co-crystal (**12**). The packing is characterised by a 1:2 dumb-bell-shaped molecular complex. (C–H···O, $d=2.096$ Å, $D=3.172$ Å, $\theta=172°$; C=O···C, $\theta=172°$).

Again we find the ring of the methyl C–H···O ($d=2.777$ Å) and a second C–H···O ($d=2.632$ Å) from a methyl group and an acetylene molecule ($D_{CC}=3.986$ Å). These five contacts, together with the intramolecular sixth, form a distorted octahedron.

Polymorphism of co-crystals is important because of its relationship to single-component crystals. This indicates that the phenomenon exists in the co-crystal; the situation of intermolecular interactions is in principle the same. Our result indicates that the phenomenon found in single-component crystals also exists in co-crystals, the situation of intermolecular interactions is in principle the same. Specifically, we may analyse the co-crystals of acetylene as model compounds and conclusions from them may be transferred to all crystalline systems, although with some caution.

The two different stoichiometries of the molecular complex with acetone raises the question of whether different stoichiometries for the other co-crystals may be expected. Furthermore, if there are different stoichiometries, can there also be a clathrate, an intercalate and a molecular complex at the same time? At the moment these questions must remain unanswered. During the preparation of capillaries for co-crystallisation we unintentionally varied the ratio of compounds as our method does not allow for quantitative measurement of the amounts introduced. Often some capillaries would give co-crystals whereas others would not. Sometimes when we obtained co-crystals of a lower quality in one capillary the next would give better quality co-crystals of the same type. In general capillaries with higher amounts of acetylene would grow co-crystals more easily

© 2009 Wiley-VCH Verlag GmbH & Co. KGaA, Weinheim

These are not the final page numbers!

UM00016684
NOVARTIS EXHIBIT 1517
Novartis v. Regents, IPR2023-01347
Page 3666 of 4460

than those with less acetylene. In one case (2,5-dimethylpyrazine) we felt that a different stoichiometry should be possible and tried to vary the content of acetylene, that is, by adding more acetylene, but to no avail.

The molecular complexes formed with acetone do have a practical importance as acetylene for welding is usually shipped in steel cylinders filled with acetone. At 12 bar in the cylinder the molecular ratio is about 2:3. It is quite likely that the motifs discussed here are also found in solution.

Trigonal bipyramidal

Formaldehyde: For acetone the methyl groups are essential for the packing in both the neat compound and in the molecular complexes. Formaldehyde must interact with acetylene without additional methyl C–H···O hydrogen bridges and chooses a far simpler packing system. In fact, the packing of formaldehyde with acetylene is such as would be expected by most experts based on crystal engineering principles. With formaldehyde small is simple!

In the molecular complex with formaldehyde the molar ratio of acetylene to formaldehyde is 1:1, the molecules are positioned with *mm* symmetry for formaldehyde and with $-1m$ symmetry for acetylene. The structure is a straightforward zigzag chain with two equal C=O···C angles ($\theta = 125°$). The molecules of the planar chain are interdigitated. The adjacent planes are stacked with a shift of half a chain width (Figure 15).

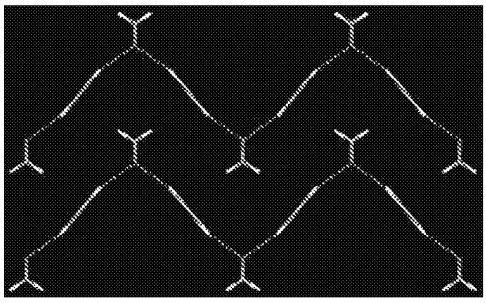

Figure 15. Packing of the 1:1 acetylene and formaldehyde co-crystal (**13**), characterised by a zigzag chain (C–H···O, $d = 2.253$ Å, $D = 3.314$ Å, $\theta = 166°$; C=O···C, $\theta = 129°$). The chains are ordered into layers with an interlayer distance of 2.715 Å.

Each oxygen atom has one intramolecular contact to a carbon atom and two intermolecular contacts to acetylene C–H···O ($d = 2.253$ Å). These form a triangle that is capped above and below by the next molecule of formaldehyde C–H···O ($D_{cc} = 3.379$ Å). The coordination geometry is that of a distorted trigonal-bipyramid.

2,5-Dimethylpyrazine: The only other molecular complex of acetylene that crystallises in planar sheets is the molecular complex with 2,5-dimethylpyrazine (**14**).[16] This molecular complex has a number of features that are special. One of the pyrazine molecules together with the acetylene molecule forms a one-dimensional linear chain along the [$\bar{1}$11] direction (Figure 16). The acetylene molecule is only 1° out of the plane of the aromatic system although it is 10° out of line with the lone-pair forming a C–H···N hydrogen bridge ($d = 2.261$ Å, $D = 3.337$ Å, $\theta = 174°$).

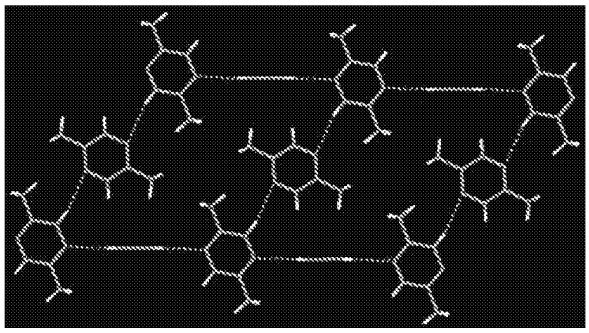

Figure 16. Packing of the co-crystal of 2,5-dimethylpyrazine with acetylene (**14**). The acetylene forms a hydrogen bridge ($d = 2.261$ Å, $D = 3.337$ Å, $\theta = 174°$) to only one of the pyrazine molecules.

The second molecule of dimethylpyrazine does not interact with acetylene. This is the only example in which the acceptor molecules in a co-crystal are simultaneously bound and unbound to acetylene. This is comparable to the situation of the clathrated acetylene in the molecular complex formed with DMSO (**1**).

The molecules are stacked and the molecular planes are tilted by only 7° with a minimum distance of 3.337 Å between them, which indicates a strong π-stacking interaction. The molecules are turned 43° against each other to avoid steric crowding of the methyl substituents and to achieve an optimal arrangement for the quadrupole interactions. An additional hydrogen bridge of the methyl group to the nitrogen atom can be identified in the π-stacked molecule C–H···O ($d = 2.974$ Å).

Similar to formaldehyde, 2,5-dimethylpyrazine forms a planar packing. There are two intramolecular contacts and one intermolecular contact with acetylene, which form a trigonal base. The π system of a pyrazine molecule on one side and a C–H···N hydrogen bridge on the other form the apexes of a trigonal-bipyramid.

2,6-Di-tert-butylpyridine: Neat 2,6-di-*tert*-butylpyridine crystallises in space group $P2_1/c$. There are no hydrogen bridges due to the steric requirement of the *tert*-butyl substituents that shield the acceptor.

We co-crystallised this compound with acetylene in the hope of synthesising a strong molecular complex (**15**). We found space group $P\bar{4}2_1c$ with the nitrogen atom and the *para*-carbon atom located on a two-fold axis and the *para*-hydrogen atom in a position to form a weak hydrogen bridge C–H···N ($d = 2.968$ Å).[16] According to the tetragonal

 © 2009 Wiley-VCH Verlag GmbH & Co. KGaA, Weinheim

UM00016685
NOVARTIS EXHIBIT 1517
Novartis v. Regents, IPR2023-01347
Page 3667 of 4460

symmetry, each chain is surrounded by four others and weak sp^3-C–H···π interactions form the dominant motif.

Surrounded by eight molecules, spherical cavities are formed. Each has a volume of 49 $Å^3$ and a mean diameter of 4.5 Å.[17] Within the cavity residual electron density is found with an almost spherical distribution of 5.3 electrons. Attributing this to acetylene, it equates to 0.38 molecules per cavity or a molecular ratio of 0.19:1 acetylene to 2,6-di-*tert*-butylpyridine. The co-crystal is a clathrate (Figure 17).

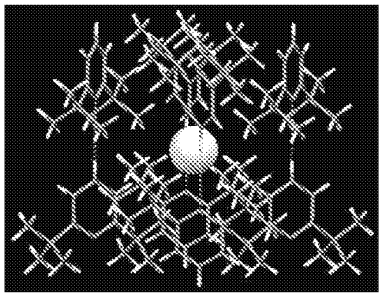

Figure 17. Co-crystal of 2,6-di-*tert*-butylpyridine with acetylene (**15**). The pyridine molecules form chains with weak C–H···N interactions (d = 2.968 Å, D = 4.051 Å, θ = 180°), the position of the disordered acetylene molecule is indicated by the white sphere.

Linear aromatic

Benzene: The following four systems are different from an acceptor point of view. They are pure aromatics and the acceptor is the π system on both sides of the aromatic ring. An additional heteroaromatic acceptor, as in pyridine, pyrazine and their derivatives, is not available. Each side may accept one hydrogen bridge from an acetylene molecule. The variation in this group of co-crystals stems from the competition between acetylene C–H and other aliphatic or aromatic C–H donors rather than different octahedral/tetrahedral geometries or different donor-to-acceptor ratios.

In the co-crystal with benzene (**16**) the molecular ratio is 1:1 and both sides of the benzene ring form a C–H···π interaction with acetylene.[18] The benzene ring lies in a special position with space group $R\bar{3}m$ and D_{3d} point-group symmetry, whereas the acetylene molecule lies on an axis perpendicular to the centre of the benzene plane, also in a special position.

The acetylene molecule reveals an unusually short triple bond. The equally unusual expansion of the C–C bond distance at lower temperature (1.097(10) Å at 201 K and 1.152(4) Å at 123 K) suggests an essentially dynamic disorder in which the acetylene molecule rotates along a double cone between benzene molecules. Assuming 1.20 Å as the "real" triple-bond length, the deviation from the axial position is 24° at 201 K and 15° at 123 K.

The crystal packing is shown in Figure 18. The distance between parallel benzene molecules corresponds to the length of the cell c axis so that, based on the X-ray intramolecular bond distances for the acetylene molecule, the C–H···π bridge (centroid) distance is 2.447 Å at 123 K and 2.462 Å at 201 K (normalised C–H distances applied). The closest intermolecular C···C distances for the benzene molecules are 5.724 Å (123 K) and 5.839 Å (201 K) and the C-(sp^2)···C(sp) contacts are 3.853 Å (123 K) and 3.918 Å (201 K).

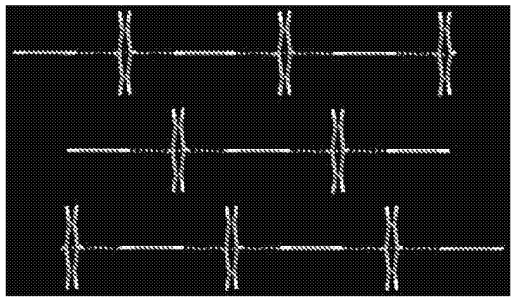

Figure 18. Co-crystal of benzene with acetylene (**16**). The high symmetry leads to a linear arrangement of the molecules. The rotational disorder does not allow the hydrogen-bridge distances to be measured directly.

1,3-Xylene: In the 1:1 co-crystal with 1,3-xylene (**17**) the acetylene forms a zigzag-chain of C–H···π interactions (2.757 Å, 3.812 Å, 165°). The other side of each acetylene is bonded by an aromatic C–H···π interaction (d_{rc} = 2.378 Å, D = 3.421 Å, θ = 161°) to the centre of a xylene molecule (Figure 19).

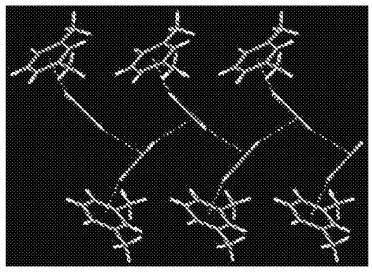

Figure 19. Co-crystal of 1,3-xylene with acetylene (**17**). The homogenic zigzag chain is formed of the C–H···π interaction (2.757 Å, 3.812 Å, 165°) as well as the heterogenic C–H···π interaction (d_{rc} = 2.378 Å, D = 3.421 Å, θ = 161°).

This is somewhat different to the situation in benzene. Although acetylene and benzene both have C–H donor and π acceptor abilities, in benzene they form heterogenic interactions. In xylene, however, they form heterogenic (acetylene–xylene) and homogenic (acetylene–acetylene and xylene–xylene) interactions. This shows that the interaction energies are in the same range and, depending on the steric requirements of the participating molecules, may be interchanged.

Mesitylene: In the co-crystal with mesitylene (**18**) we find two molecules of acetylene in two rather different environ-

© 2009 Wiley-VCH Verlag GmbH & Co. KGaA, Weinheim

These are not the final page numbers!

UM00016686
NOVARTIS EXHIBIT 1517
Novartis v. Regents, IPR2023-01347
Page 3668 of 4460

ments of weak hydrogen-bridge interactions. The first is directly comparable to benzene as it forms hydrogen bridges to two π systems, pointing nearly perpendicular (d_{rc} = 2.386 Å, θ = 159°; d_{rc} = 2.460 Å, θ = 163°) to the centre of the benzene planes. The angle between planes is 23.29°. The length of the C–C bond at 153 K is 1.144(4) Å.

In the packing with benzene, the benzene hydrogen atoms surround the acetylene and lead to a hexagonal space group. In mesitylene this kind of packing is sterically impossible due to the methyl groups. Instead, the second acetylene bridges the π system of the first acetylene. The C–H···C distance is short (2.700/2.746 Å, 167/164°). The length of the C≡C triple bond is 1.115(8) Å. A third mesitylene molecule forms another C–H···π hydrogen bridge (2.714 Å, 160°) with the first acetylene molecule to complete the molecular complex of three molecules of acetylene and six molecules of mesitylene (Figure 20). Further aromatic and aliphatic (i.e., from the methyl group) C–H···π interactions might be identified.

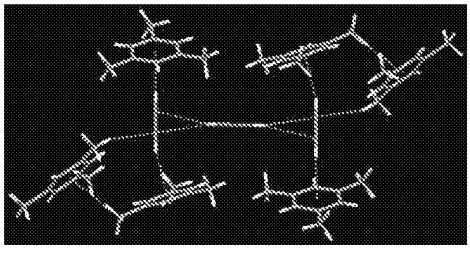

Figure 20. Co-crystal of mesitylene with acetylene (**18**). Please see the text for the length of intermolecular interactions.

The molecular complex of mesitylene with acetylene is the most complex so far. The asymmetric unit contains two molecules of acetylene and three molecules of mesitylene. The two molecules of acetylene form different types of interactions, one to the mesitylene the other to acetylene. Similarly, the three molecules of mesitylene form different types of interactions. Two accept hydrogen bridges from acetylene on one side of the π system but differ in the aromatic and aliphatic character of the donor to the other side of the π system. The third molecule does not accept any acetylene donor but only aliphatic C–H···π interactions from the other two mesitylene molecules.

Hexafluorobenzene: Methyl substituents change the packing of co-crystals of aromatic compounds with acetylene as the geometrical strain is increased and more elaborate modes of interaction are explored in the structures. But by substitution of the aromatic system there is also an influence on the strength and character of the bridge itself.

In the packing of the 1:2 co-crystal of acetylene with hexafluorobenzene (**19**) the acetylene is trapped in a cage of eight molecules of hexafluorobenzene (Figure 21). There are no hydrogen bridges between the molecules. The structure therefore is closer to a clathrate if the weak interactions

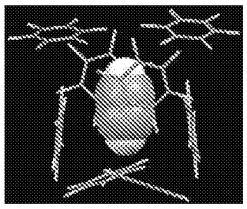

Figure 21. Co-crystal of hexafluorobenzene with acetylene (**19**). The co-crystal is a clathrate with the guest molecule tightly surrounded by eight molecules and therefore is ordered.

could be said to form a clathrating network. The C–F···C distance is 3.195 Å.

In hexafluorobenzene the six fluoro substituents exert a strong influence on the π system by withdrawing electron density. This has a marked effect on the acceptor properties of hexafluorobenzene as the charge transfer stabilisation in the molecular complex with benzene exemplifies.[19] The diminished acceptor ability of hexafluorobenzene would weaken a hydrogen bridge in a possible co-crystal with acetylene. A clathrate is therefore formed featuring typically weak C–F···π interactions, which form a loose host network in which acetylene is enclathrated without any short interactions to the host (C–H···F d = 3.252 Å, C···C D = 3.542 Å). The main difference to most other clathrates of acetylene discussed before is that the cage is small and fits closely around the guest. Therefore the acetylene is not disordered.

The five co-crystallisation partners to form a clathrate with acetylene are DMSO (**1**), water (**4**), phenol (**6**), 2,6-*tert*-butylpyridine (**15**) and hexafluorobenzene (**19**). These are rather different molecules in terms of both their size and intermolecular contacts. The extremes are water, which forms a strongly hydrogen-bridged O–H···O network into which disordered guest molecules of different sizes are inserted, and hexafluorobenzene, which forms a weakly bound host with cavities just large enough to fit acetylene. The other three are intermediate situations. Another clathrate of acetylene with hydroquinone is known from the literature.[20]

DMSO forms a two-dimensional C–H···O bridged network (**1**) with acetylene. The void between two DMSO and six acetylene molecules is filled with an additional molecule of acetylene that is ordered. Two C–H···π interactions to the other acetylene molecules are to be found but with rather small intermolecular angles (d = 2.871/2.877 Å, D = 3.677/3.571 Å, θ = 131/122°). The clathration of acetylene in DMSO is closest to a molecular complex.

In the clathrate with 2,6-*tert*-butylpyridine (**15**), acetylene is fully disordered in a cavity of 4.5 Å mean diameter. 2,6-Di-*tert*-butylpyridine forms a weak C–H···N hydrogen-bridged one-dimensional network but otherwise there is no strong intermolecular network as with water or DMSO. The clathrate is not stable without the guest. The disorder demonstrates that there is no specific hydrogen-bridge interaction between guest and host. The only requirement on the guest is to be of appropriate size to fit into the cavity left by the host.

 © 2009 Wiley-VCH Verlag GmbH & Co. KGaA, Weinheim

UM00016687
NOVARTIS EXHIBIT 1517
Novartis v. Regents, IPR2023-01347
Page 3669 of 4460

Phenol does not form a strong O–H···O intermolecular network but hexagonal prisms of 12 molecules. Acetylene is incorporated into the cages like a water cage and into the voids between prisms as in 2,6-di-*tert*-butylpyridine. The molecules are disordered over more than one orientation in their respective positions.

Compounds that did not form co-crystals: When analysing the packing of co-crystals it is always advisable to compare compounds with only small variations in chemical composition. The relative similarities and differences between them are more conclusive than absolute features of single unrelated structures. This is especially evident when looking at homologous series of compounds.[3] For co-crystallisation with acetylenes we tried to prepare analogues: formaldehyde–acetone–DMSO, ammonia–water–methanol–phenol, benzene–xylene–mesitylene and the N-heterocyclic family. It is one of the difficulties that these families of chemically similar compounds co-crystallise into rather different molecular complexes or even clathrates.

However, some compounds would not form co-crystals with acetylene. Usually we made some effort to force unyielding compounds into a co-crystal by variation of the ratio of acetylene or by changing the temperature of crystallisation but for some we were unexpectedly unsuccessful. This is especially frustrating for the preparative crystallographer as there is no rule to predict co-crystallisation partners. Even closely related compounds might yield different results: toluene, *o*- and *p*-xylene do not co-crystallise, but benzene, *m*-xylene and mesitylene do. Benzonitrile does not, acetonitrile does. Ethanol does not, methanol does. Dioxane does form a co-crystal with acetylene, furan was predicted by theoretical calculations and spectroscopic evidence to give a molecular adduct but did not yield a co-crystal.[21] In the same way diethyl ether, diacetyl, ethyleneglycol, carbon dioxide, bromine and chloroform do not co-crystallise.

The most probable explanation for this behaviour is the lattice energies of the neat compounds relative to the co-crystal. If the co-crystallisation partner has a low-energy structure of its own the formation of a co-crystal is less favourable.

To save some time in the preparative effort we used Raman spectroscopy. In general the spectra showed marked band shifts when complexes were found. On the other hand, for example, furan did not have an effect on the spectra of co-condensation, which hints that a co-crystal is not formed by our method.

Conclusion

The most respected principle in chemical structural sciences is the prediction of structures from structural knowledge. At the moment this turns out to be an impossible task for co-crystals of acetylene even if only general features of the packing are considered.

The difficulty starts with the predictability of complex formation. At present it is unclear which substances will co-crystallise and which will prefer to form one-component crystals. The difference in melting points does not seem to be an important factor. The solubility of acetylene in the corresponding neat compound is probably a good indicator. Binary mixtures with gases pose additional problems due to phase segregation at the boundary interface. As a rule, compounds forming distinct molecular complexes with strong interactions tend to form mixtures without a visible phase interface which makes the growth of single crystals easier.

Further, the chosen stoichiometry of the molecular complexes cannot be rationalised as they are a consequence of the versatility and size of acetylene to fit the available donors and optimise the overall packing. In some cases we felt that other stoichiometric ratios should be available but, except in the molecular complexes with acetone, we were not able to find conditions to synthesise different forms, usually not by lack of effort. On the other hand, although some compounds easily yield co-crystals in seemingly any ratio of mixture, temperature and growth conditions, others have to be carefully coerced maintaining specific conditions, as is well known with other co-crystallisation systems. Generally we feel that acetylene is a very convenient co-crystal former.

Acetylene forms hydrogen bridges with the strongest available acceptor that is not incorporated into stronger hydrogen bridges. Acetylene may act as a bifunctional donor or only with one side. The angle at the hydrogen atom is usually linear but may deviate from linearity as the C–H hydrogen bridge from acetylene is weaker and less directional than O–H and N–H hydrogen bridges. Equally, the distance may vary in the range between 2.085 and 2.482 Å. We found a bimodal distribution in intermolecular bridge distances with oxygen and nitrogen atoms, the aromatic partners form longer bridges above 2.36 Å.

Furthermore, acetylene is a small molecule that might be enclathrated into cavities to stabilise a host network. Owing to the size and versatility of acetylene in its interactions the molecular complexes formed and the dimensionality of the network are not predictable at present. On the other hand, because of this the packing motifs are optimised with regard to intermolecular interactions. This allows a detailed study of the interplay of weak and strong hydrogen bridges.

When classifying the molecular complexes by their coordination spheres at the acceptor site we focused on the geometrical availability of binding sites. For the most common type of coordination sphere, which is the tetrahedral, we find four contacts around the acceptor, one or two intramolecular and one to three of them intermolecularly form acetylene. The remaining are other intermolecular contacts from neighbouring molecules. The molecular complexes with acetone, pyridine and 2,5-dimethylpyridine might also be classified as tetrahedral in a simplified approach. Taking a more detailed view, two further intermolecular contacts upgrade the acceptor sphere to a distorted octahedron. The reason for an increased number of intermolecular contacts is the

© 2009 Wiley-VCH Verlag GmbH & Co. KGaA, Weinheim

These are not the final page numbers!

UM00016688
NOVARTIS EXHIBIT 1517
Novartis v. Regents, IPR2023-01347
Page 3670 of 4460

overall flatness of the acceptor molecules permitting additional perpendicular approaches to the acceptor. The same happens with formaldehyde and 2,3-dimethylpyrazine, which have three contacts in a trigonal arrangement in-plane and two additional contacts from above and below the plane leading to a trigonal-bipyramidal arrangement.

Special cases are the molecular complexes with the aromatic compounds benzene, mesitylene and xylene. They are quite different from the N-heteroaromatic systems and accept one hydrogen bridge donor on each side of the π system. The structures gain versatility by using aliphatic and aromatic C–H as donors for hydrogen bridges in competition with acetylenic C–H.

In conclusion we feel that it is not possible at the moment to predict the structure of acetylene co-crystals from a few simple rules. For true crystal structure prediction of the structures presented here, the results are too different and the geometry around acetylene as a co-crystal former is probably too variable. The classification applied above simply indicates that some of the possible alternatives for structures of new co-crystals exist, but in general the results are too unexpected. The prediction of the experimental structure from a bundle of ab initio calculated, energetically similar structures seems to be as impossible as any other intuitive approach. However, the molecular complexes are suggested as benchmarks and as a challenge for theoretical methods and simulations because acetylene is small and has no intramolecular flexibility, as are most of the partners selected for our experiments, as demonstrated with the acetylene–ammonia case.

Table 2. Crystal data for new co-crystals.

	2	**6**	**13**	**17**	**18**	**19**
partner of acetylene	acetonitrile	phenol	formaldehyde	xylene	mesitylene	hexafluorobenzene
SG	$Cmc2_1$	$R\bar{3}$	$Cmcm$	$Pnma$	$P\bar{1}$	$I4_1/a$
a [Å]	11.616(3)	16.4516(3)	5.429(12)	5.964(5)	8.4511(13)	15.536(2)
b [Å]	8.239(2)	16.4516(3)	6.346(15)	10.677(10)	11.3288(15)	15.536(2)
c [Å]	7.5017(19)	21.8494(4)	11.69(3)	14.036(14)	14.796(2)	11.173(3)
α [°]	90	90	90	90	85.351(4)	90
β [°]	90	90	90	90	75.488(2)	90
γ [°]	90	120	90	90	80.641(3)	90
V [Å^3]	718.0(3)	5121.37(16)	402.6(16)	893.8(14)	1351.9(3)	2696.9(9)
Z	4	6	4	4	3	4
ρ [g cm^{-3}]	0.861	1.189	0.925	0.982	0.982	1.897
T [K]	159(2)	143(2)	123(2)	168(2)	153(2)	213(2)
reflections	358	32394	564	3314	5472	5591
data	358	3082	179	1008	4468	1732
parameters	49	161	15	53	271	116
μ [mm^{-1}]	0.052	0.079	0.069	0.055	0.055	0.228
abs. corr.	multi-scan	multi-scan	none	multi-scan	multi-scan	multi-scan
T_{min}	0.86	0.79	–	0.86	0.85	0.68
T_{max}	0.97	0.86	–	0.98	0.98	0.93
R_1	0.0328	0.0955	0.1019	0.1739	0.1177	0.0960
wR_2	0.0719	0.1564	0.1338	0.1267	0.2186	0.0921
GOF	1115	1045	968	947	1023	988
r^+ [e Å^{-3}]	0.092	0.604	0.211	0.228	0.343	0.143
r^- [e Å^{-3}]	−0.067	−0.322	−0.206	−0.166	−0.219	−0.147
CCDC no.[a]	735040	735041	735042	735043	735044	735045

[a] The CCDC references contain the supplementary crystallographic data for this paper. These data can be obtained free of charge from The Cambridge Crystallographic Data Centre via www.ccdc.cam.ac.uk/data_request/cif.

Experimental Section

The crystals were usually grown and measured inside a 0.3 mm quartz capillary with a SMART1000 CCD system with $Mo_{K\alpha1}$ radiation. Cell determination, data collection and reduction was performed with APEX2 (versions from 2004 to 2008). Multiscan absorption correction was performed with SADABS 2004/2008, solution and refinement with SHELXLT 12.1 ($F_o = 4\sigma(F)$, LS against F^2) and the preparation of figures with Mercury 2.[22] Hydrogen atoms were refined in riding positions except for acetylenic hydrogen where possible. Further crystal data are collected in Table 2.

Acknowledgements

M.T.K. and R.B. thank the Deutsche Forschungsgemeinschaft (DFG-FOR 618).

[1] a) J. D. Dunitz, *Pure Appl. Chem.* **1991**, *63*, 177; b) J.-M. Lehn, *Supramolecular Chemistry: Concepts and Perspectives*, VCH, Weinheim, **1995**.

[2] a) M. T. Kirchner, R. Boese, W. E. Billups, L. R. Norman, *J. Am. Chem. Soc.* **2004**, *126*, 9407–9412; b) E. D. Sloan, *Clathrate Hydrates of Natural Gases*, Dekker, New York, **1997**; c) G. A. Jeffrey, R. K. McMullan, *Prog. Inorg. Chem.* **1967**, *8*, 43–108.

[3] a) R. Boese, H.-C. Weiß, D. Bläser, *Angew. Chem.* **1999**, *111*, 1042–1045; *Angew. Chem. Int. Ed.* **1999**, *38*, 988–992; b) V. R. Thalladi, R. Boese, H.-C. Weiss, *Angew. Chem.* **2000**, *112*, 942–946; *Angew. Chem. Int. Ed. Engl*, **2000**, *39*, 918–922; c) V. R. Thalladi, R. Boese, H.-C. Weiss, *J. Am. Chem. Soc.* **2000**, *122*, 1186–1190; d) V. R. Thalladi, M. Nüsse, R. Boese, *J. Am. Chem. Soc.* **2000**, *122*, 9227–9236.

[4] G. R. Desiraju, *Angew. Chem.* **1995**, *107*, 2541–2558; *Angew. Chem. Int. Ed. Engl.* **1995**, *34*, 2311–2327.

[5] a) G. R. Desiraju, T. Steiner, *The Weak Hydrogen Bond: In Structural Chemistry and Biology*, Oxford University Press, Oxford, **2001**; b) G. R. Desiraju, *Acc. Chem. Res.* **2002**, *35*, 565–573.

[6] a) *Ullmann's Encyclopedia*, 7th ed., Wiley-VCH, **2005**, Weinheim; b) *Modern Acetylene Chemistry* (Eds.: P. J. Stang, F. Diederich), VCH, Weinheim, **1995**.

[7] R. K. McMullan, A. Kvick, P. Popelier, *Acta Crystallogr. Sect. B* **1992**, *48*, 726.

[8] Cited from Ullmann:[6] "Gleichgewicht der Absorption von Gasen in Flüssigkeiten": A. Kruis in *Landolt–Börnstein Zahlenwerte und Funktionen, 4. Teil, Bestandteil c* (Ed.: H. Hausen), Springer, Berlin, **1976**.

[9] a) "In Situ Crystallisation Techniques": R. Boese, M. Nussbaumer in *Organic Crystal Chemistry* (Ed.: D. W. Jones), Oxford University

© 2009 Wiley-VCH Verlag GmbH & Co. KGaA, Weinheim

UM00016689
NOVARTIS EXHIBIT 1517
Novartis v. Regents, IPR2023-01347
Page 3671 of 4460

Press, Oxford, **1994**, pp. 20–37; b) V. R. Thalladi, H.-C. Weiss, D. Bläser, R. Boese, A. Nangia, G. R. Desiraju, *J. Am. Chem. Soc.* **1998**, *120*, 8702–8710.

[10] R. Boese, M. T. Kirchner, W. E. Billups, L. R. Norman, *Angew. Chem.* **2003**, *115*, 2005–2007; *Angew. Chem. Int. Ed.* **2003**, *42*, 1961–1963.

[11] Structural data and Raman spectra of of dioxane acetylene complex, unpublished results.

[12] M. T. Kirchner, D. Das, R. Boese, *Cryst. Growth Des.* **2008**, *8*, 763–765.

[13] a) P. Groth, O. Hassel, *Acta Chem. Scand.* **1964**, *18*, 402; b) O. Hassel, K. O. Strømme, *Acta Chem. Scand.* **1959**, *13*, 275; c) O. Hassel, K. O. Strømme, *Acta Chem. Scand.* **1954**, *8*, 873.

[14] a) A. C. Legon, *Angew. Chem.* **1999**, *111*, 2850–2880; *Angew. Chem. Int. Ed.* **1999**, *38*, 2686–2714; b) O. Hassel, *Science* **1970**, *170*, 497.

[15] R. Boese, D. Bläser, G. Jansen, *J. Am. Chem. Soc.* **2009**, *131*, 2104–2106.

[16] M. T. Kirchner, R. Boese, A. Gehrke, D. Bläser, *CrystEngComm* **2004**, *6*, 360–366.

[17] PLATON, A Multipurpose Crystallographic Tool, A. L. Spek, Utrecht, **2009**.

[18] R. Boese, T. Clark, A. Gavezzotti, *Helv. Chim. Acta* **2003**, *86*, 1085–1100.

[19] J. H. Williams, J. K. Cockcroft, A. N. Fitch, *Angew. Chem.* **1992**, *104*, 1666–1669; *Angew. Chem. Int. Ed. Engl.* **1992**, *31*, 1655–1657.

[20] Cited from CSD Refcode ZZZVKY as: D. E. Palin, H. M. Powell, *J. Chem. Soc.* **1947**, 208–221.

[21] a) E. Sánches-García, A. Mardyukov, A. Tekin, R. Crexpo-Otero, L. A. Montero, W. Sander, G. Jansen, *Chem. Phys.* **2008**, *343*, 168–185; b) A. Metzelthin, E. Sánchez-García, Ö. Birer, W. Sander, M. Havenith unpublished results; c) A. Metzelthin, Ö. Birer, E. Sánchez-García, M. Havenith, *J. Chem. Phys.* **2008**, *129*, 114307.

[22] C. F. Macrae, I. J. Bruno, J. A. Chisholm, P. R. Edgington, P. McCabe, E. Pidcock, L. Rodriguez-Monge, R. Taylor, J. van de Streek, P. A. Wood, *J. Appl. Cryst.* **2008**, *41*, 466–470.

Received: May 16, 2009
Revised: October 7, 2009
Published online: ■■ ■■, 2009

 © 2009 Wiley-VCH Verlag GmbH & Co. KGaA, Weinheim

These are not the final page numbers!

UM00016690
NOVARTIS EXHIBIT 1517
Novartis v. Regents, IPR2023-01347
Page 3672 of 4460

Complicated versatility: Acetylene is an amazingly versatile component for the formation of co-crystals. It requires careful handling and special techniques for crystallisation, but the efforts seem to be rewarding when attaining co-crystals with small molecules as partners (see figure). Many basic questions such as the dominance of specific heterogeneous intermolecular interactions and their driving force for the formation of multicomponent crystals are expected to be easily analysed.

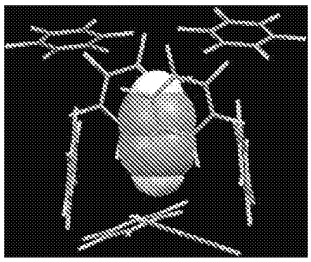

Co-crystal Interactions

*M. T. Kirchner, D. Bläser, R. Boese** ..... ▮▮▮▮–▮▮▮▮

Co-crystals with Acetylene: Small Is not Simple!

© 2001 Wiley-VCH Verlag GmbH & Co. KGaA, Weinheim

UM00016691
NOVARTIS EXHIBIT 1517
Novartis v. Regents, IPR2023-01347
Page 3673 of 4460

November 1985
Volume 74, Number 11

Journal of Pharmaceutical Sciences

A publication of the American Pharmaceutical Association

RESEARCH ARTICLES

Molecular Structure of Two Conformationally Restrained Fentanyl Analogues: cis- and trans-Isomers of *N*-{3-Methyl-1-[2-(1,2,3,4-tetrahydro)naphthyl]-4-piperidinyl}-*N*-phenylpropanamide

CHERYL L. KLEIN*×, EDWIN D. STEVENS*§, E. KIM FIFER‡, AND RONALD F. BORNE‡

Received December 5, 1984, from the *Department of Chemistry, Xavier University, New Orleans, LA 70125, §Department of Chemistry, University of New Orleans, New Orleans, LA 70148, and the ‡Department of Medicinal Chemistry, University of Mississippi, University, MS 38677. Accepted for publication July 11, 1985.

Abstract □ The X-ray crystallographic structures of two analogues of the potent analgetic fentanyl in which the *N*-phenethyl substituent is restrained through incorporation into a tetrahydronaphthyl ring system are reported. The tetrahydronaphthyl moiety exists in an equatorial conformation with respect to the piperidine ring which exists in the chair conformation. The propanilido group is also equatorial and antiperiplanar. The orientation of the *N*-phenyl group with respect to the *N*-acyl moiety is essentially invariant with an approximately 90° dihedral angle. The implications of these conformations in the interaction of fentanyl-type analgetics with opiate receptors are discussed. The following data were obtained: *cis*-[$C_{25}H_{33}N_2O^+$]Cl^- · 1/2 $C_2O_4H_2$, triclinic, $P\bar{1}$, a = 7.005(7), b = 13.189(2), c = 14.312(4)Å, α = 111.27(2), β = 99.15(5), γ = 93.52(4)°, V = 1205.9Å, Z = 2, T = 110K, R = 0.0596, R_w = 0.0760; *trans*-[$C_{25}H_{33}N_2O^+$] $C_2O_4H^-$ · 1/2 $C_2O_4H_2$ · 2 H_2O, triclinic, $P\bar{1}$, a = 8.235(6), b = 10.546(8), c = 17.108(9)Å, α = 107.72(5), β = 95.73(5), γ = 90.63(6)°, V = 1406.8Å^3, Z = 2, T = 110K, R = 0.0737, R_w = 0.0934.

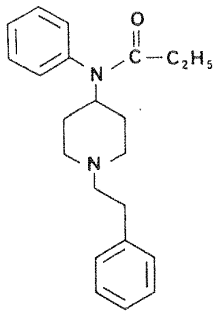

1

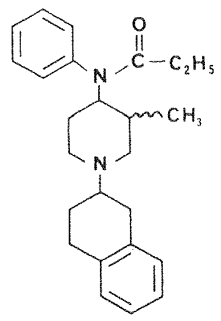

2 a = cis

b = trans

Fentanyl (1) is a potent narcotic analgetic agent which is representative of the 4-anilidopiperidine class of synthetic analgetics. This class of analgetics has been the subject of numerous structural and conformational studies. In an effort to clarify structure–activity relationships for analgetic activity there have been many reports regarding the synthesis of compounds related to fentanyl.[1–10] Several studies relating to the importance of conformational factors in the action of these analgetics have also been reported including efforts to restrict the *N*-propanilido group[11–13], the piperidine ring[14,15], and the *N*-phenethyl substituent.[16,17] Based on the reports that a 3-methyl substituent enhances activity[6,7] compounds **2a** and **b** were prepared as analogues of 3-methylfentanyl in which the *N*-phenethyl substituent is restricted in an antiperiplanar conformation. The observation that **2a** possesses approximately three times the analgetic activity of fentanyl and the proposal that the conformation of the *N*-phenyl rings plays an important role in the binding of fentanyl-type analgetics to the opiate receptor[13] prompted an investigation of its crystal structure.

Experimental Section

Compounds **2a** and **b** were prepared as described previously.[16] Single crystals of both compounds were obtained separately from solutions of aqueous ethanol, and the structure was determined by X-ray crystallographic techniques as described below.

Crystal Data—cis-[$C_{25}H_{33}N_2O^+$]Cl^- · 1/2 $C_2O_4H_2$, triclinic space group, $P\bar{1}$, a = 7.005(7), b = 13.189(2), c = 14.312(4)Å, α = 111.27(2)°, β = 99.15(5)°, γ = 93.52(4)°, V = 1205.9Å^3, Z = 2, λ = 0.70930Å, D_x = 1.23 g/mL. *trans*-[$C_{25}H_{33}N_2O^+$] · 1/2 $C_2O_4H_2$, $C_2O_4H^-$ · $2H_2O$, triclinic space group, $P\bar{1}$, a = 8.235(6), b = 10.546(8), c = 17.108(9)Å, α = 107.72(5)°, β = 95.73(5)°, γ = 90.63(6)°, V = 1406.8Å^3, Z = 2, λ = 0.70930Å, D_x = 1.25 g/mL.

***cis*-*N*-{3-Methyl-1-[2-(1,2,3,4-tetrahydro)naphthyl]-4-piperidinyl}-*N*-phenylpropanamide (2a)**—A single colorless plate-like

0022-3549/85/1100-1147$01.00/0
© 1985, American Pharmaceutical Association

UM00016692
NOVARTIS EXHIBIT 1517
Novartis v. Regents, IPR2023-01347
Page 3674 of 4460

crystal (0.06 × 0.48 × 0.30 mm) was mounted on an Enraf-Nonius CAD-4 diffractometer with a molybdenum target X-ray tube and a graphite crystal monochromator. All three-dimensional intensity data were collected at 110 K in the ω:2θ scan mode. Independent reflections (5138) were collected to a 2θ maximum of 52° Reflections with $I > 3\sigma(I)$ were considered observed (3059) and were included in the refinement. The data were corrected for Lorentz and polarization effects. Absorption as a function of psi was observed to be minimal and, therefore, not corrected. Three standard reflections measured every 2 h during data collection showed no significant change in intensity.

The structure was solved by direct methods using the MULTAN[18] series of programs which revealed the location of 31 non-hydrogen atoms, corresponding to the cis-isomer of the fentanyl analogue and one-half of an oxalic acid molecule which is located on an inversion center on the E map. These 31 atoms were refined isotropically using a full-matrix least-squares program to R = 0.131%. All hydrogen atoms, with the exception of the nitrogen proton and the oxalic acid hydrogens, were calculated on the basis of sp^2 or sp^3 geometry and a C — H bond distance of 0.95Å. The oxalic acid hydrogen and the hydrogen on the piperidine nitrogen atom were located on a difference Fourier map. Continued refinement of all-nonhydrogen atoms with anisotropic thermal parameters and hydrogen atoms with isotropic thermal parameters led to a final R = 0.0596 and R_w = 0.0760.[19]

***trans*-*N*-(3-Methyl-1-[2-(1,2,3,4-tetrahydro)naphthyl]-4-piperidinyl)-*N*-phenylpropanamide (2b)**—A single, colorless, plate-like crystal (0.42 × 0.27 × 0.08 mm) was mounted on the instrument described above. Independent reflections (3727) were collected at 110 K to a 2θ maximum of 44°. Reflections with $I > 5\sigma(I)$ were considered observed (1243) and included in the refinement. The data were corrected for Lorentz and polarization effects. Absorption as a function of psi was observed to be minimal and therefore not corrected. Three standard reflections measured every 2 h showed a 15.8% loss in intensity over a 10-d data collection period which was corrected assuming a linear decay model.

The structure was solved using the MULTAN series of programs which revealed the location of all atoms in the trans-isomer, one hydrogen oxalate anion, one-half of an oxalic acid molecule, and two water oxygen atoms. Isotropic full-matrix least-squares refinement led to an R value of 0.136. All hydrogen atoms except those on the water molecules and those on the oxalates were calculated on the basis of sp^2 or sp^3 geometry and a C — H bond distance of 0.95Å. Two of the remaining hydrogen positions were located on a subsequent Fourier map. The remaining hydrogens could not be located. Continued refinement with all non-hydrogen atoms with anisotropic temperature factors and all hydrogen atom positions and thermal parameters fixed led to a final value of R = 0.0737 and R_w = 0.0934.

All computer programs used for data collection and refinement are part of the CAD-4 SDP package.[20] Scattering factors were taken from the International Tables for X-ray Crystallography[21] and included corrections for anomalous scattering contributions.

Results and Discussion

Final fractional coordinates for both isomers are given in Table I. The numbering system and bond lengths may be found in Fig. 1 for the cis-isomer and Fig. 2 for the trans-isomer. Bond lengths and bond angles may be found in Table II.[22] Crystals of the trans-isomer **2b** were of lower quality than those of the cis-isomer **2a**, leading to a lower ratio of observations with significant intensity. In addition, the crystals of the trans-isomer showed significant decay during the data collection. The overall precision of the structural results for the trans-isomer is therefore somewhat lower than for the cis-isomer, which is reflected in estimated SD of position thermal parameters, and bond distances and angles which are 3–4 times higher. Despite the lower precision, the basic information of chemical connectivity and molecular conformation of the trans-isomer are well defined.

The cis-isomer 2a crystallized as the hydrochloride salt with the piperidine nitrogen atom protonated and the methyl group bonded axially. An oxalic acid molecule, located on an inversion center in the unit cell, participated in an extensive

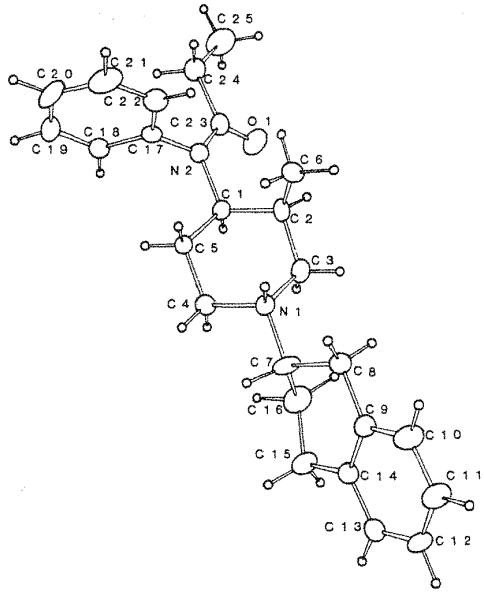

Figure 1—*Numbering system and bond lengths for **2a**, the cis-isomer.*

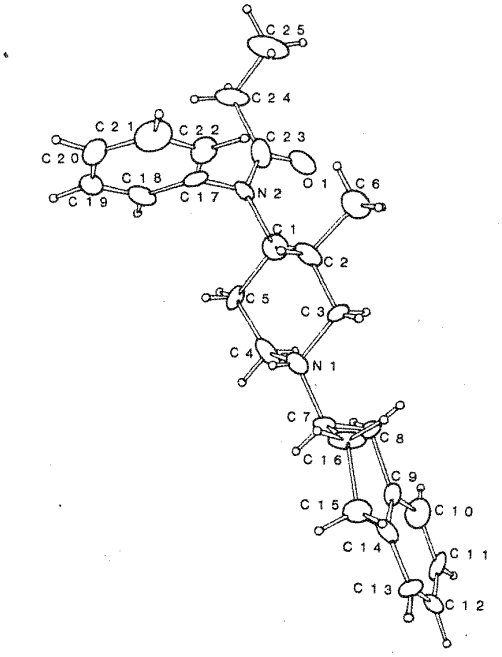

Figure 2—*Numbering system and bond lengths for **2b**, the trans-isomer.*

intermolecular hydrogen bonding network. The trans-isomer 2b crystallized as the oxalate salt, with the piperidine nitrogen atom also protonated and the methyl group bound equatorially. The unit cell contains two molecules of 2b, one oxalic acid molecule located on an inversion center, two monohydrogen oxalate anions, and four water molecules, all participating in an extensive intermolecular hydrogen bonding network.

Both the cis- and trans-isomers (2a and b) represent conformationally restrained analogues of fentanyl in which

Table

Atom

Cl(1)
O(1)
O(3)
O(4)
N(1)
N(2)
C(1)
C(2)
C(3)
C(4)
C(5)
C(6)
C(7)
C(8)
C(9)
C(10)
C(11)
C(12)
C(13)
C(14)
C(15)
C(16)
C(17)
C(18)
C(19)
C(20)
C(21)
C(22)
C(23)
C(24)
C(25)
C(26)

[a] E

UM00016693
NOVARTIS EXHIBIT 1517
Novartis v. Regents, IPR2023-01347
Page 3675 of 4460

Table I—Fractional Coordinates for 2a and 2b[a]

Atom	2a x	2a y	2a z	2a B_{equiv}(Å^2)	Atom	2b x	2b y	2b z	2b B_{equiv}(Å^2)
Cl(1)	0.3450(1)	0.85783(9)	0.15771(7)	2.47(2)	O(1)	0.846(1)	−0.1869(8)	0.5661(5)	3.3(2)
O(1)	−0.2122(4)	−0.2113(2)	0.7814(2)	2.99(7)	O(2)	0.270(1)	0.0749(7)	0.8034(5)	2.2(2)
O(3)	0.3673(4)	0.0884(2)	0.5803(2)	2.05(6)	O(3)	0.375(1)	0.2780(8)	0.8165(5)	3.6(2)
O(4)	0.6325(4)	0.0127(2)	0.6190(2)	2.23(6)	O(4)	0.106(2)	0.0811(9)	0.6653(7)	7.9(4)
N(1)	0.2572(4)	0.1626(2)	0.9051(2)	1.41(6)	O(5)	0.144(2)	0.2914(9)	0.6968(6)	5.4(3)
N(2)	0.0042(4)	−0.1632(2)	0.6990(2)	1.54(6)	O(6)	0.290(1)	0.0083(7)	0.9833(5)	2.2(2)
C(1)	0.1493(6)	0.0923(3)	0.9461(3)	1.99(8)	O(7)	0.481(1)	0.0520(7)	0.9120(5)	2.0(2)
C(2)	0.1279(6)	−0.0290(3)	0.8788(3)	2.17(8)	O(8)	−0.027(1)	0.274(1)	0.5623(6)	5.4(3)
C(3)	0.0213(5)	−0.0468(3)	0.7698(3)	1.53(7)	O(9)	−0.190(2)	0.036(1)	0.4947(7)	8.0(4)
C(4)	0.1261(5)	0.0282(3)	0.7295(3)	1.43(7)	N(1)	0.663(1)	−0.1994(8)	0.6529(5)	2.0(3)
C(5)	0.1471(5)	0.1479(3)	0.8008(3)	1.62(7)	N(2)	0.806(1)	0.0906(9)	0.8892(5)	2.0(2)
C(6)	0.3170(7)	−0.0774(3)	0.8831(3)	3.2(1)	C(1)	0.761(2)	0.139(1)	0.8154(6)	2.0(3)
C(7)	0.3094(6)	0.2823(3)	0.9741(3)	2.33(9)	C(2)	0.669(2)	0.035(1)	0.7452(7)	2.2(3)
C(8)	0.4727(5)	0.2944(3)	1.0629(3)	1.77(8)	C(3)	0.762(2)	−0.093(1)	0.7211(7)	2.2(3)
C(9)	0.5306(5)	0.4128(3)	1.1335(3)	1.83(8)	C(4)	0.802(2)	−0.139(1)	0.7979(7)	2.0(3)
C(10)	0.7058(6)	0.4427(3)	1.2035(3)	2.7(1)	C(5)	0.898(2)	−0.030(1)	0.8650(7)	2.7(3)
C(11)	0.7594(6)	0.5482(3)	1.2740(3)	2.8(1)	C(6)	0.640(2)	0.092(1)	0.6725(8)	3.4(4)
C(12)	0.6383(6)	0.6272(3)	1.2756(3)	2.34(9)	C(7)	0.891(2)	0.197(1)	0.9636(6)	1.8(3)
C(13)	0.4673(6)	0.5996(3)	1.2042(3)	2.04(8)	C(8)	1.050(2)	0.248(1)	0.9503(7)	1.7(3)
C(14)	0.4101(5)	0.4931(3)	1.1339(3)	1.73(8)	C(9)	1.132(2)	0.349(1)	1.0327(7)	1.6(3)
C(15)	0.2186(6)	0.4647(3)	1.0579(3)	2.59(9)	C(10)	1.297(2)	0.373(1)	1.0416(8)	2.7(3)
C(16)	0.1426(6)	0.3400(4)	1.0109(3)	2.9(1)	C(11)	1.377(2)	0.459(1)	1.1128(8)	2.3(3)
C(17)	0.0944(5)	−0.1921(3)	0.6112(3)	1.55(7)	C(12)	1.279(2)	0.522(1)	1.1745(7)	2.3(3)
C(18)	0.2765(6)	−0.2289(3)	0.6133(3)	2.24(9)	C(13)	1.117(2)	0.502(1)	1.1656(7)	2.4(3)
C(19)	0.3598(6)	−0.2552(4)	0.5291(4)	3.0(1)	C(14)	1.034(2)	0.413(1)	1.0945(7)	2.3(3)
C(20)	0.2652(6)	−0.2463(4)	0.4412(3)	2.9(1)	C(15)	0.852(2)	0.387(1)	1.0864(7)	2.3(3)
C(21)	0.0849(6)	−0.2083(3)	0.4390(3)	2.36(9)	C(16)	0.775(2)	0.310(1)	0.9976(7)	2.5(3)
C(22)	−0.0007(5)	−0.1821(3)	0.5229(3)	1.83(8)	C(17)	0.515(2)	−0.254(1)	0.6674(7)	1.7(3)
C(23)	−0.1240(6)	−0.2372(3)	0.7109(3)	2.08(8)	C(18)	0.516(2)	−0.362(1)	0.6965(7)	2.8(3)
C(24)	−0.1464(7)	−0.3541(3)	0.6331(3)	2.48(9)	C(19)	0.371(2)	−0.413(1)	0.7109(7)	3.1(4)
C(25)	−0.2812(9)	−0.4315(4)	0.6550(4)	4.6(1)	C(20)	0.222(2)	−0.362(1)	0.6906(8)	3.6(4)
C(26)	0.4917(5)	0.0307(3)	0.5557(3)	1.63(7)	C(21)	0.228(2)	−0.250(1)	0.6630(9)	3.9(4)
					C(22)	0.374(2)	−0.198(1)	0.6514(8)	2.9(3)
					C(23)	0.716(2)	−0.238(1)	0.5802(8)	2.6(3)
					C(24)	0.630(2)	−0.343(1)	0.5091(8)	4.3(4)
					C(25)	0.525(2)	−0.277(1)	0.4505(8)	5.3(5)
					C(26)	0.288(2)	0.185(1)	0.7836(8)	2.3(3)
					C(27)	0.164(2)	0.179(1)	0.7069(8)	3.8(4)
					C(28)	0.429(1)	0.015(1)	0.9708(6)	1.2(3)

[a] Estimated standard deviations are given in parentheses.

the *N*-phenethyl moiety is restricted to an antiperiplanar conformation by incorporation of this moiety as part of a tetrahydronaphthyl group. In the cis-isomer, the analgetic activity was slightly increased[16] and it was found to be approximately three times as potent as fentanyl. This is analogous to the effect observed in the increased potency of fentanyl upon addition of a *cis*-3-methyl group[6,7]. The trans-isomer, however, displays a slightly decreased activity relative to fentanyl. These data indicate that the conformation of the phenethyl group of fentanyl and related 4-anilidopiperidine analogues is most probably equatorial and antiperiplanar when interacting with the opiate receptor. This contradicts another model derived from molecular models which suggested a "folded" fentanyl conformation where the orientation of a phenyl ring of the phenethyl group is equivalent to the orientation of the comparable phenyl ring in other, more rigid, opiates.[23]

The piperidine ring in both the cis- and trans-isomers exists in a chair conformation with the 4-propanilido group extended and equatorially oriented. This is also the case in the crystal structure of fentanyl[24] itself and a 4-methoxymethyl derivative of fentanyl which shows analgetic activity 460 times that of fentanyl.[25] The *N*-acyl functions in all four of these compounds are essentially planar with nearly perpendicular dihedral angles between the *N*-acyl plane and the plane of the *N*-phenyl ring (fentanyl, 89°; **2a**, 87.9°, **2b**, 93.3°; and 4-CH_2OCH_3-fentanyl, 85°). In all cases, the orientation of the *N*-phenyl ring with respect to the *N*-acyl plane is essentially constant and the conformational differences result from the rotation of the *N*-phenyl/*N*-acyl groups about the C(3) — N(2) bond.

The torsion angles, C(17) — N(2) — C(3) — C(2), vary considerably (**2b**, −67.2°; fentanyl, −81.9°; and **2a**, −118.1°). This must be a result of the orientation of the 3-methyl substituent with respect to the *N*-phenyl and propanilido substituents. This can be seen more clearly in Fig. 3. Figure 3a shows that rotation of the *N*-phenyl/propanilido groups around the C(3) — N(2) bond in **2a** is hindered by the close proximity of an *N*-phenyl hydrogen atom and a methyl hydrogen atom [H(18) — H(6'), 2.32Å]. Rotation around the C(3) — N(2) bond in **2b** is also hindered by the close proximity of an *N*-phenyl hydrogen atom and a methyl hydrogen atom [H(22) — H(6'), 2.32Å] (Fig. 3c). The comparable torsion angles in the 4-methoxymethyl fentanyl derivative [C(17) — N(2) — C(3) — C(2)] are −122.0° and −120.8° (for two unique molecules in the asymmetric unit).[25] These are similar to the torsion angles in the cis-isomer **2a**.

In summary this structural investigation has resulted in the following information concerning the conformation of **2a** and **b**. The apparently preferred conformation of the piperidine ring is a chair with the propanilido group equatorial and planar with respect to the C(3) — N(2) — C(23) —C(24)

UM00016694
NOVARTIS EXHIBIT 1517
Novartis v. Regents, IPR2023-01347
Page 3676 of 4460

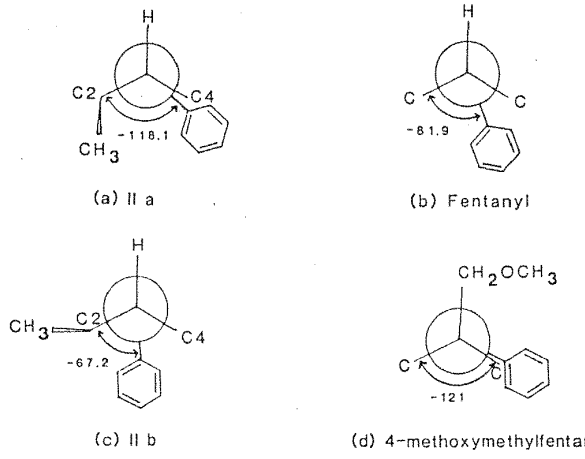

Figure 3—*Newman projections showing the degree of rotation of the N-phenyl/propanilido groups around the C3 — N2 bond (or comparable) in: a) **2a**, b) fentanyl, c) **2b**,and d) 4-methoxymethyl fentanyl.*

bond. The preferred conformation of the *N*-phenethyl moiety in fentanyl is, most probably, equatorial when interacting with the opiate receptor. This is confirmed by the observed effects on analgetic activity upon substitution of the *N*-phenethyl group with a tetrahydro naphthalene derivative which conformationally restrains the phenethyl group into an equatorial and antiperiplanar conformation. The orientation of the *N*-phenyl ring with respect to the *N*-acyl group is essentially invariant with an approximately 90° dihedral angle. Any variations that occur in the conformation of the *N*-phenyl and propanilido groups apparently result from rotation about the N(2) — C(3) bond. The increased activity of the *cis*-3-methyl derivative (**2a**) when compared with the corresponding trans-isomer (**2b**) and fentanyl (**1**) suggests that the axial *cis*-3-methyl substituent may allow the phenyl ring to assume a preferred conformation for interaction with the opiate receptor by avoiding unfavorable interactions between the phenyl ring and the methyl group. Likewise, the *N*-phenyl group in the trans-isomer is also forced into a conformation that avoids unfavorable interactions between the phenyl ring and the methyl groups. However, this orientation in the case of **2b** is apparently not one which is favorable to enhanced analgetic activity.

Table II—Bond Lengths (Å) and Bond Angles (°) for 2a and 2b

Atom 1	Atom 2	Distance	Atom 1	Atom 2	Atom 3	Angle
			2a			
O(1)	O(23)	1.222(4)	C(1)	N(1)	C(5)	109.2(2)
N(1)	C(1)	1.491(4)	C(1)	N(1)	C(7)	115.9(2)
N(1)	C(5)	1.507(3)	C(5)	N(1)	C(7)	111.9(2)
N(1)	C(7)	1.525(4)	C(3)	N(2)	C(17)	120.5(2)
N(2)	C(3)	1.487(4)	C(3)	N(2)	C(23)	117.5(2)
N(2)	C(17)	1.435(4)	C(17)	N(2)	C(23)	121.1(2)
N(2)	C(23)	1.360(4)	N(1)	C(1)	C(2)	112.3(3)
C(1)	C(2)	1.523(4)	C(1)	C(2)	C(3)	109.3(3)
C(2)	C(3)	1.547(4)	C(1)	C(2)	C(6)	113.3(3)
C(2)	C(6)	1.509(5)	C(3)	C(2)	C(6)	114.4(3)
C(3)	C(4)	1.519(4)	N(2)	C(3)	C(2)	111.9(2)
C(4)	C(5)	1.522(4)	N(2)	C(3)	C(4)	110.5(2)
C(7)	C(8)	1.524(4)	C(2)	C(3)	C(4)	110.0(2)
C(7)	C(16)	1.496(4)	C(3)	C(4)	C(5)	111.8(2)
C(8)	C(9)	1.509(4)	N(1)	C(5)	C(4)	109.9(2)
C(9)	C(10)	1.389(4)	N(1)	C(7)	C(8)	109.5(2)
C(9)	C(14)	1.395(4)	N(1)	C(7)	C(16)	115.5(3)
C(10)	C(11)	1.376(4)	C(8)	C(7)	C(16)	111.3(3)
C(11)	C(12)	1.382(5)	C(7)	C(8)	C(9)	111.4(2)
C(12)	C(13)	1.378(4)	C(8)	C(9)	C(10)	119.2(3)
C(13)	C(14)	1.387(4)	C(8)	C(9)	C(14)	122.2(3)
C(14)	C(15)	1.517(4)	C(10)	C(9)	C(14)	118.5(3)
C(15)	C(16)	1.554(5)	C(10)	C(9)	C(14)	118.5(3)
C(17)	C(18)	1.393(4)	C(9)	C(10)	C(11)	121.5(3)
C(17)	C(22)	1.387(4)	C(10)	C(11)	C(12)	119.9(3)
C(18)	C(19)	1.365(5)	C(11)	C(12)	C(13)	119.1(3)
C(19)	C(20)	1.374(5)	C(12)	C(13)	C(14)	121.5(3)
C(20)	C(21)	1.388(5)	C(7)	C(14)	C(13)	119.4(3)
C(21)	C(22)	1.370(5)	C(9)	C(14)	C(15)	120.4(3)
C(23)	C(24)	1.521(4)	C(13)	C(14)	C(15)	120.2(3)
C(24)	C(25)	1.495(5)	C(14)	C(15)	C(16)	113.4(3)
			C(7)	C(16)	C(15)	106.6(3)
			N(2)	C(17)	C(18)	121.3(3)
			N(2)	C(17)	C(22)	119.3(3)
			C(18)	C(17)	C(22)	119.4(3)
			C(17)	C(18)	C(19)	120.1(3)
			C(18)	C(19)	C(20)	120.7(3)
			C(19)	C(20)	C(21)	119.5(3)
			C(20)	C(21)	C(22)	120.5(3)
			C(17)	C(22)	C(21)	119.9(3)
			O(1)	C(23)	N(2)	121.6(3)
			O(1)	C(23)	C(24)	122.3(3)
			N(2)	C(23)	C(24)	116.1(3)
			C(23)	C(24)	C(25)	112.7(3)

continued

UM00016695
NOVARTIS EXHIBIT 1517
Novartis v. Regents, IPR2023-01347
Page 3677 of 4460

Table II—Continued

Atom 1	Atom 2	Distance	Atom 1	Atom 2	Atom 3	Angle
			2b			
O(1)	C(23)	1.27(1)	C(3)	N(2)	C(17)	121.0(8)
N(1)	C(1)	1.52(1)	C(3)	N(2)	C(23)	118.0(9)
N(1)	C(5)	1.46(1)	C(17)	N(2)	C(23)	121.0(9)
N(1)	C(7)	1.52(1)	C(1)	N(1)	C(5)	110.6(7)
N(2)	C(3)	1.50(1)	C(1)	N(1)	C(7)	113.5(6)
N(2)	C(17)	1.41(1)	C(5)	N(1)	C(7)	112.8(8)
N(2)	C(23)	1.30(1)	N(1)	C(1)	C(2)	112.6(7)
C(1)	C(2)	1.49(1)	C(1)	C(2)	C(3)	111.3(8)
C(2)	C(3)	1.53(1)	C(1)	C(2)	C(6)	107.9(8)
C(2)	C(6)	1.54(1)	C(3)	C(2)	C(6)	111.5(8)
C(3)	C(4)	1.54(1)	N(2)	C(3)	C(2)	110.3(8)
C(4)	C(5)	1.51(1)	N(2)	C(3)	C(4)	111.0(7)
C(7)	C(8)	1.47(1)	C(2)	C(3)	C(4)	109.6(7)
C(7)	C(16)	1.53(1)	C(3)	C(4)	C(5)	109.5(7)
C(8)	C(9)	1.57(1)	N(1)	C(5)	C(4)	111.4(9)
C(9)	C(10)	1.36(1)	N(1)	C(7)	C(8)	114.9(7)
C(9)	C(14)	1.39(1)	N(1)	C(7)	C(16)	110.7(8)
C(10)	C(11)	1.38(1)	C(8)	C(7)	C(16)	112.2(8)
C(11)	C(12)	1.39(1)	C(7)	C(8)	C(9)	110.4(8)
C(12)	C(13)	1.33(1)	C(8)	C(9)	C(10)	119.1(9)
C(13)	C(14)	1.40(1)	C(8)	C(9)	C(14)	119.3(9)
C(14)	C(15)	1.50(2)	C(10)	C(9)	C(14)	121.7(9)
C(15)	C(16)	1.56(1)	C(9)	C(10)	C(11)	122.(1)
C(17)	C(18)	1.38(1)	C(10)	C(11)	C(12)	116.(1)
C(17)	C(22)	1.34(1)	C(11)	C(12)	C(13)	122.(1)
C(18)	C(19)	1.38(1)	C(12)	C(13)	C(14)	123.(1)
C(19)	C(20)	1.39(1)	C(9)	C(14)	C(13)	115.(1)
C(20)	C(21)	1.41(1)	C(9)	C(14)	C(15)	122.6(9)
C(21)	C(22)	1.37(2)	C(13)	C(14)	C(15)	122.(1)
C(23)	C(24)	1.49(1)	C(14)	C(15)	C(16)	115.2(8)
C(24)	C(25)	1.58(2)	N(2)	C(17)	C(18)	121.(1)
			N(2)	C(17)	C(22)	118.2(9)
			C(18)	C(17)	C(22)	121.(1)
			C(17)	C(18)	C(19)	120.(1)
			C(18)	C(19)	C(20)	120.3(9)
			C(19)	C(20)	C(21)	117.(1)
			C(20)	C(21)	C(22)	122.(1)
			C(17)	C(22)	C(21)	119.5(9)
			O(1)	C(23)	N(2)	121.(1)
			O(1)	C(23)	C(24)	116.(1)
			N(2)	C(23)	C(24)	123.(1)
			C(23)	C(24)	C(25)	109.8(8)

References and Notes

1. Janssen, P. A. J.; Van der Eycken, C. A. M. in "Drugs Affecting the Central Nervous System," vol. 2; A. Burger, Ed.; Marcel Dekker: New York, 1968; chap. 2.
2. Maryanoff, B. E.; Simon, E. J.; Gioannini, T.; Gorissen, H. *J. Med. Chem.* 1982, *25*, 913.
3. Grossman, S.; Moser, U.; Mutschler, E. *Arch. Pharm. (Weinheim, Ger.)* 1978, *311*, 1010.
4. Lobbezoo, M. W.; Soudijn, W.; Van Wijngaarden, I. *Eur. J. Med. Chem.–Chim. Ther.* 1980, *15*, 357.
5. Lobbezzo, M. W.; Soudijn, W.; Van Wijngaarden, I. *J. Med. Chem.* 1981, *24*, 777.
6. Van Bever, W. F. M.; Niemegeers, C. J. E.; Janssen, P. A. J. *J. Med. Chem.* 1974, *17*, 1047.
7. Riley, T. N.; Hale, D. B.; Wilson, M. C. *J. Pharm. Sci.* 1973, *62*, 983.
8. Van Wijngaarden, I.; Soudijn, W. *Life Sci.* 1968, *7*, 1239.
9. Van Bever, W. F. M.; Neimegeers, C. J. E.; Schellekens, K. H. L.; Janssen, P. A. J. *Arzneim.–Forsch.* 1976, *26*, 1548.
10. Helsley, G. C.; Lunsford, D. C.; Welstead, W. J., Jr.; Boswell, R. F., Jr.; Funderburk, W. H.; Johnson, D. N. *J. Med. Chem.* 1969, *12*, 583.
11. Klein, W.; Back, W.; Mutschler, E. *Arch. Pharm. (Weinheim, Ger.)* 1975, *308*, 910.
12. Berger, J. G.; Davidson, F.; Langford, G. E. *J. Med. Chem.* 1977, *20*, 600.
13. Borne, R. F.; Fifer, E. K.; Waters, I. W. *J. Med. Chem.* 1984, *27*, 1271.
14. Borne, R. F.; Law, S.-J.; Kapeghian, J.; Masten, L. W. *J. Pharm. Sci.* 1980, *69*, 1104.
15. Riley, T. N.; Bagley, J. R. *J. Med. Chem.* 1979, *22*, 1167.
16. Fifer, E. K.; Davis, W. M.; Borne, R. F. *Eur. J. Med. Chem.–Chim. Ther.* in press.
17. Maryanoff, B. E.; McComsey, D. F.; Taylor, R. J., Jr.; Gardocki, J. F. *J. Med. Chem.* 1981, *24*, 79.
18. Main, P.; Woolfson, M. M.; Germain, G. *Acta Crystallogr.* 1971, *A27*, 368.
19. Conventional reliability indices $R = \Sigma||F_o| - |F_c||/\Sigma|F_o|$, $R_w = (\Sigma(|F_o| - |F_c|)^2/\Sigma w|F_o|^2)^{1/2}$, where F_o and F_c are observed and calculated structure factors, $w = 1/\sigma(F)^2$, and where $\sigma(F)$ is the estimated SD in F_o.
20. CAD-4 SDP package of computer programs written by B. Frenz (1982).
21. "International Tables for X-Ray Crystallography," vol. 4; Birmingham, England: Kynoch Press, 1974.
22. Observed and calculated structure factors, fractional coordinates for hydrogen atoms, and anistropic thermal parameters have been deposited with the British Lending Division. Copies may be obtained through The Executive Secretary, International Union of Crystallography, 13 White Friar, Chester Ch1 INZ, England.
23. Feinberg, A. P.; Creese, I.; Snyder, S. H. *Proc. Natl. Acad. Sci. U.S.A.* 1976, *73*, 4215.
24. D. Duchamp, the UpJohn Company, provided fractional coordinates of fentanyl citrate.
25. Koch, M. H. J.; DeRanter, C. J.; Rolies, M.; Dideberg, O. *Acta Crystallogr.* 1976, *B32*, 2529.

Acknowledgments

Partial support of this research by the National Institutes of Health (NS19789) is gratefully acknowledged. The authors would like to thank Dr. Dave Duchamp for providing fractional coordinates of fentanyl citrate prior to publication and Cathy Gatchell for recrystallizing the samples.

UM00016696
NOVARTIS EXHIBIT 1517
Novartis v. Regents, IPR2023-01347
Page 3678 of 4460

Best Copy Available

Reprinted with permission by the Publisher. This material is protected by copyright and cannot be further reproduced or stored electronically without publisher permission and payment of a royalty fee for each copy made. All rights reserved.

Journal of Pharmacy (Lahore) (1979), 1(1), 59-66
CODEN: JOUPD7; ISSN: 0253-8288

POLYMORPHISM AND DRUG AVAILABILITY. A REVIEW

N. A. MUZAFFAR AND M. AFZAL SHEIKH
Faculty of Pharmacy, University of the Punjab, Lahore—Pakistan.

POLYMORPHISM AND DRUG AVAILABILITY

Drug availability is the primary concern of every individual concerned with research, design, manufacture or clinical evaluation of drugs. In the field of pharmacy, the term availity, has, however transformed into 'bioavailability' in recent ysars. The American Pharmaceutical Association [1] defines bioavailability as a term used to indicat measurement of both the relative amount of an administered drug that reaches the general circulation and the rate at which it occurs. Bioavailability is controlled by many factors which include the route of administration, dosage form, particle size, and methods of preparation, etc as well as physicochemical properties of the drugs.

In the field of drug design, the consideration of certain physical and chemical parameters is of prime impartanc. Certain physical factors of drugs would play a great role in their bioavailability as well as pharmaceutical manufacture. Polymorphism, if not properly studied and taken into consideration, can bring about a great number of complications during the process of drug design, manufacture or its shelf life. Polymorphism is a possible complication which needs careful and prolonged studies to determine the most suitable polymorphic form for the preparation of a drug dosage form. Polymorphism has been defined by many Workers and summarized by Barth [2] as follows, "Polymorphism includes every possible difference encountered in the crystalline lattice of a substance of constant chemical composition excepting homogeneous deformations."

The polymorphic forms usually but not always belong to different crystal systems. When the change from one polymorphic form to another is reversible, it is said to be enantiotropic. When the transition takes place in one direction only

UM00016697
NOVARTIS EXHIBIT 1517
Novartis v. Regents, IPR2023-01347
Page 3679 of 4460

i.e., from a metstable form to a stable form the change is said to be monotropic [3].

A variety of phenomena often confused with polymorphism may be termed as pseudo-polymorphism. They include desolvation, second order transitions, dynamic isomerism and boundary migration of lattice strain effects [4].

Many substances exist in two or more crystalline forms and are said to be polymorphic. Brandstettr-Kuhnert has stated that about one in every three organic compounds exhibits polymorphic behaviour [5]. The differences are primarily in crystalline structure which give rise to difference in physical properties. The molecules of drugs exhibit different space-lattice arrangements in the crystal from one polymorph to the other, and have physical properties such as density, melting point, dissolution rate, solubility, hardness, crystal shape, crystal habit, friability and optical properties, etc. [6].

At any one temperature and pressure only one crystal form of a drug is stable and any other polymorph existing under these conditions will convert to the stable form and when the conversion, i.e., ti is greater than one day, the polymorph is said to be metastable rather than unstable. Metastable state is one in which equilibrium persists with respect to all but one phase. The molecules in a metastable crystal form are in a high energy level than those in the stable form of the drug, hence, the metastable form has a lower melting point and higher solubility [7].

Dissolution rates and solubilities of 3 polymorphic forms of chloramphenicol palmitate and mefanamic acid were measured [8] and it was suggested that the drugs having free energy content may significantly effect the absorption and resulting blood levels.

When the rate of conversion of a metastable form is so slow as to be negligible, the solubility of the compound will be maximal and will have a faster rate of dissolution and hence absorption. This biopharmacentical property of the metastable polymorphs could be explained for achieving better results in the formulation of drugs, especially in the unit dosage foms of the drugs. An interesting example is that of riboflavin which exists in three metastable forms which differ in thier water solubility. The therapeutic efficacy increases with the increase in solubility [9]. the phenomenon of increased absorption has also been demonstrated by the administration of the two forms of methylprednisolone wherein *in vivo* studies of polymorphic Form II showed 1.7 times higher absorption rate than Form I and *in vitro* dissolution rate was 1.4 times higher [7].

Mesley has confirmed [10] the existence of two species of the low temperature forms (II A and II B) of sulphathiazole postulated

UM00016698
NOVARTIS EXHIBIT 1517
Novartis v. Regents, IPR2023-01347
Page 3680 of 4460

by Moustafa and Carless [11] and by Shenoude [12]. Form II contains a mixture of II A with varying proportion of the other low temperature Form II B. Both Forms II A and the mixture (conveneintly called Form II) can be converted wholly to Form I by heating in an oven at about 180°C. Kuhnert-Brandstatter and Wunsch [13] stated that on long standing Form I usually reverts to the mixture of Forms II A and II B. The same phenomenon takes place in II A over a period of months. Thus it seems probie that the most stable Form of sulphathiazole is the Form II mixture. A study of 16 sulphonamides showed that 8 exhibited polymorphism [14]. Milsovich [15] stated that normal solubility determintions of sulphathiazole showed both forms I and II to have the same solubility.

Different polymorphic forms of drugs having varying and diverse nature have been prepared and utilized in the preparation of pharmaceuticals. There is a wide variety of drugs having different polymorphic forms of varying behaviour. These drugs range from prednisolone and cortisone to asprin which can be prepared in differnet polymopha by using 95 percent alcohol rand n-hexane. The two forms of asprin thus produced have different melting points but the important point is that the form produced form n-hexane dissolves much more quickly.

In certain drugs, the incidence of more than two polymorphic forms is not uncommon. Out of 22 barbiturates and 16 steroids [5], studied to find out the polymorphic behaviour, 11 compounds from each class showed polymorphism. Cortisone acetate and riboflavin also showed more than 2 forms [16]. It has been concluded that there are at least two distinct polymorphic form of sulphathiazole having different lattice strutures which can be distinguished by x-ray diffraction patterns and infrared spectra. After recrystallization from different solvents four polymorphic modifications of sulphanilamide have been obtained and studied [17]. In a screening study of 16 sulphonamides [14] polymorphism was identified in eight compounds and solvates in two compounds. The p-amino group, the acidic N¹-hydrogen atom and the oxygens of the sulphonamides group were found to be involved in various hydrogen-bonding arrangements.

Amorphous & Crystalline Drugs:

A consideration of amorphous and crystalline behaviour of the drugs is also imporatant. Some drugs in addition to showing polymorphic forms may also exist in amorphous as well as crystalline forms. The energy required for a molecule of drug to leave the lattice of its crystal is more than the energy required for a molecule of drug to leave its powder. (6). As such, amorphous form of a compound is always solube than the corresponding crystalline form and therefore may exhibit different therapeutic level.

UM00016699
NOVARTIS EXHIBIT 1517
Novartis v. Regents, IPR2023-01347
Page 3681 of 4460

The structural units of crystalline solids are arranged in fixed geometric patterns or lattices and these units which constitute the crystal structur can be atomic, ionic or molecular. In general, based on the bonding behaviour, ionic and atomic crystals are hard and brittle having higher melting points as compared to molecular crystals which are softer and have lower melting points [18]. The very prominent examples of crystalline and characteristics in drugs are those of Novobiocin [19] and chloramphenicol palmitate [20]. Both these pharmaceutically important antibiotics when administered in crystalline form do not show effective blood levels and hence no biological activity; this is mainly due to the extremely low solubilites of the two drugs. However, their amorphous forms show reasonably good and effective results.

New compounds are sometimes obtained in crystalline forms which are metastable in nature and prove to be so in the final formulation, especially in suspension preparations. Transformations of metastable compounds to more stable forms specially in aquous preparations create considerable changes in the final formulations and cause difficulties in their manufacture. These changes taking place in the liquid preparations include growth in particle size, changes in viscocity, excessive sedimentation and cementation and as such can destroy or deteriorate the product and adversely affect the bio-availability [21].

Drugs as Solvates and Hydrates:

Some drugs when crystallized as hydrates or solvates show definite chemical composition and distinct physical properties. This may be well understood that solvates and hydrates of a compound are not and cannot be represented as the polymorphic forms of that compound. It is not correct to use the term polymorphism or crystal modification to refer to crystals of substances which just represent structures in connection with varying degrees of solvation. [22].

The state of hydration of drugs can affect some physical, chemical and biological properties of drugs. More than often the anhydrous forms of an organic compound is more soluble than the hydrate. Anhydrous and trihydrate forms of ampicillin were studied [23] on dogs as suspension and capsules. The results showed that anhydrous form had better absorption and greater bioavailability than the trihydrate. The hydrates or solvates of such drugs would show comparatively much lesser *in vivo* absorption and *in vitro* dissolution. Prednisolone tert butyl acetate [24] when compressed as tablets and implanted subcutaneously in rats showed the difference between the anhydrous and monoethanol solvate. The solvate showed 4 times higher absorption rate in the animals. A 13.4 percent ethanol-water,

UM00016700
NOVARTIS EXHIBIT 1517
Novartis v. Regents, IPR2023-01347
Page 3682 of 4460

mixture was used to obtain hydarted form of glutethimide having melting point of 68C and was compared with the anhydrous drug having melting point of 83C. For the *in vitro* dissolution behaviour, the anhydrous form was 1.6 times faster in its dissolution as compared to the hydrate [21].

Thermodynamic relationships of methyl prednisolone involving polymorphism and solubility were examined [25] in water, decyl alcohol and dodecyl alcohol at various temperatures. The two forms showed independent solubility ratios in respect of solvents. At room temperatures the activity of the more energetic form II of the drug was found to be about 80 percent greater than that of the more stable form I.

EFFECT OF POLYMORPHISM IN PHARMACEUTICAL PREPARATIONS

(a) Chemical stability:

Different crystalline Phases of the same compound have different chemical stabilities. Corticosteroid suspensions when industrially prepared showed batch to batch difference in their stability. However, an x-ray differaction analysis of the starting raw material disclosed the polymorphic differences and explained the stability behaviour which could be due to the solvents occluded or the absorbed mother liquor [26].

Crystalline potassum penicillin can withstand dry heat for quite some time without considerable decomoposition but amorphous type looses its activity to quite an extent. This property is very important in preparation which require penicillin to be coated or deposited. Penicillin suspension prepared with crystalline powder would be in a much finer state of sub-division with greater stability than those prepared with amorphous powder.

(b) Tablet Compression :

Polymorphism is a function of internal structure of crystals whereas the outer appearance of a crystal is termed as its habit. In the compression of tablets when the major portion or bulk of a formulation is the active ingredient, then all other conditions being equal, the correct choice of right polymorph is the one with a habit that can be compressed easily into tablet form. Different habits of the same compound can create hurdles in each batch when the habit of the drug changes [27].

(c) Particle Size :

Polymorphism can be used in pharmaceutical industry in the preparation of fine particles by using the density difference for enantiotropic polymorph. Different polymorphs of the same compound have different densities and so when one polymorphic form is heated above its conversion temperature to

UM00016701
NOVARTIS EXHIBIT 1517
Novartis v. Regents, IPR2023-01347
Page 3683 of 4460

form another polymorph, strains will be developed in this later polymorphic form on cooling to room temperature. The strains produced in the crystal give rise to fracturing into finer particles. This operation will hold good only when suitable polymorphic forms do exist in a compound and also when repeated temperature cycling would not produce chemical degradation. This method can in certain instances be even more useful and preferentiel over micronization [4].

(d) Polymerization :

Tributylvinylphosphonium [28] bromide exists in three phases out of which phase II is metastable and polymerizes faster than the other two phases. The rapid polymerization is due to steric and collision factors which are governed by crystaline structures.

(e) Suppositories :

Polymorphic changes of a supporting base can lead to absolutely unfit preparation impossible to be used because of its melting behaviour which is the most important characteristic of the suppositories. Theobroma oil which is the most popular and widely used supporting base has three unstable forms which melt at 18, 22 & 28°C and one stable form melting at 34.5°C. An ultimate transformation of unstable form to stable form may take place if the suppositories are left in the moulde for few days. Unnecessary heating of the base at relatively higher temperature and ultimate immediate chilling causes the unstable form to appear. Suppositories so prepared will melt at about 39°C. The overheating of the oil also causes sedimentation of the active ingredient and excessive contraction on chilling bearing a depression in the product. Properly heating the base only a few degrees above its melting point (34.5C) and congealing permits the crystallization nuclei of the more stable, bigger and suitable form crystals to remain in the liquid. This on chilling encouragas further crystallization of crystals [2].

(f) Parenteral Preparations :

The polymorphic behaviour of drugs also plays a big role in the absorption rates of parenteral preparations. The differences in water solubilities cause pronounced effects on the absorption rates and change the entire expected bioavailability. Examples of compounds like methylprednisolone, glutethimide, novobiocin, ampicillin and different hormones have been cited invariably wherein polymorphism plays a big role. Crystal growth not only effects the oral preparations but can also cause difficulties in parenteral products specially the problem of syringability.

(g) Solution & Mixtures :

In solution or mixture type of pharmaceuticals, the primary consideration should be to determine the solubility of the drug in the vehicle. A thermodynamically unstable formulation will result if a metastable form

UM00016702
NOVARTIS EXHIBIT 1517
Novartis v. Regents, IPR2023-01347
Page 3684 of 4460

of the drug is used and if the quantity of the drug in the system exceeds the equilibrium. Solubility determinations for this class of preparations should be made with a most stable as well as most soluble form The most soluble form may not necessarily be most stable. Chance nucleation of the stable form may however quickly result in recrystallization. Steroidal drugs which are sparingly water soluble frequently cause such problems. These problems [4] can be minimised by formulating the drug with a suitable cosolvent.

(h) Creams Suspensions :

Certain suspensions of cortisone acetate polymorphs were prepared and it was found that a physically stable aqueous suspension is difficult to make ; crystal growth of the durg occured invariably with subsequent caking and sedimentation.

Polymorphic behaviour in the case of pharmaceutical creams is not very different from that of suspensions wherein a phase inversion takes place from that of metastable to a stable form resulting in crystal growth and the vehicle yielding gritty unac ceptable cream. Unevenly distributed active ingredient proves that an undesirable polymorphic form of the drug has been used. The best method to avoid such a performance is to choose the polymorphic phase which is least soulble in the base. However, if the phase conversion is very slow, a more soluble, metastable form can safely be used.

The transformation from metastable to stable form is a rather tricky point and can only be detected through or thorough and complete study of product formulation and stability. They are difficult to predict in the earlier stages and can be detected after x-ray differaction, hot stage microscopy, differenential thermal analysis and other appropriate techniques.

References.

[1] American Pharmaceutical Association Academy of Pharmaceutical Sciences, Washington, D.C. "Guidelines for Pharmaceutical Studies in Man", Ist. Ed. (1972).

[2.] Barth, J.F.W., Amer. J. Sc. (Fifth Series), 27 273 (1934).

[3.] Martin, A.N., Swarbrick. J., and Commarata, A., "Physical Pharmacy", 2nd Ed., Lea and Fabiger, Philadelphia, Pa. (1969).

[4.] Haleblian, J., and Mc Crone, W., J. Pharm. Sci. 58.8, 911, (1957).

[5.] Brandstattar-Kuhnert, M., Ost. Apoth. Ztg., 13 (19), 297 (1959).

[6.] Marson, S.M., and Prutton, C.F., "Principles of Physical Chemistry", 3rd Ed., Mac Millan Co., New York. N.V. (1959).

[7.] Gibaldi, M., "Introduction to Biopharmaceutics", Lea and Febiger, Philadelphia (1971).

[8.] Aguiar, A.J., and Zelmer, J.E., "Dissolution behaviour of Polymorphs of Chloramphenical Palmitate and Mefenamic Acid", J. Pharm Sci., 58 8, 983-987 (1969),

[9.] Dale, J.K., "Crystalline form of Riboflavin", U.S. Patent 2603633 1952 through Lachman, L., Lieberman, H.A., and Kanig, J.L, "Theory and Practice of Industrial Pharmacy", Lea & Febiger, Philadelphia (1970).

UM00016703
NOVARTIS EXHIBIT 1517
Novartis v. Regents, IPR2023-01347
Page 3685 of 4460

[10]. Mesley, R.J., J. Pharm. Pharmacol., 23, 687 (1973).

[11.] Moustafa, M.A., and Carless, J.E., J. Pharm. Pharmacol., 21, 359 (1969).

[12.] Shenouda, L.S., J. Pharm. Sc., 59, 785 (1970).

[13.] Kuhnert-Brandstatter, M., and Wunsch, S., Mikrochim Acta, 1297 (1969.)

[14.] Yang, S.S., and Guillory, J.K., "Polymorphism in Sulfonamides", J. Pharm. Sc., 61,1, 26 (1972).

[15.] Milsovich, G., J. Pharm. Sc., 53, 484 (1964).

[16.] Callow, R.K., and Kennard, O., "Polymorphism of Cortison Acetate", J. Pharmacol 13, 723 (1961).

[17] Lin. H.O., and Guillory, J.K., "Polymorphism in Sulfonamides-d" 4; J. Pharm. Sc., 59, 7, 972 (1970).

[18] Van Hook, A., "Crystallization, Theory and Practice", Reinhold Publishing Corp., New York, N.V. (1963).

[19.] Mullins, J.D. and Macek, T.J., J. Pharm. Sc, 49, 245 (1960).

[20]. Cadwallador, D.E., "Biopharmaceutics and Drug Interaction" 1st. Ed, Roch Laboratories, Nutley, J.J (1971).

[21.] Remingtons "Practice Book of Pharmaceutical Science", XIV Ed., (1970).

[22] Waldmann, H., "Alleged Polymorphism in Chlordiazepoxide Hydrochloride", Canad. J. Pharm. Sc., 6, 3 (1971).

[23] Poole, J.W., Owens, G., Silverin, j., Freyhof, J and Rosenman, S.B., Current Therap Res., 10, 292 (1968).

[24.] Ballard, B.E., and Biles., Steroids, 4, 273 (1964).

[25] Higuchi, W.I., Lau, P.K., Higuchi, I., Shell, J.W., "Polymorphism and Drug Availability", Solubility Relationships in the Methylprednisolone System, j. Pharm. Sc., 52, 150 (1963).

[26.] Macek, T.J., U.S. Pat. 2671750, (1954)

[27.] Shell, J., J. Pharm. Sc., 52, 100 (1963).

[28.] Haimahon, C., and Grabar, D., J. Polymer. Sc. C., 4, 849 (1964).

UM00016704
NOVARTIS EXHIBIT 1517
Novartis v. Regents, IPR2023-01347
Page 3686 of 4460

Available online at www.sciencedirect.com
SCIENCE DIRECT®
Tetrahedron: Asymmetry 15 (2004) 3811–3815
Tetrahedron: Asymmetry

Synthesis and determination of the absolute stereochemistry of the enantiomers of adrafinil and modafinil

Antonio Osorio-Lozada, Thomas Prisinzano and Horacio F. Olivo*

Division of Medicinal & Natural Products Chemistry, College of Pharmacy, The University of Iowa, Iowa City, IA 52242-1112, USA

Received 7 October 2004; accepted 15 October 2004

Abstract—Both enantiomers of modafinil, adrafinil, modafinic acid and ethyl modafinate were prepared from the diastereomers formed by reacting racemic β-sulfinyl carboxylic acid with (4*R*)-phenyl-thiazolidinethione. The absolute stereochemistry of the sulfoxide group was confirmed via X-ray analysis of one of the thiazolidinethione diastereomers.
© 2004 Elsevier Ltd. All rights reserved.

1. Introduction

Modafinil [Provigil] (±)-**1** is a psychostimulant used in the treatment of narcolepsy.[1] Adrafinil [Olmifon] (±)-**2**, the hydroxamic acid derivative of modafinil, is currently in phase III clinical trials for the same disorder. Recent work has suggested that **1** and **2** might also be effective treatments for ADHD as well as treating opioid-induced sedation.[2,3] The exact mechanisms through which (±)-**1** and (±)-**2** exert their effects are currently unclear. However, its mechanism of action appears different from that of other CNS stimulants such as *d*-amphetamine.[4–6] Given their unique pharmacological properties, clinical work has begun to explore the utility of these agents as pharmacological treatments for stimulant dependence.[7]

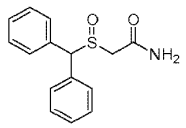

Modafinil **1**

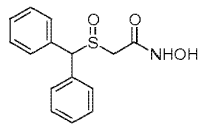

Adrafinil **2**

Modafinil **1** and adrafinil **2** each possess a stereogenic sulfoxide group, however, they are marketed as racemic materials. Recently, Prisinzano et al. reported the diastereomeric salt resolution of a β-sulfinyl carboxylic acid with each of the two enantiomers of α-methylbenzylamine.[8] This method provided the enantiomeric forms of β-sulfinyl carboxylic acid **4** in less than 21% yield and 44%, respectively. In order to improve the preparation of both enantiomeric forms of modafinil and adrafinil, we selected a chiral thiazolidinethione auxiliary to carry out a chemical resolution of the β-sulfinyl carboxylic acid. The chiral auxiliary was selected to provide two enantiomerically pure synthetic intermediates in one single operation. Herein, we report our results and also confirm the absolute stereochemistry of the enantiomeric forms via X-ray analysis of one of the diastereomeric thiazolidinethione derivatives.

2. Results and discussion

We selected an aminoacid-derived thiazolidinethione as the chiral auxiliary for the resolution of a racemic mixture of β-sulfinyl carboxylic acid **4** based on our experience with these versatile molecules (Scheme 1).[9] Diastereomeric mixtures with chiral thiazolidinethiones can be easily separated by column chromatography because of their different R_f values, their yellow colour and also the ability to recycle the silica gel. These chiral auxiliaries have also proved superior to others, because they are easily displaced by several nucleophilic reagents.[10]

Chiral thiazolidinethione auxiliary (−)-**3**,[11] derived from phenyl glycine, was coupled with racemic sulfinyl carboxylic acid **4** (Scheme 1),[12,13] and the two diastereomeric

* Corresponding author. Tel.: +1 319 335 8849; fax: +1 319 335 8766; e-mail: horacio-olivo@uiowa.edu

0957-4166/$ - see front matter © 2004 Elsevier Ltd. All rights reserved.
doi:10.1016/j.tetasy.2004.10.019

UM00016705
NOVARTIS EXHIBIT 1517
Novartis v. Regents, IPR2023-01347
Page 3687 of 4460

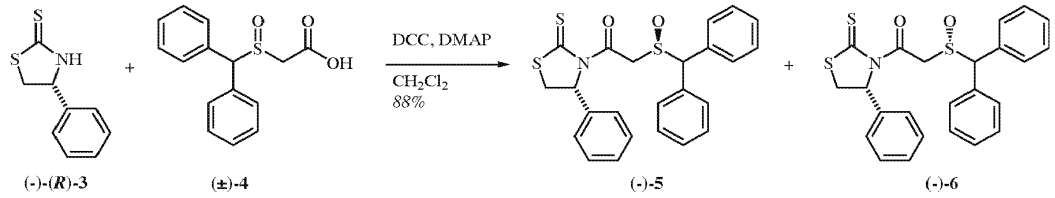

Scheme 1. Resolution of β-sulfinyl carboxylic acid **4**.

products were easily separated by column chromatography. An X-ray crystallographic analysis of diastereomer (−)-**5** showed the absolute stereochemistry of the sulfinyl group to be *R* (Fig. 1).[14] Thus, the stereochemistries of the sulfinyl groups in the two diastereomers were unequivocally assigned as illustrated in Scheme 1.

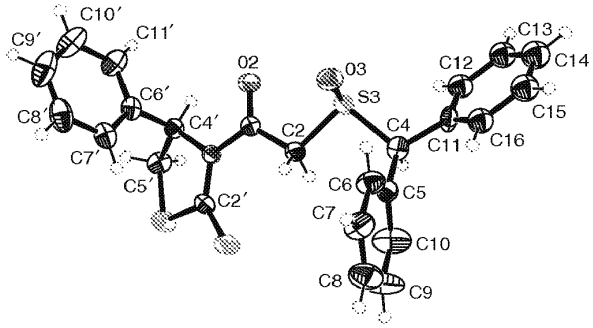

Figure 1. X-ray crystal structure of compound (−)-**5**.

With both diastereomers in hand, our efforts shifted to the preparation of adrafinil. Diastereomeric thiazolidinethione **5** was treated with a solution containing a mixture of chloroform–methanol and ammonium hydroxide (78:20:2) (Scheme 2). The reaction was monitored by TLC; when no more starting material was observed, the solvent was evaporated and the resulting mixture of chiral auxiliary and modafinil separated by silica gel column chromatography. Modafinil (−)-(*R*)-**1** was obtained in very good yield while chiral thiazolidinethione was also recovered. The same thiazolidinethione **5** was then treated with hydroxylamine hydrochloride to yield adrafinil (+)-(*R*)-**2** in 91% yield. It is noteworthy that this method provides the desired targets directly from the diastereomeric thiazolidinethiones and the chiral auxiliaries can be recovered and recycled. Thiazolidinethione **5** was also hydrolyzed and esterified to show its synthetic versatility. Adrafinil (+)-(*R*)-**2** was also obtained from ethyl modafinate (−)-(*R*)-**7** in moderate yield (75%).

In the same manner, the addition of ammonia to diastereomeric thiazolidinethione **6** yielded modafinil (+)-(*S*)-**1**, while the addition of hydroxylamine to compound **6** furnished adrafinil (−)-(*S*)-**2**, both in excellent yields (Scheme 3). Hydrolysis of thiazolidinethione **6** delivered

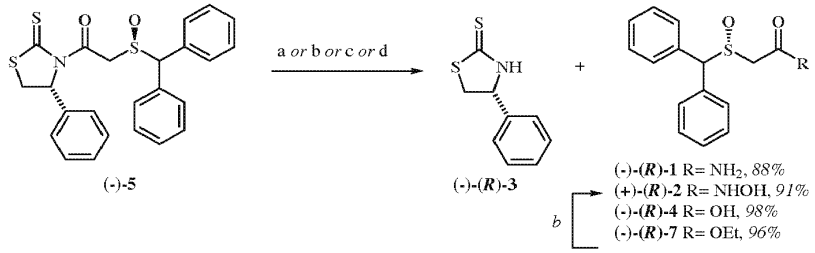

Scheme 2. Synthesis of (*R*)-modafinil and (*R*)-adrafinil. Reagents: (a) $CHCl_3$–MeOH–NH_4OH (78:20:2); (b) NH_2OH–HCl, Et_3N, THF–H_2O; (c) LiOH, THF–H_2O; (d) DCC, EtOH.

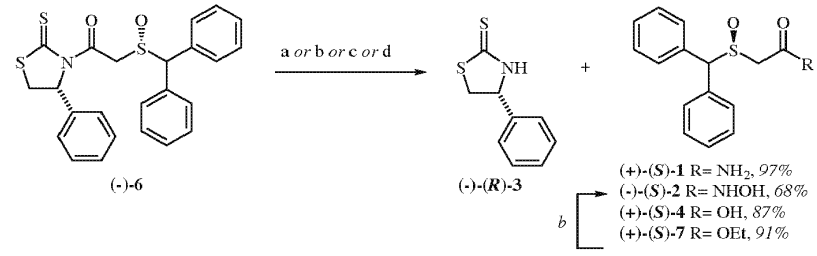

Scheme 3. Synthesis of (*S*)-modafinil and (*S*)-adrafinil. Reagents: (a) NH_4OH–MeOH–$CHCl_3$ (78:20:2); (b) NH_2OH–HCl, Et_3N, THF–H_2O; (c) LiOH, THF–H_2O; (d) DCC, EtOH.

UM00016706
NOVARTIS EXHIBIT 1517
Novartis v. Regents, IPR2023-01347
Page 3688 of 4460

modafinic acid (+)-(*S*)-**7**, and esterification furnished ethyl modafinate (+)-(*S*)-**7**.

3. Conclusions

In summary, we have prepared both enantiomers of modafinil, adrafinil, modafinic acid and ethyl modafinate employing a chemical resolution of a diastereomeric mixture formed by reacting racemic β-sulfinyl carboxylic acid with a chiral thiazolidinethione. The absolute stereochemistry of the sulfoxide group was confirmed via X-ray analysis of one of the thiazolidinethione diastereomers. Thiazolidinethiones were shown to be easily displaced by ammonia and hydroxylamine providing modafinil and adrafinil in one operation. This strategy will be useful to prepare other analogues to further explore the pharmacological activity of these compounds. The biological evaluation of these single enantiomeric compounds is currently underway and will be reported in due course.

4. Experimental

4.1. General remarks

Melting points were determined on Thomas Hoover apparatus. Optical rotations were measured on a Jasco P-1020 polarimeter at room temperature. NMR spectra were recorded in a Bruker Avance-300 spectrometer. IR spectra were recorded on a Nicolet-210 spectrophotometer. HRMS was conducted by Dr. Blake Watkins at the University of Mississippi.

4.2. Coupling of thiazolidinethione 3 and carboxylic acid 4

A solution of (−)-(*R*)-phenylthiazolidinethione (410.2 mg, 2.1 mmol) in dichloromethane (15 mL) was treated with racemic modafinic acid (548.6 mg, 2.0 mmol). 4-Dimethylaminopyridine (45 mg, 0.37 mmol) and 1,3-dicyclohexylcarbodiimide (454 mg, 2.2 mmol) were then added under a nitrogen atmosphere. The solution was stirred overnight. The reaction was quenched with a 2 M solution of hydrochloric acid (20 mL) and extracted with diethyl ether (2 × 25 mL). The combined organic layers were washed with a satd solution of $NaHCO_3$ and brine, dried over Na_2SO_4, filtered and concentrated. The residue was purified by chromatography on silica gel (5 × 13 cm) eluting with petroleum ether–ethyl acetate (3:2). Thiazolidinethione **5** was obtained as a yellow solid: 403 mg (44.5% yield) with thiazolidinethione **6** was obtained as a yellow foam: 395 mg (43.5% yield).

4.2.1. (−)-[(4*R*)-Phenyl-2-thioxo-thazolidine-3-yl]-(*R*)-(diphenylmethanesulfinyl)acetamide (−)-5. R_f 0.38 (3:2, petroleum ether/ethyl acetate); mp 134–136 °C (dec); $[\alpha]_D^{22} = -230.4$ (*c* 0.99, $CHCl_3$); ^1H NMR ($CDCl_3$): δ 7.53–7.27 (15H, m), 6.13 (1H, dd, $J = 8.1$, 1.2 Hz), 5.20 (1H, s), 5.10 (1H, d, $J = 14.2$ Hz), 4.13 (1H, d, $J = 14.2$ Hz), 3.93 (1H, dd, $J = 11.2$, 8.1 Hz), 3.09 (1H, dd, $J = 11.2$, 1.2 Hz); ^{13}C NMR ($CDCl_3$): δ 202.7 (C), 165.4 (C), 138.5 (C), 135.3 (C), 134.1 (C), 129.65 (2CH), 129.29 (2CH), 129.16 (2CH), 129.07 (2CH), 128.93 (2CH), 128.72 (CH), 128.67 (CH), 128.57 (CH), 125.4 (2CH), 71.8 (CH), 69.71 (CH), 57.5 (CH_2), 37.2 (CH_2); IR *v* 1677, 1495, 1450, 1357, 1304, 1248, 1170, 1158, 1045 cm^{-1}; ES HRMS *m/z* $(M+H)^+$ calcd 452.0813, obsd 452.0821.

4.2.2. (−)-[(4*R*)-Phenyl-2-thioxo-thazolidine-3-yl]-(*S*)-(diphenylmethanesulfinyl)acetamide (−)-6. R_f 0.24 (3:2, petroleum ether/ethyl acetate); mp 69 °C (dec); $[\alpha]_D^{22} = -216.5$ (*c* 1.0, $CHCl_3$); ^1H NMR ($CDCl_3$): δ 7.49–7.29 (15H, m), 6.17 (1H, d, $J = 8.1$ Hz), 5.07 (1H, s), 4.55 (1H, d, $J = 16.0$ Hz), 4.28 (1H, d, $J = 16.0$ Hz), 3.96 (1H, dd, $J = 11.2$, 8.1 Hz), 3.09 (1H, dd, $J = 11.2$, 1.1 Hz); ^{13}C NMR ($CDCl_3$): δ 202.6 (C), 165.8 (C), 138.5 (C), 135.7 (C), 133.9 (C), 129.77 (2CH), 129.40 (2CH), 129.23 (2CH), 129.01 (2CH), 128.94 (2CH), 128.89 (CH), 128.77 (CH), 128.61 (CH), 125.7 (2CH), 71.5 (CH), 69.6 (CH), 59.7 (CH_2), 37.3 (CH_2); IR *v* 3063, 3028, 3004, 1694, 1495, 1451, 1299, 1160, 1046, 743, 697 cm^{-1}; ES HRMS *m/z* $(M+H)^+$ calcd 452.0813, obsd 452.0818.

4.2.3. (−)-(*R*)-(Diphenylmethanesulfinyl)acetamide (−)-(*R*)-1. A mixture of chloroform–methanol, ammonium hydroxide (78:20:2, 5 mL) was added directly to thiazolidinethione (−)-**5** (179 mg, 0.396 mmol). The solution was stirred until the yellow colour disappeared and TLC did not show the presence of starting material. The solvent was evaporated and the residue purified by column chromatography (2.5 × 12.5 cm) eluting with a gradient of 1–4% methanol in dichloromethane. Modafinil was obtained as a white solid: 95 mg (88% yield). R_f 0.30 (5% methanol in dichloromethane); mp 158–159 °C; $[\alpha]_D^{22} = -79$ (*c* 1.0, $CHCl_3$); ^1H NMR ($CDCl_3$): δ 7.51–7.48 (2H, m), 7.45–7.32 (8H, m), 7.07 (1H, br s), 5.88 (1H, br s), 5.24 (1H, s), 3.47 (1H, d, $J = 14.2$ Hz), 3.14 (1H, d, $J = 14.2$ Hz); ^{13}C NMR ($CDCl_3$): δ 166.5 (C), 134.7 (C), 134.3 (C), 129.62 (2CH), 129.58 (2CH), 129.1 (2CH), 128.98 (3CH), 128.8 (CH), 71.6 (CH), 52.0 (CH_2); IR 3383, 3314, 3257, 3191, 1690, 1617, 1495, 1376, 1027, 702 cm^{-1}; ES HRMS *m/z* $(M+Na)^+$ calcd 296.0721, obsd 296.0713.

4.2.4. (+)-(*S*)-(Diphenylmethanesulfinyl)acetamide (+)-(*S*)-1. The title compound was obtained in 97% yield from compound (−)-**6** following the same procedure as above. $[\alpha]_D^{22} = +81$ (*c* 1.0, $CHCl_3$).

4.2.5. (+)-(*R*)-(Diphenylmethanesulfinyl)acetohydroxamic acid (+)-(*R*)-2. To a solution of hydroxylamine-hydrochloride (578.6 mg, 8.3 mmol) in a mixture of THF–H_2O (10 mL, 5:1) was added triethylamine (1.5 mL, 10.7 mmol). The mixture was stirred for 15 min, filtered through a small plug of cotton and added to a solution of thiazolidinethione (−)-**5** (376.1 mg, 0.83 mmol). The solution was stirred until no more starting material was observed by TLC. The solution was concentrated and the residue purified by column chromatography on silica gel (2 × 13 cm), eluting with a gradient using 2–6% methanol in dichloromethane. Adrafinil was

UM00016707
NOVARTIS EXHIBIT 1517
Novartis v. Regents, IPR2023-01347
Page 3689 of 4460

isolated as a slightly brown solid: 218.5 mg (91% yield). R_f 0.42 (10% MeOH in $CHCl_3$); mp 159–160 °C; $[\alpha]_D^{22} = +14$ (*c* 0.85, CH_3OH); ^1H NMR (CD_3OD): δ 7.56–7.51 (4H, m), 7.44–7.32 (6H, m), 5.40 (1H, s), 3.41 (1H, d, $J = 13.7$ Hz), 3.23 (1H, d, $J = 13.7$ Hz); ^{13}C NMR (CD_3OD): δ 163.5 (CO), 137.2 (C), 135.6 (C), 130.9 (2CH), 130.3 (2CH), 129.9 (2CH), 129.8 (2CH), 129.6 (2CH), 72.1 (CH), 54.0 (CH_2); IR 3209, 3027, 1686, 1656, 1496, 1451, 1061, 1005, 703 cm^{-1}; ES HRMS *m/z* $(M+Na)^+$ calcd 312.0670, obsd 312.0659.

4.2.6. (−)-(*S*)-(Diphenylmethanesulfinyl)acetohydroxamic acid (−)-(*S*)-2. The title compound was obtained in 98% yield from compound (−)-**6** following the same procedure as above. $[\alpha]_D^{22} = -14$ (*c* 1.0, CH_3OH).

4.2.7. (−)-(*R*)-(Diphenylmethanesulfinyl)acetic acid (−)-(*R*)-4. A 0.1 M THF/H_2O (2.5:1) solution of LiOH (15 mL, 1.5 mmol) was added to thiazolidinethione imide (−)-**5** (180 mg, 0.398 mmol) at 0 °C. The solution was then stirred at room temperature until no imide was observed by TLC. Water (15 mL) was added to solution and washed with dichloromethane (4 × 10 mL). The aqueous solution was acidified (1 mL of concd HCl) and extracted with ethyl acetate (2 × 25 mL). The organic layer was dried over Na_2SO_4, filtered and concentrated. The title compound was obtained as an amorphous solid: 105 mg (96% yield). R_f 0.21 (10% MeOH in $CHCl_3$); mp 118–120 °C; $[\alpha]_D^{22} = -41.7$ (*c* 0.85, CH_3OH); ^1H NMR ($CDCl_3$): δ 7.56–7.51 (4H, m), 7.44–7.32 (6H, m), 5.40 (1H, s), 3.41 (1H, d, $J = 13.7$ Hz), 3.23 (1H, d, $J = 13.7$ Hz); ^{13}C NMR (acetone-d_6): δ 167.3 (CO), 137.6 (C), 135.8 (C), 129.8 (2CH), 129.1 (2CH), 128.7 (2CH), 128.5 (2CH), 128.2 (CH), 128.1 (CH), 71.4 (CH), 55.4 (CH_2); IR 2925, 2778, 2527, 1716, 1500, 1451, 1287, 1187, 1016, 750, 704 cm^{-1}; ES HRMS *m/z* $(M+Na)^+$ calcd 297.0561, obsd 297.0559.

4.2.8. (+)-(*S*)-(Diphenylmethanesulfinyl)acetic acid (+)-(*S*)-4. The title compound was obtained in 87% yield from compound (−)-**6** following the same procedure as above. $[\alpha]_D^{22} = +39.3$ (*c* 1.0, CH_3OH).

4.2.9. (−)-(*R*)-Ethyl (diphenylmethanesulfinyl)acetate (−)-(*R*)-7. A solution of thiazolidinethione imide (−)-**5** (242 mg, 0.53 mmol) in ethanol (10 mL), was treated with dicyclohexylcarbodiimide (166.2 mg, 0.80 mmol) and 4-dimethylaminopyridine (6 mg, 0.05 mmol). The solution was stirred until the yellow colour disappeared and TLC showed no more starting material. The solvent was evaporated, and the residue purified by column chromatography on silica gel (2 × 12 cm), eluting with petroleum ether–ethyl acetate (55:45). The ethyl ester (−)-**7** was eluted after the phenyl-thiazolidinethione and obtained as a white paste: 158.4 mg (98% yield). R_f 0.23 (7:3, petroleum ether–ethyl acetate); mp 84–85 °C; $[\alpha]_D^{22} = -58.5$ (*c* 0.85, $CHCl_3$); ^1H NMR ($CDCl_3$): δ 7.52–7.46 (4H, m), 7.43–7.30 (6H, m), 5.20 (1H, s), 4.20 (2H, q, $J = 7.2$ Hz), 3.51 (1H, d, $J = 14.0$ Hz), 3.99 (1H, d, $J = 14.0$ Hz), 1.28 (3H, t, $J = 7.2$ Hz); ^{13}C NMR (CD_3OD): δ 165.5 (CO), 135.5 (C), 134.0 (C), 129.8 (2CH), 129.4 (2CH), 128.9 (4CH), 128.7 (CH), 128.6 (CH), 71.6 (CH), 62.2 (CH_2), 54.4 (CH_2), 14.2 (CH_3); IR 3061, 3029, 2983, 2932, 1732, 1495, 1451, 1286, 1053 cm^{-1}; ES HRMS *m/z* $(M+Na)^+$ calcd 325.0874, obsd 325.0874.

4.2.10. (+)-(*S*)-Ethyl (diphenylmethanesulfinyl)acetate (+)-(*S*)-7. The title compound was obtained in 87% yield from compound (−)-**6** following the same procedure as above. $[\alpha]_D^{22} = +56.2$ (*c* 1.0, $CHCl_3$).

Acknowledgements

Financial support for this work was provided by the National Science Foundation (CHE-0111292 and EEC-0310689). We thank Mr. John Podobinski for the preparation of compound **4** and Dr. Dale Swenson for obtaining the crystallographic analysis of compound (−)-**5**. We are indebted to Dr. Blake Watkins (University of Mississippi) for obtaining all the HRMS.

References

1. Teitelman, E. *Am. J. Psychiat.* **2001**, *158*, 970–971.
2. (a) Pliszka, S. R. *CNS Spectr.* **2003**, *8*, 253–258; (b) Spencer, T.; Biederman, J. *J. Atten. Disord.* **2002**, *6*(Suppl. 1), S109–S119; (c) Webster, L.; Andrews, M.; Stoddard, G. *Pain Med.* **2003**, *4*, 135–140.
3. (a) Gold, L. H.; Balster, R. L. *Psychopharmacology* **1996**, *126*, 286–292; (b) Teitelman, E. *Am. J. Psychiat.* **2001**, *158*, 1341.
4. Ferraro, L.; Antonelli, T.; O'Connor, W. T.; Tanganelli, S.; Rambert, F. A.; Fuxe, K. *Biol. Psychiat.* **1997**, *42*, 1181–1183.
5. Mignot, E.; Nishino, S.; Guilleminault, C.; Dement, W. C. *Sleep* **1994**, *17*, 436–437.
6. (a) Ferraro, L.; Antonelli, T.; O'Connor, W. T.; Tanganelli, S.; Rambert, F.; Fuxe, K. *Neuroreport* **1997**, *8*, 2883–2887; (b) Ferraro, L.; Fuxe, K.; Tanganelli, S.; Fernandez, M.; Rambert, F. A.; Antonelli, T. *Neuropharmacology* **2000**, *39*, 1974–1983.
7. (a) Malcolm, R.; Book, S. W.; Moak, D.; DeVane, L.; Czepowicz, V. *Am. J. Addict.* **2002**, *11*, 247–249; (b) Dackis, C. A.; Lynch, K. G.; Yu, E.; Samaha, F. F.; Kampman, K. M., et al. *Drug Alcohol Depend.* **2003**, *70*, 29–37; (c) Camacho, A.; Stein, M. B. *Am. J. Psychiat.* **2002**, *159*, 1947–1948.
8. (a) Prisinzano, T.; Podobinski, J.; Tidgewell, K.; Luo, M.; Swenson, D. *Tetrahedron: Asymmetry* **2004**, *15*, 1053–1058; For a racemic synthesis of modafinil, see: (b) Chatterjie, N.; Stables, J. P.; Wang, H.; Alexander, G. J. *Neurochem. Res.* **2004**, *29*, 1481–1486.
9. (a) Velázquez, F.; Olivo, H. F. *Curr. Org. Chem.* **2002**, *6*, 303–340; (b) Romero-Ortega, M.; Colby, D. A.; Olivo, H. F. *Tetrahedron Lett.* **2002**, *43*, 6439–6441; (c) Hodge, M. B.; Olivo, H. F. *Tetrahedron* **2004**, *60*, 9397–9403.
10. (a) Wu, Y.; Sun, Y.-P.; Yang, Y.-Q.; Hu, Q.; Zhang, Q. *J. Org. Chem.* **2004**, *69*, 6141–6144; (b) Smith, T. E.; Djang, M.; Velander, A. J.; Downey, C. W.; Carroll, K. A.; van Alphen, S. *Org. Lett.* **2004**, *6*, 2317–2320; (c) Crimmins, M. T.; Siliphaivanh, P. *Org. Lett.* **2003**, *5*, 4641–4644; (d) Crimmins, M. T.; Chaudhary, K. *Org. Lett.* **2000**, *2*, 775–777.

UM00016708
NOVARTIS EXHIBIT 1517
Novartis v. Regents, IPR2023-01347
Page 3690 of 4460

11. (a) Delaunay, D.; Toupet, L.; Le Corre, M. *J. Org. Chem.* **1995**, *60*, 6604–6607; (b) Wu, Y.; Yang, Y.-Q.; Hu, Q. *J. Org. Chem.* **2004**, *69*, 3990–3992.
12. Andrade, C. K. Z.; Rocha, R. O.; Vercillo, O. E.; Silva, W. A.; Matos, R. A. F. *Synlett* **2003**, 2351–2352.
13. Nagao, Y.; Miyamoto, S.; Hayashi, K.; Mihira, A.; Sano, S. *Chem. Pharm. Bull.* **2002**, *50*, 558–562.
14. CCDC 245174 contains the supplementary crystallographic data for this paper. These data can be obtained free of charge via www.ccdc.cam.ac.uk/data_request/cif, by emailing data_request@ccdc.cam.ac.uk, or by contacting The Cambridge Crystallographic Data Centre, 12, Union Road, Cambridge CB2 1EZ, UK; fax: +44 1223 336033.

UM00016709
NOVARTIS EXHIBIT 1517
Novartis v. Regents, IPR2023-01347
Page 3691 of 4460

Acta Crystallographica Section B
Structural
Science
ISSN 0108-7681

The formation of paracetamol (acetaminophen) adducts with hydrogen-bond acceptors

Iain D. H. Oswald,[a] David R. Allan,[b] Pamela A. McGregor,[b] W. D. Samuel Motherwell,[c] Simon Parsons[a]* and Colin R. Pulham[a]

[a]School of Chemistry, The University of Edinburgh, King's Buildings, West Mains Road, Edinburgh EH9 3JJ, UK, [b]School of Physics and Astronomy, The University of Edinburgh, King's Buildings, West Mains Road, Edinburgh EH9 3JZ, UK, and [c]Cambridge Crystallographic Data Centre, 12 Union Road, Cambridge CB2 1EZ, UK

Correspondence e-mail: s.parsons@ed.ac.uk

Received 29 July 2002
Accepted 4 September 2002

The crystal structures of five hemiadducts of paracetamol with 1,4-dioxane, *N*-methylmorpholine, morpholine, *N*,*N*-dimethylpiperazine and piperazine and a related 1:1 adduct of paracetamol with 4,4′-bipyridine are described. All structures are characterized by the formation of chains of paracetamol molecules, which are linked *via* either OH···O=C interactions [*C*(9) chains in graph-set notation] or NH···O=C interactions [*C*(4) chains], depending on the presence or absence of substituent groups on the guest molecule. In all cases except for the morpholine and bipyridine adducts these chains are connected by hydrogen-bond interactions with the guest molecules, which reside on crystallographic inversion centres. In the bipyridine adduct this linkage also involves a π-stacking interaction; in the morpholine adduct it is formed between the OH groups of two opposed paracetamol molecules. Most adducts (that with 4,4′-bipyridine is an exception) decompose on heating to give monoclinic paracetamol. This is the first systematic study of a series of co-crystals containing paracetamol.

1. Introduction

There have been a number of detailed studies on the polymorphic behaviour of paracetamol (acetaminophen, *p*-hydroxylacetanilide or Tylenol). Form I, which is monoclinic, was first characterized by Haisa *et al.* (1976), and has since been shown to be the thermodynamically more stable form. Form II is orthorhombic and was also described by Haisa *et al.* in 1974 (Haisa *et al.*, 1974). The orthorhombic form can be grown using a single orthorhombic crystal as a seed from a super-saturated aqueous solution of paracetamol. This method, however, can result in the crystals changing to the monoclinic form if left in contact with the solution for any length of time (Nichols & Frampton, 1998). The same authors showed that the only method that gives the orthorhombic polymorph reproducibly is growth from the melt. They also showed that this form is stable if dried and stored in a stoppered vial and that neither grinding nor compression induces a transition to the monoclinic form. In a very careful study, Boldyreva *et al.* (2000) have shown that application of hydrostatic pressures up to 4.2 GPa does not induce a transition from the monoclinic to the orthorhombic form. The behaviour of the orthorhombic form is of interest for its ability to undergo plastic deformation when compressed, thereby facilitating the production of tablets of paracetamol.

With the exception of our own recent report of paracetamol trihydrate (McGregor *et al.*, 2002), little structural work appears to have been carried out on solvates or other co-crystals of paracetamol, although a thermochemical study showed the existence of a hemisolvate of paracetamol with

© 2002 International Union of Crystallography
Printed in Great Britain – all rights reserved

UM00016710
NOVARTIS EXHIBIT 1517
Novartis v. Regents, IPR2023-01347
Page 3692 of 4460

XP009014505

1,4-dioxane (Fachaux *et al.*, 1995). In this report, we describe the preparation and characterization of six new adducts of paracetamol with 1,4-dioxane, 4,4′-bipyridine, *N*-methylmorpholine, *N*,*N*-dimethylpiperazine, morpholine and pip razine (these are referred to as *guest molecules* below; see Schemes). All these molecules, except for morph line, can be considered to be at least pseudo-centrosymmetric with respect to their hydrogen-bonding properties.

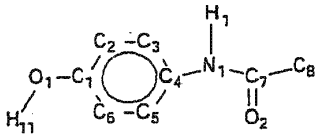

Paracetamol, with atomic numbering scheme.

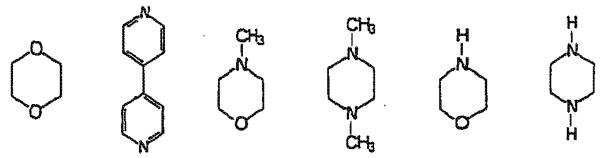

Guest molecules used to form adducts with paracetamol. Left to right: dioxane, bipyridine, *N*-methylmorpholine, *N*,*N*-dimethylpiperazine, morpholine and piperazine.

2. Experimental

2.1. Synthesis

All starting materials were obtained from Sigma-Aldrich except for 1,4-dioxane (May & Baker) and were used as received.

Paracetamol:0.5 1,4-dioxane. A saturated solution of paracetamol (1.51 g, 10 mmol) in 1,4-dioxane (2 cm^3, 23 mmol) was refluxed and allowed to cool. Colourless crystals were formed overnight at 293 K according to the published procedure (Fachaux *et al.*, 1995).

Paracetamol:4,4′-bipyridine. Paracetamol (0.51 g, 3.40 mmol) was refluxed with an equimolar amount of 4,4′-bipyridine (0.52 g, 3.33 mmol) in ethanol (1 cm^3). Pale-yellow needle-like crystals were formed on standing overnight at room temperature.

Paracetamol:0.5 N-methylmorpholine. Paracetamol (0.43 g, 2.85 mmol) and *N*-methylmorpholine (1 cm^3, 9.11 mmol) were refluxed and allowed to cool. The flask was maintained at 277 K, leading to the formation of colourless rod-shaped crystals.

Paracetamol:0.5 N,N-dimethylpiperazine. Paracetamol (0.55 g, 3.64 mmol) and *N*,*N*-dimethylpiperazine (3 cm^3, 22.2 mmol) were refluxed together and allowed to cool. A large excess of dimethylpiperazine was required to dissolve the paracetamol completely. The flask was maintained at 277 K leading to the formation of colourless rod-shaped crystals.

Paracetamol:0.5 piperazine. Paracetamol (0.62 g, 4.1 mmol) was refluxed together with piperazine (0.35 g, 4.1 mmol) in ethanol (1 cm^3). Colourless crystals formed on cooling to 293 K.

Paracetamol:0.5 morpholine. Paracetamol (0.57 g, 3.8 mmol) was refluxed with morpholine (0.37 g, 4.3 mmol). Colourless crystals formed directly from the reaction mixture after a week at 277 K.

Ethanol was required in the reactions of paracetamol with piperazine and 4,4′-bipyridine because these compounds are both solids at room temperature.

2.2. Differential scanning calorimetry (DSC)

DSC traces were recorded using a Perkin Elmer Pyris DSC 1. Samples were contained in open aluminium pans and purged with helium during the temperature scans to facilitate the removal of any volatile products of thermal decomposition. Samples were heated from 298 K to 453 K at a rate of 10 K min^{-1}.

2.3. Crystallography

X-ray diffraction intensities were collected on either a Stoe Stadi-4 diffractometer with Cu $K\alpha$ radiation or a Bruker SMART APEX CCD diffractometer with Mo $K\alpha$ radiation. Both instruments were equipped with Oxford Cryosystems low-temperature devices. An absorption correction for the four-circle data was applied using ψ scans [*SHELXTL* (Sheldrick, 1997*a*), based on the procedure described by North *et al.* (1968)]; the multiscan procedure *SADABS* [(Sheldrick, 1997*b*), based on the procedure described by Blessing (1995)] was applied to the CCD data sets. All structures were in space group $P2_1/c$, except the morpholine adduct, which formed in $P2_12_12_1$. All structures were solved by direct methods and refined by full-matrix least squares against F^2 using all data (*SHELXTL*). H atoms were placed in calculated positions and allowed to ride on their parent atoms; methyl groups were treated with the Sheldrick (1997) rotating rigid group model. H atoms involved in hydrogen bonding were located in difference maps and refined freely. All non-H atoms were modelled with anisotropic displacement parameters.

One of the two crystallographically independent dioxane molecules in the 1,4-dioxane adduct was disordered over two orientations about a crystallographic inversion centre. The occupancies of the two components were fixed at 0.75 and 0.25 after competitive refinement. Similarity restraints were applied to the geometries and displacement parameters of the two components. The program *ROTAX* (Cooper *et al.*, 2002) suggested that the crystal may have been twinned by a twofold rotation about the [100] direct lattice direction. Incorporation of this into the model reduced *R*1 slightly from 7.02% to 6.86%, with a twin scale factor of 2.6 (3)%. This is barely significant, and the twinning is omitted in the model presented here.

In the *N*-methylmorpholine adduct, the *N*-methylmorpholine is disordered over a crystallographic inversion centre with

UM00016711
NOVARTIS EXHIBIT 1517
Novartis v. Regents, IPR2023-01347
Page 3693 of 4460

Table 1
Experimental details.

All data were collected at 150 K.

	1,4-Dioxane adduct	Dimethylpiperazine adduct	*N*-methylmorpholine adduct
Crystal data			
Chemical formula	$2[C_6H_9O_2N][C_4H_8O_2]$	$2[C_8H_9NO_2][C_6H_{14}N_2]$	$2[C_8H_9NO_2][C_5H_{11}NO]$
Chemical formula weight	390.43	416.52	403.47
Cell setting, space group	Monoclinic, $P2_1/c$	Monoclinic, $P2_1/c$	Monoclinic, $P2_1/c$
a, b, c (Å)	12.421 (5), 12.056 (4), 13.396 (3)	10.6970 (9), 11.0240 (9), 9.4896 (8)	10.5749 (8), 11.0221 (8), 9.3894 (7)
β (°)	91.51 (3)	100.684 (2)	101.145 (2)
V (Å^3)	2005.4 (11)	1099.65 (16)	1073.77 (14)
Z	4	2	2
D_x (Mg m^{-3})	1.293	1.258	1.248
D_m (Mg m^{-3})	Not measured	Not measured	Not measured
Radiation type	Cu $K\alpha$	Mo $K\alpha$	Mo $K\alpha$
No. of reflections for cell parameters	80	3488	2729
θ range (°)	20–22	2.5–29	2.5–27.5
μ (mm^{-1})	0.795	0.088	0.090
Temperature (K)	220 (2)	150 (2)	150 (2)
Crystal form, colour	Lath, colourless	Plate, colourless	Rod, colourless
Crystal size (mm)	0.78 × 0.19 × 0.16	0.56 × 0.18 × 0.08	0.34 × 0.09 × 0.07
Data collection			
Diffractometer	Stoe Stadi-4	Bruker SMART APEX CCD	Bruker SMART APEX CCD
Data collection method	ω–θ scans	φ and ω scans	φ and ω scans
Absorption correction	Empirical	Multiscan	Multiscan
T_{min}	0.602	0.833	0.792
T_{max}	0.826	1	0.962
No. of measured, independent and observed reflections	4865, 3499, 2508	7034, 2724, 2512	6517, 2444, 1890
Criterion for observed reflections	$I > 2\sigma(I)$	$I > 2\sigma(I)$	$I > 2\sigma(I)$
R_{int}	0.0532	0.0164	0.0221
θ_{max} (°)	69.79	29.08	27.49
Range of h, k, l	$-15 \rightarrow h \rightarrow 15$ $0 \rightarrow k \rightarrow 14$ $0 \rightarrow l \rightarrow 15$	$-8 \rightarrow h \rightarrow 14$ $-15 \rightarrow k \rightarrow 14$ $-12 \rightarrow l \rightarrow 12$	$-13 \rightarrow h \rightarrow 13$ $-14 \rightarrow k \rightarrow 14$ $-11 \rightarrow l \rightarrow 12$
No. and frequency of standard reflections	3 every 60 min	Not measured	Not measured
Intensity decay (%)	10.9	0	0
Refinement			
Refinement on	F^2	F^2	F^2
$R[F^2 > 2\sigma(F^2)]$, $wR(F^2)$, S	0.0702, 0.2243, 1.078	0.0525, 0.1339, 1.059	0.0408, 0.1082, 0.973
No. of reflections and parameters used in refinement	3499, 285	2724, 146	2444, 147
H-atom treatment	Riding	Riding/All H-atom parameters refined	Riding/All H-atom parameters refined
Weighting scheme	$w = 1/[\sigma^2(F_o^2) + (0.125P)^2 + 1.1494P]$ where $P = (F_o^2 + 2F_c^2)/3$	$w = 1/[\sigma^2(F_o^2) + (0.069P)^2 + 0.4625P]$ where $P = (F_o^2 + 2F_c^2)/3$	$w = 1/[\sigma^2(F_o^2) + (0.0658P)^2]$ where $P = (F_o^2 + 2F_c^2)/3$
$(\Delta/\sigma)_{max}$	0.002	0.009	0.000
$\Delta\rho_{max}$, $\Delta\rho_{min}$ (e Å^{-3})	0.503, −0.260	0.401, −0.193	0.216, −0.220
Extinction method	*SHELXL*	None	*SHELXL*
Extinction coefficient	0.0019 (6)	0	0.008 (3)

	Piperazine adduct	4,4′-Bipyridine adduct	Morpholine adduct
Crystal data			
Chemical formula	$2[C_8H_9NO_2][C_4H_{10}N_2]$	$[C_8H_9NO_2][C_{10}H_8N_2]$	$2[C_8H_9NO_2][C_4H_9O]$
Chemical formula weight	388.46	307.35	389.45
Cell setting, space group	Monoclinic, $P2_1/c$	Monoclinic, $P2_1/c$	Orthorhombic, $P2_12_12_1$
a, b, c (Å)	15.893 (5), 5.1664 (17), 12.993 (4)	11.2906 (10), 24.103 (2), 11.5526 (10)	7.2791 (9), 14.6277 (18), 18.303 (2)

the N and O atoms sharing an equivalent site. A composite scattering factor $[0.5f(N) + 0.5f(O)]$ was used for this site; the occupancy of the methyl group was fixed at 0.5.

A consistent numbering scheme was used for the paracetamol molecules in all structures and this is shown in the schemes above. Where there is more than one paracetamol molecule in the asymmetric unit the labels in the schemes are augmented with the letters *A* and *B*. Labels for atoms forming part of the guest molecules carry the letters *S*, *T etc.* A full listing of crystal, data collection and refinement parameters is given in Table 1; a set of hydrogen-bonding parameters is given in Table 2.[1] The figures were produced using *CAMERON* (Watkin *et al.*, 1993). Other analyses utilized the PC version of the program *PLATON* (Spek, 2002; Farrugia, 1999).

3. Results

3.1. Paracetamol

Crystal structures of the monoclinic and orthorhombic polymorphs of paracetamol have been reported several times, but here we have used the structures reported by Nichols & Frampton (1998) [Cambridge Structural Database (CSD; Allen *et al.*, 1983) reference codes HXACAN07 and HXACAN08]. Our motive for discussing them here is to highlight certain features of their graph sets that enable structural relationships to be drawn between them and the adducts that form the subject of the rest of this paper.

Packing in both polymorphs is dominated by the formation of NH···OH and OH···O=C hydrogen bonds (Fig. 1) giving rise to layered two-dimensional networks. Both polymorphs of paracetamol have identical graph sets (Bernstein *et al.*, 1995), in which the

[1] Supplementary data for this paper are available from the IUCr electronic archives (Reference: AN0622). Services for accessing these data are described at the back of the journal.

UM00016712
NOVARTIS EXHIBIT 1517
Novartis v. Regents, IPR2023-01347
Page 3694 of 4460

XP009014505

Table 1 (continued)

	Piperazine adduct	4,4'-Bipyridine adduct	Morpholine adduct
β (°)	113.633 (5)	96.1484 (16)	90
V (Å^3)	977.4 (6)	3125.8 (5)	1948.9 (4)
Z	2	8	4
D_x (Mg m^{-3})	1.320	1.306	1.327
D_m (Mg m^{-3})	Not measured	Not measured	Not measured
Radiation type	Mo $K\alpha$	Mo $K\alpha$	Mo $K\alpha$
No. of reflections for cell parameters	1227	5375	3801
θ range (°)	2.5–29	2–28.5	2.5–24.5
μ (mm^{-1})	0.093	0.087	0.096
Temperature (K)	150 (2)	150 (2)	150 (2)
Crystal form, colour	Plate, colourless	Block, colourless	Block, colourless
Crystal size (mm)	0.77 × 0.28 × 0.11	0.46 × 0.28 × 0.18	0.54 × 0.52 × 0.28
Data collection			
Diffractometer	Bruker Smart Apex CCD	Bruker SMART APEX CCD	Bruker SMART APEX CCD
Data collection method	ω and φ scans	ω and φ scans	φ and ω scans
Absorption correction	Multiscan	Multiscan	Multiscan
T_{min}	0.690	0.830	0.868
T_{max}	1	1	1
No. of measured, independent and observed reflections	5628, 2309, 1778	20270, 7766, 6044	12312, 4733, 4265
Criterion for observed reflections	$I > 2\sigma(I)$	$I > 2\sigma(I)$	$I > 2\sigma(I)$
R_{int}	0.0458	0.0220	0.0308
θ_{max} (°)	28.55	29.18	28.97
Range of h, k, l	$-17 \rightarrow h \rightarrow 21$ $-6 \rightarrow k \rightarrow 6$ $-17 \rightarrow l \rightarrow 16$	$-14 \rightarrow h \rightarrow 14$ $-19 \rightarrow k \rightarrow 31$ $-15 \rightarrow l \rightarrow 15$	$-9 \rightarrow h \rightarrow 7$ $-19 \rightarrow k \rightarrow 18$ $-24 \rightarrow l \rightarrow 22$
No. and frequency of standard reflections	Not measured	Not measured	Not measured
Intensity decay (%)	0	0	0
Refinement			
Refinement on	F^2	F^2	F^2
$R[F^2 > 2\sigma(F^2)]$, $wR(F^2)$, S	0.0779, 0.1652, 1.179	0.0471, 0.128, 1.038	0.0462, 0.1028, 1.066
No. of reflections and parameters used in refinement	2309, 140	7766, 433	4733, 276
H-atom treatment	Riding/All H-atom parameters refined	Riding/All H-atom parameters refined	Riding/All H-atom parameters refined
Weighting scheme	$w = 1/[\sigma^2(F_o^2) + (0.052P)^2 + 0.5663P]$ where $P = (F_o^2 + 2F_c^2)/3$	$w = 1/[\sigma^2(F_o^2) + (0.0676P)^2 + 0.569P]$ where $P = (F_o^2 + 2F_c^2)/3$	$w = 1/[\sigma^2(F_o^2) + (0.049P)^2 + 0.2716P]$ where $P = (F_o^2 + 2F_c^2)/3$
$(\Delta/\sigma)_{max}$	0.002	0.001	0.001
$\Delta\rho_{max}$, $\Delta\rho_{min}$ (e Å^{-3})	0.336, −0.447	0.357, −0.246	0.256, −0.270
Extinction method	None	None	*SHELXL*
Extinction coefficient	0	0	0.0031 (7)

Computer programs used: Stoe *DIF4* (Stoe & Cie, 1990*a*), Stoe *REDU4* (Stoe & Cie, 1990*b*), Bruker *SMART* (Bruker, 2001), Bruker *SAINT* (Bruker, 2002), *SHELXTL* (Sheldrick, 1997*a*).

OH···O=C and NH···OH hydrogen bonds, respectively, form $C(9)$ and $C(7)$ motifs at the unitary level.[2] In both polymorphs, these are disposed about crystallographic glide planes. In the monoclinic form, the hydrogen-bonded layers are arranged parallel to the (010) planes, which means that the layers are polar: in Fig. 1(*a*) all the molecules have the methyl group on the left. This polarity is reversed in neighbouring layers by crystallographic inversion centres. In the orthorhombic form, glide planes run perpendicular to the layers, so that the layers are non-polar: in Fig. 1(*b*) the methyl groups lie on the left- and right-hand sides of the molecules in alternate $C(9)$ chains.

The angles between mean planes of the amide and phenyl groups in orthorhombic and monoclinic paracetamol are 17.7° and 20.5°, respectively. Analogous angles observed in this work are given in the figure captions and range from 3.03° to 41.72°. pπ-pπ bonding between the phenyl ring and the amide group favours a dihedral angle of zero, and some correlation between this angle and the N—C(phenyl) bond length might have been expected, though none is evident at the precision of these structure determinations. This angle is evidently a rather easily deformed structural parameter, and is presumably at the mercy of crystal-packing forces. As we show in the following sections, hydrogen bonding is the dominant feature in these structures, and the torsion observed is presumably a consequence of the optimization of these interactions.

3.2. The paracetamol:1,4-dioxane adduct

The asymmetric unit in the crystal structure of the dioxane adduct of paracetamol consists of two paracetamol molecules and two half molecules of dioxane. The latter both reside on crystallographic inversion centres. One of the dioxane molecules (labelled *T*/*U* in the tables and supplemental data) is disordered, although both components participate in hydrogen bonding. The occupancy ratio is 0.75:0.25 and in the discussion that follows we have ignored the minor component (*U*). There is some evidence from electron-density difference maps that the other dioxane molecule (labelled *S*) is disordered as well, although, if present, the distinction between the components is at the limit of the resolution of our data set. An ordered model for this part of the structure is therefore presented here. The structure is depicted in Fig. 2. Primary bond lengths and angles are normal and have been deposited; hydrogen-bonding parameters are listed in Table 2.

[2] Note that where no sub- and superscripts appear in the graph-set descriptor, one donor and one acceptor are implied.

UM00016713
NOVARTIS EXHIBIT 1517
Novartis v. Regents, IPR2023-01347
Page 3695 of 4460

The $C(9)$ chains formed by hydrogen bonding between OH···O=C moieties of neighbouring molecules described above with regard to the crystal structures of paracetamol are also observed in the structure of the 1,4-dioxane adduct. In order to accommodate the dioxane molecules these chains are sinusoidal, with the two crystallographically independent paracetamol molecules alternating along the chain. The NH groups point towards the O atoms of dioxane molecules forming NH···O hydrogen bonds. Since both dioxane molecules reside on inversion centres, the space-group symmetry builds up two-dimensional sheets in which chains of paracetamol are linked by dioxane bridges (Fig. 2). In graph-set notation, the bridges can be described as $D_2^2(6)$. The two-dimensional sheets are parallel to the (210) lattice planes, and the rather open structure depicted in Fig. 2 is 'filled in' by symmetry-equivalent sheets parallel to $(2\bar{1}0)$.

Table 2
Hydrogen-bonding parameters.

Standard uncertainties are omitted in the case of the dioxane adduct because the H-atom positions were calculated and not refined. N—H and O—H distances were normalized to 1.009 Å and 0.983 Å, respectively, to aid comparison with Cambridge Structural Database search results (Fig. 7).

Adduct	Donor	Acceptor	Observed distance (Å)	Normalized distance (Å)	Typical normalized distance (Å)
1,4-Dioxane	N1*A*—H1*A*	O1*S*	2.03	1.90	1.96
	O1*A*—H1*A*	O2*B*	1.82	1.67	1.78
	O1*B*—H1*B*	O2*A*^{i}	1.86	1.71	1.78
	N1*B*—H1*B*	O1*U*	1.92	1.77	1.96
	N1*B*—H1*B*	O1*T*	2.13	2.00	1.96
4,4′-Bipyridine	O1*A*—H1*A*	O2*B*	1.755 (19)	1.68	1.78
	N1*A*—H1*A*	N1*S*	2.047 (18)	1.92	1.96
	O1*B*—H1*B*	O2*A*^{ii}	1.81 (2)	1.71	1.78
	N1*B*—H1*B*	N1*T*^{iii}	2.100 (18)	2.01	1.96
N,*N*-dimethylpiperazine	N1—H1	O2^{iv}	1.98 (2)	1.84	1.92
	O1—H11	N1*S*^{v}	1.81 (2)	1.82	1.82
N-methylmorpholine	O1—H11	O1*S*/N1*S*^{vi}	1.88 (2)	1.81	1.81/1.82
	N1—H1	O2^{vii}	1.925 (16)	1.80	1.92
Piperazine	O1—H11	N1*S*	1.79 (3)	1.74	1.82
	N1—H1	O2^{viii}	2.14 (3)	2.06	1.92
	N1*S*—H1*S*	O1^{viii}	2.30 (3)	2.21	2.03
Morpholine	O1*A*—H11*A*	O1*B*^{ix}	1.97 (2)	1.76	1.87
	N1*A*—H1*A*	O2*B*^{x}	2.033 (18)	1.87	1.92
	O1*B*—H11*B*	N4*S*^{xi}	1.79 (3)	1.69	1.82
	N1*B*—H1*B*	O2*A*^{xii}	2.061 (19)	1.86	1.92

(i) $x, y, z+1$; (ii) $x-1, y, z-1$; (iii) $-x, y-\frac{1}{2}, -z+\frac{1}{2}$; (iv) $x, -y+\frac{1}{2}, z-\frac{1}{2}$; (v) $-x+1, -y, -z$; (vi) $-x+1, -y+2, -z$; (vii) $x, -y+\frac{1}{2}, z-\frac{1}{2}$; (viii) $x, y+1, z$; (ix) $x+\frac{1}{2}, -y+\frac{1}{2}, -z$; (x) $x+\frac{1}{2}, -y+\frac{1}{2}, -z$; (xi) $-x+1, y+\frac{1}{2}, -z+\frac{1}{2}$; (xii) $-x+1, y-\frac{1}{2}, -z+\frac{1}{2}$

3.3. The paracetamol:4,4′-bipyridine adduct

The O atoms in 1,4-dioxane formally have two lone pairs of electrons, each of which could potentially act as a hydrogen-bond acceptor. In practice, however, motifs in which ethers act as double hydrogen-bond acceptors occur rarely, and so for practical crystal-packing purposes it can be considered to be a centrosymmetric molecule containing two hydrogen-bond acceptors. 4,4′-Bipyridine is similar, although a torsion about the central C—C bond breaks the inversion symmetry. Recrystallization of paracetamol from a solution of 4,4′-bipyridine in ethanol yields a 1:1 co-crystal rather than the hemisolvate obtained with dioxane, a possible effect of the greater basicity of bipyridine.

The crystal structure of paracetamol:bipyridine contains two independent molecules each of paracetamol and bipyridine. Primary bond lengths and angles are normal and have been deposited; hydrogen-bonding parameters are listed in Table 2. As in the dioxane adduct, the paracetamol molecules form $C(9)$ chains through OH···O=C hydrogen bonds (Fig. 3). The two crystallographically independent paracetamol molecules alternate along the chain. The disposition of the molecules within the chains is rather similar to that in orthorhombic paracetamol, except that alternate molecules are rotated through 180° about the chain axis in order to accommodate the bipyridine molecules.

The NH bonds of paracetamol act as hydrogen-bond donors to the aromatic N atoms of the bipyridine molecules, forming a discrete (D) graph set. However, since this crystal is a 1:1 adduct there are insufficient hydrogen-bond donors for the number of acceptors present, and only one of the two N atoms in each bipyridine acts as an acceptor. The result is that there are no hydrogen-bonded pathways connecting the $C(9)$ paracetamol chains. The structure thus consists of a paracetamol backbone with attached bipyridine molecules. These motifs are interconnected by π-stacking between the bipyridine molecules, building up sheets than run parallel to the $(10\bar{1})$ planes.

3.4. The paracetamol adducts with *N*-methylmorpholine and *N*,*N*-dimethylpiperazine

N,*N*-dimethylpiperazine and *N*-methylmorpholine are closely related to 1,4-dioxane by the substitution of one or both O atoms by N—Me; paracetamol forms 2:1 adducts with both compounds, as it does with dioxane. The *N*,*N*-dimethylpiperazine adduct consists of one crystallographically independent paracetamol molecule with the *N*,*N*-dimethylpiperazine residing on a crystallographic inversion centre. The *N*-methylmorpholine adduct is isostructural with this, with the guest molecule disordered about the inversion centre. Primary bond lengths and angles are unremarkable and have been deposited; hydrogen-bonding parameters are listed in Table 2

The crystal structures are similar to those of the dioxane and bipyridine adducts in that the packing can be described with reference to chains of paracetamol molecules. However, rather than $C(9)$ motifs formed through OH···O=C H bonds, the paracetamol molecules define a $C(4)$ graph set through NH···O=C bonds (Fig. 4). The NH moiety of the para-

UM00016714
NOVARTIS EXHIBIT 1517
Novartis v. Regents, IPR2023-01347
Page 3696 of 4460

XPO09014505

cetamol now fulfils the role of the OH groups in the dioxane structure, and *N*,*N*-dimethylpiperazine and *N*-methylmorpholine are similar to dioxane with regard to their hydrogen-bonding properties. Therefore, although the nature of the paracetamol chain differs from that of the dioxane adduct, the roles of the *N*-methylmorpholine and dimethylpiperazine molecules are similar, and both act to link paracetamol chains *via* the $D_2^2(6)$ graph set. Overall, this structure consists of a two-dimensional network, although the sheets formed have a corrugated or zigzag appearance in cross section. Alternate regions of the network are approximately parallel to the (310) and (3$\bar{1}$0) planes. Just as in the dioxane adduct, the open structure of Fig. 4 is filled in by symmetry-equivalent networks.

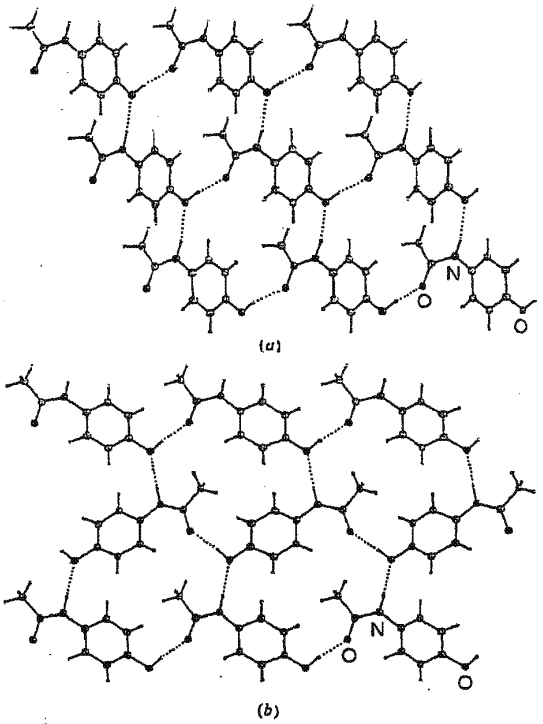

Figure 1
(*a*) Monoclinic paracetamol (Form I) viewed along the *b* axis; the *c* axis runs diagonally from top left to bottom right, so that the *C*(9) chains are established by the *n*-glide. (*b*) Orthorhombic paracetamol (Form II) viewed along the *c* axis; the *a* axis runs horizontally, the *b* axis runs from top to bottom. The *C*(9) chains referred to in the text run from left to right and the *C*(7) chains run approximately vertically. [Colour versions of this and the other figures are available in the online edition of this journal.]

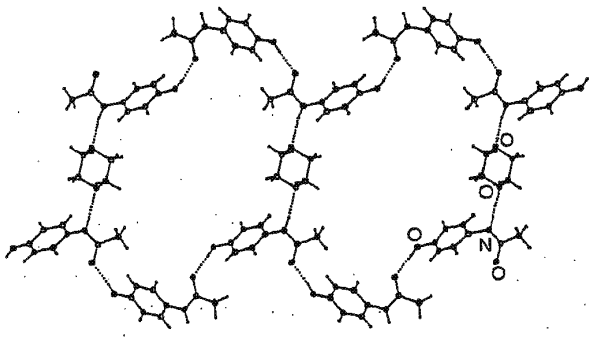

Figure 2
Paracetamol:1,4-dioxane adduct viewed perpendicular to (210); the *c* axis runs horizontally. The *C*(9) chains referred to in the text run from left to right and are linked together by dioxane molecules. The dihedral angles between the amide and phenyl mean planes in the two independent paracetamol molecules are 41.72 (15)° and 39.37 (14)° for molecules *A* and *B*, respectively.

3.5. The paracetamol:morpholine adduct

Morpholine is related to *N*-methylmorpholine by the substitution of the methyl group for hydrogen, and it is unique in this series because the hydrogen-bonding characteristics of the two hetero-centres are not the same: the NH group is a donor and acceptor, the ether O atom potentially a double, but more usually a single, acceptor. The asymmetric unit of the morpholine hemiadduct consists of two crystallographically independent paracetamol molecules (labelled *A* and *B*) and one molecule of morpholine (labelled *S* in the tables). Primary bond lengths and angles are normal and have been deposited; hydrogen-bonding parameters are listed in Table 2.

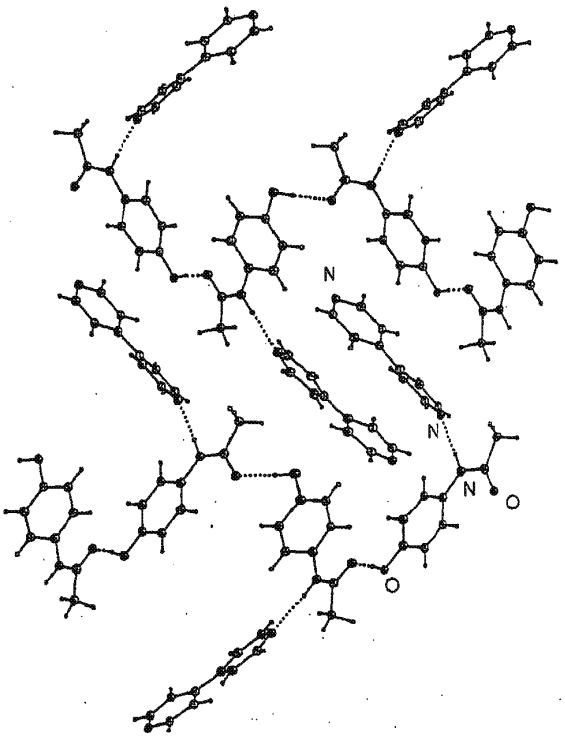

Figure 3
Paracetamol:4,4-bipyridine viewed perpendicular to (10$\bar{1}$); the *b* axis runs from top to bottom. The *C*(9) chains referred to in the text run from left to right and are linked together by a pair of π-stacked bipyridine molecules. The dihedral angles between the amide and phenyl mean planes in the two independent paracetamol molecules are 14.68 (8)° and 13.27 (9)° for molecules *A* and *B*, respectively.

UM00016715
NOVARTIS EXHIBIT 1517
Novartis v. Regents, IPR2023-01347
Page 3697 of 4460

The crystallographically independent paracetamol molecules alternate in the pattern ...*ABABAB*... along a chain formed by ···HNCO···NHCO··· linkages between neighbouring amide groups. Because these molecules are crystallographically independent, these hydrogen bonds formally constitute discrete graphs at the unitary level, although it is clear from Fig. 5 that they are closely related to the *C*(4) graphs observed in the crystal structures of the *N*-methylmorpholine and *N*,*N*-dimethylpiperazine adducts described above. For consistency we continue to use this designation, although it is not formally correct [the binary graph $C_2^2(8)$ takes proper account of symmetry].

The chains are formed by 2_1 operations parallel to *c*, leading to a pairwise alternation of the centres of the paracetamol molecules above and below the chain. This pattern is reminiscent of the structures of the *N*-methylmorpholine and *N*,*N*-dimethylpiperazine adducts, except that in these cases the alternation applies to single molecules. The potential for this arrangement to lead to some steric hindrance between the phenyl groups of neighbouring molecules is avoided by adjacent molecules veering slightly away from each other and an increase in the torsional angle between the phenyl group and amide group from 3.04 (3)° in molecule *B* to 36.03 (6)° in molecule *A*.

Lattice translation along the *b* direction generates further *C*(4) chains, and these are linked together by discrete [*D*] hydrogen bonds in which an OH group from an '*A*' molecule in one chain acts as a donor to an OH group of a '*B*' molecule in a neighbouring chain. This is the only structure in the series in which pairs of paracetamol molecules interact *via* their hydroxyl moieties.

The two sets of hydrogen bonds described above – the *C*(4) chains and the *D* links between chains – form a grid-like network parallel to the (100) planes. The morpholine molecules fit into the cavities of the grid. As in the *N*-methylmorpholine adduct, the amine N atom acts as an acceptor to the OH group of one of the paracetamol molecules (*B*), but this is the only hydrogen-bonding interaction formed by the morpholine. The NH group of the morpholine is in an axial position to accommodate this interaction.

This scheme satisfies all the hydrogen-bonding potential of the two paracetamol molecules, with the exception of the hydroxyl acceptor of molecule *A*. The weakest acceptor in the system (the ether function of the morpholine) does not

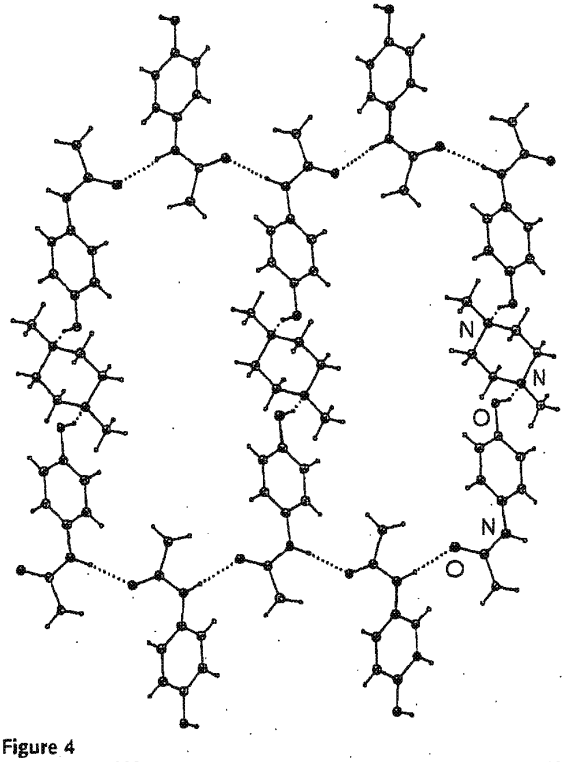

Figure 4
Paracetamol:*N*,*N*-dimethylpiperazine adduct (isostructural to the *N*-methylmorpholine adduct) viewed along the *a* axis; the *c* axis runs from left to right and the *b* axis from top to bottom. The *C*(4) chains referred to in the text run from left to right and are linked together by *N*,*N*-dimethylpiperazine molecules. The dihedral angles between the amide and phenyl mean planes in the paracetamol molecules are 33.75 (7)° and 34.11 (6)° in the *N*,*N*-dimethylpiperazine and *N*-methylmorpholine adducts, respectively.

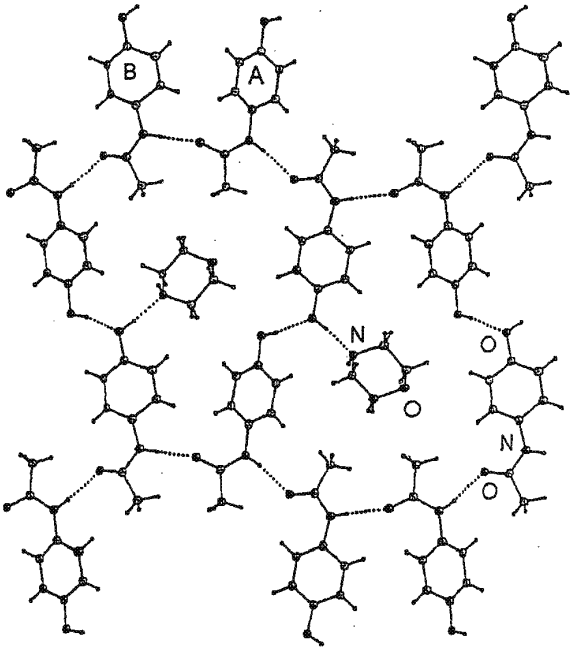

Figure 5
Paracetamol:morpholine adduct viewed along the *a* axis. The *c* direction runs from left to right, the *b* direction up and down. The labels *A* and *B* refer to the crystallographically independent paracetamol molecules referred to in the text. The *C*(4) chains referred to in the text run from left to right and are linked together by hydrogen bonds between opposed OH groups. This forms a grid-like array with the morpholine molecules residing in the grid cavities. The dihedral angles between the amide and phenyl mean planes in the two independent paracetamol molecules are 36.03 (6)° and 3.04 (3)° for molecules *A* and *B*, respectively.

UM00016716
NOVARTIS EXHIBIT 1517
Novartis v. Regents, IPR2023-01347
Page 3698 of 4460

XP009014505

participate in hydrogen bonding at all. A rather surprising feature of this structure, given the excess of acceptors present, is that the NH donor functionality of the morpholine amine moiety is also unsatisfied. However, this is consistent with the relatively long NH···OH hydrogen bonds observed in the piperazine adduct (which is described in the next section) and the generally poor hydrogen-bond-donor ability of secondary amines (see below).

3.6. The paracetamol:piperazine adduct

Piperazine is related to *N,N*-dimethylpiperazine by substitution of the two methyl groups by hydrogen. The asymmetric unit of the piperazine adduct, in common with the *N,N*-dimethylpiperazine adduct, consists of one paracetamol molecule and a molecule of piperazine on a crystallographic inversion centre. Primary bond lengths and angles are normal and have been deposited: hydrogen-bonding parameters are listed in Table 2. There are $C(4)$ chains, consisting of NH···O=C hydrogen bonds, linked *via* $D_2^2(6)$ motifs consisting of OH···N bonds (Fig. 6). Piperazine is a weak hydrogen-bond donor as well as an acceptor, and the extra NH-donor moiety is satisfied by rotating alternate paracetamol molecules about the $C(4)$ chain axis, leading to *D*-type NH···OH hydrogen bonds. This rotation produces ribbons that run parallel to the *b* axis rather than the infinite two-dimensional networks.

3.7. Differential scanning calorimetry

Decomposition of a co-crystal of paracetamol is a potential strategy for the production of the orthorhombic polymorph. In all cases except for the 4,4′-bipyridine adduct, DSC traces exhibited thermal events attributable to loss of the guest molecule followed by a strong endotherm, corresponding to melting, at 438–444 K. The melting point of monoclinic paracetamol is 442 K (Nichols & Frampton, 1998). The same authors showed that DSC traces for orthorhombic paracetamol show either melting at 430 K or a phase transition to the monoclinic form at the same temperature, depending on the method of preparation. The DSC traces observed in this study can therefore be interpreted in terms of decomposition leading to formation of the monoclinic polymorph.

Thermal decomposition temperatures follow the trend that might be predicted on the basis of the boiling points of 1,4-dioxane (374 K), *N*-methylmorpholine (388 K), morpholine (401 K), *N,N*-dimethylpiperazine (404 K) and piperazine (419 K). Two exotherms were observed for the dioxane solvate at 299 K and 338 K, in agreement with the previous study (Fachaux *et al.*, 1995). This is plausibly interpreted as sequential loss of the two crystallographically independent dioxane molecules. Dioxane is readily lost at room temperature from a crystalline sample of this adduct, and the DSC trace of a sample that had been allowed to stand for 10 min showed only one exotherm with an onset temperature of 330 K. Decomposition of the morpholine, *N*-methylmorpholine and *N,N*-dimethylpiperazine adducts occur as broad exotherms with onsets at approximately 327, 335 and 373 K, respectively. The DSC trace of the piperazine adduct showed one endotherm at 413 K.

4,4′-Bipyridine sublimes at 578 K under ambient pressure, and it is the least volatile compound to have been studied in this work. The DSC trace of the co-crystal exhibits a weak endotherm at 399 K followed by a strong endotherm at 402 K; no thermal event attributable to the melting of pure paracetamol was observed. The strong endotherm occurs at a similar temperature to the decomposition events observed for the other adducts, and it is likely to correspond to a melting process forming paracetamol solvated by liquid bipyridine (m.p. 374–377 K). Unlike the other solvents studied here, bipyridine is not lost to leave pure paracetamol, because its boiling point is well beyond the temperature of adduct decomposition. It is likely that the small peak corresponds to a phase transition.

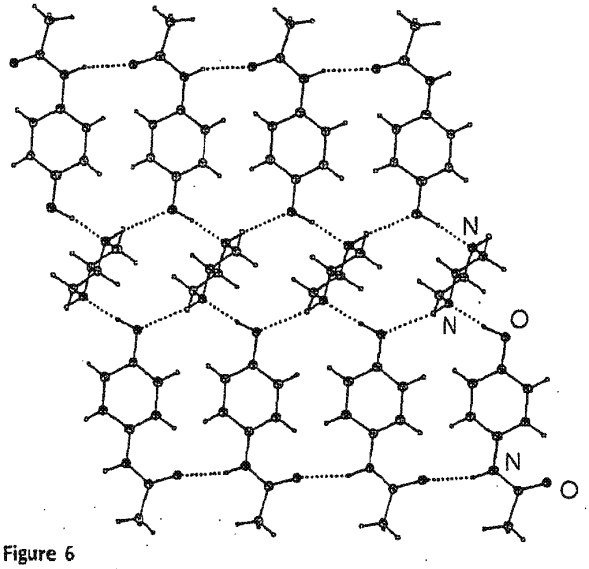

Figure 6
Paracetamol:piperazine adduct viewed perpendicular to (302); the *b* axis runs from left to right. The $C(4)$ chains referred to in the text run from left to right and are linked together by piperazine molecules. The latter also act as weak hydrogen-bond donors. The dihedral angles between the amide and phenyl mean planes in the paracetamol molecule is 33.21 (14)°.

4. Discussion and conclusions

This paper has described the formation of five new paracetamol hemiadducts with 1,4-dioxane, *N,N*-dimethylpiperazine, *N*-methylmorpholine, morpholine and piperazine and a 1:1 adduct with 4,4′-bipyridine. This is the first such systematic study of paracetamol co-crystals to have been undertaken. As is to be expected, the crystal structures of all adducts are dominated by hydrogen-bond formation, and comparisons between them were much facilitated by the use of graph-set analysis in the form described in the illuminating review by Bernstein *et al.* (1995).

Although ether oxygen can potentially act as a double acceptor, it rarely does so, and so with the exception of

UM00016717
NOVARTIS EXHIBIT 1517
Novartis v. Regents, IPR2023-01347
Page 3699 of 4460

Donor (NH or OH)	Acceptor (O or N in each case)					
		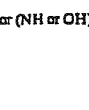	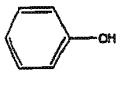	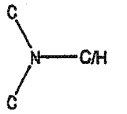	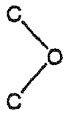	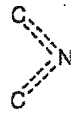
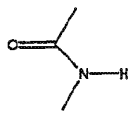	Sample size	1250	14	11	31	40
	Max NH..A /Å	(2.2) *	2.14	2.17	2.19	2.19
	Min NH..A /Å	1.73	1.79	1.80	1.83	1.81
	Mean NH..A /Å	1.92	2.01	1.96	2.03	1.96
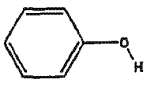	Sample size	49	256	49	53	76
	Max OH..A /Å	2.19	2.20	2.19	2.20	2.18
	Min OH..A /Å	1.60	1.67	1.66	1.62	1.53
	Mean OH..A /Å	1.78	1.87	1.82	1.90	1.81
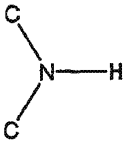	Sample size	5	1 (HOLZOD)	12	4	Not applicable
	Max NH..A /Å	2.17	-	2.20	2.18	
	Min NH..A /Å	2.08	-	2.00	2.11	
	Mean NH..A /Å	2.13	2.03	2.14	2.13	

Figure 7
Summary of the results of searches of the CSD (Version 5.23, April 2002) for typical distances (in Å) in hydrogen-bonded systems containing identical functional groups to the paracetamol adducts studied. The distances to H atoms were normalized to typical neutron distances (C—H 1.803, N—H 1.009 and O—H 0.983 Å). Only 'organic' structures where the *R* factor is less than 0.05 with no errors or disorder were included, and ionic or polymeric structures were excluded. The C atoms attached to the amine moieties were specified to be sp^3 hybridized. The donor-H-to-acceptor distance was specified to be 1.50–2.20 Å. The asterisk denotes the limit of search.

morpholine all the guest molecules studied are at least pseudo-centrosymmetric with respect to their hydrogen-bonding properties. The dioxane, *N*-methylmorpholine, *N*,*N*-dimethylpiperazine and piperazine adducts all consist of hydrogen-bonded chains of paracetamol molecules linked together by the guest molecules, which all reside on crystallographic inversion centres. In the bipyridine adduct the chains are linked *via* a pair of π-stacked pyridine rings, though the structure as a whole is still centrosymmetric. The morpholine adduct does not conform to this pattern, although chains of paracetamol are still present. The arrangements of paracetamol chains described in this paper tend to lend themselves to the formation of centrosymmetric crystal structures, and this seems to favour adduct formation in the centrosymmetric guest molecules. It is perhaps significant that we have been unable to prepare an adduct with 1,3,5-trioxane, a molecule closely related to dioxane but which lacks inversion symmetry.

The donor groups that appear in this series are amidic NH, phenol OH and secondary amine NH; the acceptors are amidic O, phenolic O, secondary or tertiary amine N, ether O, and pyridine N. The results of searches of the CSD for typical hydrogen-bond geometries involving these functionalities are shown in Fig. 7; searching criteria are given in the legend to that figure. The pattern of adduct formation observed in this study is quite consistent with the data in Fig. 7 if the reasonable assumption is made that the hydrogen-bond strength is related to the average donor-hydrogen—acceptor distance. The donor group O—H or N—H to acceptor distances observed in this study were normalized to typical neutron values (O—H 0.983 Å and N—H 1.009 Å) to aid ready comparison with typical H-to-acceptor distances derived from our CSD search, and this comparison is made in Table 2. Our hydrogen-bond distances agree tolerably well with typical values; they are often on the short side, as might be expected with low-temperature data.

The strongest hydrogen bonds in Fig. 7 are formed between phenolic OH (as donor) and amide O (as acceptor). These are observed in the *C*(9) chains formed in structures of both polymorphs of paracetamol. In pure paracetamol, hydrogen bonds are formed between the remaining NH donor and OH acceptor to form *C*(7) chains, but on adduct formation with 1,4-dioxane and 4,4′-bipyridine it is these, weaker, interactions that break to accommodate the guest molecules, preserving the strongly bound *C*(9) chains and forming hydrogen bonds between the amide NH of paracetamol and either the ether O or the pyridyl N atoms of the guest molecule. These observations are consistent with the results obtained in the variable-pressure study of monoclinic paracetamol by Boldyreva *et al.* (2000), where the NH···O contacts were found to be more compressible than the OH···O contacts.

Neither dioxane nor bipyridine has any group attached to the donor O or N atoms. All of the other molecules studied carry either hydrogen or methyl groups in these positions, and reference to Fig. 2 or Fig. 3 shows that a structure based on the *C*(9) paracetamol chains would suffer some steric crowding

UM00016718
NOVARTIS EXHIBIT 1517
Novartis v. Regents, IPR2023-01347
Page 3700 of 4460

XP009014505

between these groups and either the phenyl or the methyl group attached to the amide moiety. In order to avoid steric overcrowding in the m rpholine, piperazine, *N*,*N*-dimethylpiperazine and *N*-methylmorpholine adducts, the paracetamol utilizes its NH group as a donor. Fig. 7 shows that the most effective acceptor for this group is amide CO and this explains the formation of *C*(4) paracetamol chains in all four of these structures.

In the structures of *N*-methylmorpholine and *N*,*N*-dimethypiperazine, hydrogen bonds are formed between the OH group of paracetamol and the N or O of the guest molecule. In morpholine and piperazine, both the OH group of paracetamol and the NH group(s) of the guest could act as either donors or acceptors. Fig. 7 shows that secondary aliphatic amines are particularly poor hydrogen-bond donors, and so the hydroxyl group acts as the donor in both cases. In fact, so poor a donor is secondary amine NH that it is left unsatisfied in the morpholine adduct, even in the presence of excess acceptor functions. The weakness of these NH···N hydrogen bonds relative to OH···O or NH···O systems may be a consequence of the size of N relative to O, a feature recently emphasized by Brown (2002). However, in piperazine the NH groups do act as weak donors, and this induces a change in conformation of these *C*(4) chains relative to the *N*,*N*-dimethylpiperazine adduct that condenses the sheets into ribbons.

In the case of morpholine, the *C*(4) chains are linked by the OH group of a paracetamol molecule in one chain acting as a hydrogen-bond donor to a similar group in a neighbouring chain. On the basis of the structures of the other adducts, the role might have been expected to be fulfilled by the ether m iety of the morpholine. Fig. 7 shows that these interactions are of rather similar strength, and this might explain the apparently anomalous behaviour observed in this adduct.

In the 1,4-dioxane adduct, alternate *C*(9) paracetamol chains have reversed polarity. In the adducts based on *C*(4) chains, the resemblance to orthorhombic paracetamol is less obvious, although inspection of Fig. 1(*b*) shows that removal of alternate molecules along the *C*(7) graph followed by a small displacement would yield NH···O=C *C*(4) chains. Viewed in this light, desolvation might have been predicted to yield the orthorhombic polymorph of paracetamol, although in practice it was shown by DSC that in all cases except for paracetamol:bipyridine (for which we did not observe desolvation at all) the therm dynamically more stable monoclinic polymorph was formed.

We thank Mrs A. Dawson and Dr A. Parkin for assistance with data collection, and the EPSRC, the Cambridge Crystallographic Data Centre and the University of Edinburgh for funding.

References

Allen, F. H., Kennard, O. & Taylor, R. (1983). *Acc. Chem. Res.* 16, 146–153.

Bernstein, J., Davis, R. E., Shimoni, L. & Chang, N-L. (1995). *Angew. Chem. Int. Ed. Engl.* 34, 1555–1573.

Blessing, R. H. (1995). *Acta Cryst.* A51, 33–38.

Boldyreva, E. V., Shakhtshneider, T. P., Vasilchenko, M. A., Ahsbahs, H. & Uchtmann, H. (2000). *Acta Cryst.* B56, 299–309.

Brown, I. D. (2002). *The Chemical Bond in Inorganic Chemistry*, ch. 7. IUCr Monographs on Crystallography. Oxford University Press.

Bruker (2001). *SMART*. Bruker-AXS, Madison, Wisconsin, USA.

Bruker (2002). *SAINT*. Bruker-AXS, Madison, Wisconsin, USA.

Cooper, R. I., Gould, R. O., Parsons, S. & Watkin, D. J. (2002). *J. Appl. Cryst.* 35, 168–174.

Fachaux, J.-M., Guyot-Hermann, A.-M., Guyot, J.-C., Confiant, P., Drache, M., Veesler, S. & Boistelle, R. (1995). *Powder Technol.* 82, 123–128.

Farrugia, L. J. (1999). *J. Appl. Cryst.* 32, 837–838.

Haisa, M., Kashino, S., Kawaii, R. & Maeda, H. (1976). *Acta Cryst.* B32, 1283–1285.

Haisa, M., Kashino, S. & Maeda, H. (1974). *Acta Cryst.* B30, 2510–2512.

McGregor, P. A., Allan, D. R., Parsons, S. & Pulham, C. R. (2002). *J. Pharm. Sci.* 91, 1308–1311.

Nichols, G. & Frampton, C. S. (1998). *J. Pharm. Sci.* 87, 684–693.

North, A. C. T., Phillips, D. C. & Mathews, F. S. (1968). *Acta Cryst.* A24, 351–359.

Sheldrick, G. M. (1997*a*). *SHELXTL*. Bruker-AXS, Madison, Wisconsin, USA.

Sheldrick, G. M. (1997*b*). *SADABS*. Bruker-AXS, Madison, Wisconsin, USA.

Spek, A. L. (2002). *PLATON. A Multipurpose Crystallographic Tool*. Utrecht University, The Netherlands.

Stoe & Cie (1990*a*). *DIF4. Diffractometer Control Program*. Stoe & Cie, Darmstadt, Germany.

Stoe & Cie (1990*b*). *REDU4. Data Reduction Program*. Stoe & Cie, Darmstadt, Germany.

Watkin, D. J., Pearce, L. & Prout, C. K. (1993). *CAMERON – A Molecular Graphics Package*. Chemical Crystallography Laboratory, University of Oxford, UK.

UM00016719
NOVARTIS EXHIBIT 1517
Novartis v. Regents, IPR2023-01347
Page 3701 of 4460

Chem. Pharm. Bull. 47(6) 852—856 (1999) Vol. 47, No. 6 June 199

Effect of Polymorphic Forms of Bulk Powders on Pharmaceutical Properties of Carbamazepine Granules

Makoto Otsuka,* Hitoshi Hasegawa, and Yoshihisa Matsuda

Department of Pharmaceutical Technology, Kobe Pharmaceutical University, Motoyama-Kitamachi, Higashi-Nada, Kobe 658–5885, Japan. Received February 4, 1999; accepted March 3, 1999

The effects of polymorphic forms of bulk powder on the pharmaceutical properties of carbamazepine (CBZ) granules were investigated by using X-ray diffraction analysis, thermal analysis and Brunauer-Emmett-Teller surface area measurement. A mixture consisting of 50% CBZ forms I, II, III or IV (dihydrate) as a bulk powder, 35% crystalline α-lactose monohydrate and 15% corn starch was used as a pharmaceutical powder, with binder aqueous solutions containing 5% hydroxypropylcellulose (HPC). After kneading with the binder solution, granules were obtained using an extruding granulator. After granulation forms I, II and III were 2.5, 80.3 and 35.2% transformed into dihydrate, respectively. Next, the wet granules were dried at 60 °C for 24 h, and the transformed dihydrates were dehydrated into fine particles containing form III. The yield of granules obtained from forms I, II, III and IV was 73.8, 0.0, 0.0 and 76.3%, respectively. The lower granule yields of forms II and III appeared to be due to a lack of kneading water due to absorption of CBZ as crystalline water. Therefore, to the granules of forms II and III was added extra water (60 and 30 ml/kg) to the mixture, respectively, which improved yield markedly, (to 65.1 and 69.2%), indicating the decrease in granule yield was caused by the absorption of water on transformation of dihydrate. The specific surface area (Sw) results suggested that the granules obtained from form II bulk powder had the largest Sw, and those from form I the lowest. In the order of Sw and tablet hardness of the granules, the powders ranked form II>III>IV>I. This indicated that the mechanical strength of the tablet was proportional to the Sw of the particles. The dissolution profiles of the CBZ tablets were investigated in JP XIII, 1st fluid (pH 1.2, 37±0.5 °C), and the time required for 50% dissolution (T50) was measured. In the order of T50 the ranking was IV≤I<III<II. These results suggested that the polymorphic transformation during the granulation and drying processes induced a change in pharmaceutical properties.

Key words polymorphism; carbamazepine; preformulation study; an extruding granulation; specific surface area; polymorphic transformation

Preparations of high quality granules offer a number of potential advantages to the pharmaceutical industry in the production of beads or granules as both finished and intermediate products. As such, various kinds of formulations, techniques and equipment have been developed to obtain high quality granular materials.[1] However, the polymorphic form of insoluble drugs influences the bioavailability of preparations by affecting the dissolution rate.[2] Thus, the polymorphic forms affect the pharmaceutical properties of the preparations.[3] Carbamazepine (CBZ) is widely used as a potent anticonvulsant, and there have been reports concerning its polymorphic form.[4—6] The physicochemical stability of the polymorphic form at high humidity[7] and in suspension[8] has been investigated in formulation studies, and the method of preparing CBZ has been shown to affect the drug's pharmaceutical properties through the polymorphic phase transformation of the bulk CBZ powder during the manufacturing process. In a previous study,[9] we investigated the effects of solvent systems on polymorphic transformation of CBZ during the extrusion-granulation process and the pharmaceutical properties of the granules. Their dissolution behaviors and the mechanical strength of the CBZ granules and/or tablets were affected by the characteristics of the solvent systems in the binder solution, since the metastable polymorphic form was transformed into other crystalline forms during granulation. In this study therefore, we investigated the effect of the polymorphic form of bulk CBZ powders on the pharmaceutical properties of granules and/or tablets obtained by extrusion-granulation.

Materials and Methods

Materials CBZ bulk powder of Japanese Pharmacopoeia (JP) XIII grade (lot No. CEE-9-5) was obtained from Katsura Chem. Co., Tokyo, Japan. The bulk powders were identified as polymorphic forms I, II, III and IV[7] by X-ray diffraction analysis and differential scanning calorimetry (DSC) measurement. Crystalline α-lactose monohydrate (Pharmatose 200M, DeMelkindustrie Veghel Co., the Netherlands) and corn starch (Matsuya Chem. Co., Japan) were used as a diluent and a disintegrator, respectively. Hydroxypropylcellulose (HPC) (HPC-L, Nihon Soda Co., Japan) and magnesium stearate (Kishida Chem. Co., Japan) were used as a binder and a lubricant, respectively. All other chemicals were of analytical grade.

Preparation of Polymorphs The CBZ bulk powder was identified as form I (anhydrate, monoclinic CBZ).[7] Form II (anhydride) was precipitated from a saturated chloroform solution of the drug by the addition of ethyl ether, and stirring for 1 h at room temperature. The separated crystals were then filtered and dried *in vacuo* in a desiccator containing P_2O_5 at room temperature for 3 h. Form III (anhydride) was obtained by heating dihydrate at 115 °C *in vacuo* for 6 h. Dihydrate form (form IV)[7] was obtained by recrystallization as follows: CBZ bulk powder was dissolved in 50% ethanol solution in a water bath at 70 °C, and filtered. After cooling the saturated CBZ solution to room temperature, the crystalline samples were filtered and dried in a desiccator containing silica gel at room temperature *under vacuo* for 3 h. All of the CBZ samples were passed through a No. 200 mesh (75 μm) screen.

Micrometric Characterization The true densities of the powders were determined using an air comparison pycnometer (model 930, Beckman-Toshiba Co., Tokyo, Japan). Specific surface area (Sw) measurement: The Sw was measured with a gas adsorption apparatus (one point method, Flow sorb, model 2300, Shimadzu Co.) using Brunauer-Emmett-Teller gas adsorption. The adsorption gas used for measurement contained 30% N_2 and 70% He. All values represent averages of 4 measurements.

X-Ray Powder Diffraction Analysis Diffractograms were taken at room temperature with an X-ray diffractometer (XD-3A, Shimadzu Co., Kyoto, Japan). The operating conditions were as follows: Target, Cu; filter, Ni; voltage 20 kV, current, 20 mA; receiving slit, 0.1 mm; time constant, 1 s; counting range, 1 kcps; scanning speed 4° 2θ/min.

Thermal Analysis DSC was performed with a type 3100 instrument

Fig.

* To whom correspondence should be addressed.

© 1999 Pharmaceutical Society of Japan

UM00016720
NOVARTIS EXHIBIT 1517
Novartis v. Regents, IPR2023-01347
Page 3702 of 4460

(Mac Science Co., Tokyo). The operating conditions in the open-pan system were as follows: Sample weight, 5 mg; heating rate, 10 °C/min; N_2 gas flow rate, 30 ml/min.

Granulation Process The manufacturing process for CBZ granules and tablets is summarized in Chart 1. Two hundred and fifty grams of CBZ bulk powder, 175 g of crystalline lactose and 75 g of corn starch were mixed in a twin-shell type mixer (Model 5DMr, Sanei Ind. Co., capacity: 4.7 liters, mixing speed 28 rpm) for 60 min. The HPC binder solutions were obtained by mixing with 5 g of HPC and 100 ml of distilled water. After adding HPC binder solution (150 ml/kg), the mixed powder was kneaded at 107 rpm in a Multipurpose mixer (Shinagawa Ind. Co., 10 liter) for 10 min. The wet mass was immediately transferred to an extruding granulator equipped with a 0.5-mm mesh (Dorm Gran, Type DG-L1, Fuji Powdal Co., Japan) where the wet mass was extruded at 20 rpm. All procedures were performed at 25 °C, and 50±10% relative humidity (RH). Completed, processed granules were dried at 60 °C for 24 h. The sample granules between a No. 12 mesh screen (1400 μm) and a No. 42 mesh (355 μm) were used.

In order to evaluate the amount transformed dihydrate one gram of granule was sampled after granulation, and stored at 30 °C, 47% RH for 24 h to measure DSC.

Measurement of the Dihydrate Content of Granules The dihydrate (form IV) content of the granules was measured by DSC based on the endothermic peak at around 70 °C due to dehydration. Briefly, known quantities of standard mixtures were obtained by physically mixing anhydrate and dihydrate at various ratios (0, 25, 50, 75 and 100% crystal content) in a mortar. The DSC curves of the standard samples were measured in triplicate. The standard deviation of the data were within 5%. The plots gave good linear correlation and the linear regression equation is as follows:

$$Y=308.4X+5.8 \quad (R=0.998) \qquad (1)$$

Y (J/g) is a latent heat due to dehydration of dihydrate CBZ. X is the dihydrate concentrations (%). R is the correlation coefficient.

Tabletting Compression Process Sample granules were mixed with 1.0% magnesium stearate in a twin-shell mixer (Tokujyu Ind. Co., Model V-1, capacity, 2 L, mixing speed, 28 rpm) for 10 min. A compression/tension tester (Autograph, model IS-5000, Shimadzu Co., Kyoto, Japan) was used at 25±1 °C. An 8-mm diameter die and punches compressed samples of 200 mg at 147 MPa (maximum upper punch pressure) at a flat surface compression speed of 15 mm/min. The tablet hardness was measured 3 times using a hardness tester (Toyama Co.).

Dissolution Test Drug dissolution was investigated in JP XIII 1st (pH 1.2) fluids. The sample tablet was introduced into 800 ml of dissolution medium at 37+0.5 °C. The test solution was stirred with a paddle (JP XIII) at 100 rpm. Aliquots (3 ml) of the solution were withdrawn through a 0.8 μm membrane filter at appropriate time intervals using a syringe and suitably diluted with dissolution medium for measurement of the CBZ concentration. The concentration of the drug was measured spectrophotometrically (model UV-160A, Shimadzu Co.) at 285 nm. The tablet disintegration time was evaluated by visible observation. All values are reproducible and represent the average of three runs.

Results and Discussion

Physicochemical Properties of CBZ Figures 1 and 2 shows the X-ray diffraction profiles and DSC curves of CBZ powders and excipients. CBZ was prepared by several means, as previously reported.[6,7] The X-ray diffraction patterns and the DSC curves of all crystalline CBZ forms were significantly different and identical to these reported.[6,7] The lactose was identical to α-crystalline monohydrate, and the corn starch was amorphous. The X-ray diffraction profiles and DSC curves of lactose and cornstarch did not change after granulation of the formulation without bulk CBZ powder.

Preparation of CBZ Granules from Polymorphic Forms of CBZ by Extrusion–Granulation The granule yield of all granules obtained by adding 150 ml/kg of the binder solution is shown in Table I. The yield of granules obtained from each of the forms I and IV was more than 70%

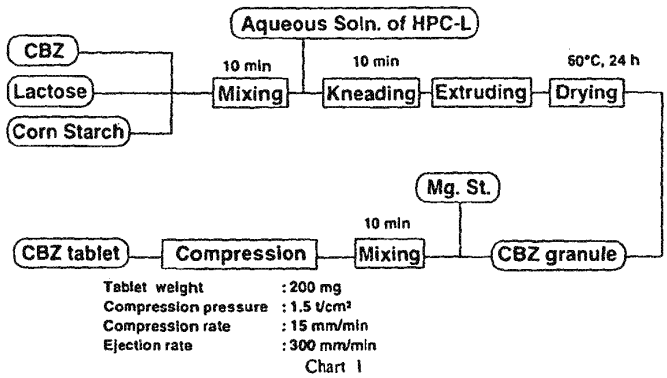

Chart 1

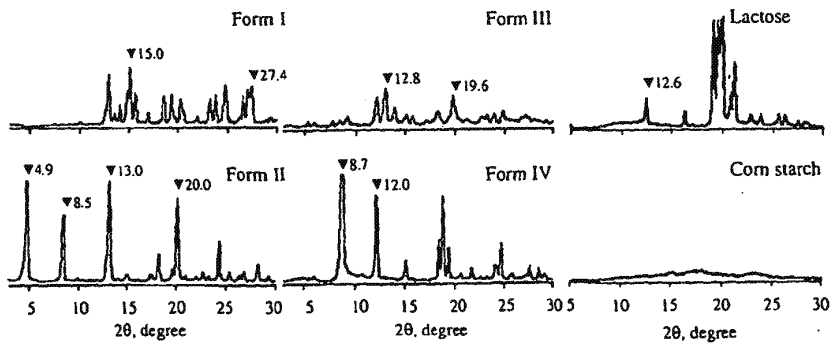

Fig. 1. Powder X-Ray Diffraction Profiles of CBZ Powders and Excipients

NOVARTIS EXHIBIT 1517
Novartis v. Regents, IPR2023-01347
Page 3703 of 4460

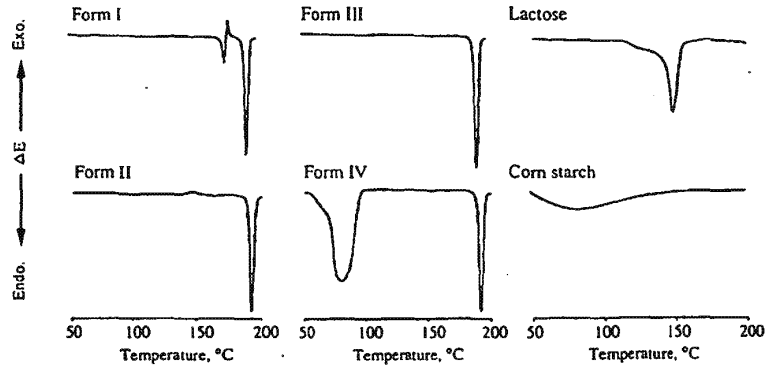

Fig. 2. DSC Curves of CBZ Powders and Excipients

Table 1. Yield of CBZ Granules by Extrusion–Granulation

Sample name	Crystalline form	Binder solution (ml/kg)	Added water (ml/kg)	Transformed (%)	Yield (%)
A	Form I	150	0	2.5	73.8
B	Form II	150	0	80.3	0.0
C	Form II	150	60	82.5	65.1
D	Form III	150	0	35.2	0.0
E	Form III	150	30	38.1	69.2
F	Form IV	150	0	98.8	76.3

The transformed value was based on the latent heat of dehydration in DSC, the yield is the percent amount of the sample granules that passed through a No. 12 mesh screen (1400 μm) but not a No. 42 mesh (355 μm).

yield. However, the yields of forms II and III were almost zero, since the mixed powders were not wet after kneading with the binder solution by the mixer, and did not mass even when treated with the granular instrument. Young *et al.*[8] reported first-order kinetics of CBZ polymorphic transformation in aqueous suspension, suggesting that anhydrate CBZ transformed into dihydrate in aqueous suspension. Anhydrate CBZ absorbed water into its crystalline structure and transformed into dihydrate during granulation, meaning that the decrease of free water in the wet powder mass made difficult the granulation process.

Figure 3 shows the DSC curves of the CBZ forms in the granules during granulation. After granulation forms I, II and III were 2.5, 80.3 and 35.2% transformed into dihydrate, respectively. Next, the wet granules were dried at 60 °C, after which the transformed dihydrate was transformed into form III, but form I did not change. Thus, CBZ was transformed into dihydrate, and dehydrated into fine particles of anhydrate form III, and the amount transformed depended on the stability of the crystalline phase of the bulk powder in water. The amount (Table 1) transformed suggested the order of the stability: CBZ form I>III≥II. Kaneniwa *et al.*[5] reported the rate of phase transition of forms I, II and III in distilled water at 20 °C by the rotating disk method to be 0.151, 0.369 and 0.130 min^{-1}, respectively, and suggested that CBZ form I was the most stable in distilled water. This result is partially consistent with the present data, but the order was not the same. This is because the previous results were obtained by the rotating disk method in distilled water, whereas the present results were obtained by the powder suspending method in water. The difference may be related to the variation between particle size and/or the shape of the forms. The results clearly indicated that the decrease of granule yields of forms II and III (samples B and D) were caused by a lack of kneading water due to absorption of CBZ as crystalline water. Therefore, to the granules of forms II and III (samples C and E) was added extra water in order to supplement that absorbed during the dihydrate transformation. The amount of water added was considered to represent the amount of dihydrate transformed during granulation, respectively. The granule yields of forms II and III (samples C and E) were improved markedly as shown in Table 1, indicating that the decrease of granule yield caused by the water absorption was due to transformation of dihydrate.

Characteristics of the Granules and Tablet Obtained from the Various CBZ Polymorphic Forms as Bulk Powders Table 2 shows the Sw of CBZ granules and their tablet hardness. The Sw result suggested that the granules obtained from form II bulk powder had the largest Sw, and those from form I the lowest. From the value of Sw of the granules, the powders are ranked as form II>III>IV>I. Sekiguchi *et al.* reported[10] that particle size reduction in several medical compounds was accomplished by forming solvates and then removing the solvent from the solvate. The present results suggested that the metastable forms transformed into fine monohydrate during granulation, and then the hydrate dehydrated and transformed into very fine anhydrate particles during the drying process. The particle size of the less stable CBZ was more reduced than that of the stable form after granulation and drying, since the amount of dihydrate transformed from the starting materials depended on the stability in the binder solution.

From the mechanical strength of the tablet obtained from the granules, the ranking was the same as that for the Sw: form II>III>IV>I. The relationship between the Sw and tablet is shown in Figure 4. The plot produced a linear line, indicating that the mechanical strength of the tablet was proportional to the Sw of the particles. The granules obtained from form II bulk powder had the highest tablet hardness and Sw values, and those from form I the lowest Sw and tablet hardness values. This is because most of form II was transformed into fine particles *via* dihydrate during the manufacturing process, but little of form I was transformed. Previously,[9] the effect of solvent systems in binder solution on the

UM00016722
NOVARTIS EXHIBIT 1517
Novartis v. Regents, IPR2023-01347
Page 3704 of 4460

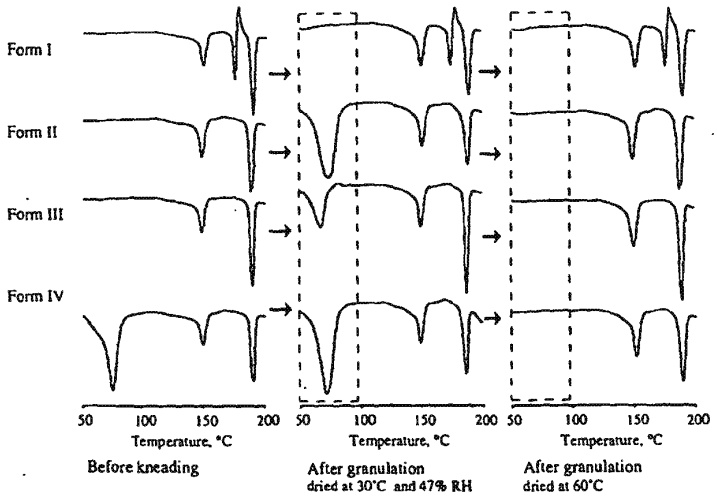

Fig. 3. Change of DSC Curves of CBZ Forms during Granulation and Drying Processes

Table 2. Pharmaceutical Properties of CBZ Granules and Their Tablet Obtained by Extrusion–Granulation.

Sample name	Crystalline form	Sw ($m^2/g \pm$S.D.)	Tablet hardness (kg±S.D.)	T50 (min±S.D.)	DT (min±S.D.)
A	Form I	0.952±0.021	7.7±0.2	3.2±0.2	2.1±0.2
C	Form II	2.87±0.016	14.6±0.3	64.4±5.2	72.2±6.1
E	Form III	2.075±0.025	12.1±0.2	9.8±1.3	11.4±2.2
F	Form IV	1.788±0.044	10.7±0.3	3.1±0.1	5.2±1.2

Sw, specific surface area of CBZ granules; T50, time required for 50% dissolution for tablets; DT, tablet disintegration time.

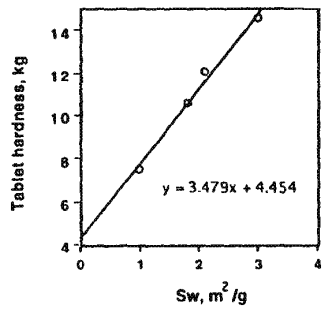

Fig. 4. Relationship between Sw and Tablet Hardness of the Granules Obtained from Various Polymorphic Forms of CBZ

tablet hardness of CBZ tablets was investigated. A large amount of the metastable CBZ (form I) was transformed into fine anhydrate particles *via* a dihydrate form in a soluble solution (50% ethanol) during extruding granulation, but this did not occur with distilled water or ethanol solutions in a less soluble solution. The tablet hardness improved by the phase change reflects the increasing of Sw. In the present study, the tablet hardness was affected by the stability of the CBZ polymorphic powders in the kneading solution, and depended on the amount of fine particle transformed during granulation and drying. The least stable crystalline form was the most effective in improving tablet hardness as a bulk powder for tablet production. This implies that the tablet hardness can be controlled by the degree of phase transformation.

Dissolution Behavior of the CBZ Tablets Obtained from the Various Polymorphic Forms Figure 5 shows the dissolution behavior of the CBZ tablets prepared by compressing the granules obtained from the polymorphic forms as starting bulk powder, and the times required for 50% dissolution (T50) are summarized in Table 2. The tablets A and F disintegrated and dissolved very rapidly, but tablet C dissolved very slowly. Since tablet C had a relatively large Sw, it seems that the geometrical structure of the tablet was more complex than that of the others. Tablet C has fine particles due to transformation of a large amount of form II, but tablets A, E and F do not.

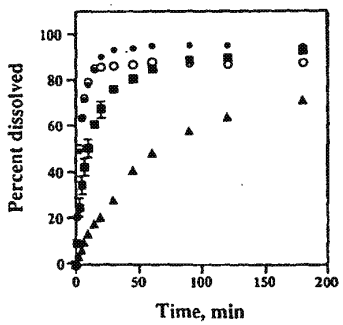

Fig. 5. Dissolution Profiles of the CBZ Granules Obtained from the Polymorphic Forms

●, Tablet A; ▲, tablet C; ■, tablet E; ○, tablet F.

In the order of T50, the ranking was table F≤A<E<C. Kaneniwa *et al.*[5] reported the solubility of forms I, II, III and IV to be 785, 531, 504 and 269 $\mu g \cdot ml^{-1}$ at 40 °C, respectively. In the present study, tablets C, E and F consisted of form III, but tablet A is of form I. The ranking of T50 of tablets is not consistent with that of the solubility of CBZ polymorphs. This result suggests that the dissolution rate for

UM00016720
NOVARTIS EXHIBIT 1517
Novartis v. Regents, IPR2023-01347
Page 3705 of 4460

the various CBZ tablets depends on the crystalline forms of the starting material, which is clearly consistent with the results for Sw and hardness of tablet.

Conclusions

The pharmaceutical properties and yield of granules and/or tablets containing metastable polymorphic forms of CBZ as bulk powder were affected by the stability of crystalline transformation during the manufacturing processes. Because the free water content changed depending on the extent of absorption during the transformation to dihydrate, the granulation process was affected. On the other hand, particle size was reduced by forming the hydrate and removing the crystalline water. The particle size reduction changed the mechanical strength of the tablet and their dissolution behavior. The nature of the bulk powders and excipients, such as polymorphic form, particle size and distribution, crystallinity *etc.*, reflect the history of the chemical and physical treatments of the raw materials. Therefore, to prepare better quality granules it is necessary to monitor and control the characteristics of the powder materials.

Acknowledgments This work was supported in part by a Grant-in-Aid for Scientific Research from the Ministry of Education, Science, Sports and Culture, Japan.

References

1) *a*) Otsuka M., Gao J., Matsuda Y., *Drug Devel. Ind. Pharm.*, 20, 2977—2992 (1994); *b*) Woodruff C. W., Nuessle, N. O., *J. Pharm. Sci.*, 61, 787—790 (1972).
2) *a*) Ebian A. E. A. R., Moustafa R. M. A., Abul-Enin, E. B. *Egypt. J. Pharm. Sci.*, 26, 287—300 (1985); *b*) Ebian A. E. A. R., Fikrat H. T., Moustafa R. M. A., Abul-Enin, E. B., *Egypt. J. Pharm. Sci.*, 27, 347—358 (1986); *c*) *Pharm. Tech. Japan*, 1, 835.
3) *a*) Haleblian J. K., *J. Pharm. Sci.*, 64, 1269—1288 (1975); *b*) Gouda H. W., Moustafa M. A., Al-Shora H. I., *Int. J. Pharm.*, 18, 213 (1984).
4) *a*) Polmann H., Gulde C., Jahn R., Pfeifer S., *Pharmazie*, 30, 709—711 (1975); *b*) Lefebvre C., Guyot-Hermann A. M., Draguet-Brughmans M., Bouché R., *Drug Devl. Ind. Pharm.*, 12, 11—13 (1986).
5) Kaneniwa N., Ichikawa J., Yamaguchi T., Hayashi K., Watari N., Sumi M., *Yakugaku Zasshi*, 107, 808—813 (1987).
6) Kahela P., Aaltonen R., Lewing E., Anttila M., Kristoffersson E., *Int. J. Pharm.*, 14, 103—120 (1983).
7) Kaneniwa N., Yamaguchi T., Watari N., Otsuka M., *Yakugaku Zasshi*, 104, 184—190 (1984).
8) Young W. W. L., Suryanarayanan R., *J. Pharm. Sci.*, 80, 496—500 (1991).
9) Otsuka M., Hasegawa H., Matsuka Y., *Chem. Pharm. Bull.*, 45, 894—898 (1997).
10) Sekiguchi K., Shirotani K., Kanke M., Furukawa H., Iwatsuru M., *Chem. Pharm. Bull.*, 24, 1621—130 (1976).

UM00016724
NOVARTIS EXHIBIT 1517
Novartis v. Regents, IPR2023-01347
Page 3706 of 4460

本複製物は、特許庁が著作権法第４２条第２項第１号の規定により複製したものです。
取扱にあたっては、著作権侵害とならないよう十分にご注意ください。

Pergamon

Tetrahedron Letters 39 (1998) 9831–9834

TETRAHEDRON LETTERS

Layered Structures Formed by Dinitrobenzoic Acids

V. R. Pedireddi, Anuparna Rangarajan and Swati Chatterjee*

Chemistry & Physics of Materials Unit,
Jawaharlal Nehru Centre for Advanced Scientific Research,
Jakkur P.O., Bangalore 560 064, India.

Received 27 August 1998; accepted 19 October 1998

Abstract: 3,5-dinitrobenzoic acid, 1 and 3,5-dinitro-4-methylbenzoic acid, 2, form co-crystals with 4,4'-bipyridyl but only the latter forms a layered structure, which can incorporate anthracene molecules. Furthermore, 2 forms a pillared type structure with thionicotinamide. © 1998 Elsevier Science Ltd. All rights reserved.

A variety of nanoporous inorganic structures are known.[1] Recently, there has been some effort to explore whether organic porous structures can be designed and synthesized by making use of supramolecular organization.[2] Thus, Yaghi et al.[3] have reported a microporous metal-organic framework based on a trimesic acid-pyridine-cobalt complex. Recently, novel layered and channel structures formed by trithiocyanuric acid (TTCA) were reported from this laboratory.[4] Crystallization of TTCA from acetone gave a layered structure, comparable to clays, pillared by acetone molecules while co-crystallization of TTCA from benzene solution gave a novel channel structure which could accommodate benzene. Encouraged by these findings, we wanted to examine other possible organic porous structures obtained by noncovalent synthesis.[5] In this context, it appeared to us that 3,5-dinitrobenzoic acid, 1 and 3,5-dinitro-4-methylbenzoic acid, 2 were well suited to form such structures. This is because, 1 is known to form a structure with cavities when crystallized from benzene solution, the cavities accommodating molecules such as anthracene.[6] In the absence of benzene, 1 does not form a layered structure. Crystallization of 2, from most solvents, yields structures with cavities in a two-dimensional arrangement, which can accommodate anthracene.[6a] We have investigated whether the cavities formed by 1 and 2 could be modified by incorporating an azaaromatic donor molecule such as 4,4'-bipyridyl, 3. In addition, we have examined the possibility of formation of layered structures by 1 and 2 by co-crystallization with other compounds.

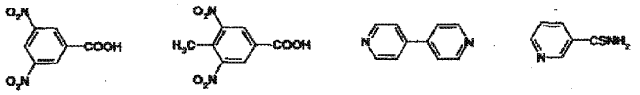

Crystallization of 1 and 2 in the presence of 3 gave complexes **1a** and **2a** respectively with 2:1 stoichiometry.[7] In both **1a** and **2a**, bipyridyl molecules break up the hydrogen bonds between the carboxyl groups as shown in Figure 1. Interestingly, interaction between the carboxylic acid and the bipyridyl molecule in these complexes occurs through the formation of a single O-H…N hydrogen bond[8] (see Figure 1) unlike the pair-wise hydrogen bond coupling, consisting of O-H…N and C-H…O bonds as shown below, observed in other related systems.[9] The H…N distances in **1a** and **2a** are 1.61 and 1.58-1.65Å respectively. Furthermore, molecules of **2a** are arranged in two dimensions to yield planar sheets (Figure 2) which in turn are stacked in the three-dimensional packing while molecules of **1a** adopts a herringbone packing pattern.

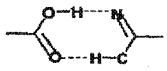

0040-4039/98/$ - see front matter © 1998 Elsevier Science Ltd. All rights reserved.
PII: S0040-4039(98)02244-8

本複製物は、特許庁が著作権法第４２条第２項第１号の規定により複製したものです。
取扱にあたっては、著作権侵害とならないよう十分にご注意ください。

Although both **1a** and **2a** do not possess cavities, the two-dimensional arrangement in **2a**, (Figure 1), which is similar to that of the structure of pure acid, **2**[6a] encouraged us to investigate the co-crystallization of **1a** and **2a** in the presence of anthracene. **1a** did not yield any co-crystals with anthracene, but **2a** gave crystals of a quality suitable for single crystal X-ray diffraction studies.

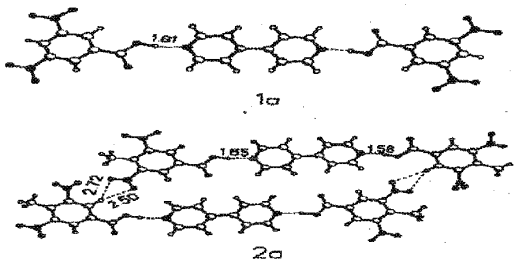

Figure 1: 1a) Recognition pattern between acid, **1** and 4,4'-bipyridyl in the molecular complex, **1a**. The dashed lines represent hydrogen bonds and unique H...O distance is quoted. 2a) Two-dimensional arrangement of supermolecules of acid, **2** and 4,4'-bipyridyl in **2a**. Notice the formation of a six membered ring formed through hydrogen bonds.

The complex of **2a** with anthracene (designated as **2b**[7]) is stabilized by the formation of O-H...N and C-H...O hydrogen bonds coupling[9] (Figure 2), not found either in **2a** or **1a**. The H...N and H...O distances between **2** and **3** in the anthracene adduct, **2b**, are 1.68 and 2.57Å respectively. Figure 2 shows that the supermolecules are arranged in two dimensions in a hexagonal mode through the formation of C-H...O hydrogen bonds between anthracene and the neighbouring molecules of carboxylic acid, **2** such that a cavity of dimension 10 x 12Å results. The anthracene molecules are accommodated in these cavities through the formation of C-H...O hydrogen bonds. The H...O distances are in the range of 2.76 – 2.93Å. A comparison of the structure of **2b** (Figure 2) with the anthracene adduct formed by the parent carboxylic acid, **2**[6a] alone indicates that the recognition pattern between anthracene and the acid **2** is not perturbed with the presence of bipyridyl molecule in **2b**.

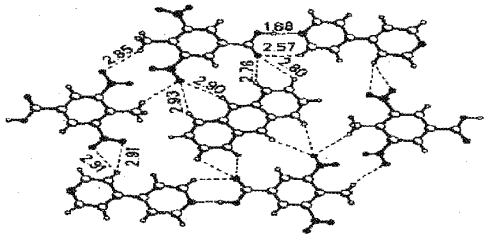

Figure 2: Two-dimensional arrangement of a cavity, formed by acid **2** and 4,4'-bipyridyl, which is filled by molecules of anthracene in the complex **2b**.

UM00016726
NOVARTIS EXHIBIT 1517
Novartis v. Regents, IPR2023-01347
Page 3708 of 4460

本複製物は、特許庁が著作権法第４２条第２項第１号の規定により複製したものです。
取扱にあたっては、著作権侵害とならないよう十分にご注意ください。

We have investigated the formation of pillared structures of **2** which forms layer structures even in the absence of guest molecules such as benzene. Crystallization of **2** from acetone gave a layered structure with no pillaring. We, therefore, crystallized **2** with compounds containing different types of hydrogen-bond donating and accepting sites. Crystallization of **2** with pyridine carboxylic acid or nicotinamide did not yield a molecular complex. We then examined the co-crystals of **2** with thionicotinamide, **4**, since the presence of sulfur could change the recognition pattern. It is known that sulfur-mediated hydrogen bonds such as N-H...S are indeed different from O-H...O, N-H...O and such hydrogen bonds.[4,10] Thus, **2** and **4** yield a complex **2c** upon co-crystallization from methanol.

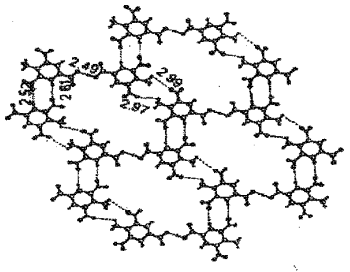

Figure 3: Two-dimensional arrangement of a layer of acid, **2** in the complex with thionicotinamide. The H...O bonds are shown in dashed lines and unique H...O distances are quoted for C-H...O hydrogen bond and O...O distance is quoted for O-H...O hydrogen bond.

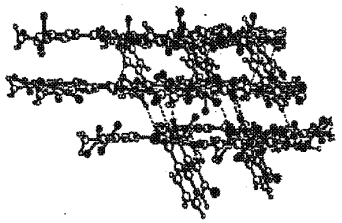

Figure 4: Stacking of layers in a three-dimensional arrangement in the complex, **2c**. Notice the pillaring of thionicotinamide molecules between the layers.

Crystal structure determination of the 2:1 adduct, **2c**[7], formed by **2** with thionicotinamide reveals that the asymmetric unit contains two symmetry independent molecules. Packing analysis shows that the co-crystals of **2** and **4** adopt a pillared type structure.[11] Each of the symmetry dependent molecules of **2** interacts with neighbouring molecules to form two-dimensional planar sheets (Figure 3) which in turn stack alternately in a three-dimensional arrangement through π-π interaction. It is clear from Figure 3 that in each sheet, molecules are held together through formation of O-H...O and C-H...O hydrogen bonds. The H...O distances are in the 2.55 - 3.00Å range. The -COOH groups of adjacent molecules form only a single O-H...O hydrogen bond rather than the well known cyclic hydrogen bonded system, as one of the acids is deprotonated. The mutual association of the molecules in each sheet, however, results in the formation of cavities of 7 x 12Å. The molecules of **4** are intercalated in between the sheets, to yield a pillared type structure, as shown in Figure 4. It is evident from Figure 4 that the molecules of **4** are inclined to the layers of acid, **2** unlike anthracene molecules which are coplanar with the sheets observed in the crystal structure of complex, **2b** (see Figure 2).

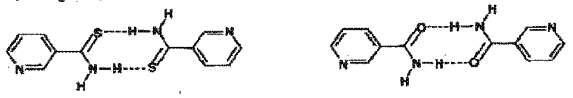

(a)　　(b)

Scheme 1

UM00016727
NOVARTIS EXHIBIT 1517
Novartis v. Regents, IPR2023-01347
Page 3709 of 4460

本複製物は、特許庁が著作権法第４２条第２項第１号の規定により複製したものです。
取扱にあたっては、著作権侵害とならないよう十分にご注意ください。

It is rather surprising that thionicotinamide and nicotinamide show such different behaviour with respect to interaction with **2**. It appears that hydrogen bonding pattern shown in Scheme 1 plays a significant role. It is known that molecules with amide or thioamide groups exist as dimers rather than monomers. However, it is evident from Figure 4 that in the complex **2c**, the molecules of **4** intercalated in between the acid sheets are single. It is easier to obtain such single molecular units from **4** rather than nicotinamide as the dimers in the former are formed through weak N-H...S hydrogen bonds (Scheme 1a) whereas the dimers in nicotinamide result from the strong N-H…O hydrogen bonds (Scheme 1b).

Acknowledgements:

We are grateful to Professor C. N. R. Rao, F.R.S. for his encouragement and interest in this work.

References:

1) (a) Oliver, S., Kuperman, A. and Ozin, G. A., *Angew. Chem. Int. Ed.* **1998**, *37*, 46. (b) Thomas, J. M., *Chem. Eur. J.*, **1997**, *3*, 1557. (c) Davies, M. E., *Chem. Eur. J.*, **1997**, *3*, 1745.

2) Gardner, G. B., Venkataraman, D., Moore, J. S. and Lee, S., *Nature*, **1995**, *374*, 792.

3) (a) Yaghi, O. M., Li, G. and Li, H., *Nature*, **1995**, *378*, 703. (b) Yaghi, O. M. and Li, H., *J. Am. Chem. Soc.*, **1996**, *118*, 295.

4) Pedireddi, V. R., Chatterjee, S., Ranganathan, A. and Rao, C. N. R., *J. Am. Chem. Soc.*, **1997**, *119*, 10867.

5) *For highlighted articles on noncovalent synthesis see* (a) Whitesides, G. M., Simanek, E. E., Mathias, J. P., Seto, C. T., Chin, D. N., Mammen, M. and Gordon, D. M., *Acc. Chem. Res.*, **1995**, *28*, 37. (b) Etter, M. C., *J. Phys. Chem.*, **1991**, *95*, 4601. (c) Desiraju, G. R., *Angew. Chem. Int. Ed. Engl.* **1995**, *34*, 2311. (d) Ankeroy, C. B., *Acta Cryst.*, **1997**, *B53*, 569. (e) Ranganthan A. and Pedireddi, V. R., *Tetrahedron Letters*, **1998**, *13*, 1803.

6) (a) Pedireddi, V. R., Jones, W., Chorlton, A. P. and Docherty, R., *Chem. Commun.*, **1996**, 987. (b) Pedireddi, V. R., Jones, W., Chorlton, A. P. and Docherty, R., *Tetrahedron Letters*, **1998**, *39*, 5409.

7) Crystal structure determination procedure: Data were collected for all the crystals (**1a**, **2a** - **2c**) on Smart. CCD area detector using MoKα (λ=0.7107) at T=293 K. Structures were determined using SHELXTL-PLUS package (Sheldrick, G. M., SHELXTL, Users Manual, Siemens Analytical X-ray Instruments Inc., Madison, Wisconsin, U. S. A., 1993). Crystal Data for **1a**: $2(C_7H_6N_2O_6):C_{10}H_8N_2$, M=580.43, monoclinic, $P2_1/n$, a=6.226(1), b=22.150(2), c=9.417(1)Å, β=99.17(1)°, Z=2, F(000)=596, R_1=0.065 and wR_2=0.087. Crystal Data for **2a**: $2(C_8H_6N_2O_4):C_{10}H_8N_2$, M=608.48, triclinic, $P\bar{1}$, a=9.852(1), b=11.297(1), c=14.827(1)Å, α=67.72(1), β=89.77(2), γ=64.85(1)°, Z=2, F(000)=628, R_1=0.049 and wR_2=0.098. Crystal Data for **2b**: $2(C_8H_6N_2O_4):(C_{14}H_{10}):(C_{10}H_8N_2)$, M=786.70, triclinic, $P\bar{1}$, a=9.121(1), b=9.260(1), c=11.199(1)Å, α=73.83(1), β=89.58(1), γ=81.78(1)°, Z=1, F(000)=408, R_1=0.055 and wR_2=0.085. Crystal Data for **2c**: $2(C_8H_6N_2O_4):C_8H_6N_2S_2$, M=590.48, triclinic, $P\bar{1}$, a=12.840(1), b=14.270(1), c=15.506(1)Å, α=69.24(1), β=74.18(1), γ=82.07(1)°, Z=4, F(000)=1216, R_1=0.064 and wR2=0.124.

8) Ferguson, G., Glidewell, C., McManus, G. D. and Meehan, P. R., *Acta Cryst.* 1998, *CS4*, 418.

9) (a) Pedireddi, V. R., Jones, W., Chorlton, A. P. and Docherty, R. *Chem. Commun.*, **1996**, 997. (b) Chatterjee, S., Pedireddi, V. R. and Rao, C. N. R., *Tetrahedron Letters*, **1998**, *39*, 2843.

10) Allen, F. H., Bird, C. M., Rowland, R. S. and Raithby, P. R., *Acta Cryst.* **1997**, *B53*, 680.

11) Kooli, F., Chisem, I. C., Vucelice., M and Jones, W., *Chem. Mater.* **1996**, *8*, 1969.

UM00016728
NOVARTIS EXHIBIT 1517
Novartis v. Regents, IPR2023-01347
Page 3710 of 4460

Electronic Acknowledgement Receipt

EFS ID:	8731500
Application Number:	10378956
International Application Number:	
Confirmation Number:	4742
Title of Invention:	Multiple-component solid phases containing at least one active pharmaceutical ingredient
First Named Inventor/Applicant Name:	Michael J. Zaworotko
Customer Number:	23557
Filer:	Glenn Ladwig/J'Nese Williams
Filer Authorized By:	Glenn Ladwig
Attorney Docket Number:	USF.106XC1
Receipt Date:	29-OCT-2010
Filing Date:	03-MAR-2003
Time Stamp:	13:47:35
Application Type:	Utility under 35 USC 111(a)

Payment information:

Submitted with Payment	no

File Listing:

Document Number	Document Description	File Name	File Size(Bytes)/ Message Digest	Multi Part /.zip	Pages (if appl.)
1		SIDS7.pdf	2449838 0d744cb1d3cc117374acff5b7a26e5863c9cc966	yes	13

	Multipart Description/PDF files in .zip description				
	Document Description		Start	End	
	Transmittal Letter		1	2	
	Information Disclosure Statement (IDS) Filed (SB/08)		3	13	
Warnings:					
Information:					
2	Foreign Reference	FR2849029.pdf	3394992 6c743ea4839a5ae5236b34d1839b1d19c7828c9d	no	86
Warnings:					
Information:					
3	Foreign Reference	JP-46-33588.pdf	329178 976c23a726f5a1fe7950757fd347ceb7a811795a	no	3
Warnings:					
Information:					
4	Foreign Reference	JP54095589.pdf	242796 5c86a7aa085e64aa88223d1283682d71b2936521	no	5
Warnings:					
Information:					
5	Foreign Reference	EP1167355.pdf	445281 3322b715028e15030227828 71acfeb1e177d1be1	no	14
Warnings:					
Information:					
6	Foreign Reference	GB1297261A.pdf	330137 19d2e76abc6479196d78c97da324414ab4af4d80	no	4
Warnings:					
Information:					
7	Foreign Reference	GB2169601A.pdf	231774 232d7bf0f1d99788addf2b1abfb5606263b05c44	no	6
Warnings:					
Information:					
8	Foreign Reference	WO95-023596.pdf	1187100 925b4bbedafc421d097fd5940b682b24a18993e0	no	35
Warnings:					
Information:					

9	Foreign Reference	WO96-033193.pdf	998489 a20b221937233ac198a8da9d8966b3d16b29406e	no	23
Warnings:					
Information:					
10	Foreign Reference	WO00-07583.pdf	4193821 07070b3b562eb4bdeccbccce63ae30893f9fc48f	no	105
Warnings:					
Information:					
11	Foreign Reference	WO00-32189.pdf	3706679 49ef22696d171aacb4c07dffe2c40b059798f2a0	no	79
Warnings:					
Information:					
12	Foreign Reference	WO00-50020.pdf	1414899 08750c558f2cc636dd5125e6f6a5bcc7d8fd1cc7	no	38
Warnings:					
Information:					
13	Foreign Reference	WO00-72841.pdf	1013664 d25f5c3e6f40f1621785db4a453bb86541bc4a24	no	23
Warnings:					
Information:					
14	Foreign Reference	WO01-41536.pdf	1639050 be4e655af0062c330b69ab5a6aaa54c4468e1629	no	40
Warnings:					
Information:					
15	Foreign Reference	WO01-41760.pdf	3338601 f33c0455cbf0ea30bf7d6745ecb1a83a71b5f6a8	no	59
Warnings:					
Information:					
16	Foreign Reference	WO01-42222.pdf	3242114 609883a04b51efa43449d65893eeb50d7a6f1ca8	no	89
Warnings:					
Information:					
17	Foreign Reference	WO01-45706.pdf	3356250 07d33f373b7b7acd3fd3fe07273ac7767b088b3a	no	66
Warnings:					
Information:					

18	Foreign Reference	WO01-51919.pdf	11567650 9fcced6c6ebb4d2861db9da102a1a489cec80fb8	no	228
Warnings:					
Information:					
19	Foreign Reference	WO01-78724.pdf	2371566 d6681d47cb2e325f142ea94653bce8ce41d8e876	no	48
Warnings:					
Information:					
20	Foreign Reference	WO01-91750.pdf	1943299 59da680f92cac0e8c9e9fd1276f11d2823b23192	no	39
Warnings:					
Information:					
21	Foreign Reference	WO02-00627.pdf	617468 35dae4afdf700719d700cfb06f76ee7040d36d9a	no	23
Warnings:					
Information:					
22	Foreign Reference	WO02-56878.pdf	2838984 c814947fc78f68f39cd15fe9e211f70a0ef236fb	no	73
Warnings:					
Information:					
23	Foreign Reference	WO02-056915.pdf	1178158 3002d8c361563cb3eb26c429c204b413bd3283ba	no	25
Warnings:					
Information:					
24	Foreign Reference	WO02-102376.pdf	3360090 3c13c40d90f23e515029c22fb14beb36f5099a075	no	65
Warnings:					
Information:					
25	Foreign Reference	WO02-010125.pdf	1488036 44cc4561d6cd268be1cb60563d7ba82510b1c0ee	no	35
Warnings:					
Information:					
26	Foreign Reference	WO03-033462.pdf	2278239 accd2aa950963e762ee085d8ad60e35b2c431a59	no	49
Warnings:					
Information:					

27	Foreign Reference	WO05-053612.pdf	1474912 addb68cbe8045c9d545d8a0b3fff2294316f528a	no	38
Warnings:					
Information:					
28	Foreign Reference	WO05-077894.pdf	2304159 75afd8d175fe65bae2430bc0ed064a85058616c2	no	53
Warnings:					
Information:					
29	Foreign Reference	WO05-118577.pdf	3900866 9bf2af967719bee7a77a4eb09cf96f6673eb9e5c	no	86
Warnings:					
Information:					
30	Foreign Reference	WO04-060347.pdf	14670483 7365951dcc06b94c306b7d7c9f0a32053e66dc43	no	317
Warnings:					
Information:					
31	NPL Documents	Aakeroy-DoPolymorphic.pdf	783918 e8dec735cea086276173306 9f3378c83b8cc c2f5	no	7
Warnings:					
Information:					
32	NPL Documents	Bastin.pdf	2096987 0860c25cf63e191ea18cd8455ebfac6c0fc71de7	no	9
Warnings:					
Information:					
33	NPL Documents	Brader.pdf	685764 b6fe96f82bc719f85780b05aec9c125d9c9259a2	no	5
Warnings:					
Information:					
34	NPL Documents	Brittain.pdf	1001878 f8779de073146dbede4ee4a5a00eee3aec70d123	no	11
Warnings:					
Information:					
35	NPL Documents	Cowan.pdf	436901 2bae35c44fcdbe391b21ee031ce63cc0555364a4	no	5
Warnings:					
Information:					

36	NPL Documents	Database.pdf	46909 a6ea18e4c8fbba462934ae435002090f927d5022	no	1
Warnings:					
Information:					
37	NPL Documents	Davidovich.pdf	952974 e1ed2aadadec90c7d95c63159fc7687a9a030c41	no	5
Warnings:					
Information:					
38	NPL Documents	Davies.pdf	176568 bc90e8f89b38de2912bbdf100a1c80024cba4515	no	19
Warnings:					
Information:					
39	NPL Documents	Dean.pdf	771860 77d9cd0d2e4440bfbdc9ba80b81c6f442b3a9b88	no	4
Warnings:					
Information:					
40	NPL Documents	DefSolvate.pdf	76254 f554053aa60b9466076f2540c97301109306f42f	no	3
Warnings:					
Information:					
41	NPL Documents	Doelker-2002.pdf	721331 013e03f7ab7bf960be662f9dedca46651abf5538	no	10
Warnings:					
Information:					
42	NPL Documents	Doelker-2000.pdf	1227944 b3037fb0c0b4aaf1661ddfc2fe8579847cdf08ba	no	13
Warnings:					
Information:					
43	NPL Documents	Dunitz-2003.pdf	1311104 e086682e5248598102b23e47b430a4256247d448	no	4
Warnings:					
Information:					
44	NPL Documents	Dvorkin.pdf	331196 47f8ee4ad1915b68a410211addced6168630d4f7	no	6
Warnings:					
Information:					

45	NPL Documents	El-Nahhas.pdf	295893 f011aa5fa5512c6fe6a0e87c56de2ad99ef750fe	no	4
Warnings:					
Information:					
46	NPL Documents	Faught.pdf	74841 bf22a122f45715c4a5e0faf4bb7b8bc3310c7302	no	1
Warnings:					
Information:					
47	NPL Documents	Fitzgerald.pdf	152934 e7e94b17c9e2fda620e75c58525114c1c57f5cb4	no	10
Warnings:					
Information:					
48	NPL Documents	Fleischman.pdf	1236039 02179015e638385a027427fa314a8be3d0436714	no	11
Warnings:					
Information:					
49	NPL Documents	Fung.pdf	619074 69c06272bd796a7cf4a95849ae254448db5fde17	no	5
Warnings:					
Information:					
50	NPL Documents	deJong-1999.pdf	1177764 b0adfef3639e3d7014b66320c4fd2b08f6deada0	no	6
Warnings:					
Information:					
51	NPL Documents	Jain.pdf	995737 4674c88ad65b8c4acbab56efdcba398c0e02d500	no	15
Warnings:					
Information:					
52	NPL Documents	JP-OfficeAction.PDF	885502 a3f83728c348f4a218196c2a469b2bc2b277273c	no	11
Warnings:					
Information:					
53	NPL Documents	Kirchner.pdf	1520726 d62fe9f8cb00e48f2e300176bda1ee02883cd33b	no	17
Warnings:					
Information:					

54	NPL Documents	Klein.pdf	769798 7cea67fc43e1ff498cc80e07521033543f194479	no	5
Warnings:					
Information:					
55	NPL Documents	Muzaffar.pdf	505774 28610c99de6c2debc4225c395f4abb4b623c64b6	no	8
Warnings:					
Information:					
56	NPL Documents	Osorio-Lozada.pdf	329913 55fae9b65d05d36c11f99e5f6b93f3ae577572c8	no	5
Warnings:					
Information:					
57	NPL Documents	Oswald-2002.pdf	807519 b664e56aa098084ed716588b35d07cb4f92f494a	no	10
Warnings:					
Information:					
58	NPL Documents	Otsuka.pdf	349079 82e1a6129b3566422de40167b4dc11ec75b8482b	no	5
Warnings:					
Information:					
59	NPL Documents	Pedireddi.pdf	360900 0e8e9d9b6d0b937f35dd8af35be5492b85360e1d	no	4
Warnings:					
Information:					
		Total Files Size (in bytes):	102211654		

This Acknowledgement Receipt evidences receipt on the noted date by the USPTO of the indicated documents, characterized by the applicant, and including page counts, where applicable. It serves as evidence of receipt similar to a Post Card, as described in MPEP 503.

New Applications Under 35 U.S.C. 111
If a new application is being filed and the application includes the necessary components for a filing date (see 37 CFR 1.53(b)-(d) and MPEP 506), a Filing Receipt (37 CFR 1.54) will be issued in due course and the date shown on this Acknowledgement Receipt will establish the filing date of the application.

National Stage of an International Application under 35 U.S.C. 371
If a timely submission to enter the national stage of an international application is compliant with the conditions of 35 U.S.C. 371 and other applicable requirements a Form PCT/DO/EO/903 indicating acceptance of the application as a national stage submission under 35 U.S.C. 371 will be issued in addition to the Filing Receipt, in due course.

New International Application Filed with the USPTO as a Receiving Office
If a new international application is being filed and the international application includes the necessary components for an international filing date (see PCT Article 11 and MPEP 1810), a Notification of the International Application Number and of the International Filing Date (Form PCT/RO/105) will be issued in due course, subject to prescriptions concerning national security, and the date shown on this Acknowledgement Receipt will establish the international filing date of the application.

I hereby certify that this correspondence is being electronically filed in the United States Patent and Trademark Office on October 29, 2010.

Glenn P. Ladwig, Patent Attorney, Reg. #46,853

SUPPLEMENTAL INFORMATION DISCLOSURE STATEMENT
Patent Application
Docket No. USF.106XC1
Serial No. 10/378,956

IN THE UNITED STATES PATENT AND TRADEMARK OFFICE

Examiner	:	Sahar Javanmard
Art Unit	:	1627
Applicants	:	Michael J. Zaworotko, Brian Moulton, Nair Rodriguez-Hornedo
Serial No.	:	10/378,956
Filed	:	March 3, 2003
Conf. No.	:	4742
For	:	Multiple-Component Solid Phases Containing at Least One Active Pharmaceutical Ingredient

Mail Stop RCE
Commissioner for Patents
P.O. Box 1450
Alexandria, VA 22313

SUPPLEMENTAL INFORMATION DISCLOSURE STATEMENT
UNDER 37 C.F.R. §§ 1.97 AND 1.98

Sir:

In accordance with 37 C.F.R. § 1.56, the references listed on the attached form PTO/SB/08 are being brought to the attention of the Examiner for consideration in connection with the examination of the above-identified patent application. A copy of each cited reference is enclosed. However, Applicants have not submitted copies of the U.S. Patents or published U.S. Patent Applications cited on attached Form PTO/SB/08 pursuant to 37 CFR 1.98(a)(2)(ii).

It is respectfully requested that the references cited on the attached form PTO/SB/08 be considered in the examination of the subject application and that their consideration be made of record. If any additional fee is required, or to credit any overpayment, please use Deposit Account No. 19-0065.

J:\USF\106XC1\PTO\SIDS7.doc/DNB/jnw

Applicants note that French Patent No. 2849029, cited as F1 on the attached form PTO/SB/08, was written in a foreign language. However, an English language abstract is provided in the reference. Applicants respectfully request that the reference be made of record and considered in the examination of the subject application.

Applicants note that Japanese Patent No. 46-33588 cited as F2 on the attached form PTO/SB/08, was written in a foreign language. However, an English language abstract is provided in the reference. Applicants respectfully request that the reference be made of record and considered in the examination of the subject application.

Applicants note that Japanese Patent No. 54-095589, cited as F3 on the attached form PTO/SB/08, was written in a foreign language. However, an English language translation is provided of the relevant section within in the reference. Applicants respectfully request that the reference be made of record and considered in the examination of the subject application.

This information is being submitted subsequent to the filing of a Request for Continued Examination, therefore no fees are associated with this filing. Please charge any additional fees to Deposit Account No. 19-0065.

Respectfully submitted,

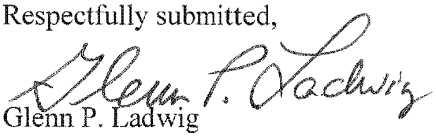

Glenn P. Ladwig
Patent Attorney
Registration No. 46,853
Phone No.: 352-375-8100
Fax No.: 352-372-5800
Address: P.O. Box 142950
Gainesville, FL 32614-2950

GPL/jnw
Attachments: Form PTO/SB/08; copies of references cited therein.

J:\USF\106XC1\PTO\SIDS7.doc/DNB/jnw

Tolectin—Cont.

used with caution in patients with compromised cardiac function, hypertension, or other conditions predisposing to fluid retention.

The antipyretic and anti-inflammatory activities of the drug may reduce fever and inflammation, thus diminishing their utility as diagnostic signs in detecting complications of presumed non-infectious, non-inflammatory painful conditions.

As with other nonsteroidal anti-inflammatory drugs, borderline elevations of one or more liver tests may occur in up to 15% of patients. These abnormalities may progress, may remain essentially unchanged, or may be transient with continued therapy. The SGPT (ALT) test is probably the most sensitive indicator of liver dysfunction. Meaningful (3 times the upper limit of normal) elevations of SGPT or SGOT (AST) occurred in controlled clinical trials in less than 1% of patients. A patient with symptoms and/or signs suggesting liver dysfunction, or in whom an abnormal liver test has occurred, should be evaluated for evidence of the development of more severe hepatic reaction while on therapy with TOLECTIN. Severe hepatic reactions, including jaundice and fatal hepatitis, have been reported with TOLECTIN as with other nonsteroidal anti-inflammatory drugs. Although such reactions are rare, if abnormal liver tests persist or worsen, if clinical signs and symptoms consistent with liver disease develop, or if systemic manifestations occur (e.g. eosinophilia, rash, etc.), TOLECTIN should be discontinued.

Carcinogenesis, Mutagenesis, Impairment of Fertility

Tolmetin sodium did not possess any carcinogenic liability in the following long-term studies: a 24-month study in rats at doses as high as 75 mg/kg/day, and an 18-month study in mice at doses as high as 50 mg/kg/day.

No mutagenic potential of tolmetin sodium was found in the Ames Salmonella-Microsomal Activation Test.

Reproductive studies revealed no impairment of fertility in animals. Effects on parturition have been shown, however, as with other prostaglandin inhibitors. This information is detailed in the Pregnancy section below.

Pregnancy

Pregnancy Category C. Reproduction studies in rats and rabbits at doses up to 60 mg/kg (1.5 times the maximum clinical dose based on a body weight of 60 kg) revealed no evidence of teratogenesis or impaired fertility due to TOLECTIN. However, TOLECTIN is an inhibitor of prostaglandin synthetase. Drugs in this class have known effects on the fetal cardiovascular system which may cause constriction of the ductus arteriosus *in utero* during the third trimester of pregnancy, which may result in persistent pulmonary hypertension of the newborn.

There are no adequate and well-controlled studies in pregnant women. TOLECTIN should be used during pregnancy only if the potential benefit justifies the potential risk to the fetus.

Non-Teratogenic Effects

Prostaglandin inhibitors have also been shown to increase the incidence of dystocia and delayed parturition in animals.

Nursing Mothers

TOLECTIN has been shown to be secreted in human milk. Because of the possible adverse effects of prostaglandin inhibiting drugs on neonates, use in nursing mothers should be avoided.

Pediatric Use

The safety and effectiveness of TOLECTIN in children under 2 years of age have not been established.

Drug Interactions

The *in vitro* binding of warfarin to human plasma proteins is unaffected by tolmetin, and tolmetin does not alter the prothrombin time of normal volunteers. However, increased prothrombin time and bleeding have been reported in patients on concomitant TOLECTIN and warfarin therapy. Therefore, caution should be exercised when administering TOLECTIN to patients on anticoagulants.

In adult diabetic patients under treatment with either sulfonylureas or insulin there is no change in the clinical effects of either TOLECTIN or the hypoglycemic agents.

Caution should be used if TOLECTIN is administered concomitantly with methotrexate. TOLECTIN and other nonsteroidal anti-inflammatory drugs have been reported to reduce the tubular secretion of methotrexate in an animal model, possibly enhancing the toxicity of methotrexate.

Laboratory Tests

Because serious GI tract ulceration and bleeding can occur without warning symptoms, physicians should follow chronically treated patients for the signs and symptoms of ulceration and bleeding and should inform them of the importance of this follow-up (see WARNINGS—Risk of GI Ulceration, Bleeding and Perforation with NSAID Therapy).

Drug/Laboratory Test Interaction

The metabolites of tolmetin sodium in urine have been found to give positive tests for proteinuria using tests which rely on acid precipitation as their endpoint (e.g. sulfosalicylic acid). No interference is seen in the tests for proteinuria using dye-impregnated commercially available reagent strips (e.g., Albustix®, Uristix®, etc.).

Drug-Food Interaction

In a controlled single dose study, administration of TOLECTIN with milk had no effect on peak plasma tolmetin concentrations, but decreased total tolmetin bioavailability by 16%. When TOLECTIN was taken immediately after a meal, peak plasma tolmetin concentrations were reduced by 50% while total bioavailability was again decreased by 16%.

Information for Patients

TOLECTIN, like other drugs of its class, is not free of side effects. The side effects of these drugs can cause discomfort and, rarely, there are more serious side effects, such as gastrointestinal bleeding, which may result in hospitalization and even fatal outcomes.

NSAIDs (Nonsteroidal Anti-Inflammatory Drugs) are often essential agents in the management of arthritis, but they also may be commonly employed for conditions which are less serious.

Physicians may wish to discuss with their patients the potential risks (see WARNINGS, PRECAUTIONS, and ADVERSE REACTIONS sections) and likely benefits of NSAID treatment, particularly when the drugs are used for less serious conditions where treatment without NSAID's may represent an acceptable alternative to both the patient and physician.

ADVERSE REACTIONS

The adverse reactions which have been observed in clinical trials encompass observations in about 4370 patients treated with TOLECTIN (tolmetin sodium), over 800 of whom have undergone at least one year of therapy. These adverse reactions, reported below by body system, are among those typical of nonsteroidal anti-inflammatory drugs and, as expected, gastrointestinal complaints were most frequent. In clinical trials with TOLECTIN, about 10% of patients dropped out because of adverse reactions, mostly gastrointestinal in nature.

Incidence Greater Than 1%

The following adverse reactions which occurred more frequently than 1 in 100 were reported in controlled clinical trials.

Gastrointestinal: Nausea (11%), dyspepsia,* gastrointestinal distress,* abdominal pain,* diarrhea,* flatulence,* vomiting,* constipation, gastritis, and peptic ulcer. Forty percent of the ulcer patients had a prior history of peptic ulcer disease and/or were receiving concomitant anti-inflammatory drugs including corticosteroids, which are known to produce peptic ulcerations.

Body as a Whole: Headache,* asthenia,* chest pain

Cardiovascular: Elevated blood pressure,* edema*

Central Nervous System: Dizziness,* drowsiness, depression

Metabolic/Nutritional: Weight gain,* weight loss*

Dermatologic: Skin irritation

Special Senses: Tinnitus, visual disturbance

Hematologic: Small and transient decreases in hemoglobin and hematocrit not associated with gastrointestinal bleeding have occurred. These are similar to changes reported with other nonsteroidal anti-inflammatory drugs.

Urogenital: Elevated BUN, urinary tract infection

* Reactions occurring in 3% to 9% of patients treated with TOLECTIN. Reactions occurring in fewer than 3% of the patients are unmarked.

Incidence Less Than 1%
(Causal Relationship Probable)

The following adverse reactions were reported less frequently than 1 in 100 in controlled clinical trials or were reported since marketing. The probability exists that there is a causal relationship between TOLECTIN and these adverse reactions.

Gastrointestinal: Gastrointestinal bleeding with or without evidence of peptic ulcer, perforation, glossitis, stomatitis, hepatitis, liver function abnormalities

Body as a Whole: Anaphylactoid reactions, fever, lymphadenopathy, serum sickness

Hematologic: Hemolytic anemia, thrombocytopenia, granulocytopenia, agranulocytosis

Cardiovascular: Congestive heart failure in patients with marginal cardiac function

Dermatologic: Urticaria, purpura, erythema multiforme, toxic epidermal necrolysis

Urogenital: Hematuria, proteinuria, dysuria, renal failure

Incidence Less Than 1%
(Causal Relationship Unknown)

Other adverse reactions were reported less frequently than 1 in 100 in controlled clinical trials or were reported since marketing, but a causal relationship between TOLECTIN and the reaction could not be determined. These rarely reported reactions are being listed as alerting information for the physician since the possibility of a causal relationship cannot be excluded.

Body as Whole: Epistaxis

Special Senses: Optic neuropathy, retinal and macular changes

MANAGEMENT OF OVERDOSAGE

In the event of overdosage, the stomach should be emptied by inducing vomiting or by gastric lavage followed by the administration of activated charcoal.

DOSAGE AND ADMINISTRATION

In adults with rheumatoid arthritis or osteoarthritis, the recommended starting dose is 400 mg three times daily (1200 mg daily), preferably including a dose on arising and a dose at bedtime. To achieve optimal therapeutic effect the dose should be adjusted according to the patient's response after one to two weeks. Control is usually achieved at doses of 600–1800 mg daily in divided doses (generally t.i.d.). Doses larger than 1800 mg/day have not been studied and are not recommended.

The recommended starting dose for children (2 years and older) is 20 mg/kg/day in divided doses (t.i.d. or q.i.d.). When control has been achieved, the usual dose ranges from 15 to 30 mg/kg/day. Doses higher than 30 [illegible] been studied and, therefore, are not recommended.

A therapeutic response to TOLECTIN [illegible] can be expected in a few days to a week. [illegible] provement can be anticipated during subsequent therapy. If gastrointestinal symptoms occur, [illegible] can be administered with antacids other than [illegible] bonate. TOLECTIN bioavailability and [illegible] are not significantly affected by acute co-administration of magnesium and aluminum hydroxide [illegible] availability is affected by food or milk [illegible] TIONS—Drug-Food Interaction).

HOW SUPPLIED

TOLECTIN® 200 (tolmetin sodium) tablets [illegible] scored, imprinted "TOLECTIN," "200" and "[illegible]" NDC 0045-0412, bottles of 100.

TOLECTIN® DS (tolmetin sodium) capsules [illegible] ored orange opaque, with contrasting [illegible] printed "TOLECTIN DS" and "MCNEIL", NDC [illegible] bottles of 100, 500.

TOLECTIN® 600 (tolmetin sodium) tablets [illegible] orange, film coated, imprinted "TOLECTIN 600" [illegible] NEIL", NDC 0045-0416, bottles of 100 and 500.

Dispense in tight, light-resistant container as [illegible] official compendium.

Store at controlled room temperature (15°–30° [illegible]

Protect from light.

McNeil Pharmaceutical, McNEIL-PAL, Inc.
Spring House, PA 19477
Revised June 1997

Shown in Product Identification Guide, page [illegible]

TOPAMAX®
(to 'pa-ma-mix)
(topiramate)
Tablets

TOPAMAX®
(topiramate capsules)
Sprinkle Capsules
Prescribing Information

DESCRIPTION

Topiramate is a sulfamate-substituted monosaccharide [illegible] is intended for use as an antiepileptic drug. TOPAMAX® (topiramate) Tablets are available as 25 mg, 100 mg and 200 mg round tablets for oral administration. TOPAMAX® (topiramate capsules) Sprinkle Capsules are available as 15 mg and 25 mg sprinkle capsules for oral administration as whole capsules or opened and sprinkled on a small amount of soft food. Topiramate is a white crystalline powder with a bitter taste. Topiramate is most soluble in alkaline solutions containing sodium hydroxide or sodium phosphate and being [illegible] 9 to 10. It is freely soluble in acetone, chloroform, dimethylsulfoxide, and ethanol. The solubility in water is 9.8 mg/mL. Its saturated solution has a pH of 6.3. Topiramate has the molecular formula $C_{12}H_{21}NO_8S$ and a molecular weight of 339.37. Topiramate is designated chemically as 2,3:4,5-Di-O-isopropylidene-β-D-fructopyranose sulfamate and has the following structural formula:

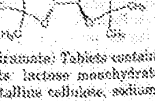

TOPAMAX® (topiramate) Tablets contain the following active ingredients: lactose monohydrate, [illegible] starch, microcrystalline cellulose, sodium starch [illegible] magnesium stearate, purified water, carnauba wax, [illegible] ypropyl methylcellulose, titanium dioxide, polyethylene [illegible] col, synthetic iron oxide (100 and 200 mg tablets) and [illegible] sorbate 80.

TOPAMAX® (topiramate capsules) Sprinkle Capsules [illegible] tain topiramate coated beads in a hard gelatin capsule. [illegible] inactive ingredients are: sugar spheres (sucrose and [illegible] povidone, cellulose acetate, gelatin, silicone dioxide, [illegible] lauryl sulfate, titanium dioxide, and black pharmaceutical [illegible] ink.

CLINICAL PHARMACOLOGY

Mechanism of Action

The precise mechanism by which topiramate exerts its [illegible] tiseizure effect is unknown; however, electrophysiological and biochemical studies of the effects of topiramate on cultured neurons have revealed three properties that may contribute to topiramate's antiepileptic efficacy. First, [illegible] potentials elicited repetitively by a sustained depolarization of the neurons are blocked by topiramate in a time-dependent manner, suggestive of a state-dependent sodium channel blocking action. Second, topiramate increases the frequency at which γ-aminobutyrate (GABA) activates GABA$_A$ receptors, and enhances the ability of GABA to induce influx of chloride ions into neurons, suggesting that topiramate potentiates the activity of this inhibitory neurotransmitter. This effect was not blocked by flumazenil, a benzodiazepine antagonist, nor did topiramate increase the duration of GABA channel open time, differentiating topiramate from barbiturates that modulate GABA$_A$ receptors. Third, topiramate antagonizes the ability of kainate to activate the kainate/AMPA (α-amino-3-hydroxy-5-methylisoxazole-4-propionic

UM00016740

NOVARTIS EXHIBIT 1517
Novartis v. Regents, IPR2023-01347
Page 3722 of 4460

non-NMDA) subtype of excitatory amino acid (glutamate) receptor, but has no apparent effect on the activity of N-methyl-D-aspartate (NMDA) at the NMDA receptor subtype. These effects of topiramate are concentration-dependent within the range of 1 µM to 200 µM.

Topiramate also inhibits some isoenzymes of carbonic anhydrase (CA-II and CA-IV). This pharmacologic effect is generally weaker than that of acetazolamide, a known carbonic anhydrase inhibitor, and is not thought to be a major contributing factor to topiramate's antiepileptic activity.

Pharmacodynamics:

Topiramate has anticonvulsant activity in rat and mouse maximal electroshock seizure (MES) tests. Topiramate is also readily effective in blocking clonic seizures induced by the $GABA_A$ receptor antagonist, pentylenetetrazole. Topiramate is also effective in rodent models of epilepsy, which include tonic and absence-like seizures in the spontaneous epileptic rat (SER) and tonic and clonic seizures induced in mice by kindling of the amygdala or by global ischemia.

Pharmacokinetics:

The sprinkle formulation is bioequivalent to the immediate release tablet formulation and, therefore, may be substituted on a therapeutic equivalent.

Absorption of topiramate is rapid, with peak plasma concentrations occurring at approximately 2 hours following a 400 mg oral dose. The relative bioavailability of topiramate from the tablet formulation is about 80% compared to a solution. The bioavailability of topiramate is not affected by food.

The pharmacokinetics of topiramate are linear with dose proportional increases in plasma concentration over the dose range studied (200 to 800 mg/day). The mean plasma elimination half-life is 21 hours after single or multiple dose. Steady state is thus reached in about 4 days in patients with normal renal function. Topiramate is 13–17% bound to human plasma proteins over the concentration range of 1–250 µg/mL.

Metabolism and Excretion:

Topiramate is not extensively metabolized and is primarily eliminated unchanged in the urine (approximately 70% of administered dose). Six metabolites have been identified in humans, none of which constitutes more than 5% of an administered dose. The metabolites are formed via hydroxylation, hydrolysis, and glucuronidation. There is evidence of renal tubular reabsorption of topiramate. In rats, given probenecid to inhibit tubular reabsorption, along with topiramate, a significant increase in renal clearance of topiramate was observed. This interaction has not been evaluated in humans. Overall, oral plasma clearance (CL/F) is approximately 20 to 30 mL/min in humans following oral administration.

Pharmacokinetic Interactions (see also Drug Interactions):

Antiepileptic Drugs

Potential interactions between topiramate and standard AEDs were assessed in controlled clinical pharmacokinetic studies in patients with epilepsy. The effect of these interactions on mean plasma AUCs are summarized under **PRECAUTIONS** (Table 3).

Special Populations:

Renal Impairment:

The clearance of topiramate was reduced by 42% in moderately renally impaired (creatinine clearance 30–69 mL/min/1.73m²) and by 54% in severely renally impaired subjects (creatinine clearance <30 mL/min/1.73m²) compared to normal renal function subjects (creatinine clearance >70 mL/min/1.73m²). Since topiramate is presumed to undergo significant tubular reabsorption, it is uncertain whether this decrease can be generalized to all situations of renal impairment. It is conceivable that some forms of renal disease could differentially affect glomerular filtration rate and tubular reabsorption resulting in a clearance of topiramate not predicted by creatinine clearance. In general, however, use of one-half the usual dose is recommended in patients with moderate or severe renal impairment.

Hemodialysis:

Topiramate is cleared by hemodialysis. Using a high efficiency, counterflow, single pass-dialysate hemodialysis procedure, topiramate dialysis clearance was 120 mL/min with blood flow through the dialyzer at 400 mL/min. This high clearance (compared to 20–30 mL/min total oral clearance in healthy adults) will remove a clinically significant amount of topiramate from the patient over the hemodialysis treatment period. Therefore, a supplemental dose may be required (see **DOSAGE AND ADMINISTRATION**).

Hepatic Impairment:

In hepatically impaired subjects, the clearance of topiramate may be decreased; the mechanism underlying the decrease is not well understood.

Age, Gender, and Race:

Clearance of topiramate in adults was not affected by age (15–87 years), gender, or race.

Pediatric Pharmacokinetics:

Pharmacokinetics of topiramate were evaluated in patients ages 4 to 17 years receiving one or two other antiepileptic drugs. Pharmacokinetic profiles were obtained after one week at doses of 1, 3, and 9 mg/kg/day. Clearance was independent of dose.

Pediatric patients have a 50% higher clearance and consequently shorter elimination half-life than adults. Consequently, the plasma concentration for the same mg/kg dose

Table 1: Topiramate Dose Summary During the Stabilization Periods of Each of Five Double-Blind, Placebo-Controlled, Add-On Trials in Adults with Partial Onset Seizures[a]

			Target Topiramate Dosage (mg/day):				
Protocol	Stabilization Dose	Placebo[b]	200	400	600	800	1,000
YD	N	42	42	46	41	---	---
	Mean Dose	5.9	200	390	556	---	---
	Median Dose	6.0	200	400	600	---	---
YE	N	44	---	---	40	45	40
	Mean Dose	9.7	---	---	544	739	796
	Median Dose	10.0	---	---	600	800	1,000
Y1	N	28	---	19	---	---	---
	Mean Dose	5.8	---	386	---	---	---
	Median Dose	4.0	---	400	---	---	---
Y2	N	30	---	---	28	---	---
	Mean Dose	5.7	---	---	522	---	---
	Median Dose	6.0	---	---	600	---	---
Y3	N	28	---	---	---	25	---
	Mean Dose	7.3	---	---	---	368	---
	Median Dose	8.0	---	---	---	600	---

[a] Placebo dosages are given as the number of tablets. Placebo target dosages were as follows: Protocol Y1, 4 tablets/day; Protocol YD and Y2, 6 tablets/day; Protocol Y3, 8 tablets/day; Protocol YE, 10 tablets/day.
[b] Dose ranging studies were not conducted for other indications or pediatric partial onset seizures.

Table 2: Key Efficacy Results in Double-Blind, Placebo-Controlled, Add-On Trials

			Target Topiramate Dosage (mg/day):					
Protocol	Efficacy Results	Placebo	200	400	600	800	1,000	~6 mg/kg/day[c]
Partial Onset Seizures								
Studies in Adults								
YD	N	45	45	45	46	---	---	---
	Median % Reduction	11.6	27.2[a]	47.5[a]	44.7[a]	---	---	---
	% Responders	18	24	44[a]	46[a]	---	---	---
YE	N	47	---	---	48	48	47	---
	Median % Reduction	1.7	---	---	40.8[a]	41.9[a]	36.8[a]	---
	% Responders	9	---	---	40[a]	42[a]	36[a]	---
Y1	N	24	---	23	---	---	---	---
	Median % Reduction	1.1	---	46.7[a]	---	---	---	---
	% Responders	8	---	35[a]	---	---	---	---
Y2	N	30	---	---	30	---	---	---
	Median % Reduction	-12.2	---	---	46.4[a]	---	---	---
	% Responders	10	---	---	47[a]	---	---	---
Y3	N	28	---	---	---	28	---	---
	Median % Reduction	-20.6	---	---	---	34.3[a]	---	---
	% Responders	0	---	---	---	43[a]	---	---
Studies in Pediatric Patients								
YP	N	45	---	---	---	---	---	41
	Median % Reduction	16.8	---	---	---	---	---	33.3[a]
	% Responders	20	---	---	---	---	---	39
Primary Generalized Tonic-Clonic[d]								
YTC	N	46	---	---	---	---	---	39
	Median % Reduction	9.0	---	---	---	---	---	36.7[a]
	% Responders	20	---	---	---	---	---	38[a]

Comparisons with placebo: [a]p≤0.050; [b]p≤0.010; [c]p≤0.001, [d]p≤0.060; [e]p=0.066; [f]p=0.005. [g] Median % reduction and % responders are reported for PGTC Seizures

[c] For Protocols YP and YTC, protocol-specified target dosages (~9.3 mg/kg/day) were assigned based on subject's weight to approximate a dosage of 6 mg/kg per day; these dosages corresponded to mg/day dosages of 125, 175, 225, and 400 mg/day.

Table 3: Summary of AED Interactions with TOPAMAX®

AED Co-administered	AED Concentration	Topiramate Concentration
Phenytoin	NC or 25% increase[a]	48% decrease
Carbamazepine (CBZ)	NC	40% decrease
CBZ epoxide[b]	NC	NE
Valproic acid	11% decrease	14% decrease
Phenobarbital	NC	NE
Primidone	NC	NE

[a] = Plasma concentration increased 25% in some patients, generally those on a b.i.d. dosing regimen of phenytoin.
[b] = is not administered but is an active metabolite of carbamazepine.
NC = Less than 10% change in plasma concentration.
AED = Antiepileptic drug.
NE = Not Evaluated.

CLINICAL STUDIES

The results of controlled clinical trials established the efficacy of TOPAMAX® (topiramate) as adjunctive therapy in adults and pediatric patients ages 2–16 years with partial onset seizures or primary generalized tonic-clonic seizures.

Controlled Trials in Patients With Partial Onset Seizures

Adults With Partial Onset Seizures

The studies described in the following section were conducted using TOPAMAX® (topiramate) Tablets.

The effectiveness of topiramate as an adjunctive treatment for adults with partial onset seizures was established in five multicenter, randomized, double-blind, placebo-controlled trials, two comparing several dosages of topiramate and placebo and three comparing a single dosage with placebo, in

lets or placebo. In each study, patients were stabilized on optimum dosages of their concomitant AEDs during an 8–12 week baseline phase. Patients who experienced at least 12 (or 8, for 8-week baseline studies) partial onset seizures, with or without secondary generalization, during the baseline phase were randomly assigned to placebo or a specified dose of TOPAMAX® Tablets in addition to their other AEDs. Following randomization, patients began the double-blind phase of treatment. Patients received active drug beginning at 100 mg per day; the dose was then increased by 100 mg or 200 mg/day increments weekly or every other week until the assigned dose was reached, unless intolerance prevented increases. After titration, patients entered an 8 or 12-week stabilization period. The numbers of patients ran-

UM00016741
NOVARTIS EXHIBIT 1517
Novartis v. Regents, IPR2023-01347
Page 3723 of 4460

Topamax—Cont.

Pediatric Patients Ages 2–16 Years With Partial Onset Seizures

The effectiveness of topiramate as an adjunctive treatment for pediatric patients with partial onset seizures was established in a multicenter, randomized, double-blind, placebo-controlled trial, comparing topiramate and placebo in patients with a history of partial onset seizures, with or without secondarily generalized seizures.

Patients in this study were permitted a maximum of two antiepileptic drugs (AEDs) in addition to TOPAMAX® Tablets or placebo. In this study, patients were stabilized on optimum dosages of their concomitant AEDs during an 8 week baseline phase. Patients who experienced at least six partial onset seizures, with or without secondarily generalized seizures, during the baseline phase were randomly assigned to placebo or TOPAMAX® Tablets in addition to their other AEDs.

Following randomization, patients began the double-blind phase of treatment. Patients received active drug beginning at 25 or 50 mg per day; the dose was then increased by 25 mg to 150 mg/day increments every other week until the assigned dosage of 125, 175, 225, or 400 mg/day based on patients' weight to approximate a dosage of 6 mg/kg per day was reached, unless intolerance prevented increases. After titration, patients entered an 8-week stabilization period.

Controlled Trials in Patients With Primary Generalized Tonic-Clonic Seizures

The effectiveness of topiramate as an adjunctive treatment for primary generalized tonic-clonic seizures was established in a multicenter randomized, double-blind, placebo-controlled trial, comparing a single dosage of topiramate and placebo.

Patients in this study were permitted a maximum of two antiepileptic drugs (AEDs) in addition to TOPAMAX® or placebo. Patients were stabilized on optimum dosages of their concomitant AEDs during an 8 week baseline phase. Patients who experienced at least three primary generalized tonic-clonic seizures during the baseline phase were randomly assigned to placebo or TOPAMAX® in addition to their other AEDs.

Following randomization, patients began the double-blind phase of treatment. Patients received active drug beginning at 50 mg per day for four weeks; the dose was then increased by 50 mg to 150 mg/day increments every other week until the assigned dose of 175, 225, or 400 mg/day based on patients' body weight to approximate a dosage of 6 mg/kg per day was reached, unless intolerance prevented increases. After titration, patients entered a 12-week stabilization period.

[See table 1 at top of previous page]

In all add-on trials, the reduction in seizure rate from baseline during the entire double-blind phase was measured. The median percent reductions in seizure rates and the responder rates (fraction of patients with at least a 50% reduction) by treatment group for each study are shown below in Table 2.

[See table 2 on previous page]

Subset analyses of the antiepileptic efficacy of TOPAMAX® Tablets in these studies showed no differences as a function of gender, race, age, baseline seizure rate, or concomitant AED.

Table 4: Incidence (1%) of Treatment-Emergent Adverse Events in Placebo-Controlled, Add-On Trials in [illegible] TOPAMAX® Dosage Range

Body System/ Adverse Event*	Placebo (N=251)	200–400 (N=153)	[illegible] (N=[illegible])
Body as a Whole—General Disorders			
Fatigue	13	15	[illegible]
Asthenia	1	6	[illegible]
Back Pain	4	5	[illegible]
Chest Pain	3	4	[illegible]
Influenza-Like Symptoms	2	3	[illegible]
Leg Pain	2	2	[illegible]
Hot Flushes	1	2	[illegible]
Allergy	1	2	[illegible]
Edema	1	2	[illegible]
Body Odor	0	1	[illegible]
Rigors	0	1	[illegible]
Central & Peripheral Nervous System Disorders			
Dizziness	13	25	[illegible]
Ataxia	7	16	[illegible]
Speech Disorders/Related Speech Problems	2	13	[illegible]
Paresthesia	4	13	[illegible]
Nystagmus	7	10	[illegible]
Tremor	6	9	[illegible]
Language Problems	1	6	[illegible]
Coordination Abnormal	2	4	[illegible]
Hypoesthesia	1	2	[illegible]
Gait Abnormal	1	3	[illegible]
Muscle Contractions Involuntary	1	2	[illegible]
Stupor	0	2	[illegible]
Vertigo	1	1	[illegible]
Gastro-intestinal System Disorders			
Nausea	8	10	[illegible]
Dyspepsia	6	7	[illegible]
Abdominal Pain	4	6	[illegible]
Constipation	2	4	[illegible]
Gastroenteritis	1	3	[illegible]
Dry Mouth	1	3	[illegible]
Gingivitis	<1	1	[illegible]
GI Disorder	<1	1	[illegible]
Hearing and Vestibular Disorders			
Hearing Decreased	1	2	[illegible]
Metabolic and Nutritional Disorders			
Weight Decrease	3	9	[illegible]
Muscle-Skeletal System Disorders			
Myalgia	1	2	[illegible]
Skeletal Pain	0	1	[illegible]
Platelet, Bleeding, & Clotting Disorders			
Epistaxis	1	2	[illegible]
Psychiatric Disorders			
Somnolence	12	29	[illegible]
Nervousness	6	16	[illegible]
Psychomotor Slowing	2	13	[illegible]
Difficulty with Memory	3	12	[illegible]
Anorexia	4	10	[illegible]
Confusion	5	11	[illegible]
Depression	5	5	[illegible]
Difficulty with Concentration/Attention	2	8	[illegible]
Mood Problems	2	4	[illegible]
Agitation	2	3	[illegible]
Aggressive Reaction	2	3	[illegible]
Emotional Lability	1	3	[illegible]
Cognitive Problems	1	3	[illegible]
Libido Decreased	1	2	[illegible]
Apathy	1	1	[illegible]
Depersonalization	1	1	[illegible]

(Table continued on next page)

INDICATIONS AND USAGE

TOPAMAX® (topiramate) Tablets and TOPAMAX® (topiramate capsules) Sprinkle Capsules are indicated as adjunctive therapy for adults and pediatric patients ages 2–16 years with partial onset seizures, or primary generalized tonic-clonic seizures.

CONTRAINDICATIONS

TOPAMAX® is contraindicated in patients with a history of hypersensitivity to any component of this product.

WARNINGS

Withdrawal of AEDs

Antiepileptic drugs, including TOPAMAX®, should be withdrawn gradually to minimize the potential of increased seizure frequency.

Cognitive/Neuropsychiatric Adverse Events

Adults

Adverse events most often associated with the use of TOPAMAX® were central nervous system-related. In adults, the most significant of these can be classified into two general categories: 1) psychomotor slowing, difficulty with concentration, and speech or language problems, in particular, word-finding difficulties and 2) somnolence or fatigue. Additional nonspecific CNS effects occasionally observed with topiramate as add-on therapy include dizziness or imbalance, confusion, memory problems, and exacerbation of mood disturbances (e.g., irritability and depression).

Reports of psychomotor slowing, speech and language problems, and difficulty with concentration and attention were common in adults. Although in some cases these events were mild to moderate, they at times led to withdrawal from treatment. The incidence of psychomotor slowing is only marginally dose-related, but both language problems and difficulty with concentration or attention clearly increased in frequency with increasing dosage in the five double-blind trials (see **ADVERSE REACTIONS, Table 5**).

Somnolence and fatigue were the most frequently reported adverse events during clinical trials with TOPAMAX®. These events were generally mild to moderate and occurred early in therapy. While the incidence of somnolence does not appear to be dose-related, that of fatigue increases at dosages above 400 mg/day.

Pediatric Patients

In double-blind clinical studies, the incidences of cognitive/neuropsychiatric adverse events in pediatric patients were generally lower than previously observed in adults. These events included psychomotor slowing, difficulty with concentration/attention, speech disorders/related speech problems and language problems. The most frequently reported neuropsychiatric events in this population were somnolence and fatigue. No patients discontinued treatment due to adverse events in double-blind trials.

Sudden Unexplained Death in Epilepsy (SUDEP)

During the course of premarketing development of TOPAMAX® (topiramate) Tablets, 10 sudden and unexplained deaths were recorded among a cohort of treated patients (2,796 subject years of exposure). This represents an incidence of 0.0035 deaths per patient year. Although this rate exceeds that expected in a healthy population matched for age and sex, it is within the range of estimates for the incidence of sudden unexplained deaths in patients with epilepsy not receiving TOPAMAX® (ranging from 0.0005 for the general population of patients with epilepsy, to 0.003 for a clinical trial population similar to that in the TOPAMAX® program, to 0.005 for patients with refractory epilepsy).

PRECAUTIONS

General:

Kidney Stones

A total of 32/2,086 (1.5%) of adults exposed to topiramate during its development reported the occurrence of kidney stones, an incidence about 2–4 times that expected in a similar, untreated population. As in the general population, the incidence of stone formation among topiramate treated patients was higher in men. Kidney stones have also been reported in pediatric patients.

An explanation for the association of TOPAMAX® and kidney stones may lie in the fact that topiramate is a weak carbonic anhydrase inhibitor. Carbonic anhydrase inhibitors (e.g., acetazolamide or dichlorphenamide, promote stone formation by reducing urinary citrate excretion and by increasing urinary pH. The concomitant use of TOPAMAX® with other carbonic anhydrase inhibitors or potentially in patients on a ketogenic diet may create a physiological environment that increases the risk of kidney stone formation, and should therefore be avoided.

Increased fluid intake increases the urinary output, reducing the concentration of substances involved in stone formation. Hydration is recommended to reduce new stone formation.

Paresthesia

Paresthesia, an effect associated with the use of other carbonic anhydrase inhibitors, appears to be a common effect of TOPAMAX®.

Adjustment of Dose in Renal Failure

The major route of elimination of unchanged topiramate and its metabolites is via the kidney. Dosage adjustment may be required (see **DOSAGE AND ADMINISTRATION**).

Decreased Hepatic Function

In hepatically impaired patients, topiramate should be administered with caution as the clearance of topiramate will be decreased.

Information for Patients

Patients, particularly those with predisposing factors, should be instructed to maintain adequate fluid intake to

UM00016742
NOVARTIS EXHIBIT 1517
Novartis v. Regents, IPR2023-01347
Page 3724 of 4460

...minimize the risk of renal stone formation **PRECAUTIONS: General**, for support regarding hydration as a preventive measure).

...should be warned about the potential for somnolence, dizziness, confusion, and difficulty concentrating and ...not to drive or operate machinery until they have gained sufficient experience on topiramate to gauge whether it adversely affects their mental and/or motor performance.

...additional food intake may be considered if the patient is losing weight while on this medication.

...refer to the end of the product labeling for important information on how to take TOPAMAX® (topiramate capsules) Sprinkle Capsules.

Drug Interactions:

Antiepileptic Drugs

Potential interactions between topiramate and standard AEDs were assessed in controlled clinical pharmacokinetic studies in patients with epilepsy. The effects of these interactions on mean plasma AUCs are summarized in the following table:

In Table 3, the second column (AED concentration) describes what happens to the concentration of the AED listed in the first column when topiramate is added.

The third column (topiramate concentration) describes how the coadministration of a drug listed in the first column affects the concentration of topiramate in experimental studies when TOPAMAX® was given alone.

See table 3 on page 2601)

Other Drug Interactions

Digoxin: In a single-dose study, serum digoxin AUC was reduced by 12% with concomitant TOPAMAX® administration. The clinical relevance of this observation has not been established.

CNS Depressants: Concomitant administration of TOPAMAX® and alcohol or other CNS depressant drugs has not been evaluated in clinical studies. Because of the potential of topiramate to cause CNS depression, as well as other cognitive and/or neuropsychiatric adverse events, topiramate should be used with extreme caution if used in combination with alcohol and other CNS depressants.

Oral Contraceptives: In a pharmacokinetic interaction study with oral contraceptives using a combination product containing norethindrone and ethinyl estradiol, TOPAMAX® did not significantly affect the clearance of norethindrone. The mean oral clearance of ethinyl estradiol at 200 mg/day dose was increased by 47% (range: 13–1078). The mean total exposure to the estrogenic component decreased by 18%, 21%, and 30% at daily doses of 200, 400, and 800 mg/day, respectively. Therefore, efficacy of oral contraceptives may be compromised by topiramate. Patients using oral contraceptives should be asked to report any change in their bleeding patterns. The effect of oral contraceptives on the pharmacokinetics of topiramate is not known.

Other: Concomitant use of TOPAMAX®, a weak carbonic anhydrase inhibitor, with other carbonic anhydrase inhibitors, e.g., acetazolamide or dichlorphenamide, may create a physiological environment that increases the risk of renal stone formation, and should therefore be avoided.

Laboratory Tests: There are no known interactions of topiramate with commonly used laboratory tests.

Carcinogenesis, Mutagenesis, Impairment of Fertility:

An increase in urinary bladder tumors was observed in mice given topiramate (20, 75, and 300 mg/kg) in the diet for 21 months. The elevated bladder tumor incidence, which was statistically significant in males and females receiving 300 mg/kg, was primarily due to the increased occurrence of transitional muscle tumor considered histomorphologically unique to mice. Plasma exposures in mice receiving 300 mg/kg were approximately 0.5 to 1 times steady state exposures measured in patients receiving topiramate monotherapy at the recommended human dose (RHD) of 400 mg, and 1.5 to 2 times steady state topiramate exposures in patients receiving 800 mg of topiramate plus phenytoin. The relevance of this finding to human carcinogenic risk is unknown. No evidence of carcinogenicity was seen in rats following oral administration of topiramate for 2 years at doses up to 120 mg/kg (approximately 3 times the RHD on a mg/m² basis).

Topiramate did not demonstrate genotoxic potential when tested in a battery of *in vitro* and *in vivo* assays. Topiramate was not mutagenic in the Ames test or the *in vitro* mouse lymphoma assay, it did not increase unscheduled DNA synthesis in rat hepatocytes *in vitro*, and it did not increase chromosomal aberrations in human lymphocytes *in vitro* or in rat bone marrow *in vivo*.

No adverse effects on male or female fertility were observed in rats at doses up to 100 mg/kg (2.5 times the RHD on a mg/m² basis).

Pregnancy: Pregnancy Category C.

Topiramate has demonstrated selective developmental toxicity, including teratogenicity, in experimental animal studies. When oral doses of 20, 100, or 500 mg/kg were administered to pregnant mice during the period of organogenesis, the incidence of fetal malformations (primarily craniofacial defects) was increased at all doses. The low dose is approximately 0.2 times the recommended human dose (RHD=400 mg/day) on a mg/m² basis. Fetal body weights and skeletal ossification were reduced at 500 mg/kg in conjunction with decreased maternal body weight gain.

In rat studies (oral doses of 20, 100, and 500 mg/kg or 0.2, 1.2, 30 and 300 mg/kg), the frequency of limb malformations (micromelia, micromelia, and amelia) was increased among the offspring of dams treated with 300 mg/kg (10 times the RHD on a mg/m² basis) or greater during the organogenesis period of pregnancy. Embryotoxicity (reduced fetal body weights, increased incidence of structural variations) was observed at doses as low as 20 mg/kg (0.5 times the RHD on a mg/m² basis). Clinical signs of maternal toxicity were seen at 300 mg/kg and above, and maternal body weight gain was reduced during treatment with 100 mg/kg or greater.

In rabbit studies (20, 60, and 180 mg/kg or 10, 35, and 120 mg/kg orally during organogenesis), embryofetal mortality was increased at 35 mg/kg (2 times the RHD on a mg/m² basis) or greater, and teratogenic effects (primarily rib and vertebral malformations) were observed at 120 mg/kg (6 times the RHD on a mg/m² basis). Evidence of maternal toxicity (decreased body weight gain, clinical signs, and/or mortality) was seen at 35 mg/kg and above.

When female rats were treated during the latter part of gestation and throughout lactation (0.2, 4, 20, and 100 mg/kg or 2, 20, and 200 mg/kg), offspring exhibited decreased viability and delayed physical development at 200 mg/kg (5 times the RHD on a mg/m² basis) and reductions in pre- and/or postweaning body weight gain at 2 mg/kg (0.05 times the RHD on a mg/m² basis) and above. Maternal toxicity (decreased body weight gain, clinical signs) was evident at 100 mg/kg or greater.

In a rat embryo/fetal development study with a postnatal component (0.2, 2.5, 30 or 400 mg/kg during organogenesis, noted above), pups exhibited delayed physical development at 400 mg/kg (10 times the RHD on a mg/m² basis) and persistent reductions in body weight gain at 30 mg/kg (1 times the RHD on a mg/m² basis) and higher.

There are no studies using TOPAMAX® in pregnant women. TOPAMAX® should be used during pregnancy only if the potential benefit outweighs the potential risk to the fetus.

In post-marketing experience, cases of hypospadias have been reported in male infants exposed *in utero* to topiramate, with or without other anticonvulsants; however, a causal relationship with topiramate has not been established.

Labor and Delivery:

In studies of rats where dams were allowed to deliver pups naturally, no drug-related effects on gestation length or parturition were observed at dosage levels up to 200 mg/kg/day. The effect of TOPAMAX® on labor and delivery in humans is unknown.

Nursing Mothers:

Topiramate is excreted in the milk of lactating rats. It is not known if topiramate is excreted in human milk. Since many drugs are excreted in human milk, and because the potential for serious adverse reactions in nursing infants to TOPAMAX® is unknown, the potential benefit to the mother should be weighed against the potential risk to the infant when considering recommendations regarding nursing.

Pediatric Use:

Safety and effectiveness in patients below the age of 2 years have not been established.

Geriatric Use:

In clinical trials, 2% of patients were over 60. No age related difference in effectiveness or adverse effects were seen. There were no pharmacokinetic differences related to age alone, although the possibility of age-associated renal functional abnormalities should be considered.

Race and Gender Effects:

Evaluation of effectiveness and safety in clinical trials has shown no race or gender related effects.

ADVERSE REACTIONS

The data described in the following section were obtained using TOPAMAX® (topiramate) Tablets.

Continued on next page

Table 4 *(cont.)*: Incidence (%) of Treatment-Emergent Adverse Events in Placebo-Controlled, Add-On Trials in Adults[a,b]

Body System/ Adverse Event[c]	Placebo (N=291)	TOPAMAX® Dosage (mg/day) 200–400 (N=183)	600–1,000 (N=414)
Reproductive Disorders, Female			
Breast Pain	2	4	6
Amenorrhea	1	2	2
Menorrhagia	0	2	1
Menstrual Disorder	1	2	1
Reproductive Disorders, Male			
Prostatic Disorder	<1	2	0
Resistance Mechanism Disorders			
Infection	1	2	1
Infection Viral	1	2	<1
Moniliasis	<1	1	0
Respiratory System Disorders			
Pharyngitis	2	6	3
Rhinitis	6	7	8
Sinusitis	4	5	6
Dyspnea	1	1	2
Skin and Appendages Disorders			
Skin Disorder	<1	2	1
Sweating Increased	<1	1	<1
Rash Erythematous	<1	1	<1
Special Sense Other, Disorders			
Taste Perversion	0	2	4
Urinary System Disorders			
Hematuria	1	2	<1
Urinary Tract Infection	1	2	2
Micturition Frequency	1	1	3
Urinary Incontinence	<1	2	1
Urine Abnormal	0	1	<1
Vision Disorders			
Vision Abnormal	2	13	10
Diplopia	5	10	10
White Cell and RES Disorders			
Leukopenia	1	2	1

[a] Patients in these add-on trials were receiving 1 to 2 concomitant antiepileptic drugs in addition to TOPAMAX® or placebo.

[b] Values represent the percentage of patients reporting a given adverse event. Patients may have reported more than one adverse event during the study and can be included in more than one adverse event category.

[c] Adverse events reported by at least 1% of patients in the TOPAMAX® 200–400 mg/day group and were common than in the placebo group are listed in this table.

Table 5: Incidence (%) of Dose-Related Adverse Events From Placebo-Controlled, Add-On Trials in Adults with Partial Onset Seizures[a]

Adverse Event	Placebo (N = 216)	TOPAMAX® Dosage (mg/day) 200 (N = 45)	400 (N = 66)	600–1,000 (N = 414)
Fatigue	13	11	12	20
Nervousness	7	13	15	19
Difficulty with Concentration/Attention	1	7	9	14
Confusion	3	5	10	14
Depression	6	9	7	13
Amnesia	4	4	6	12
Language problems	<1	2	9	10
Anxiety	6	2	3	10
Mood problems	2	0	6	9
Weight decrease	3	4	9	13

[a] Dose-ranging studies were not conducted for other indications or for pediatric population.

UM00016743
NOVARTIS EXHIBIT 1517
Novartis v. Regents, IPR2023-01347
Page 3725 of 4460

Topamax—Cont.

The most commonly observed adverse events associated with the use of topiramate at dosages of 200 to 400 mg/day in controlled trials in adults with partial-onset seizures, primary generalized tonic-clonic seizures, or Lennox-Gastaut syndrome, that were seen at greater frequency in topiramate-treated patients and did not appear to be dose-related were: somnolence, dizziness, ataxia, speech disorders and slowed speech, problems, psychomotor slowing, abnormal vision, difficulty with memory, paresthesia and diplopia (see Table 4). The most common dose-related adverse events at dosages of 200 to 1,000 mg/day were: fatigue, nervousness, difficulty with concentration or attention, confusion, depression, anorexia, language problems, anxiety, mood problems, and weight decrease (see Table 5).

Adverse events associated with the use of topiramate at dosages of 5 to 9 mg/kg/day in controlled trials in pediatric patients with partial-onset seizures, primary generalized tonic-clonic seizures, or Lennox-Gastaut syndrome, that were seen at greater frequency in topiramate-treated patients were: fatigue, somnolence, anorexia, nervousness, difficulty with concentration/attention, difficulty with memory, aggressive reaction, and weight decrease (see Table 6).

In controlled clinical trials in adults, 11% of patients receiving topiramate 200 to 400 mg/day as adjunctive therapy discontinued due to adverse events. This rate appeared to increase at dosages above 400 mg/day. Adverse events associated with discontinuing therapy included somnolence, dizziness, anxiety, difficulty with concentration or attention, fatigue, and paresthesia and increased at dosages above 400 mg/day. None of the pediatric patients who received topiramate adjunctive therapy at 5 to 9 mg/kg/day in controlled clinical trials discontinued due to adverse events.

Approximately 28% of the 1,757 adults with epilepsy who received topiramate at dosages of 200 to 1,600 mg/day in clinical studies discontinued treatment because of adverse events; an individual patient could have reported more than one adverse event. These adverse events were: psychomotor slowing (4.0%), difficulty with memory (3.2%), fatigue (3.2%), confusion (3.1%), somnolence (3.2%), difficulty with concentration/attention (2.8%), anorexia (2.7%), depression (2.6%), dizziness (2.6%), weight decrease (2.5%), nervousness (2.3%), ataxia (2.1%), and paresthesia (2.0%). Approximately 13% of the 316 pediatric patients who received topiramate at dosages up to 30 mg/kg/day discontinued due to adverse events. Adverse events associated with discontinuing therapy included aggravated convulsions (2.8%), difficulty with concentration/attention (1.6%), language problems (1.3%), personality disorder (1.3%), and somnolence (1.3%).

Incidence in Controlled Clinical Trials - Add-On Therapy

Table 4 lists treatment-emergent adverse events that occurred in at least 1% of adults treated with 200 to 400 mg/day topiramate in controlled trials that were numerically more common at this dose than in the patients treated with placebo. In general, most patients who experienced adverse events during the first eight weeks of these trials no longer experienced them by their last visit. Table 5 lists treatment-emergent adverse events that occurred in at least 2% of pediatric patients treated with 5 to 9 mg/kg topiramate in controlled trials that were numerically more common than in patients treated with placebo.

The prescriber should be aware that these data were obtained when TOPAMAX® was added to concurrent antiepileptic drug therapy and cannot be used to predict the frequency of adverse events in the course of usual medical practice where patient characteristics and other factors may differ from those prevailing during clinical studies. Similarly, the cited frequencies cannot be directly compared with data obtained from other clinical investigations involving different treatments, uses, or investigators. Inspection of these frequencies, however, does provide the prescribing physician with a basis to estimate the relative contribution of drug and non-drug factors to the adverse event incidences in the population studied.

[See table 4 on page 2592 and previous page]
[See table 5 on previous page]
[See table 6 at top of page]

Other Adverse Events Observed

Other events that occurred in more than 1% of adults treated with 200 to 400 mg of topiramate in placebo-controlled trials but with equal or greater frequency in the placebo group were: headache, injury, anxiety, rash, pain, convulsions aggravated, coughing, fever, diarrhea, vomiting, muscle weakness, insomnia, personality disorder, dysmenorrhea, upper respiratory tract infection, and eye pain.

Other Adverse Events Observed During All Clinical Trials

Topiramate, initiated as adjunctive therapy, has been administered to 1,757 adults and 316 pediatric patients with epilepsy during all clinical studies. During these studies, all adverse events were recorded by the clinical investigators using terminology of their own choosing. To provide a meaningful estimate of the proportion of individuals having adverse events, similar types of events were grouped into a smaller number of standardized categories using modified WHOART dictionary terminology. The frequencies presented represent the proportion of patients who experienced an event of the type cited on at least one occasion while receiving topiramate. Reported events are included except those already listed in the previous table or text, those too general to be informative, and those not reasonably associated with the use of the drug.

Table 6: Incidence (%) of Treatment-Emergent Adverse Events in Placebo-Controlled, Add-On Trials in Pediatric Patients Ages 2–16 Years[a,b]

(Events that Occurred in at Least 1% of Topiramate-Treated Patients and Occurred More Frequently in Topiramate-Treated Than Placebo-Treated Patients)

Body System/ Adverse Event	Placebo (N=101)	Topiramate (N=92)
Body as a Whole—General Disorders		
Fatigue	5	16
Injury	13	18
Allergic Reaction	1	2
Back Pain	0	2
Pallor	0	1
Cardiovascular Disorders, General		
Hypertension	0	2
Central & Peripheral Nervous System Disorders		
Gait Abnormal	5	8
Ataxia	2	5
Hyperkinesia	4	5
Dizziness	2	4
Speech Disorder/Related Speech Problems	2	4
Hypoesthesia	0	2
Convulsions Grand Mal	0	2
Fecal Incontinence	0	1
Paresthesia	0	1
Gastro-Intestinal System Disorders		
Nausea	5	9
Saliva Increased	4	5
Constipation	3	4
Gastroenteritis	2	3
Dysphagia	0	2
Flatulence	0	2
Gastroesophageal Reflux	0	2
Gingivitis	0	1
Gum Hyperplasia	0	1
Heart Rate and Rhythm Disorders		
Bradycardia	0	1
Metabolic and Nutritional Disorders		
Weight Decrease	1	6
Thirst	1	3
Hypoglycemia	0	1
Weight Increase	0	1
Platelet, Bleeding, & Clotting Disorders		
Purpura	4	5
Epistaxis	1	4
Hematoma	0	1
Prothrombin Increased	0	1
Thrombocytopenia	0	1
Psychiatric Disorders		
Somnolence	16	36
Anorexia	15	31
Nervousness	7	16
Personality Disorder (Behavior Problems)	9	13
Difficulty with Concentration/Attention	2	10
Aggressive Reaction	4	9
Insomnia	7	8
Difficulty with Memory NOS	6	8
Confusion	3	4
Psychomotor Slowing	2	3
Appetite Increased	0	1
Neurosis	0	1
Reproductive Disorders, Female		
Leukorrhoea	0	3
Resistance Mechanism Disorders		
Infection Viral	3	7
Respiratory System Disorders		
Pneumonia	1	5
Respiratory Disorder	0	1
Skin and Appendages Disorders		
Skin Disorder	2	3
Alopecia	1	3
Dermatitis	0	2
Hypertrichosis	1	2
Rash Erythematous	0	2
Eczema	0	1
Seborrhoea	0	1
Skin Discoloration	0	1
Urinary System Disorders		
Urinary Incontinence	2	4
Nocturia	0	1
Vision Disorders		
Eye Abnormality	1	3
Vision Abnormal	1	2
Diplopia	0	1
Lacrimation Abnormal	0	1
Myopia	0	1
White Cell and RES Disorders		
Leukopenia	0	2

[a] Patients in these add-on trials were receiving 1 to 2 concomitant antiepileptic drugs in addition to TOPAMAX® or placebo.
[b] Values represent the percentage of patients reporting a given adverse event. Patients may have reported more than an adverse event during the study and can be included in more than one adverse event category.

Events are classified within body system categories and enumerated in order of decreasing frequency using the following definitions: *frequent* occurring in at least 1/100 patients; *infrequent* occurring in 1/100 to 1/1000 patients; *rare* occurring in fewer than 1/1000 patients.

Autonomic Nervous System Disorders: *Infrequent:* vasodilation.

Body as a Whole: *Frequent:* fever, malaise. *Infrequent:* syncope, halitosis, abdomen enlarged. *Rare:* alcohol intolerance, substernal chest pain.

Cardiovascular Disorders, General: *Infrequent:* hypotension, postural hypotension.

Central & Peripheral Nervous System Disorders: *Frequent:* hypertonia. *Infrequent:* leg cramps, neuropathy, vertigo, apraxia, hypoesthesia, dyskinesia, dysphonia, hemiplegia, ptosis, dystonia, visual field defect, coma, encephalitis, upper motor neuron lesion, EEG abnormal, hemiparesis, cerebellar syndrome, tongue paralysis.

Endocrine Disorders: *Infrequent:* goiter. *Rare:* thyroid disorder.

UM00016744
NOVARTIS EXHIBIT 1517
Novartis v. Regents, IPR2023-01347
Page 3726 of 4460

Gastrointestinal System Disorders: *Frequent:* diarrhea, nausea, hemorrhoids. *Infrequent:* tooth caries, stomatitis, dysphagia, gastritis, hiccough, tongue edema, esophagitis, rectal hemorrhage.

Hearing and Vestibular Disorders: *Frequent:* tinnitus. *Infrequent:* deafness, hyperacusis.

Heart Rate and Rhythm Disorders: *Frequent:* palpitation. *Infrequent:* AV block, bradycardia, bundle branch block, cardiomegaly, arrhythmia, arrhythmia atrial, fibrillation atrial.

Hepatic and Biliary System Disorders: *Infrequent:* SGPT increased, SGOT increased, gall bladder disorders including cholelithiasis, gamma-GT increased.

Hypo/Hyperglycemic and Nutritional Disorders: *Frequent:* dehydration. *Infrequent:* hypokalemia, alkaline phosphatase increased, hypocalcemia, hyperlipemia, acidosis, hyperglycemia, hypercholesteremia, xerophthalmia. *Rare:* diabetes mellitus, hypernatremia, abnormal serum folate, hyponatremia, hypercalciuria, hypophosphatemia, creatinine increased.

Musculoskeletal System Disorders: *Frequent:* arthralgia, muscle weakness. *Infrequent:* arthrosis, osteoporosis.

Myo-, Endo-, Pericardial & Valve Disorders: *Infrequent:* angina pectoris.

Neoplasms: *Infrequent:* basal cell carcinoma, thrombocythemia. *Rare:* polycythemia.

Platelet, Bleeding, and Clotting Disorders: *Infrequent:* gingival bleeding, pulmonary embolism.

Psychiatric Disorders: *Frequent:* impotence, hallucination, depression, psychosis. *Infrequent:* paranoid reaction, delusion, paresis, delirium, abnormal dreaming, neurosis, libido decreased, manic reaction, suicide attempt.

Red Blood Cell Disorders: *Frequent:* anemia. *Rare:* macrocytic anemia, pancytopenia.

Reproductive Disorders, Female: *Frequent:* intermenstrual bleeding, vaginitis.

Reproductive Disorders, Male: *Infrequent:* ejaculation disorder, breast discharge.

Respiratory System Disorders: *Frequent:* coughing, bronchitis. *Infrequent:* asthma, bronchospasm, laryngismus.

Skin and Appendages Disorders: *Frequent:* acne, nail disorder, folliculitis, dry skin, urticaria. *Infrequent:* photosensitivity reaction, sweating decreased, abnormal hair texture. *Rare:* chloasma.

Special Senses Other, Disorders: *Infrequent:* taste loss, anosmia.

Urinary System Disorders: *Frequent:* dysuria, renal calculus. *Infrequent:* urinary retention, face edema, renal pain, albuminuria, polyuria, oliguria.

Vascular (Extracardiac) Disorders: *Infrequent:* flushing, deep vein thrombosis, phlebitis. *Rare:* vasospasm.

Vision Disorders: *Frequent:* conjunctivitis. *Infrequent:* abnormal accommodation, photophobia, strabismus, color blindness, mydriasis, cataract. *Rare:* corneal opacity, iritis.

White Cell and Reticuloendothelial System Disorders: *Infrequent:* lymphadenopathy, eosinophilia, lymphopenia, granulocytopenia, lymphocytosis.

Postmarketing and Other Experience

In addition to the adverse experiences reported during clinical testing of TOPAMAX®, the following adverse experiences have been reported in patients receiving marketed TOPAMAX® from worldwide use since approval. These adverse experiences have not been listed above and data are inadequate to support an estimate of their incidence or to establish causation. The listing is alphabetized: hepatic failure, hepatitis, pancreatitis, and renal tubular acidosis.

DRUG ABUSE AND DEPENDENCE

The abuse and dependence potential of TOPAMAX® has not been evaluated in human studies.

OVERDOSAGE

In acute TOPAMAX® overdose, if the ingestion is recent, the stomach should be emptied immediately by lavage or by induction of emesis. Activated charcoal has not been shown to adsorb topiramate *in vitro*. Therefore, its use in overdose is not recommended. Treatment should be appropriately supportive. Hemodialysis is an effective means of removing topiramate from the body. However, in the few cases of acute overdosage reported, hemodialysis has not been necessary.

DOSAGE AND ADMINISTRATION

TOPAMAX® has been shown to be effective in adults and pediatric patients with partial onset seizures or primary generalized tonic-clonic seizures. In the controlled add-on trials, no correlation has been demonstrated between trough plasma concentrations of topiramate and clinical efficacy. No evidence of tolerance has been demonstrated in humans. Doses above 400 mg/day (600, 800, or 1000 mg/day) have not been shown to improve responses in dose-ranging studies in adults with partial onset seizures.

It is not necessary to monitor topiramate plasma concentrations to optimize TOPAMAX® therapy. On occasion, the addition of TOPAMAX® to phenytoin may require an adjustment of the dose of phenytoin to achieve optimal clinical response. Addition or withdrawal of phenytoin and/or carbamazepine during adjunctive therapy with TOPAMAX® may require adjustment of the dose of TOPAMAX®. Because of the bitter taste, tablets should not be broken.

TOPAMAX® can be taken without regard to meals.

Adults ≥17 Years of Age and Over

The recommended total daily dose of TOPAMAX® as adjunctive therapy is 400 mg/day in two divided doses. In studies of adults with partial onset seizures, a daily dose of 400 mg/day, It is recommended that therapy be initiated at 25–50 mg/day followed by titration to an effective dose in increments of 25–50 mg/week. Titrating in increments of 25 mg/week may delay the time to reach an effective dose. Daily doses above 1,600 mg have not been studied.

In the study of primary generalized tonic-clonic seizures the initial titration rate was slower than in previous studies, the assigned dose was reached at the end of 8 weeks (see **CLINICAL STUDIES, Controlled Trials in Patients With Primary Generalized Tonic-Clonic Seizures**).

Pediatric Patients Ages 2–16 Years

The recommended total daily dose of TOPAMAX® (topiramate) as adjunctive therapy is approximately 5 to 9 mg/kg/day in two divided doses. Titration should begin at 25 mg (or less, based on a range of 1 to 3 mg/kg/day) nightly for the first week. The dosage should then be increased at 1- or 2-week intervals by increments of 1 to 3 mg/kg/day (administered in two divided doses), to achieve optimal clinical response. Dose titration should be guided by clinical outcome. In the study of primary generalized tonic-clonic seizures the initial titration rate was slower than in previous studies; the assigned dose of 6 mg/kg/day was reached at the end of 8 weeks (see **CLINICAL STUDIES, Controlled Trials in Patients With Primary Generalized Tonic-Clonic Seizures**).

Administration of TOPAMAX® Sprinkle Capsules

TOPAMAX® (topiramate capsules) Sprinkle Capsules may be swallowed whole or may be administered by carefully opening the capsule and sprinkling the entire contents on a small amount (teaspoon) of soft food. This drug/food mixture should be swallowed immediately and not chewed. It should not be stored for future use.

Patients with Renal Impairment:

In renally impaired subjects (creatinine clearance less than 70 mL/min/1.73m^2), one half of the usual adult dose is recommended. Such patients will require a longer time to reach steady-state at each dose.

Patients Undergoing Hemodialysis:

Topiramate is cleared by hemodialysis at a rate that is 4 to 6 times greater than a normal individual. Accordingly, a prolonged period of dialysis may cause topiramate concentration to fall below that required to maintain an anti-seizure effect. To avoid rapid drops in topiramate plasma concentration during hemodialysis, a supplemental dose of topiramate may be required. The actual adjustment should take into account 1) the duration of dialysis period, 2) the clearance rate of the dialysis system being used, and 3) the effective renal clearance of topiramate in the patient being dialyzed.

Patients with Hepatic Disease:

In hepatically impaired patients topiramate plasma concentrations may be increased. The mechanism is not well understood.

HOW SUPPLIED

TOPAMAX® (topiramate) Tablets is available as debossed, coated, round tablets in the following strengths and colors:

25 mg white (coded "TOP" on one side; "25" on the other)

100 mg yellow (coded "TOPAMAX" on one side; "100" on the other)

200 mg salmon (coded "TOPAMAX" on one side; "200" on the other)

They are supplied as follows:

25 mg tablets—bottles of 60 count with desiccant (NDC 0045-0638-65)

100 mg tablets—bottles of 60 count with desiccant (NDC 0045-0641-65)

200 mg tablets—bottles of 60 count with desiccant (NDC 0045-0642-65)

TOPAMAX® (topiramate capsules) Sprinkle Capsules contain small, white to off white spheres. The gelatin capsules are white and clear.

They are marked as follows:

15 mg capsule with "TOP" and "15 mg" on the side

25 mg capsule with "TOP" and "25 mg" on the side

The capsules are supplied as follows:

15 mg capsules—bottles of 60 (NDC 0045-0647-65)

25 mg capsules—bottles of 60 (NDC 0045-0645-65)

TOPAMAX® (topiramate) Tablets should be stored in tightly-closed containers at controlled room temperature, 59 to 86°F, 15 to 30°C). Protect from moisture.

TOPAMAX® (topiramate capsules) Sprinkle Capsules should be stored in tightly-closed containers at or below 25°C (77°F). Protect from moisture.

TOPAMAX® (topiramate) and TOPAMAX® (topiramate capsules) are trademarks of Ortho-McNeil Pharmaceutical.

HOW TO TAKE

TOPAMAX® (topiramate capsules) SPRINKLE CAPSULES

A Guide for Patients and Their Caregivers

Your doctor has given you a prescription for TOPAMAX® (topiramate capsules) Sprinkle Capsules. Here are your instructions for taking this medication. Please read these instructions prior to use.

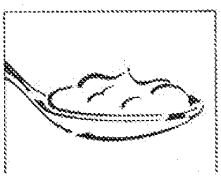

To Take With Food

You may sprinkle the contents of TOPAMAX® Sprinkle Capsules on a small amount (teaspoon) of soft food, such as applesauce, custard, ice cream, oatmeal, pudding, or yogurt.

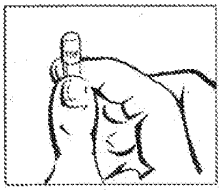

Hold the capsule upright so that you can read the word "TOP".

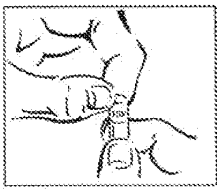

Carefully twist off the clear portion of the capsule. You may find it best to do this over the small portion of the food onto which you will be pouring the sprinkles.

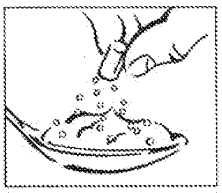

Sprinkle all of the capsule's contents onto a spoonful of soft food, taking care to see that the entire prescribed dosage is sprinkled onto the food.

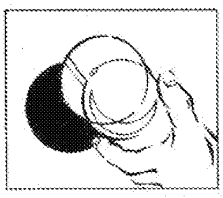

Be sure the patient swallows the entire spoonful of the sprinkle/food mixture immediately. Chewing should be avoided. It may be helpful to have the patient drink fluids immediately in order to make sure all of the mixture is swallowed.

IMPORTANT: Never store any sprinkle/food mixture for use at a later time.

To Take Without Food

TOPAMAX® Sprinkle Capsules may also be swallowed as whole capsules.

For more information about TOPAMAX® Sprinkle Capsules, ask your doctor or pharmacist.

ORTHO-McNEIL
OMP DIVISION
ORTHO-McNEIL PHARMACEUTICAL, INC.
Raritan, NJ 08869
© OMP 1998
Revised May 2000 648-19-445-3
Shown in Product Identification Guide, page 930

TYLENOL® with Codeine ℞

(ti 'len-gael co' dein)

tablets
(acetaminophen and codeine phosphate tablets)
elixir
(acetaminophen and codeine phosphate oral solution USP)

Analgesic For Oral Use

DESCRIPTION

Each tablet contains:	
No. 3 Codeine Phosphate	30 mg
Acetaminophen	300 mg
No. 4 Codeine Phosphate	60 mg
Acetaminophen	300 mg
Each 5 mL of elixir contains:	
Codeine Phosphate	12 mg
Acetaminophen	120 mg

Alcohol 7%.

Inactive ingredients: tablets—powdered cellulose, magnesium stearate, sodium metabisulfite†, pregelatinized starch, starch (corn); elixir—alcohol, citric acid, propylene glycol, sodium benzoate, saccharin sodium, sucrose, natural and artificial flavors, FD&C Yellow No. 6.

Acetaminophen, 4'-hydroxyacetanilide, is a non-opiate, non-salicylate analgesic and antipyretic which occurs as a white, odorless, crystalline powder, possessing a slightly bitter taste. Its structure is as follows:

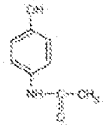

$C_8H_9NO_2$ M.W. 151.16

Clinical Development of Topiramate for Obesity Extended to Simplify Dosing, Improve Tolerability
714 words
4 February 2002
08:31
PR Newswire
PRN
English
(Copyright (c) 2002, PR Newswire)

RARITAN, N.J., Feb. 4 /PRNewswire-FirstCall/ -- Johnson & Johnson Pharmaceutical Research & Development, L.L.C. (JJPRD), a Johnson & Johnson company (NYSE: JNJ), said it will revise its clinical development program for the use of topiramate in obesity to enhance the compound's profile. The current clinical trial program will be discontinued in order to develop a new, controlled release formulation using drug delivery technology from ALZA Corporation, which merged with Johnson & Johnson in 2001.

The company said its intent is to enhance the tolerability and simplify the dosing of the resulting treatment for obesity. In recent years, ALZA technology has demonstrated the potential to achieve these objectives with a variety of existing medicines. If successful, the company said these changes could result in a better treatment than it originally contemplated for this serious health condition.

Preliminary data has demonstrated that topiramate has resulted in weight loss in obese individuals. However, at the higher doses being studied in this patient population the tolerability profile was not acceptable to the company and, as a result, JJPRD will pursue a new formulation.

The company said that the decision to revise the obesity clinical trial program does not impact the use of topiramate in any currently marketed indications, or for any of the other clinical development programs currently underway.

TOPAMAX(R) (topiramate / topiramate capsules) is indicated as adjunctive therapy for adults and pediatric patients ages two-16 years with partial onset seizures or primary generalized tonic-clonic seizures, and in patients two years of age and older with seizures associated with Lennox-Gastaut syndrome. In clinical trials for these indications, the most common side effects observed in children included excessive drowsiness, loss of appetite, fatigue, nervousness, difficulty with concentration / attention, weight loss, aggressive reaction and memory difficulties. In adults, the most common side effects were sleepiness, dizziness, poor coordination, speech difficulties, slowed thinking (psychomotor slowing), blurred or double vision, memory difficulties and changes in sensation. However, these effects were generally temporary.

TOPAMAX is marketed in the United States by Ortho-McNeil Pharmaceutical, Inc., and is approved for marketing in more than 75 countries, including the United Kingdom, France, Sweden, Australia, Hong Kong, China, Germany and Canada. To date, TOPAMAX has been used to treat approximately one million patients worldwide. Clinical studies are underway to determine the safety and efficacy of topiramate in the treatment of bipolar disorder and for the prevention of migraine headaches.

Based in Raritan, New Jersey, Johnson & Johnson Pharmaceutical Research & Development, L.L.C. conducts pharmaceutical research and development for the pharmaceutical companies of Johnson & Johnson. For more information about TOPAMAX, please see full U.S. prescribing information or go to www.topamax.com.

This press release contains "forward-looking statements" as defined in the Private Securities Litigation Reform Act of 1995. These statements are based on current expectations of future events. If underlying assumptions prove inaccurate or unknown risks or uncertainties materialize, actual results could vary materially from the Company's expectations and projections. Risks and uncertainties include general industry conditions and competition; economic conditions, such as interest rate and currency exchange rate fluctuations; technological advances and patents attained by competitors; challenges inherent in new product development, including obtaining regulatory approvals; domestic and foreign health care reforms and governmental laws and regulations; and trends toward health care cost containment. A further list and description of these risks, uncertainties and other factors can be found in Exhibit 99(b) of the Company's Annual Report on Form 10-K for the fiscal year ended December 31, 2000. Copies of this Form 10-K are available online at www.sec.gov<http://www.sec.gov> or on request from the Company. The Company assumes no obligation to update any forward-looking statements as a result of new information or future events or developments.

D.6 **CONCENTRATION RELATED EFFECTS OF VIGABATRIN ON GABA UPTAKE IN CULTURED RODENT ASTROCYTES**

John Paul Leach, Graeme Sills, George Thompson, Gerard Forrest, Elaine Butler, and Martin J Brodie.
Epilepsy Research Unit, Western Infirmary, Glasgow, UK

Rationale
Vigabatrin is an effective anticonvulsant when used as add-on therapy. The clinical efficacy of vigabatrin was previously believed to be due solely to the inhibition of GABA-transaminase (GABA-T) activity. We have shown that vigabatrin also inhibits the reuptake of GABA by astrocytes. Here we describe how this effect varies with the concentration of vigabatrin.

Methods
Astrocytes were cultured from the cerebral cortices of 1-day old rat pups. After three weeks in culture, the rate of GABA uptake was assessed by exposure to [^{14}C]-labelled GABA. GABA uptake into cells following 1 hour pre-treatment with vigabatrin (1 to 500uM) was compared to that of cells exposed to control conditions.

Results
At concentrations of 1uM,10uM, and 50uM, vigabatrin did not significantly alter the rate of GABA uptake. At 100uM however, vigabatrin significantly decreased GABA uptake, the mean values at 100uM being 80% of the mean control values ($p<0.05$), an effect that persists at 250uM. Exposure to vigabatrin at 500uM, however, significantly *increased* the mean rate of GABA uptake by 32% ($p<0.01$).

Conclusions
While it was previously felt that vigabatrin had only one action on the GABAergic system, it is now clear that it also has significant dose-dependant effects on the rate of GABA uptake. The clinical relevance of this is unclear, but this inhibition at levels known to decrease GABA-T activity may be at least partly responsible for the anticonvulsant action of vigabatrin.

D.8 **TOPIRAMATE: DOUBLE-BLIND TRIAL AS MONOTHERAPY**

Authors: S. K. Sachdeo, MD, Rajesh C. Sachdeo, MD, UMDNJ, New Brunswick, NJ, Ross A. Reife, MD, Pilar Lim, Gordon Pledger, Ph.D., RWJ Pharmaceutical Research Institute, Raritan, NJ.

Rationale: Topiramate has shown efficacy in treating adults with refractory partial-onset seizures in five trials. In these double-blind trials, patients were randomized to add either topiramate or placebo to their existing anti-epileptic drug (AED) regimen. The percent reduction in seizures over baseline was compared for the two groups. The current trial assessed efficacy in the same population using a different design.
Methods: In this double-blind trial, 48 patients were randomized to receive either the minimum efficacious dose of topiramate [100 mg/day] or a higher dose [1000 mg/day or maximum tolerated dose (MTD)]. Concomitant AEDs were withdrawn during the first 35 days of the double-blind period. The patient continued monotherapy of either 100 mg/day or 1000 mg/day (or MTD) of topiramate for the duration of the 112-day double-blind phase or until the patient met exit criteria. The exit criteria were pre-defined to indicate a worsening of seizures over baseline.
Results: The time to exit was longer in the 1000 mg/day group than in the 100 mg/day group ($p=0.0017$). The number of patients who remained in the trial for the entire 112 days was also greater in the 1000 mg/day group ($p=0.002$).
Conclusions: In a different trial design than those previously reported with topiramate, 1000 mg/day (or MTD) of topiramate monotherapy is effective as treatment for refractory partial onset seizures in adults.

Supported by RWJ Pharmaceutical Research Institute

Ross A. Reife, Pilar Lim, and Gordon Pledger, Ph.D., are employees of RWJ Pharmaceutical Research Institute, the sponsor of the research. As such they receive salaries from RWJ Pharmaceutical Research Institute and may hold equity positions and/or receive stock options. Drs. S. K. Sachdeo and Rajesh C. Sachdeo have received a grant for doing the above study.

D.7 **DOSE-RANGING TRIAL WITH HIGHER DOSES OF TOPIRAMATE IN PATIENTS WITH RESISTANT PARTIAL SEIZURES** Michael Privitera,[1] Richard Fincham,[2] J. Kiffin Penry,[3] Ross Reife,[4] Lynn Kramer,[5] Gordon Pledger,[4] R. Karim,[4] and the Topiramate YE Study Group 1.University of Cincinnati Medical Center, 2.University of Iowa Hospitals, 3.Bowman Gray School of Medicine, 4.R.W. Johnson Pharmaceutical Research Institute, 5.Ciba-Geigy Pharmaceuticals Division

RATIONALE: We conducted a double-blind, parallel group, placebo-controlled trial in 190 patients to evaluate the safety and efficacy of three dosages of topiramate, an investigational antiepileptic drug (AED) as adjunctive therapy for refractory partial epilepsy. **METHODS**: During a 12 week baseline period, patients were required to have at least one partial-onset seizure per week while receiving one or two standard AEDs at therapeutic concentrations. Patients were randomized to 600 mg/day, 800 mg/day, 1000 mg/day or placebo in a bid regimen. A 6 week titration period was followed by a 12-week maintenance period. **RESULTS**: Median percent reductions from baseline in monthly seizure rates were 1% for placebo, 41% for topiramate 600 mg/day and topiramate 800 mg/day, and 38% for topiramate 1000 mg/day. A 50% or greater reduction in baseline seizure frequency during the treatment phase was observed in 9% of placebo, 44% of topiramate 600 mg/day, 40% of topiramate 800 mg/day and 35% of topiramate 1000 mg/day patients. No placebo patients improved by 75-100%, but 20% of topiramate patients had this degree of improvement. All analyses were intent-to-treat drug-placebo comparisons and significantly ($p \leq 0.02$) favored topiramate. Treatment-emergent adverse events consisted mainly of neurological symptoms commonly observed during standard AED therapy. Sixteen percent of topiramate patients discontinued due to adverse events. **CONCLUSIONS**: Topiramate is a highly efficacious and generally well tolerated new AED. When large groups of patients are compared, incremental efficacy in the add-on setting is not observed above 600 mg/day; however, higher doses may prove beneficial to individual patients who tolerate them.

Dr. Privitera has performed consulting for R.W. Johnson PRI. Drs. Reife, Pledger, and Karim are currently employees of R.W. Johnson PRI. Dr. Kramer was an employee of R.W. Johnson PRI at the time the trial was completed, however, he no longer works for them.

D.9 TOPIRAMATE DOSE-RANGING TRIAL IN REFRACTORY PARTIAL EPILEPSY. Edward Faught, B.J. Wilder, R. Eugene Ramsay, Ross A. Reife, Lynn D. Kramer, Gordon W. Pledger, Rezaul M. Karim and the Topiramate YD Study Group. University of Alabama at Birmingham, Birmingham, AL 35294.

RATIONALE: We conducted a randomized, double-blind comparison of three dosages of topiramate to placebo as adjunctive therapy in refractory partial onset epilepsy.
METHODS: 181 patients completed a 12-week baseline during which they had at least one partial-onset seizure per week. All received one or two other drugs at therapeutic concentrations. Patients were randomized to 200 mg/day, 400 mg/day, 600 mg/day or placebo. A four-week titration preceded a 12-week maintenance period.
RESULTS: The median percent seizure reductions relative to baseline, using an intent to treat analysis, were: 30% for topiramate 200 mg/day ($p = 0.051$), 48% for topiramate 400 mg/day ($p = 0.007$), 45% for topiramate 600 mg/day ($p = 0.001$) and 13% for placebo. Percent responders (> 50% reduction in seizure frequency) were 27% for topiramate 200 mg/day, 47% for topiramate 400 mg/day ($p = 0.013$), 46% for topiramate 600 mg/day ($p = 0.027$) and 18% for placebo. A significant ($p = 0.003$) reduction in secondarily generalized tonic clonic seizures with topiramate was demonstrated.
Mild or moderate central nervous system symptoms were the primary treatment-emergent adverse events, but treatment-limiting adverse events occurred in only 9% of topiramate patients compared to 7% of placebo patients.
CONCLUSIONS: Topiramate is effective and well-tolerated in refractory partial epilepsy.

Edward Faught, M.D., received research support and an honorarium for speaking from R.W. Johnson Pharmaceutical Research Institute.

UM00016748
NOVARTIS EXHIBIT 1517
Novartis v. Regents, IPR2023-01347
Page 3730 of 4460

MARTINDALE

The Extra Pharmacopoeia

Thirtieth Edition

Edited by James E. F. Reynolds

Deputy Editor
Kathleen Parfitt

Assistant Editors
Anne V. Parsons
Sean C. Sweetman

95 / 0610
EPA EPO OEB

Published by direction of the Council of the Royal Pharmaceutical Society of Great Britain and prepared in the Society's Department of Pharmaceutical Sciences

London
THE PHARMACEUTICAL PRESS
1993

UM00016749
NOVARTIS EXHIBIT 1517
Novartis v. Regents, IPR2023-01347
Page 3731 of 4460

cepress *(Guidotti, Ital.).*
aptopril.
ypertension; congestive heart failure.

cepril *(Squibb, UK).*
aptopril.
ypertension; congestive heart failure.

cequin *(Recordati, Ital.).*
uinapril hydrochloride.
ypertension.

cerbine† *(Millot-Solac, Fr.).*
enzoic acid; salicylic acid; malic acid; opylene glycol.
ounds; bedsores.

cerbine *(Lucchini, Switz.).*
intment: Benzoic acid; malic acid; salicyl- acid; propylene glycol; propylene glycol alate; hexachlorophane.
ounds; burns.

cerbine *(Lucchini, Switz.).*
pical solution; topical gel: Benzoic acid; alic acid; salicylic acid; propylene glycol; opylene glycol malate.
ounds; burns.

cerbiol *(Vitapharm, Spain).*
enzyl alcohol; benzoic acid; malic acid; opylene glycol malate; propylene glycol; licylic acid.
ounds; burns.

cerbon *(ICI, Ger.; Rhein-Pharma, Ger.).*
sinopril.
ypertension.

cerola Complex *(Suisse, Austral.).*
scorbic acid; hesperidin-rutin-buckwheat- rus bioflavonoid complex.
tamin C deficiency.

certol *(Lacer, Spain).*
racetamol.
in: fever.

cesal *(Manzoni, Ital.).*
spirin.
in; fever.

cesistem *(Sigma-Tau, Ital.).*
alapril maleate; hydrochlorothiazide.
pertension.

cetaco *(Legere, USA).*
racetamol; codeine phosphate.

cetadeps *(Westbrook, UK).*
cetylated wool fat.

cétalgine *(Streuli, Switz.).*
racetamol.
in: fever.

cet-Am *(Organon, Canad.).*
eophylline calcium glycinate.
onchodilator.

cet-Am Expectorant *(Organon, Canad.).*
eophylline sodium glycinate; guaiphenes-

onchodilator; expectorant.

cetaminophen, Aspirin, and Caf- ine Capsules *(U.S.P. XXII).*
racetamol; aspirin; caffeine.

cetaminophen, Aspirin, and Caf- ine Tablets *(U.S.P. XXII).*
racetamol; aspirin; caffeine.

cetaminophen and Aspirin Tablets *-S.P. XXII).*
racetamol; aspirin.

cetaminophen and Caffeine Cap- les *(U.S.P. XXII).*
racetamol; caffeine.

cetaminophen and Caffeine Tablets *-S.P. XXII).*
racetamol; caffeine.

cetaminophen Capsules *(U.S.P. :II).*
racetamol.

cetaminophen with Codeine *(Pharmas- ce, Canad.; Stanley, Canad.).*
racetamol; caffeine; codeine phosphate.
in; fever; coughs.

cetaminophen and Codeine Phos- ate Capsules *(U.S.P. XXII).*
racetamol; codeine phosphate hemihy- ate.

Acetaminophen and Codeine Phosphate Elixir *(U.S.P. XXII).*
Paracetamol; codeine phosphate hemihydrate.

Acetaminophen and Codeine Phosphate Tablets *(U.S.P. XXII).*
Paracetamol; codeine phosphate hemihydrate.

Acetaminophen and Diphenhydramine Citrate Tablets *(U.S.P. XXII).*
Paracetamol; diphenhydramine citrate.

Acetaminophen for Effervescent Oral Solution *(U.S.P. XXII).*
Paracetamol.

Acetaminophen Oral Solution *(U.S.P. XXII).*
Paracetamol.

Acetaminophen Oral Suspension *(U.S.P. XXII).*
Paracetamol.

Acetaminophen and Pseudoephedrine Hydrochloride Tablets *(U.S.P. XXII).*
Paracetamol; pseudoephedrine hydrochloride.

Acetaminophen Suppositories *(U.S.P. XXII).*
Paracetamol.

Acetaminophen Tablets *(U.S.P. XXII).*
Paracetamol.

Acetamol *(Genrili, Ital.).*
Paracetamol.
Pain.

Acetard *(Benzon, Swed.).*
Aspirin.
Pain; inflammation; fever.

Acetazolamide Tablets *(B.P. 1988).*

Acetazolamide Tablets *(U.S.P. XXII).*

Acetazone Forte *(Technilab, Canad.).*
Chlorzoxazone; paracetamol.
Pain; muscle spasm.

Acetazone Forte C8 *(Technilab, Canad.).*
Chlorzoxazone; paracetamol; codeine phosphate.
Pain; muscle spasm.

Acetensil *(Andromaco, Spain).*
Enalapril maleate.
Hypertension; heart failure.

Acétest *(Ames, Fr.).*
Test for ketones in urine.

Acetest *(Ames, UK).*
Test for ketones in urine, plasma, or serum. In the *UK* these are described in the Drug Tariff as Nitroprusside Reagent Tablets (Rothera's Tablets).

Acethropan *(Hoechst, Ger.).*
Corticotrophin (porcine).
Stimulation of the adrenal glands; multiple sclerosis; glucocorticoid therapy.

Acetic Acid Irrigation *(U.S.P. XXII).*
Glacial acetic acid 0.25%.

Acetic Acid Otic Solution *(U.S.P. XXII).*
Glacial acetic acid.

Acétocaustine *(Asta, Switz.).*
Monochloroacetic acid.
Warts.

Acetohexamide Tablets *(B.P. 1988).*

Acetohexamide Tablets *(U.S.P. XXII).*

Acetohydroxamic Acid Tablets *(U.S.P. XXII).*

Acetolyt *(Madaus, Ger.).*
Hexacalcium-hexasodium-heptacitrate-hydrate complex.
Metabolic acidosis.

Acetonal *(Athenstaedt, Ger.).*
Aluminium subacetate tartrate; (2,2,2-trichlor-1,1-dimethylethyl)-salicylate.
Anorectal disorders.

Acetonal Vaginale *(Athenstaedt, Ger.).*
Aluminium acetotartrate; (2,2,2-trichlor-1,1-dimethylethyl)-salicylate; oestradiol benzoate; sulphanilamide.
Vaginitis; vaginal infections.

Acetophenazine Maleate Tablets *(U.S.P. XXII).*

Acetopt *(Sigma, Austral.).*
Sulphacetamide sodium.
Conjunctival infections.

Acetoxyl *(Stiefel, Canad.).*
Benzoyl peroxide.
Acne vulgaris.

Acetoxyl *(Stiefel, UK).*
Benzoyl peroxide.
Acne vulgaris.

Acetuber *(Hubber, Spain).*
Injection: Pituitary extract.
Acetonaemia; vomiting in pregnancy.

Acetuber *(Hubber, Spain).*
Suppositories: Cocarboxylase; dimenhydrinate; glucose; pyridoxine; potassium chloride; dibasic sodium phosphate.
Acetonaemia; vomiting in pregnancy.

Acetylcholine Chloride for Ophthalmic Solution *(U.S.P. XXII).*

Acetylcysteine and Isoproterenol Hydrochloride Inhalation Solution *(U.S.P. XXII).*
Acetylcysteine; isoprenaline hydrochloride.

Acetylcysteine Solution *(U.S.P. XXII).*

Acetylin *(Squibb-Heyden, Ger.).*
Aspirin.
Pain; fever; rheumatism.

Acetyst *(Jossa-Arznei, Ger.).*
Acetylcysteine.
Respiratory-tract disorders associated with increased or viscous mucus; otitis media.

Acezide *(Squibb, UK).*
Captopril; hydrochlorothiazide.
Hypertension.

Acfol *(Torlan, Spain).*
Folic acid.
Folic acid deficiency.

Achrocidin *(Lederle, Canad.).*
Tetracycline hydrochloride; caffeine; salicylamide; chloropyrilene citrate.
Bacterial infections.

Achromycin *(Lederle, Austral.).*
Tetracycline hydrochloride.
Bacterial infections.

Achromycin *(Lederle, Canad.).*
Intramuscular injection: Tetracycline hydrochloride; procaine hydrochloride.
Bacterial infections.

Achromycin *(Lederle, Canad.).*
Intravenous injection; ointment; eye ointment: Tetracycline hydrochloride.
Bacterial infections.

Achromycin *(Lederle, Ger.).*
Capsules; ointment; tablets: Tetracycline hydrochloride.
Bacterial infections.

Achromycin *(Lederle, Ger.).*
Eye ointment: Tetracycline hydrochloride; hydrocortisone.
Allergic and inflammatory disorders of the eye.

Achromycin *(Lederle, Swed.).*
Tetracycline hydrochloride.
Bacterial infections.

Achromycin *(Lederle, UK).*
Capsules; tablets; ointment; eye and ear ointment; intravenous injection: Tetracycline hydrochloride.
Bacterial infections.

Achromycin *(Lederle, UK).*
Intramuscular injection: Tetracycline hydrochloride; procaine hydrochloride.
Bacterial infections.

Achromycin† *(Lederle, USA).*
Intramuscular injection: Tetracycline hydrochloride; procaine hydrochloride.
Bacterial infections.

Achromycin *(Lederle, USA).*
Intravenous injection; ophthalmic suspension; ophthalmic ointment; ointment; capsules: Tetracycline hydrochloride.
Bacterial infections.

Achromycin V *(Lederle, Austral.).*
Tetracycline hydrochloride.
Bacterial infections.

Achromycin V *(Lederle, Canad.).*
Tetracycline hydrochloride.
Bacterial infections.

Achromycin V *(Lederle, S.Afr.).*
Tetracycline hydrochloride.
Bacterial infections.

Achromycin V† *(Lederle, UK).*
Tetracycline.
Bacterial infections.

Achromycin V *(Lederle, USA).*
Capsules: Tetracycline hydrochloride.
Bacterial infections.

Achromycin V *(Lederle, USA).*
Oral suspension: Tetracycline.
Bacterial infections.

Achromycine *(Lederle, Switz.).*
Tetracycline hydrochloride.
Bacterial infections.

Achrostatin *(Lederle, Austral.).*
Tetracycline hydrochloride; nystatin.
Bacterial infections.

Aci Kestomal *(Boizot, Spain).*
Aluminium hydroxide; dimethicone; magnesium carbonate; magnesium oxide; metoclopramide hydrochloride.
Gastro-intestinal disorders.

Acicloftal *(Bruschettini, Ital.).*
Acyclovir.
Herpes simplex keratitis.

Acid A Vit *(Roche, Neth.).*
Tretinoin.
Acne vulgaris.

Acid Citrate Dextrose Solution (ACD) *(B.P. 1988).*
Formula A: sodium citrate 2.2 g; citric acid monohydrate 0.8 g; glucose monohydrate 2.45 g or anhydrous glucose 2.24 g; water for injections to 100 mL. Formula B: sodium citrate 1.32 g; citric acid monohydrate 0.48 g; glucose monohydrate 1.47 g or anhydrous glucose 1.34 g; water for injections to 100 mL.
15 mL of formula A and 25 mL of formula B are used for the collection of 100 mL of blood.

Acid Gentian Mixture *(B.P. 1988).*
Concentrated Compound Gentian Infusion *(B.P.)* 10% v/v; dilute hydrochloric acid 5% v/v.
For extemporaneous preparation the *B.P.* specifies Concentrated Compound Gentian Infusion *(B.P.)* 10 mL; dilute hydrochloric acid 5 mL; Double-strength Chloroform Water *(B.P.)* 50 mL; water to 100 mL.

Acid Insulin Injection *(B.P. 1988)*
Acid Insulin.
A sterile solution of Insulin (*B.P.*) pH 3.0 to 3.5.

Acid Mantle *(Miles, Canad.).*
Aluminium acetate.
Skin irritation.

Acid Mantle *(Sandoz Consumer, USA).*
Aluminium acetate.
Minor skin disorders; pharmaceutical vehicle.

Acidac *(Alonga, Spain).*
Aluminium hydroxide; dimethicone; magnesium carbonate; magnesium hydroxide.
Hyperchlorhydria; flatulence.

Acidion *(Dibios, Spain).*
Aluminium hydroxide; dimethicone; magnesium carbonate; magnesium hydroxide.
Gastro-intestinal disorders.

Acidion Solucion *(Dibios, Spain).*
Aluminium hydroxide; magnesium hydroxide.
Hyperchlorhydria.

UM00016750
NOVARTIS EXHIBIT 1517
Novartis v. Regents, IPR2023-01347
Page 3732 of 4460

Asmaven *(Approved Prescription Services, UK).*
Salbutamol sulphate.
Bronchospasm; premature labour.

Asmaxen *(Doetsch, Grether, Switz.).*
Salbutamol.
Bronchospasm.

Asmetil *(Benvegna, Ital.).*
Protokylol hydrochloride.
Respiratory-system disorders.

Asmisul *(Inibsa, Spain).*
Eprozinol dihydrochloride.
Asthmatic and dyspnoeic disorders.

Asmo *(Hubber, Spain).*
Theophylline.
Obstructive airways disease; paroxysmal dyspnoea; heart failure.

Asmobacterial† *(Leti, Spain).*
Escherichia coli; Haemophilus influenzae; Klebsiella pneumoniae; Staphylococcus pyogenes; Moraxella (Branhamella) catarrhalis; Streptococcus sp.; Proteus vulgaris.
Respiratory-tract infections.

Asorec *(Radiumfarma, Ital.).*
Sulphaguanole.
Infective diarrhoea.

Aspac *(Inexfa, Spain).*
Paracetamol.
Pain; fever.

Aspalgin *(Fawns & McAllan, Austral.).*
Aspirin; codeine phosphate.
Pain; fever.

Aspalox *(Rorer, Ger.).*
Aspirin.
Pain; fever; rheumatism; arthritis; thrombo-embolic disorders.

Aspam *(RP-LABO, Fr.).*
Aspartame.
Sugar substitute.

Asparagin (Rōwo-119) *(Pharmakon, Ger.).*
Vitamin and electrolyte preparation with rutin.
Tonic.

Asparagus-P *(Plantina, Ger.).*
Rhiz. asparagi off. pulv.; herb. petroselini sat. pulv.
Oedema; urinary tract stones.

Aspartatol *(Eagle, Austral.).*
Potassium aspartate; magnesium aspartate; levoglutamide.
Tonic.

Aspartina *(Vick International, Ital.).*
Aspartame.
Sugar substitute.

Aspartono *(Medix, Spain).*
Adenosine triphosphate; glucose; magnesium aspartate; potassium aspartate.
Tonic; cardiopathies; liver disorders; muscular dystrophies.

Aspaserine B6 Tranq *(Roger, Spain).*
Diazepam; pyridoxine.
Anxiety; insomnia; febrile convulsions; muscle spasm; alcohol withdrawal.

Aspasmon N *(Norgine, Ger.).*
Peppermint oil; anise oil; caraway oil.
Gastro-intestinal disorders; asthma.

Aspav *(Roussel, UK).*
Aspirin; papaveretum.
Pain.
Formerly known as Soluble Aspirin and Papaveretum Tablets.

Aspecton *(Krewel, Ger.).*
Rad. liquiritiae; anise oil; greek sage oil; eucalyptus oil; fennel oil; thyme oil.
Coughs; catarrh.

Aspecton N *(Krewel, Ger.).*
Thyme; saponins from gypsophila spp.
Respiratory-tract disorders.

Aspecton-Balsam *(Krewel, Ger.).*
Camphor; ol. thymi; ol. eucalypti.
Coughs; cold symptoms.

Aspectonetten *(Krewel, Ger.).*
Butethamate citrate.
Coughs and associated respiratory-tract disorders.

Aspégic *(Synthelabo, Fr.).*
Lysine aspirin.
Pain; fever; rheumatism.

Aspegic *(Lirca, Ital.).*
Lysine aspirin.
Pain; fever; inflammation.

Aspegic *(Lorex, Neth.).*
Lysine aspirin.
Pain; fever; inflammation.

Aspegic *(Cantabria, Spain).*
Lysine aspirin.
Pain; fever; inflammation; thrombo-embolic disorders.

Aspégic *(Synthelabo, Switz.).*
Lysine aspirin; glycine.
Pain; fever.

Aspellin *(Fisons, UK).*
Methyl salicylate; ethyl salicylate; ammonium salicylate; menthol; camphor.
Pain.

Aspenil *(Chemil, Ital.).*
Amoxycillin.
Bacterial infections.

Aspercreme *(Roche, Ital.).*
Diethylamine salicylate; methyl nicotinate.
Musculoskeletal disorders.

Aspergum† *(Plough, UK).*
Aspirin.
Pain; fever.

Aspidol *(Piam, Ital.).*
Lysine aspirin.
Pain; fever.

Aspiglicina *(Antonetto, Ital.).*
Glycine; aspirin.
Neuralgia.

Aspinfantil *(Lasa, Spain).*
Aspirin.
Pain; fever.

Aspirin, Alumina, and Magnesia Tablets *(U.S.P. XXII).*
Aspirin; aluminium hydroxide; magnesium hydroxide.

Aspirin, Alumina, and Magnesium Oxide Tablets *(U.S.P. XXII).*
Aspirin; aluminium hydroxide; magnesium oxide.

Aspirin, Caffeine, and Dihydrocodeine Capsules *(U.S.P. XXII).*
Aspirin; caffeine; dihydrocodeine tartrate.

Aspirin and Caffeine Tablets *(B.P. 1988).*
Aspirin 350 mg; caffeine 30 mg.

Aspirin Capsules *(U.S.P. XXII).*
They may be enteric-coated.

Aspirin, Codeine Phosphate, Alumina, and Magnesia Tablets *(U.S.P. XXII).*
Aspirin; codeine phosphate hemihydrate; aluminium hydroxide; magnesium hydroxide.

Aspirin, Codeine Phosphate, and Caffeine Capsules *(U.S.P. XXII).*
Aspirin; codeine phosphate hemihydrate; caffeine.

Aspirin, Codeine Phosphate, and Caffeine Tablets *(U.S.P. XXII).*
Aspirin; codeine phosphate hemihydrate; caffeine.

Aspirin and Codeine Phosphate Tablets *(U.S.P. XXII)* Co-codaprin Tablets.
Aspirin; codeine phosphate hemihydrate.

Aspirin Delayed-release Capsules *(U.S.P. XXII).*
Enteric-coated aspirin.

Aspirin Delayed-release Tablets *(U.S.P. XXII).*
Enteric-coated aspirin.

Aspirin Effervescent Tablets for Oral Solution *(U.S.P. XXII).*

Aspirin Extended-release Tablets *(U.S.P. XXII).*

Aspirin forte *(Bayer, Ger.).*
Aspirin; caffeine.
Pain; inflammation.

Aspirin plus C *(Bayer, Ger.).*
Aspirin; ascorbic acid.
Light to moderate pain; fever; cold symptoms.

Aspirin Suppositories *(U.S.P. XXII).*

Aspirin Tablets *(B.P. 1988)* Acetylsalicylic Acid Tablets.

Aspirin Tablets *(U.S.P. XXII).*
They may be enteric-coated.

Aspirina *(Bayer, Ital.).*
Aspirin.
Pain; fever; inflammation.

Aspiriha C *(Bayer, Ital.).*
Aspirin; ascorbic acid.
Pain; fever; inflammation.

Aspirina C *(Bayer, Spain).*
Aspirin; ascorbic acid.
Pain; fever; musculoskeletal disorders.

Aspirine C *(Bayer, Neth.).*
Aspirin; ascorbic acid.
Pain; fever.

Aspirinetta *(Bayer, Ital.).*
Aspirin.
Pain; fever; inflammation.

Aspirinetta C *(Bayer, Ital.).*
Aspirin; ascorbic acid.
Pain; fever; inflammation.

Aspisol *(Bayer, Ger.).*
Lysine aspirin.
Pain; fever; rheumatism; thrombo-embolic disorders.

Asplin *(Roger, Spain).*
Paracetamol.
Pain; fever.

Asporin 0.25 *(MC, Ital.).*
Sodium phenolate; glutaraldehyde.
Instrument sterilisation.

Asporin 2 *(MC, Ital.).*
Glutaraldehyde.
Instrument sterilisation.

Aspro *(Nicholas, Austral.).*
Aspirin.
Pain; fever.

Aspro *(Nicholas, Ger.).*
Aspirin.
Pain; inflammation.

Aspro *(Bouty, Ital.).*
Aspirin.
Pain; fever.

Aspro *(Nicholas, Neth.).*
Aspirin.
Pain; fever.

Aspro *(Pan Quimica, Spain).*
Aspirin.
Pain; fever; inflammation; thrombo-embolism prophylaxis.

Aspro *(Nicholas, Switz.).*
Aspirin.
Pain; fever.

Aspro *(Nicholas, UK).*
Aspirin.
Pain; fever.

Aspro C *(Bouty, Ital.).*
Aspirin; ascorbic acid.
Pain; fever.

Aspro Paraclear *(Nicholas, UK).*
Paracetamol.

Asprodeine *(Nicholas, Austral.).*
Aspirin; codeine phosphate.

Asprol *(Nicholas, Austral.).*
Paracetamol.
Pain; fever.

ASS *(Stada, Ger.; Durachemie, Ger.; Woelm, Ger.; Ratiopharm, Ger.).*
Aspirin.
Pain; inflammation; fever; rheumatism; thrombo-embolic disorders.

ASS + C *(Ratiopharm, Ger.).*
Aspirin; ascorbic acid.
Pain; cold symptoms.

Assagix *(Pierre Fabre, Fr.).*
Tilia; calcium bromolactobionate.
Insomnia; irritability.

Assan *(Permamed, Switz.).*
Flufenamic acid; glycol salicylate; heparin sodium.
Musculoskeletal and joint pain; peripheral vascular disorders.

Assan-Thermo *(Permamed, Switz.).*
Flufenamic acid; glycol salicylate; benzyl nicotinate; heparin sodium.
Musculoskeletal and joint pain.

Assist Energetico *(Farmasport, Ital.).*
Vitamin preparation.

Assist Reintegratore *(Farmasport, Ital.).*
Nutritional supplement.
Fluid and electrolyte imbalance.

ASS-Kombi *(Ratiopharm, Ger.).*
Paracetamol; aspirin; ascorbic acid.
Pain.

Assocort *(Squibb, Ital.).*
Triamcinolone acetonide; neomycin sulphate; gramicidin; nystatin.
Skin disorders.

Assoral *(Glaxo, Ital.).*
Roxithromycin.
Bacterial infections.

Assugrin *(Pan Quimica, Spain).*
Sodium cyclamate; saccharin sodium; sodium bicarbonate; tartaric acid.
Sugar substitute.

Assur *(Delagrange, Fr.).*
Moroxydine hydrochloride; aspirin.
Viral infections.

Astenile *(Recordati, Ital.).*
Prasterone sodium sulphate.
Asthenia.

Astenolit *(Elmu, Spain).*
Vitamin, mineral and amino-acid preparation.
Tonic.

Aster C *(Carvi, Ital.).*
Ascorbic acid.
Vitamin C deficiency.

Asthénal *(Grassmann, Switz.).*
Sodium dimethyl aminophenylphosphinate; glutamic acid; thiamine hydrochloride; ascorbic acid.
Tonic.

Asthenopin *(Mann, Ger.).*
Pilocarpine hydrochloride.
Ophthalmic disorders.

Asthma 6 *(Hobein, Ger.).*
Ephedrine hydrochloride; caffeine; khellin; potassium iodide; potassium guaiacolsulfonate; sodium benzoate; tinct. herb. grindel.; tinct. herb. hyoscyami; rad. senegae; polysorbate 20; rad. liquiritiae.
Obstructive airways disease.

Asthma-Bisolvon *(Thomae, Ger.).*
Bromhexine hydrochloride; ephedrine hydrochloride; theophylline.
Bronchitis; emphysema; asthma.

Asthma-Bomin† *(Pfluger, Ger.).*
Ambra; ammi visnaga; arnica; blatta or.; cactus; carduus mar.; cetraria isl.; chamomilla; crataegus; dracontium foet.; drosera; dulcamara; echinacea ang.; ephedrinum; eriodictyon calif.; geisemium; grindelia rob.; ipecacuanha; menthol; mercurius cyan.; sodium sulphate; pulsatilla; spigelia; spongia; stramonium.
Homoeopathic preparation.

Asthmacolat *(Galenika, Ger.).*
Etofylline; ephedrine hydrochloride; sem. stramonii; herb. adonidis; flor. arnicae; fol. belladonnae.
Asthma; bronchitis; adjunct in whooping cough.

UM00016751
NOVARTIS EXHIBIT 1517
Novartis v. Regents, IPR2023-01347
Page 3733 of 4460

Coalgan *(Brothier, Fr.).*
Calcium alginate.
Haemorrhage.

Coalgel *(Ducray, Fr.).*
Coal tar; salicylic acid.
Dandruff.

Coalip *(ISF, Ital.).*
Coenzyme A.
Metabolic disorders.

Co-amilozide Oral Solution *(B.P. 1988)* Amiloride and Hydrochlorothiazide Oral Solution.
Anhydrous amiloride hydrochloride 1 part by weight; hydrochlorothiazide 10 parts by weight.

Co-amilozide Tablets *(B.P. 1988)* Amiloride and Hydrochlorothiazide Tablets.
Anhydrous amiloride hydrochloride 1 part by weight; hydrochlorothiazide 10 parts by weight.

CO-B1 *(Bruco, Ital.).*
Cocarboxylase.
Metabolic disorders.

CO-B12 (Cobidodici) *(Bruco, Ital.).*
Cocarboxylase; thiamine monophosphate; cyanocobalamin.
Neuralgia symptoms.

Coba-12 *(Nordic, Canad.).*
Vitamin B substances; lysine hydrochloride; lignocaine hydrochloride.
Vitamin B deficiency.

Cobadex *(Cox, UK).*
Hydrocortisone; dimethicones.
Skin disorders.

Cobaforte *(Roussel, Ital.).*
Cobamamide.
Vitamin B_{12} deficiency.

Cobalatec *(Caps, S.Afr.).*
Cyanocobalamin.
Vitamin B_{12} deficiency.

Cobaldocemetil *(Clariana, Spain).*
Mecobalamin.
Vitamin B_{12} deficiency.

Cobalin-H *(Paines & Byrne, UK).*
Hydroxocobalamin.
Anaemia due to B_{12} deficiency; tobacco amblyopia; Leber's atrophy.

Cobalparen† *(Saarsticksstoff-Fatol, Ger.).*
Cyanocobalamin.
Vitamin B deficiency.

Cobalparen-Depot† *(Saarsticksstoff-Fatol, Ger.).*
Hydroxocobalamin.
Vitamin B deficiency.

Cobalton *(Lagap, Ital.).*
Cocarboxylase; cyanocobalamin; sodium glycerophosphate.
Neuralgia symptoms.

Cobamas *(Tofir, Spain).*
Cyproheptadine hydrochloride; amino acids and vitamins.
Anorexia; weight loss; tonic.

Cobamide *(UCB, Ital.).*
Hydroxocobalamin.
Anaemias; neurological symptoms.

Cobantril *(Pfizer, Switz.).*
Pyrantel hydrogen embonate.
Nematode infections.

Cobanzyme *(Bouchara, Fr.).*
Cobamamide.
Debilitated states.

Cobazymase *(Bouchara, Switz.).*
Cobamamide.
Vitamin B_{12} deficiency.

Cobed *(Merrell, Ger.).*
Drops; syrup: Guaiphenesin; sodium camsylate.
Bronchitis; tracheobronchitis.

Cobed *(Merrell, Ger.).*
Gel: Camphor; guaiacol ethylglycolate; turpentine oil; peppermint oil; menthol; rosemary oil; thymol; methyl nicotinate.
Bronchitis; bronchopneumonia.

Cobergon *(Mendelejeff, Ital.).*
Cobamamide.
Tonic.

Co-Betaloc *(Astra, Eire).*
Metoprolol tartrate; hydrochlorothiazide.
Hypertension.

Co-Betaloc *(Astra, UK).*
Metoprolol tartrate; hydrochlorothiazide.
Hypertension.

Cobeton *(Propan, S.Afr.).*
Vitamin B substances.

cobidec n *(Parke, Davis, Ger.).*
Multivitamin and mineral preparation.

Cobiona *(Esteve, Spain).*
Oxatomide.
Hypersensitivity reactions.

Cobolin-M *(Legere, USA).*
Cyanocobalamin.

Cobutolin† *(Cox, UK).*
Inhalation: Salbutamol.
Asthma; bronchospasm.

Cobutolin† *(Cox, UK).*
Tablets: Salbutamol sulphate.
Asthma; bronchospasm.

Cocaine Eye-drops *(B.P.C. 1973).*
Cocaine hydrochloride.

Cocaine and Homatropine Eye-drops *(B.P.C. 1973).*
Cocaine hydrochloride; homatropine hydrobromide.

Cocaine Hydrochloride Tablets for Topical Solution *(U.S.P. XXII).*

Cocardoce *(Hortel, Spain).*
Cyanocobalamin; cocarboxylase.
Vitamin B deficiency; nausea and vomiting in pregnancy; tonic; alcoholism.

Cocardoce A M P *(Hortel, Spain).*
Adenosine phosphate; cyanocobalamin; cocarboxylase.
Tonic.

Co-careldopa Tablets *(B.P. 1988)* Levodopa and Carbidopa Tablets.
Levodopa; carbidopa.

Co-Carnetina B12 *(Sigma-Tau, Ital.).*
Cobamamide; L-carnitine.
Tonic.

Cocarvit *(CT, Ital.).*
Cocarboxylase.

Coccidioidin *(U.S.P. XXII).*
Contains the antigens obtained from the by-products of mycelial growth or from the spherules of the fungus *Coccidioides immitis.*

Cocculine *(Boiron, Fr.).*
Cocculus; tabacum; nux vomica; petroleum.
Homoeopathic preparation.

Cocilix *(Vernleigh, S.Afr.).*
Cocillana; senega; squill; guaiacol; terpin hydrate; menthol; codeine phosphate.
Coughs.

Cocillana Liquid Extract *(B.P.C. 1973).*

Cocillana-etyfin *(Kabi, Swed.).*
Ethylmorphine hydrochloride; senega; cocillana; cascara.
Coughs.

Co-Cillin *(Compu, S.Afr.).*
Ampicillin trihydrate.
Bacterial infections.

Cocktail Reale *(Sella, Ital.).*
Honey; pollen; ginseng; royal jelly; propolis.
Nutritional supplement.

Co-codamol Tablets *(B.P. 1988)* Codeine Phosphate and Paracetamol Tablets.
Codeine phosphate 2 parts by weight; paracetamol 125 parts by weight.

Co-codaprin Tablets *(B.P. 1988)* Aspirin and Codeine Tablets.
Codeine phosphate 1 part by weight; aspirin 50 parts by weight.

Cocois *(Biogian, UK).*
Coal tar solution; salicylic acid; precipitated sulphur; coconut oil.
Dry scalp conditions.

Cocresol *(Area, Spain).*
Feprazone.
Pain; fever; inflammation.

Codafen Continus *(Napp, UK).*
Ibuprofen; codeine phosphate.
Pain; inflammation.

Codalan *(Lannett, USA).*
Codeine phosphate; paracetamol; caffeine.

Codalax *(Regent Laboratories, UK).*
Danthron; poloxamer 188.
Constipation.
These ingredients are present in such proportion that together they can be described by the British Approved Name Co-danthramer.

Codalgin *(Fawns & McAllan, Austral.).*
Paracetamol; codeine phosphate.
Pain; fever.

Codalgina Retard *(Faes, Spain).*
Aspirin.
Pain; inflammation; fever; thrombo-embolism prophylaxis.

Coda-Med *(Broad, UK).*
Paracetamol; codeine phosphate; caffeine citrate.

Codamine *(Barre-National, USA).*
Phenylpropanolamine hydrochloride; hydrocodone tartrate.

Codan *(Warner Chilcott, USA).*
Hydrocodone tartrate; homatropine methobromide.

Codanin *(Whitehall, UK).*
Codeine phosphate; paracetamol.
Pain; fever.

Co-danthrusate Capsules *(B.P. 1988)* Danthron and Docusate Sodium Capsules.
Danthron 5 parts by weight; docusate sodium 6 parts by weight.

Codaphen *(Roxane, USA).*
Codeine phosphate; paracetamol.

Codate *(Rorer, Austral.).*
Codeine phosphate.
Pain; diarrhoea; coughs.

Code Vin† *(Vinsi, Spain).*
Suppositories: Codeine phosphate; ephedrine hydrochloride; propyphenazone.
Influenza and cold symptoms.

Code Vin† *(Vinsi, Spain).*
Tablets: Codeine phosphate; ephedrine hydrochloride.
Coughs.

Codefilona† *(Lasa, Spain).*
Aminophylline; codeine.
Coughs; bronchospasm.

Codegest Expectorant *(Great Southern, USA).*
Phenylpropanolamine hydrochloride; codeine phosphate; guaiphenesin.

Codeine Linctus *(B.P. 1988).*
Codeine phosphate hemihydrate 0.3% w/v or an equivalent concentration of the sesquihydrate.
Diabetic Codeine Linctus *(B.P.)* is formulated with a vehicle appropriate for administration to diabetics and complies with the requirements for Codeine Linctus *(B.P.).*

Codeine Phosphate Injection *(U.S.P. XXII).*
Codeine phosphate hemihydrate.

Codeine Phosphate Oral Solution *(B.P. 1988)* Codeine Phosphate Syrup.
Codeine phosphate hemihydrate 0.5% w/v or an equivalent concentration of the sesquihydrate.
This preparation replaces Codeine Phosphate Syrup *B.P.C. 1973.* For extemporaneous preparation the *B.P.* specifies codeine phosphate hemihydrate 0.5 g, water 1.5 mL, chloroform spirit 2.5 mL, and syrup to 100 mL.

Codeine Phosphate Tablets *(B.P. 1988).*
Codeine phosphate or codeine phosphate sesquihydrate.

Codeine Phosphate Tablets *(U.S.P. XXII).*
Codeine phosphate hemihydrate.

Codeine Sulfate Tablets *(U.S.P. XXII).*
Codeine sulphate trihydrate.

Codeinol *(Sabo, Ital.).*
Codeine hydrochloride; ephedrine hydrochloride.
Respiratory-tract symptoms with cough.

Codeisan *(Abello, Spain).*
Syrup: Codeine phosphate; ephedrine hydrochloride; Primula veris; sodium benzoate.
Respiratory-tract disorders.

Codeisan *(Abello, Spain).*
Tablets; suppositories: Codeine phosphate.
Coughs; pain; diarrhoea.

Codelasa *(Lasa, Spain).*
Codeine; ephedrine hydrochloride; potassium guaiacolsulfonate.
Respiratory-tract disorders.

Codelasa Infantil† *(Lasa, Spain).*
Cineole; codeine; ephedrine hydrochloride.
Respiratory-tract disorders.

Codelix *(Drug Houses Austral., Austral.).*
Codeine phosphate.
Coughs; pain; diarrhoea.

Codella *(Napp, UK).*
Glycerol; kaolin; povidone-iodine.
Dry skin.

Co-dergocrine Tablets *(B.P. 1988)* Codergocrine Mesylate Tablets.

Coderma *(Biotrading, Ital.).*
Fluocinolone acetonide.
Skin disorders.

Codetilina *(Promesa, Spain).*
Cineole; ethylmorphine.
Respiratory-tract disorders.

Codetilina-Eucaliptolo Houdé *(Lirca, Ital.).*
Ethylmorphine hydrochloride; eucalyptus oil.
Coughs.

Codex DNB *(Smith Kline & French, Ital.).*
Saccharomyces boulardii.
Gastro-intestinal disorders.

Codicaps *(Thiemann, Ger.).*
Capsules: Codeine; chlorpheniramine maleate.
Coughs and associated respiratory-tract disorders.

Codicaps *(Thiemann, Ger.).*
Oral liquid: Codeine polistirex; chlorpheniramine polistirex.
Coughs and associated respiratory-tract disorders.

Codicaps B *(Thiemann, Ger.).*
Codeine; chlorpheniramine maleate; bromhexine hydrochloride.
Coughs and associated respiratory-tract disorders.

codicept *(Sanol, Ger.).*
Codeine.
Coughs.

Codiclear DH *(Central Pharmaceuticals, USA).*
Hydrocodone tartrate; guaiphenesin.
Coughs.

Codicompren *(Cascan, Ger.).*
Codeine phosphate hemihydrate.
Coughs.

Codidoxal *(Mack, Illert., Ger.).*
Doxycycline hydrochloride; codeine polistirex.
Coughs associated with infections of the respiratory-tract.

Codimal DH *(Central Pharmaceuticals, USA).*
Hydrocodone tartrate; phenylephrine hydrochloride; mepyramine maleate.
Coughs.

The symbol † denotes a preparation no longer actively marketed

UM00016752
NOVARTIS EXHIBIT 1517
Novartis v. Regents, IPR2023-01347
Page 3734 of 4460

Furo-Puren *(Klinge-Nattermann, Ger.).*
Frusemide.
Oedema; hypertension.

Furorese *(Hexal, Ger.).*
Injection: Frusemide sodium.
Oedema; hypertension.

Furorese *(Hexal, Ger.).*
Tablets: Frusemide.
Oedema; hypertension.

Furosemide Injection *(U.S.P. XXII).*
Frusemide.
Prepared with the aid of sodium hydroxide.

Furosemide Tablets *(U.S.P. XXII).*
Frusemide.

Furospir *(Mepha, Switz.).*
Spironolactone; frusemide.
Oedema.

Furotricina *(Biomedica, Ital.).*
Tyrothricin; nitrofurazone.
Gynaecological infections.

Furoxone *(Norwich Eaton, Austral.).*
Furazolidone.
Infective diarrhoea.

Furoxone *(Formenti, Ital.).*
Furazolidone.
Intestinal infections.

Furoxone *(SmithKline Beecham, S.Afr.).*
Furazolidone.
Gastro-intestinal infections.

Furoxone *(Procter & Gamble, USA).*
Furazolidone.

Furunkulosin *(Diaberylin, Ger.).*
Faex medicinalis.
Skin disorders.

Fusaloyos *(Servier, Spain).*
Fusafungine.
Upper-respiratory-tract inflammation.

Fusid *(Winthrop, Ger.).*
Frusemide.
Oedema; hypertension.

Fusid *(ICN, Neth.).*
Frusemide.
Oedema; hypertension.

Fusidic Acid Oral Suspension *(B.P. 1988)* Fusidic Acid Mixture.

Futraful *(Taiho, Jpn).*
Tegafur.
Malignant neoplasms.

Futura *(Farmacologico Milanese, Ital.).*
Aspartame.
Sugar substitute.

Fybogel *(Reckitt & Colman, Austral.).*
Ispaghula husk.
Dietary fibre supplement.

Fybogel *(Reckitt, Eire).*
Ispaghula husk.
Diverticular disease; spastic and irritable colon; constipation.

Fybogel *(Reckitt & Colman, S.Afr.).*
Ispaghula husk.
Bowel disorders.

Fybogel *(Reckitt & Colman Pharmaceuticals, UK).*
Ispaghula husk.
Constipation.

Fybranta *(Norgine, UK).*
Bran.
Constipation.

Fynnon Calcium Aspirin *(SmithKline Beecham, UK).*
Aspirin; calcium carbonate.
Pain; fever.

Fysioquens *(Nourypharma, Neth.).*
7 Tablets, ethinyloestradiol; 15 tablets, ethinyloestradiol; lynoestrenol.
Biphasic oral contraceptive; dysmenorrhoea.

G-1 *(Hauck, USA).*
Paracetamol; butalbital; caffeine.

G 1000 Record *(Pierrel, Ital.).*
Carbohydrate, multivitamin, and mineral preparation.

G Tril *(Vinas, Spain).*
Febarbamate.
Agitation; tremor; insomnia; alcohol withdrawal.

Gabacet *(Carrion, Fr.).*
Piracetam.
Cerebral vascular disorders.

Gabakalm *(Contassium Co., UK).*
Gamma aminobutyric acid; vitamins; minerals.

Gabbroral *(Carlo Erba, Ital.).*
Paromomycin sulphate.
Bacterial infections.

Gabomade† *(Knoll, Spain).*
Aminohydroxybutyric acid.
Emotional disorders; behaviour disorders; convulsions.

Gaboril Complex *(Sigma-Tau, Spain).*
Phenytoin; phenobarbitone; aminohydroxybutyric acid.
Epilepsy.

Gaboril Sedativo† *(Sigma-Tau, Spain).*
Crataegus; aminohydroxybutyric acid; passion flower; matricaria; valerian.
Anxiety; sleep disorders.

Gabrene *(Synthelabo, Fr.).*
Progabide.
Epilepsy.

Gabroral *(Farmitalia, Spain).*
Paromomycin sulphate.
Gastro-intestinal bacterial infections; gastro-intestinal amoebiasis; tapeworm infections.

Gadional *(Cinfa, Spain).*
Phosphoric acid; cod-liver oil; minerals; calcium pantothenate; gentian; fenugreek.
Tonic.

Gafir *(Biotekfarma, Ital.).*
Niperotidine hydrochloride.
Gastro-intestinal disorders.

Gaiarsol *(Chanteaud, Fr.).*
Methylarsinic acid; guaiacol; aconite root; codeine; tolu balsam.
Coughs.

Galactogil *(Elgi, Fr.).*
Galega; tricalcium diphosphate; malt extract.
Insufficient milk production in lactating mothers.

Galactomin *(Cow & Gate, UK).*
Food for special diets.
Lactose, glucose, or galactose intolerance.

Galactomin-17 *(Medifood-Trufood, Ital.).*
Food for special diets.
Lactose intolerance.

Galactoquin *(Mundipharma, Ger.).*
Quinidine polygalacturonate.
Arrhythmias.

Galake *(Galen, UK).*
Dihydrocodeine tartrate; paracetamol.

Galantase *(Tokyo Tanabe, Jpn).*
Tilactase.
Lactose intolerance.

Galantase *(Noristan, S.Afr.).*
Tilactase.
Lactose intolerance.

Galcodine *(Galen, UK).*
Codeine phosphate.
Dry coughs.

Galenamet *(Galen, UK).*
Cimetidine.

Galenamox *(Galen, UK).*
Amoxycillin trihydrate.
Bacterial infections.

Galenavowen-N† *(Vogel & Weber, Ger.).*
Tablets: Cort. syzygii jamb.; fel tauri; fol. boldo; fruct. ammi visn.; fruct. cardui mariae; herb. cynarae; herb. hyperici; rhiz. curcumae.
Gastro-intestinal disorders.

Galenavowen-N *(Weber & Weber, Ger.).*
Oral drops: Ammi visnaga; boldo; curcuma long.; cynara scolymus; frangula; syzygium jambolanum.
Homoeopathic preparation.

Galénic *(Galenic, Fr.).*
Ruscus aculeatus; dextran sulphate; melilot.
Peripheral vascular disorders.

Galenphol *(Galen, UK).*
Pholcodine.
Coughs.
Formerly known as Galphol.

Galfer *(Galen, UK).*
Ferrous fumarate.
Iron-deficiency anaemia.

Galfer F.A. *(Galen, UK).*
Ferrous fumarate; folic acid.
Iron and folic acid deficiency in pregnancy.

Galfer-Vit *(Galen, UK).*
Ferrous fumarate; vitamin B and C substances.
Iron deficiency.

Galfloxin *(Galen, UK).*
Flucloxacillin.

Galirène *(Merck-Clevenot, Fr.).*
Calcium bromide; calcium lactate pentahydrate.
Insomnia; nervous disorders.

Galium Complex *(Blackmores, Austral.).*
Galium aparine; echinacea angustifolia; calendula officinalis; baptisia tinctoria; ascorbic acid; calcium pantothenate; pyridoxine hydrochloride; zinc amino acid chelate.
Tonic.

Gallamine Injection *(B.P. 1988).*
Gallamine triethiodide.

Gallamine Triethiodide Injection *(U.S.P. XXII).*

Gallcusan (Röwo-29) *(Pharmakon, Ger.).*
Cholesterinum; terebinthina chios; berberis; anagallis arvensis; carduus marianus; china; aesculus; leptandra; podophyllum; chelidonium; nux vomica; belladonna.
Homoeopathic preparation.

Galleb *(Hoyer, Ger.).*
Tinct. herb. chelidonii; tinct. rhiz. curcumae xanth.; tinct. rad. rubiae tinct.; tinct. sem. cardui mariae; tinct. fol. menthae pip.; tinct. rad. taraxaci c. herb.; tinct. rad. echinaceae purpur.; tinct. cort. frangulae.
Biliary disorders; post-hepatitis syndrome.

Galleb forte† *(Hoyer, Ger.).*
Herb. chelidonii; rad. rubiae tinct.; rhiz. curcumae xanth.; herb. virgaureae; fruct. ammeos visnagae; rad. taraxaci c. herb.; rad. echinaceae purpur.; fol. menthae pip.; fruct. cardui mariae; cort. frangulae; aescin.
Biliary disorders.

Gallemolan N *(Redel, Ger.).*
Herb. chelidon.; herb. absinth.; fol. boldo; rad. taraxaci c. herba; rhiz. rhei; flor. chamomillae; fel tauri.
Biliary disorders; gall stones; liver disorders.

Gallen-Leber-Tee Stada *(Stada, Ger.).*
Flor. calendulae; flor. calcatrippae; rad. gentianae; fruct. foeniculi; fruct. carvi; flor. chamomillae; rad. ononidis; cort. frangulae; herb. chelidonii; fol. menth. pip.; rad. taraxac. c. herb.; ol. carvi.
Herbal tea.

Gallensteinkapseln *(Evers, Ger.).*
Herb. hederae terrestr.
Gall stones.

Gallexier *(Salushaus, Ger.).*
Tablets: Rhiz. curcumae xanthor.; fol. cynarae scolym.; fruct. cardui mariae; rad. taraxaci c. herb.; flor. chamomillae; fol. menthae pip.
Biliary disorders.

Gallexier *(Salushaus, Ger.).*
Tea: Fol. cynarae scolym.; herb. taraxaci; rhiz. curcumae xanth.; fruct. cardui mariae; herb. cardui benedicti; fol. trifolii fibrini; herb. millefolii; rad. gentianae; herb. absinthii; rhiz. calami; flor. chamomillae; fruct. foeniculi; fructose.
Herbal tea.

Galliagène T.C.M. *(Gallia, Fr.).*
Infant feed; food for special diets.
Milk-protein intolerance; malabsorption syndromes.

Gallialite *(Gallia, Fr.).*
Glucose; potassium citrate; sodium bicarbonate; sodium chloride; potassium chloride; magnesium sulphate; calcium chloride.
Diarrhoea; oral rehydration.

Gallieva *(Gallia, Fr.).*
Infant feed; food for special diets.
Milk-protein intolerance.

Gallitophen *(Reinecke, Ger.).*
Herb. burs. past.; cort. frangul.; follic. sennae angust.; fol. betul.; herb. chelidon.; herb. equiset.; herb. card. bened.; fruct. card. mar.; flor. chamomill.; herb. nasturt.; rad. et herb. taraxac.; herb. eschscholtziae calif.; fel tauri; berberis; card. mar.; ol. menth. pip.
Biliary disorders; liver disorders.

Gallium Citrate Ga 67 Injection *(U.S.P. XXII).*
Gallium-67 in the form of gallium citrate.

Gallium(^{67}Ga) Citrate Injection *(B.P. 1988).*
Gallium-67 in the form of gallium citrate.

gallo sanol N *(Sanol, Ger.).*
Fel tauri; cort. frangulae; aloes.
Biliary disorders; post-hepatitis convalescence.

Gallolingual *(Pohl, Ger.).*
Ethaverine hydrochloride; glyceryl trinitrate.
Smooth muscle spasms.

Gallo-Merz N *(Merz, Ger.).*
Dimethicone; rhiz. curcumae.
Gastro-intestinal disorders.

Gallo-Merz Spasmolyticum† *(Merz, Ger.).*
Ethaverine hydrochloride; dehydrocholic acid; pancreatin; cellulase; dimethicone; rhiz. curcumae.
Biliary disorders; gastro-intestinal spasm.

Gallopas *(Pascoe, Ger.).*
Chelidonium majus.
Gastro-intestinal and biliary-tract disorders.

Galloselect *(Dreluso, Ger.).*
Chamomilla; carduus marianus; lycopodium; menth. pip.; chelidonium; belladonna; natrium sulfuricum; taraxacum.
Homoeopathic preparation.

Galloselect N *(Dreluso, Ger.).*
Herb. chelidonii; herba et rad. taraxaci; fruct. cardui mariae; rhei; fol. cynarae; flor. chamomillae; ol. menthae pip.; ol. carvi.
Biliary disorders; adjunct in chronic liver inflammation.

Galloway's Cough Syrup *(LRC Products, UK).*
Ipecacuanha liquid extract; squill vinegar; acetic acid; chloroform; ether.
Coughs.

Galpseud *(Galen, UK).*
Pseudoephedrine hydrochloride.
Nasal congestion.

Galpseud Plus *(Galen, UK).*
Pseudoephedrine hydrochloride; chlorpheniramine maleate.
Allergic rhinitis.

Galusan *(Almirall, Spain).*
Pipemidic acid.
Urinary-tract infections.

Gamadiabet† *(Salvat, Spain).*
Acetohexamide.
Diabetes mellitus.

Gamalate B6 *(Novag, Spain).*
Aminobutyric acid; aminohydroxybutyric acid; magnesium glutamate hydrobromide; pyridoxine.
Mental function impairment; senility.

Gamanil *(E. Merck, UK).*
Lofepramine hydrochloride.
Depression.

Gamastan *(Cutter, Canad.).*
A normal immunoglobulin.
Passive immunisation.

Gamastan *(Cutter, USA).*
A normal immunoglobulin.

UM00016753
NOVARTIS EXHIBIT 1517
Novartis v. Regents, IPR2023-01347
Page 3735 of 4460

CLINICAL THERAPEUTICS®/VOL. 19, NO. 6, 1997

Topiramate: A Review of Preclinical, Pharmacokinetic, and Clinical Data

William E. Rosenfeld, MD

The Comprehensive Epilepsy Care Center for Children and Adults, St. Louis, Missouri

ABSTRACT

The antiepileptic drug (AED) topiramate is a monosaccharide derivative with a sulfamate functionality. It modulates voltage-dependent sodium conductance, potentiates gamma-aminobutyric acid–evoked currents, and blocks the kainate/AMPA (α-amino-3-hydroxy-5-methylisoxazole-4-propionic acid) subtype of the glutamate receptor. Topiramate is rapidly absorbed and has linear, proportional, steady-state pharmacokinetics. It has no known clinically significant effect on plasma levels of carbamazepine, valproic acid, or phenobarbital, although it may increase plasma concentrations of phenytoin in some patients. When topiramate is used with hepatic enzyme–inducing AEDs, its plasma concentrations are approximately 50% lower than when it is administered alone. The efficacy of topiramate 200 to 1000 mg/d administered in two divided doses as adjunctive therapy for partial-onset seizures was investigated in five double-masked, placebo-controlled trials. The median percentage reduction in average monthly seizure frequency from baseline was 12% for placebo, compared with 30% for the 200-mg/d group and 48% for the 400-mg/d group. At a dosage of 400 mg/d, a seizure reduction of 75% or greater was seen in 22% of topiramate patients, compared with 7% of those receiving placebo; up to 9% of topiramate patients, compared with none of those receiving placebo, became seizure free. Although little additional efficacy was seen at dosages of 600, 800, and 1000 mg/d, dosing should be individualized, because some patients may respond to higher dosages. When topiramate is combined with other AEDs, the most common side effects at dosages of 200 to 400 mg/d are somnolence, dizziness, ataxia, psychomotor slowing, hesitant speech, and word-finding difficulties. Most patients who experienced adverse events during the first 8 weeks of the trials no longer experienced them by their last visit. Although

0149-2918/97/$3.50

UM00016754
NOVARTIS EXHIBIT 1517
Novartis v. Regents, IPR2023-01347
Page 3736 of 4460

there was a 1.5% incidence of renal stones that may be associated with carbonic anhydrase inhibition, more than 75% of patients experiencing a stone continued on therapy. ***Key words:*** antiepileptic drug, partial-onset seizure, pharmacokinetics, topiramate.

INTRODUCTION

The compelling need for more effective and less toxic antiepileptic drugs (AEDs) is underscored by the striking statistic that combination therapy with currently available medications does not completely control seizures in as many as 25% of patients with partial epilepsy.[1] Worldwide, perhaps 12.5 million of the 50 million people with epilepsy require two or more AEDs and still have less than total seizure control.[1] Such polytherapy is often complicated by pharmacokinetic interactions and side effects. Even patients who are seizure free with monotherapy frequently experience acute and chronic central nervous system (CNS) side effects and idiosyncratic reactions. New AEDs with greater efficacy, less toxicity (better risk-benefit ratios), and a defined mechanism of action are needed to provide rational therapeutic alternatives.

Topiramate* is a structurally novel AED indicated as add-on therapy for patients with partial-onset seizures. The structure of topiramate (2,3:4,5-bis-*O*-(1-methylethylidene)-ß-D-fructopyranose sulfamate), a monosaccharide derivative with a sulfamate functionality ($-OSO_2NH_2$), distinguishes it from other antiepileptic agents (Figure 1).[2] The drug's anticonvulsant effects, discovered in a screening protocol using the standard maximal electroshock seizure (MES) test, are similar to those of phenytoin and carbamazepine, although in animal studies, topiramate was found to be less toxic in relation to its efficacy.[3]

This comprehensive review of the topiramate literature summarizes the data from preclinical, pharmacokinetic, and clinical studies.

MECHANISM OF ACTION

Several pharmacologic properties of topiramate that may contribute to its anticonvulsant activity have been detected in cultured neurons. Specifically, three potential mechanisms of action have been identified. First, topiramate enhances gamma-aminobutyric acid type A ($GABA_A$) receptor–mediated Cl^- flux in cultured cerebellar granule cells.[4] While similar to that of the benzodiazepines, this effect is not blocked by the benzodiazepine antagonist flumazenil. White et al[5] have suggested that topiramate potentiates GABA-evoked currents through a novel interaction with the $GABA_A$ receptor ionophore.[5] These actions suggest that topiramate potentiates the activity of the inhibitory neurotransmitter, GABA. Unlike barbiturates that modulate $GABA_A$ receptors, topiramate does not increase the duration of the channel open time.

Second, topiramate modulates the voltage-dependent sodium conductance that generates action potentials, an effect also demonstrated with phenytoin and lamotrigine. This activity of topiramate is substantiated by the observation of Sombati et al[6] that reversible reductions in sustained repetitive firing and reversible decreases in epileptiform activity occur with topiramate

*Topamax® (Ortho-McNeil Pharmaceutical, Inc., Raritan, New Jersey).

UM00016755
NOVARTIS EXHIBIT 1517
Novartis v. Regents, IPR2023-01347
Page 3737 of 4460

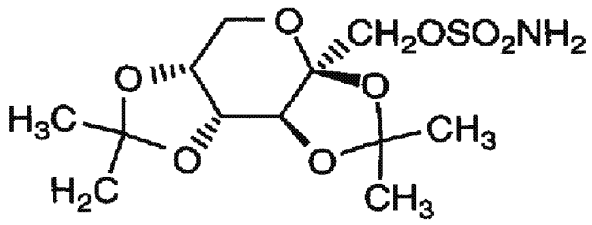

Figure 1. The chemical structure of topiramate.

at concentrations ranging from 10 to 100 μm (a range overlapping that of the free serum topiramate levels seen in patients).

Finally, topiramate has been shown to block kainate-evoked current in perforated-patch whole-cell voltage-clamp studies,[7] indicating that topiramate has antagonistic effects on glutaminate receptors of the kainate/AMPA (α-amino-3-hydroxy-5-methylisoxazole-4-propionic acid) subtype. Topiramate had essentially no effect on the activity of glutamate receptors of the NMDA (N-methyl-D-aspartate) subtype. Blockade of kainate-evoked currents is a known mechanism by which neuronal excitability can be decreased.

PRECLINICAL PHARMACOLOGY

Topiramate displayed potent and long-lasting anticonvulsant activity when evaluated using the MES test in rodents, with an oral median effective dose of 47.6 mg/kg in the mouse and 15.8 mg/kg in the rat.[8] The ability of a drug to prevent seizures during the MES test is generally accepted as correlating positively with its ability to prevent partial and secondarily generalized seizures in humans.[9] Topiramate is weakly effective in blocking clonic seizures induced by the GABA receptor antagonist pentylenetetrazol but is inactive in blocking seizures induced by picrotoxin and bicuculline.[9] Topiramate is effective in several other rodent models of epilepsy, including tonic and absence-like seizures in the spontaneously epileptic rat and tonic and clonic seizures in rats induced by kindling of the amygdala or by global ischemia.[10]

CLINICAL PHARMACOKINETICS

In humans, the pharmacokinetics of topiramate have been studied in both a single-dose study[11] and a multiple-dose study[12] (Table I[13]).

Absorption

In the single-dose study, in which healthy subjects received oral doses ranging from 100 to 1200 mg, topiramate was rapidly absorbed, with most subjects achieving levels of more than 90% of the maximum concentration (C_{max}) within 2 hours.[11] Over this dose range, topiramate showed linear but nonproportional kinetics for both C_{max} and area under the curve (AUC). In the multiple-dose study conducted in healthy volunteers, topiramate had predictable, linear, proportional steady-state pharmacokinetics at dosages up to 800 mg/d.[12] The bioavailability of topiramate is 80%. When it is adminis-

UM00016756
NOVARTIS EXHIBIT 1517
Novartis v. Regents, IPR2023-01347
Page 3738 of 4460

Table I. Pharmacokinetic characteristics of topiramate.

Characteristic	Value
Elimination half-life (h)	19–23
Peak plasma concentration (mg/L)	1.7 (100-mg single dose) 7.7 (400-mg single dose) 28.7 (1200-mg single dose)
Time to maximum concentration (h)	1.8–4.3
Fraction of systemically available drug excreted unchanged into the urine (%)	70–97
Apparent oral clearance (mL/min)	22–36
Apparent volume of distribution (L/kg)	0.6–0.8
Unbound fraction of drug in plasma (%)	Predominantly unbound

Adapted with permission from Bialer.[13]

tered with food, the rate of absorption is slowed moderately, but the extent of absorption is not affected.[14]

Distribution

In healthy volunteers, the apparent volume of distribution of topiramate is 0.6 to 0.8 L/kg. Topiramate is 13% to 17% bound to plasma proteins. It exhibits saturable low-capacity binding to erythrocytes; however, with multiple dosing, binding sites are saturated and this is no longer of clinical concern. Topiramate appears to readily cross the blood-brain barrier. The excretion of topiramate in human milk has not been studied.

Metabolism

Topiramate is not extensively metabolized. Approximately 70% of an administered dose is eliminated unchanged in the urine. Six inactive metabolites, formed via hydroxylation, hydrolysis, and glucuronidation, have been identified.

Excretion

The kidney is the major route of elimination of unchanged topiramate and its metabolites. Topiramate plasma clearance is 20 to 30 mL/min, and the mean elimination half-life is 21 hours. The mechanism of renal elimination of topiramate may involve kidney tubular reabsorption.

Special Populations

Renal Impairment

The clearance of topiramate is decreased and the elimination half-life prolonged in persons with renal impairment, as shown in a study comparing the pharmacokinetics of a single 100-mg oral dose of topiramate in adults with moderate-to-severe renal impairment (creatinine clearance <30 mL/min) with the pharmacokinetics of the same dose in adults with normal renal function.[15] Topiramate plasma concentrations fall by an average of 50.1% during hemodialysis. The mean hemodialysis plasma clearance of topira-

UM00016757
NOVARTIS EXHIBIT 1517
Novartis v. Regents, IPR2023-01347
Page 3739 of 4460

mate has been reported to be approximately nine times higher than that found in subjects not receiving hemodialysis.[16]

Hepatic Impairment

Hepatic disease appears to have minimal effects on the pharmacokinetics of topiramate. In subjects with moderate-to-severe liver disease, plasma concentrations of topiramate were increased by 29%, and plasma clearance was reduced by 26% compared with healthy volunteers.[10]

Pediatric Subjects

Topiramate pharmacokinetics in children versus adults was evaluated in 18 children (4 to 17 years of age) with epilepsy who were receiving one AED or two concomitant AEDs.[17] Topiramate was titrated over 4 weeks to 1, 3, 6, and 9 mg/kg per day. Results showed that topiramate pharmacokinetics were linear, with clearance independent of dose and steady-state plasma levels increasing in proportion to dosage. Topiramate clearance was higher for subjects receiving concomitant enzyme-inducing AEDs (grand mean = 71.1 mL/min per 70 kg) than for subjects not receiving concomitant enzyme-inducing AEDs (grand mean = 32.2 mL/min per 70 kg). Comparison to historical data from subjects with epilepsy indicates that mean topiramate plasma clearance is approximately 50% higher in children. Steady-state plasma topiramate concentrations for the same milligram-per-kilogram dose are expected to be approximately 33% lower in children than in adults.

DRUG INTERACTION STUDIES

Studies comparing the steady-state pharmacokinetics of topiramate with the most commonly prescribed AEDs—carbamazepine, phenytoin, and valproic acid—had similar designs, as shown in Figure 2. This design allowed the sequential evaluation of the topiramate steady-state pharmacokinetics as both adjunctive therapy and monotherapy. The interactions of topiramate with these AEDs and with digoxin, norethindrone–ethinyl estradiol, and CNS depressants are discussed in the sections that follow.

Topiramate and Carbamazepine

The steady-state pharmacokinetics of carbamazepine and topiramate as adjunctive therapy and monotherapy were determined in 12 adults whose epilepsy was stabilized with carbamazepine 300 to 800 mg TID.[18] No significant differences were observed in the pharmacokinetics of total or unbound carbamazepine or carbamazepine epoxide in the absence of topiramate or with topiramate 100 to 400 mg BID. Topiramate AUC, C_{max}, average concentration, and minimum concentration levels were approximately 40% lower in the presence of carbamazepine than with topiramate monotherapy.

Topiramate and Phenytoin

The steady-state pharmacokinetics of phenytoin and topiramate were determined in 12 adults with partial epilepsy who were stabilized on phenytoin.[19] During concomitant phenytoin therapy, topiramate pharmacokinetics were proportional for dosages ranging from 100 to 400 mg BID. During topiramate adjunctive therapy with phenytoin, topiramate concentrations were reduced by approximately 50%. The investigators hypothesized that the increase in topiramate clearance during concomitant phenytoin therapy was due to enzyme

UM00016758
NOVARTIS EXHIBIT 1517
Novartis v. Regents, IPR2023-01347
Page 3740 of 4460

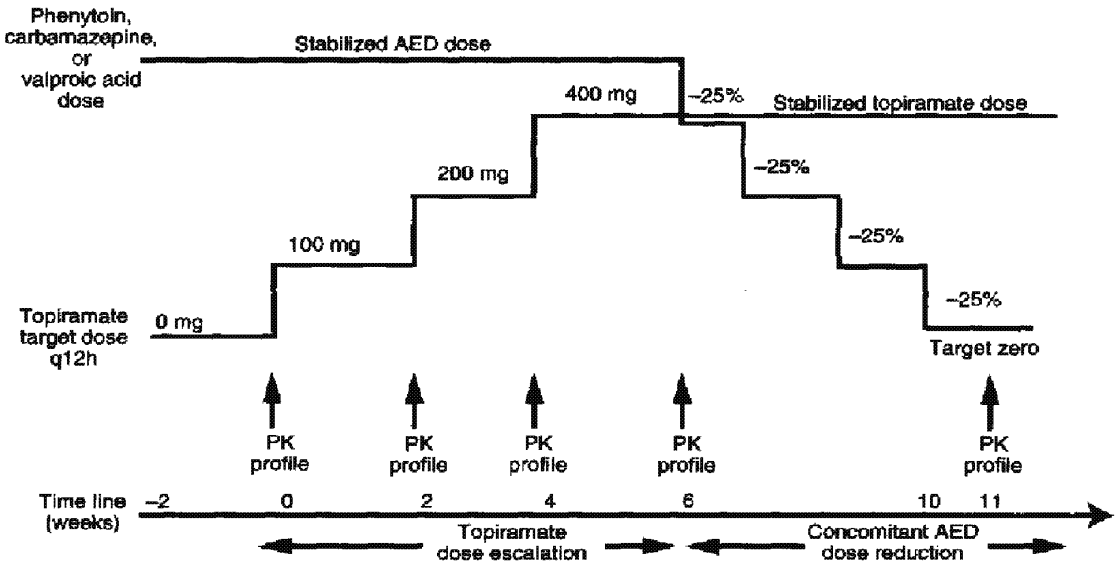

Figure 2. Pharmacokinetic interaction of topiramate with existing antiepileptic drugs (AEDs). PK = pharmacokinetic. All studies included 12 patients with epilepsy for each AED.

induction by phenytoin. In half the patients, topiramate had no measurable effect on the pharmacokinetics of phenytoin; in the other patients, however, particularly those taking phenytoin twice a day, phenytoin concentrations were approximately 25% higher. No patients required a dosage adjustment of phenytoin or discontinued the trial. In clinical practice, patients receiving dosages in the higher therapeutic ranges of phenytoin should be observed carefully, because they may be more likely to require a downward adjustment of phenytoin dosage.

Topiramate and Valproic Acid

The steady-state pharmacokinetics of valproic acid and topiramate were determined in 12 patients whose partial epilepsy was treated with valproic acid.[20] Topiramate plasma concentrations were approximately 14% lower during adjunctive therapy with valproic acid. Valproic acid concentrations decreased by 11% when topiramate 400 mg BID was added. The clinical significance of these changes is unknown but is probably minimal.

Topiramate and Digoxin

The effect of topiramate on the pharmacokinetics of a single oral dose of digoxin was evaluated by Liao and Palmer.[21] Peak plasma concentrations of digoxin decreased by approximately 12%. The clinical relevance of this interaction has not been established.

Topiramate and Norethindrone–Ethinyl Estradiol

The pharmacokinetic interaction between topiramate and norethindrone–

UM00016759
NOVARTIS EXHIBIT 1517
Novartis v. Regents, IPR2023-01347
Page 3741 of 4460

ethinyl estradiol was evaluated in 12 women with epilepsy stabilized with valproic acid.[22] Patients received topiramate doses of 200, 400, and 800 mg/d. Although the norethindrone component of the contraceptive was not affected by concomitant administration of topiramate, the mean serum estradiol AUC was reduced by 18%, 21%, and 30% for the three topiramate doses. Patients should be instructed to report abnormal bleeding patterns.

Topiramate and Central Nervous System Depressants

Concomitant administration of topiramate and alcohol or other CNS depressant drugs has not been evaluated. However, because topiramate is a centrally acting drug, caution should be exercised if it is used in combination with CNS depressant drugs.

CLINICAL EVALUATION OF TOPIRAMATE AS ADJUNCTIVE THERAPY IN PATIENTS WITH PARTIAL-ONSET SEIZURES

Five randomized, double-masked, placebo-controlled clinical trials—two in the United States[23,24] and three in Europe[25–27]—have assessed the safety and efficacy of topiramate as adjunctive therapy in adults with partial-onset seizures with or without secondary generalization. Patients who experienced at least four seizures per month while taking one or two AEDs were eligible for the studies. In each study, patients were titrated to a target dosage, even if that was not the optimal dose for the individual patient. The two US studies were dose-ranging studies that evaluated three doses of topiramate in comparison to placebo; a low-dose study by Faught et al[23] evaluated target dosages of 200, 400, and 600 mg/d, and a high-dose study by Privitera et al[24] evaluated dosages of 600, 800, and 1000 mg/d. Each of the three European studies evaluated a single dose of topiramate: 400 mg/d,[25] 600 mg/d,[26] and 800 mg/d.[27] The primary efficacy assessment was the median percentage reduction in seizure rate during the entire double-masked treatment period in relation to baseline. Secondary measures included the percentage of patients with at least a 50%, 75%, or 100% reduction in seizures. Statistical analysis was performed on all patients randomized to a treatment group (Table II).

In the low-dose US study, at a target dose of 400 mg/d, the median percentage reduction in seizure rate was 48%, compared with 12% for placebo. At a target topiramate dosage of 200 mg/d, there was a statistically significant median reduction of 30%, compared with 13% for placebo ($P = 0.051$); this indicates that some patients will see a clinical response at 200 mg/d. As shown in Table II, the response rates in groups receiving target dosages of 600, 800, and 1000 mg/d were not substantially better than the response rate in those receiving a dosage of 400 mg/d; however, in my experience, higher seizure-free rates can be obtained by using higher dosages in some patients. As with all AEDs, there are some patients who will respond best to higher doses, whereas others will respond at lower doses.

In two trials using a dosage of 400 mg/d,[23,25] 35% to 47% of patients achieved a >50% reduction in seizure frequency, compared with 8% to 18% of patients receiving placebo. A considerable number of patients achieved a 75% to 100% reduction in average monthly seizure rate (22% receiving topiramate 400 mg/d and 7% receiving placebo) (see

UM00016760
NOVARTIS EXHIBIT 1517
Novartis v. Regents, IPR2023-01347
Page 3742 of 4460

Table II. Randomized, double-masked, placebo-controlled clinical trials investigating the efficacy of topiramate (TPM) as adjunctive therapy for refractory, partial-onset seizures, showing number of patients, median percentage seizure reduction (MPSR) relative to baseline, and percentage responders (PR) to treatment (≥50% reduction in seizure frequency).

Study	Placebo	TPM 200 mg/d	TPM 400 mg/d	TPM 600 mg/d	TPM 800 mg/d	TPM 1000 mg/d
Faught et al[23]						
No. of patients	45	45	45	46	0	0
MPSR (*P*)	13	30 (0.051)	48 (0.007)	45 (<0.001)	—	—
PR (*P*)	18	27 (0.620)	47 (0.013)	46 (0.027)	—	—
Privitera et al[24]						
No. of patients	47	0	0	48	48	47
MPSR (*P*)	1	—	—	41 (<0.001)	41 (<0.001)	38 (<0.001)
PR (*P*)	9	—	—	44 (<0.001)	40 (0.001)	38 (0.001)
Sharief et al[25]						
No. of patients	24	0	23	0	0	0
MPSR (*P*)	1.1	—	40.7 (0.065)	—	—	—
PR (*P*)	8	—	35 (0.033)	—	—	—
Tassinari et al[26]						
No. of patients	30	0	0	30	0	0
MPSR (*P*)	−12.2	—	—	46.4 (0.004)	—	—
PR (*P*)	10	—	—	47 (0.001)	—	—
Ben-Menachem et al[27]						
No. of patients	28	0	0	0	28	0
MPSR (*P*)	−17.8	—	—	—	35.8 (0.001)	—
PR (*P*)	0	—	—	—	43 (0.001)	—

UM00016761

NOVARTIS EXHIBIT 1517
Novartis v. Regents, IPR2023-01347
Page 3743 of 4460

Table III. Percentage of responders (≥75% and 100% reduction in seizures) at a topiramate dosage of 200 to 400 mg/d as adjunctive therapy.

	≥75% Reduction (%)			100% Reduction (%)		
Study	Placebo	200 mg/d	400 mg/d	Placebo	200 mg/d	400 mg/d
Faught et al[23]	7	9	22	0	0	4
Sharief et al[25]	4	—	22	0	—	9

Table III). In one study,[27] at a dosage of 800 mg/d, 36% of patients had a 75% to 100% reduction in seizures; however, the most important outcome measure for a patient is seizure freedom, and at a dosage of 400 mg/d, up to 9% of patients became seizure free, compared with 0% in the placebo group. Meta-analysis of all five trials, which comprised 534 patients, indicated that the efficacy of topiramate was consistent across trials and across patient strata defined by age, sex, race, and baseline seizure rate.[28]

ADVERSE EVENTS

The safety profile of topiramate is derived from clinical studies involving 1715 patients.[10] Extensive analysis of the safety data compiled in these studies has produced information that should aid the physician and patient in obtaining the best possible result from the use of topiramate.[29]

As with other AEDs and many centrally acting drugs, the most common adverse events reported by patients taking topiramate involved the CNS. In the controlled trials of topiramate as adjunctive therapy to traditional AEDs, the most significant of these events could be divided into two groups: (1) psychomotor slowing, difficulty with concentration, and speech and language problems, and (2) somnolence and fatigue.

Somnolence and fatigue were the most frequently reported adverse events in the clinical trials. Interestingly, fatigue was more common in the placebo group than in subjects receiving topiramate dosages of 200 to 400 mg/d. Psychomotor slowing, difficulty with concentration and speech (eg, hesitancy), and language (eg, word-finding) problems were generally mild to moderate in intensity but occasionally led to discontinuation. Difficulty with concentration and language problems were dose related in the controlled trials.

The original double-masked, placebo-controlled studies were all forced-titration studies that increased each patient's dosage to a target dose, usually at weekly increments of 100 to 200 mg/d. The recommended titration rate (weekly increments of 50 mg/d) is slower and has clearly been associated with improved tolerability.[29,30] If topiramate is titrated too quickly, patients may complain of agitation, anxiety, or nervousness as well as word-finding difficulties. This can be ameliorated by slowing the rate of titration. Reduction in the dose of concomitant AEDs can further decrease side effects. Particularly in patients with high valproic acid levels, reduction of the dose of valproate can im-

UM00016762
NOVARTIS EXHIBIT 1517
Novartis v. Regents, IPR2023-01347
Page 3744 of 4460

prove cognitive side effects. Patients with thrombocytopenia while taking valproate may have a further reduction in platelet count with the addition of topiramate.[20] Platelet counts increase when the valproate dose is reduced. In most cases, side effects are manageable and do not require discontinuation of the drug.

Additional nonspecific CNS effects seen with topiramate include dizziness/imbalance, confusion, memory problems, and exacerbation of mood disturbance (eg, irritability and depression). In the controlled trials, side effects occurred early in therapy; in general, most patients who experienced adverse events during the first 8 weeks of the trials no longer experienced them by their last visit.

Long-term follow-up of patients taking topiramate indicates that the drug generally continues to be well tolerated, with no evidence of tolerance to its antiepileptic effect.[31–33] Dosages used in European studies tend to be lower than those used in US studies (Table IV).

Two adverse events of interest were examined in long-term follow-up studies: renal stones[34] and weight loss.[10] In vitro studies have shown topiramate to be a weak carbonic anhydrase inhibitor. Although this property is not considered a primary mechanism of topiramate's antiepileptic activity,[2] it may be associated with the occasional development of renal calculi. In topiramate-treated patients as well as the general population, risk factors for renal stones include a personal or family history of renal stones, male gender, and concomitant administration of other carbonic anhydrase inhibitors. In clinical trials, 1.5% of patients treated with topiramate developed renal stones, two to four times the incidence expected in a similar untreated population. Of seven stones analyzed,[34] five were composed primarily of calcium phosphate. Despite the development of renal calculi, approximately 24 of 32 (75%) patients with stones elected to continue topiramate therapy. Adequate hydration is recommended to reduce the risk of stone formation.

Weight loss of 1.6 to 6.5 kg was reported[10] in patients during the clinical trials. Patients who weighed most (>100 kg) before topiramate therapy experienced the greatest weight loss (mean weight loss, 9.6 kg) compared with those who weighed least (<60 kg) before topiramate treatment (mean weight loss, 1.3 kg). For patients receiving long-term topiramate therapy, body-weight reductions were most commonly noted during the first 3 months of treatment and peaked at 12 to 18 months. This was partially reversed in some patients who gained weight starting with the second year of therapy.

Another side effect that patients may mention is paresthesia. This adverse effect also appears to be related to the fact that topiramate is a carbonic anhydrase inhibitor. Paresthesia appears to decrease with time or with dosage reduction.

Overdosage

In acute topiramate overdose, if the ingestion is recent, the stomach should be emptied by lavage or induction of emesis. Activated charcoal has not been shown to absorb topiramate. Treatment should be appropriately supportive. Topiramate is removed by dialysis.

DOSING AND ADMINISTRATION

The recommended starting dose of topiramate is 50 mg/d in two divided doses. The

UM00016763
NOVARTIS EXHIBIT 1517
Novartis v. Regents, IPR2023-01347
Page 3745 of 4460

Table IV. Long-term efficacy of topiramate in patients with refractory partial-onset seizures: Patients entering open extensions of double-masked clinical trials or independent open-label studies.

Patient Characteristics	Fincham and Schottelius[31]	Privitera[32]	Ben-Menachem[33]
No. of patients entering study	16	27	24
No. of patients remaining in study at last follow-up	13	17	11
Time in study at last follow-up	Mean: 76.2 mo Range: 60–83 mo	24 mo	7 patients: 5 y 4 patients: 2 y
Average daily dose at last follow-up	761 mg	Not reported	295 mg
Seizure status at last follow-up	All patients had decreased seizure frequency from prestudy baseline. Mean: 14.9/mo Range: 0.9–135/mo	Ten patients had >50% seizure reduction from prestudy baseline.	There was a 57% mean seizure reduction from baseline.
Reasons for study discontinuation	Felt less comfortable on topiramate (1), moved (1), decided to try surgery (1).	No patient dropped out because of loss of seizure control only.	Lack of efficacy (6), adverse effects (8); 1 discontinued for both reasons.

UM00016764

NOVARTIS EXHIBIT 1517
Novartis v. Regents, IPR2023-01347
Page 3746 of 4460

drug can then be titrated to an effective dose at weekly increments of 50 mg/d in two divided doses. The maintenance dosage of topiramate is generally 200 to 400 mg/d. In some patients an even slower titration rate may be advantageous, for instance starting with 25 mg BID for 2 weeks, increasing to 50 mg BID for 2 weeks, and then increasing by 100 mg/wk. After 6 to 8 weeks, the dosage can usually be titrated above 400 mg/d with few side effects. Topiramate should be used in the same manner as any AED and titrated to the most effective dose that is well tolerated by the patient.[35] Daily doses above 1600 mg/d have not been studied. Topiramate can be taken with or without food. Tablets should not be cut but can be crushed.

Clinicians should be aware that when topiramate is added to phenytoin, an adjustment in the dosage of phenytoin may be necessary to achieve optimal clinical outcome. When discontinuing a hepatic enzyme–inducing drug from a regimen including topiramate, reduction of the topiramate dosage may be necessary. Higher topiramate levels at the same dosage can be obtained by reducing the dosage of a concomitant hepatic enzyme–inducing agent.

Half the usual adult dose is recommended in renally impaired patients (creatinine clearance <70 mL/min per 1.73 m^2).[13] Furthermore, it has been established that patients with epilepsy who are undergoing hemodialysis for end-stage renal failure should receive supplemental doses of topiramate.[16] In patients with hepatic impairment, topiramate clearance may be decreased.

Plasma concentrations of topiramate do not correlate with seizure reduction. Therefore, monitoring these concentrations is not necessary for optimal therapy. No special laboratory monitoring is necessary during topiramate therapy. As with any new AED, appropriate baseline laboratory testing should be conducted.

CONCLUSIONS

The antiepileptic properties of topiramate have been confirmed in five double-masked, placebo-controlled clinical trials that evaluated the safety and efficacy of this drug as adjunctive therapy for partial seizures. More topiramate-treated patients than placebo-treated patients had a 75% reduction in seizure rate or became seizure free. The results of open-label studies that included patients who had been treated with topiramate for up to 7 years indicate that topiramate appears to be safe and effective for long-term use. A brief review of comparable trials by Faught et al[23] evaluating topiramate, gabapentin, and lamotrigine suggests that topiramate is the most effective.

Most of the adverse effects associated with topiramate have been CNS effects such as dizziness, somnolence, and psychomotor slowing. Current data suggest that the adverse effects of topiramate generally resolve over time and may be related to how quickly the starting dosage of topiramate is increased to the optimal level.

Clinical trials have shown that the use of topiramate is very much like that of other AEDs. Therapy should be tailored to the individual patient's response. Once patients are stabilized and have achieved maximal seizure control, topiramate may be a low-maintenance form of long-term therapy.

Address correspondence to: William E. Rosenfeld, MD, The Comprehensive Epilepsy Care Center for Children and Adults, 222 S. Woods Mill Road, Suite 610, St. Louis, MO 63017.

UM00016765
NOVARTIS EXHIBIT 1517
Novartis v. Regents, IPR2023-01347
Page 3747 of 4460

REFERENCES

1. Rogawski MA, Porter RJ. Antiepileptic drugs: Pharmacological mechanisms and clinical efficacy with consideration of promising developmental stage compounds. *Pharmacol Rev.* 1990;42:223–286.

2. Maryanoff BE, Nortoy SO, Gardocki JF, et al. Anticonvulsant O-alkyl sulfamates. 2,3:4,5-Bis-*O*-(1-methylethylidene)-ß-D-fructopyranose sulfamate and related compounds. *J Med Chem.* 1987;30:880–887.

3. Patsalos PN, Sander JWAS. Newer antiepileptic drugs: Towards an improved risk-benefit ratio. *Drug Saf.* 1994;11: 37–67.

4. Brown SD, Wolf HH, Swinyard EA, et al. The novel anticonvulsant topiramate enhances GABA-mediated chloride flux. *Epilepsia.* 1993;34(Suppl 2):122. Abstract.

5. White HS, Brown SD, Skeen GA, Twyman RE. The investigational anticonvulsant topiramate potentiates GABA-evoked currents in mouse cortical neurons. *Epilepsia.* 1995;36(Suppl 4):34. Abstract.

6. Sombati S, Coulter DA, DeLorenzo RJ. Effects of topiramate on sustained repetitive firing and low $Mg2^{+}$-induced seizure discharges in cultured hippocampal neurons. *Epilepsia.* 1995;36(Suppl 4):38. Abstract.

7. Severt L, Coulter DA, Sombati S, DeLorenzo RJ. Topiramate selectively blocks kainate currents in cultured hippocampal neurons. *Epilepsia.* 1995;36(Suppl 4):38. Abstract.

8. Shank RP, Gardocki JF, Vaught JL, et al. Topiramate: Preclinical evaluation of a structurally novel anticonvulsant. *Epilepsia.* 1994;35:450–460.

9. Harden CL. New antiepileptic drugs. *Neurology.* 1994;44:787–795.

10. Data on file, Robert Wood Johnson Pharmaceutical Research Institute.

11. Easterling DE, Zakszewski T, Moyer MD, et al. Plasma pharmacokinetics in topiramate, a new anticonvulsant, in humans. *Epilepsia.* 1988;29:662. Abstract.

12. Doose DR, Scott VV, Margul BL, et al. Multiple-dose pharmacokinetics of topiramate in healthy male subjects. *Epilepsia.* 1988;29:662. Abstract.

13. Bialer M. Comparative pharmacokinetics of the newer antiepileptic drugs. *Clin Pharmacokinet.* 1993;24:441–452.

14. Doose DR, Gisclon LG, Stellar SM, et al. The effect of food on the bioavailability of topiramate from 100-mg and 400-mg tablets in healthy male volunteers. *Epilepsia.* 1992;33(Suppl 3):105. Abstract.

15. Gisclon LG, Riffitts JM, Sica DA, et al. The pharmacokinetics (PK) of topiramate (T) in subjects with renal impairment (RI) as compared to matched subjects with normal renal function (NRF). *Pharm Res.* 1993;10(Suppl 10):S-397. Abstract.

16. Gisclon LG, Curtin CR, Sica DA, et al. The pharmacokinetics (PK) of topiramate (T) in subjects with end-stage renal disease undergoing hemodialysis. *Clin Pharmacol Ther.* 1994;55:196. Abstract PIII-56.

17. Rosenfeld WE, Doose DR, Walker SA, Reife RA. The steady-state pharmacokinetics of topiramate as adjunctive therapy

UM00016766
NOVARTIS EXHIBIT 1517
Novartis v. Regents, IPR2023-01347
Page 3748 of 4460

in pediatric subjects with epilepsy. *Epilepsia.* 1995;36(Suppl 3):S158. Abstract.

18. Sachdeo RC, Sachdeo SK, Walker SA, et al. Steady-state pharmacokinetics of topiramate and carbamazepine in patients with epilepsy during monotherapy and concomitant therapy. *Epilepsia.* 1996;37: 774–780.

19. Gisclon LG, Curtin CR, Kramer LD. The steady-state pharmacokinetics of phenytoin (Dilantin Kapseals® brand) and of Topamax® (topiramate) in male and female epileptic patients on monotherapy, and during combination therapy. *Epilepsia.* 1994;35(Suppl 8):54. Abstract.

20. Rosenfeld WE, Liao S, Kramer LD, et al. Comparison of the steady-state pharmacokinetics of topiramate and valproate in patients with epilepsy during monotherapy and concomitant therapy. *Epilepsia.* 1997; 38:324–333.

21. Liao S, Palmer M. Digoxin and topiramate drug interaction study in male volunteers. *Pharm Res.* 1993;10(Suppl): S405. Abstract PPDM 8425.

22. Rosenfeld WE, Doose DR, Walker SA, Nayak RK. Effect of topiramate on the pharmacokinetics of an oral contraceptive containing norethindrone and ethinyl estradiol in patients with epilepsy. *Epilepsia.* 1997;38:317–323.

23. Faught E, Wilder BJ, Ramsay RE, and the Topiramate YD Study Group. Topiramate placebo-controlled dose-ranging trial in refractory partial epilepsy using 200, 400 and 600 mg daily dosages. *Neurology.* 1996;46:1684–1690.

24. Privitera M, Fincham R, Penry J, and the Topiramate YE Study Group. Topiramate placebo-controlled dose-ranging trial in refractory partial epilepsy using 600, 800 and 1000 mg daily dosages. *Neurology.* 1996;46:1678–1683.

25. Sharief M, Viteri C, Ben-Menachem E, et al. Double-blind, placebo-controlled study of topiramate in patients with refractory partial epilepsy. *Epilepsy Res.* 1996;25: 217–224.

26. Tassinari C, Michelucci R, Chauvel P, et al. Double-blind placebo-controlled trial of topiramate (600 mg/day) for the treatment of refractory partial epilepsy. *Epilepsia.* 1996;37:763–768.

27. Ben-Menachem E, Henriksen O, Dam M, et al. Double-blind, placebo-controlled trial of topiramate as add-on therapy in patients with refractory partial epilepsy. *Epilepsia.* 1996;37:539–543.

28. Pledger G, Reife R, Lim P, Karim R. Overview of topiramate efficacy from adjunctive therapy trials. *Epilepsia.* 1995;36 (Suppl 3):150. Abstract.

29. Reife RA, Lim P, Pledger G. Topiramate: Side effect profile in double-blind studies. *Epilepsia.* 1995;36(Suppl 4):34. Abstract.

30. Edward KR, Kamin MT. The beneficial effect of slowing the initial titration rate of topiramate. *Neurology.* 1997;48(Suppl): A39. Abstract.

31. Fincham RW, Schottelius DD. Long-term therapy with topiramate in patients with partial seizures. *Epilepsia.* 1995;36(Suppl 4):56. Abstract.

32. Privitera M. Long-term efficacy and safety of topiramate. *Epilepsia.* 1995;36(Suppl 3):152. Abstract.

UM00016767
NOVARTIS EXHIBIT 1517
Novartis v. Regents, IPR2023-01347
Page 3749 of 4460

33. Ben-Menachem E. Long-term follow-up of patients treated with topiramate for partial seizures. *Epilepsia.* 1995;36(Suppl 3): 152. Abstract.

34. Wasserstein AG, Rak I, Reife RA. Nephrolithiasis during treatment with topiramate. *Epilepsia.* 1995;36(Suppl 3): 153. Abstract.

35. Rosenfeld WE, Holmes GB, Hunt TL, Schaefer P. Topiramate—effective dosing enhances potential for success. *Epilepsia.* 1992;33(Suppl 13):118. Abstract.

UM00016768
NOVARTIS EXHIBIT 1517
Novartis v. Regents, IPR2023-01347
Page 3750 of 4460

XP-002282988

P.D. 00.00.1990
P. 141-145

International Journal of Pharmaceutics, 65 (1990) 141–145
Elsevier

IJP 02274

Influence of solvent composition on the solubilities and solid-state properties of the sodium salts of some drugs

Joseph T. Rubino and Elizabeth Thomas

Division of Pharmaceutics, School of Pharmacy, University of North Carolina at Chapel Hill, Chapel Hill, NC 27599-7360 (U.S.A.)

(Received 5 December 1989)
(Modified version received 30 January 1990)
(Accepted 30 January 1990)

Key words: Solubility; Solubilization; Cosolvency; Sodium salt; Crystal hydrate; Solid-state properties

Summary

The solubilities of the sodium salts of some sulfonamides, barbiturates and hydantoins have been determined in mixtures of propylene glycol and water. In many cases, the solubilities of the salts in the mixed solvents were lower than those in water, however, several compounds exhibited enhanced solubilities in the mixed solvents. This unexpected increase in solubility was not related to the lipophilicity of the acidic forms of the drugs and occurred in at least one member of each group of compounds. Analysis of the solid phase which had been equilibrated with each solvent indicated the formation of crystal hydrates for most of the solutes, and in at least one instance, mixed solvates. These compounds could be categorized on the basis of their desolvation temperatures. Those compounds with low temperatures of desolvation had increased solubilities in propylene glycol-water mixtures while compounds with high desolvation temperatures had decreased solubilities in the mixed solvents. These data indicate that crystal hydrate formation plays a significant role in determining if a cosolvent can be used to enhance the solubilities of certain sodium salts.

In the last several years considerable interest has been devoted towards understanding and quantitating the influence of solvent blending, or cosolvency, on the solubilities of lipophilic solutes (Martin et al., 1979; Williams and Amidon, 1984; Yalkowsky and Rubino, 1987). Most of these studies considered the influence of solvent composition on the solubilities of nonelectrolyte solutes. However, few studies have examined the influence of solvent composition on the solubilities of salt forms of drugs. The combination of salt formation and consolvency might, in some instances, provide an alternative method of solubilization of a poorly water soluble weak electrolyte drug in cases where either technique alone is unsuitable due to reasons of poor chemical stability of the drug, toxicity due to high concentrations of cosolvents, or the inability of a single method to achieve the desired concentrations of drug in a formulation.

In theory, the addition of a cosolvent to an aqueous salt solution would be expected to reduce the solubility of the drug due to a reduction in the dielectric constant of the medium with a corresponding reduction in the solvation of the ions (Johnson, 1968). However, some studies have demonstrated that the addition of cosolvents to aqueous solutions of the salt forms of drugs has resulted in enhanced solubilities of the drugs

Correspondence: J.T. Rubino, Division of Pharmaceutics, School of Pharmacy, University of North Carolina at Chapel Hill, Chapel Hill, NC 27599-7360, U.S.A.

0378-5173/90/$03.50 © 1990 Elsevier Science Publishers B.V. (Biomedical Division)

BEST AVAILABLE COPY

UM00016769
NOVARTIS EXHIBIT 1517
Novartis v. Regents, IPR2023-01347
Page 3751 of 4460

(Kramer and Flynn, 1972; Agharkar et al., 1976). This apparent contradiction between the observed and expected behavior of salts in semi-aqueous solvent systems prompted further study of this phenomenon.

In the present study, the influence of solvent composition on the solubilities of the sodium salts of some representative poorly water soluble weak electrolyte drugs was examined. These included the sodium salts of some sulfonamides, barbiturates and hydantoins. The determination of the solubilities of the salts was performed at 25 ± 0.2°C in a constant temperature water bath. An excess amount of salt was equilibrated with 0, 10, 30 and 50% propylene glycol in water for 24–72 h. The supernatant was filtered through a 0.45 μm solvent-resistant filter, diluted with 0.1 N NaOH and assayed spectrophotometrically. Solubility determinations were performed in triplicate. The solid phase from the solubility experiments was collected onto filter paper, blotted free of excess solvent and dried under ambient conditions. Differential thermal analysis was performed on the solid phases using a Perkin Elmer DSC-2. Examination of the solid phase by thermal analysis was performed to ensure that the acid form of the drug did not precipitate during the equilibration procedure (Anderson and Conradi, 1985). In addition, it was reported previously (Rubino, 1989) that most of the compounds included in the present studies formed crystal hydrates when equilibrated with water. Thus, the drying time for the solid phases was dependent upon the rate of water loss from the crystal hydrate. Solvates with relatively low temperatures of desolvation were dried for 3 h; drying for longer periods of time resulted in significant changes in the transition temperatures. The more stable solvated solids were allowed to dry from 24 to 48 h without significant changes in their thermograms. The solvent com-

TABLE 1

Semi-aqueous / aqueous solubilities and transition temperatures (K) for desolvation [a]

Drug	log PC [c]	Fraction of propylene glycol			ΔH (cal K^{-1} $mol)^{-1}$ [b]
		0.10	0.30	0.50	
Sodium sulfadimethoxine [d]	1.56	1.14 (335)	1.18 (320)	1.31 (320)	1800
Sodium sulfamerazine [d]	0.14	0.86 (390)	0.68 (390)	0.54 (385)	5030
Sodium sulfamethazine [d]	0.27	0.90 (385)	0.78 (385)	0.69 (385)	3100
Sodium sulfaquinoxaline [d]	1.68	0.98 [e] (385)	0.99 [e] (381)	0.98 [e] (381)	3520
Sodium sulfathiazole [d]	0.05	1.07 (336)	1.34 (336)	1.80 (347)	1050
Sodium amobarbital	2.07	1.01 [e]	1.02 [e]		
Sodium barbital	0.65	1.02 [e]	0.85 [e]	0.58	
Sodium butabarbital [d]	1.89	1.14 (350)	1.30 (350)	1.33	
Sodium phenobarbital	1.42	0.96 [e]	0.96 [e]	0.92	
Sodium 5-methyl-5-phenylhydantoin [d]	1.02	0.96 (395)	0.93 (395)	0.85 (395)	
Sodium phenytoin [d]	1.98	1.27 (330)	1.58 (345)	1.08 (345)	1070

[a] Numbers in parentheses are transition temperatures.
[b] Calculated per mole of water in crystal after equilibration in 10% propylene glycol.
[c] Log octanol/water partition coefficient of acid form.
[d] Indicates compounds which form crystal hydrates.
[e] Indicates ratio not significantly different from 1.00 at $p < 0.05$.

BEST AVAILABLE COPY

UM00016770
NOVARTIS EXHIBIT 1517
Novartis v. Regents, IPR2023-01347
Page 3752 of 4460

position of the solid phase was determined from the loss of weight after heating in the DSC, or from the spectrophotometric absorbance of a known weight of the solid phase, as reported previously (Rubino, 1989). The presence of propylene glycol in the solid phase was determined using high-performance liquid chromatography with a refractive index detector. The stationary phase was a 10 μm, 25 cm, C-18 column and the mobile phase consisted of 30% methanol in water. The flow rate was 1 ml/min. In order to verify further the presence of the sodium salt after equilibration, the solid phase in many cases was also examined using a Phillips X-ray powder diffractometer. This was also performed to detect possible structural changes in the various solvates which were identified.

The results of the solubility determinations are presented in Table 1 along with the log octanol/water partition coefficient of each drug (Leo et al., 1971). The data are listed as the ratio of the solubility of the drug in mixed solvent/water. Aqueous solubilities were reported in a previous publication (Rubino, 1989). For many of the compounds, the addition of cosolvent resulted in a reduction in the solubility of the drug as would be expected based on a reduced dielectric constant of the solution. However, four compounds unexpectedly exhibited enhanced solubility upon addition of the cosolvent. These four compounds belonged to different chemical groups of drugs, indicating that the phenomenon was not related to a particular class of compound or ionic group. Likewise, the trends in the solubility data are apparently not related to the lipophilicity of the corresponding unionized form of the drugs. For example, the order of the partition coefficients for the sulfonamides is: sulfaquinoxaline > sulfadimethoxine > sulfamethazine > sulfamerazine > sulfathiazole. However, the order of the solubility changes in 30 and 50% propylene glycol from Table 1 is: sulfathiazole > sulfadimethoxine > sulfaquinoxaline > sulfamethazine > sulfamerazine.

The rank order of the solubility changes for the barbiturate salts likewise does not follow the order of the partition coefficients of the unionized forms of the drugs. In the case of the hydantoin salts, the more lipophilic phenytoin demonstrated some enhanced solubility in the mixed solvent systems compared with the 5-methyl-5-phenyl derivative, but the solubility profile is unusual in that a maximum was reached in 30% propylene glycol. These results indicate that the magnitude and direction of change of the solubilities of these salts do not appear to depend on the lipophilic nature of the conjugate acid.

The results of the DSC analysis confirmed that in each case, the solid phase was composed of the salt form of the drug. Thus, the solubility data reported in Table 1 are representative of the salt-solution equilibrium. These results also indicate that the saturated salt solutions were sufficiently basic to prevent precipitation of the acid form of the drugs in all cases but one. It was reported previously (Rubino, 1989) that thermal and X-ray analysis of samples of sulfathiazole sodium revealed evidence of precipitation of the acid form of the drug after equilibration with water, but most of the solid phase was composed of the sodium salt. As in the case of the purely aqueous systems, most of the compounds included in the present study formed hydrates, and in the case of phenytoin sodium, evidence of mixed solvates was found (see below).

Hydrate and solvate formation have been shown previously to influence the solubilities of nonelectrolyte drugs (Pfeiffer et al., 1970; Fokkens et al., 1983; Gould et al., 1989), however few studies have reported the effects of this phenomenon on electrolyte solubility. Fung and Nealon (1974) reported that the solvent composition of the dissolution medium can have a significant effect on the dissolution behavior of a given solvated form of a drug. In purely aqueous solvent systems, crystal hydrate formation has been associated with reduced solubilities, compared to anhydrous crystals, however, in semi-aqueous solvents their behavior might be quite different if a favorable interaction takes place between the cosolvent and the solvate or hydrate molecule. This may be the case in the propylene glycol-water system where an exothermic reaction between the two components has been noted (Borghesani et al., 1989).

It is reasonable to suspect, therefore, that crystal hydrate or solvate formation might play a role in the trends in the solubility data for the sodium

BEST AVAILABLE COPY

UM00016771
NOVARTIS EXHIBIT 1517
Novartis v. Regents, IPR2023-01347
Page 3753 of 4460

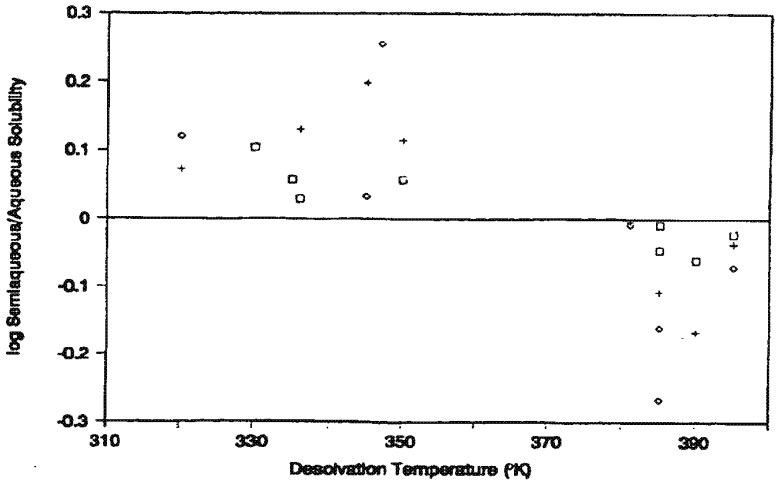

Fig. 1. Solubility in semi-aqueous/aqueous solvents vs temperature of desolvation. (□) 10% propylene glycol, (+) 30% propylene glycol, (◇) 50% propylene glycol.

salts reported in the present study. A plot of the log semi-aqueous/aqueous solubilities vs the desolvation transition temperatures is presented in Fig. 1 for those compounds that formed crystal hydrates. The temperatures for the onset of desolvation are listed in Table 1. The plot indicates that the salts appear to fall into two groups, 'low' and 'high' transition temperature solvates. Compounds which possess low temperatures of desolvation have increased solubilities in propylene glycol-water while those with high transition temperatures have decreased solubilities in the cosolvent-water mixture. The enthalpies of desolvation of the solid phase obtained after equilibration with 10% propylene glycol are reported in Table 1 for several of the compounds. These values are expressed as the enthalpy per mole of water present in the solid phase. The high transition temperature solvates were found to possess 3–5-fold greater enthalpies of desolvation per mole of water compared to the low transition temperature compounds. This observation is consistent with those of Fung and Nealon (1974) who observed that a high transition enthalpy, *t*-butylamine solvate of fluprednisolone did not demonstrate an enhanced dissolution rate in water while the lower transition enthalpy solvate of griseofulvin did show enhanced dissolution rates in water. It can also be noted from Table 1 that the solubilities of those compounds which did not show evidence of hydrate formation were either reduced or insignificantly influenced by the addition of the cosolvent. This observation agrees more closely with the anticipated effects of the addition of a polar cosolvent to an aqueous solution of a strong electrolyte.

The unusual solubility profile of phenytoin sodium in propylene glycol-water may also have been due to a change in the solid state of the drug. X-ray diffraction patterns of the solid phases were different after equilibration with each solvent system examined. Compositional analysis of the solid phase indicated a change in the crystal from a hexahydrate to a monohydrate when the solvent was changed from 10 to 30% propylene glycol, respectively. In addition, the solid phase incorporated one molecule of propylene glycol after equilibration in 30% propylene glycol. The remaining compounds retained only fractional amounts of propylene glycol in their solid phases. In 50% propylene glycol, the solid phase of phenytoin

BEST AVAILABLE COPY

sodium retained approx. 3 molecules of water and 1.5 molecules of propylene glycol.

Although the results obtained from the present studies do not provide a quantitative relationship of the effects of cosolvents on the solubilities of salts, the generality observed in Fig. 1 does seem to indicate that crystal solvation plays a significant role in determining whether the sodium salts of these drugs demonstrate enhanced solubilities in mixed solvent systems. The accurate prediction of the solubilities would most likely require numerous thermochemical data (Fokkens et al., 1983) as well as a knowledge of the dielectric constants of the saturated solutions. This might require that each drug be considered on an individual basis. Nonetheless, a consideration of solvate formation and its thermal behavior may help decide if a cosolvent will improve the solubility of a sodium salt. Finally, although the solubility increases observed for some of the compounds were relatively modest in the propylene glycol-water system, other solvent systems might result in greater solubility increases.

References

Agharkar, S., Lindenbaum, S. and Higuchi, T., Enhancement of solubility of drug salts by hydrophilic counterions: properties of organic salts of an antimalarial drug. *J. Pharm. Sci.*, 65 (1976) 747–749.

Anderson, B.D. and Conradi, R.A., Predictive relationships in the water solubility of salts of a nonsteroidal anti-inflammatory drug. *J. Pharm. Sci.*, 74 (1985) 815–820.

Borghesani, G., Pedriali, R. and Pulidori, F., Solute-solute-solvent interactions in dilute aqueous solutions of aliphatic diols. Excess enthalpies and Gibbs free energies. *J. Solution Chem.*, 18 (1989) 289–300.

Fokkens, J.G., Van Amelsfoort, J.G.M., DeBlaey, C.J., De Kruif, C.G. and Wilting, J., A thermodynamic study of the solubility of theophylline and its hydrate. *Int. J. Pharm.*, 14 (1983) 79–93.

Fung, H.L. and Nealon, T., Solvent effects on comparative dissolution of pharmaceutical solvates. *Chem. Pharm. Bull. Tokyo*, 22 (1974) 454–458.

Gould, P.L., Howard, J.R. and Oldershaw, G.A., The effect of hydrate formation on the solubility of theophylline in binary aqueous cosolvent systems. *Int. J. Pharm.*, 51 (1989) 195–202.

Johnson, D.A., The standard free energies of solution of anhydrous salts in water. *J. Chem. Educ.*, 45 (1968) 236–240.

Kramer, S.F. and Flynn, G.L., Solubility of organic hydrochlorides. *J. Pharm. Sci.*, 61 (1972) 1896–1904.

Leo, A., Hansch, C. and Elkins, D., Partition coefficients and their uses. *Chem. Rev.*, 71 (1971) 525–616.

Martin, A., Paruta, A.N. and Adjei, A., Extended Hildebrand solubility approach: Methylxanthines in mixed solvents. *J. Pharm. Sci.*, 70 (1981) 1115–1120.

Pfeiffer, R.R., Yang, K.S. and Tucker, M.A., Crystal pseudopolymorphism of cephaloglycin and cephalexin. *J. Pharm. Sci.*, 59 (1970) 1809–1814.

Rubino, J.T., Solubilities and solid state properties of the sodium salts of drugs. *J. Pharm. Sci.*, 78 (1989) 485–489.

Williams, N.A. and Amidon, G.L., An excess free energy approach to the estimation of solubility in mixed solvent systems. *J. Pharm. Sci.*, 73 (1984) 9–13.

Yalkowsky, S.H. and Rubino, J.T., Cosolvency and Cosolvent Polarity. *Pharm. Res.*, 4 (1987) 220–230.

BEST AVAILABLE COPY

UM00016773
NOVARTIS EXHIBIT 1517
Novartis v. Regents, IPR2023-01347
Page 3755 of 4460

D.6 **CONCENTRATION RELATED EFFECTS OF VIGABATRIN ON GABA UPTAKE IN CULTURED RODENT ASTROCYTES**

John Paul Leach, Graeme Sills, George Thompson, Gerard Forrest, Elaine Butler, and Martin J Brodie.
Epilepsy Research Unit, Western Infirmary, Glasgow, UK

Rationale
Vigabatrin is an effective anticonvulsant when used as add-on therapy. The clinical efficacy of vigabatrin was previously believed to be due solely to the inhibition of GABA-transaminase (GABA-T) activity. We have shown that vigabatrin also inhibits the reuptake of GABA by astrocytes. Here we describe how this effect varies with the concentration of vigabatrin.

Methods
Astrocytes were cultured from the cerebral cortices of 1-day old rat pups. After three weeks in culture, the rate of GABA uptake was assessed by exposure to [^{14}C]-labelled GABA. GABA uptake into cells following 1 hour pre-treatment with vigabatrin (1 to 500uM) was compared to that of cells exposed to control conditions.

Results
At concentrations of 1uM,10uM, and 50uM, vigabatrin did not significantly alter the rate of GABA uptake. At 100uM however, vigabatrin significantly decreased GABA uptake, the mean values at 100uM being 80% of the mean control values ($p<0.05$), an effect that persists at 250uM. Exposure to vigabatrin at 500uM, however, significantly *increased* the mean rate of GABA uptake by 32% ($p<0.01$).

Conclusions
While it was previously felt that vigabatrin had only one action on the GABAergic system, it is now clear that it also has significant dose-dependant effects on the rate of GABA uptake. The clinical relevance of this is unclear, but this inhibition at levels known to decrease GABA-T activity may be at least partly responsible for the anticonvulsant action of vigabatrin.

D.7 **DOSE-RANGING TRIAL WITH HIGHER DOSES OF TOPIRAMATE IN PATIENTS WITH RESISTANT PARTIAL SEIZURES** Michael Privitera,[1] Richard Fincham,[2] J. Kiffin Penry,[3] Ross Reife,[4] Lynn Kramer,[5] Gordon Pledger,[4] R. Karim,[4] and the Topiramate YE Study Group 1.University of Cincinnati Medical Center, 2.University of Iowa Hospitals, 3.Bowman Gray School of Medicine, 4.R.W. Johnson Pharmaceutical Research Institute, 5.Ciba-Geigy Pharmaceuticals Division

RATIONALE: We conducted a double-blind, parallel group, placebo-controlled trial in 190 patients to evaluate the safety and efficacy of three dosages of topiramate, an investigational antiepileptic drug (AED) as adjunctive therapy for refractory partial epilepsy. **METHODS**: During a 12 week baseline period, patients were required to have at least one partial-onset seizure per week while receiving one or two standard AEDs at therapeutic concentrations. Patients were randomized to 600 mg/day, 800 mg/day, 1000 mg/day or placebo in a bid regimen. A 6 week titration period was followed by a 12-week maintenance period. **RESULTS**: Median percent reductions from baseline in monthly seizure rates were 1% for placebo, 41% for topiramate 600 mg/day and topiramate 800 mg/day, and 38% for topiramate 1000 mg/day. A 50% or greater reduction in baseline seizure frequency during the treatment phase was observed in 9% of placebo, 44% of topiramate 600 mg/day, 40% of topiramate 800 mg/day and 35% of topiramate 1000 mg/day patients. No placebo patients improved by 75-100%, but 20% of topiramate patients had this degree of improvement. All analyses were intent-to-treat drug-placebo comparisons and significantly ($p \leq 0.02$) favored topiramate. Treatment-emergent adverse events consisted mainly of neurological symptoms commonly observed during standard AED therapy. Sixteen percent of topiramate patients discontinued due to adverse events. **CONCLUSIONS**: Topiramate is a highly efficacious and generally well tolerated new AED. When large groups of patients are compared, incremental efficacy in the add-on setting is not observed above 600 mg/day; however, higher doses may prove beneficial to individual patients who tolerate them.

Dr. Privitera has performed consulting for R.W. Johnson PRI. Drs. Reife, Pledger, and Karim are currently employees of R.W. Johnson PRI. Dr. Kramer was an employee of R.W. Johnson PRI at the time the trial was completed, however, he no longer works for them.

D.8 **TOPIRAMATE: DOUBLE-BLIND TRIAL AS MONOTHERAPY**

Authors: S. K. Sachdeo, MD, Rajesh C. Sachdeo, MD, UMDNJ, New Brunswick, NJ, Ross A. Reife, MD, Pilar Lim, Gordon Pledger, Ph.D., RWJ Pharmaceutical Research Institute, Raritan, NJ.

Rationale: Topiramate has shown efficacy in treating adults with refractory partial-onset seizures in five trials. In these double-blind trials, patients were randomized to add either topiramate or placebo to their existing anti-epileptic drug (AED) regimen. The percent reduction in seizures over baseline was compared for the two groups. The current trial assessed efficacy in the same population using a different design.
Methods: In this double-blind trial, 48 patients were randomized to receive either the minimum efficacious dose of topiramate [100 mg/day] or a higher dose [1000 mg/day or maximum tolerated dose (MTD)]. Concomitant AEDs were withdrawn during the first 35 days of the double-blind period. The patient continued monotherapy of either 100 mg/day or 1000 mg/day (or MTD) of topiramate for the duration of the 112-day double-blind phase or until the patient met exit criteria. The exit criteria were pre-defined to indicate a worsening of seizures over baseline.
Results: The time to exit was longer in the 1000 mg/day group than in the 100 mg/day group ($p=0.0017$). The number of patients who remained in the trial for the entire 112 days was also greater in the 1000 mg/day group ($p=0.002$).
Conclusions: In a different trial design than those previously reported with topiramate, 1000 mg/day (or MTD) of topiramate monotherapy is effective as treatment for refractory partial onset seizures in adults.

Supported by RWJ Pharmaceutical Research Institute

Ross A. Reife, Pilar Lim, and Gordon Pledger, Ph.D., are employees of RWJ Pharmaceutical Research Institute, the sponsor of the research. As such they receive salaries from RWJ Pharmaceutical Research Institute and may hold equity positions and/or receive stock options. Drs. S. K. Sachdeo and Rajesh C. Sachdeo have received a grant for doing the above study.

D.9 TOPIRAMATE DOSE-RANGING TRIAL IN REFRACTORY PARTIAL EPILEPSY. Edward Faught, B.J. Wilder, R. Eugene Ramsay, Ross A. Reife, Lynn D. Kramer, Gordon W. Pledger, Rezaul M. Karim and the Topiramate YD Study Group. University of Alabama at Birmingham, Birmingham, AL 35294.

RATIONALE: We conducted a randomized, double-blind comparison of three dosages of topiramate to placebo as adjunctive therapy in refractory partial onset epilepsy.
METHODS: 181 patients completed a 12-week baseline during which they had at least one partial-onset seizure per week. All received one or two other drugs at therapeutic concentrations. Patients were randomized to 200 mg/day, 400 mg/day, 600 mg/day or placebo. A four-week titration preceded a 12-week maintenance period.
RESULTS: The median percent seizure reductions relative to baseline, using an intent to treat analysis, were: 30% for topiramate 200 mg/day ($p = 0.051$), 48% for topiramate 400 mg/day ($p = 0.007$), 45% for topiramate 600 mg/day ($p = 0.001$) and 13% for placebo. Percent responders (> 50% reduction in seizure frequency) were 27% for topiramate 200 mg/day, 47% for topiramate 400 mg/day ($p = 0.013$), 46% for topiramate 600 mg/day ($p = 0.027$) and 18% for placebo. A significant ($p = 0.003$) reduction in secondarily generalized tonic clonic seizures with topiramate was demonstrated.
Mild or moderate central nervous system symptoms were the primary treatment-emergent adverse events, but treatment-limiting adverse events occurred in only 9% of topiramate patients compared to 7% of placebo patients.
CONCLUSIONS: Topiramate is effective and well-tolerated in refractory partial epilepsy.

Edward Faught, M.D., received research support and an honorarium for speaking from R.W. Johnson Pharmaceutical Research Institute.

UM00016774
NOVARTIS EXHIBIT 1517
Novartis v. Regents, IPR2023-01347
Page 3756 of 4460

10/747,742

ELSEVIER

International Journal of Pharmaceutics 141 (1996) 257–259

international journal of pharmaceutics

Preparation, characterisation and transformation of terfenadine polymorphic forms

M. Sheikh Salem[a,*], G.K. Pillai[a], L. Nabulsi[b], H.N. Al-Kaysi[a], T.A. Arafat[c], A. Abu. Malooh[b], M. Saleh[b], A.A. Badwan[b]

[a] *Faculty of Pharmacy, Jordan University of Science and Technology, Irbid, Jordan*
[b] *Jordanian Pharmaceutical, Manufacturing Company, Naor, Jordan*
[c] *Women's University Amman, Amman, Jordan*

Received 22 April 1996; accepted 30 May 1996

Abstract

Polymorphic modifications of terfenadine as well as solvates from various solvents have been prepared and characterised by X-ray powder diffraction (XRPD), infrared (IR) spectroscopy, differential scanning calorimetry (DSC) and thermogravimetric analysis. Crystallization of terfenadine from *n*-alkanols, except methanol and ethanol, resulted in the stable polymorph 1 (m.p. 151°C) while the iso-alkanols yielded the corresponding solvates. Water content, temperature of incubation and duration were found to have significant effect on transformation.

Keywords: Terfenadine; Polymorphic form; Preparation; Characterisation; Transformation

Terfenadine is a relatively new H1-receptor antagonist, (Sorkin and Heel, 1985; Guill et al., 1986). The US Pharmacopeia XXII (1990) monograph indicates that the melting range of terfenadine is 145–151°C. Differential scanning colorimetry (DSC) of several commercial samples of terfenadine revealed that their melting peaks lies within the wide range specified in the officia-compendia (US Pharmacopeia XXII, 1990). However, deviation from symmetrical peaks shown by some of the samples suggested the existence of different polymorphic forms within the USP melting range specification. Three distinct polymorphs and two solvates were then identified and characterised (Badwan et al., 1990).

The aim of this study was to evaluate the effect of different proportions of water in alcohol–water mixtures, temperature, duration of incubation and homogenisation on transformation of unstable to the most stable polymorph and effect of position

* Corresponding author. Tel.: +962 2 295111 ext. 3523; fax: +962 2 295123.

0378-5173/96/$15.00 © 1996 Elsevier Science B.V. All rights reserved
PII S0378-5173(96)04626-1

UM00016775
NOVARTIS EXHIBIT 1517
Novartis v. Regents, IPR2023-01347
Page 3757 of 4460

of hydroxyl group in a series of alkanols on formation of polymorphs and solvates.

Terfenadine (m.p. 151°C) was obtained from the Jordanian Pharmaceutical Manufacturing Co., Jordan. All solvents used in this study were obtained from May and Baker, Germany and propylene glycol from Dow Chemicals, USA. Polymorph 1 was obtained by dissolving commercial terfenadine in *n*-alkanols with aid of heating. The solution was filtered and cooled in a refrigerator. Polymorph 2 was obtained by cooling a solution of commercial terfenadine in propylene glycol for 3 days in a refrigerator and the glass form by rapid cooling of the melt. The thermograms of different crystalline modifications were obtained using Mettler TA 3000 DSC 20 unit (Mettler, Switzerland). The heating rate was 10°C/min and the sample size ranged between 4 and 10 mg.

To study the effect of water content in alcohol and the position of hydroxyl groups on the formation of polymorph and solvate, a different proportion of water and a series of *n*-alkanols and iso-alkanols were used. In addition, the effect of temperature, duration and homogenisation on transformation of the glass form as well as polymorph 2 was studied using DSC pattern.

DSC and X-ray diffraction (XRD) pattern of terfenadine polymorphs 1 and 2 were reported previously (Badwan et al., 1990). A single endothermic peak at 151.1°C (polymorph 1, stable form) and at 143.5°C (polymorph 2) indicated that no decomposition occurs at their melting points. X-ray diffractogram of the glass form indicated lack of crystallinity. The possibility of any chemical degradation was excluded after analysis by thin layer chromatography (TLC), high performance liquid chromatography (HPLC), IR spectroscopy and also by mass spectroscopy.

The melting point of terfenadine polymorphs and solvates crystallized from different solvents are as follows: terfenadine (starting material) 151.1, methanol (solvate) 149.3, methanol–water (50%) 150. Propylene glycol 143.5, ethanol (solvate) 152.3, ethanol–water (50%) 148.3, propanol 151.6, isopropanol (solvate) 150.0, butanol 152.0, isobutanol (solvate) 149.2, pentanol 153.4, 2-pentanol (solvate) 150.8 crystallization from pure methanol or ethanol yielded solvates. However, in the presence of water in these alcohols, polymorph 1 is readily formed. As the water content is increased in these mixtures (i.e. from 20 to 60% water) the desolvation peak in the DSC profile (87°C) starts to disappear. The material obtained from a mixture of 40% methanol and 60% water showed only one endothermic peak at 151°C corresponding to that of the stable polymorph. Thus, it appears that the proportion of water in these alcohol water mixtures is a crucial factor determining formation of solvate or the stable polymorph.

Methanol and ethanol yielded the corresponding solvates while *n*-propanol, *n*-butanol, *n*-pentanol, and *n*-octanol have led to the formation of the stable polymorph 1. However, the use of isopropanol and isobutanol always resulted in the formation of the metastable solvate as evidenced by the desolvation peak at 70, 85°C and an endothermic peak at 149.5°C (iso-propanol) and at 71, 100 and 149°C (iso-butanol). Allyl alcohol and tetrahydrofuran also yielded solvate peak in their DSC profile. Thus, it appears that in a series of alkanols, the iso-alkanols tends to favour formation of the solvate while the *n*-alcohols favour formation of stable polymorph 1. The solvate formed from isopropanol was shown to contain a stoichiometric amount of crystallisation solvent (1:1) by spectrophotometric estimation of terfenadine and by comparison with the theoretical amount for a (1:1) solvate.

Transformation of glass form of terfenadine was studied by incubating a water dispersion at 25°C. Fig. 1a shows the DSC profile of samples of glassy material at various time periods from 6 h to 15 days. The thermogram obtained at 6 h shows shoulder on the main peak at 147°C (metastable) which, by 24 h have clearly split into a second peak at 151°C. As the duration of incubation is increased, a steady increase in peak height at 151°C and the gradual disappearance of peak at 147°C is apparent. Homogenisation of the dispersion on the 14th day completed the transformation as shown by a single peak at 151°C.

UM00016776
NOVARTIS EXHIBIT 1517
Novartis v. Regents, IPR2023-01347
Page 3758 of 4460

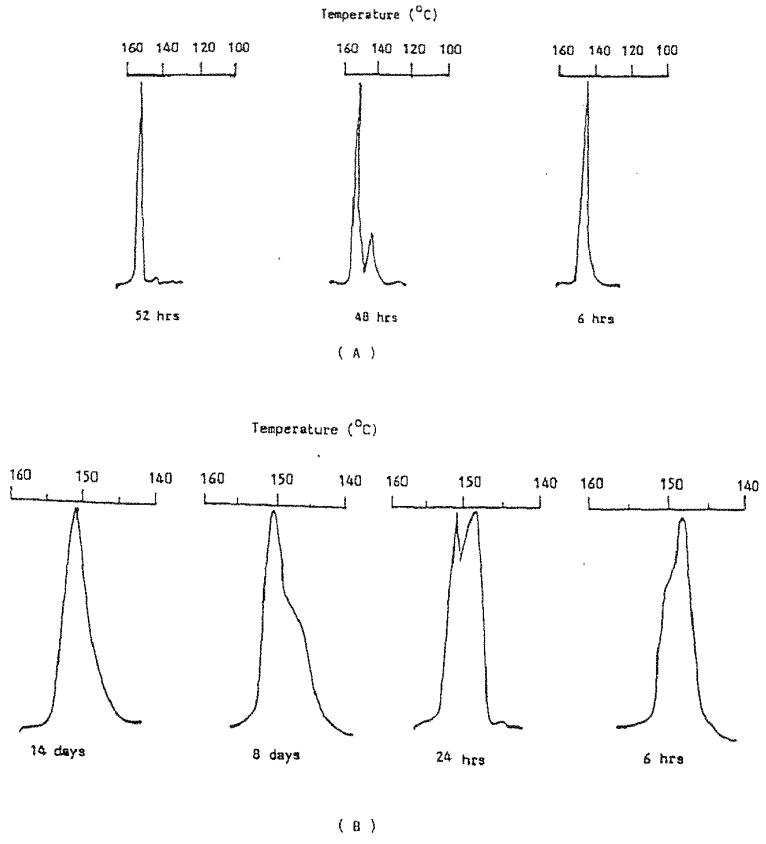

Fig. 1. DSC profile of transformation of (A) glass form of terfenadine with time at 25°C. (B) Polymorph 2 of terfenadine with time at 60°C.

The transformation of polymorph 2 by incubating a dispersion in water at 60°C for a period of 52 h is shown in Fig. 1b. A second peak in the thermogram corresponding to 151°C begins to appear alongside the main peak at 143°C and by 48 h, the proportion of the stable polymorph is increased significantly in the mixture. By 52 h, peak at 151°C with a small hump at 143°C indicated that the polymorph 2 is almost completely transformed into stable polymorph 1. Using an elevated temperature of 60°C has obviously accelerated the transformation to the stable form.

References

Badwan, A.A., Al.Kaysi, H.N., Owais, L.B., Salem, M.S. and Arafat, T.A., Terfenadine. *Anal. Profile Drug Subst.*, 19 (1990) 627–662.

Guill, M.F., Buckley, R.H., Rocha, W., Kemp, J.P., Segal, A.T., Shirley, L.R., Thinkelman, D.G., Shaath-Schwen, Z., Dietrich, K.K., Wille, L.J. and Tsai, T.H., Multicenter, double-blind, placebo-controlled trial of terfenadine. Suspension in the treatment of allergic rhinitis in children. *J. Allergy Clin. Immunol.*, 78 (1986) 4–9.

Sorkin, E.M. and Heel, R.C., Terfenadine: a review of its pharmacodynamic properties and therapeutic efficacy. *Drugs*, 29 (1985) 34–35.

US Pharmacopeia XXII, *US Pharmacopeial Convention*, Rockville, MD, 1990, p. 2173.

UM00016777
NOVARTIS EXHIBIT 1517
Novartis v. Regents, IPR2023-01347
Page 3759 of 4460

Chemical & Engineering News
Serving the chemical, life sciences and laboratory worlds

Cover Story

June 18, 2007
Volume 85, Number 25
pp. 17-30

Form And Function

The choice of pharmaceutical crystalline form can be used to optimize drug properties, and cocrystals are emerging as new alternatives

Ann M. Thayer

"TAKE TWO ASPIRIN and call me in the morning," the medical adage goes. To most people, this means simply washing down two tablets. Until late 2005, "take two aspirin" didn't have any different connotation for crystallographic researchers either; as far as anyone knew, after 40 years of study, only one crystalline phase, or polymorph, of acetylsalicylic acid had been found.

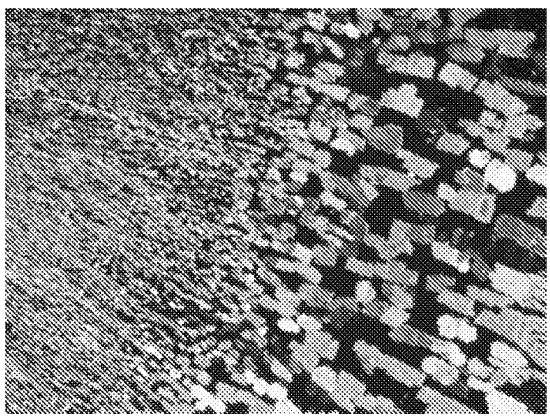

Scott Childs/SSCI

Ch-Ch-Changes Metformin hydrochloride polymorph forms under thermal microscopy.

Then a reported second polymorph unleashed a rancorous dispute over the subtleties of how molecules pack in crystals (C&EN, Jan. 1, page 27). Although the discovery isn't expected to have practical ramifications, it underscored the importance of identifying, making, and controlling the crystal forms of pharmaceuticals. A drug's behavior depends on much more than the molecular structure; its solid form dictates its properties, including stability, hygroscopicity, dissolution rate, solubility, and bioavailability.

Pharmaceutical developers usually search for a crystal form with the best properties for therapeutic use and manufacturability. As a material, the selected form must be amenable to handling and processing, and as a drug, it must be effective and safe. One problem is that the most stable polymorph is also the least soluble. In addition, one can't know beforehand exactly how many polymorphs exist and under what conditions they'll appear.

The industry took note of this in 1998 when Abbott Laboratories had to halt sales of its HIV protease inhibitor, Norvir. It had commercialized a metastable form of ritanovir, the active pharmaceutical ingredient (API), in solution-filled gelcaps. When a more stable, previously unknown polymorph suddenly crystallized, the company had to reformulate the drug, which cost it an estimated $250 million in lost sales.

Meanwhile, the U.S. Food & Drug Administration became concerned about the effect that different solid forms could have on API quality and performance. Consequently, international regulators now require manufacturers to screen for polymorphs. When it comes to getting approval, beyond the usual safety and efficacy considerations, drugmakers may have to prove they understand the form they've chosen and can reliably

UM00016778
NOVARTIS EXHIBIT 1517
Novartis v. Regents, IPR2023-01347
Page 3760 of 4460

control its production and stability.

Besides single-component polymorphs, drugs can also exist as salts and other multicomponent crystalline phases. For example, solvates and hydrates may contain an API host and either solvent or water molecules, respectively, as guests. Analogously, when the guest compound is a solid at room temperature, the resulting form is often called a cocrystal. Salts, solvates, hydrates, and cocrystals may show polymorphism as well.

According to a recent analysis by SSCI, the solid-state chemistry business of Aptuit, polymorph screens of 245 compounds revealed that about 90% of them exhibit multiple solid forms. These data are consistent with those from other sources. Overall, half the compounds were polymorphic, often having one to three forms. About one-third of the compounds formed hydrates, and about one-third formed solvates. Data from cocrystal screens of 64 compounds showed that 60% formed cocrystals other than hydrates or solvates.

Faced with so much variety, pharmaceutical companies choose their solid forms carefully. "We're interested in getting the right properties for a compound to be a good medicine," says Simon Black, crystallization scientist in process R&D at AstraZeneca.

"We always prefer to develop the most thermodynamically stable form, provided its other properties are acceptable," he says. If, however, a compound is insoluble, hygroscopic, or difficult to crystallize, they'll consider making salts or possibly cocrystals.

Apart from the regulatory obligations, polymorph screening is common practice to avoid surprises later in development, Black notes. Drug developers also want to identify and characterize as many forms of their proprietary compounds as possible. Beyond offering choices for optimal physical properties, each form may be patentable.

Drug companies usually file patents on all the different forms during development. Thus, when initial patents on the compound itself expire, they can conceivably extend a product's life by moving to another form. In turn, generic drugmakers will target unprotected forms to avoid patent infringement. Nevertheless, high-profile lawsuits???around GlaxoSmithKline's Zantac and Paxil and Bristol-Myers Squibb's cefadroxil???have hinged on solid-form issues.

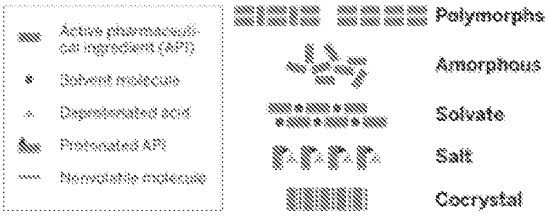

adapted from rolf hilfiker/solvias

Construction Drug molecules can be crystallized in different solid forms.

Mounting litigation, Abbott's Norvir experience, regulatory changes, and other factors have all converged within the past decade. They have elevated concerns about solid forms and the desire to explore alternatives to salts and polymorphs. Although researchers have studied crystalline molecular complexes for more than 100 years, drug developers have only intermittently exploited cocrystal forms of pharmaceuticals.

In the past, there had been a lack of experience making cocrystals with APIs, along with a limited understanding of how cocrystals can change drug properties. No drug that can be definitively described as a cocrystal and not a salt has been approved, those working in the field say. But greater interest is emerging as both understanding and experience grow, and the need for new and better-performing solid forms increases. Cocrystals are potentially attractive for improving properties while leaving an API unaltered.

In a Molecular Pharmaceutics special section this month on pharmaceutical cocrystals, Andrew V. Trask, a legal intern at Jones Day law firm in New York City, lays out arguments he and others believe support why pharmaceutical cocrystals will continue to be an active area of scientific investigation. He also describes how they might offer commercial and legal opportunities and advantages over other solid forms (*Mol. Pharmaceutics* **2007**, 4, 301).

As a former scientist at Pfizer, Trask himself is a co-inventor on patents related to crystal forms of APIs. After receiving his Ph.D. in chemistry in 2006 from Cambridge University, where he worked with chemistry professor William Jones, he now attends law school and is registered to practice before the U.S. Patent & Trademark Office (PTO).

"There's been a lot of legal activity around salts and polymorphs, but not yet for pharmaceutical cocrystals," Trask tells C&EN. Although there is a growing number of patent applications on cocrystals, PTO has yet to issue many patents. But similar forms, such as salts, hydrates, and solvates, have proven to be patentable.

TO BE PATENTABLE, a new crystal form must have utility, which is not usually an obstacle for most APIs. It must also be nonobvious and novel—that is, not previously appearing in the prior art. Fortunately for pharmaceutical cocrystals, the prior art is limited, says Eyal Barash, a chemist and Aptuit's chief patent counsel.

UM00016779
NOVARTIS EXHIBIT 1517
Novartis v. Regents, IPR2023-01347
Page 3761 of 4460

Prior art can be tricky, Barash explains, because it needs to only "inherently anticipate" a form's existence. For example, a patented method to make an anhydrate may also yield trace amounts of a hydrated form; even if the hydrate is never identified, it's still considered to have appeared in the prior art because the method makes it.

This catch has been the basis of litigation around polymorphs, hydrates, and solvates. "Cocrystals offer a better shot at surviving such an attack," Barash says, "because if you reproduce a method, and a component is not included, then you're never going to have made a cocrystal of the API with a component that's not there."

Crystallizing a salt may be attempted if an ionizable group is present. And the drug industry has a lot of experience screening for and making salts; according to Trask, more than 24,000 U.S. patents contain the term "pharmaceutically acceptable salt." But salt and cocrystal forms are not predictable, Trask and Barash say.

Salts of APIs are limited to acceptable counterions, but cocrystals can potentially be made using a broader range of guests or cocrystal formers. Although you can choose logical combinations to start with, you can't know in advance whether a salt or cocrystal will form, and it's impossible to predict the structure and its properties, Trask and Barash explain. Thus, researchers may resort to even more extensive screening to discover cocrystals.

"Cocrystals have the same advantages that polymorphs do from an obviousness perspective in being less predictable," Barash says. He recommends supporting any solid-form claim with high-quality, reproducible data drawn often from multiple analytical techniques.

This may be good for the overall patentability of cocrystals, but it means coverage will probably be narrow rather than over broad classes of compounds. "If you find and claim a really good cocrystal, that won't protect you against someone else claiming a different one," Barash says. "You'd have to do more experimental work to find as many cocrystals as you can and then protect each of them."

Others take a different view. Michael J. Zaworotko, chemistry department chairman at the University of South Florida, says he and collaborators at Johnson & Johnson's TransForm Pharmaceuticals are awaiting decisions on patent applications covering cocrystal classes. "Once you have established that you can make cocrystals of a particular drug with a particular type of cocrystal former, you should be able to claim a series," Zaworotko says.

"It's long established that you can claim a series of salts before they have been made," he says. "There's little rhyme or reason to why polymorphs or solvates form, and until you've made one, you really can't predict whether the crystal morphology, dissolution profile, and stability will be superior.

"With cocrystals, there's a bit more crystal engineering or design possible," he continues. "Before our work came along, it wasn't obvious that drugs would form cocrystals and that the cocrystals would have superior properties." In a 2004 article, Zaworotko and TransForm's Örn Almarsson highlighted the potential of pharmaceutical cocrystals (*Chem. Commun.* **2004**, 1889).

Cocrystals have sparked the interest of many researchers in the crystal engineering field as a way to tailor material properties. Intermolecular interactions between neutral molecules hold these crystals together in well-defined and ordered crystalline arrays. To assemble cocrystals, scientists have been exploring molecular recognition events.

One place Zaworotko looks for these events is among the more than 130,000 organic crystal structures in the Cambridge Structural Database. Fewer than 1,500 are cocrystals held together by hydrogen bonding (*J. Pharm. Sci.* **2006**, 95, 499). By evaluating the 1,500 structures, chemists can determine the occurrence and geometries of "supramolecular heterosynthons," or intermolecular pairings, which can be starting points for cocrystal design.

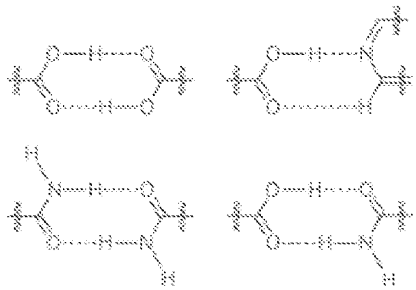

Connections Supramolecular synthons, such as those involving carboxylic acids, pyridinium nitrogens, and amides, can hold cocrystals together.

"Carboxylic acids, alcohols, and amides are quite prevalent in drugs," Zaworotko points out, "so you choose a cocrystal former that has better hydrogen-bonding complementarity with the drug than the drug with itself." The assumption is that a cocrystal will assemble if a favorable supramolecular heterosynthon forms.

But which heterosynthon pairing-for example, hydroxyl-pyridine, hydroxyl-amine, and hydroxyl-cyano-prevails among competing options can be determined only by characterizing the resulting cocrystals. Zaworotko and coworkers recently delineated such a hierarchy with a series of 17 cocrystals (*Mol. Pharmaceutics* **2007**, 4, 401).

SIMILAR WORK on heterosynthons is under way in other research groups. At the University of Hyderabad, in India, Ashwini Nangia and

UM00016780
NOVARTIS EXHIBIT 1517
Novartis v. Regents, IPR2023-01347
Page 3762 of 4460

collaborators have explored temperature effects and the reactivity of hydrogen-bonding groups in aromatic carboxylic acid and carboxamide cocrystals (*Chem.-Asian J.* **2007**, 2, 505). Further work of theirs has looked specifically at cocrystal preparation with model APIs such as carbamazepine and barbituric acid that involve amide-N-oxide heterosynthons (*Mol. Pharmaceutics* **2007**, 4, 417).

Interest in multicomponent crystals is actually decades old, with many research groups having laid the groundwork. The field's research portfolio spans studies focused on intermolecular interactions and crystal structures to applications in specialty chemicals, advanced materials, and, more recently, APIs. Still, the field of supramolecular chemistry is quite young compared with traditional organic or covalent chemistry.

Christer B. Aakeröy, a professor of chemistry at Kansas State University, sees parallels to the historical development of organic reactions and synthetic methods. "We are trying to replicate that and come up with a reliable synthetic paradigm for noncovalent synthesis," he says. "But it's not going to happen overnight or have the same kind of reliability, because we are dealing with weaker and reversible interactions.

"We are still looking to develop a drawer full of supramolecular reactions that we can pull out every time we see a molecule with certain functionalities," he adds. Eventually, he believes the odds can be stacked in the chemist's favor to give good supramolecular yields by better understanding which functional groups to bring together to form cocrystals with the desired connectivity.

To this end, Aakeröy's research group has undertaken systematic cocrystallization studies of hydrogen-bond-based synthons (*CrystEngComm* **2005**, 7, 439 and 2007, 9, 46). A wide variety of synthons is needed to determine which ones can operate side by side without interfering with each other, thus providing the foundation for modular supramolecular synthesis based upon hierarchies of intermolecular interactions, he explains.

To further increase the options and chances for success, Aakeröy's group often covalently modifies the supramolecular reagents. Such synthetic changes can adjust the strength of hydrogen-bond donors or acceptors (*CrystEngComm* **2006**, 8, 586; *Chem. Commun.* **2006**, 1445) to fine-tune the compatibility between functional groups on the cocrystal former and an API.

Although most efforts at making cocrystals center on two components, there is no reason that multiple sites on an API can't be targeted. Aakeröy and coworkers have made ternary cocrystals of carboxylic acids with isonicotinamide (*Angew. Chem. Int. Ed.* **2001**, 40, 3240) and with tailor-made pyridyl/benzimidazol-1-yl-based reagents (*Chem. Commun.* **2005**, 2820).

Likewise, Nangia has made carboxylic acid-bipyridine ternary systems (*Cryst. Growth Des.* **2005**, 5, 1683). And Joel Bernstein at Ben-Gurion University, in Israel, has explored a hydrogen-bonding synthon that could potentially involve up to four different molecules. He and graduate student Mazal Wenger attempted to make this synthon in cocrystals of γ-aminobutyric acid with oxalic or benzoic acid (*Angew. Chem. Int. Ed.* **2006**, 45, 7966).

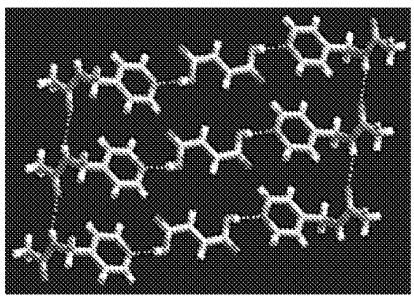

Courtesy of Christer Aakeröy

Alignment Hydrogen bonds create a ladder structure in a 4-(acetaminomethyl)pyridine-fumaric acid cocrystal.

Because the number of possible combinations can quickly get out of hand, researchers believe systematic approaches are crucial when designing and making cocrystals. Drug company researchers often look for potential cocrystal formers among the hundreds of compounds on FDA's Generally Recognized as Safe (GRAS) list because they anticipate regulators may find these more acceptable in drug forms.

Others, such as Zaworotko, believe the list is creating "a certain amount of tunnel vision." His research group doesn't focus on using GRAS list compounds, but does choose cocrystal formers on the basis of melting point, cost, and toxicity.

From a chemistry point of view, Aakeröy believes there won't be much headway made by staying with compounds on the GRAS list. "The pharmaceutical industry is particularly keen to do that," he says, "but there is no reason to believe that those compounds would be perfect for interacting in a targeted way with complicated APIs."

Taking a different approach, Mino R. Caira, professor of chemistry at the University of Cape Town, in South Africa, has studied the possibility of using "old" drugs as cocrystal formers. In a recent paper, Caira reviews the cocrystallization of antimicrobial sulfonamide drugs with drugs in other classes (*Mol. Pharmaceutics* **2007**, 4, 310).

ALONG WITH attempts to design cocrystals, other researchers are investigating methods to synthesize and screen them. Cambridge University's Jones is among those exploring making cocrystals by simply grinding components together.

His group has extended the method by adding tiny, nonstoichiometric amounts of solvent that can enhance the rate and selectivity of cocrystal formation. With liquid-assisted grinding, they have even made ternary systems and found they could make more by grinding than from solution

UM00016781
NOVARTIS EXHIBIT 1517
Novartis v. Regents, IPR2023-01347
Page 3763 of 4460

crystallization (*Angew. Chem. Int. Ed.* **2006**, 45, 7546).

Grinding avoids the need to have all the components soluble in the same solvent. "In the vast majority of cases, we can get the same product by grinding as you can from solution," Jones says. "It's not that grinding is better, but it's a quick way of getting information." During grinding, the components mix intimately and homogeneously to yield structures that can be characterized by X-ray powder diffraction, he explains.

Jones's group uses grinding to screen for cocrystals and to check for polymorph and hydrate stability. For example, simply by changing the liquid used, they have reproducibly made different polymorphs (*Chem. Commun.* **2004**, 890). In a screen for pharmaceutical salts, grinding using methanol had the same efficiency as solution crystallization and even yielded a few new salts (*Chem. Commun.* **2006**, 51).

Because many APIs are optically active, his group "started playing with chiral molecules," Jones says, and tested combinations of racemic, right- and left-handed drugs, and cocrystal formers (*Faraday Discuss.*, DOI: 10.1039/b616399h). One observation with implications for drug forms was that the symmetry of the cocrystal formers changed the thermal properties of the resulting cocrystals.

To test for hydrate stability, Jones and coworkers studied caffeine and theophylline as model APIs and citric acid as the guest (*Mol. Pharmaceutics* **2007**, 4, 347). Liquid-assisted grinding using water proved most useful in making cocrystal hydrates. If they switched to hydrated APIs, however, theophylline formed a stable hydrated cocrystal with citric acid, whereas caffeine and citric acid resulted in an anhydrous one.

Cocrystal studies often generate different solid forms and even new polymorphs. In fact, this is how Zaworortko's group and collaborators at TransForm found the proposed second polymorph of aspirin (*J. Am. Chem. Soc.* **2005**, 127, 16802). "There are always surprises," Bernstein says, based on his experience with oxalic acid (*Mol. Pharmaceutics* **2007**, 4, 355). "This is going to happen because you are creating crystallization conditions that haven't really been tried before."

Given that different methods can produce the same or different cocrystals, most researchers resort to using several means in their discovery efforts. They frequently use grinding, evaporation, sublimation, and melt crystallization. Some focus on solution-based approaches because these are typically used on an industrial scale for crystallization and purification.

"In general, crystallizations by cooling are by far the simplest to develop and scale up, because the fundamentals of the process are thermodynamic and thus scale-independent," AstraZeneca's Black says. And once you know which solid form you want to make, cooling crystallization is the easiest way to ensure that you make these desired crystals, he adds. A common practice is to seed, or initiate, crystallization with small amounts of the desired crystal, a process that also works for cocrystals.

But cocrystallization may run counter to how most people think about crystallization, where the goal is usually to get a pure compound, not two or more coming out of solution together. Black and other researchers emphasize the importance of knowing the system's phase diagram, including the solubility curve, to pinpoint where one needs to be in terms of temperature and composition to make the desired product.

"If you want to control the process to make sure you get the right polymorph or crystallize a salt or cocrystal, you have to know something about how a molecule gets from the solution to the crystal," says Roger J. Davey, professor in the chemical engineering department at the University of Manchester, in England. His research group has been looking at nucleation processes for solid forms, including salts, polymorphs, and cocrystals (*Faraday Discuss.*, DOI: 10.1039/b616164m).

"We try to choose systems where we can do in situ measurements to explore simple questions about the relationship between the solution chemistry in a particular solvent and the crystal structure that appears," he explains. Although one can monitor what's happening, predicting the kinetics and outcome is just too hard.

Lacking the ability to predict outcomes, most pharmaceutical cocrystals are found by taking an API and a range of solvents and potential salt or cocrystal formers and screening combinations. This can be a hit-or-miss approach, but if something does form, it's likely to be fairly robust, or it wouldn't have appeared, many researchers say. At the same time, they admit, depending on the extent of screening, it's possible that something will be missed.

Nair Rodríguez-Hornedo, pharmaceutical sciences professor at the University of Michigan, aspires to a mechanistic, nonempirical approach to understanding cocrystal formation and stability. Thinking practically about how cocrystals could be made and handled industrially, "we want to find methods that are transferable to large scale and understand how vulnerable cocrystals are to processing and storage," she says.

COCRYSTALLIZATION generally involves the slow evaporation of solutions with equimolar or stoichiometric concentrations of the components. In this process, there's always the risk of crystallizing only the single components.

UM00016782
NOVARTIS EXHIBIT 1517
Novartis v. Regents, IPR2023-01347
Page 3764 of 4460

In analogy to precipitating salts by changing the pH, Rodr??guez-Hornedo finds conditions under which cocrystals become less soluble and form from solutions or other wet phases. She has shown mathematically how solubility depends on the equilibrium between the cocrystal and its components (*Cryst. Growth. Des.* **2006**, 6, 592).

Based on this solubility behavior, her group has been able to rapidly generate carbamazepine-nicotinamide and other cocrystals by reaction crystallization (*Mol. Pharmaceutics* **2006**, 3, 362). The process entails either mixing solutions of the reactants to achieve nonstoichiometric amounts or dissolving a nonstoichiometric excess of one in a solution of the other.

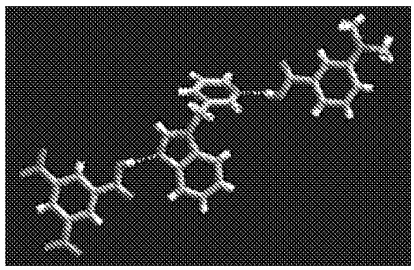

Courtesy of Christer Aakeröy

Supermolecule Ternary structure of a pyridyl/benzimidazol-1-yl and two carboxylic acids.

At a certain point, the mixture is supersaturated with respect to the cocrystal complex, which precipitates out because it is less soluble than the reactants. Nonstoichiometric concentrations and supersaturation can also be achieved in small quantities of solvent by using solid reactants with different dissolution rates.

"We have not been able to find an existing cocrystal that we cannot make," Rodríguez-Hornedo claims. Her group has shown that even in solvents where the cocrystal is more soluble than the pure API, the reaction can be reversed to form the cocrystal by increasing the concentration of the cocrystal former above a critical value. "The ability to change the thermodynamic relationship between the cocrystal phase and pure API crystal is valuable to control cocrystal formation and stability," she says.

These methods work in both organic and aqueous solvents, although both components must be at least somewhat soluble. Her students typically test methanol, ethanol, and water. The methods are also easily scaled up, applicable to high-throughput crystallization screens, and offer prospects for greener synthetic routes, she points out.

To test stability, Rodr??guez-Hornedo has found that moisture, simply from the air, facilitates cocrystal formation in physical mixtures that contain a deliquescent component, which dissolves as it absorbs moisture in the air. Cocrystal ingredients dissolve in this deliquesced solution and then cocrystallize (*Mol. Pharmaceutics* **2007**, 4, 360). She says moisture can also increase molecular mobility via amorphous phases made during grinding (*Pharm. Res.* **2006**, 23, 2381) or, as she learned in work with collaborators at Schering-Plough and Amgen, in melts and films (*J. Pharm. Sci.* **2007**, 96, 1147).

Meanwhile, other researchers are finding that cocrystal forms can be more stable than the pure API, but the relative stability varies from case to case. Jones and Trask, for example, found that the physical stability of caffeine and the asthma drug theophylline could be increased in cocrystals with oxalic acid (*Int. J. Pharm.* **2006**, 320, 11).

Such factors are important considerations, Rodríguez-Hornedo explains, because drug formulation frequently involves mechanical stress from grinding, milling, or blending. And products may be exposed to different levels of humidity during storage. These changes could either induce cocrystal formation or lead to degradation.

The driver behind making cocrystals is, of course, to improve upon the properties of an API, and many more comparisons are being reported. Rodríguez-Hornedo's group, for example, has found that cocrystals with an ionizable guest can impart pH solubility dependence to nonionizable APIs. "It offers the possibility of tailoring the pH dependence of the dissolution," she notes.

For many years, crystal engineering focused on optical and mechanical properties of materials, says Matthew L. Peterson, a senior scientist and group leader at TransForm. "It has taken some time to recognize that something as simple as dissolution is a very important property to enhance through cocrystals," he says. This realization has opened up a whole new area of looking at what other changes can be made, he adds.

Another driver, suggests TransForm principal investigator Julius F. Remenar, has been the advent of high-throughput drug discovery methods. These methods have resulted in many more poorly soluble compounds that need solid-state engineering. By about 2002, this problem-along with legal, regulatory, and business issues, as well as with emerging work in cocrystals-made the drug industry "ready for cocrystals," he says.

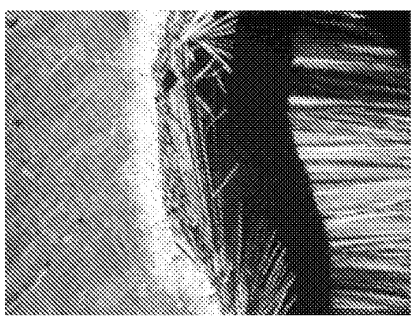

Remenar, Peterson, and coworkers published an early example involving the antifungal drug itraconazole, which is extremely insoluble and not suited to salt formation (a common and generally straightforward route to increase solubility). J&J had made an amorphous form to achieve a usable bioavailability. With a high-throughput crystallization screen, the researchers discovered stable cocrystals using 1,4-dicarboyxlic acids as the cocrystal formers (*J. Am. Chem.*

UM00016783
NOVARTIS EXHIBIT 1517
Novartis v. Regents, IPR2023-01347
Page 3765 of 4460

Soc. **2003**, 125, 8456).

scott childs/ssci

Togetherness Cocrystal needles form in the center from the mixing of melted (black area) crystalline nabumetone (on left) and crystalline 2,3-naphthalenediol (on right).

With Zaworotko, these scientists have recently compared a carbamazepine cocrystal with the marketed carbamazepine polymorph (*Eur. J. Pharm. Biopharm.*, DOI: 10.1016/j.ejpb.2006.12.016). The drug is an antiepileptic that is water-insoluble and thus requires high doses. It is a favorite in the crystal engineering field because it crystallizes in at least four polymorphs and forms several salts, solvates, and hydrates, though it is a simple molecule with one primary amide hydrogen-bonding site.

Their carbamazepine-saccharin cocrystal could be made by a cooling crystallization from alcohol solution without seeding and was scaled up to a 30-g batch size. With polymorph screening, they found only one polymorph of the cocrystal, which had comparable stability to the marketed form, as well as favorable dissolution properties and comparable oral adsorption.

The TransForm researchers have also looked at cocrystals in aqueous media and in the presence of materials, called excipients, used in formulating products. The API was celecoxib, the well-known analgesic drug that has been studied extensively to improve its absorption. Excipients were found to stabilize a celecoxib-nicotinamide cocrystal with good properties and help direct its conversion into more bioavailable intermediates (*Mol. Pharmaceutics* **2007**, 4, 386).

Formulated cocrystals haven't received much attention, the TransForm scientists say, but are expected to as cocrystals move through drug company pipelines. And although most published examples involve nonproprietary or model APIs, researchers tell C&EN there are indications that several cocrystal drugs are likely to be coming to the market.

Merck researchers recently reported what they say is the first case of a stable cocrystal formed between an API and an inorganic acid (*Chem. Commun.* **2007**, 419). By using a monophosphate salt of the API and phosphoric acid, they say their cocrystal allowed them to avoid the need to use an unstable amorphous drug or salts to get an optimal solid dosage form.

Previously, another Merck group prepared and characterized cocrystals of a phosphodiesterase-IV inhibitor with L-tartaric acid (*Cryst. Growth. Des.* **2006**, 6, 690). The free compound had insufficient bioavailability to develop it for safety studies, but a series of stable nonstoichiometric acid-base cocrystals demonstrated as much as 20-fold improvement in blood plasma concentrations.

Similarly, Pfizer scientists formed complexes of a sparingly soluble anticancer drug candidate containing multiple basic nitrogens and hydrogen-bonding sites with three different dicarboxylic acids (*J. Am. Chem. Soc.* **2006**, 128, 8199). Resulting acid-base complexes, depending on the difference in pK_a's of the acids and bases, ranged from neutral complexes to fully ionic salts. Characterization and analysis of these complexes showed significantly enhanced properties needed for drug delivery.

Researchers at Purdue Pharma and SSCI recently reported on the development of a cocrystal to improve the bioavailability of another low-solubility API (*Pharm. Res.* **2006**, 23, 1888). Using a crystal engineering approach, they screened 26 pharmaceutically acceptable carboxylic acids and found a stable API-glutaric acid cocrystal that had an 18-times-greater dissolution rate in water and three-times-higher blood plasma concentrations. Similarly, Scott L. Childs at SSCI and Kenneth I. Hardcastle at Emory University conducted a broad study in which 50 cocrystals of the API piroxicam were made with 23 carboxylic acids (*Cryst. Growth Des.*, DOI: 10.1021/cg060742p).

"COCRYSTAL SCREENING is going to be an empirical process," says G. Patrick Stahly, former chief operating officer of SSCI, "but we start with an initial evaluation of the API in terms of its structure and properties, along with careful selection of potential guests, experimental techniques, and screening protocols." Stahly, who is starting his own consulting firm called Chemfocus, describes the entire solid-form discovery and characterization process in a recent article (*Cryst. Growth Des.* **2007**, 7, 1007).

SSCI is also known for its work on carboxylic acid cocrystals of fluoxetine hydrochloride, the API in the antidepressant Prozac (*J. Am. Chem. Soc.* **2004**, 126, 13335). An estimated 50% of all API salts are made with the chloride ion, and cocrystallization of these salts provides the opportunity to alter physical properties while retaining the salt form in the cocrystal structure, Stahly explains.

"There's also a bit of a debate about whether something is a cocrystal or a salt," he says. In a salt, the components are ionizable and differ enough in pK_a that a proton is transferred. When this doesn't happen, as with very weak acids or bases, it's a cocrystal. One can miss forming cocrystals, Stahly warns, if the components are chosen based on large differences in pK_a.

But there's another hitch. "If the components are close in pK_a, whether the proton is transferred or not depends on the crystal environment," he explains. SSCI researchers explored this "salt-cocrystal continuum" and the influence crystal structure has on the ionization state in 20 complexes of theophylline (*Mol. Pharmaceutics* **2007**, 4, 323).

UM00016784
NOVARTIS EXHIBIT 1517
Novartis v. Regents, IPR2023-01347
Page 3766 of 4460

Similarly, Aakeröy has analyzed 86 salts and cocrystals synthesized from carboxylic acids and N-heterocycles (*Mol. Pharmaceutics* **2007**, 4, 317). "We found that the stoichiometric composition of cocrystals was more predictable than that of certain salts," he says. "In principle, this indicates that cocrystal structures would be more controllable, and, of course, that's key to controlling physical properties."

BUT NOT ALL cocrystals show improved properties, and they are not a panacea for all problems. Although pharmaceutical industry interest is on the rise, many researchers believe drug developers are still waiting for the first big cocrystal product to emerge. It's not yet clear how regulators will treat these new forms and what testing will be required, nor have generic drug firms used a cocrystal form to challenge a related product.

Researchers at TransForm say they have become concerned in the past few years about hype surrounding cocrystals. "When you put it in perspective, the opportunities to make a cocrystal into something useful are rather limited, given the number of possibilities of other forms and how hard it is to actually make a new drug anyway," Peterson says.

The question also arises of the necessity for having a cocrystal form in the first place. "If making a cocrystal of a specific molecule helps to enable an application or solve a problem, then it's the right thing to do," Remenar adds. "But you don't design a molecule in the real world simply because you are looking for a cocrystal strategy."

Cover Story

- Form And Function
- The choice of pharmaceutical crystalline form can be used to optimize drug properties, and cocrystals are emerging as new alternatives
- War Of The Words
- Dispute Over Crystal Structure Nomenclature Takes Center Stage
- Solid-State Services
- Specialized companies help drug developers find crystalline forms with the right properties

[Top of Page]

UM00016785
NOVARTIS EXHIBIT 1517
Novartis v. Regents, IPR2023-01347
Page 3767 of 4460

Procedure—Place in the dry flask a quantity of the substance, weighed accurately to the nearest centigram, which is expected to yield 2 to 4 mL of water. If the substance is of a pasty character, weigh it in a boat of metal foil of a size that will just pass through the neck of the flask. If the substance is likely to cause bumping, add enough dry, washed sand to cover the bottom of the flask, or a number of capillary melting-point tubes, about 100 mm in length, sealed at the upper end. Place about 200 mL of toluene in the flask, connect the apparatus, and fill the receiving tube *E* with toluene poured through the top of the condenser. Heat the flask gently for 15 minutes and, when the toluene begins to boil, distil at the rate of about 2 drops per second until most of the water has passed over, then increase the rate of distillation to about 4 drops per second. When the water has apparently all distilled over, rinse the inside of the condenser tube with toluene while brushing down the tube with a tube brush attached to a copper wire and saturated with toluene. Continue the distillation for 5 minutes, then remove the heat, and allow the receiving tube to cool to room temperature. If any droplets of water adhere to the walls of the receiving tube, scrub them down with a brush consisting of a rubber band wrapped around a copper wire and wetted with toluene. When the water and toluene have separated completely, read the volume of water, and calculate the percentage that was present in the substance.

METHOD III (GRAVIMETRIC)

Procedure for Chemicals—Proceed as directed in the individual monograph preparing the chemical as directed under *Loss on Drying* ⟨731⟩.

Procedure for Biologics—Proceed as directed in the individual monograph.

Procedure for Vegetable Drugs—Place about 10 g of the drug, prepared as directed (see *Vegetable Drugs—Methods of Analysis* (561)) and accurately weighed, in a tared evaporating dish. Dry at 105° for 5 hours, and weigh. Continue the drying and weighing at 1-hour intervals until the difference between two successive weighings corresponds to not more than 0.25%.

⟨941⟩ X-RAY DIFFRACTION

Every crystal form of a compound produces its own characteristic X-ray diffraction pattern. These diffraction patterns can be derived either from a single crystal or from a powdered specimen (containing numerous crystals) of the material. The spacings between and the relative intensities of the diffracted maxima can be used for qualitative and quantitative analysis of crystalline materials. Powder diffraction techniques are most commonly employed for routine identification and the determination of relative purity of crystalline materials. Small amounts of impurity, however, are not normally detectable by the X-ray diffraction method, and for quantitative measurements it is necessary to prepare the sample carefully to avoid preferred orientation effects.

The powder methods provide an advantage over other means of analysis in that they are usually nondestructive in nature (specimen preparation is usually limited to grinding to ensure a randomly oriented sample, and deleterious effects of X-rays on solid pharmaceutical compounds are not commonly encountered). The principal use of single-crystal diffraction data is for the determination of molecular weights and analysis of crystal structures at the atomic level. However, diffraction established for a single crystal can be used to support a specific powder pattern as being truly representative of a single phase.

Solids—A solid substance can be classified as being crystalline, noncrystalline, or a mixture of the two forms. In crystalline materials, the molecular or atomic species are ordered in a three-dimensional array, called a lattice, within the solid particles. This ordering of molecular components is lacking in noncrystalline material. Noncrystalline solids sometimes are referred to as glasses or amorphous solids when repetitive order is nonexistent in all three dimensions. It is also possible for order to exist in only one or two dimensions, resulting in mesomorphic phases (liquid crystals). Although crystalline materials are usually considered to have well-defined visible external morphologies (their habits), this is not a necessity for X-ray diffraction analysis.

The relatively random arrangement of molecules in noncrystalline substances makes them poor coherent scatterers of X-rays, resulting in broad, diffuse maxima in diffraction patterns. Their X-ray patterns are quite distinguishable from crystalline specimens, which give sharply defined diffraction patterns.

Many compounds are capable of crystallizing in more than one type of crystal lattice. At any particular temperature and pressure, only one crystalline form (polymorph) is thermodynamically stable. Since the rate of phase transformation of a metastable polymorph to the stable one can be quite slow, it is not uncommon to find several polymorphs of crystalline pharmaceutical compounds existing under normal handling conditions.

In addition to exhibiting polymorphism, many compounds form crystalline solvates in which the solvent molecule is an integral part of the crystal structure. Just as every polymorph has its own characteristic X-ray patterns, so does every solvate. Sometimes the differences in the diffraction patterns of different polymorphs are relatively minor, and must be very carefully evaluated before a definitive conclusion is reached. In some instances, these polymorphs and/or solvates show varying dissolution rates. Therefore, on the time scale of pharmaceutical bioavailability, different total amounts of drug are dissolved, resulting in potential bioinequivalence of the several forms of the drug.

Fundamental Principles—A collimated beam of monochromatic X-rays is diffracted in various directions when it impinges upon a rotating crystal or randomly oriented powdered crystal. The crystal acts as a three-dimensional diffraction grating to this radiation. This phenomenon is described by Bragg's law, which states that diffraction (constructive interference) can occur only when waves that are scattered from different regions of the crystal, in a specific direction, travel distances differing by integral numbers (n) of the wavelength (λ). Under such circumstances, the waves are in phase. This condition is described by the Bragg equation:

$$\frac{n\lambda}{2 \sin \theta} = d_{hkl},$$

in which d_{hkl} denotes the interplanar spacings and θ is the angle of diffraction.

A family of planes in space can be indexed by three whole numbers, usually referred to as Miller indices. These indices are the reciprocals, reduced to smallest integers, of the intercepts that a plane makes along the axes corresponding to three nonparallel edges of the unit cell (basic crystallographic unit). The unit cell dimensions are given by the lengths of the spacings along the three axes, a, b, c, and the angles between them, α, β, and γ. The interplanar spacing for a specific set of parallel planes hkl is denoted by d_{hkl}. Each such family of planes may show higher orders of diffraction where the d values for the related families of planes nh, nk, nl are diminished by the factor $1/n$ (n being an integer: 2, 3, 4, etc.). Every set of planes throughout a crystal has a corresponding Bragg diffraction angle associated with it (for a specific λ).

The amplitude of a diffracted X-ray beam from any set of planes is dependent upon the following atomic properties of the crystal: (1) position of each atom in the unit cell; (2) the respective atomic scattering factors; and (3) the individual thermal motions. Other factors that directly influence the intensities of the diffracted beam are: (1) the intensity and wavelength of the incident radiation; (2) the volume of crystalline specimen; (3) the absorption of the X-radiation by the specimen; and (4) the experimental arrangement utilized to record the intensity data. Thus, the experimental conditions are especially important for measurement of diffraction intensities.

Only a limited number of Bragg planes are in a position to diffract when monochromatized X-rays pass through a single crystal. Techniques of recording the intensities of all of the possible diffracting hkl planes involve motion of the single crystal and the recording media. Recording of these data is accomplished by photographic techniques (film) or with radiation detectors.

A beam passing through a very large number of small, randomly oriented crystals produces continuous cones of diffracted rays from each set of lattice planes. Each cone corresponds to the diffraction from various planes having a similar interplanar spacing. The intensities of these Bragg reflections are recorded by either film or radiation detectors. The Bragg angle can be measured easily from a film, but the advent of radiation detectors

BEST AVAILABLE COPY